FOSSIL

DOE/PC/90544-T9
(DE94002026)

DESIGN VERIFICATION AND COLD-FLOW MODELING TEST REPORT

July 1993

Work Performed Under Contract No. FC22-91PC90544

For
U.S. Department of Energy
Pittsburgh Energy Technology Center
Pittsburgh, Pennsylvania

By
TRW Applied Technology Division
Redondo Beach, California

DOE/PC/90544-T9
(DE94002026)
Distribution Category UC-105

TRW Applied Technology Division
One Space Park
Redondo Beach, CA 90278

Design Verification and Cold-Flow Modeling Test Report

July 1993

Submitted to:

Alaska Industrial Development & Export Authority
280 West Tudor
Anchorage, Alaska 99503-6690

Professional Service Agreement HCP-008

Under DOE Cooperative Agreement No. DE-FC22-91PC-90544

SN 57024
93.HP.SKU-714

ABSTRACT

This report presents a compilation of the following three test reports prepared by TRW for Alaska Industrial Development and Export Authority (AIDEA) as part of the Healy Clean Coal Project, Phase 1 Design of the TRW Combustor and Auxiliary Systems, which is co-sponsored by the Department of Energy under the Clean Coal Technology 3 Program:

(1) Design Verification Test Report, dated April, 1993
(2) Combustor Cold Flow Model Report, dated August 28, 1992
(3) Coal Feed System Cold Flow Model Report, October 28, 1992

In this compilation, these three reports are included in one volume consisting of three parts, and TRW proprietary information has been excluded.

Part 1

Design Verification Test Report

Table of Contents: Part 1
Design Verification Test Report

1.0 Abstract

This report covers the activities associated with the design, fabrication, installation and testing of a full-scale precombustor, rated at 130 MMBTU/hr, and a one-third scale direct coal feed system (DCFS), also rated at 130 MMBTU/hr, at TRW's Fossil Energy Test Site in San Juan Capistrano, California, as part of the design of two 350 MMBTU/hr coal combustion systems for the Healy Clean Coal Project under the sponsorship of Alaska Industrial Development and Export Authority (AIDEA). These design verification tests (DVT) were performed during the period August 1992 to February 1993.

It was recognized early on that the most critical components of the TRW coal combustion system were the precombustor and the coal feed system. The slagging combustor scaling and operation was well understood, both from analytical and operational viewpoints after the successful completion of the testing of a 40 MMBTU/hr system at TRW's Cleveland facility during 1990-1991 time frame under the sponsorship of AIDEA. The limestone feed system was operated successfully at TRW's Cleveland Facility. This experience was sufficient to allow scaling to Healy requirements without further testing of these components. The coal feed system at Cleveland was a storage type of system. During the first quarter of 1992, AIDEA directed TRW to abandon the storage type of system and change to a non-storage, or direct coal feed system.

The precombustor design was scaled from TRW's design of the 40 MMBTU/hr system in Cleveland, a scaleup by a factor of approximately 8. A significant change in the design approach was necessitated by the requirement that the precombustor be used for boiler warm-up and that during that time all the coal fines from the mill be combusted prior to entering the cold furnace. Also, because of scaling, it was recognized early that a multiple coal injector would be advantageous and to this end a commercial Foster Wheeler (low NO_x) burner was incorporated into this design. The new DCFS was conceived, designed, fabricated, installed and tested all within a span of approximately one year. The successful completion of the tests mitigated the concerns on scaleup and operation of the total system.

Both the combustor and coal feed system hardware design were supported by cold-flow tests conducted TRW's Space Park facility. The results of these tests are presented in Parts 2 and 3.

Over 200 tons of Performance Blend coal was supplied gratis by Usibelli Coal Mine Company for these tests. The coal was transported from Usibelli mine to EER, Inc. in Irvine, California by barge and rail cars. EER pulverized this coal to TRW's specifications and a total of 160 tons was delivered to TRW's test site in hopper cars. This pulverized coal was stored in tanks called guppies and blanketed with a nitrogen atmosphere, for safety

reasons, and used during the tests as needed.

All of the pulverized coal was utilized in a series of 28 tests. The total run time on coal was approximately 43 hours. The oil burner was operated for approximately 50 hours.

The details of the hardware, the test facility, testing, the data accumulated and the analyses of the data are presented in this report.

The DVT on the precombustor and the DCFS fully satisfied the objectives of the test program. Sufficient data were accumulated to validate the performance predictions and to verify the proposed operating conditions and sequences. Several operational problems were encountered during the DVT series, and the experience gained while correcting these problems provided the guidelines for improving the design and operating procedures.

2.0 Executive Summary

2.1 Objectives

The design verification tests (DVT) were performed as part of the total design of the TRW coal combustion system for the Healy plant primarily to mitigate the uncertainties associated with two critical subsystems, namely, the precombustor and the direct coal feed system. The risks associated with the operation and scalability of the slagging combustor and the limestone feed system were significantly less, and hence DVT on these subsystems were not performed.

The tests were grouped into two major categories: (1) Full-scale precombustor tests only, using an existing coal feed system at TRW's Capistrano Test Site (CTS), (2) Flow, checkout and hot-fire tests of the one-third scale direct coal feed system coupled to the precombustor.

The major objectives of the precombustor tests were to:

- Mitigate risks associated with scaleup and meet the new requirements of the HCCP.
- Validate precombustor ignition, stability and performance.
- Investigate and verify the absence of slagging and fouling in the precombustor.
- Verify that the vent air with coal fines rejected by the direct coal feed system can be burned in the precombustor during startup without adverse effects on its performance.
- Operate the precombustor through the entire startup and shutdown sequences, and investigate and correct anomalies, if any.
- Measure heat fluxes in water-cooled areas in the precombustor and validate these measurements with the design values.
- Measure pressures (and pressure drops) in critical regions of the precombustor.
- Demonstrate operation of the 70 MMBTU/hr Forney ignitor through the four-to-one firing range and document the lessons learned for use at Healy.
- Prove that the precombustor can be operated safely with the coal and oil flame scanners as designed and tested.

The major objectives of the combined coal feed system and precombustor tests were to:

- Demonstrate the overall operation, stability and controllability of the coal feed system

- Validate the operation and design of the splitter drum, the blowdown cyclones and the transport piping downstream of the cyclones.

- Investigate and validate the following features of the variable splitter: Split control, stability, accuracy, repeatability, pressure drop (with and without coal) and accumulation of coal (if any).

- Investigate and validate the following features of the blowdown cyclones: Effect of blowdown on cyclone efficiency, blowdown pressure drop, cyclone pressure drop, blowdown control, accumulation of coal (if any) and deswirling the blowdown flow.

- Investigate and validate the following features of the transport system downstream of the cyclones: Line sizes and layout including bends, pressure drops, saltation (if any) control and pressure balancing the two legs downstream of the two cyclones.

2.2 Design Verification Test Schedule

The Design Verification Test (DVT) Program was completed at the TRW Fossil Energy Test Site (FETS) close to the planned schedule as shown in Figure 2-1. The objectives of the original test plan were met. The design and performance of the Precombustor (PC), and the concept and arrangement of the Direct Coal Feed System (DCFS) were verified to be acceptable for the Healy application.

2.3 Design Verification Test Logic

A detailed test logic and test plan was developed by TRW prior to the tests and presented to AIDEA and DOE in March 1992. This test plan was subsequently approved. At the conclusion of the DVT series, all proposed activities, except one (discussed below), were completed. Figure 2-2 shows the overall logic. Since the precombustor was designed, fabricated and installed significantly earlier than the DCFS, the precombustor tests were first performed using the existing facility coal feed system, and in parallel, the DCFS was fabricated and installed at CTS. This was accomplished by operating the site on two shifts. The timing was important to complete the installation of the DCFS just prior to the time the precombustor testing was completed. This is shown in both Figures 2-1 and 2-2. The precombustor testing consisted of the following major blocks of activities, as shown in Figure 2-3:

- Coal Lightoff
- Coal Firing
- Burner Tuning
- Swirl Damper Checkout

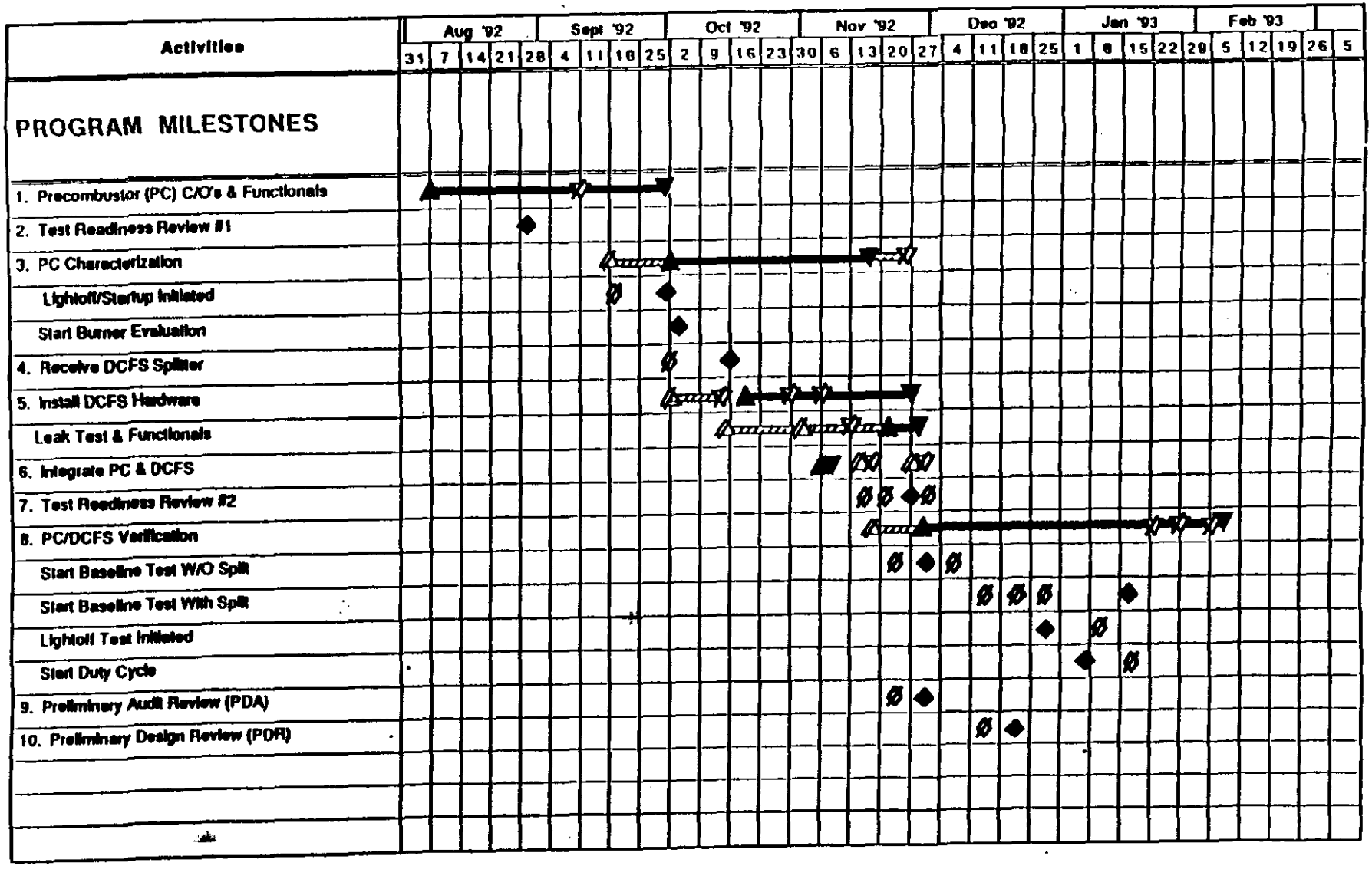

Figure 2-1 DVT Schedules - Milestones

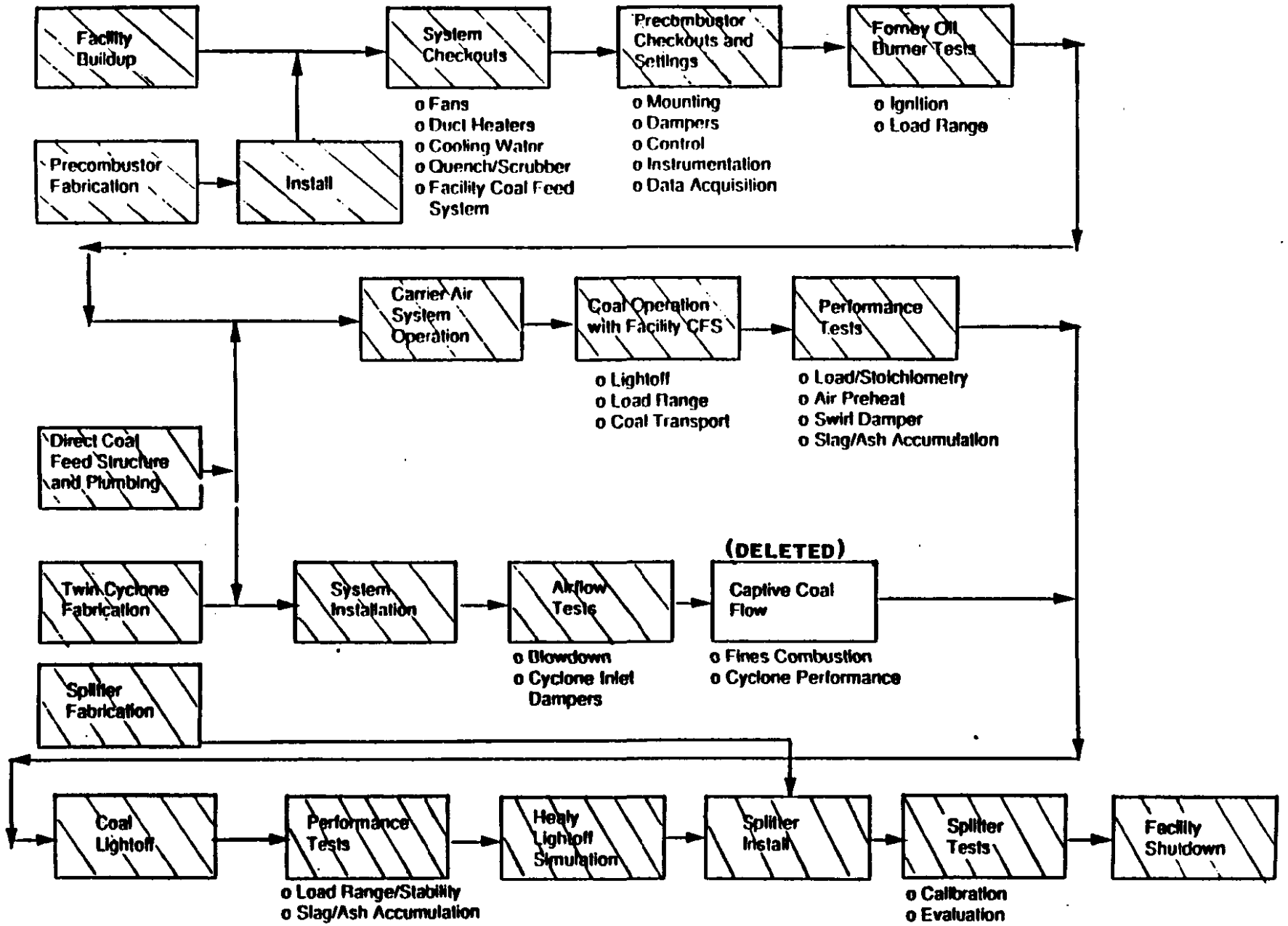

Figure 2-2 DVT Logic Chart

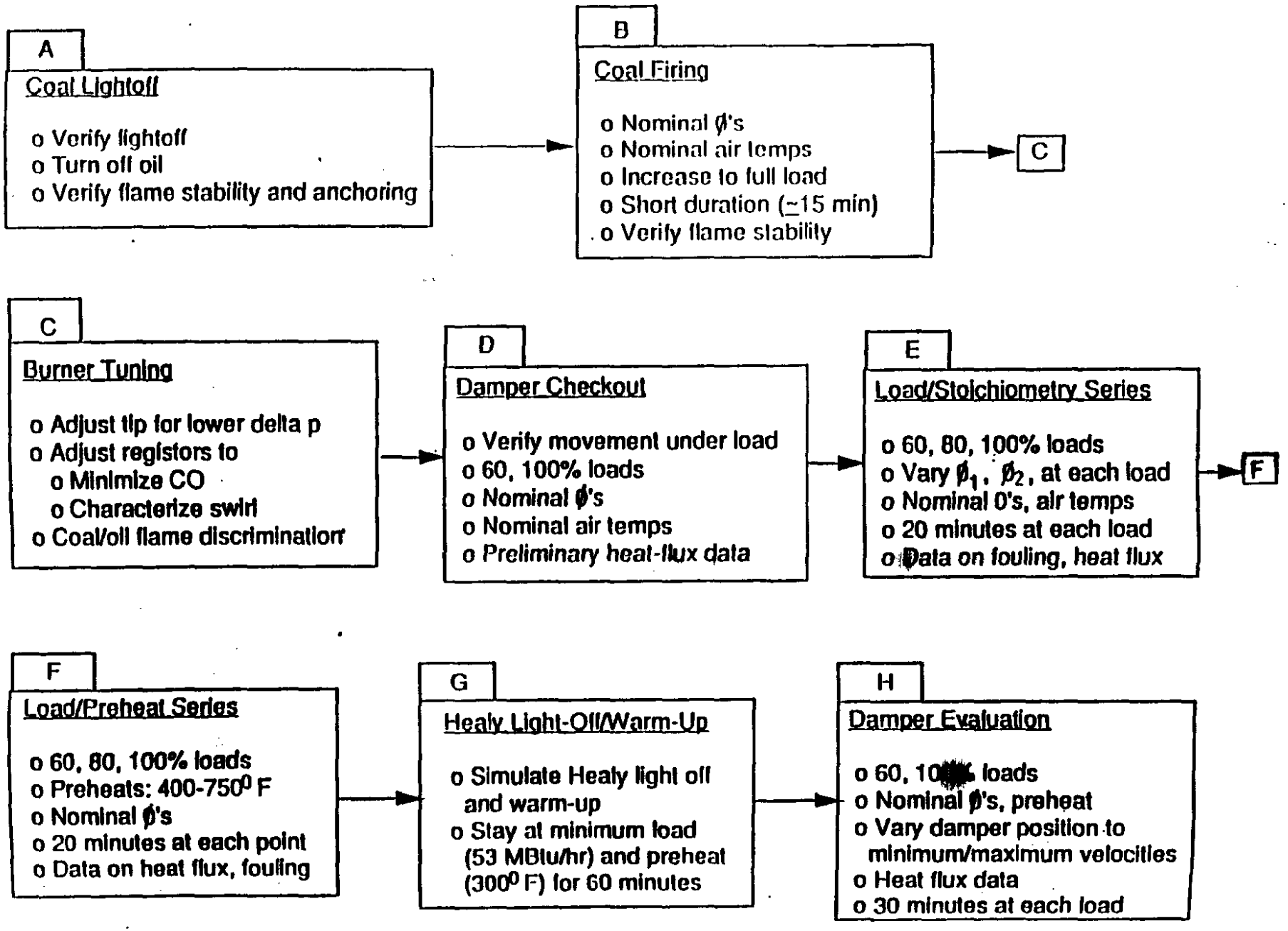

Figure 2-3 DVT Precombustor Test Sequence

- Load/Stoichiometry Series
- Load/Preheat Series
- Healy Light-off/Warmup Sequences
- Swirl Damper Evaluation

The tests on the DCFS were preceded by cold flow modeling tests of a one-tenth scale Plexiglas model. The data and results from these tests helped in the design of the DVT DCFS hardware, as shown in Figure 2-4. There were two major modes of operation for the DCFS. When the output legs of the two cyclones were combined, the total throughput capacity of the one-third scale DCFS was equal to 100% throughput capacity of the precombustor, since the precombustor burns approximately one-third of the total coal throughput. This allowed full-load operation of the precombustor. The next major configuration was the split mode, when one cyclone was directly connected to the precombustor and the other was connected to a catch tank (called the "pup") for evaluating the splitter performance. The following blocks of activities were performed during the DCFS tests:

- Cyclone Efficiency Evaluation
- Blowdown Control and Evaluation
- Evaluation and Improvement of Flow Stability
- Evaluation and Elimination of Coal Accumulation in the Lines
- Evaluation and Minimization of Pressure Drops

The only activity which was eliminated from the original plan was the Captive Flow Test. The original plan called for evaluating cyclone performance with coal prior to the actual hot firing into the precombustor. However, it was determined that it was more expeditious, safer and less expensive to perform these tests while firing the precombustor. This was possible because by the time the DCFS was ready for operation, the precombustor had been completely checked out and could be operated reliably.

2.4 Results

Section 3 includes a description of the hardware utilized for the DVT. Prior to the hot-firing of the precombustor and the DCFS, checkout tests of the various systems and subsystems were performed, and these tests are summarized in Section 4.0. The details of the precombustor and DCFS tests are presented in Sections 5 and 6. The modifications made to the Healy design based on the DVT data and observations, which was the objective of the DVT, are presented in Sections 7 and 8. The last section gives a narrative of the physical status of the hardware after the completion of the tests.

The appendices include the analyses of the Performance Coal tested, a summary of important data from all tests conducted, and the sound level data of selected hardware components.

The highlights of the precombustor and DCFS operation and performance are summarized below:

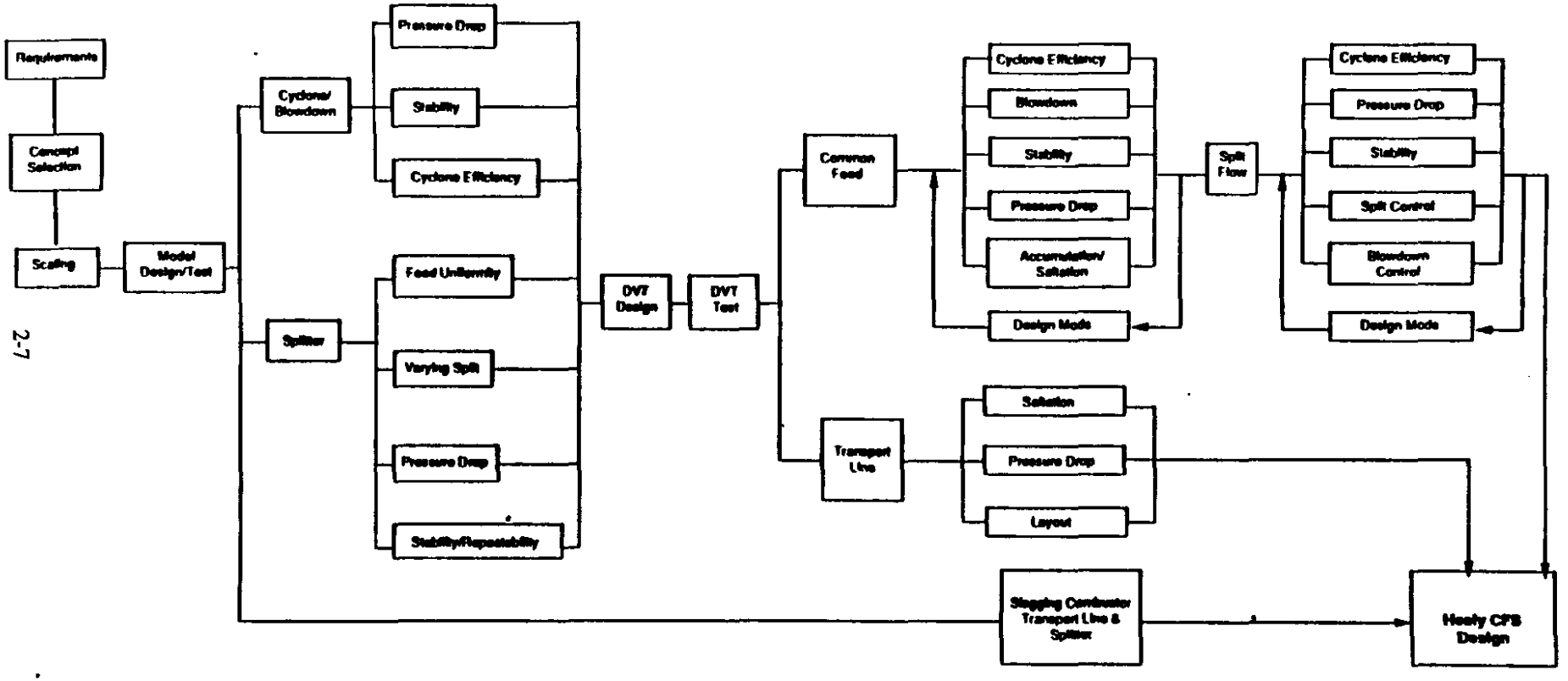

Figure 2-4. Direct Coal Feed System DVT Logic

2.4.1 Precombustor Operation and Performance

- After some initial problems with the Forney oil ignitor, the Foster Wheeler burner oil and coal lightoffs could be achieved within 10 minutes consistently. The burner could be lighted off with primary air from room temperature to 550° F.

- The flame scanner provided by Forney could not discriminate between the oil and coal flames. However, safe operation and continuous monitoring of either the coal or oil flame was still achieved. Whether this meets NFPA requirements is still an issue which needs to be addressed. Since at several Forney installations the same problem exists, and since such installations continue to be in service, the applicability of NFPA requirements in this specific application needs further study.

- The precombustor test results verified the design of the precombustor from the viewpoints of geometry, physical dimensions, pressure drops and heat fluxes.

- Introduction of the mill air (with coal fines) did not adversely impact the operation or performance of the precombustor. This was one of the most important changes to the precombustor design from prior TRW experience.

- The applicability of the Foster Wheeler burner was verified successfully.

- Based on the CO and O_2 levels measured at the stack, the carbon conversion was about the same as that for the smaller scale precombustor tested by TRW in earlier programs.

- Several thermal stress induced cracks were identified in the precombustor windbox. The Healy design has provisions to eliminate this problem.

- Slag deposits in the lowermost region of the combustion can were observed after the tests. This slagging is attributed to the lower-than-expected T_{250} of the slag. However, to prevent the mill air ports in this region from filling with slag (if any) the 8 ports were reduced to 6 upper ports in the Healy design.

- The swirl damper blades were moved in and out during several tests, and were exercised to their design limits. Operationally there were no problems. Higher than designed cooling loads were measured. In the Healy design plasma coating of the blades with a refractory will be considered for reducing this cooling load.

2.4.2 Coal Feed System Operation and Performance

- Tests utilizing the first hardware configuration, which was based on cold flow modeling test, were not entirely successful because at loads higher than 50%, unacceptable fluctuations in coal flow were measured. This was later attributed to coal accumulations in the splitter legs downstream of the splitter drum. This region was modified to increase the velocity, and the modified design was verified successfully by cold flow modeling.

- The DVT hardware was later modified to reflect the flow sections successfully modeled by cold flow and was tested. The coal flow fluctuations diminished considerably to within acceptable levels.

- The pressure drops through the entire DCFS-precombustor system were measured and in the final configuration, the total pressure requirement was below the 60" water limit set for Healy.

- The operation of the modified DCFS was smooth, controllable and was safe. Several "hard" shutdowns followed by a startup were performed to see if the coal remaining in the system after a hard shutdown would affect the next startup. No adverse peaks or operational problems were encountered during the startups.

- The CO levels in the DCFS were below 10 ppm throughout the test series, indicating the absence of smoldering coal particles.

- The splitter dampers were exercised in the range 44%:56% to 50%:50%. The split coal was collected and weighed, and the split was within 2% of the set values.

- The DVT series provided extremely valuable data and operational experience to proceed with the design of the Healy DCFS. The final design configuration for the Healy system is presented in Section 8 of this report.

2.5 Conclusions

Prior to the DVT, TRW's test experience had been on the small-scale 40 MMBTU/hr combustion system. The Healy combustion system is approximately 8 times larger in firing rate, and this posed concerns on scaling to a significantly larger size. Hence, there was a need to mitigate this concern by conducting design verification tests of critical components of the system. TRW identified that only the precombustor and the coal feed system needed to be tested to mitigate the scaling concerns. Furthermore, since the coal feed system was a new innovative system, the DVT was all the more significant.

At the conclusion of the DVT, all concerns related to scaling and operation had been addressed. The objectives of the DVT program were successfully met, and the results of the tests provided the HCCP the confidence needed to proceed with the fabrication, installation and operation at Healy.

3.0 Test Hardware

The Healy design verification test (DVT) program was conducted at TRW's Capistrano Test Site (CTS), located about 65 miles south of Los Angeles, California. Figure 3-1 depicts a three-dimensional overview of Cell No. 3 at the Fossil Energy Test Site (FETS), a facility dedicated to fossil fuel combustion research and development. A photograph of the test arrangement is shown in Figure 3-2.

3.1 DVT Precombustor

A full-scale DVT precombustor (PC) was used to verify the Healy PC design by actual hot-firing with Performance Blend coal. The precombustor consists of five subassemblies: Foster Wheeler burner with primary windbox and Forney ignitor, combustion chamber with secondary windbox, mill air spool (including splitter), transition section, and swirl dampers. A cross sectional view of the DVT precombustor is shown in Figures 3-3. Each subassembly is described separately in the following sections. The DVT precombustor overall dimensions, including the burner, are 18' as measured from burner flange to transition flange, with a maximum diameter of 10'. The dry weight of entire assembly, including refractory is approximately 38,000 lbs.

3.1.1 Installation

The design of the Precombustor and the DVT System were completed during September 1991 - March 1992. The fabrication of the PC was subcontracted to Monroe Inc. in the interest of meeting the DVT program schedule requirements. Monroe had also previously fabricated the combustor hardware for the Cleveland combustor for TRW. Figure 3-4 shows a view of the combustion can during fabrication. A very tight schedule was maintained to deliver the hardware by truck from Pittsburgh and install it on time.

Lifting and installing the PC without incidents was a major concern to the program. A mounting system designed to accommodate thermal expansion was prepared in which the mounting beam could be removed for installation of the PC. Figure 3-5 shows the precombustor as it was lifted into place on the test stand.

The downstream transition and mount sections were installed first without refractory which was provided later. The precombustor, Foster Wheeler coal burner, and Forney oil burner were preassembled on the ground and refractory was installed. An overhead crane lifted and held the assembled unit in place while it was secured to the mount system. The final connections of air supply ducts, cooling water supply and return lines, etc. were field fabricated to assure fitup. The mounting beam and support arrangement is shown in the photograph of Figure 3-6. Figures 3-7 and 3-8 show the fully installed views of the precombustor on Cell No. 3 test stand. Leak and cold flow checks were performed prior to the first

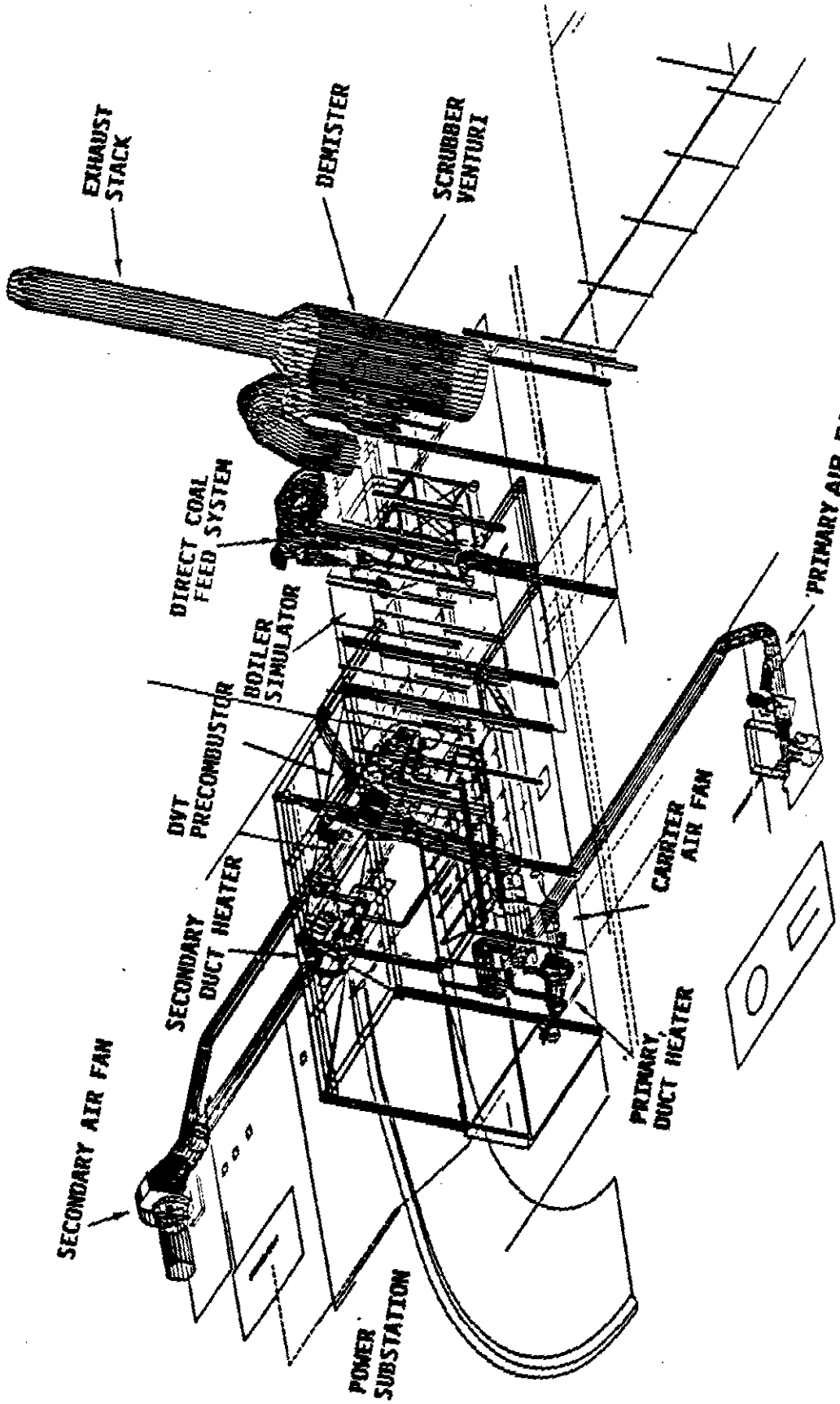

Figure 3-1 FETS Cell #3 Overview

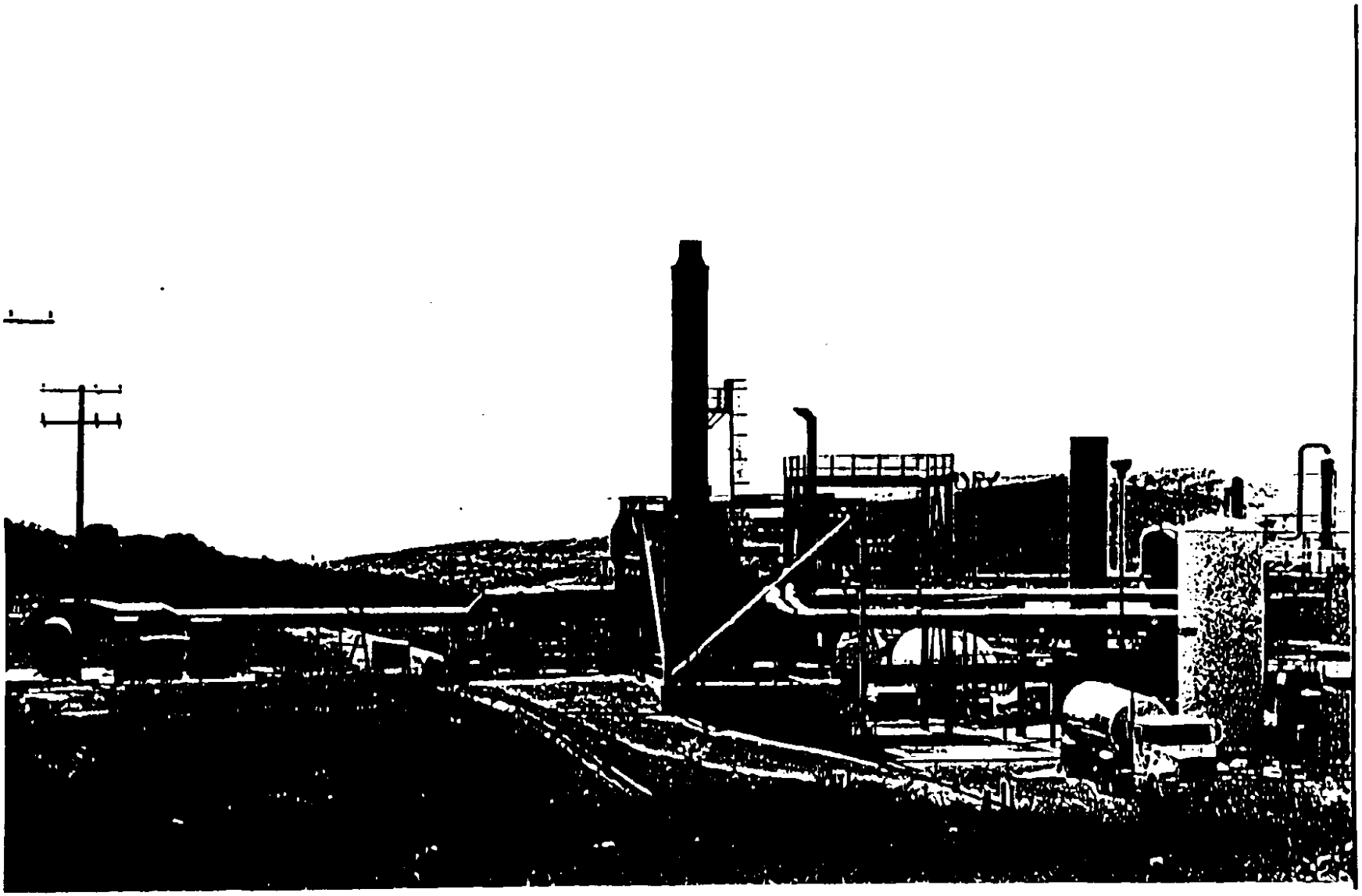

Figure 3-2 Photograph of Test Cell #3 at FETS

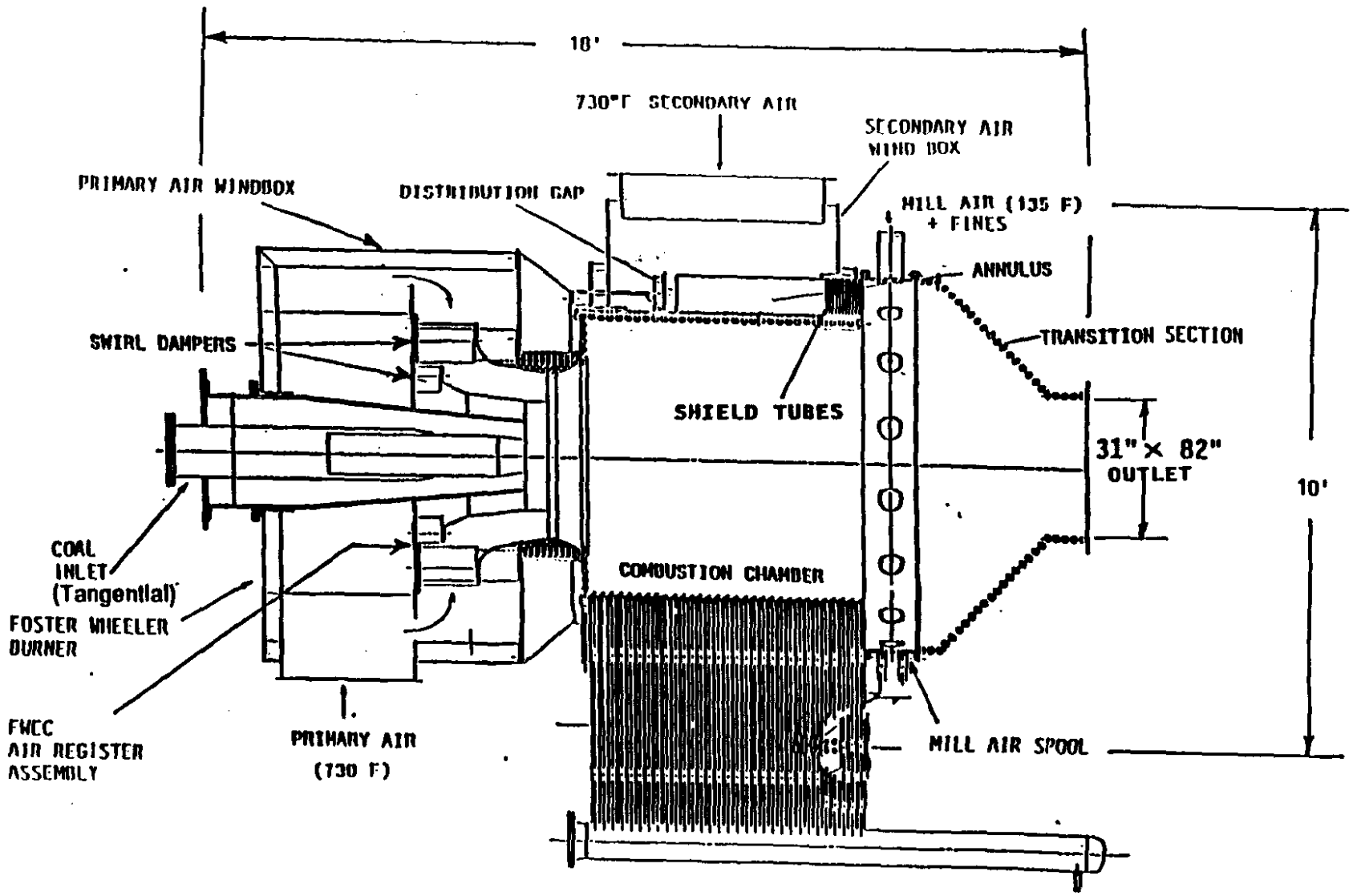

Figure 3-3 DVT Precombustor Configuration

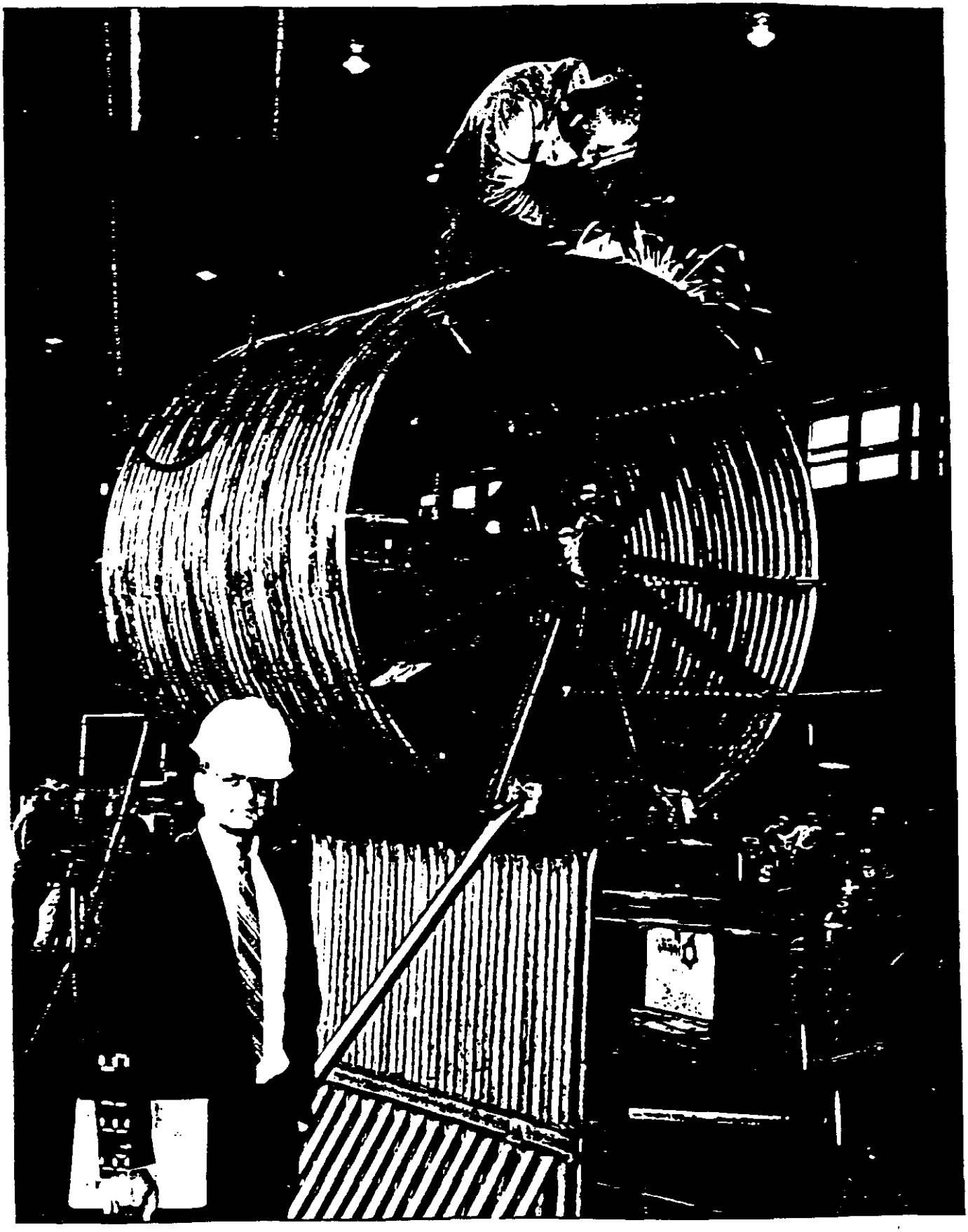

Figure 3-4 DVT Precombustor Combustor Shell During Fabrication

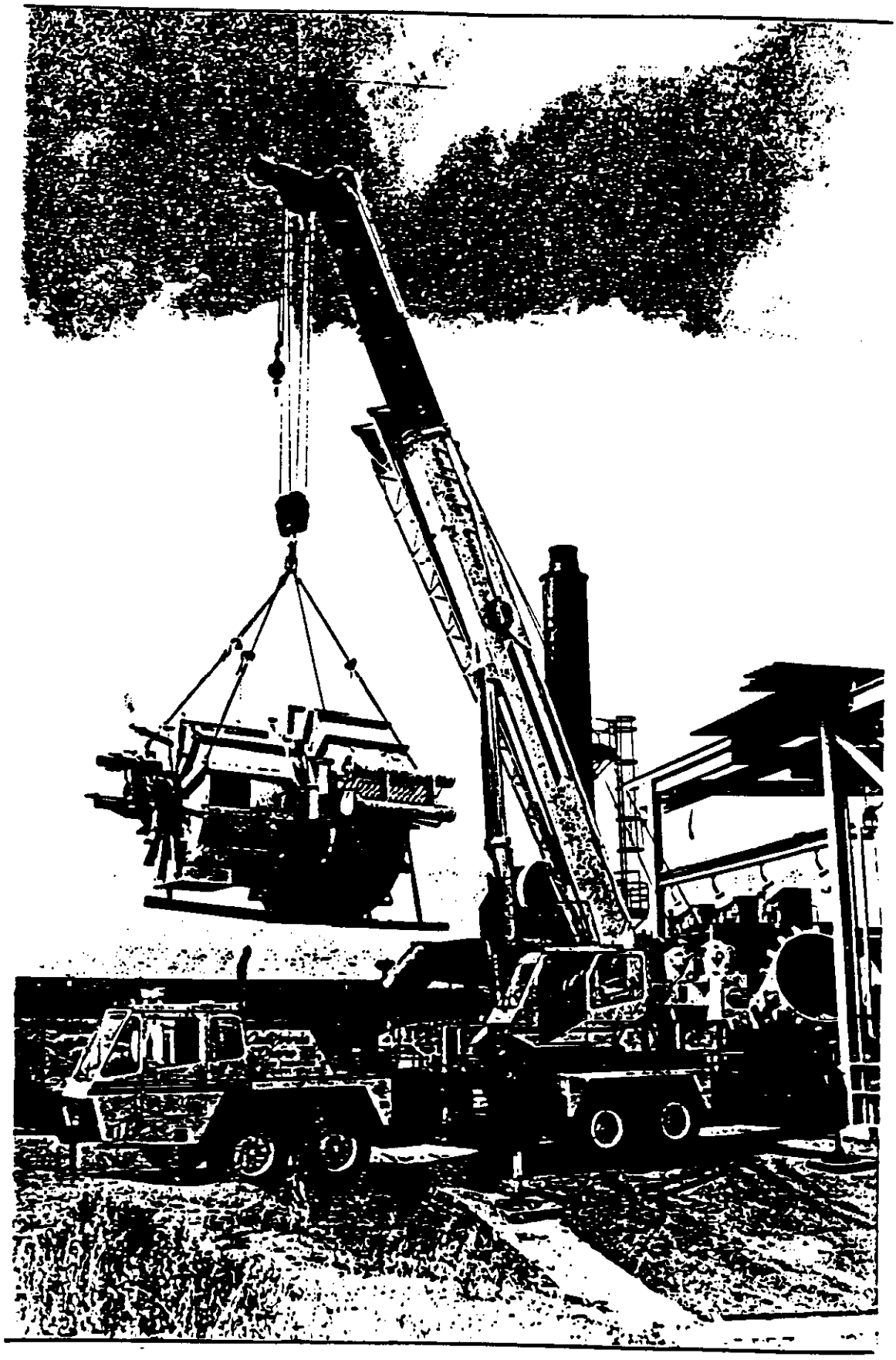

Figure 3-5 DVT Precombustor Installation

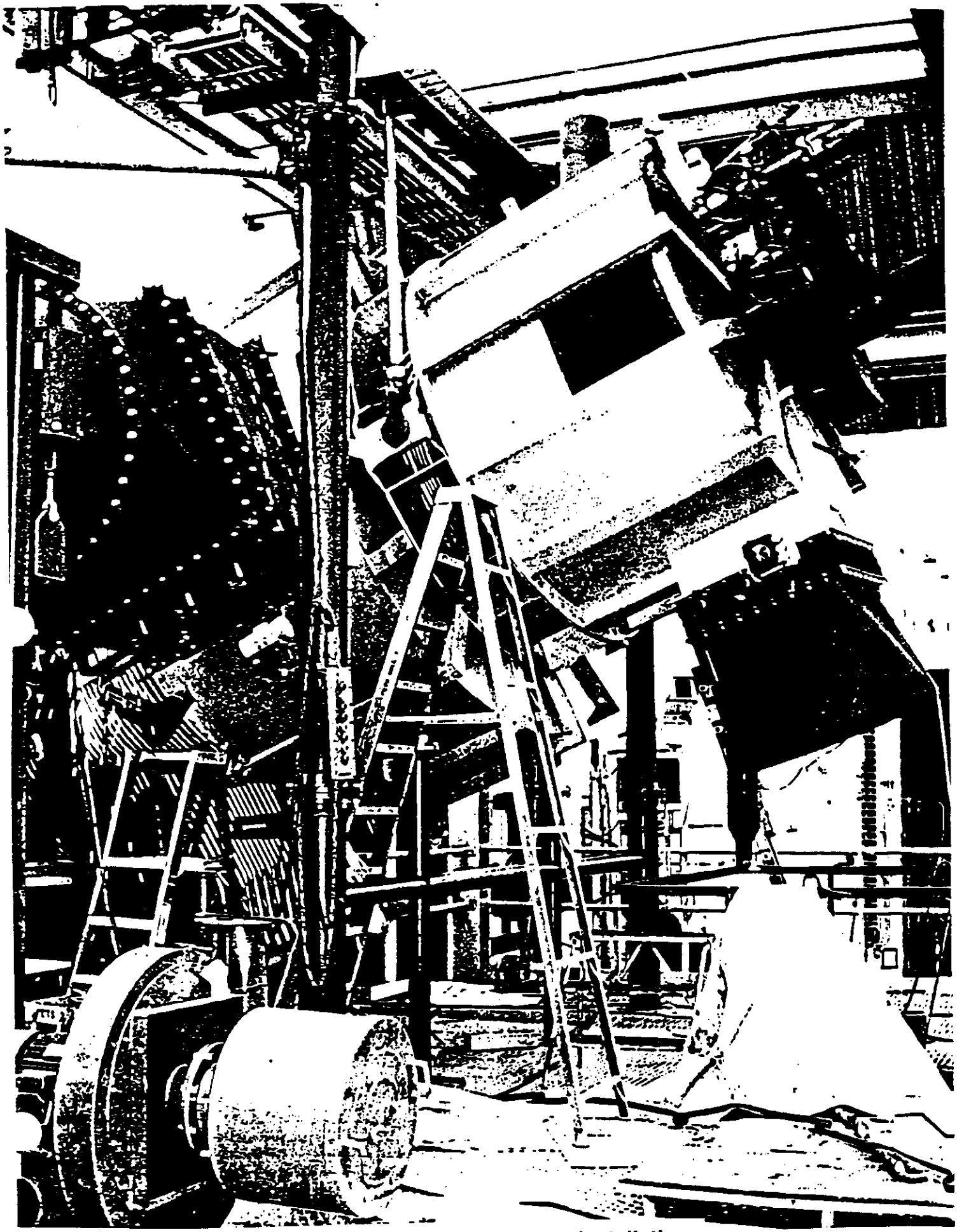

Figure 3 - 6 DVT Precombustor Installation

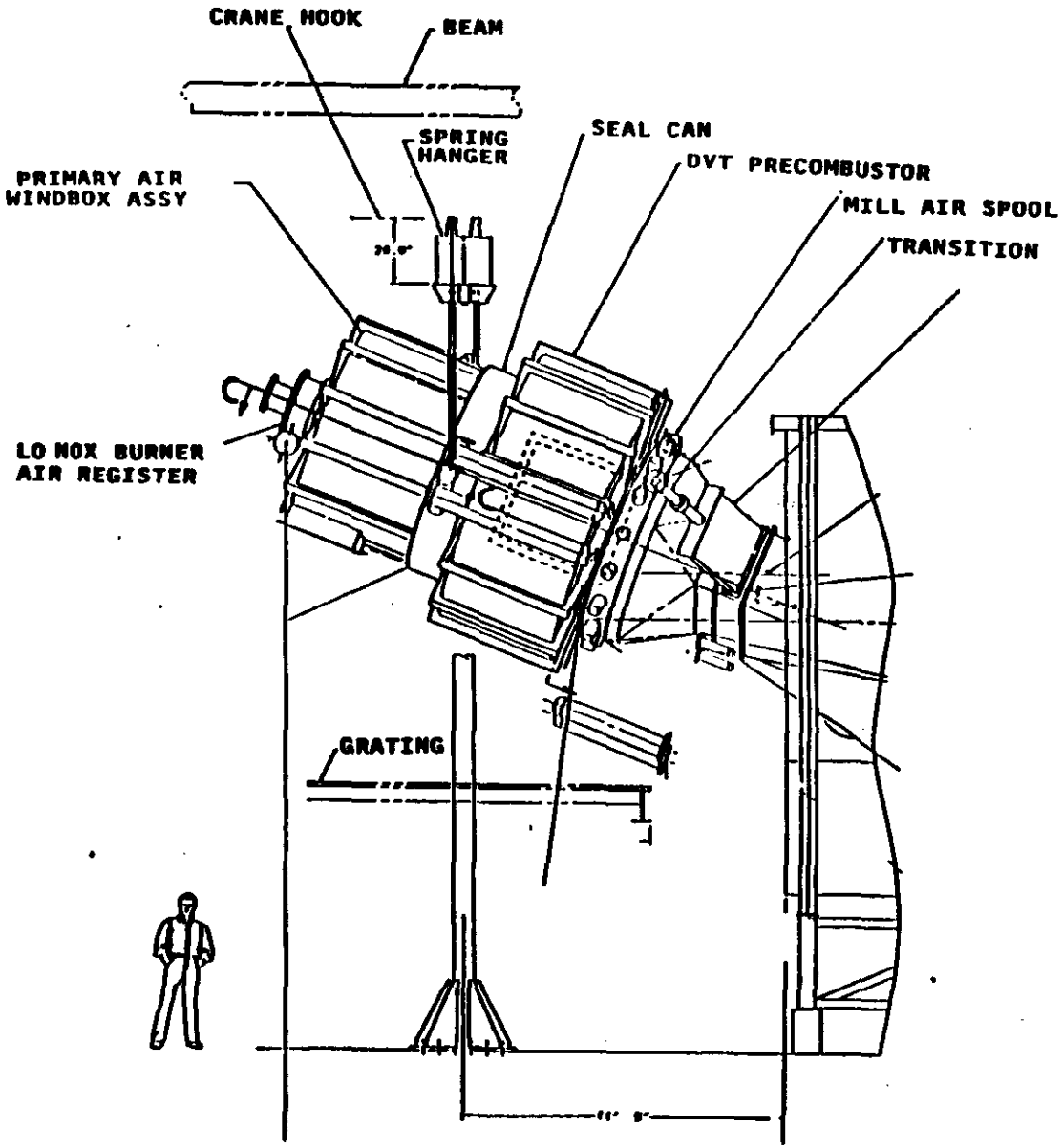

Figure 3-7 Precombustor Installation - Side View

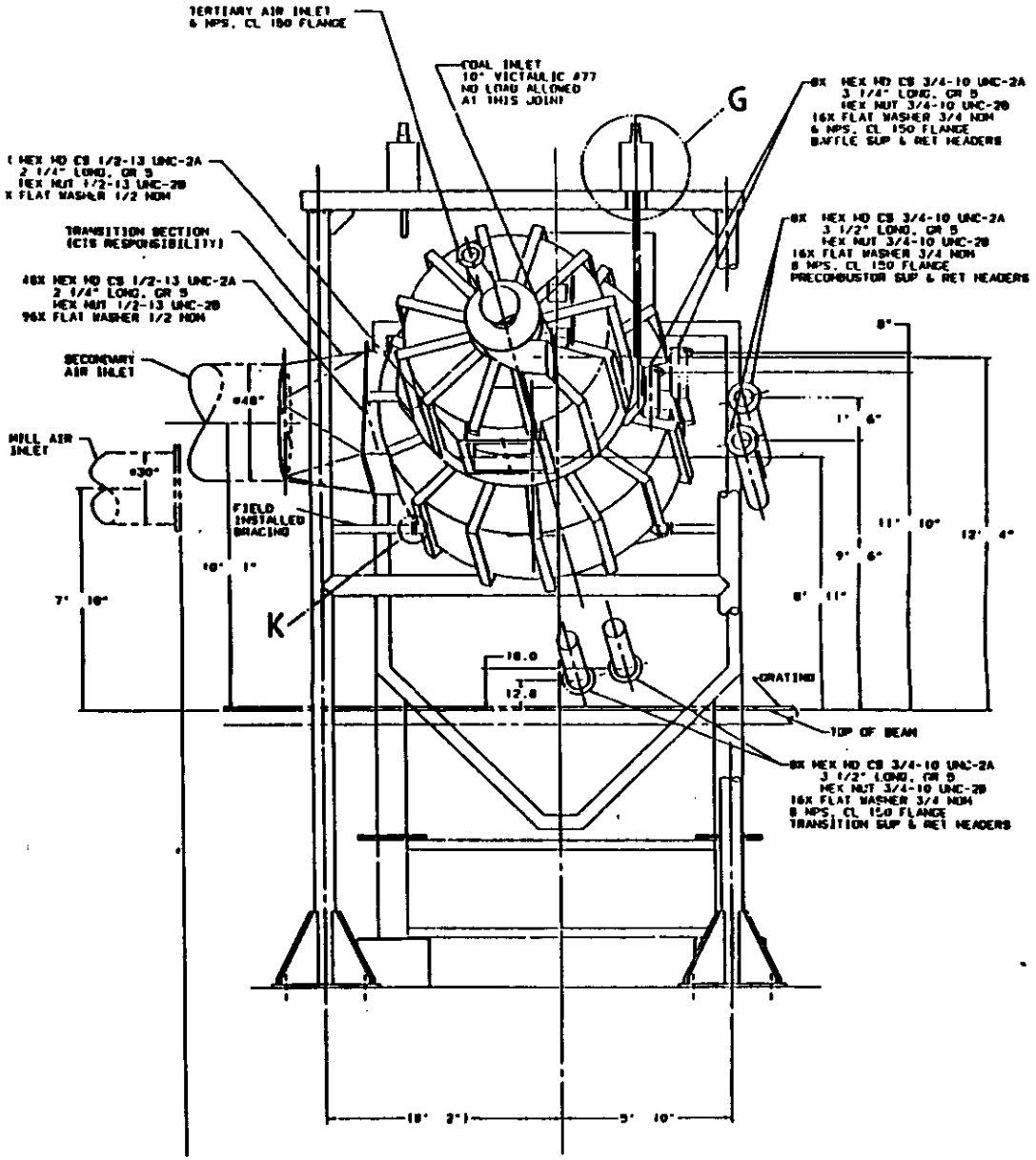

Figure 3-8 DVT Precombustor Installation - End Elevation

lightoff.

Most of the features of the DVT precombustor were identical to the Healy design. Figure 3-9 compares features of the DVT and Healy designs. To meet cost and schedule constraints, some design compromises were made. However, these compromises had no impact on the DVT objectives and test results. The primary differences between the two designs are as follows:

- Low temperature and pressure water (100°F, 150 psi) used at DVT.
- DVT precombustor used single 360° loop cooling circuits as opposed to drainable 180° for the Healy design.
- Separately cooled mill air spool. Healy design incorporates an integral design.
- DVT mix annulus windbox used single air inlet, Healy uses two inlets.
- Slightly different tube and membrane dimensions.
- Use of bolted flanges between sections at DVT. Healy will use all-welded design.
- The Foster Wheeler burner had no ceramic liners, whereas the Healy design will have such liners.

A schematic of the precombustor showing its full instrumentation is presented later in Section 3.8

3.1.2 Foster Wheeler Burner/Primary Air Windbox

This subassembly consisted of a Foster Wheeler Low NO_x burner and primary air windbox. The primary air windbox interfaced with the facility air system to provide air to the Foster Wheeler burner. A Foster Wheeler dual air register within the primary windbox controlled both swirl and distribution of air to the burner.

Figures 3-10 illustrate the Foster Wheeler burner subassembly consisting of a coal burner, oil-fired ignitor and spark ignitor. A coal splitter is internal to the burner. The subassembly is complete with oil and coal flame scanners which interface to facility instrumentation and control systems.

The Foster Wheeler coal burner system as delivered consisted of a dual air register with adjustment wheels, a coal injector with inlet scroll, a (peripheral) coal injector scanner, and a set of thermocouples for monitoring critical metal temperatures. The system was mounted on the primary air windbox (separately supplied by TRW). The coal injector converts a single inlet stream into six separate coal/air jets through a cyclone shaped arrangement. The

FEATURE(S)	DVT	HEALY
Combustion chamber dimensions	62" I.D. x 62" L	62" I.D. x 62" L
Burner throat diameter	37"	37"
Coal burner type	FWEC split flame w/o wear liners	FWEC split flame w/wear liners
Oil ignitor type	Forney 70 MBtu/hr	Forney 70 MBtu/hr
P.C. exit dimensions	31" x 82"	31" x 82"
Cooling water	100°F, 150 psi	592°F, 1405 psi
Cooling circuit geometry	Single full loop (360°)	Two half loops (180°)
Mill air injection cooling	Separately cooled spool	Integral with water wall
Mill air injection ports	16 - 4.813" I.D.	8 - 5.50" I.D.
Mix annulus windbox inlet	1 - 45" x 45"	2 - 40" I.D.
Tube dimensions	1.50" O.D. x 0.250" MWT	1.50" O.D. x 0.180" MWT
Tube inside surface	Ribbed	Smooth
Tube material	SA-210 Gr A-1	SA-213 T2
Membrane dimensions	0.50" wide x 0.50" thick	0.75" wide x 0.250" thick
Membrane material	SA-515 Gr 60	SA-387 Gr 11

Figure 3-9 Precombustor-DVT Versus Healy

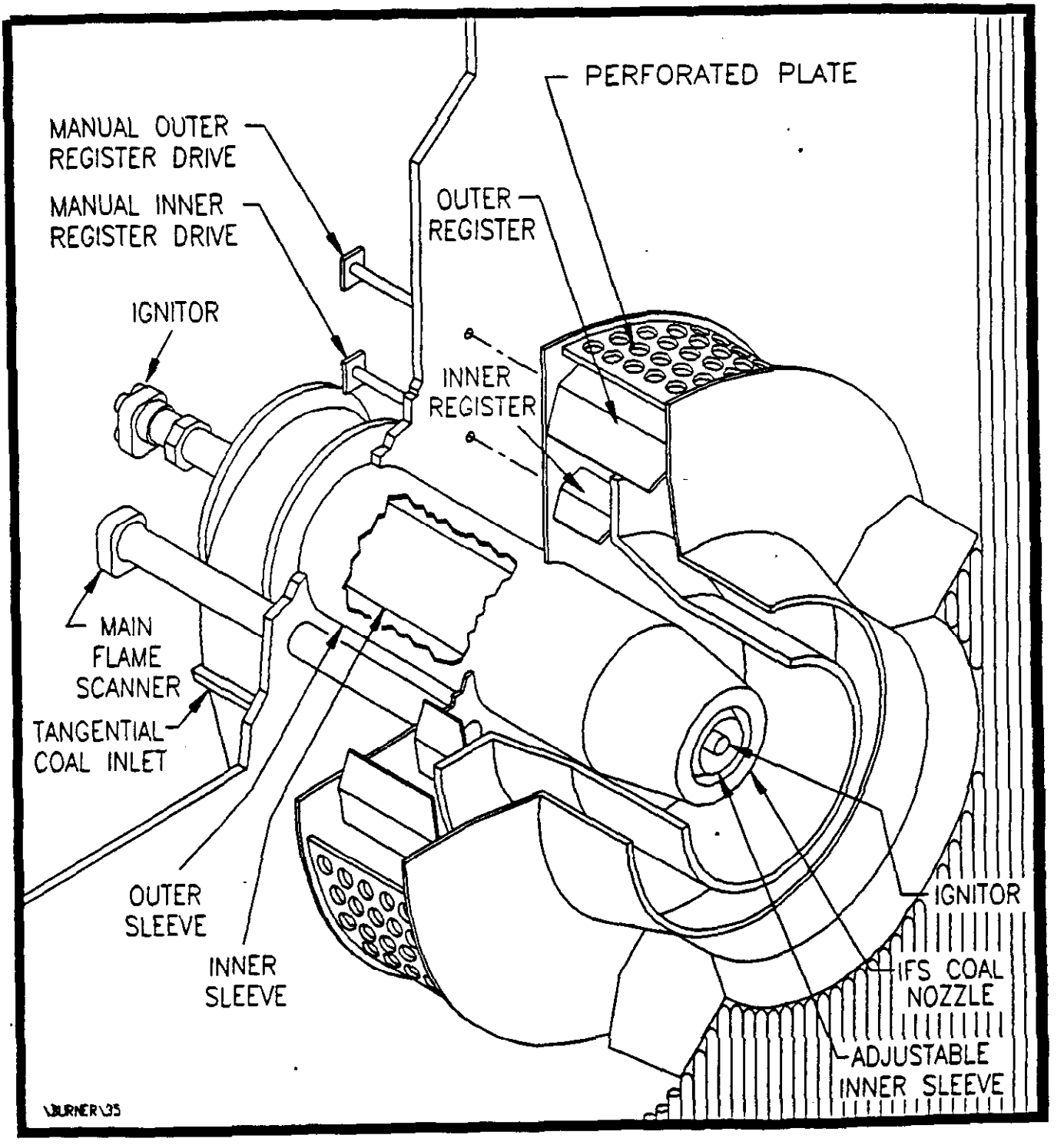

Figure 3-10 Foster Wheeler Internal Fuel Staged Low NO_x Coal Burner

injector was supplied without ceramic liners for the short DVT series, however, liners will be installed for long term operation at Healy.

3.1.3 Forney Oil Burner

The Forney oil burner system as delivered consisted of a retractable oil gun assembly with removable tip and swirler. Cold tertiary air was supplied by a separate fan. The air flowed into a housing which is part of the Foster Wheeler burner assembly surrounding the oil gun. The air provided external cooling for the oil gun, purged the housing cavity, and added swirling air into the oil flame for flame stabilization purposes. Figure 3-11 shows the oil burner as installed on the precombustor.

The atomizing arrangement for the oil burner initially featured a Cashco regulator which maintained a preset air pressure differential above the oil pressure at the tip. Nitrogen was used for atomization instead of air. A retractable high energy spark ignitor (HESI) was mounted in the gun assembly. A separate valve package provided on/off control of oil and air for lightoff, shutdown, and purge functions. An infra-red (IR) oil flame scanner was provided. It viewed the oil flame parallel to the burner axis through holes in the burner support ring. A hard wired control cabinet provided sequence control of the equipment.

The oil burner system as supplied did not have an oil flow control feature. Oil flow control was obtained with a regulator and a Fox cavitating venturi arrangement installed in the supply line pressurized by a pump. Oil flowrate was measured with a turbine meter in the supply line. A three way valve established either a recirculation or firing mode of oil flow. The three way valve was switched simultaneously with the Forney valve package to startup or shutdown the burner.

3.1.4 Combustion Chamber/Secondary Air Windbox

The schematic previously shown in Figure 3-3 also shows the secondary air windbox and water-cooled combustion chamber. The windbox interfaces with facility air system to provide air downstream of the chamber. A refractory-lined combustion chamber was constructed using a tube membrane design with 1.5" ribbed tubing (0.24" MWT) illustrated in Figure 3-12. The 62" diameter chamber is enclosed by the secondary air windbox.

3.1.5 Mill Air Spool

The 82" diameter mill air spool, shown in Figure 3-13, is constructed with a water-cooled, double wall design. The function of this spool is to direct mill air laden with coal fines to the precombustor downstream of the Foster Wheeler burner. A coal splitter upstream of the mill air spool distributes coal fines to precombustor through 8 individual 5" diameter ports. Diagnostic precombustor gas pressure was measured in this component.

Figure 3-11 Forney Oil Burner Installation

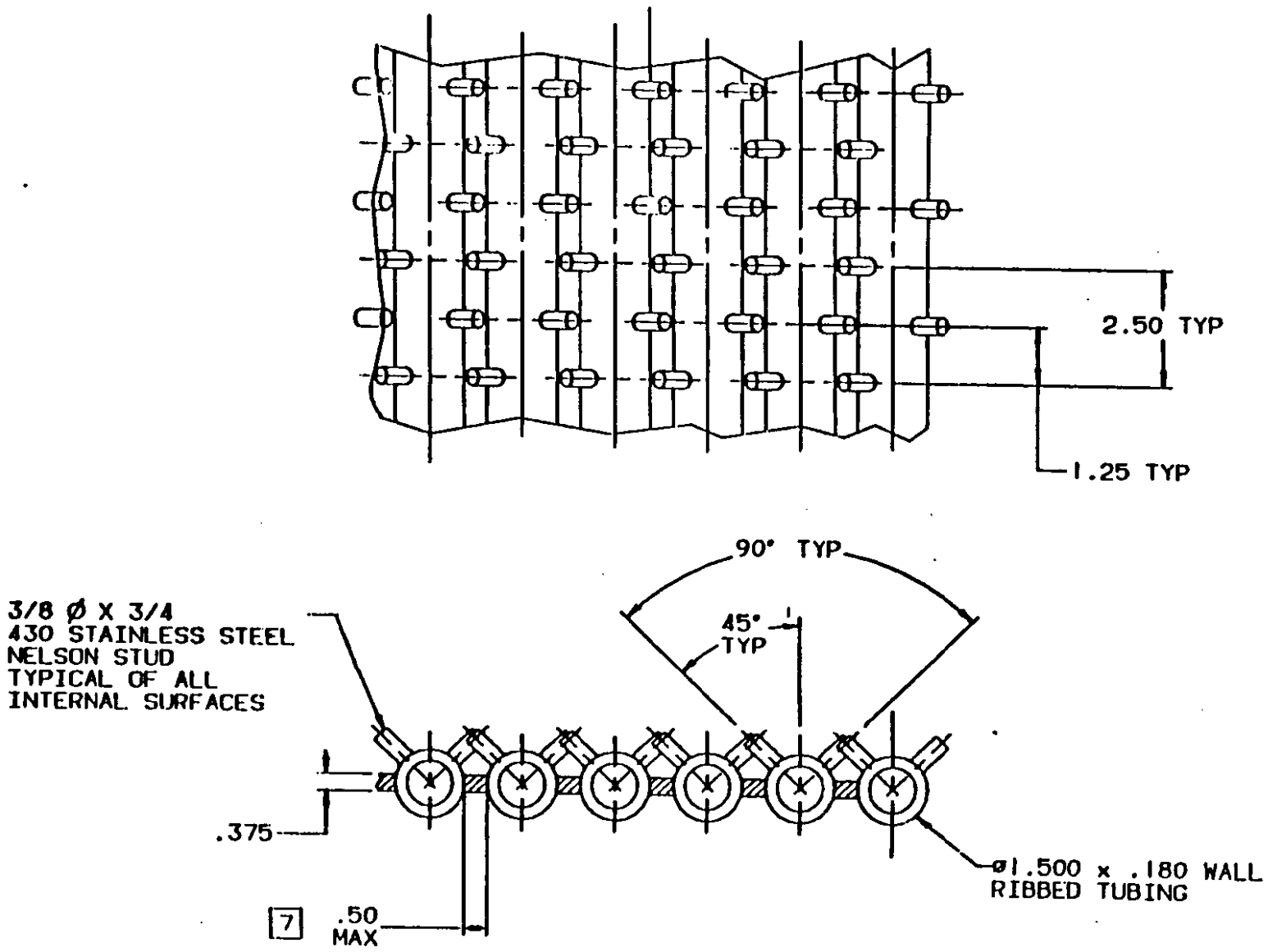

Figure 3-12 Refractory Retention Stud Pattern

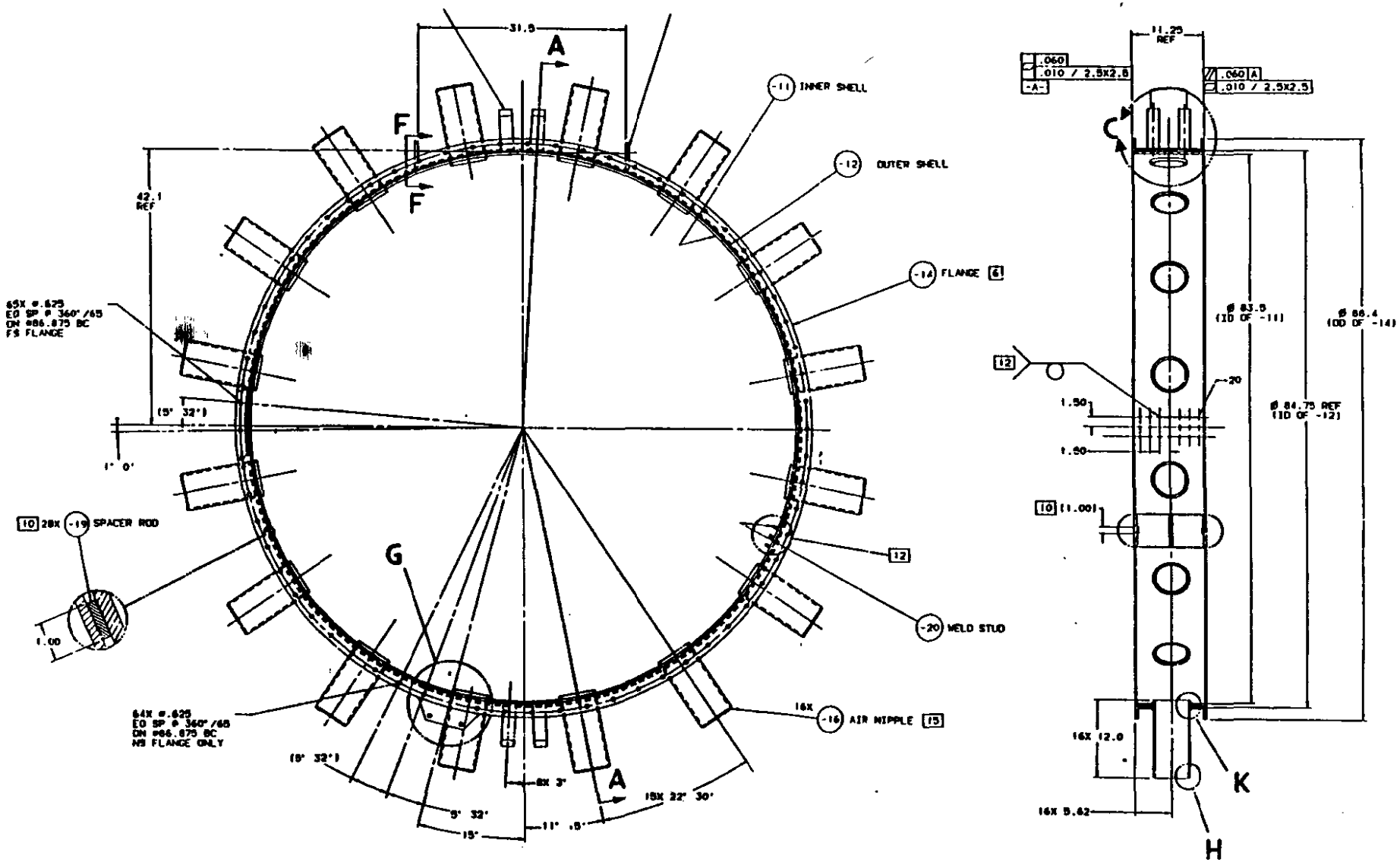

Figure 3-13 Mill Air Spool

3.1.6 Transition Section

This subassembly provides a transition from a 82" diameter chamber to a 31"x82" rectangle required at the slagging combustor inlet, as shown in Figure 3-14. The mechanical design is based on a water-cooled tube membrane design similar to the combustion chamber construction (Figure 3-3).

3.1.7 Swirl Damper Assembly

As shown in Figure 3-15, this assembly consists of a housing and two damper blades. Each component is constructed based on a water-cooled tube membrane design. The damper blades utilize 0.75" diameter tubing (0.095" MWT). A key function of the blades is to maintain minimum gas velocity through precombustor for stable slagging stage operation. Remote actuation of blade position allows operators to control blade position individually, or as a pair, during 100% MCR load conditions.

A video camera located in swirl housing sidewall provided a useful diagnostic tool for evaluating flame stability over various operating conditions. In addition, the camera images confirmed both damper blades and housing remained free of ash attachment during the entire DVT series.

3.2 DVT Direct Coal Feed System

The DCFS variable splitter, vent manifold, and cyclones were subcontracted from Delta/Ducon, who had worked with TRW during the concept development stage when the coal feed system approach was changed from indirect to direct. An extensive subscale cold flow model test effort was conducted at TRW to gain the engineering design data needed for scaling and validation of the concept selected.

The variable splitter design was specified by TRW to Delta Ducon using specification control drawings for all critical performance dimensions. This input was based on TRW's analytical calculations and cold flow model data. Delta Ducon subsequently prepared the final detailed design and fabrication drawings from which the variable splitter was manufactured.

The blowdown cyclone designs were also specified by TRW to Delta Ducon based on cold flow model results and analytical design calculations. Delta Ducon provided conventional cyclone design input and subsequently prepared detailed design and fabrication drawings from which the blowdown cyclones were fabricated.

The DVT system was sized to handle full load precombustor coal flow with both cyclones connected in parallel with a deswirl configuration to a common precombustor transport line. This arrangement was tested initially in a one-tenth scale cold flow model prior to the DVT hardware fabrication. The deswirl interconnection was removed for subsequent splitter evaluation

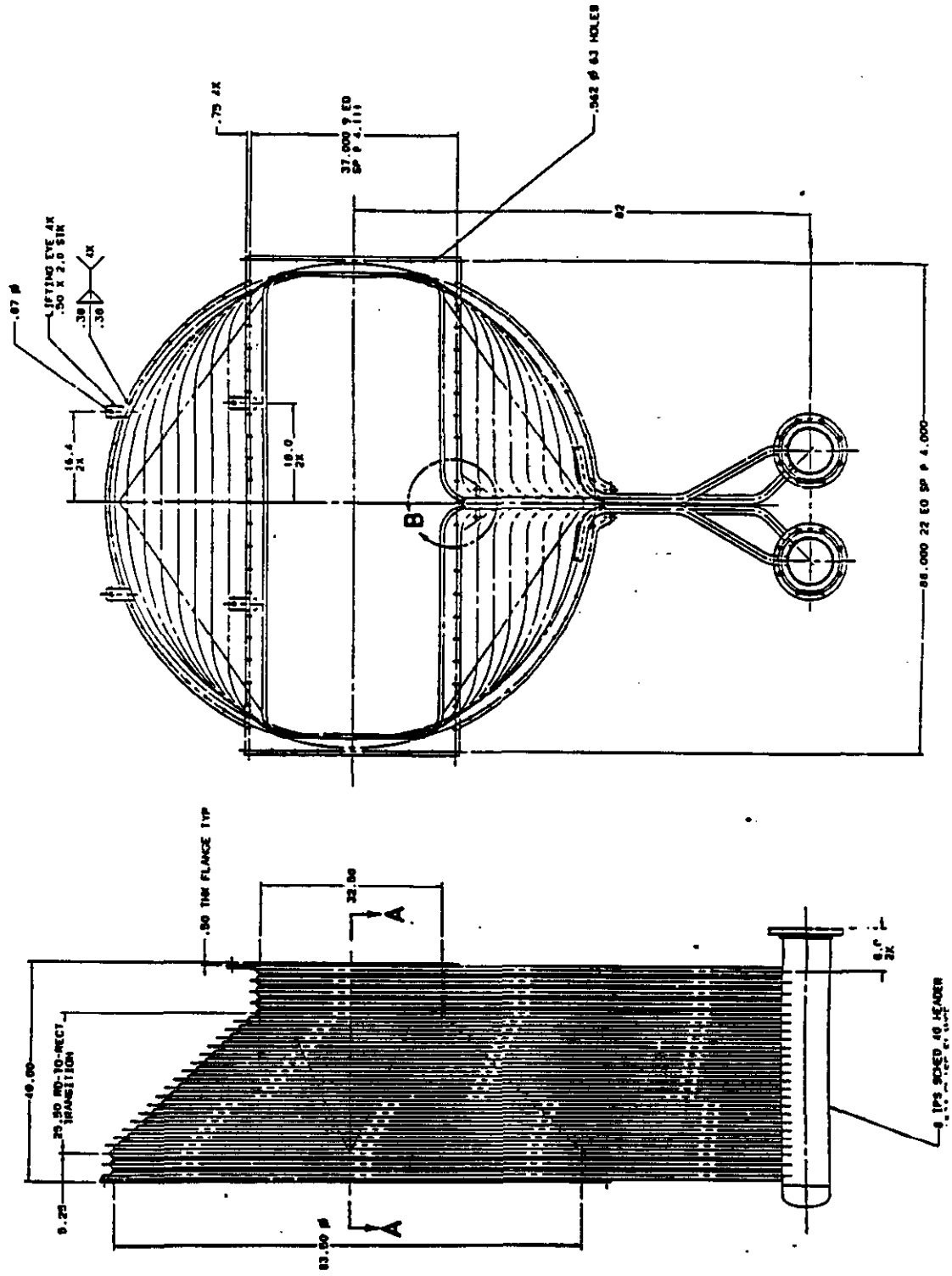

Figure 3-14 DVT Precombustor Transition Section

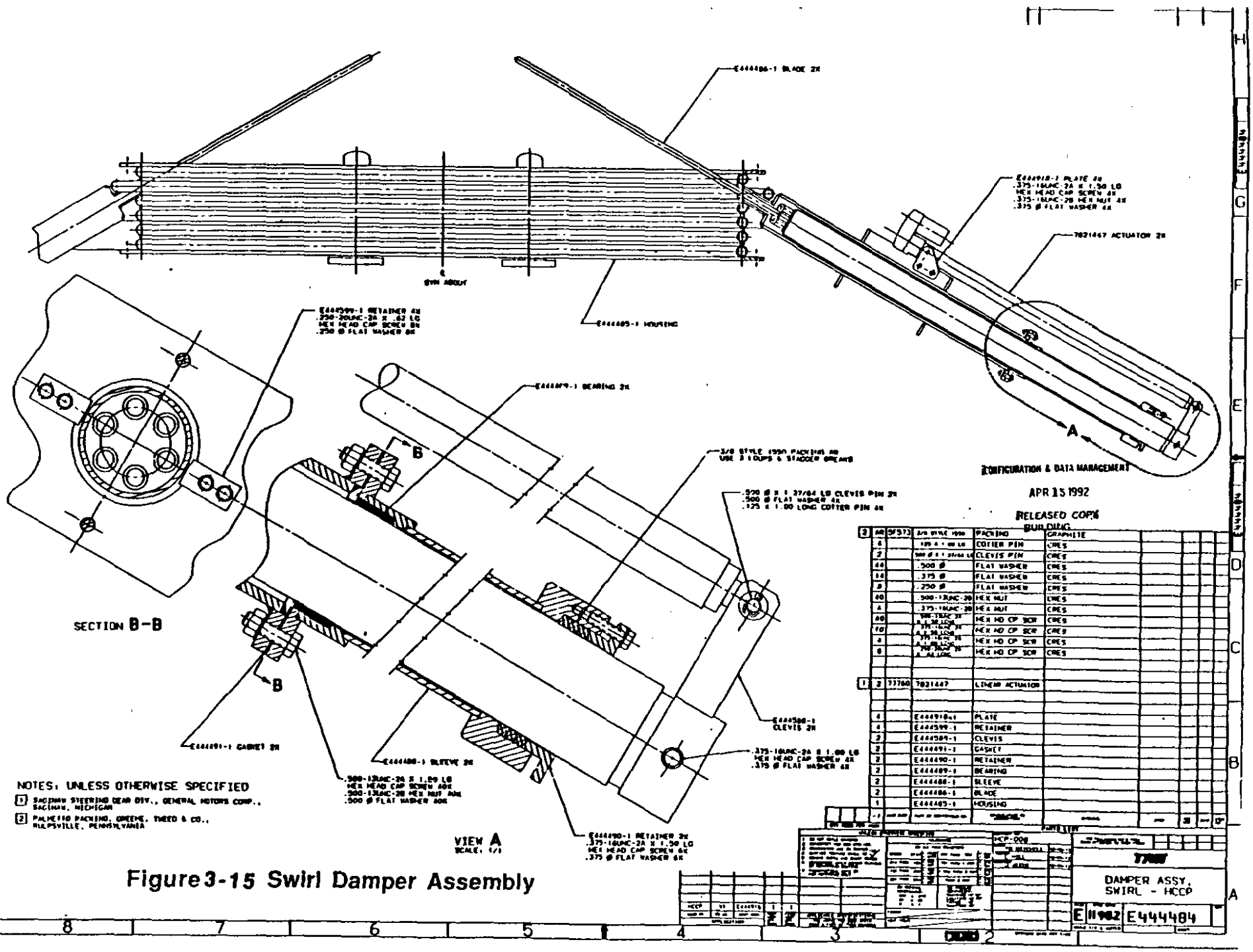

Figure 3-15 Swirl Damper Assembly

tests in which the split to the slagging combustor was collected and weighed. Talcum powder was used to simulate coal in the cold flow modeling tests. After the successful completion of the cold flow tests (presented in Part 3) the design of the DCFS was finalized.

3.2.1 Configuration

A one-third scale DVT Direct Coal Feed System (DCFS) was fabricated, installed and tested to demonstrate the design planned for the Healy plant. The total throughput of the DCFS matched the full-scale rating of the precombustor since the precombustor utilizes approximately one-third of the total coal flow. Therefore, the DVT series was planned for two DCFS configurations: One configuration was for firing the precombustor at full load with the total coal flow from both the outlet legs of the DCFS, while the other was in the split mode, with only the split coal stream was used to fire the precombustor while the other (which would have fired the slagging combustor) was just collected and weighed.

Both configuration requirements were included in one DCFS design. Flow through two cyclone blowdown ports (coal discharge) could both be added and directed to the precombustor in the configuration called common blowdown configuration. The second, split blowdown configuration, directed flow from one cyclone to the precombustor and the flow from the second cyclone to a coal collection system. This collection system replaced what would have been a slagging combustor in the Healy design. The collection system consisted of a calibration cyclone that separated the air and coal, a collection tank ("pup") used to collect the split stream, a weight monitoring assembly used to measure the coal split collected in the collection tank, and all instrumentation and controls.

The DVT DCFS was designed and constructed so that in the event problems were encountered with the DCFS, precombustor testing could still be continued simply by closing and opening manual valves without any hardware changes. This was accomplished by a design that would allow parallel operation with a facility transport system that could direct coal from the facility coal supply system (described later) to the precombustor without flowing through the DCFS.

A CO monitor was installed in the vent line of the DCFS to monitor CO levels during testing for fires. A CO_2 fire extinguishing system was also connected to the coal feed system in the event a problem occurred. Water deluge ports were also incorporated into the design for fire extinguishing.

Access and observation ports were installed at critical locations to inspect for coal accumulations.

3.2.2 Installation

The precombustor coal transport line assembly was installed at the same time as the precombustor was installed to allow testing just the precombustor. The rest of the DCFS components were installed during night shifts on a non-interference basis while the precombustor test series was being completed. The installation tasks consisted of:

- providing mounting and access platforms
- installing the splitter with inlet transition rectangular elbow
- installing the cyclones and splitter ducts with splitter dampers
- cross connecting the cyclones to the transport system
- interconnecting the carrier air supply system
- installing a cyclone vent duct across the simulator to connect the cyclone manifold to the coal fines injection system
- installing a parallel circuit to the DCFS allowing firing of the precombustor directly from the facility coal feed system.

A schematic of the DCFS, including all instrumentation is presented in Section 3.8

3.3 Facility Coal Supply System

Initial testing of the DVT precombustor was conducted by using the existing facility coal supply system at the test site, without using the DCFS. The facility dense phase supply system was connected to the DCFS coal transport assembly which furnished additional air to simulate the Healy air flow rates and coal/air ratios to the precombustor of the precombustor. The DCFS variable splitter and cyclones, not installed during precombustor tests, were isolated as a parallel circuit from the transport assembly by manual valves. A schematic of this system, including all instrumentation is shown later in Section 3.8.

Performance coal supplied by Usibelli Mine Company was transported from Alaska to a EERC Inc., a pulverizing and drying facility located near the test site. Prepulverized coal was transported to the test site in 25 ton trailers and stored in 100 ton guppy trailers at the test site. An inerting blanket of nitrogen was maintained on the pulverized coal at all times. A CO detection system continuously monitored the storage system. Some of the coal was stored for several months without indicating any significant CO level increases. A CO_2 fire extinguishing system was installed and was available for use had there been any fires in the guppies.

During testing intermediate coal storage was provided in a 10 ton storage hopper. The coal transfer equipment was capable of transferring coal from the storage hopper to a 5 ton run hopper at a rate of 1500 lb every 5-6 minutes during a test. The 5 ton run hopper was suspended from a load cell to enable measurement of coal flow rate. An eductor with a 2.5" diameter outlet was supplied with nitrogen for dense phase coal transport out of the run hopper.

The coal transport line was then subsequently expanded to 3" diameter prior to injection into the precombustor coal transport line. A controlled nitrogen flow of 1600 lb/hr was needed to convey coal from the 5 ton hopper. The 5 ton hopper was preloaded prior to a test and filled as needed with 1500 lb transfers to support the test duration. Minor disturbances in coal flow control occurred when coal was transferred into the hopper while running. Coal flow rate was indicated by the load cell readings and by a venturi throat pressure measurements in the dense phase feed line. The load cell readings were invalid during a transfer. The hopper was not filled to capacity to smooth out operation.

A new Phelps mill air fan was installed which was sized to deliver more than the 40,000 pounds per hour of air at pressure levels up to 85 inches water sufficient for operation of the DCFS. The dense phase flow stream of coal from the run hopper was injected into this mill air flowing in a vertical riser intended to simulate mill transport conditions. At that point, carrier air from the mill air fan was added to achieve the desired coal/air ratio to the precombustor. Coal flow characteristics obtained at the lock hopper were satisfactory throughout the test program once the tank ullage controls were worked out.

At 100% MCR conditions, 15,000 lb/hr of coal was delivered to the coal feed system via dense phase using 1,600 lb/hr of nitrogen carrier.

Coal flow rate was averaged over 2 seconds using a fixed-area venturi located in the dense phase system calibrated with hopper load cells. Air carrier flow rate was recorded using annubars while nitrogen carrier was measured with a sonic venturi.

A CO detector was used to monitor the DCFS and transport lines. A carbon dioxide fire extinguishing system was installed on the facility supply system in the event a fire did develop. Such an event never occurred during the DVT series.

During operation without the DCFS about 10,000 lb/hr of carrier air was required from the mill air fan to transport coal to the precombustor. Unneeded air (about 30,000 lb/hr) was vented to atmosphere through a flow control vent. Transport air flow was measured as the difference between flow measurements at the fan and vent. After installation of the DCFS, the vent flow was measured out of the cyclone vent manifold. In the initial setup, all flow measurements involved clean air. After the DCFS was installed, the vent flow measurement involved dealing with coal fines.

3.4 Combustion Air Systems

Combustion air for DVT precombustor testing was provided by the primary and secondary air systems. Each system is complete with electric fan, power substation, oil-fired duct heater, flow control and diagnostic measurement equipment.

Three dimensional views of the primary and secondary air systems are shown in Figures 3-16 and 3-17 respectively. A schematic of this system with all instrumentation is presented later in Section 3.8. Primary air was supplied by two 125 HP, 3560 RPM fans. Secondary air was supplied by a single 300 HP, 1800 RPM fan. Determination of mass air flow rates were based on Dietrich Standard annubars with associated absolute and differential pressure transducers. Blade louver dampers provide remote actuation for desired flow rate settings as indicated by the annubar. Oil-fired duct heater systems, rated for max 12-15 MMBTU/hr, were complete with power cabinets, controls and logic sequence to enable heating of air from ambient to 740° F. Gaseous oxygen is injected upstream of both heaters to replenish oxygen consumed in the duct heater combustion process.

The primary and secondary combustion air was supplied by separate fans. A new power supply substation and Phelps secondary air fan were purchased and installed using TRW capital funds. The primary air was supplied from two existing fans rearranged in parallel. North American oil fired duct burners were purchased and installed using TRW capital. They were capable of maintaining the combustion air temperature within a range of 300 to 800°F at all required combustion airflow rates. The oxygen consumed by firing the oil was replenished from a liquid oxygen system to provide combustion air properties as close to Healy conditions as practical.

Prior to installation of the DCFS, secondary air was used to purge the coal fines injection ports on the precombustor. This air was diverted from the cold upstream duct supplying the duct heater. A splitter and flex hoses connected the source to each of the eight coal fines injection ports (Figure 3-18). The purge flow was maintained near 15,000 pounds per hour. This system operated without incident.

The duct heater combustion chambers and downstream ducting were supported on hanger systems to accommodate thermal expansion. Simple cloth bellows were used to isolate the cold air supply ducts. Combustion air temperature measurement thermocouples were located in the precombustor windboxes. The temperature control thermocouples were located adjacent to the monitors. Combustion air and carrier air supply and vent flowrates were measured using annubar systems. Sufficient duct lengths were provided to obtain accurate measurements. Flowrate control was provided at the fans by inlet dampers. Flowrate control by backpressure was provided at the primary and secondary air inlets to the precombustor using close coupled louver dampers.

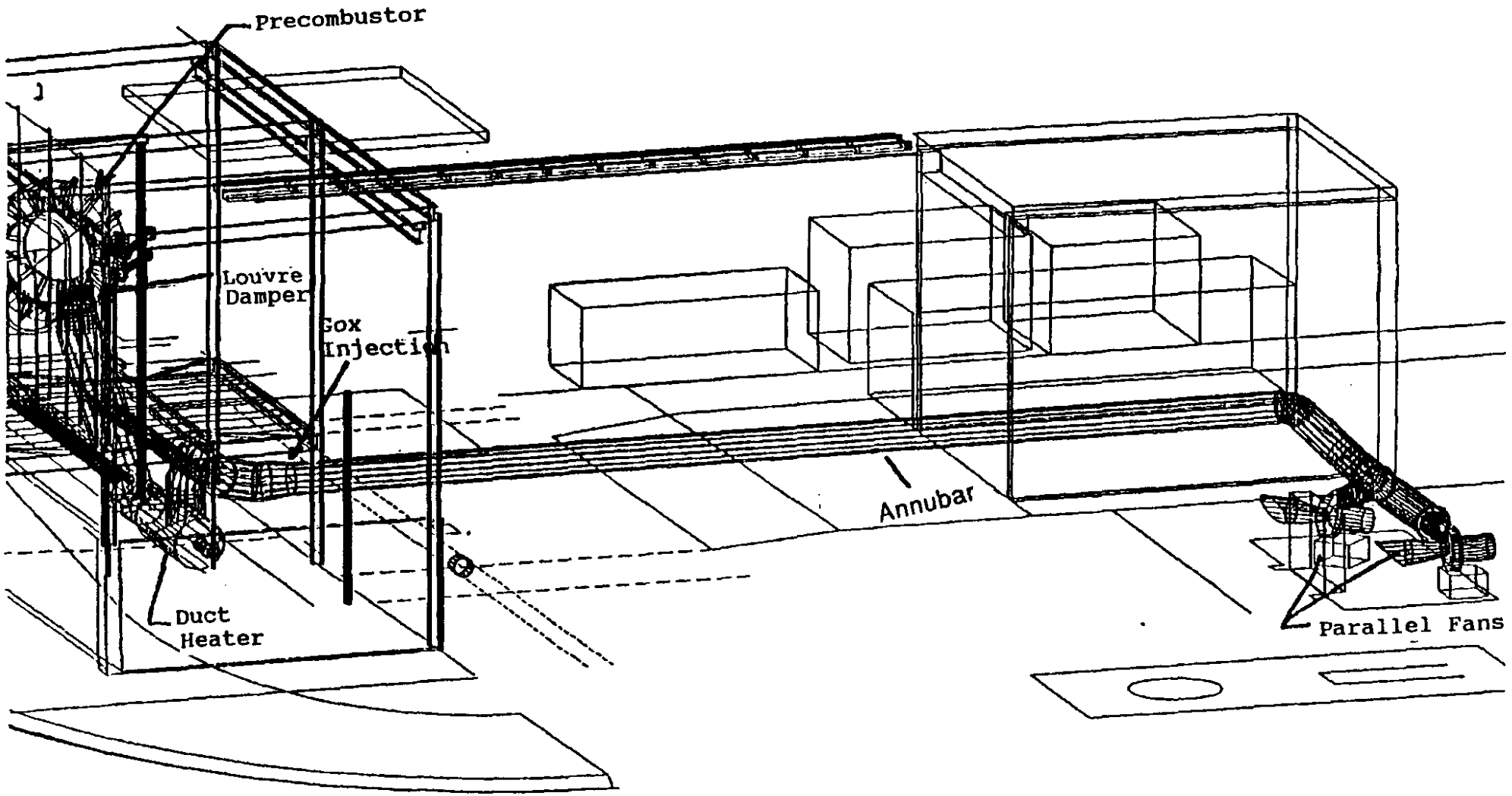

Figure 3-16 Primary Air Subsystem

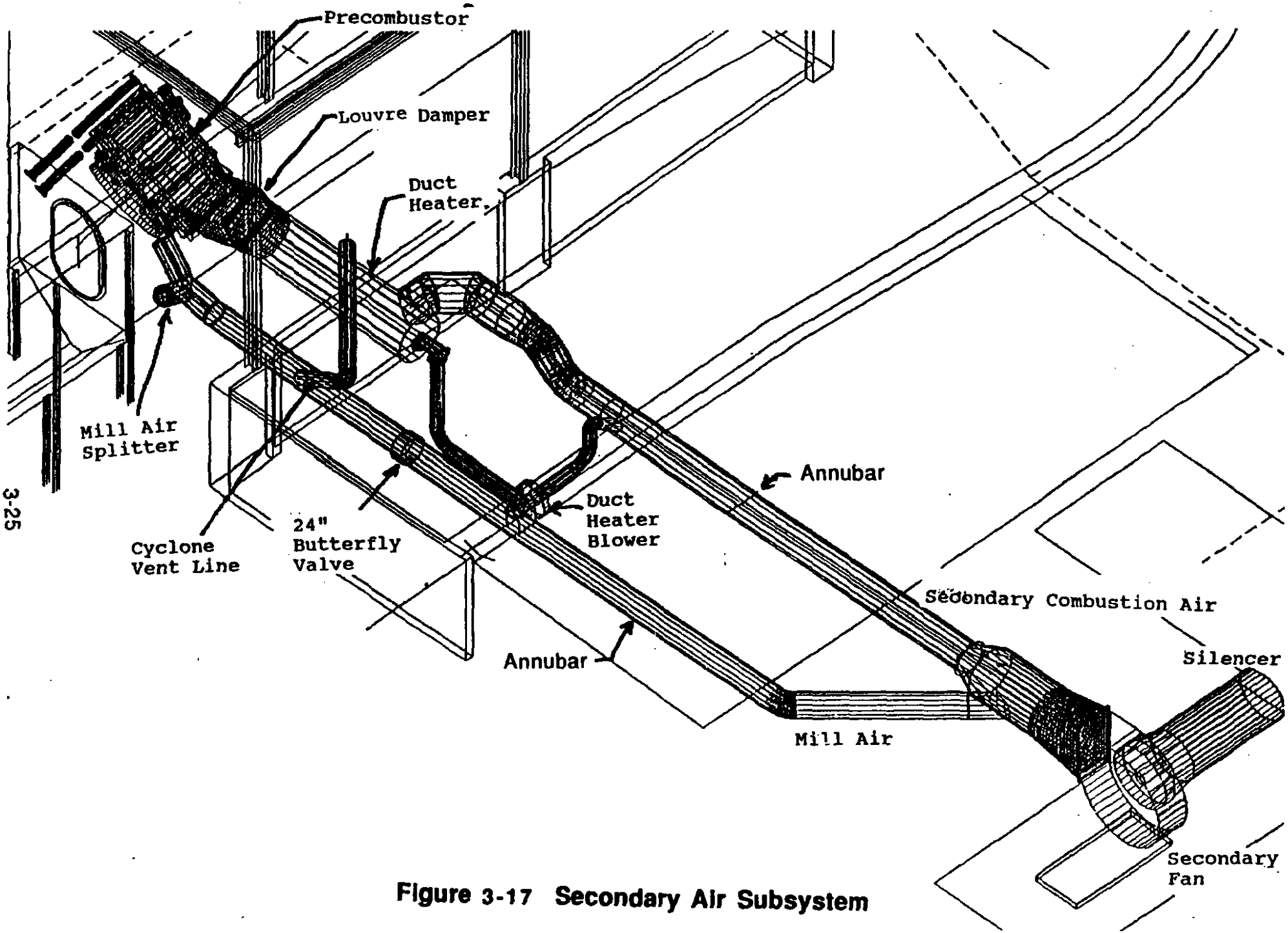

Figure 3-17 Secondary Air Subsystem

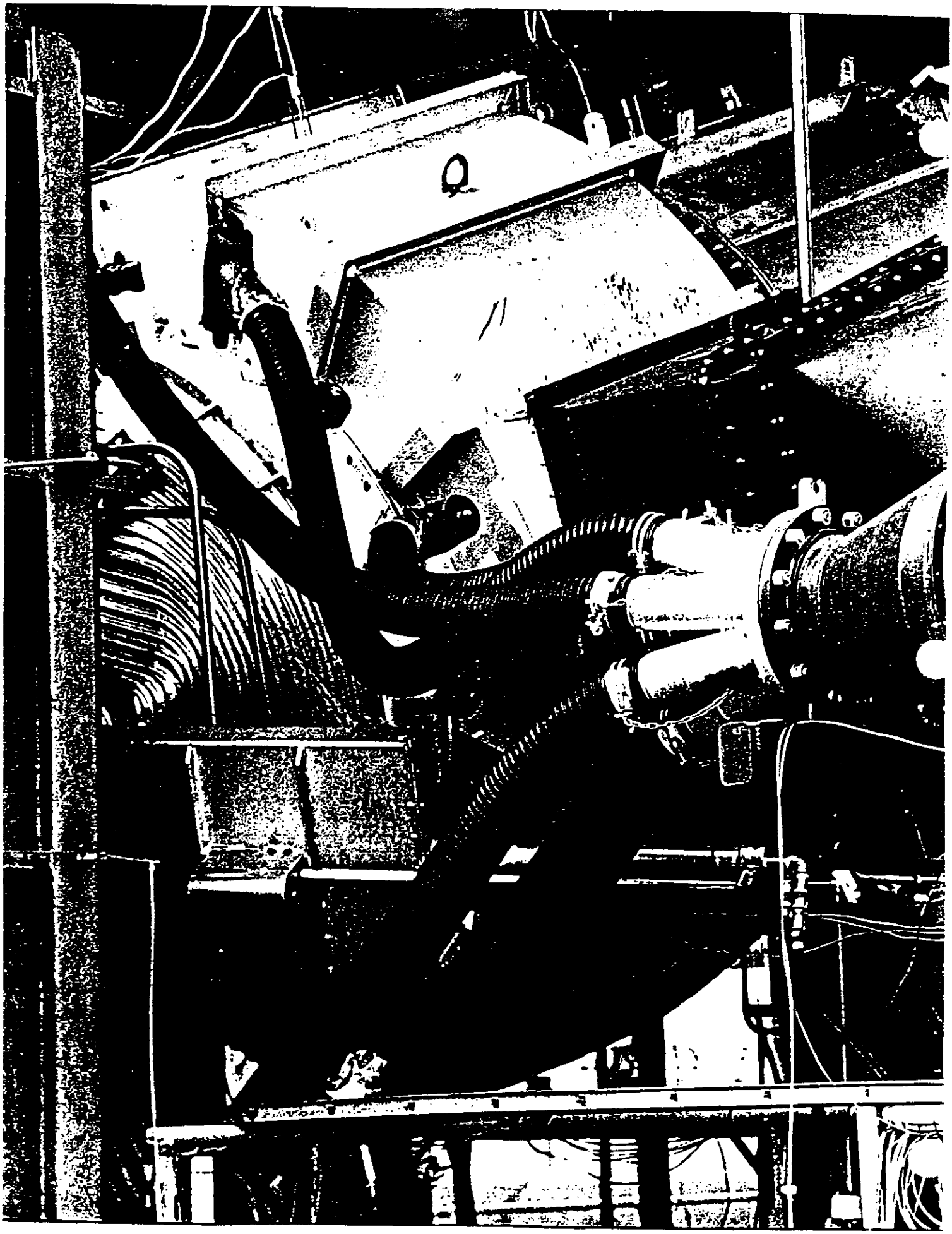

Figure 3-18 Mill Air Connections to Precombustor

3.5 Boiler Simulator

The DVT precombustor was mounted to a boiler simulator, as shown in Figures 3-7 and 3-8 in the same orientation relative to gravity, as in the Healy application. The boiler simulator was a rectangular chamber with flood-cooled water walls. The simulator provided residence time for complete carbon conversion of exhaust gases prior to a water quench. A photograph of the boiler simulator is shown in Figure 3-19.

The front face of boiler simulator was rebuilt to mount the precombustor. The peak gas temperature entering the simulator was approximately 2500°F, well within the limit supported by the pool cooled design of the simulator walls and the internal refractory which covered all surfaces except the modified front face. Ash deposits in the simulator did not require removal during the test program.

3.6 Exhaust, Quench and Scrubber Systems

The downstream support equipment required to met the Southern California Air Quality Management District (SCAQMD) regulations consisted of a quench system, scrubber system, and exhaust stack.

The quench and scrubber systems are shown schematically in Figure 3-20. A photographic view of this equipment is shown in Figure 3-19. A schematic of this system including all instrumentation is presented in later in Section 3.8. Exhaust gases leaving the boiler simulator entered a quench chamber where approximately 300 GPM was sprayed through 20 nozzles to cool the combustion gases below 200° F. After quench, the cooled gases were routed to the venturi scrubber. A fabric expansion joint is located in this duct to absorb approximately 0.5" axial thermal growth in the boiler simulator. The venturi scrubber was supplied with 800 GPM of water to remove particulates down to 0.5 micron with an overall efficiency of 98.5%. After scrubbing, the water and exhaust gases were directed to the cyclonic separator, where the entrained water droplets were separated from the gas due to centrifugal force. Additional moisture was removed from gases within a demister located downstream of the separator. At this point, gases are sampled for CO, NO_x, CO_2, O_2 and HC before being driven out the exhaust stack. The emissions were monitored and recorded in a dedicated TRW emissions van. Water used in the quench and scrubber processes were circulated back to filtering and conditioning equipment.

The scrubber unit and stack were moved to Cell 3 from Cell 2 which had supported an earlier DOE sponsored test program. Airpol Inc. was contracted to modify the scrubber and stack as required to meet the Southern California Air Quality Management District's particulate emissions limitations. Ash collected in the scrubber flowed with return scrubber water to an existing pond system. The

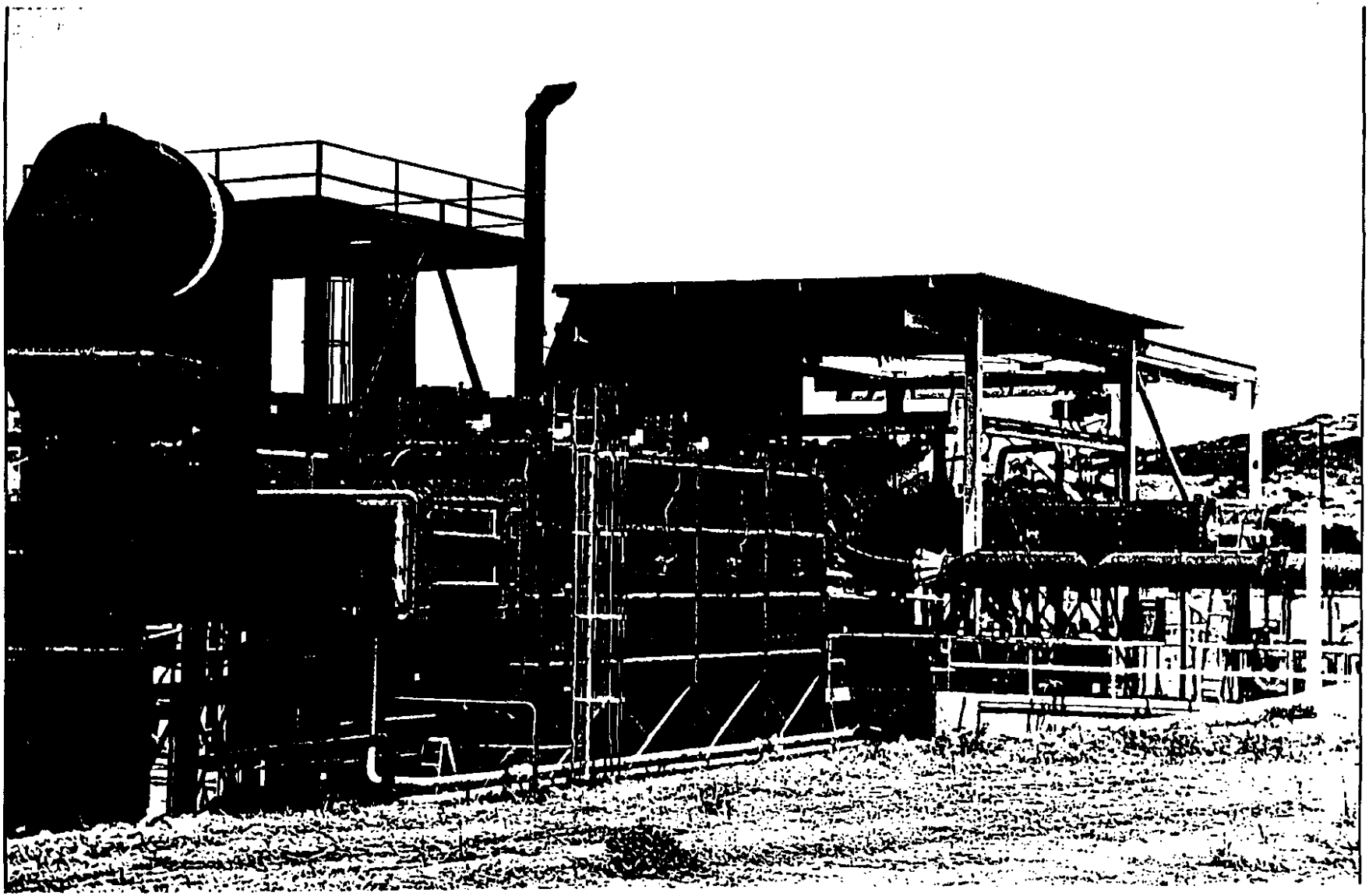

Figure 3-19 Photograph of Boiler Simulator and Scrubber

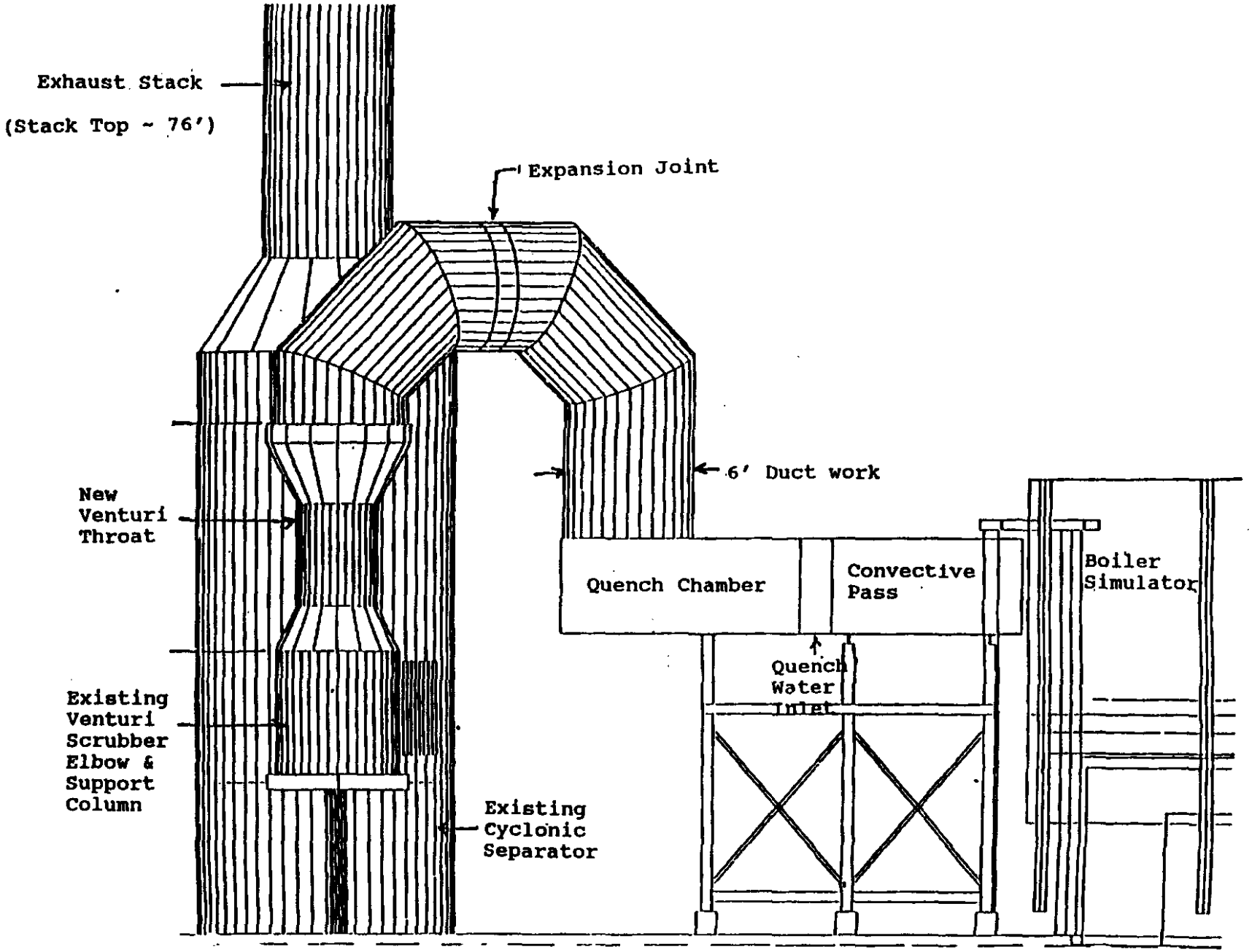

Figure 3-20 Quench Scrubber Subsystem

ash in the scrubber ponds was compressed for drying and disposed of in a landfill at the conclusion of the program.

Pressure losses in the downstream support equipment were identified at the outset of the test series. The higher than expected backpressure appeared to be caused primarily by the scrubber. A restriction in the stack at its outlet was left intact after it was determined that its loss contribution of less than 2 inches did not warrant its removal. The quench system resulted in a significant stack plume which achieved satisfactory elevation as a result of the restriction.

The facility was operated in strict compliance with all SCAQMD and EPA regulations. Test periods were restricted to 3 hours of coal firing on any given day from midnight to midnight. If coal consumption was planned to exceed ten tons during the test period, an acceptable PM10 (particulate matter having sizes greater than 10 microns) sample taken at the site during a preceding period was available.

3.7 Auxiliary Systems

Number 2 diesel fuel oil was required for the DVT precombustor oil gun, primary and secondary duct heaters. Oil was received and stored in a 4,000 gallon storage tank and pumped to a 1600 gallon run tank as required. Maximum oil flow capacity for 100% MCR conditions was approximately 4,800 lb/hr at 300 psia.

The facility cooling water system consists of a pumping station, storage tank, filtration and water treatment equipment. This system provided a flow rate of 2300 GPM at 122 psia to water-cooled precombustor hardware circuits.

Gaseous oxygen was required on both primary and secondary air systems to replenish oxygen consumed during the duct heater combustion process. Facility liquid oxygen storage capacity was 676,500 ft^3 (NTP), with a maximum vaporizer flow rate of 77,675 ft^3/hr.

Gaseous nitrogen was required for coal feed system inerting, coal transfer between storage vessels, hopper ullage pressurization, eductor carrier flow, viewport purges and remote valve actuation. Facility liquid nitrogen storage capacity was 1,027,030 cft (NTP), with a maximum vaporizer flow rate of 230,400 cfh.

Schematics of these systems including all instrumentation are shown in the next section.

3.8 Instrumentation, Control and Data Systems

A complete set of schematics showing the instrumentation used during the DVT is included in this section. Each instrument is identified by a specific acronym, as indicated in the schematics.

The following figures illustrate the schematics:

Figure 3-21: Precombustor Primary and Secondary Air Systems Instrumentation.
Figure 3-22: Cell 3 Cooling, Quench and Scrubber Water System Instrumentation.
Figure 3-23: Precombustor Instrumentation.
Figure 3-24: Direct Coal Feed System Instrumentation.
Figure 3-25: Cell 3 Nitrogen System Instrumentation
Figure 3-26: Facility Coal Supply System Instrumentation.
Figure 3-27: Facility Cooling, Quench and Scrubber Water System Instrumentation.
Figure 3-28: Facility Cooling, Quench and Scrubber Water System Instrumentation (continued)
Figure 3-29: Facility Oil Supply System Instrumentation.
Figure 3-30: Facility CO_2 Supply System Instrumentation.
Figure 3-31: Facility Nitrogen Supply System Instrumentation.

A General Automation host computer controlled all systems and provided the capability of recording and displaying the outputs from the instrumentation depicted in the foregoing schematics during testing. Data acquisition capability was 256 analog inputs, each parameter being sampled every 100 msec. Real-time data display consisted of 10 stripcharts, video monitoring and CRT displays. In addition to diagnostic and control capabilities, a computer interlock abort sequence was utilized to provide maximum safety for personnel, DVT hardware and the facility. The red lines for the abort sequences were established by the chief and test engineers of the project, and were reviewed by a safety committee during the test readiness reviews prior to the commencement of each test series.

A telephone line data link was established between the test site and TRW's offices at Space Park for rapid transfer of data for analysis. These data were analyzed using a PC-based software package developed specifically for the DVT series. The software performed all post-test diagnostic engineering calculations and generated various plots, summary tables and bar charts. Examples of such charts are included in Sections 5 and 6.

3.9 TRW Capital Equipment

In support of the DVT series, TRW invested $536K of capital funds for installing the following equipment at FETS: (1) A secondary air fan system, complete with acoustic enclosure, (2) Two oil-fired duct heaters, one in the primary air line, and the other in the secondary air line and (3) A 750 KVA substation to power the newly installed equipment. In addition, an existing scrubber in the FETS area was refurbished and moved to Cell # 3 for the Healy project. Since this scrubber was originally procured under a Department of Energy project, appropriate permission was secured from DOE for this specific use.

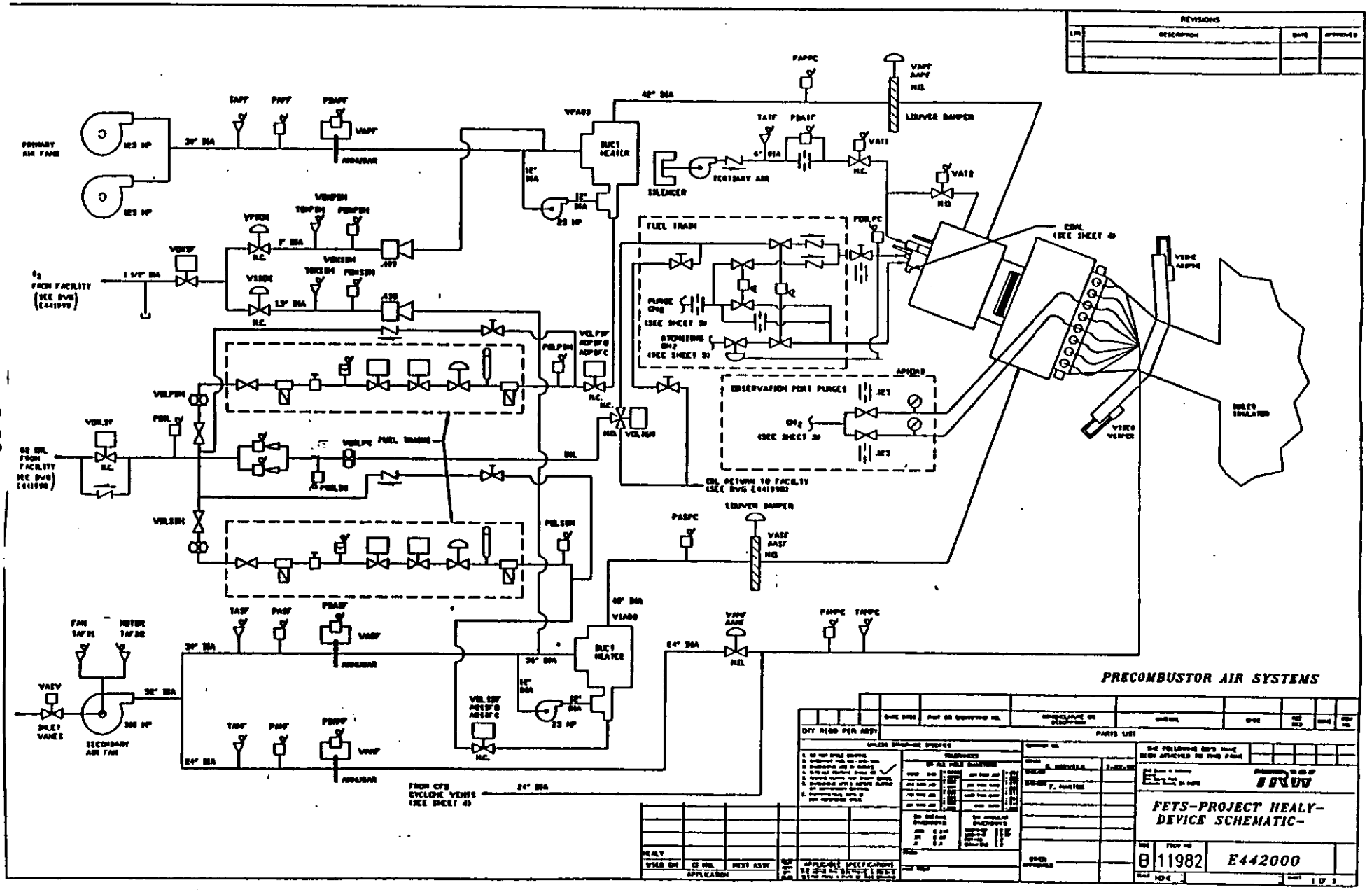

Figure 3-21 Precombustor Primary and Secondary Air Systems Instrumentation

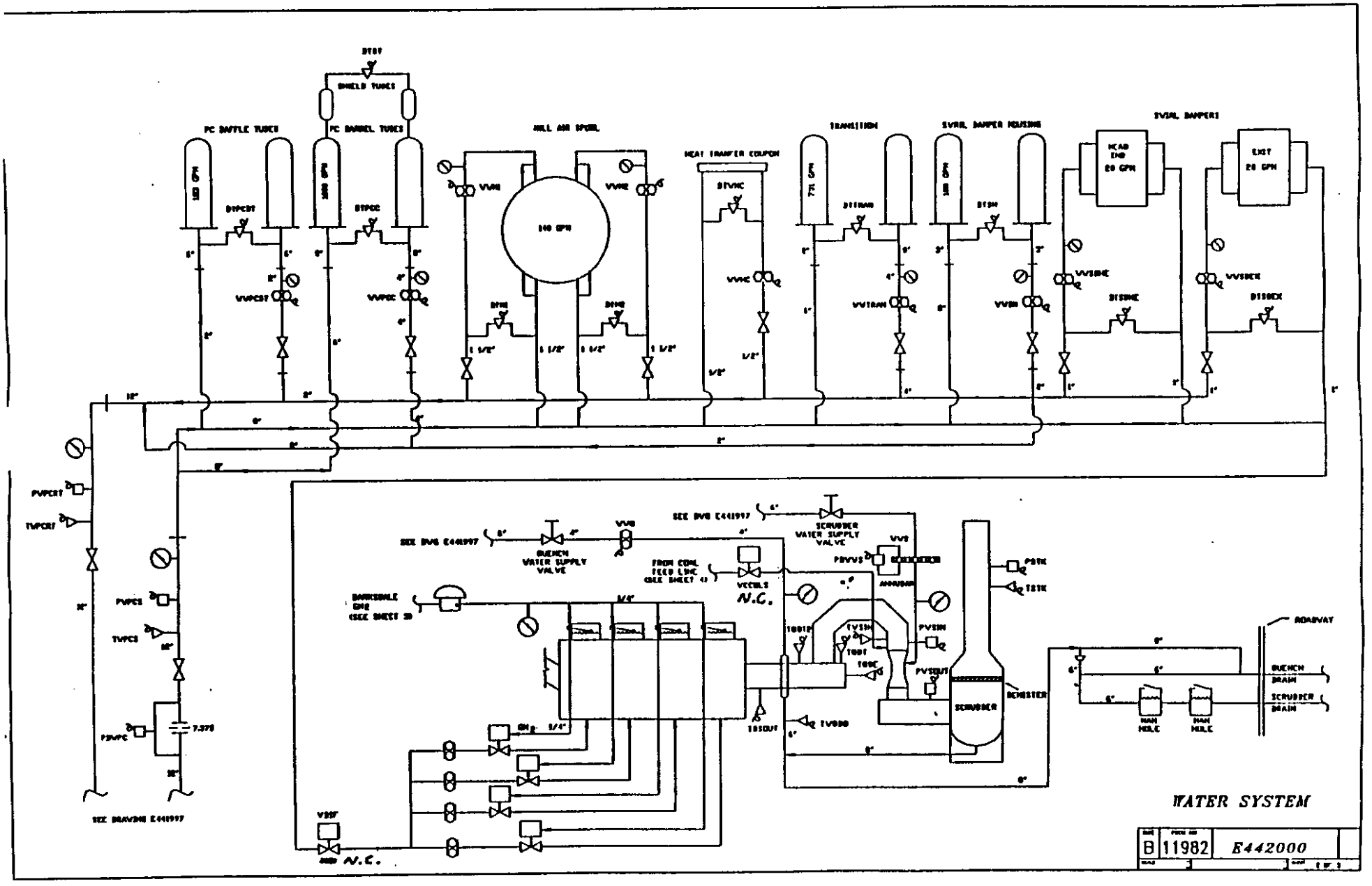

Figure 3-22 Cell 3 Cooling, Quench and Scrubber System Instrumentation

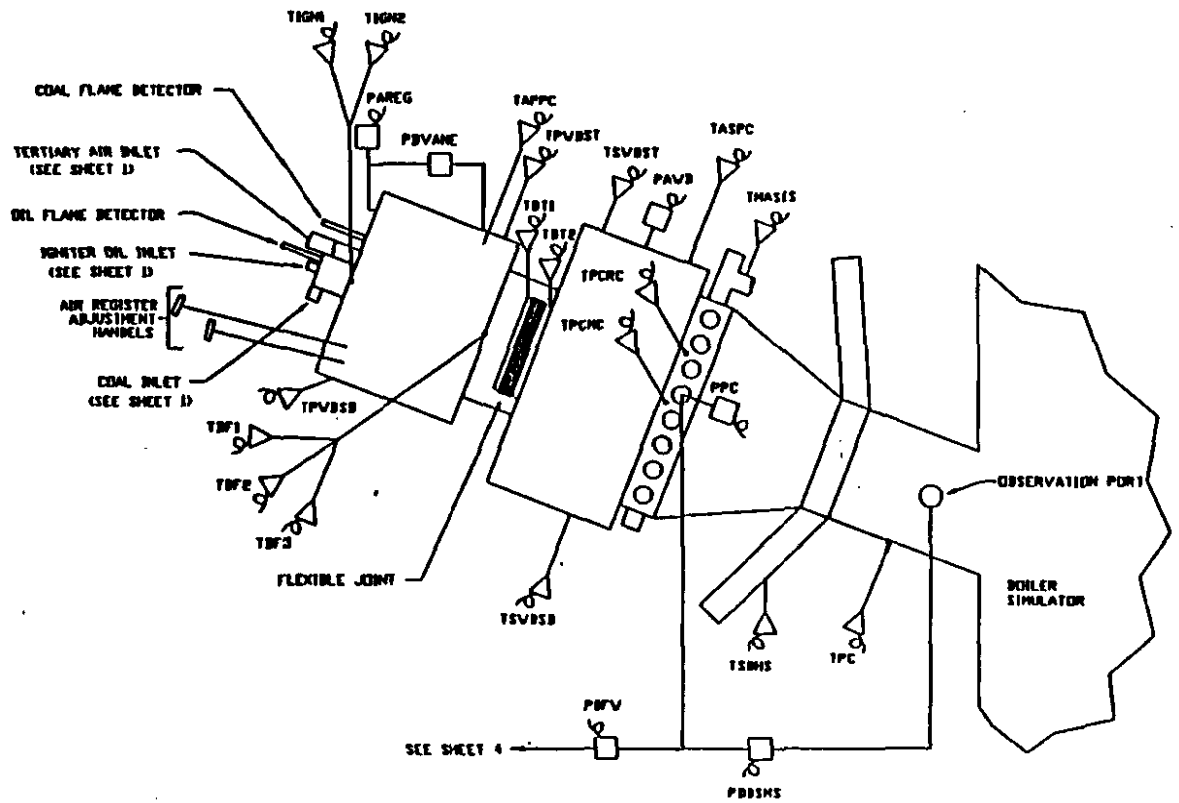

PRECOMBUSTOR INSTRUMENTATION

B	11982	E442000

Figure 3-23 Precombustor Instrumentation

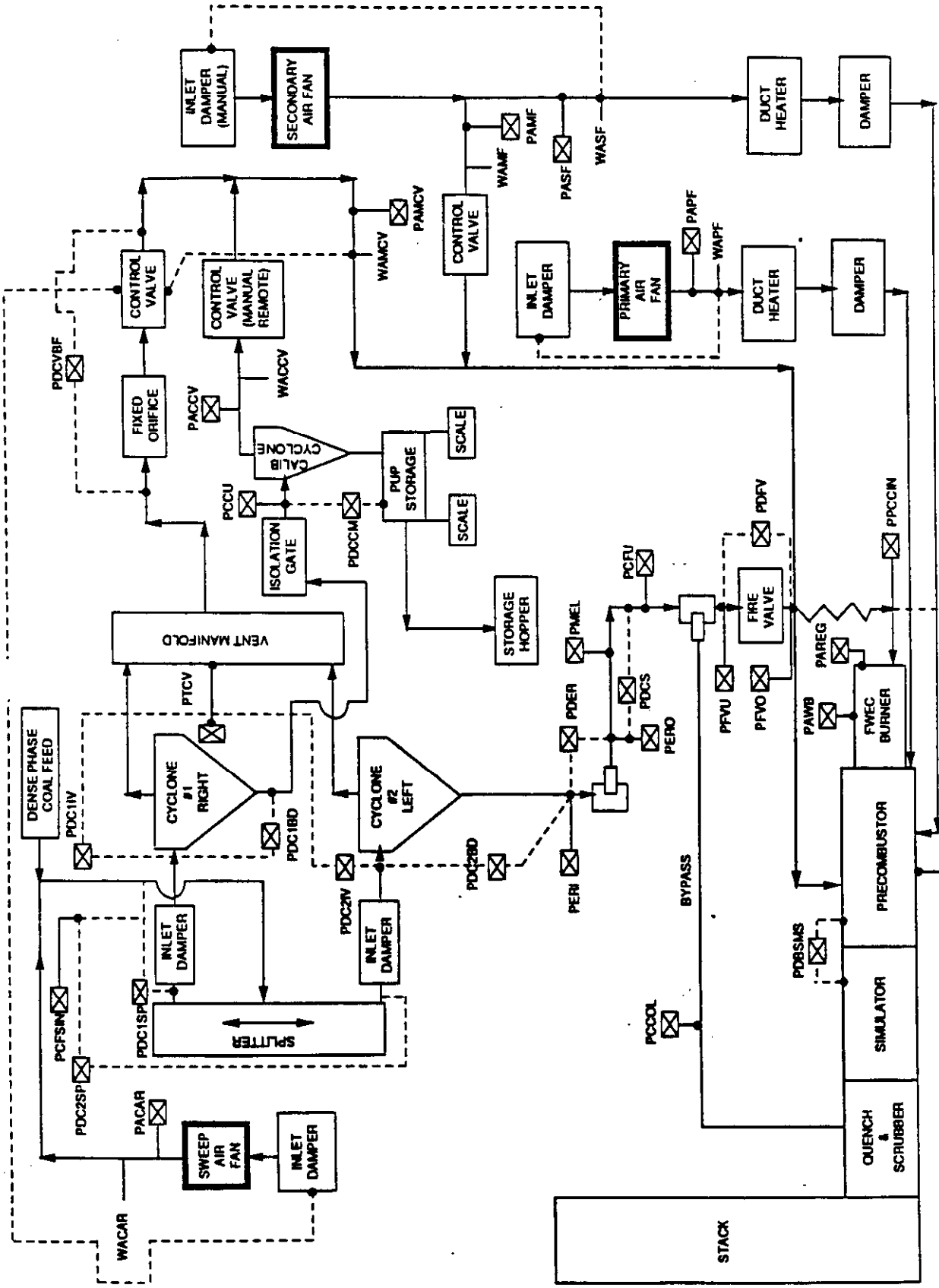

Figure 3-24 Direct Coal Feed System Instrumentation

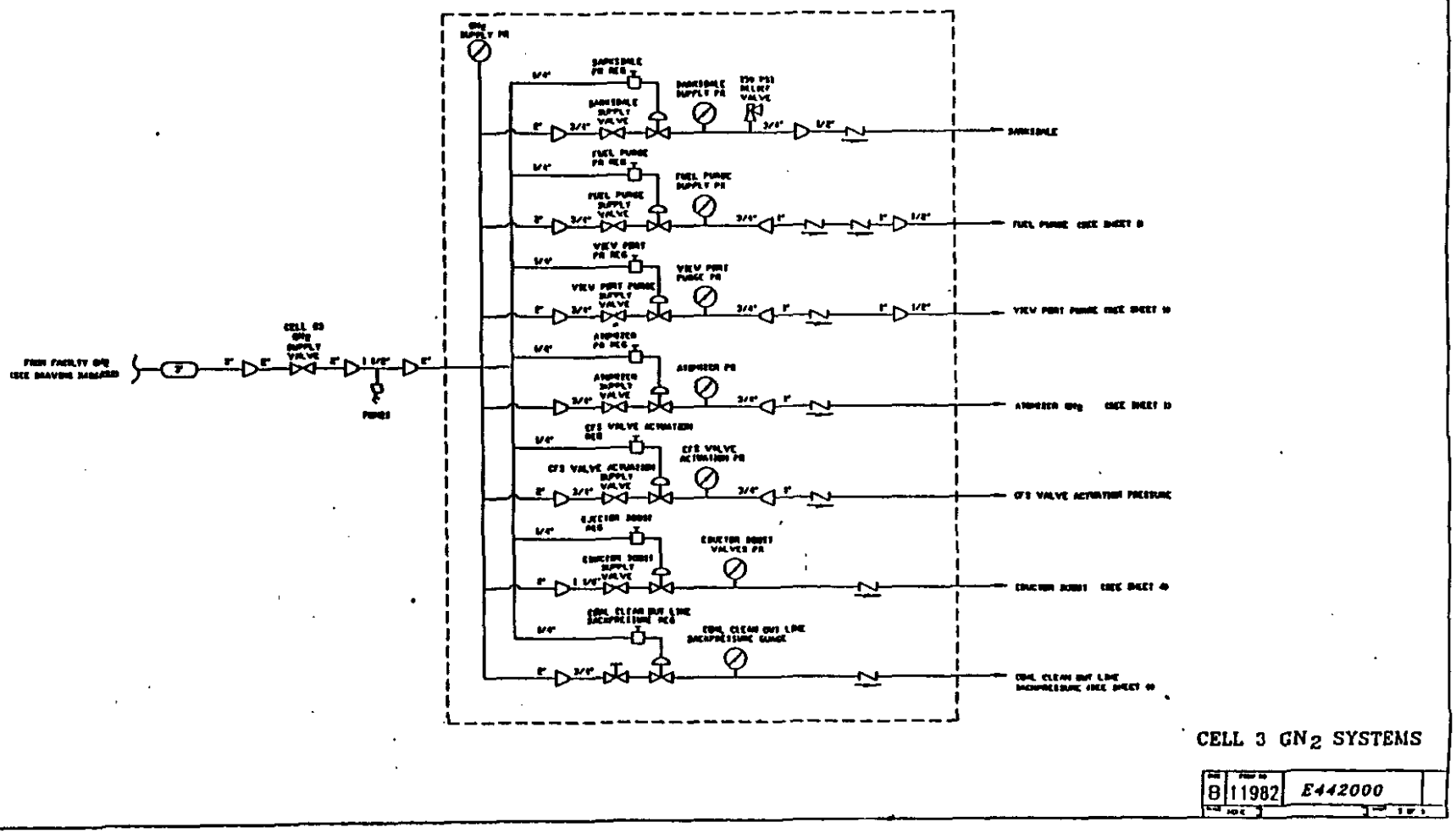

Figure 3-25 Cell 3 Nitrogen System Instrumentation

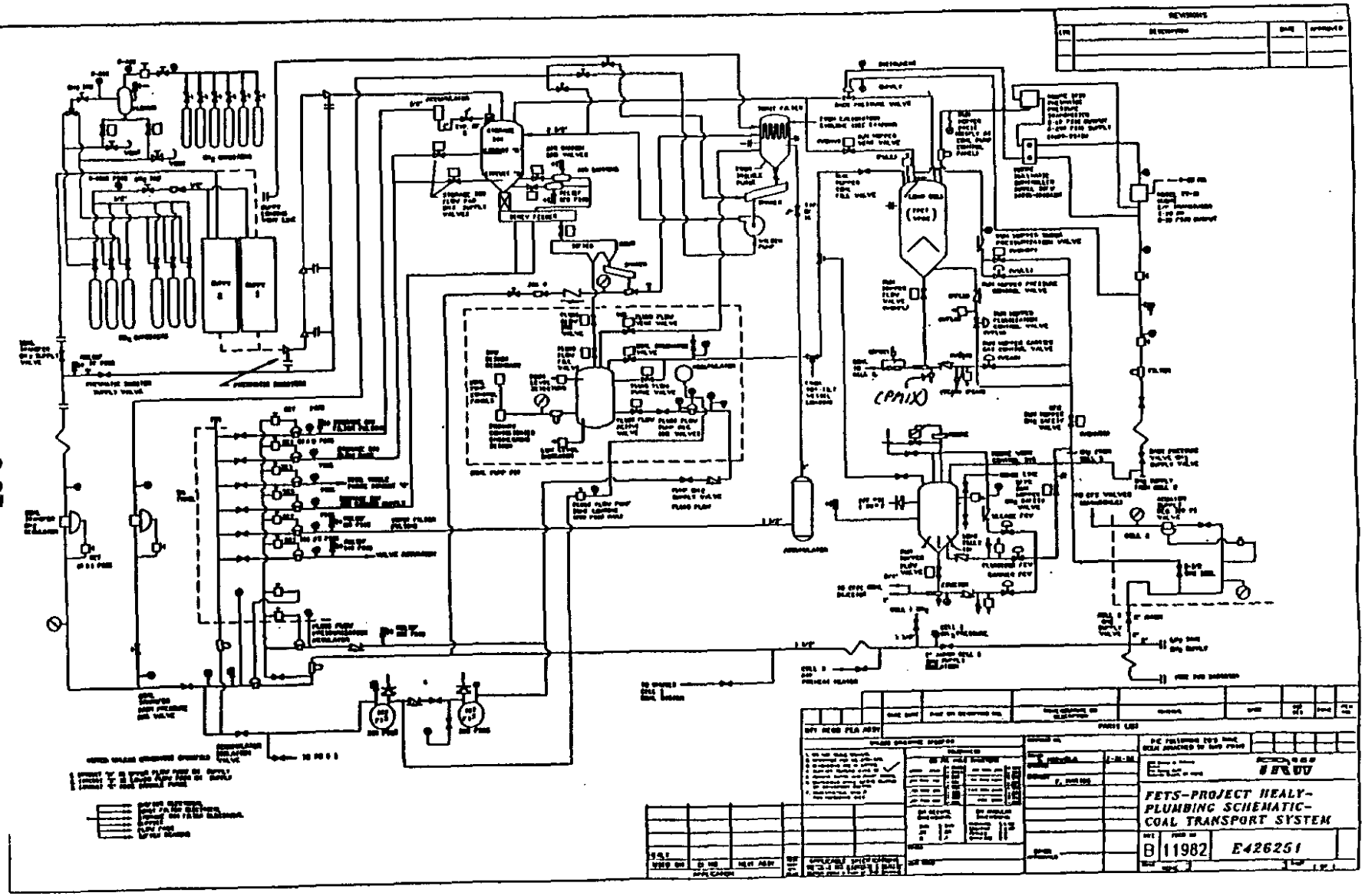

Figure 3-26 Facility Coal Supply System Instrumentation

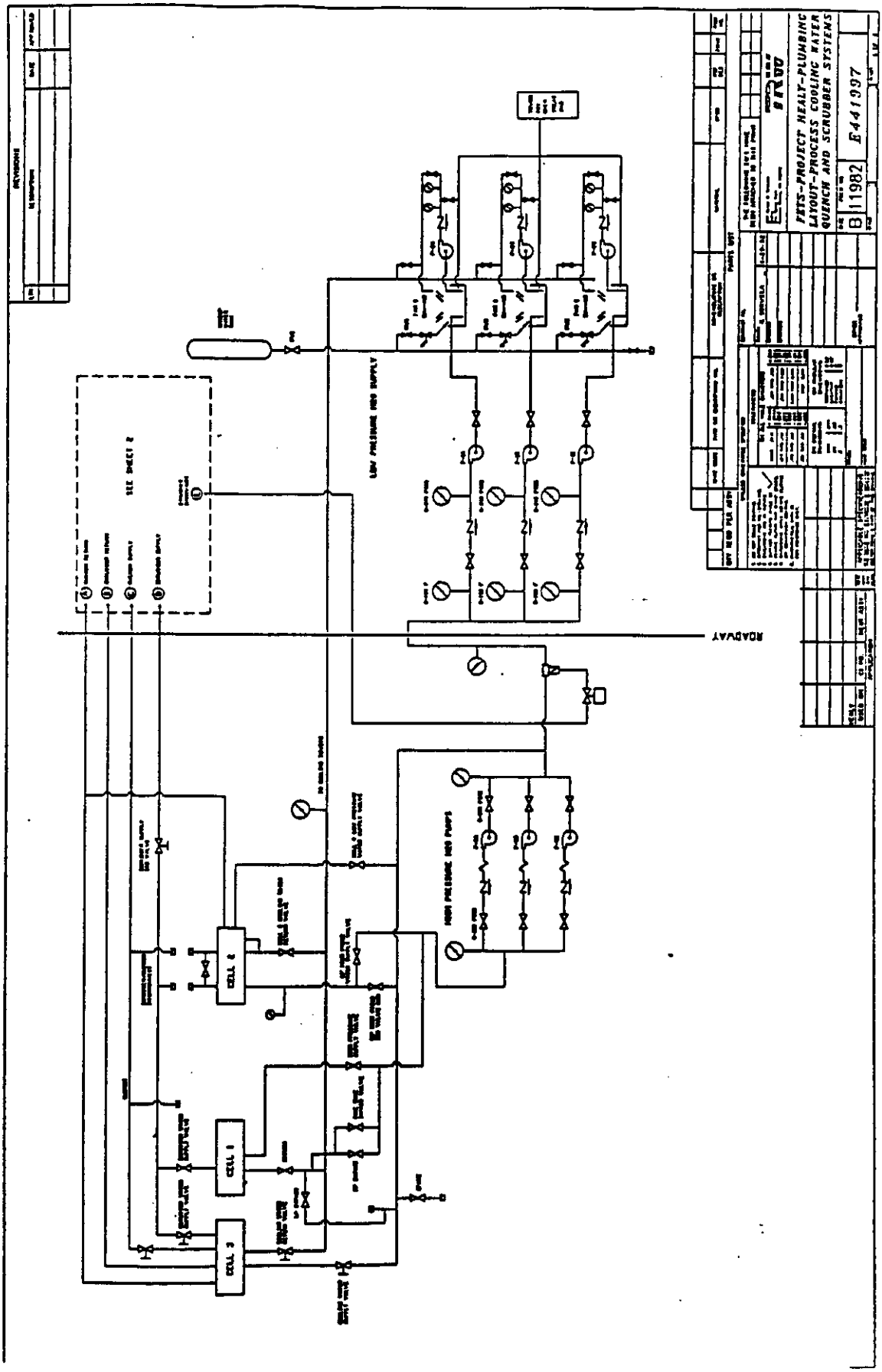

Figure 3-27 Facility Cooling Water, Quench and Scrubber System Instrumentation

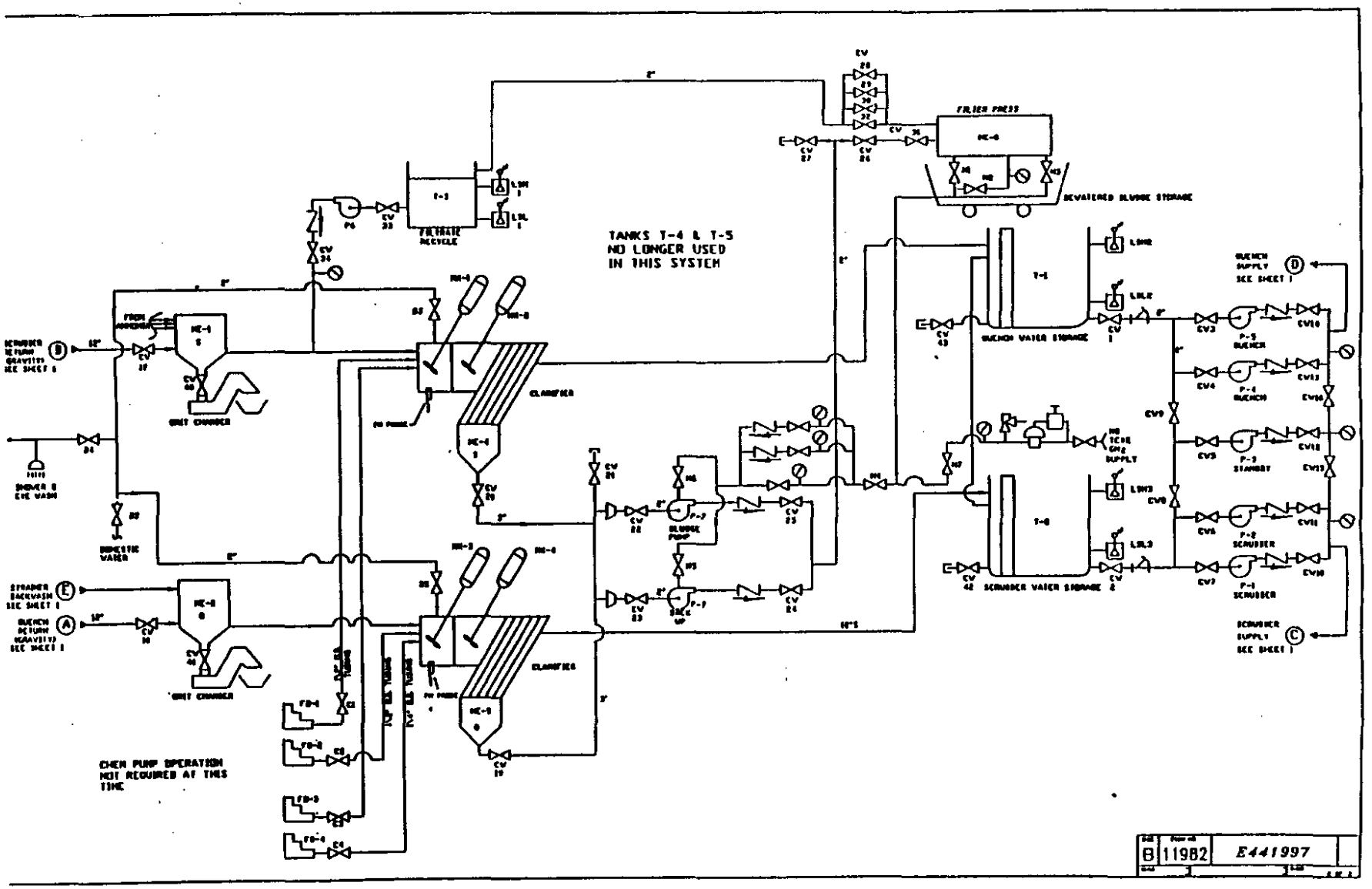

Figure 3-28 Facility Cooling Water, Quench and Scrubber System Instrumentation - Continued

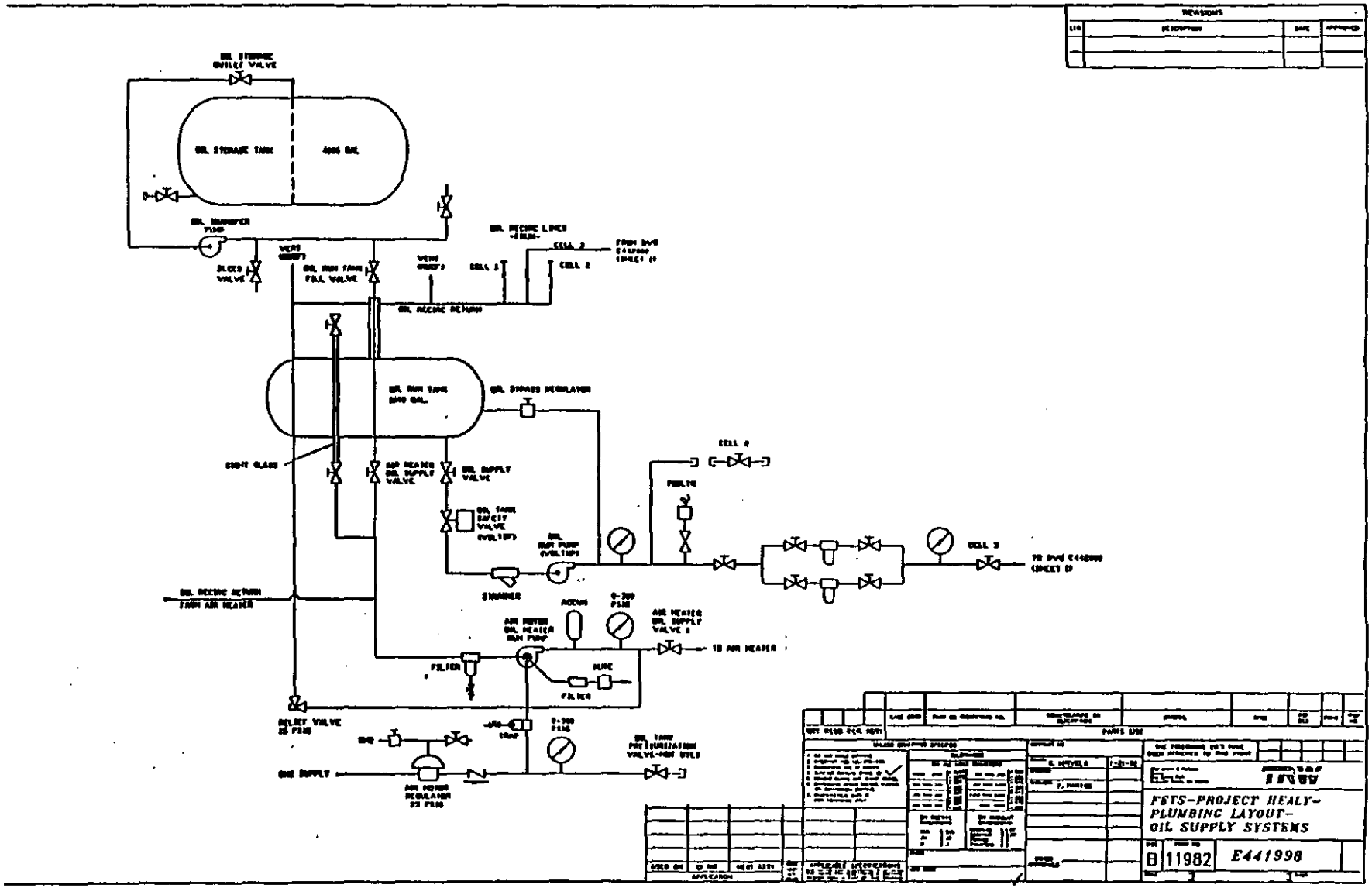

Figure 3-29 Facility Oil Supply System Instrumentation

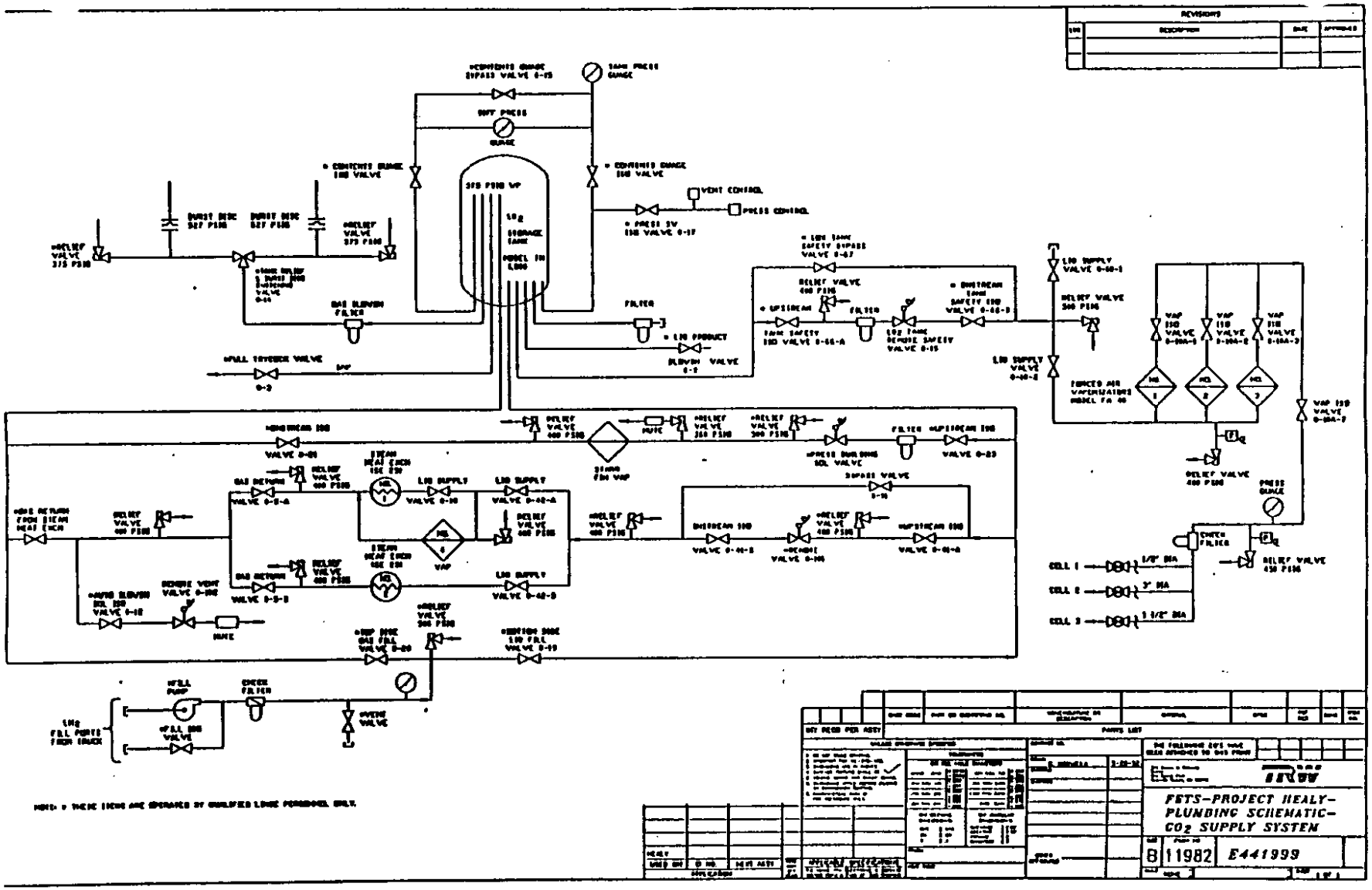

Figure 3-30 Facility CO_2 Supply System Instrumentation

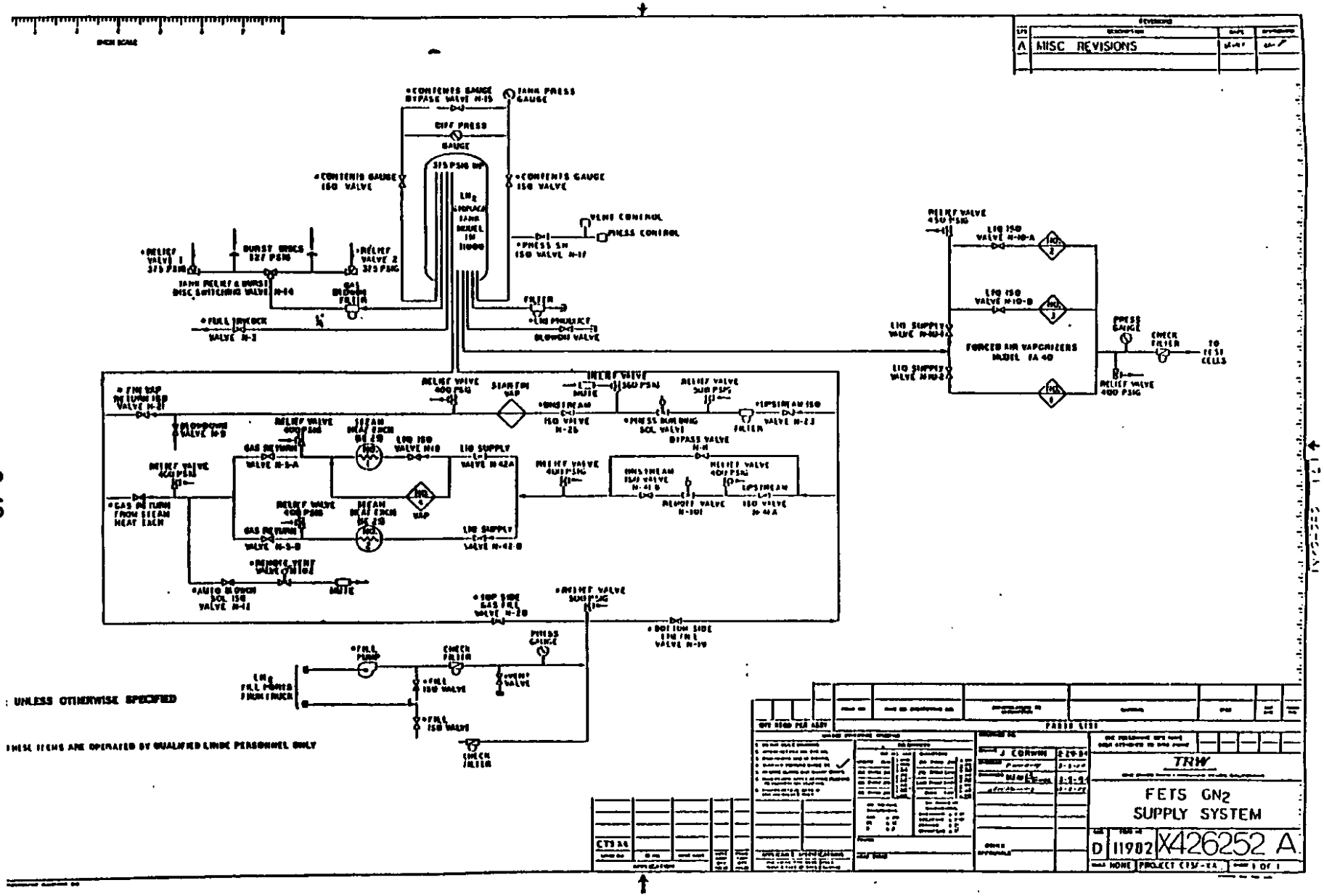

Figure 3-31 Facility Nitrogen Supply System Instrumentation

4.0 Checkout Tests

The checkout tests performed prior to hot-firing of the precombustor and the combined DCFS-precombustor system are described in this section. Complete test data, analyses and hardware modifications made during the test series are presented in Sections 5 and 6.

4.1 Precombustor Checkout Tests

During this test phase, a considerable amount of time was spent in the initial operation, trouble-shooting and checkout of the Forney oil burner, and to a lesser extent, the Foster Wheeler coal burner. A number of facility related systems also required checkout, including the facility coal feed system, combustion air supply and heaters, cooling water, oil supply and exhaust. The following provides a narrative of this effort.

4.1.1 Forney Oil Burner Checkout

Initial oil lightoffs of the Forney oil burner involved positioning the oil gun assembly relative to the Foster Wheeler burner and determining the lightoff location of the HESI. Several startups were impaired by dirt in the burner tip until the entire system consisting of supply tank, pump, valves, lines, and regulators had been run sufficiently to clean itself up. External tip deposits never appeared to interfere with tip operation. Initial startups were conducted with the firing position of the oil gun tip flush with the face of the Foster Wheeler burner assembly. Later, this position was retracted by 3.5 inches, the maximum permitted by the mechanical arrangement of the equipment. This increased the probability of lightoff and reduced the stack smoke level.

Initially, the HESI was positioned 8 inches beyond the oil gun assembly for lightoff. Several startup cycles were frequently required before a flame could be obtained. Extending the HESI lightoff location to 10 inches resulted in reliable startups.

A flame scanner signal of only marginal strength could be obtained at the Forney recommended centerline scanner location. With the scanner in a peripheral location, the oil flame was readily confirmed as ignition occurred. The centerline flame scanner was moved early in the test program to the peripheral location not used for the coal flame scanner.

Oil flow required to support a 20 MMBTU/hr firing rate was established in the recirculation loop prior to lightoff. Oil gun assembly insertion to the firing position was confirmed by position switch contact. A delay of approximately 30 seconds after the oil gun was extended was normal before oil ignition occurred. Lightoff sequences obtained by viewing up the PC centerline have been preserved on video tape. Oil frequently obscured the HESI spark for several seconds before ignition occurred. Once ignited, six

fingers of flame quickly expanded to fill the headend of the combustion chamber. No voids in the final flame were apparent.

Before any lightoffs could be attempted, the mechanical function of the equipment and the control logic wired into the cabinet as supplied required rework. It was necessary to remove equipment interferences which prevented full retraction of the oil gun assembly. A ramp was added to the configuration of the alignment ring which supports the oil gun in the extended position. This was required to eliminate hangup from preventing full extension of the oil gun assembly. The Cashco regulator failed to regulate reliably until internal clearances were reworked. The flex lines for supplying oil and air to the oil gun were initially crossed at the oil gun ports as a result of improper callouts on the Forney drawings. These attach points should be permanently marked as "oil" and "air" on the oil gun. The sequence logic as wired in the control cabinet caused the system to bypass the startup phase and initiate a purge sequence. This situation was resolved during discussions with Forney. All the above mechanical changes are recommended for the Healy installation.

Once lightoff was achieved, the next step was operation over a load range from 20 MMBTU/hr (oil lightoff) to 70 MMBTU/hr. Two major problems had to be resolved before a coal lightoff was attempted:

- Oil and atomizing air pressure requirements. The oil and air supply pressure requirements (near 400 psig) needed to reach full load greatly exceeded Forney predictions and the capability of the installed CTS facility equipment. A review of orifice arrangement and sizing by TRW indicated that the test data results were correct. The atomization mode of operation was changed from a constant differential to a constant pressure regulation at 95 psig. As a result of this change, the oil pressure requirement was reduced to less than 150 psig at full load. Figure 4-1 shows the relationship between oil pressure, oil firing rate and the atomizing air pressures.

  This modified arrangement started up satisfactorily and produced the cleanest burning conditions over the load range. This arrangement eliminates the requirement for the Cashco pressure differential regulator, and has been implemented for the Healy design.

- Visual smoke levels at the stack. In the original installation, a tertiary air fan supplied cold air to the housing surrounding the oil gun. The system was designed to switch to hot combustion air from the primary air windbox after coal ignition was completed. Increasing tertiary air diminished the visual stability of the oil flame and increased smoke levels at the stack.

  Sixteen coal lightoffs and a flame scanner evaluation series were completed before a changeover eliminating the switching

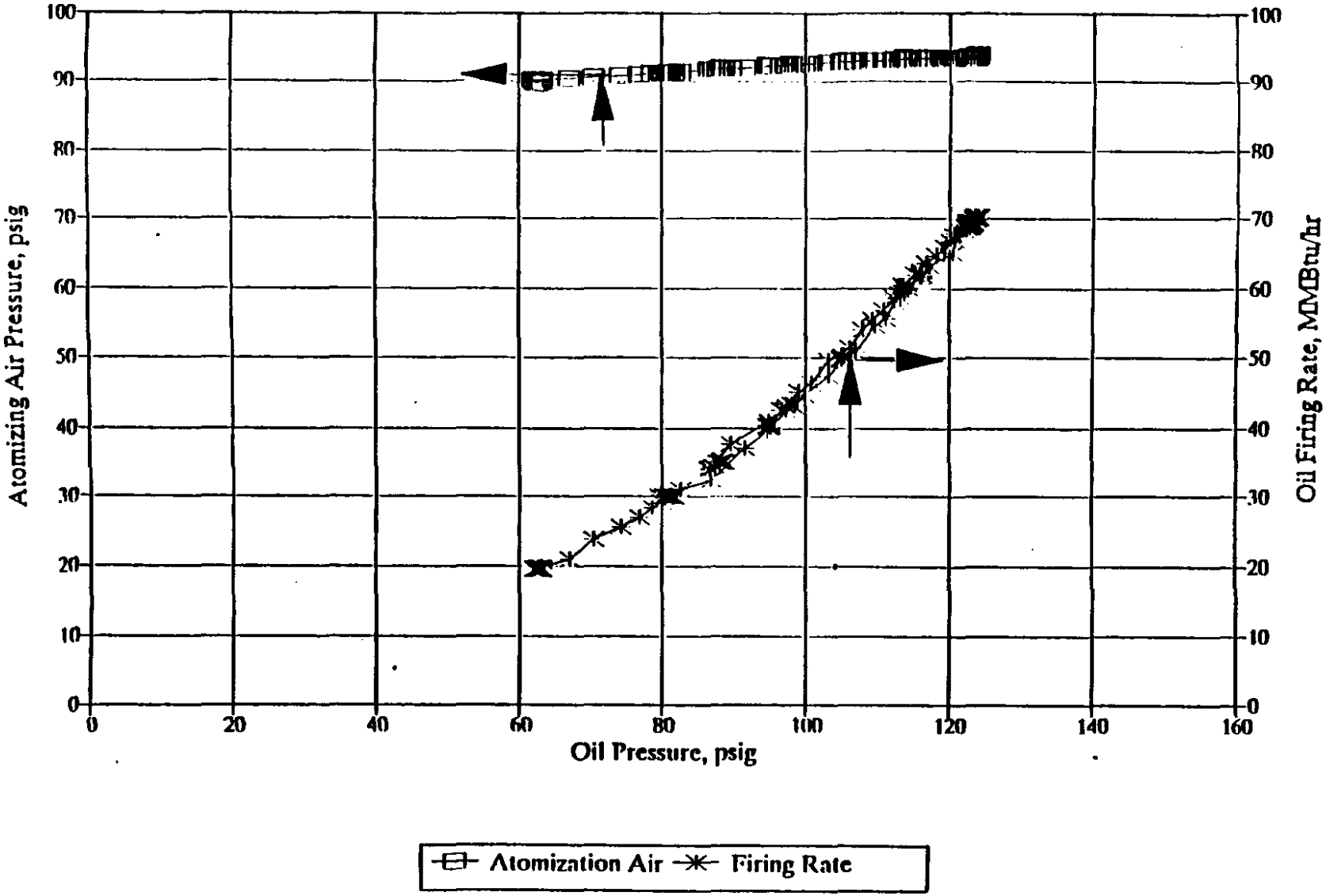

Figure 4-1 Forney Igniter Pressure Data

mode was implemented. The intent of the changeover was to use air ducted from the primary air windbox as the tertiary air. This inadvertently eliminated tertiary air from all future tests because the tertiary air fan was used for coal injector purging prior to coal lightoff and was left on throughout the duration of all subsequent tests. The windbox duct valve switched closed whenever the fan was turned on and switched open when the fan was turned off. This wiring arrangement had been installed for the original setup.

However, the changeover resulted in a significant reduction in stack smoke levels. Prior to the change, different combinations of Foster Wheeler dual air register settings and cold air flows were tried to improve ignition and reduce smoke levels. These efforts were met with limited success. The best operation was obtained without tertiary air flow. For Healy, tertiary air flow may be reduced during oil burner operation. However, tertiary air is still required for purging the burner cavity, and for cooling prior to lightoff or restart.

During DVT, internal cooling of the oil gun was performed prior to lightoff by initiating three successive startup and purge cycles with the three way oil divert valve closed. This procedure was implemented after the tertiary air change.

Oil burner performance was improved during the DVT program. Smokeless operation occurred at both lightoff and full load. A slight stack haze consistently occurred at intermediate loads. The necessity to make step changes in air and oil flowrates with the control system available at FETS aggravated the problem. Changes in air to fuel ratios did alter the intensity of the haze. If required, minor changes in burner settings, ramping air and fuel at near constant air/fuel ratio should help eliminate the problem. The oil flame obtained was very stable and never flamed out except during the initial phase of coal lightoff during the DVT program. Ignition of oil into an existing coal flame always occurred.

As previously described, the signal strength of the central axis flame scanner was always only marginal even with an oil only flame. Oil flame signal strength diminished significantly whenever coal was introduced into the system. This situation with coal also prevented confirmation of oil flame ignition during the shutdown sequence when the coal flame was present. Stack emissions confirmed that oil ignition was always obtained. A number of steps were taken without success to resolve the problem. Signal strength was improved slightly by changing the scanner mounting arrangement to view a wider angle and adding view openings in the burner support ring. None of the steps taken resolved the problem to the point where a reliable indication of oil flame status could be obtained. It is recommended that a flame management scheme using separate peripheral oil and coal flame scanners be implemented at Healy rather than the on-axis location.

4.1.2 Foster Wheeler Coal Burner Checkout

The as-supplied Foster Wheeler coal burner arrangement exhibited desirable operating pressure loss characteristics (5-6 inches of water at full load). The pressure loss characteristic proved to be dependent primarily upon transport airflow with little change occurring with coal flow. (See Section 5 for burner pressure drop data.) Because of this characteristic, this pressure loss measurement can be used to monitor PC transport airflow during operation at Healy. Subtracting the PC transport airflow from total blowdown flow will provide an indirect measurement of the slagging combustor transport airflow.

The injector was sized to operate with a transport air to coal ratio near 0.66 at full load. The coal transport flowrate was held near 10,600 pounds per hour. Conventional pulverized coal systems are operated typically closer to a ratio of 2.5. Diversion of a major fraction of the mill air to the boiler NO_x ports is required at Healy in order to achieve the temperature levels required for slagging. This produces a substantial fuel rich condition in the center of the burner.

The mechanical function of the Foster Wheeler hardware was acceptable as supplied. Initially, the air registers were adjusted for the best visual oil flame characteristics. This resulted in dual air register settings of 25% full travel clockwise for the inner registers and 30% full travel clockwise for the outer registers.

Figure 4-2 shows a sketch of the adjustment indicator on the register drives, indicating a 30% position. There is not a one-to-one correspondence between the indicator setting and the actual open area of the registers, as shown in Figure 4-3. For example, an actuator position of 30° corresponds to an open area of approximately 55%.

A number of air register adjustments were subsequently tried while operating on coal. The same 25% and 30% settings gave the best results for oil and coal thereby establishing them as nominal for the test program.

The burner demonstrated that the air register settings could be set over a wide range without encountering unacceptable operation. The combustion airflow rate was held constant during register setting evaluation tests. Opening the outer register setting to 60% open with the inner at nominal resulted in a pulsing flame condition. Closing the outer register to 15% resulted in a dark flame as viewed along the centerline axis. Opening the inner register to 60% with the outer register at 50% resulted in a pulsing darker flame and weakened the scanner signal. Closing the inner damper to 15% with the outer at 30% resulted in an acceptable oil flame. The operational envelope for the outer and inner register settings is illustrated in Figure 4-4.

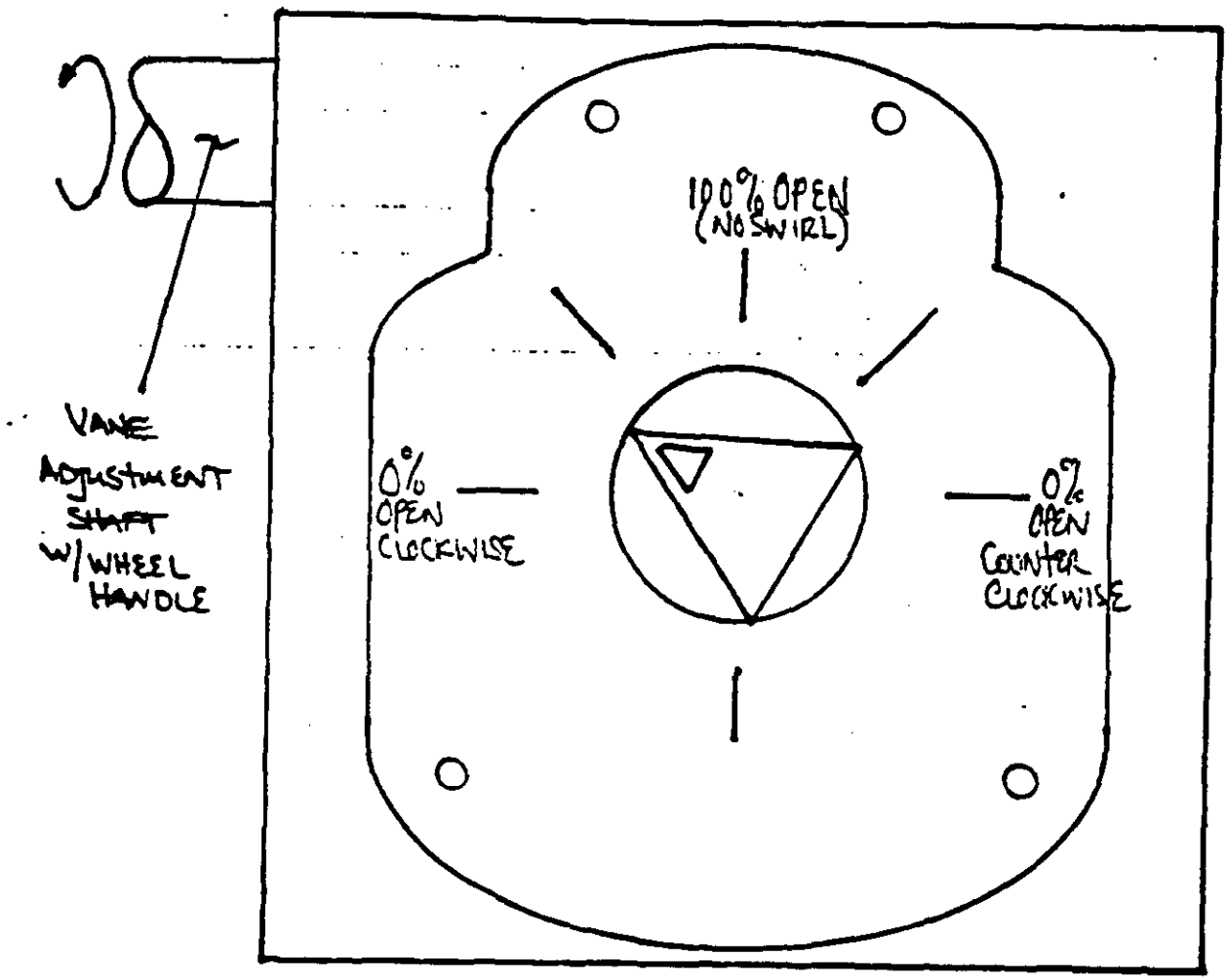

NOTE - THIS SKETCH DEPICTS A VANE SETTING OF 30% OPEN, CLOCKWISE.

Figure 4-2 Dual Register Vane Adjustment Indicator

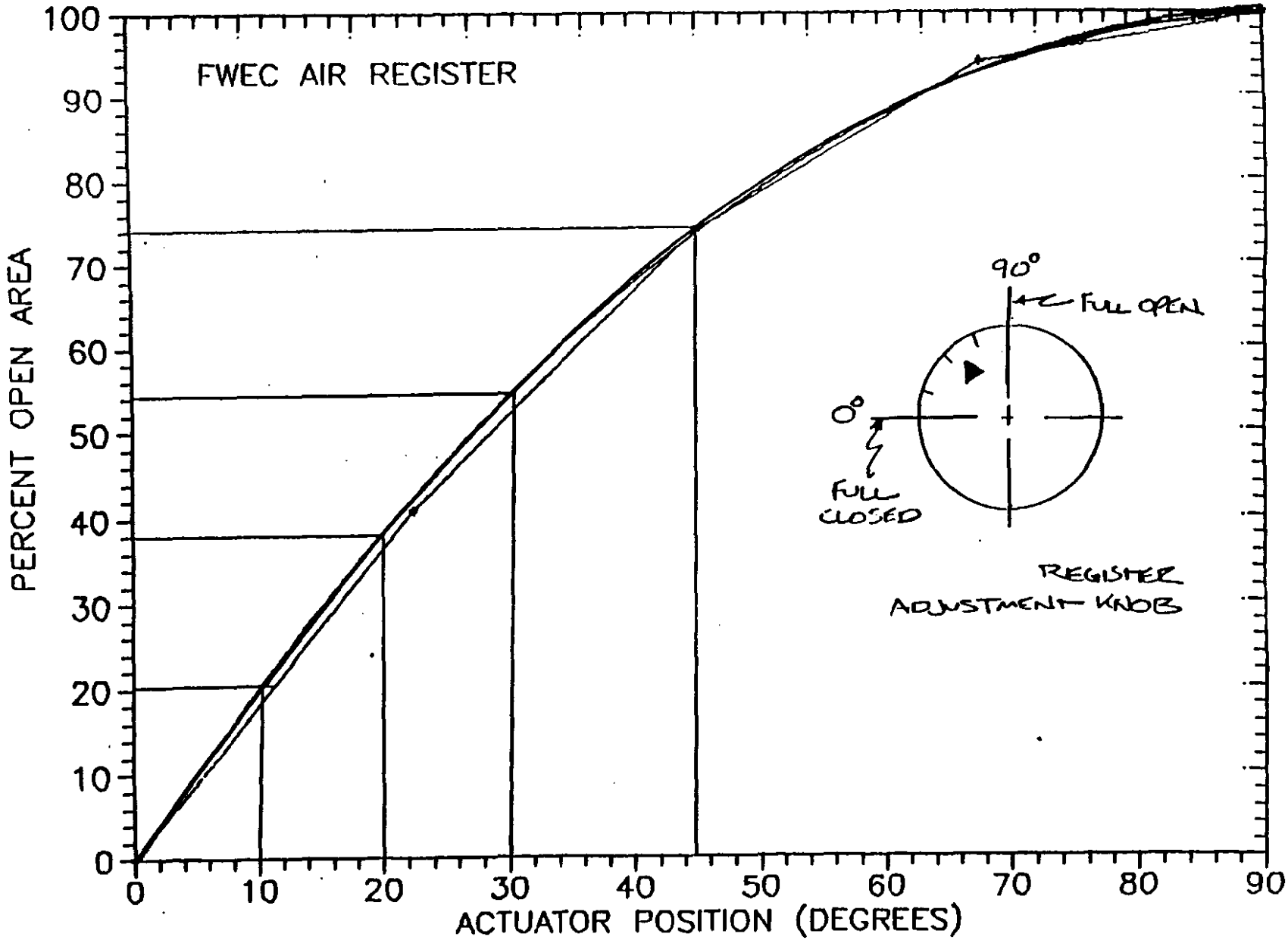

Figure 4-3 Air Register Open Area Versus Indicator Position

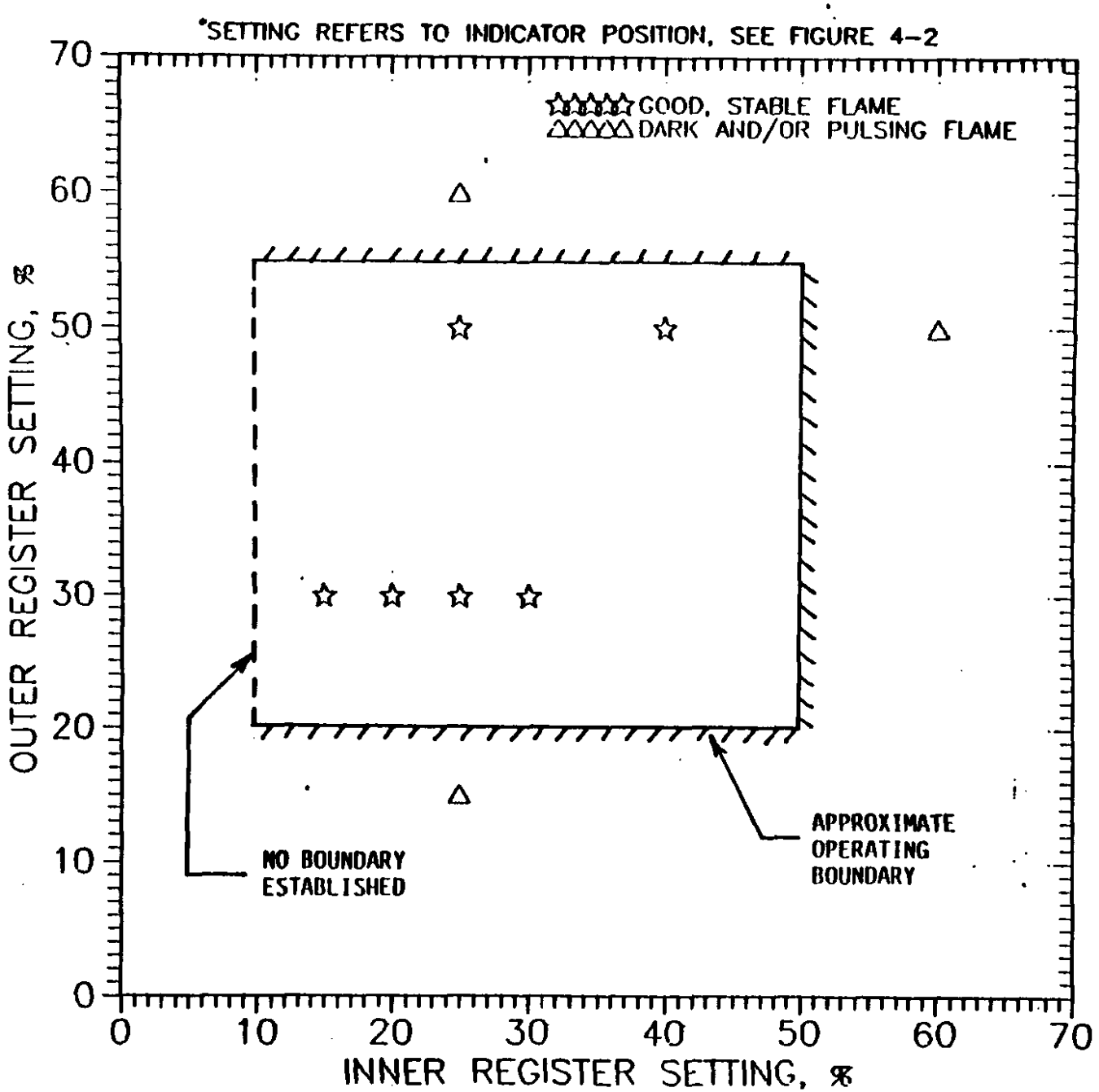

Figure 4-4 Approximate Operating Map for FWEC Air Register Settings*

Initially, a cold air purge through a 2 inch line from the carrier air fan was established to the coal injector downstream of the fire valve prior to lightoff. Later the tertiary air fan provided this source (see discussion in Section 4.1.1). The purge prevented the circulation of hot gas within the housing cavity during startup of the combustion air supply system and/or during oil only firing. The purge was terminated at coal lightoff by simultaneously switching the purge and fire valves. A similar purge arrangement has been implemented for the Healy design.

The Foster Wheeler coal burner performed well without incident. No loss of coal flame ever occurred. The burner operated over a load range from 1000 to 15000 pounds per hour of coal without encountering any major problems. The peripheral coal flame scanner provided a strong signal under all conditions whether firing oil only, oil and coal, or coal only.

4.1.3 Oil/Coal Flame Discrimination

During initial attempts to introduce carrier air to the oil flame, the scanner signal was lost and the burner tripped. This lightoff problem was resolved by slowing the opening response of the fire valve and reducing the preset transport air flowrate in the bypass line. The transport air flowrate was increased to the run level after opening the valve and before introducing any coal.

A major effort was undertaken with a spectrum analyzer to find any differences between the three firing conditions which could lead to discrimination between the coal and oil flames. Figure 4-5 shows typical frequency spectrum data for coal firing only and oil firing only. The data were obtained with a scanner located in the coal flame scanner (peripheral) port. Although there is some difference in signal strength, the basic frequency spectrum is the same for the two flames, making discrimination difficult.

Despite the lack of flame discrimination ability, reliable ignition of both coal and oil was always obtained. The firing duty of the system was near half load (70 MMBTU/hr) when ignition of a new fuel was required. As long as the presence of the half load flame is assured, the probability of a flame failure is extremely low. The NFPA code requires that ignition and flame propagation from a 4 to 10% duty ignitor be verified. It also requires that only the continuous presence of a flame be verified when increasing load. The concentric arrangement of the oil and coal flames within the refractory lined combustion chamber virtually assures that all zones of the newly introduced alternate fuel will be ignited. Hence flame discrimination requirement may not be necessary. Yet, it is necessary to establish that the present system will meet NFPA requirements. In fact, we have learned from Forney that lack of flame discrimination is a problem common to all of their installations, and despite this problem those installations continue to be in service.

Coal ignition was visually observed repeatedly within 6 seconds of

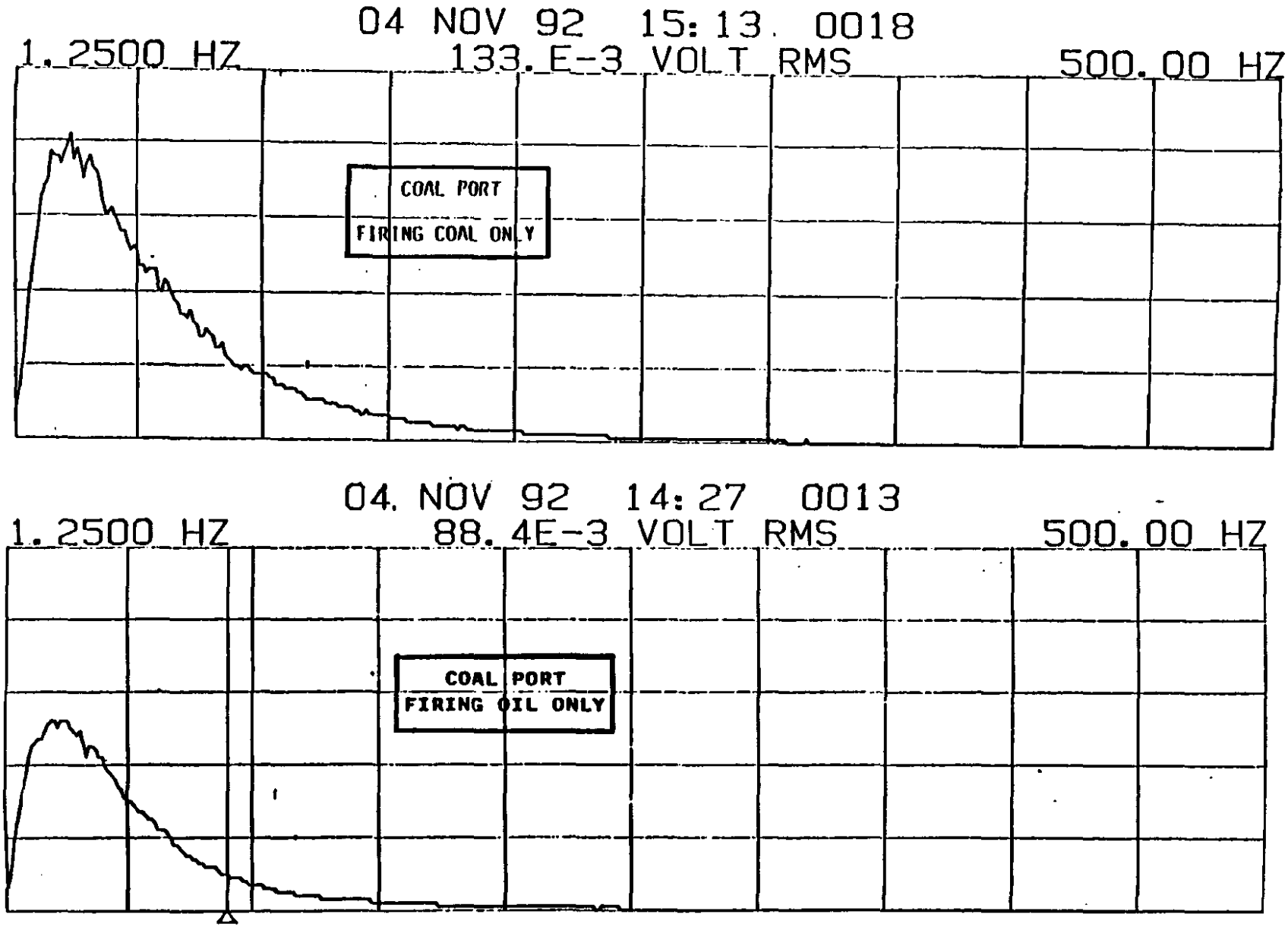

Figure 4-5 Flame Scanner Spectrum Analysis

opening the supply valve under the lock hopper. This time period is the transit time in the system. Oil ignition by the coal flame always occurred without any effects observed visually. In this situation igniting the fuel is analogous to increasing load. When firing coal, an observer was always dedicated to visually monitor the flame condition on a video monitor. View ports were modified as necessary to always be able to view the flame. Not one instance of coal flame failure occurred throughout the entire DVT Program.

4.2 DCFS Checkout Tests

A series of cold air flow tests were conducted prior to introducing coal. The system was completely leak checked under cold flow conditions. Blowdown flowrate was indicated as the difference between carrier air delivered to the splitter and vent air leaving the cyclones. The flow rate, absolute pressure, and pressure loss data obtained agreed closely with the laboratory subscale model results. This provided considerable confidence concerning the scaling principles which had been used.

4.3 Checkout of Other Systems

Cooling, quench, and scrubber system water flowrates were established and checked prior to the introduction of any fuel to the system. The primary and secondary fans were turned on next. The carrier air fan was turned on last to avoid blowing coal back through the duct heaters and fans. Prior to installation of the DCFS, the transport/carrier air system was isolated by the fire valve. After installation of the DCFS, a cloud of coal was consistently produced at the carrier air fan inlet by air back flow through the cyclone vent connection. This condition was always required clean up before starting the duct heaters. It is recommended that avoiding the back flow situation be assured at all times at Healy, especially if the combustion air supplied to the PC is hot.

The coal transport system to the Foster Wheeler burner incorporated a bypass tee which allowed transport air (and coal) to be blown into the quench scrubber system when the fire valve was closed. This bypass also served as a coal cleanout line for any large coal accumulations in the transport system and/or DCFS and allowed the transport air flowrate to be preset prior to opening the fire valve. The fire and bypass valves were switched in opposite directions simultaneously. The carrier air fan flowrate not used for transport was vented both before and after lightoff.

5. Precombustor Test Data

The Precombustor Test Series consisted of a total of 17 tests not including oil and coal lightoff and checkout activities. A total of 83.6 tons of pulverized coal was consumed by the time the series was completed. Several complete simulations of Healy duty cycles were performed.

This section presents data collected during the precombustor test series. These tests utilized the existing facility coal supply system described in Section 3.0 to deliver coal to the precombustor. This allowed testing of the precombustor to proceed in parallel with installation of the direct coal feed system.

The precombustor test sequence is illustrated in Figure 5-1. Test series A through D were used for initial verification of oil and coal lightoff, burner tuning and swirl damper mechanical checkout. This was followed by specific tests to address the parameters listed in blocks E through H of Figure 5-1.

5.1 Oil and Coal Light-off Tests

Oil and coal lightoffs were performed with the primary windbox combustion air temperature preset within a range from room temperature to 550°F. Initial coal lightoffs were performed with an oil firing rate near 50 MMBTU/hr established in the precombustor. This was later raised to 70 MMBTU/hr (the actual Healy requirement) after the Forney burner supply pressure problem was resolved.

A similar technique can be used at Healy to establish the mill sweep air split for transport and vent flowrates prior to starting coal feed to the mill. Any residual coal in the system from the previous shutdown will be consumed in the oil flame. Increasing the sweep air flowrate to lightoff values should be done at a low ramp rate to minimize the rate at which coal is picked up.

5.2 Precombustor Test Series

The Precombustor Test Series progressed smoothly once the Forney oil burner and initial coal lightoff sequences were worked out. The overall system handled the pulverized coal without any major problems. Trouble free operation of the facility coal supply system was achieved early in the test series after a scheme of backpurging the tank prior to startup was worked out. An effort concentrated on increasing the reliability of the coal transfers to the lock hopper reduced the number of empty (dummy) transfers which enabled sustained operation at full load.

The precombustor test results verified the design of the complete precombustor package and the operating conditions tested covered the operating envelope expected at Healy.

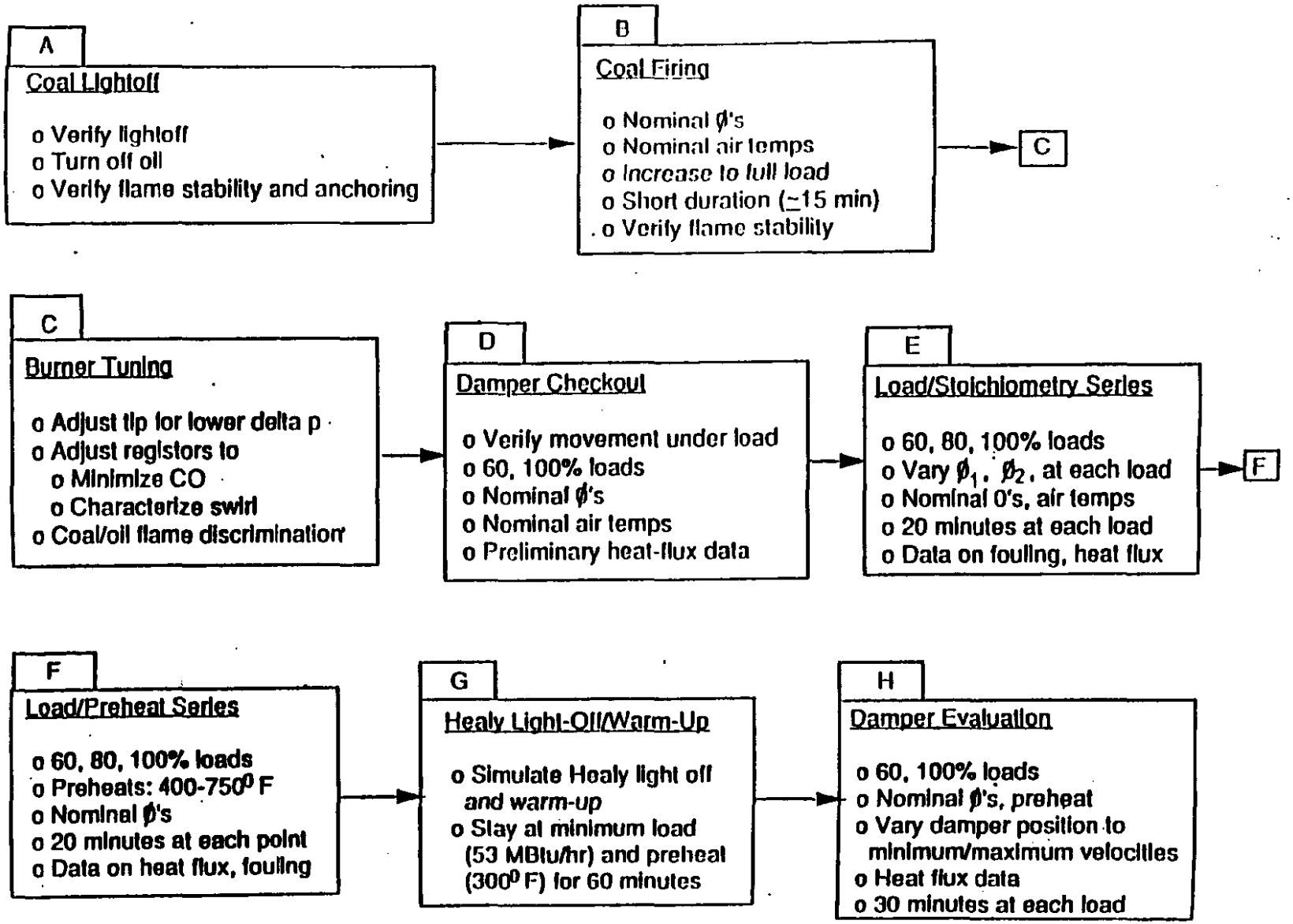

Figure 5-1 DVT Precombustor Test Sequence

All the mechanical features of the Precombustor operated without any significant problems. The swirl dampers were inserted and retracted without incident. The mounting design of the precombustor, interconnecting ducts, and duct heater chambers worked without requiring any modifications.

5.2.1 Operating Conditions

The test matrix which was used to develop operating conditions for testing is shown in Table 5-1. The conditions listed in the table provided "target" values for parameters such as load, preheat, stoichiometry, etc. The actual values obtained are listed in Appendix B. (Note that matrix conditions from Table 5-1 are referred to in the tables of Appendix B.)

Figure 5-2 illustrates the range of operating conditions for the precombustor tests, showing exit stoichiometry versus load at various air preheat levels. Also indicated is the stoichiometry versus load line which will be followed for operation at Healy.

5.2.2 Stack Oxygen Levels

Measured stack oxygen levels versus exit stoichiometry are plotted in Figure 5-3 and compared to predicted values. Predictions are shown for combustion of rapid volatiles only, and for complete combustion of the coal. The close agreement between the data and predictions is a good indication that the precombustor was operating with high combustion efficiency.

5.2.3 Heat Fluxes and Cooling Loads

The determination of heat fluxes on the various precombustor components is important in verifying the Healy design. The magnitude of heat flux has a direct effect on the choice of tube and membrane sizes, material selection and refractory specification. The magnitude of precombustor cooling loads affects the temperature of the combustion gas products entering the slagging stage, as well as the overall thermal-hydraulic design of the combustor.

The DVT precombustor had 7 separate water cooled circuits with flow and temperature measurements for obtaining calorimetry data. The circuits are (Figure 5-4): baffle, combustion can, mill air spool, transition, swirl damper housing, and swirl damper blades (2). Heat flux values were obtained by dividing the component cooling load by the component surface area. This provides an average heat flux and does not account for possible peak values.

In addition to the above measurements, a small (5 inch diameter) water cooled coupon was installed in one of the unused mill air spool ports. The coupon was left bare (no refractory) and thus indicates the level of "bare wall" heat fluxes in this zone of the precombustor.

Table 5-1 DVT Precombustor Test Matrix

SERIES	LOAD % MCR	PHI 1	PHI 2	T1 DEG F	T2 DEG F	URATIO MINUTES	DAMPER POSITION	NOTES
C1	60-100	0.85	1.75/2.12	500	500	TBD	NOM	BURNER DP REDUCTION
C2	60-100	0.85	1.75/2.12	500	500	TBD	NOM	AIR REGISTER TUNING
D1	60	0.85	1.75	500	500	20	+/- TBD%	DAMPER CHECKOUT UNDER LOAD
D2	100	0.85	2.12	500	500	20	+/- TBD%	DAMPER CHECKOUT UNDER LOAD
E1	60	0.85	1.75	700	700	20	NOM	LOAD/PHI 1 SERIES
E2	60	0.70	1.75	700	700	20	NOM	LOAD/PHI 1 SERIES
E3	60	1.00	1.75	700	700	20	NOM	LOAD/PHI 1 SERIES
E4	100	0.85	2.12	740	740	20	NOM	LOAD/PHI 1 SERIES
E5	100	0.70	2.12	740	740	20	NOM	LOAD/PHI 1 SERIES
E6	100	1.00	2.12	740	740	20	NOM	LOAD/PHI 1 SERIES
E7	80	0.85	1.94	725	725	20	NOM	LOAD/PHI 1 SERIES
E8	60	0.85	1.50	700	700	20	NOM	LOAD/PHI 2 SERIES
E9	60	0.85	2.40	700	700	20	NOM	LOAD/PHI 2 SERIES
E10	100	0.85	1.50	740	740	20	NOM	LOAD/PHI 2 SERIES
E11	100	0.85	2.40	740	740	20	NOM	LOAD/PHI 2 SERIES
F1	60	0.85	1.75	400	400	20	NOM	LOAD/PREHEAT SERIES
F2	60	0.85	1.75	500	500	20	NOM	LOAD/PREHEAT SERIES
F3	60	0.85	1.75	600	600	20	NOM	LOAD/PREHEAT SERIES
F4	60	0.85	1.75	750	750	20	NOM	LOAD/PREHEAT SERIES
F5	80	0.85	1.94	400	400	20	NOM	LOAD/PREHEAT SERIES
F6	80	0.85	1.94	750	750	20	NOM	LOAD/PREHEAT SERIES
F7	100	0.85	2.12	500	500	20	NOM	LOAD/PREHEAT SERIES
F8	100	0.85	2.12	600	600	20	NOM	LOAD/PREHEAT SERIES
F9	100	0.85	2.12	750	750	20	NOM	LOAD/PREHEAT SERIES
G1	40	0.85	2.12	300	300	60	NOM	HEALY LIGHT-OFF SIMULATION
H1	60	0.85	1.75	700	700	30	+TBD%	DAMPER EVALUATION
H2	60	0.85	1.75	700	700	30	-TBD%	DAMPER EVALUATION
H3	80	0.85	1.94	740	740	30	+TBD%	DAMPER EVALUATION
H4	80	0.85	1.94	740	740	30	-TBD%	DAMPER EVALUATION

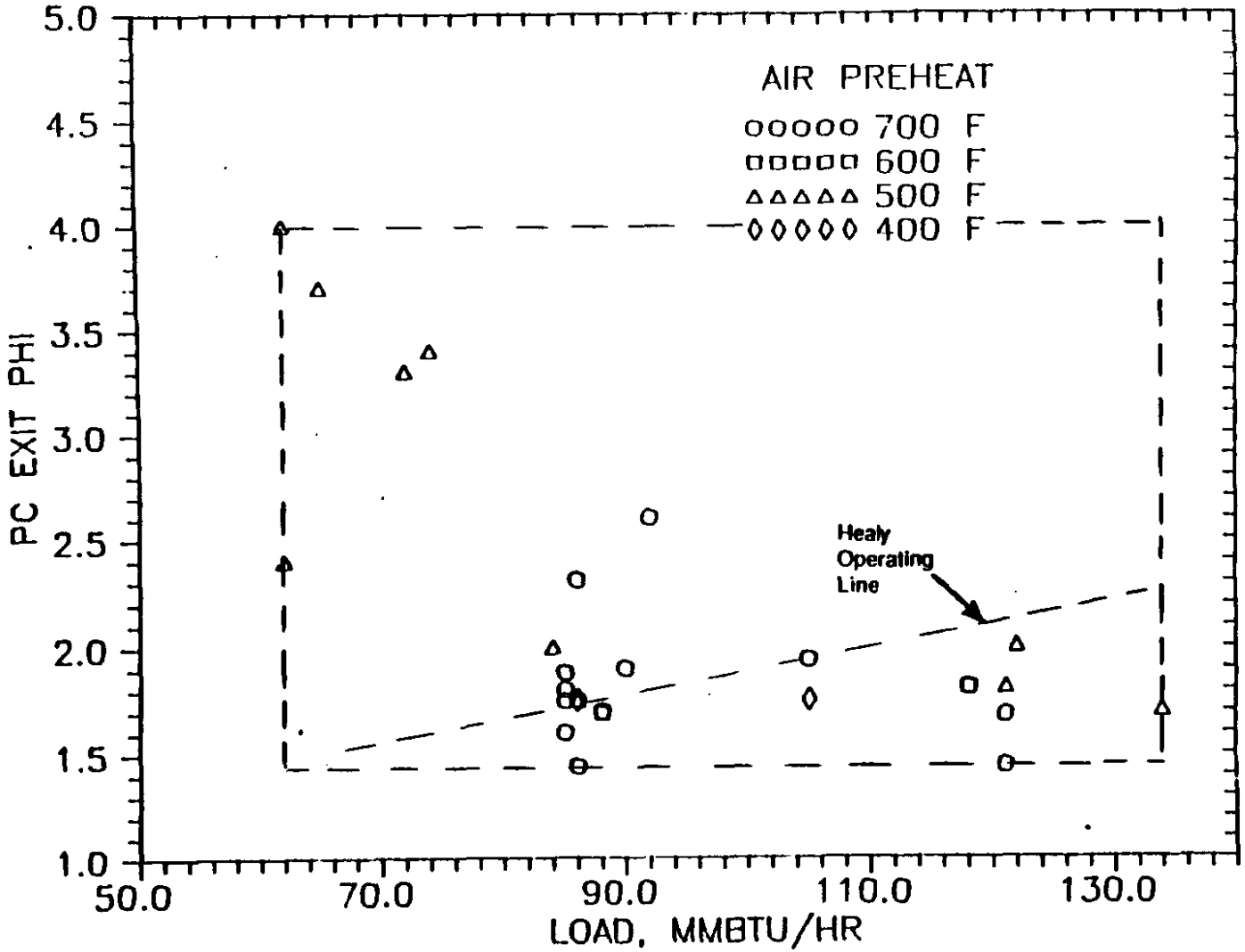

Figure 5-2 DVT Precombustor Test Conditions Map

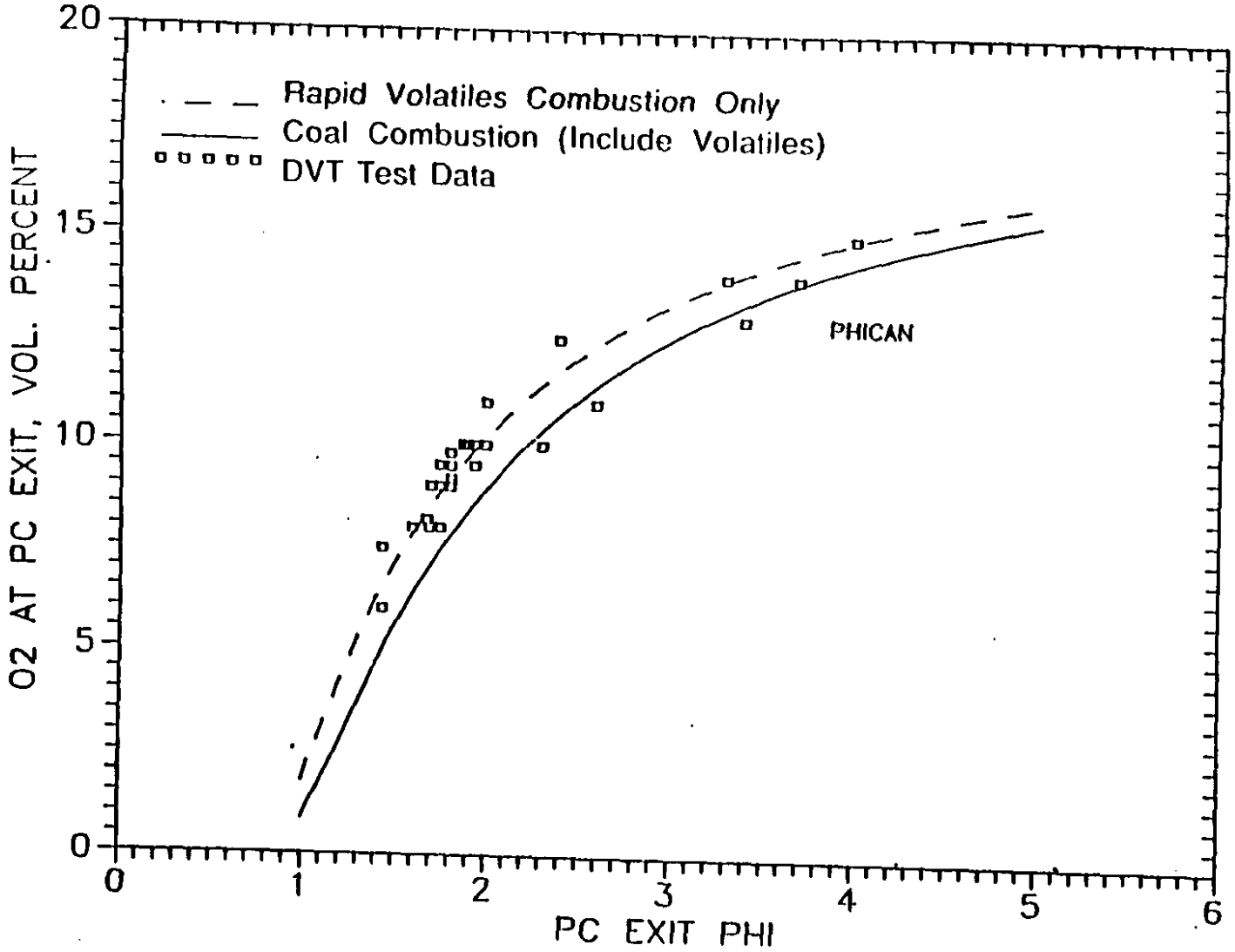

Figure 5-3 Measured versus Predicted Stack Oxygen Levels

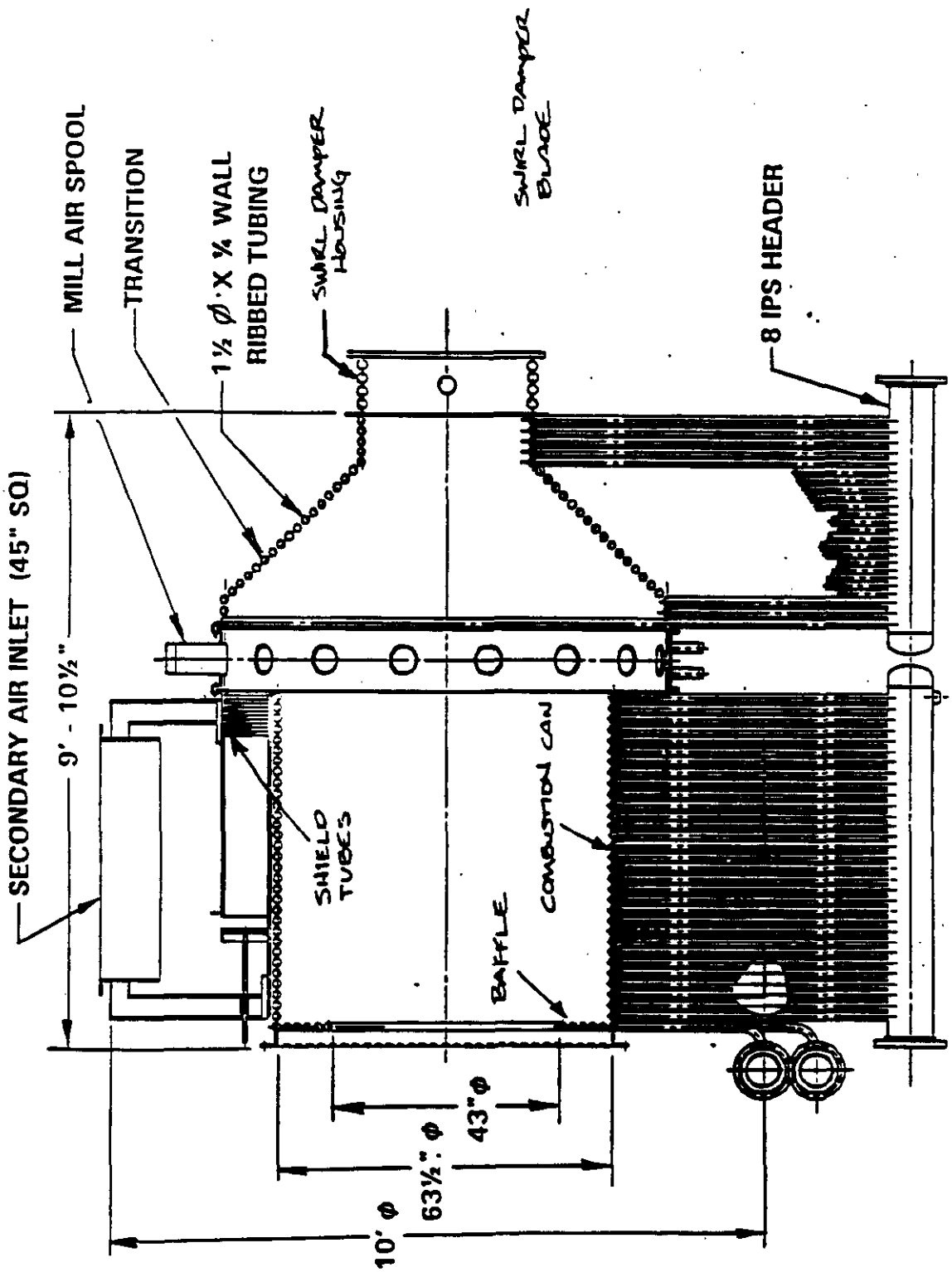

Figure 5-4 Combustor Cooling Circuits

5.2.4 Effect of Precombustor Load

Figure 5-5 shows component heat loss (cooling load) data as a function of precombustor load (% MCR). (Data for the swirl damper blades are presented separately since they will be cooled with low pressure water at Healy.) The air preheat and stoichiometry for each load were set at the levels consistent with the Healy heat and material balance conditions (see Table 5-1). Because of its lack of refractory coating, the swirl damper housing heat loss (Figure 5-4) is higher than will be the case at Healy. Figure 5-5 addresses this by showing total heat loss with and without the housing included. The actual heat loss at Healy will be somewhere between these two curves, or close to 3.0 MMBtu/hr at 100% MCR, which is the value used in TRW's heat and material balance.

Figure 5-6 shows component heat fluxes as a function of precombustor load. Predicted values are shown for the transition, the "neck" (the rectangular duct just downstream of the transition) and the combustion can. Heat fluxes are highest in the can, ranging 4 to 5 Btu/ft^{2}sec, and are lowest in the transition at 1 to 2 Btu/ft^{2}sec. The heat flux predictions are in relatively good agreement with the data. The increase in heat flux in going from 80 to 100% MCR may be due to a movement of the flame front downstream in the precombustor. Note that the heat flux on the baffle (located at the burner throat) shows no such increase, which supports this assumption.

Heat fluxes for the damper blades and damper blade housing are plotted in Figure 5-7 and show a similar increase in heat flux with load. The predicted value of 40 Btu/ft^{2}sec is based on previous test experience at CTS and Cleveland. The heat flux to the blades is calculated assuming all heat input is on the upstream side of the blade only. Since there is some heating of the downstream side, this approach results in a conservative (high) heat flux. At Healy, the downstream side of the blades will receive some radiative heating from the slagging stage of the combustor. To be conservative, the Healy design values used for damper blade heat loss assume two-sided heating with the maximum DVT heat flux on both sides.

Figure 5-7 also shows heat flux values for the swirl damper housing described earlier. Since the housing did not have a refractory lining, the heat flux of 20 Btu/ft^{2}sec at 100% MCR provides a good estimate of the "bare wall" heat flux in this zone of the precombustor, i.e. the heat flux which would be seen if the refractory is lost locally.

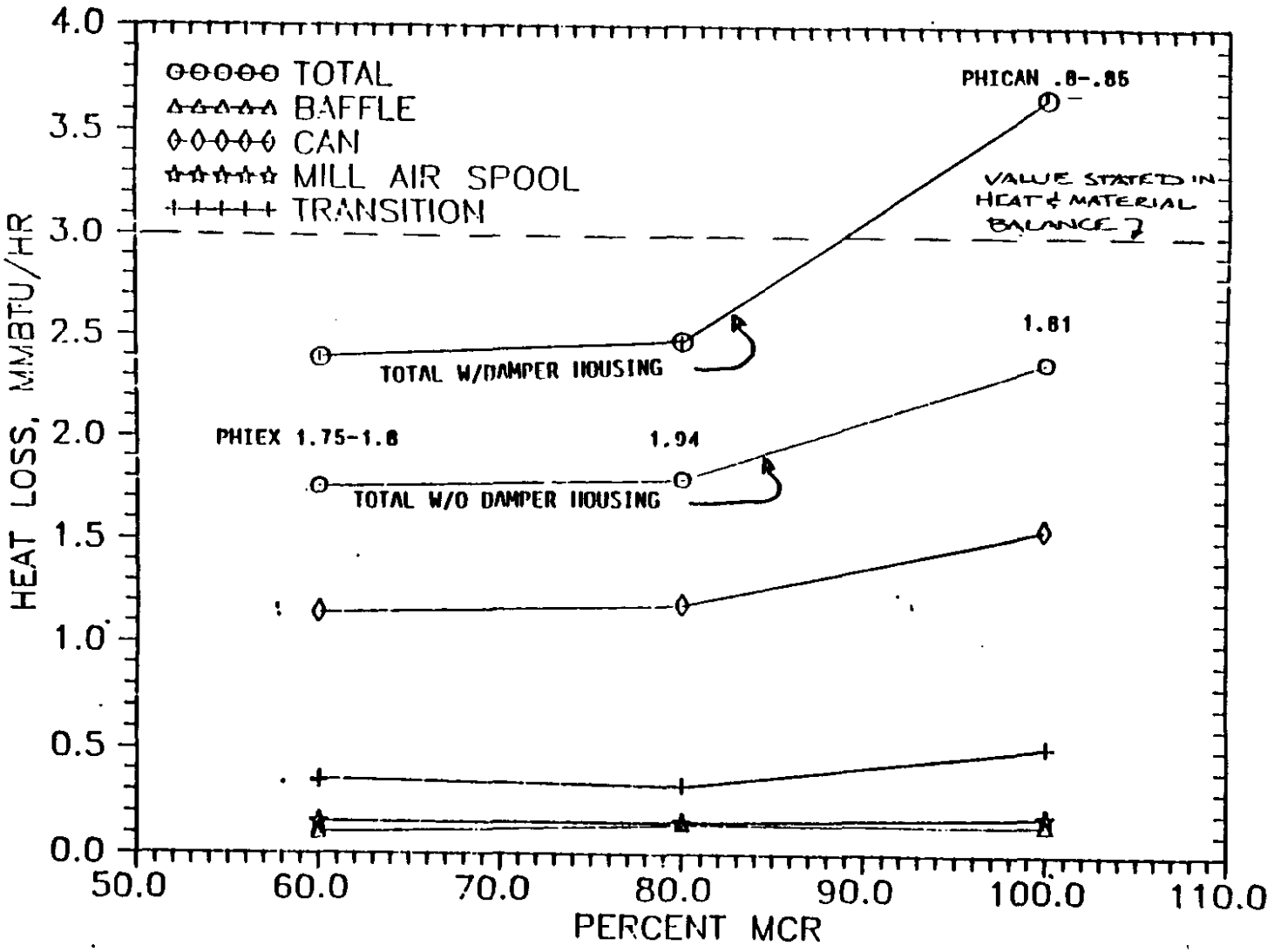

Figure 5-5 DVT Precombustor Heat Loss versus Load

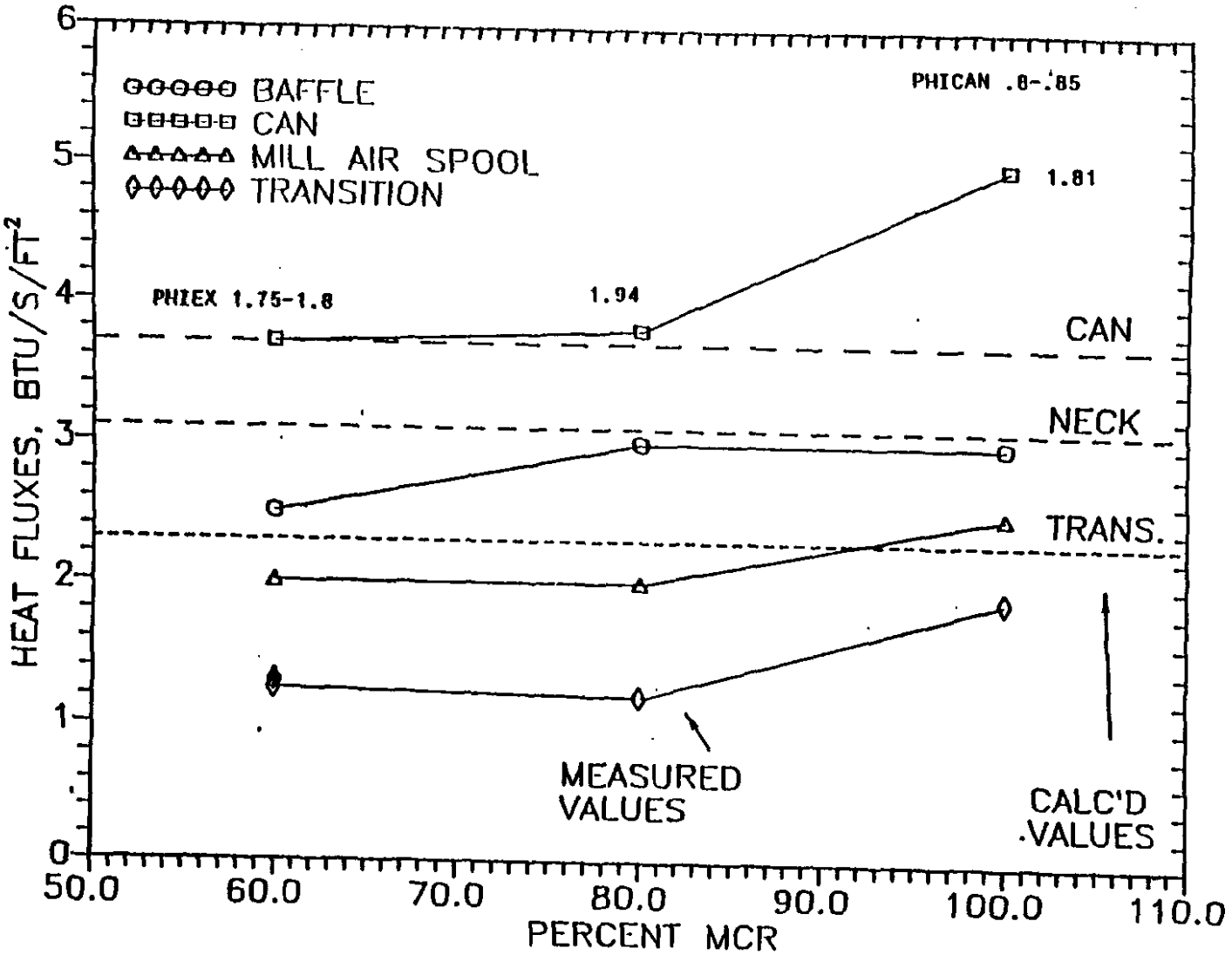

Figure 5-6 Heat Flux versus Load

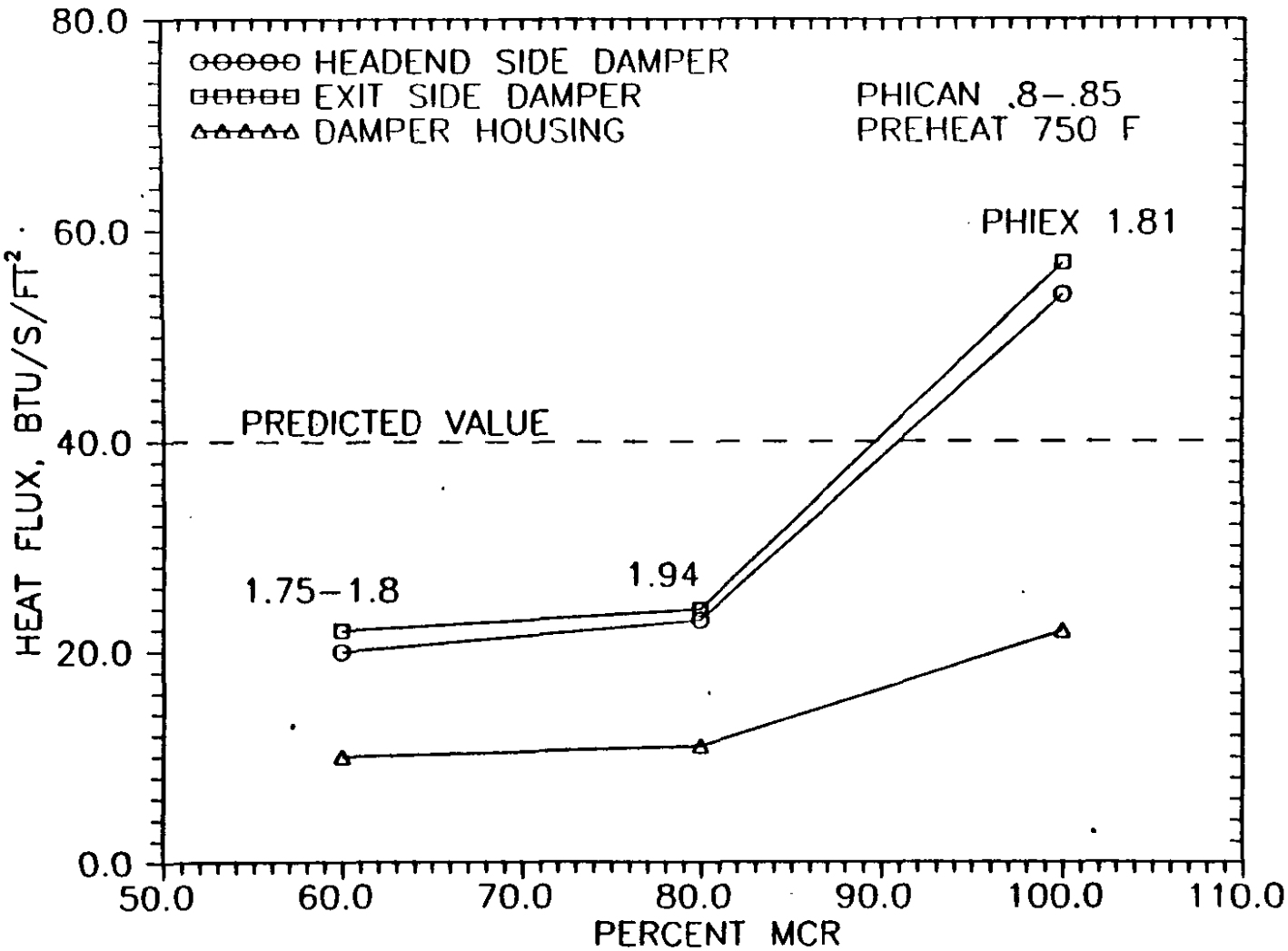

Figure 5-7 Damper Blade and Housing Heat Fluxes

5.2.5 Effect of Combustion Air Preheat

Figures 5-8a, 5-8b and 5-8c show the effect of combustion air preheat on component heat fluxes for loads of 60, 80 and 100% MCR, respectively. With the exception of the damper blade housing and mill air port coupon, the heat fluxes are relatively insensitive to preheat over the load range. The damper housing heat flux is relatively insensitive to load at 60 and 80% MCR, but at 100% MCR increases by a factor of 2.4 in the range of preheat from 500 to 740°F.

Similar results are seen for the damper blade heat fluxes as shown in Figures 5-9a-c for the same three loads. Air preheat has a minor effect on heat fluxes at 60 and 80% MCR, but has a significant impact at 100% MCR (Figure 5-9c). At 100% MCR, the damper blade heat flux increases by nearly a factor of three with an air preheat increase of 240°F (500°F to 740°F).

The damper blade (and housing) heat flux results indicate that the damper blade heating is strongly dominated by convection at full load. With a 240°F air temperature increase, radiation could be responsible for, at most, a 50% increase in heat flux. If one assumes that the damper blades are primarily heated by a layer of secondary air which is not well-mixed with the core combustion products, then a small increase in air temperature can have a large impact on the heat flux.

This result is important because it indicates that the damper blade heat loss (i.e. cooling load to low temperature condensate) can be reduced by coating the damper blades with a thin layer of refractory. For example, preliminary calculations show that a 0.060 inch thick plasma spray coating of alumina could reduce the damper blade heat loss by more than 50%. This is being considered for the Healy hardware.

The total PC heat loss (excluding damper blades), shown in Figures 5-10a-c, shows results consistent with the heat flux data presented above. Note that the heat loss increase at 100% MCR (Figure 5-10c) is driven mainly by the lack of refractory on the damper housing. With refractory installed in this zone at Healy, this increase will not occur.

5.2.6 Effect of Combustion Can Stoichiometry

Combustion can stoichiometry is determined by the amount of air added to the burner windbox, plus the coal carrier air. Figures 5-11a and 5-11b show the effect of can stoichiometry on component heat fluxes at a fixed preheat of 740°F, exit stoichiometry of 1.75-2.12 and loads of 60 and 100% MCR. As with air preheat, the heat fluxes are relatively insensitive to can stoichiometry, with the exception of the damper housing and coupon. Figures 5-12a and 5-12b shown similar data for the damper blades.

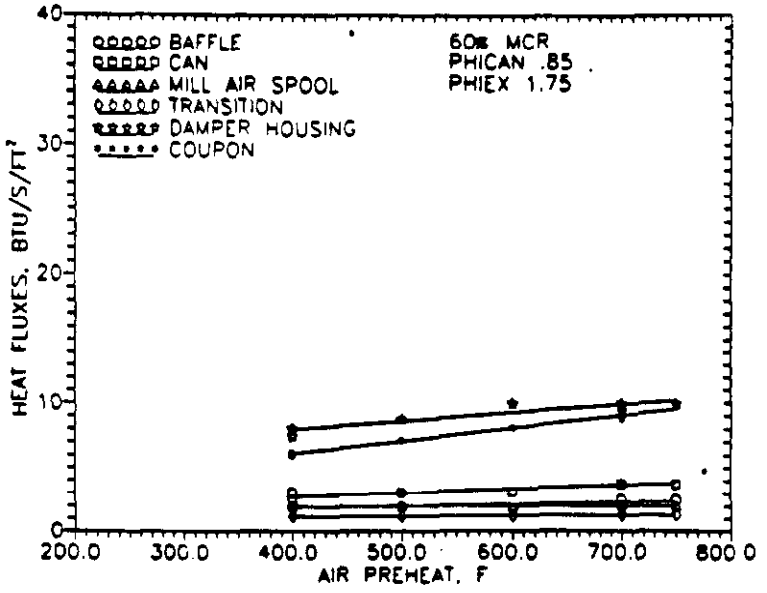

Figure 5-8a Heat Flux Versus Air Preheat - 60% MCR

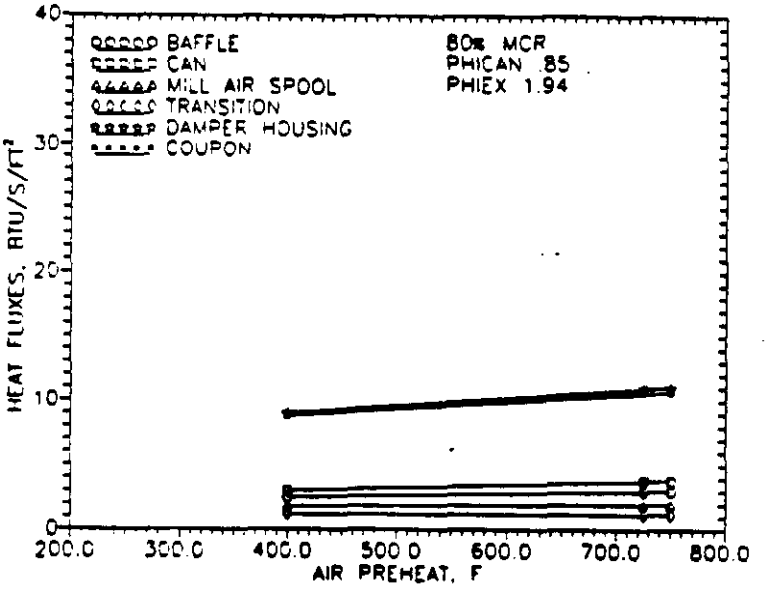

Figure 5-8b Heat Flux Versus Air Preheat - 80% MCR

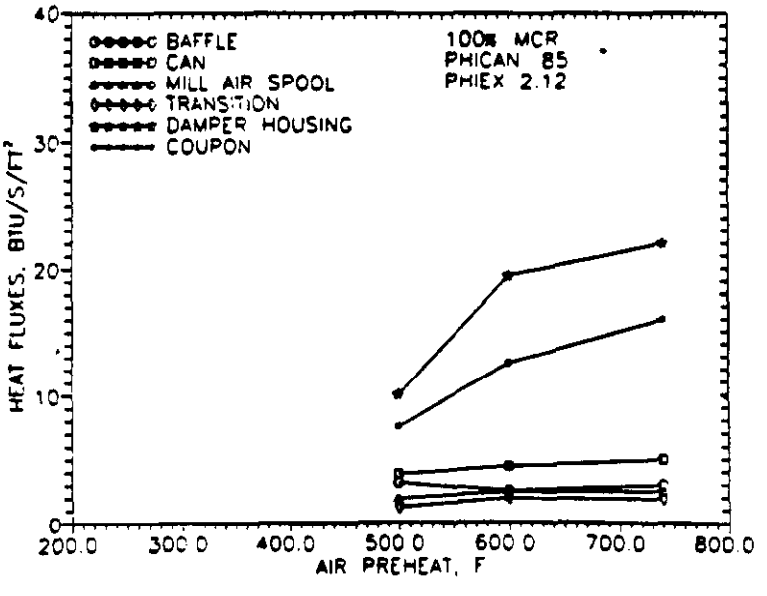

Figure 5-8c Heat Flux Versus Air Preheat - 100% MCR

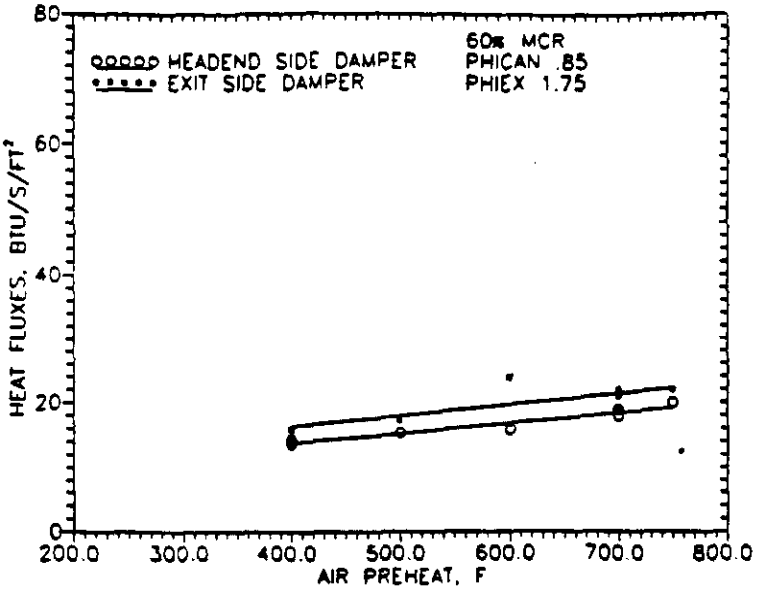

Figure 5-9a Damper Blade Heat Flux Versus Air Preheat - 60% MCR

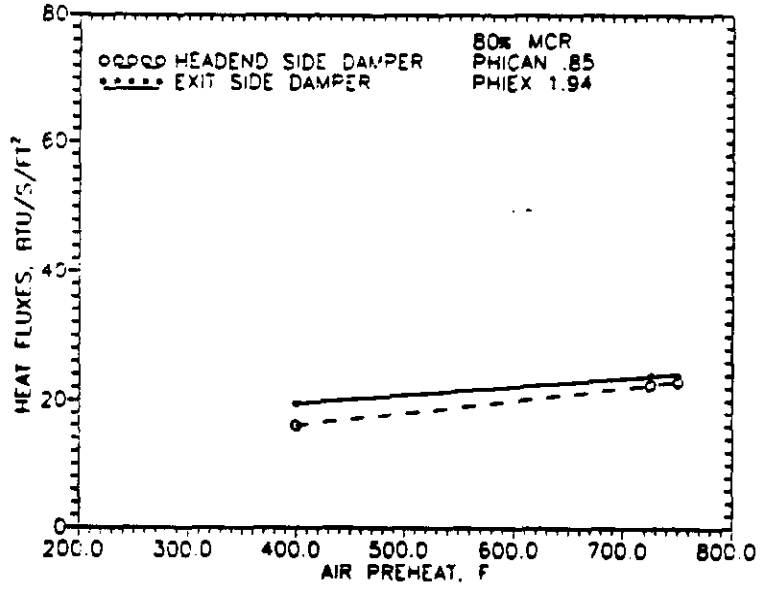

Figure 5-9b Damper Blade Heat Flux Versus Air Preheat - 80% MCR

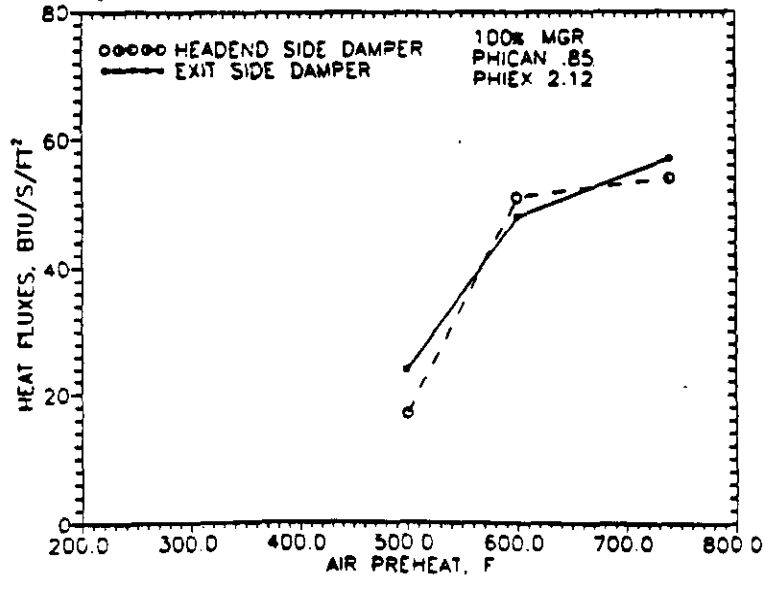

Figure 5-9c Damper Blade Heat Flux Versus Air Preheat - 100% MCR

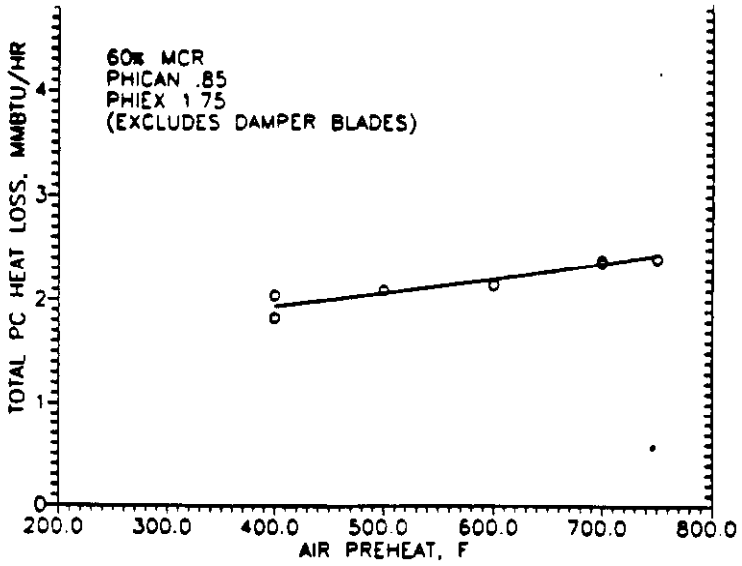

Figure 5-10a Total PC Heat Loss Versus Air Preheat - 60% MCR

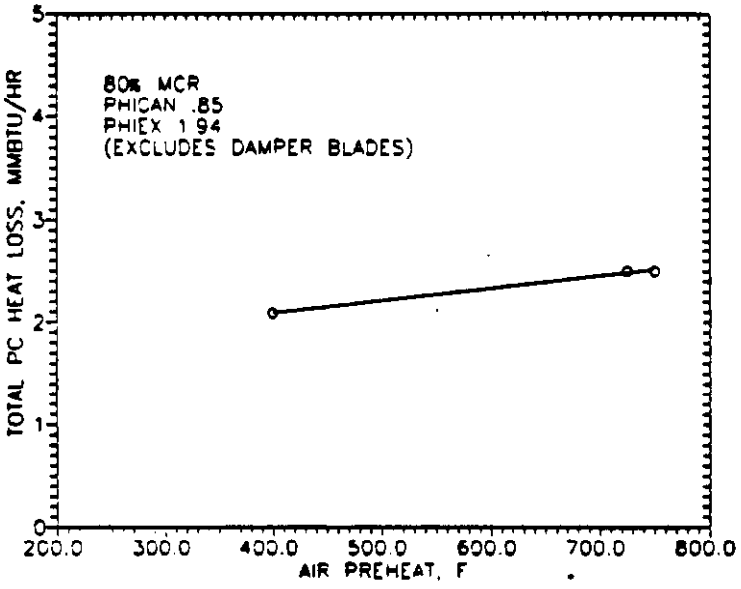

Figure 5-10b Total PC Heat Loss Versus Air Preheat - 80% MCR

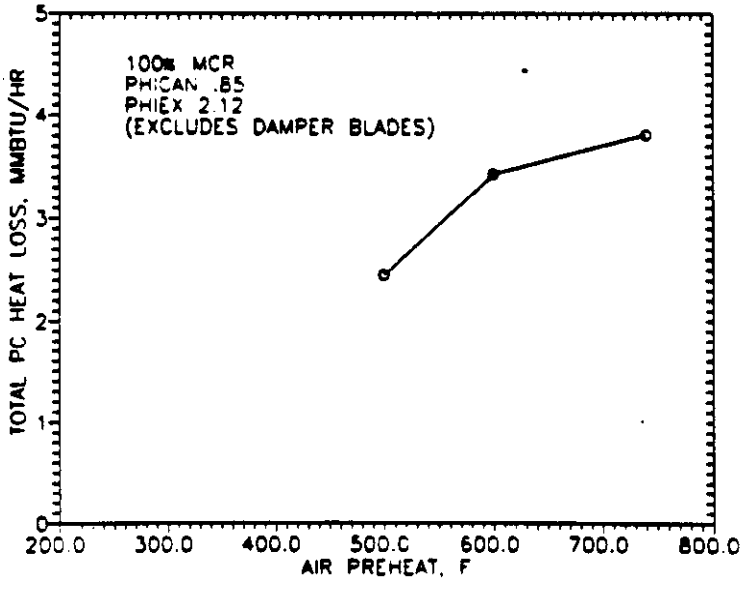

Figure 5-10c Total PC Heat Loss Versus Air Preheat - 100% MCR

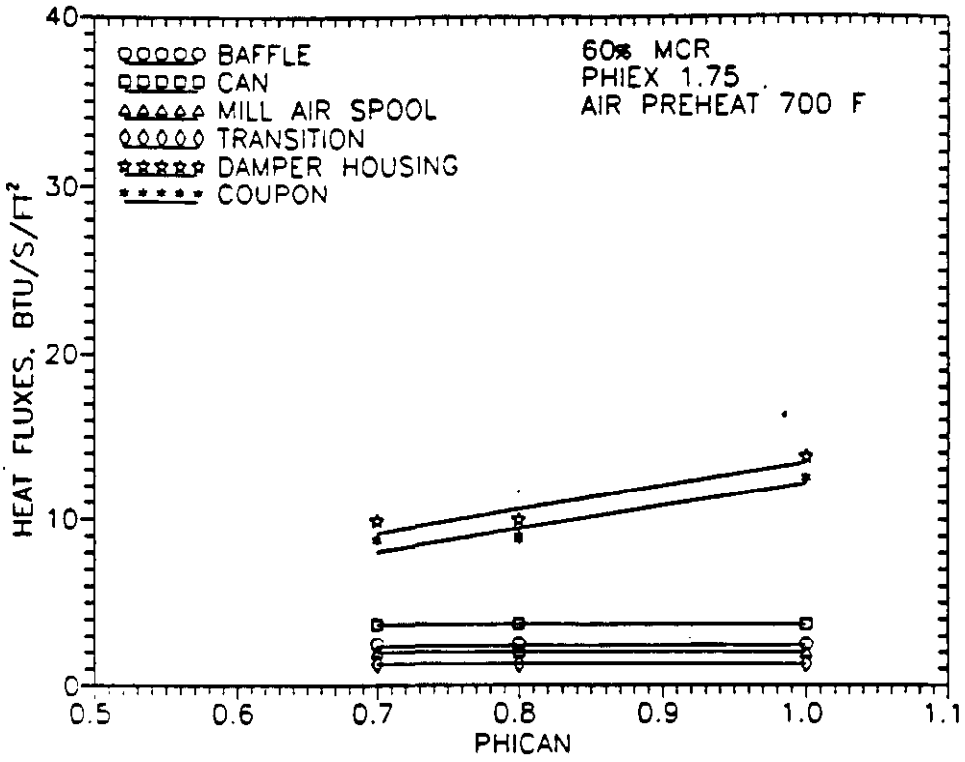

Figure 5-11a Heat Fluxes Versus Can Stoichiometry - 60% MCR

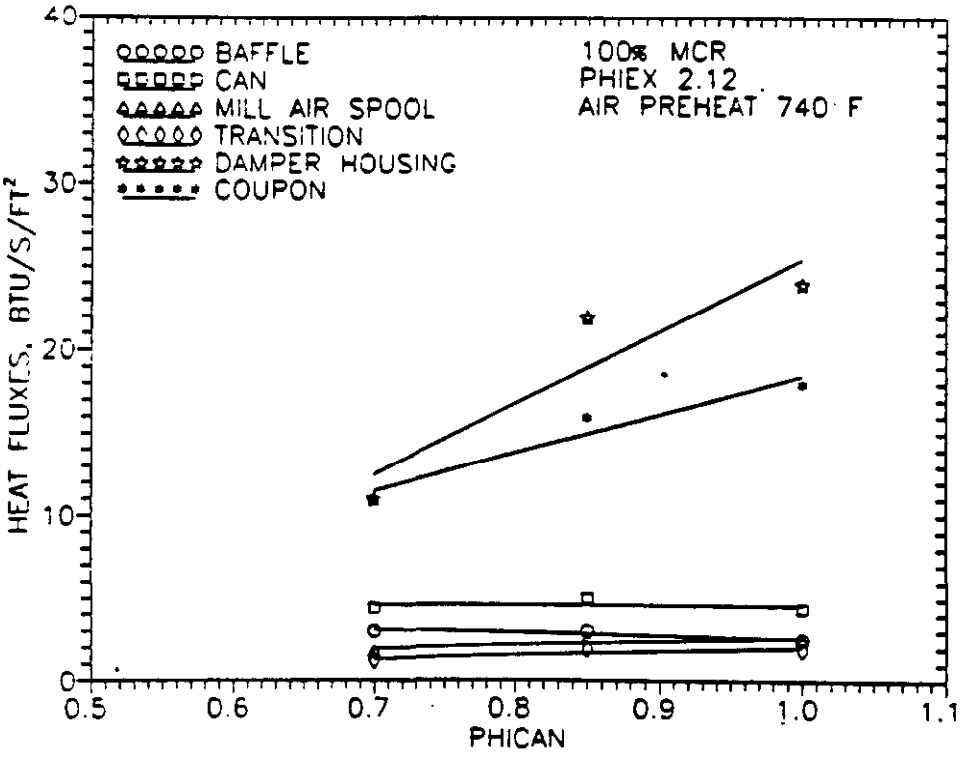

Figure 5-11b Heat Fluxes Versus Can Stoichiometry - 100% MCR

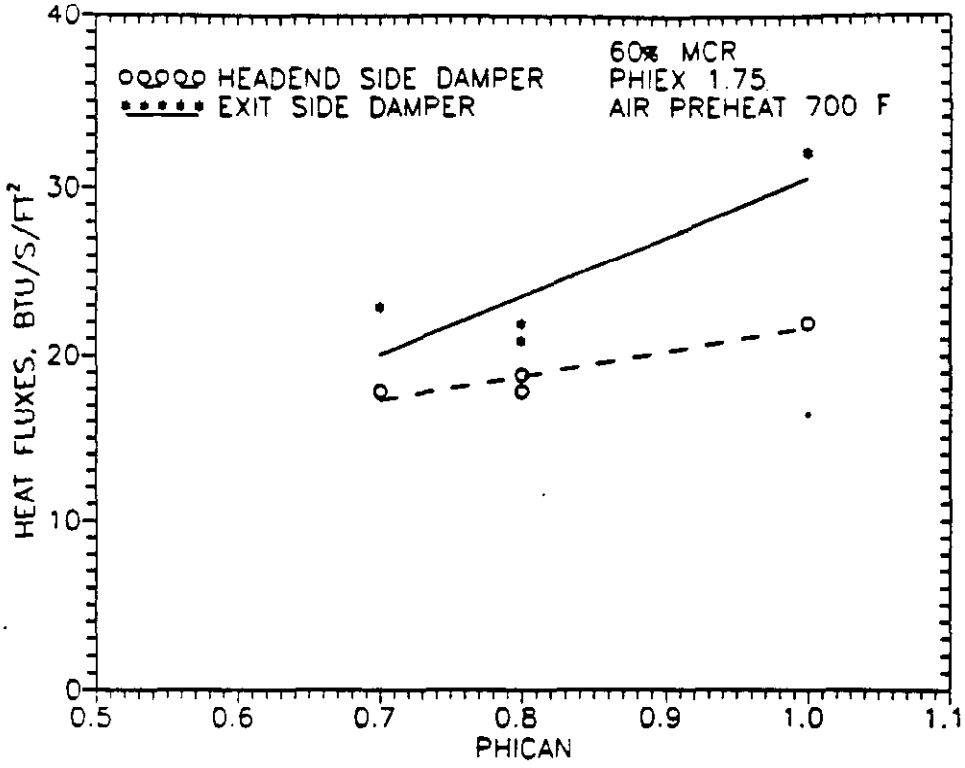

Figure 5-12a Damper Blade Heat Fluxes Versus Can Stoichiometry - 60% MCR

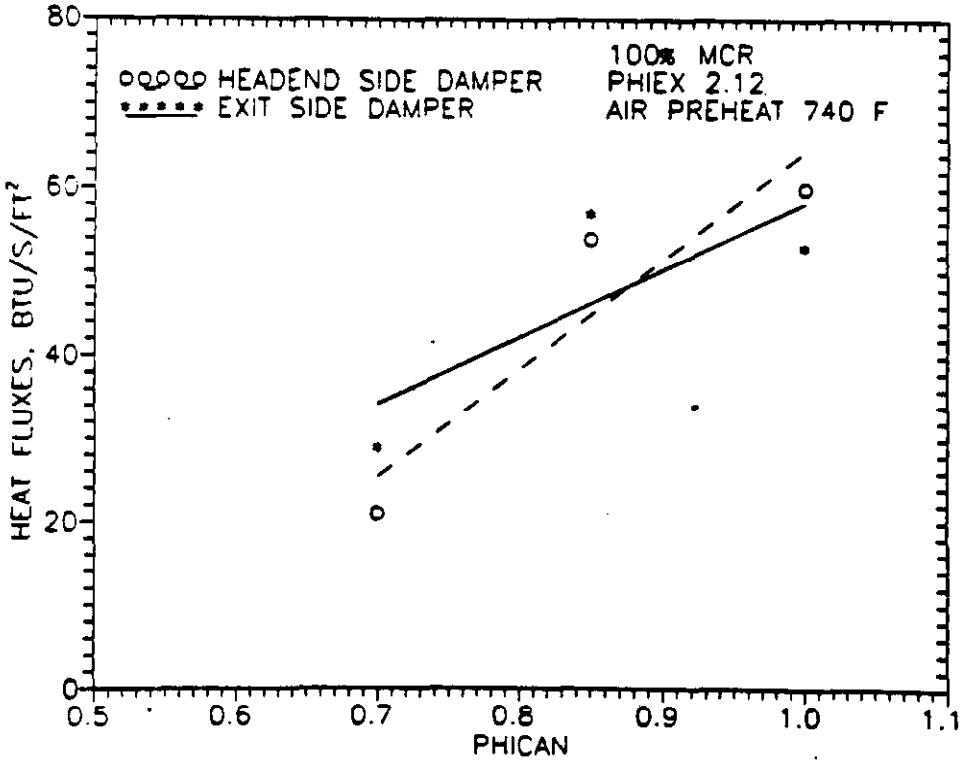

Figure 5-12b Damper Blade Heat Fluxes Versus Can Stoichiometry - 100% MCR

Figures 5-13a and 5-13b show the effect of can stoichiometry on total PC heat loss (excluding damper blades).

5.2.7 Effect of Exit Stoichiometry

Heat flux data were obtained over a range of exit stoichiometry and are plotted in Figures 5-14a and 5-14b for loads of 60% and 100% MCR, respectively. Again, the primary effect is on the damper housing and coupon, with the effect much more pronounced at 100% MCR. Figures 5-15a and 5-15b show similar data for the damper blades.

Figures 5-16a and 5-16b show the effect of exit stoichiometry on total PC heat loss (excluding damper blades) for different loads. Again note that the increase in heat loss at 100% MCR is driven by the non-refractory lined damper housing.

5.2.8 Damper Blade Heat Loss - Effect of Insertion Depth

Damper blade heat loss as a function of insertion depth is shown at a nominal load of 100% MCR (118-123 MMBtu/hr) in Figure 5-17. Data are shown for two ranges of exit stoichiometry: phi_e=1.79-1.97 and phi_e=1.45 (nominal phi_e=2.05). The nominal insertion depth at 100% MCR is 47%, which produces an inlet velocity to the slagging stage of approximately 375 ft/sec. The large scatter at 10% insertion depth is due to the relatively small exposed area of the blade at this setting. Note that the dependence on exit stoichiometry is similar to that seen in Figure 5-15.

5.2.9 Other Thermal Data

Shield Tubes

Cooling tubes were installed in the downstream portion of the mix annulus windbox to provide protection against possible radiative heating from the combustion products. These tubes were called "shield tubes", and are indicated on Figure 5-4. Since the tubes add a measure of complexity to the PC design, an effort was made during DVT to determine if the shield tubes were required for Healy.

Two uncooled coupons were installed in the shield tube region (see Figure 5-4) to give an indication of the equilibrium temperature of an uncooled windbox surface. One coupon was bare metal, and the other had a 1" thick refractory coating attached to its surface. As shown in Figure 5-18, for loads below 80% MCR, both coupons stayed within reasonable temperature limits (<850°F). At 100% MCR, however, the coupons reached temperatures >1100°F. For this reason, the shield tubes will be retained for the Healy design.

Cooling water was fed to the shield tubes from a common manifold with the combustion can, so direct calorimetry was not possible. However, thermocouples were installed in the shield tube sub-

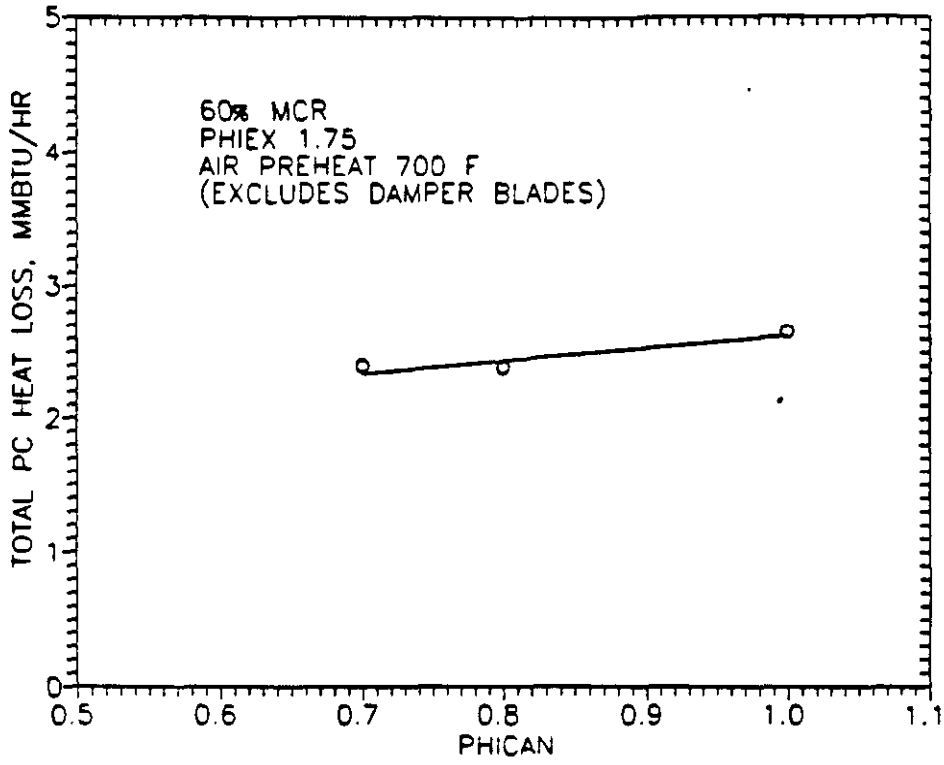

Figure5-13a Total PC Heat Loss Versus Can Stoichiometry - 60% MCR

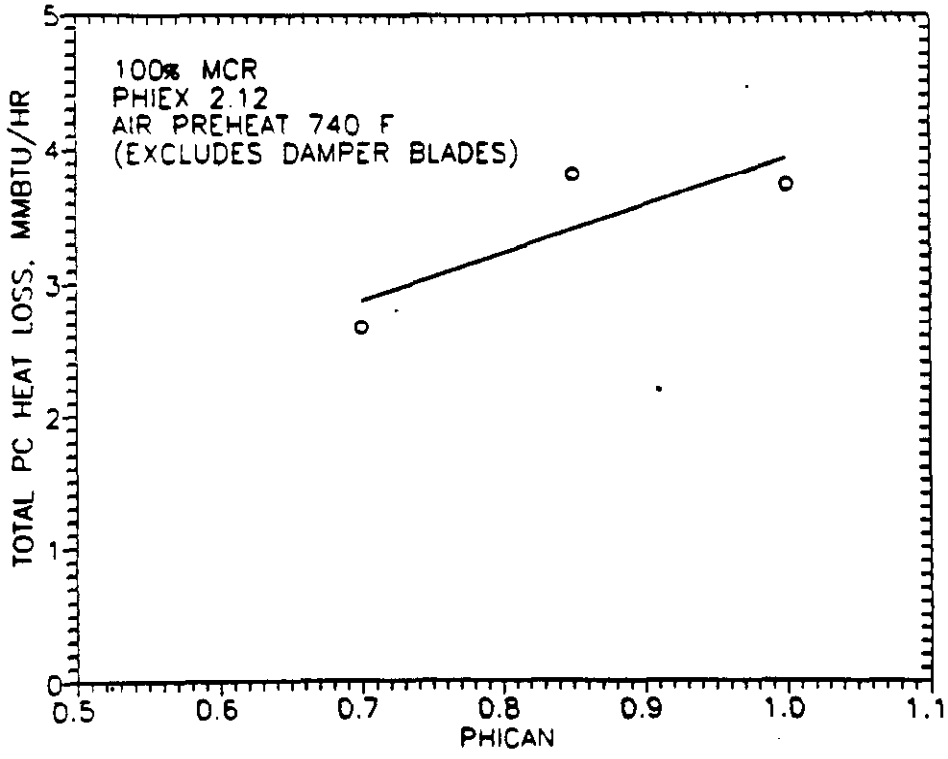

Figure5-13b Total PC Heat Loss Versus Can Stoichiometry - 100% MCR

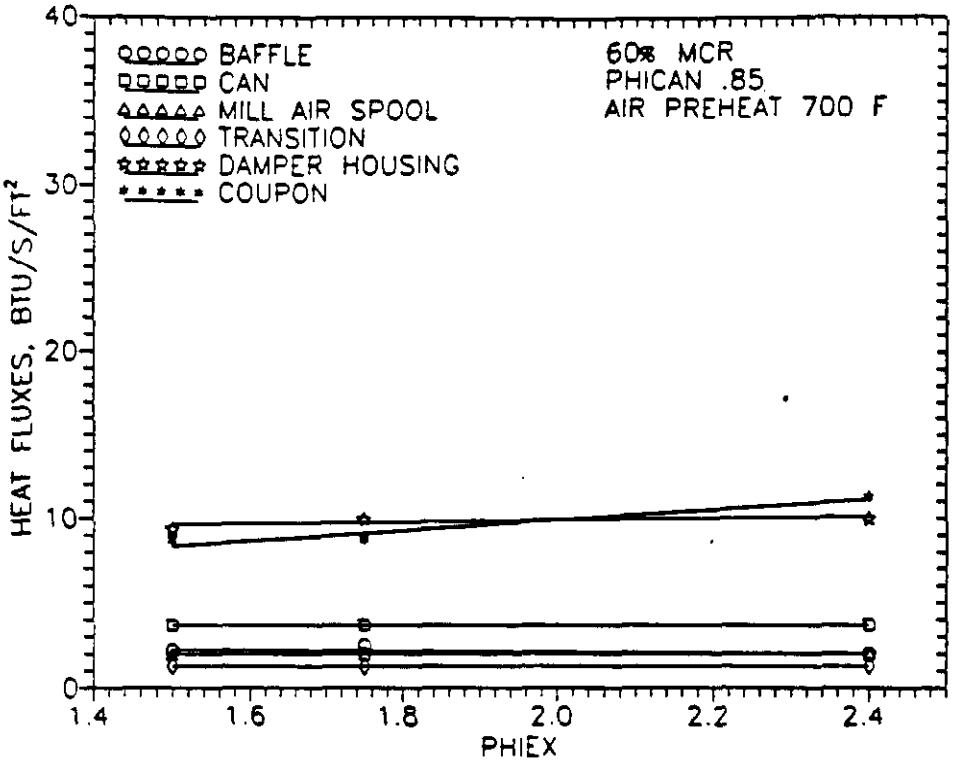

Figure 5-14a Heat Fluxes Versus Exit Stoichiometry - 60% MCR

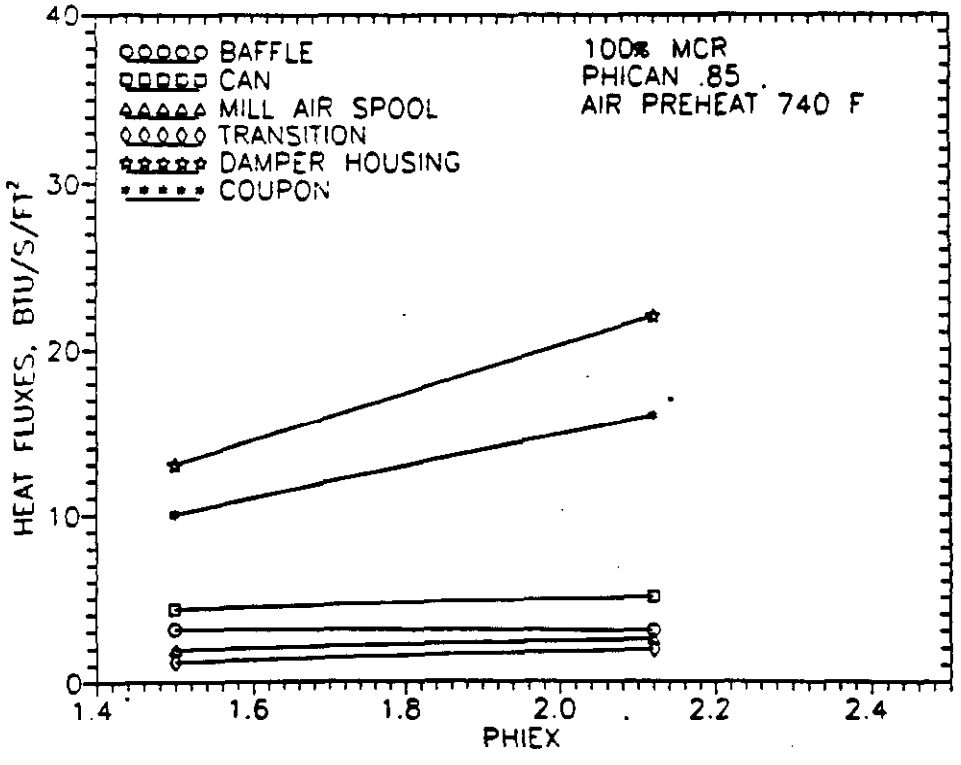

Figure 5-14b Heat Fluxes Versus Exit Stoichiometry - 100% MCR

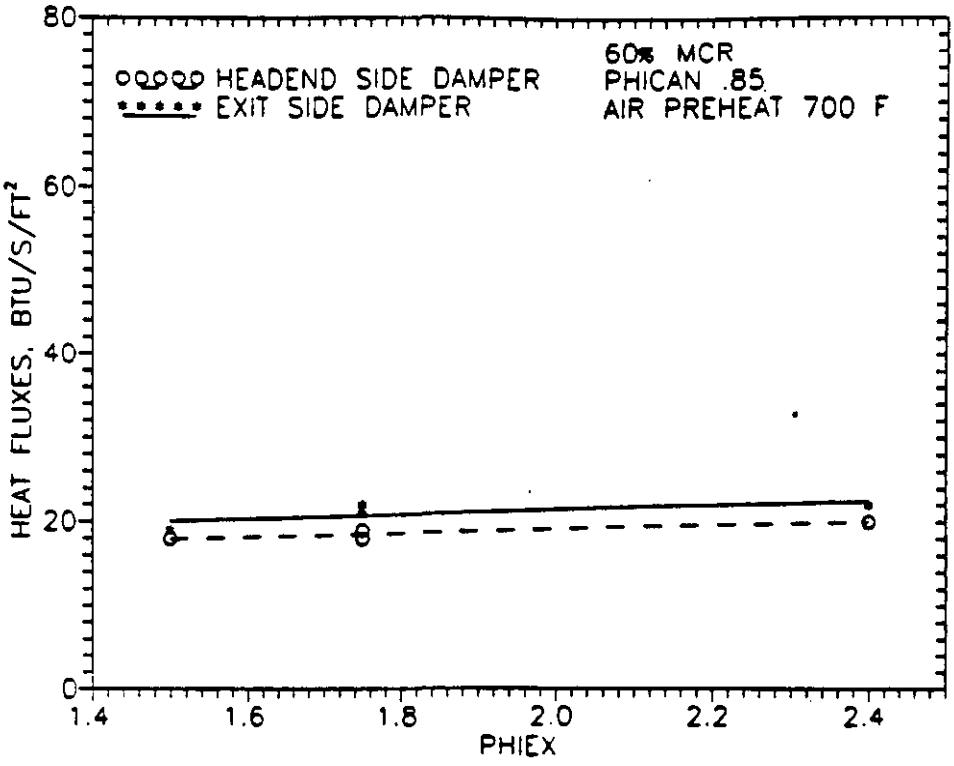

Figure5-15a Damper Blade Heat Flux Versus Exit Stoichiometry - 60% MCR

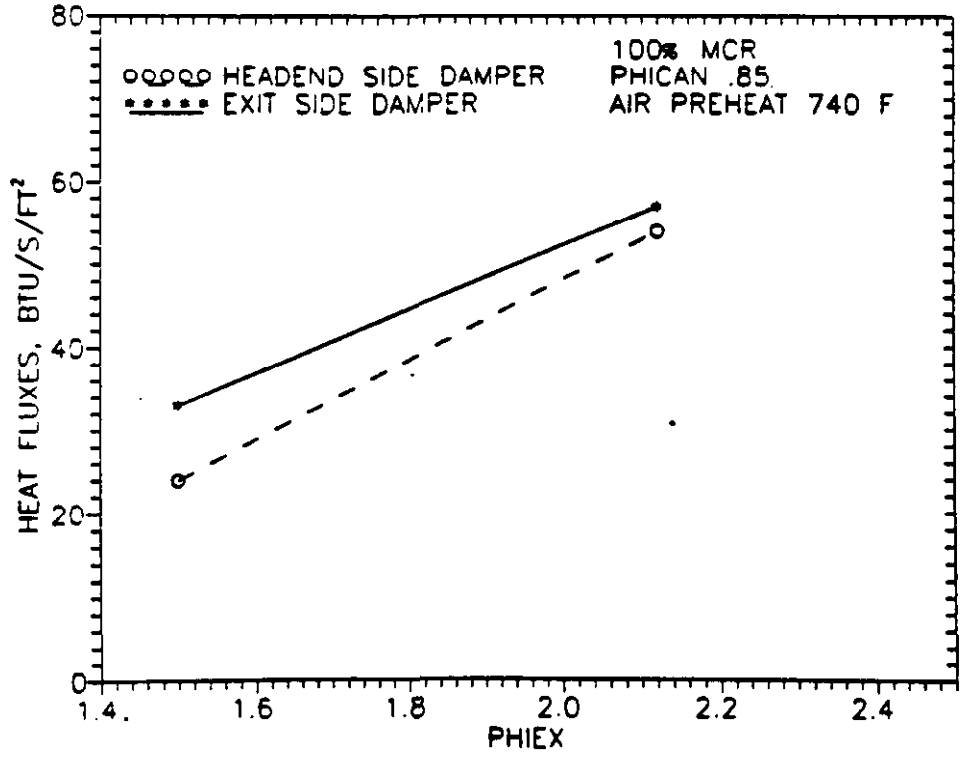

Figure5-15b Damper Blade Heat Flux Versus Exit Stoichiometry - 100% MCR

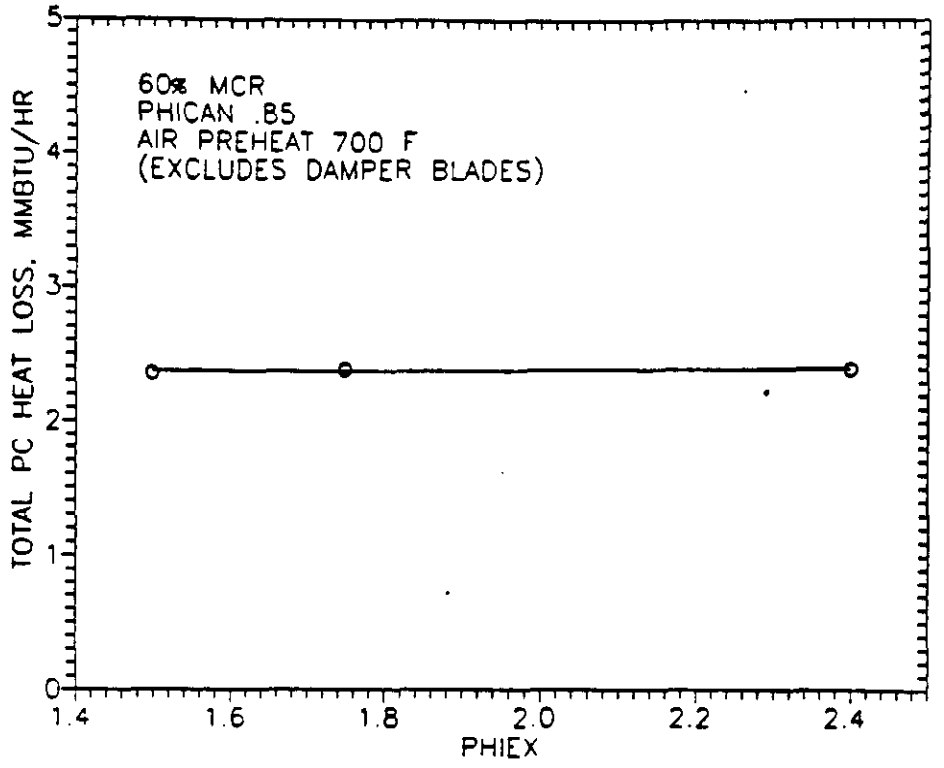

Figure 5-16a Total PC Heat Loss Versus Exit Stoichiometry - 60% MCR

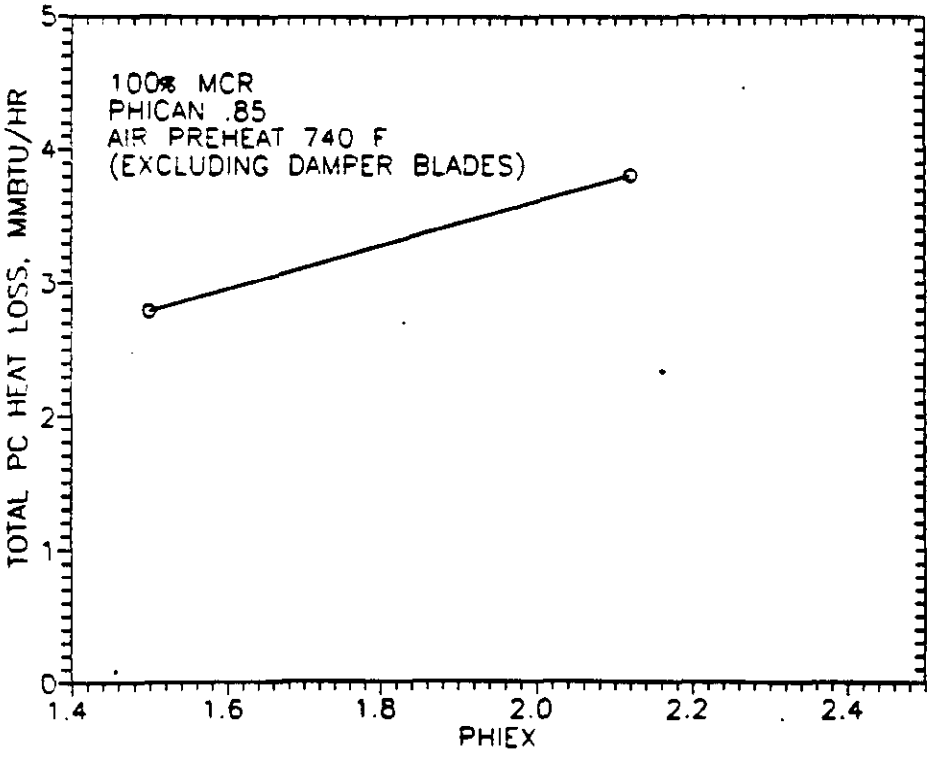

Figure 5-16b Total PC Heat Loss Versus Exit Stoichiometry - 100% MCR

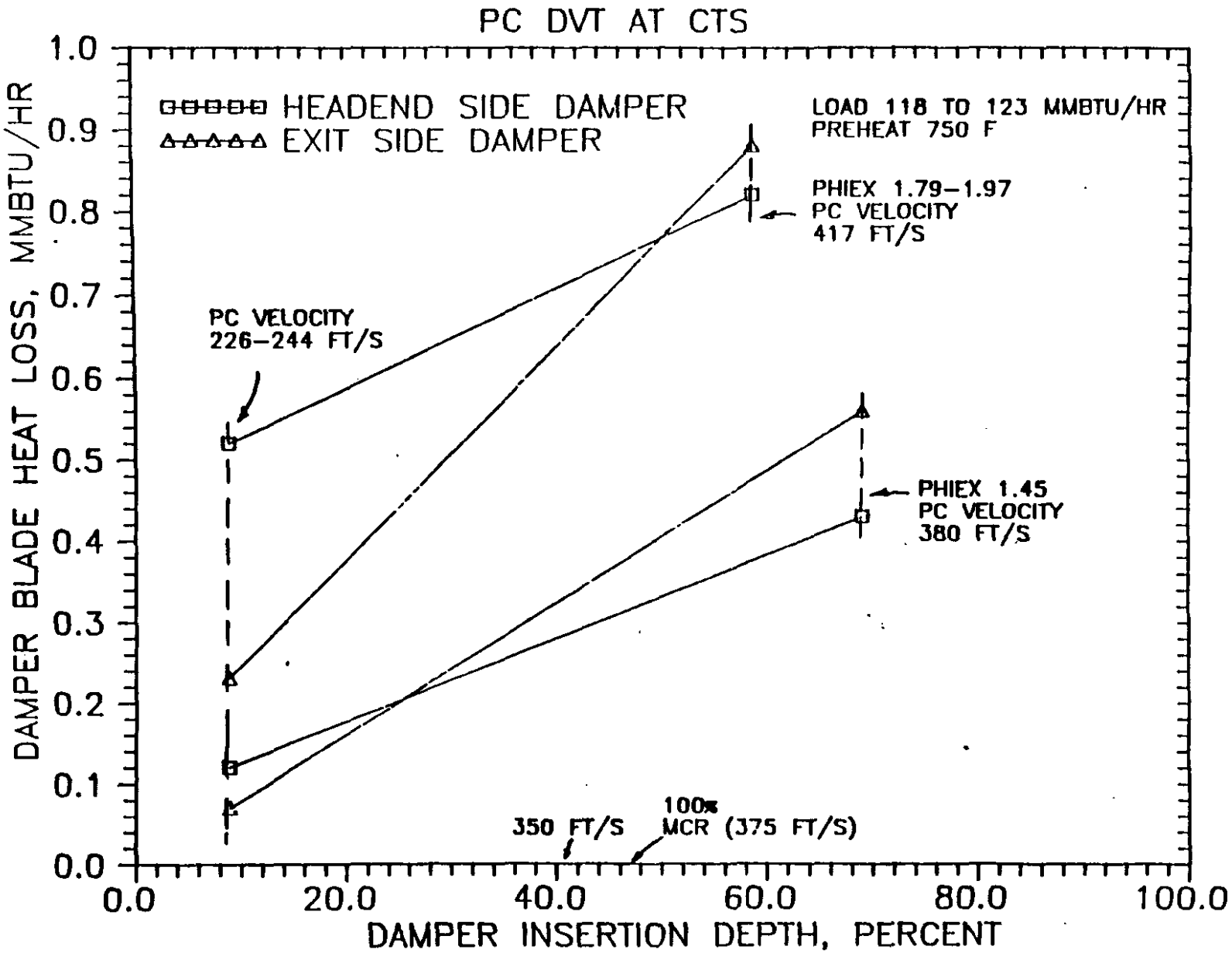

Figure 5-17 Damper Blade Heat Loss Versus Insertion Depth

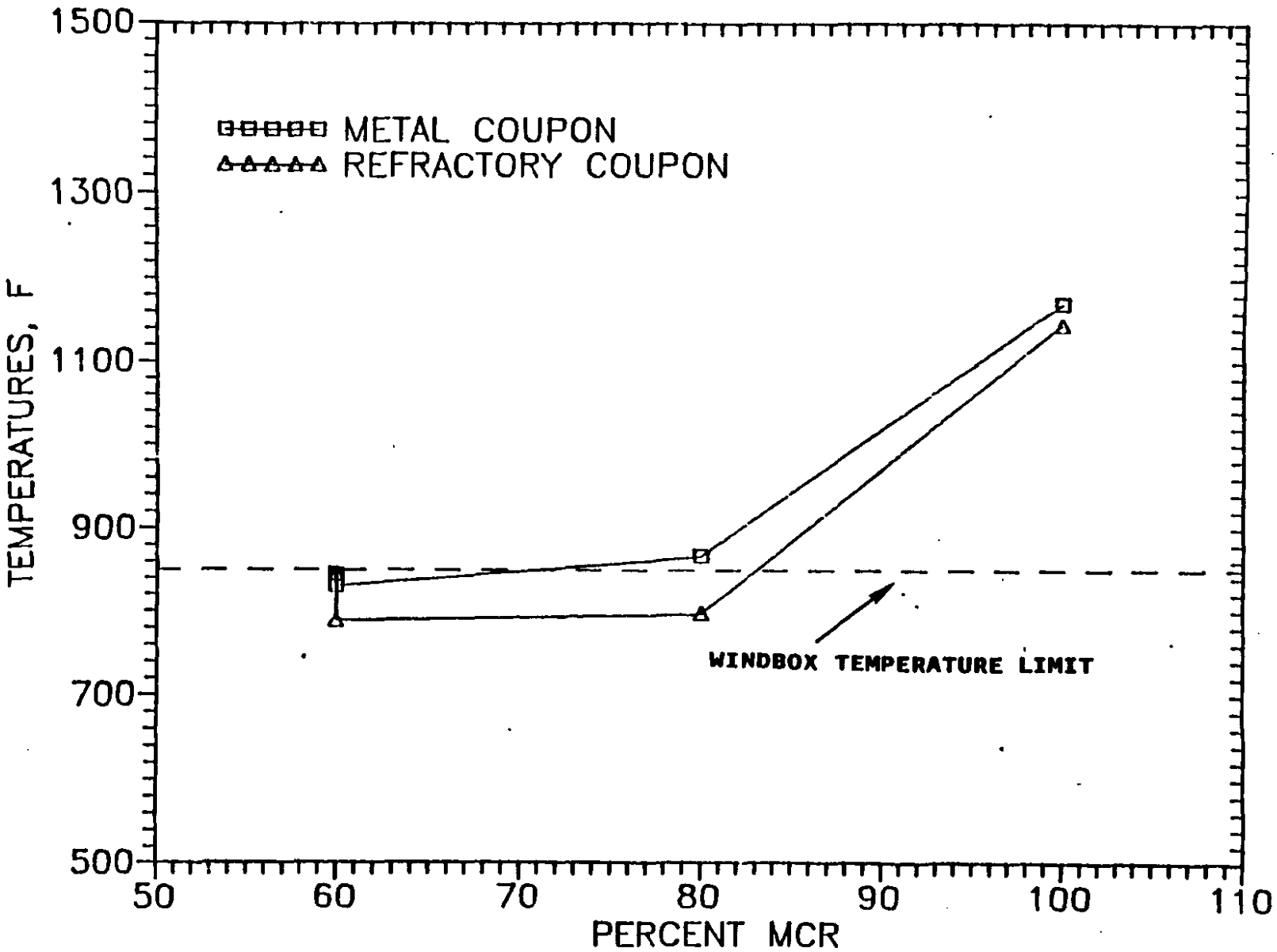

Figure 5-18 Shield Tube Coupon Temperatures Verus Load

manifolds and an estimate of the flow was made based on pressure drop measurements. Based on this method, the average heat flux on the shield tubes is about 1 Btu/ft^{2}sec at 100% MCR (Figure 5-19).

Burner Temperatures

Thermocouples were provided with the Foster Wheeler burner for monitoring temperature of the nozzle and sleeves. These temperatures remained below Foster Wheeler prescribed limits for all tests. The temperatures were independent of coal load (Figure 5-20) and tracked combustion air temperature (Figure 5-21). Changes in stoichiometry over the ranges previously discussed had no impact on the temperatures.

5.2.10 Pressure Drop Measurements

Air side pressure drop measurements were made for a number of components on the precombustor. These measurements are important in establishing an overall pressure budget for the Healy combustion system.

Figure 5-22 shows the pressure drop across the Foster Wheeler coal burner as a function of cyclone blowdown flow (i.e. carrier flow). At the nominal carrier flow of 12,000 lb/hr, the pressure drop is 5-6 inches H_2O.

Pressure drop across the Foster Wheeler burner air register is shown in Figure 5-23 as a function of combustion air flow, for outer register settings of 50% and 30% (refer to Section 4.3 for a discussion of air register settings). At 100% MCR, the combustion air flow rate to the burner windbox is 63,000 lb/hr, and the air register pressure drop will be 4-5 inches H_2O.

The impact of air register settings on pressure drop is shown in Figures 5-24 and 5-25 for the inner and outer registers, respectively. Although there is a large amount of scatter in the data, the pressure drop change is relatively small. Thus small changes in register settings should not impact the overall pressure budget for Healy.

A summary of the pressure drop data is shown schematically on Figure 5-26. Nominal and maximum pressures are shown for each location for 100% MCR conditions. The pressure provided upstream of the combustion air dampers (points 2 and 5 on Figure 5-26) will be 40 inches H_2O at Healy. Therefore, the dampers will have 10-15 inches H_2O drop available, which should be sufficient for control purposes.

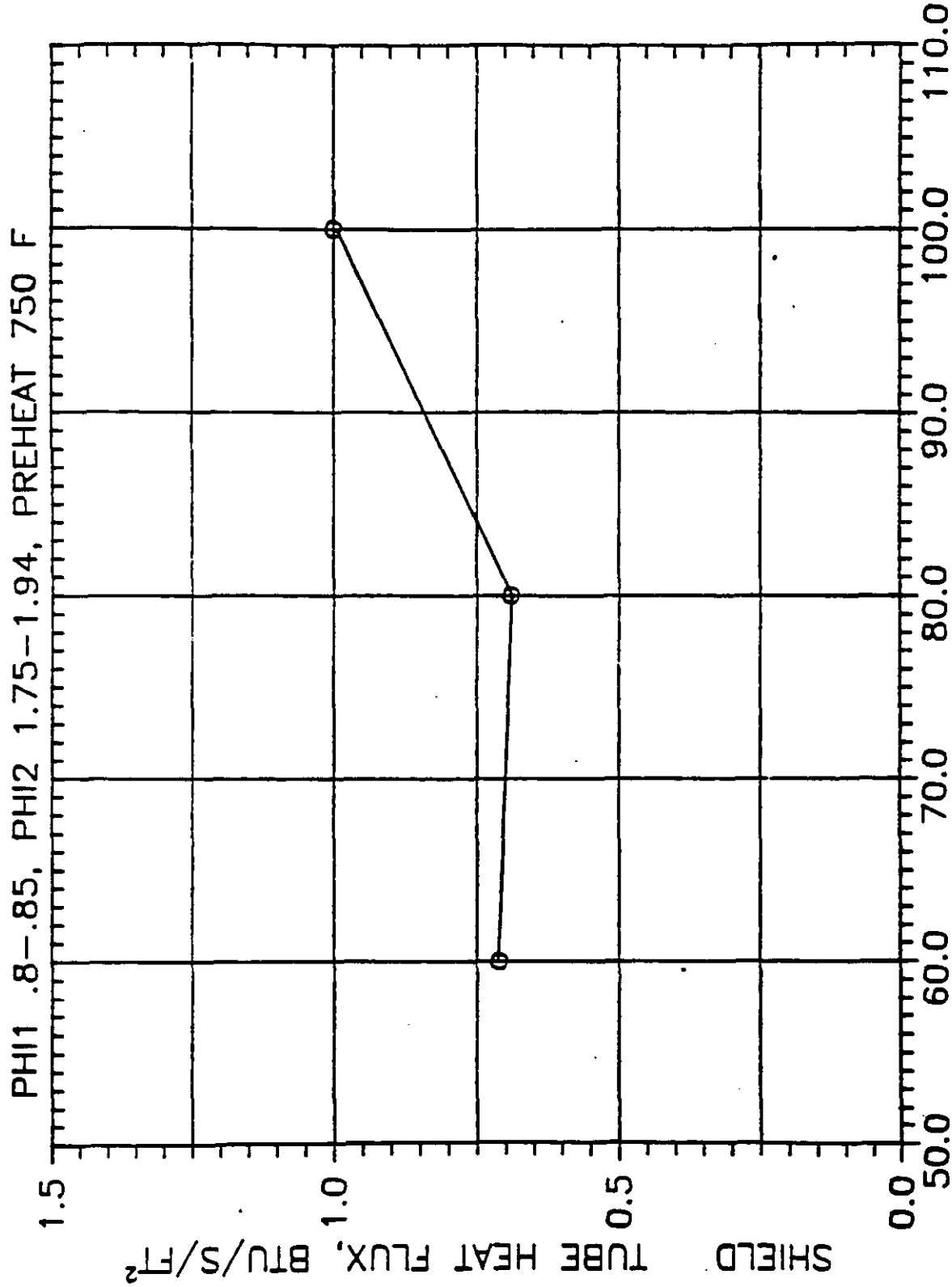

Figure5-19 Shield Tuhe Heat FLux Versus Load

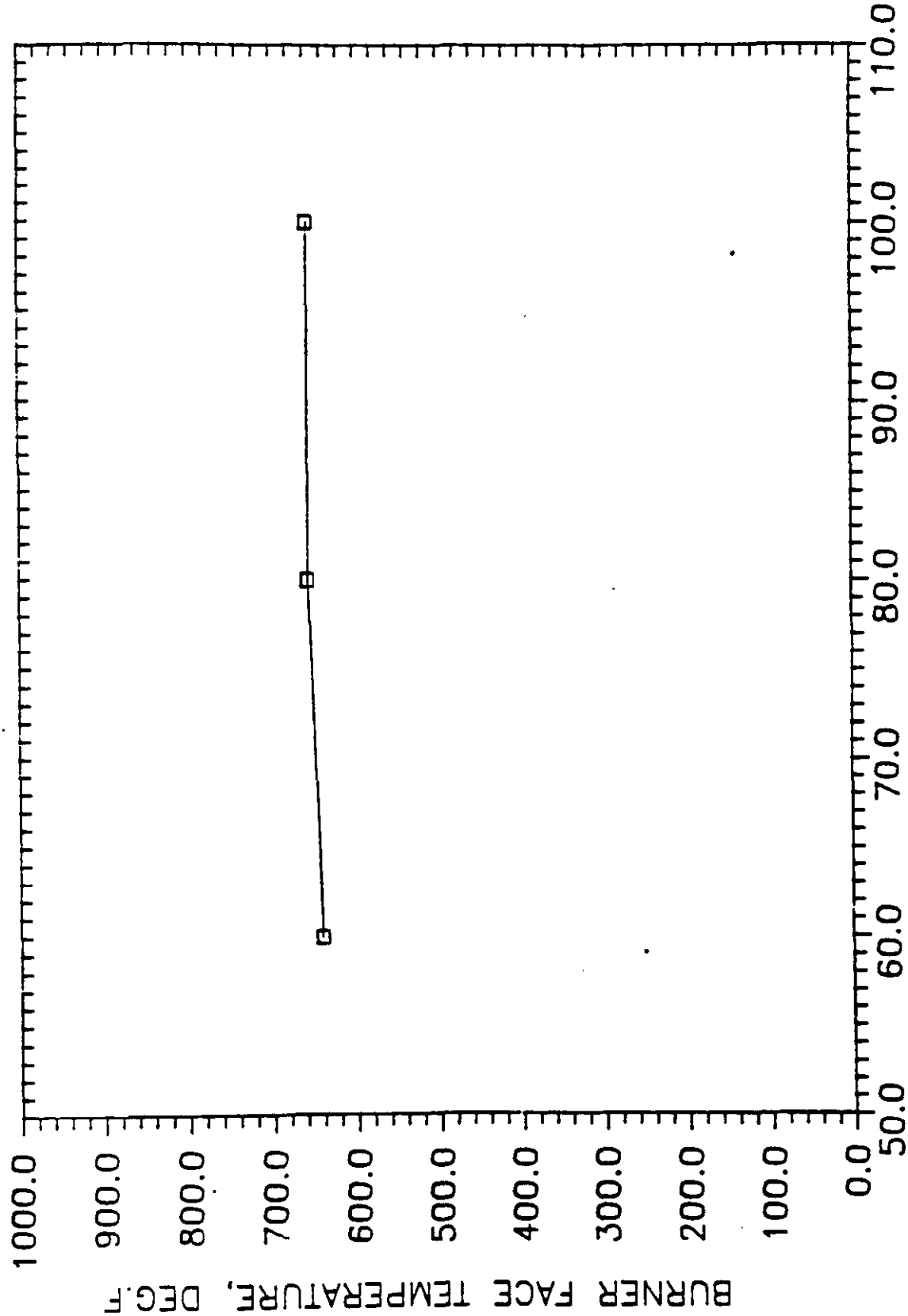

Figure 5-20 Burner Face Temperature Versus Load

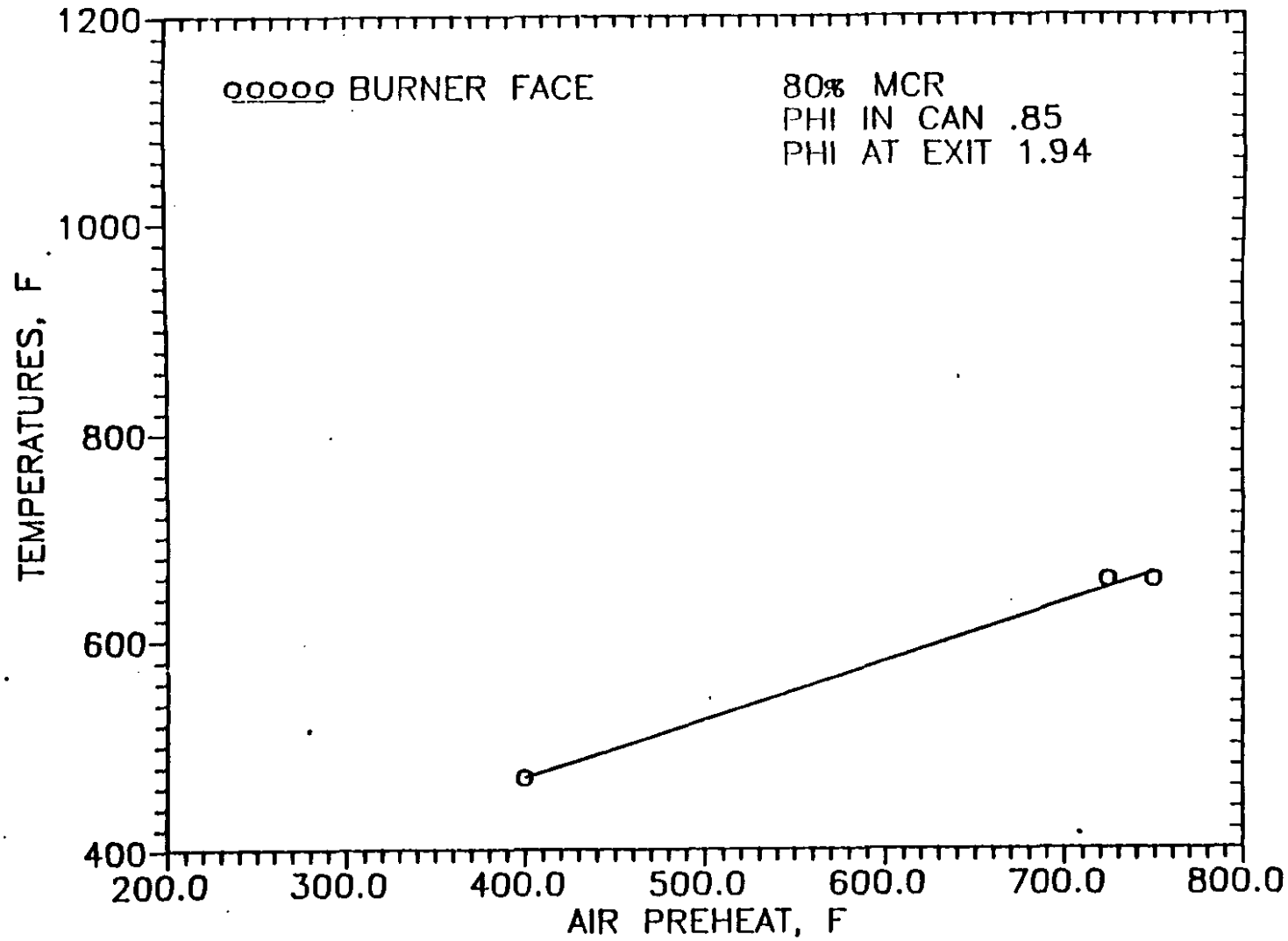

Figure 5-21 Burner Face Temperate Versus Air Preheat - 80% MCR

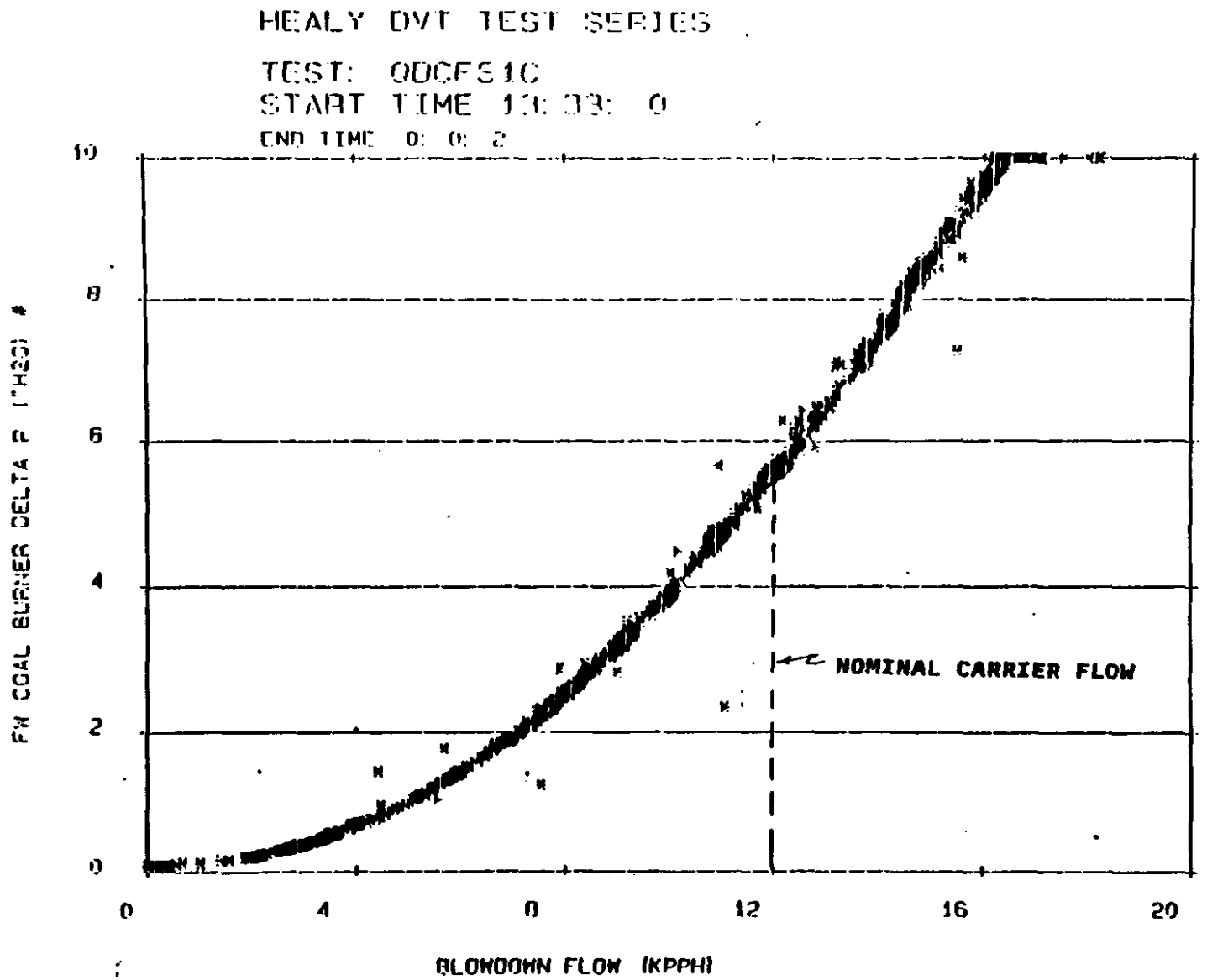

Figure 5-22 FWEC Coal Burner Pressure Drop Versus Air Flow

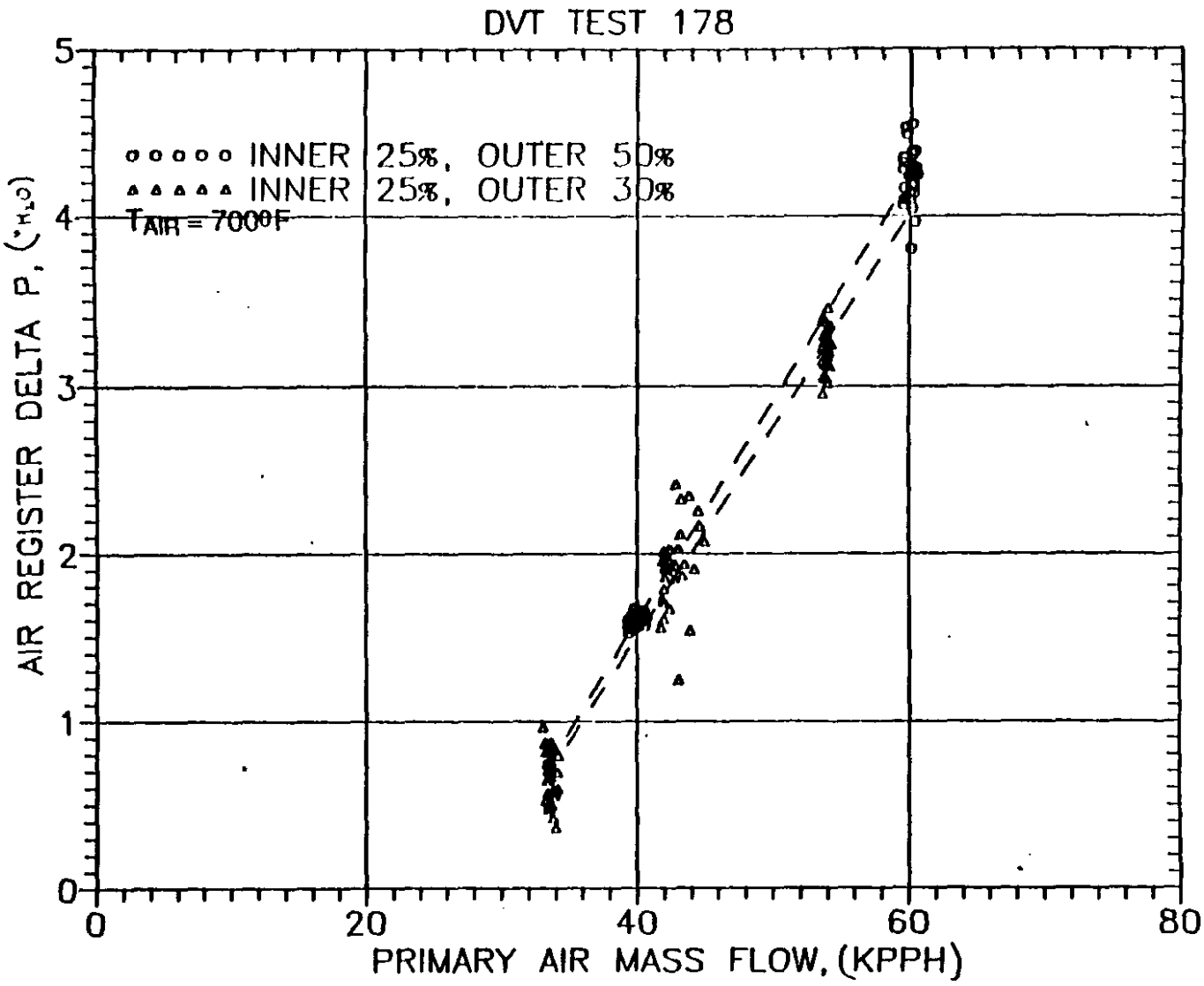

Figure 5-23 Pressure Drop Versus Air Flow for FWEC Air Register

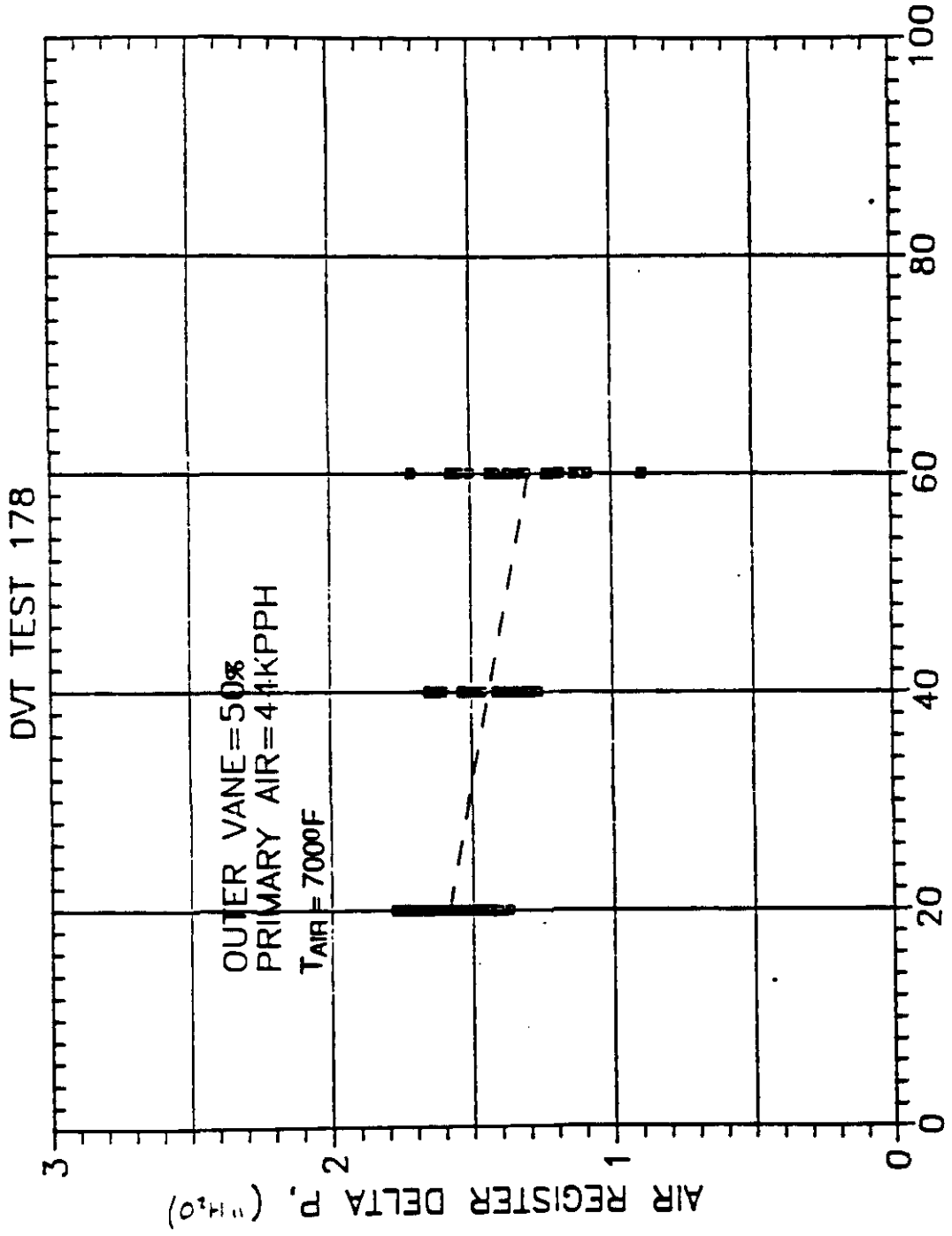

Figure 5-24 Effect of Inner Register Setting on Pressure Drop

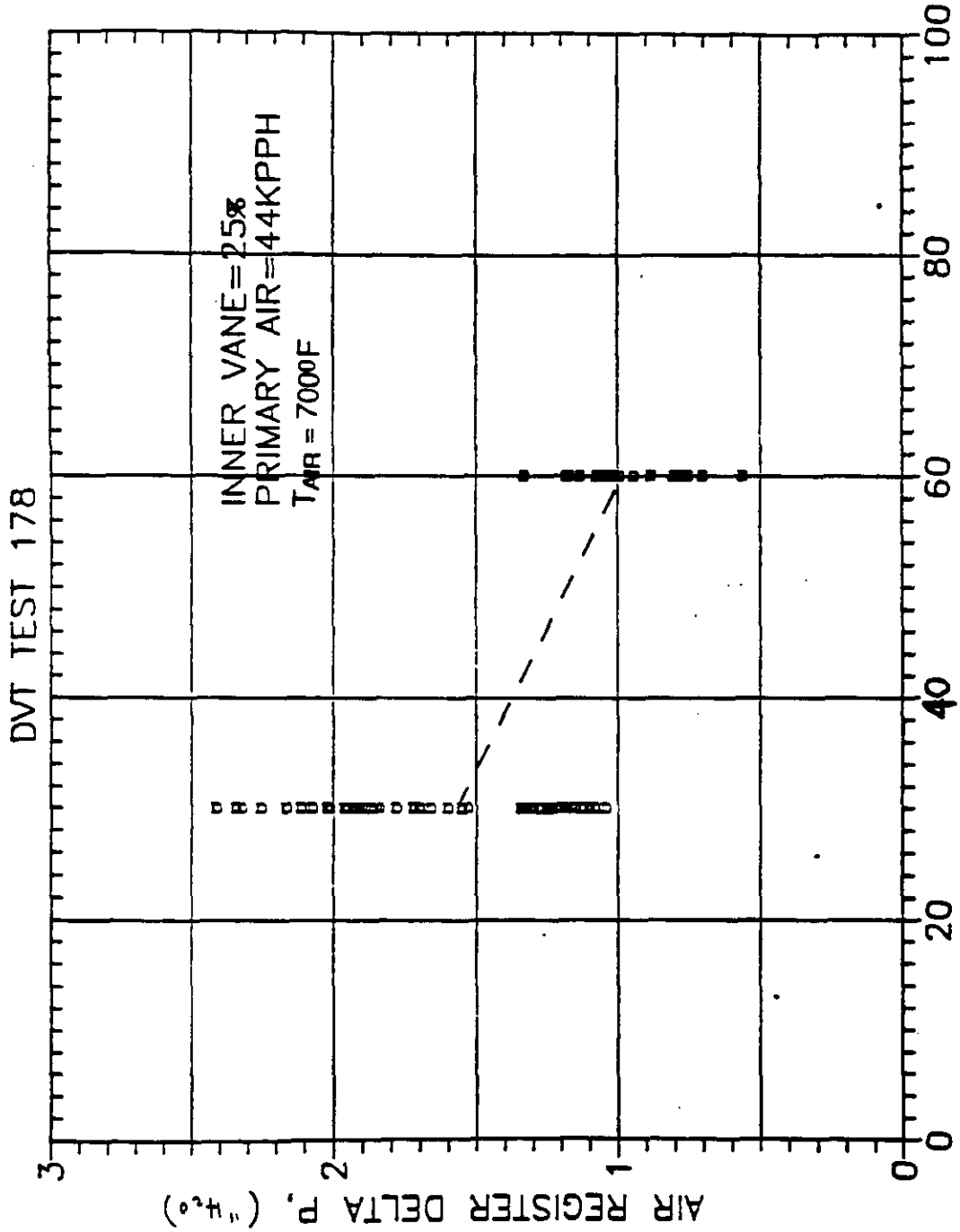

Figure 5-25 Effect of Outer Register Setting on Pressure Drop

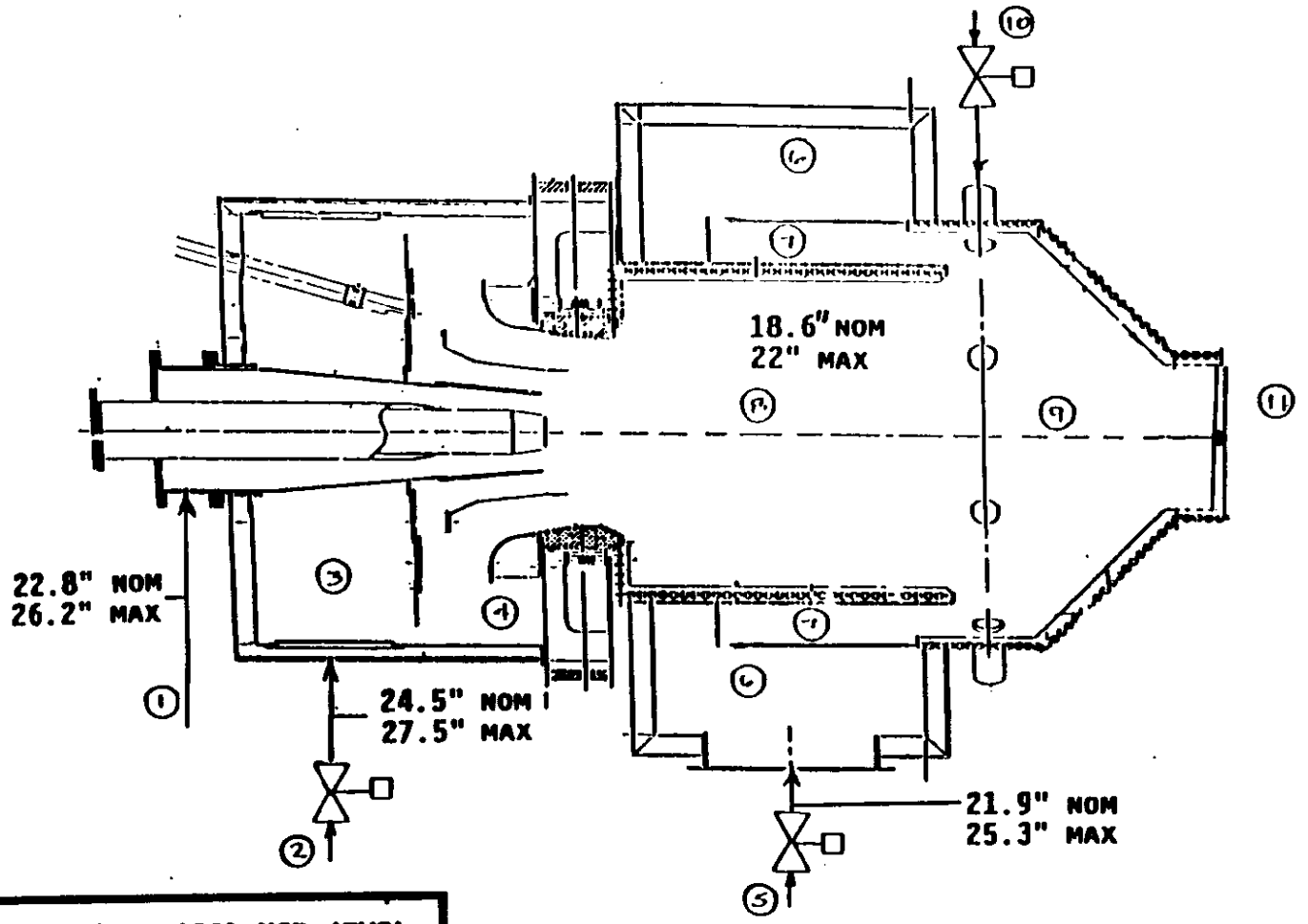

Location	ΔP @ 100% MCR (IWG) Measured	Calculated
1-8	4.2	6.8
3-4	1.2	1.8
4-8	4.7	3.0
6-9	3.0	3.3
9-11	9.2	6.6

Figure 5-26 Summary of DVT Precombustor Pressure Drop Data

5.3 Startup and Shutdown Sequences

The run conditions used for start-up and shut-down are shown in Figure 5-27. The Forney ignitor was first fired at 20 MMBTU/hr, and this was accomplished within about 4 minutes; this could be achieved with the primary air temperature at room temperature, as well as at temperatures up to the maximum 550° F. Then the ignitor was ramped up first to 30 MMBTU/hr, and then to its maximum of 70 MMBTU/hr within the next five to six minutes. The burner could be held at this position as long as was necessary. For coal firing, the coal flow was established from the facility supply system and ramped up first to about 30 MMBTU/hr. At this point, the oil flow was decreased to 35 MMBTU/hr. Then the oil flow was reduced to zero over a period of about ten minutes while the coal was ramped up to 70 MMBTU/hr. At this point, the burner was completely sustained on only coal, and could be held under such a condition as long as was necessary. The burner could then be ramped up on coal to the precombustor MCR, as required by the specific test sequence. The shutdown sequence was the reverse of the startup sequence as indicated in Figure 5-27.

5.4 Combined DCFS-Precombustor Tests

Test results for the Direct Coal Feed system as tested together with the precombustor are described in Section 6. In this section, only the data from this test series which are specific to the precombustor are presented.

In general, there were no major changes in precombustor performance in changing from operation with the facility coal feed system to operation with the DCFS. Heat fluxes, pressures, temperatures and other measurements were consistent with the data obtained during testing with the facility coal feed system. No increase in heat fluxes or cooling loads were observed due to the burning of coal fines from the cyclone vents.

Total heat loss for the precombustor is compared for testing with and without the DCFS in Figure 5-28. Although there is some scatter due to a range of test conditions, there is no significant difference between the two sets of data.

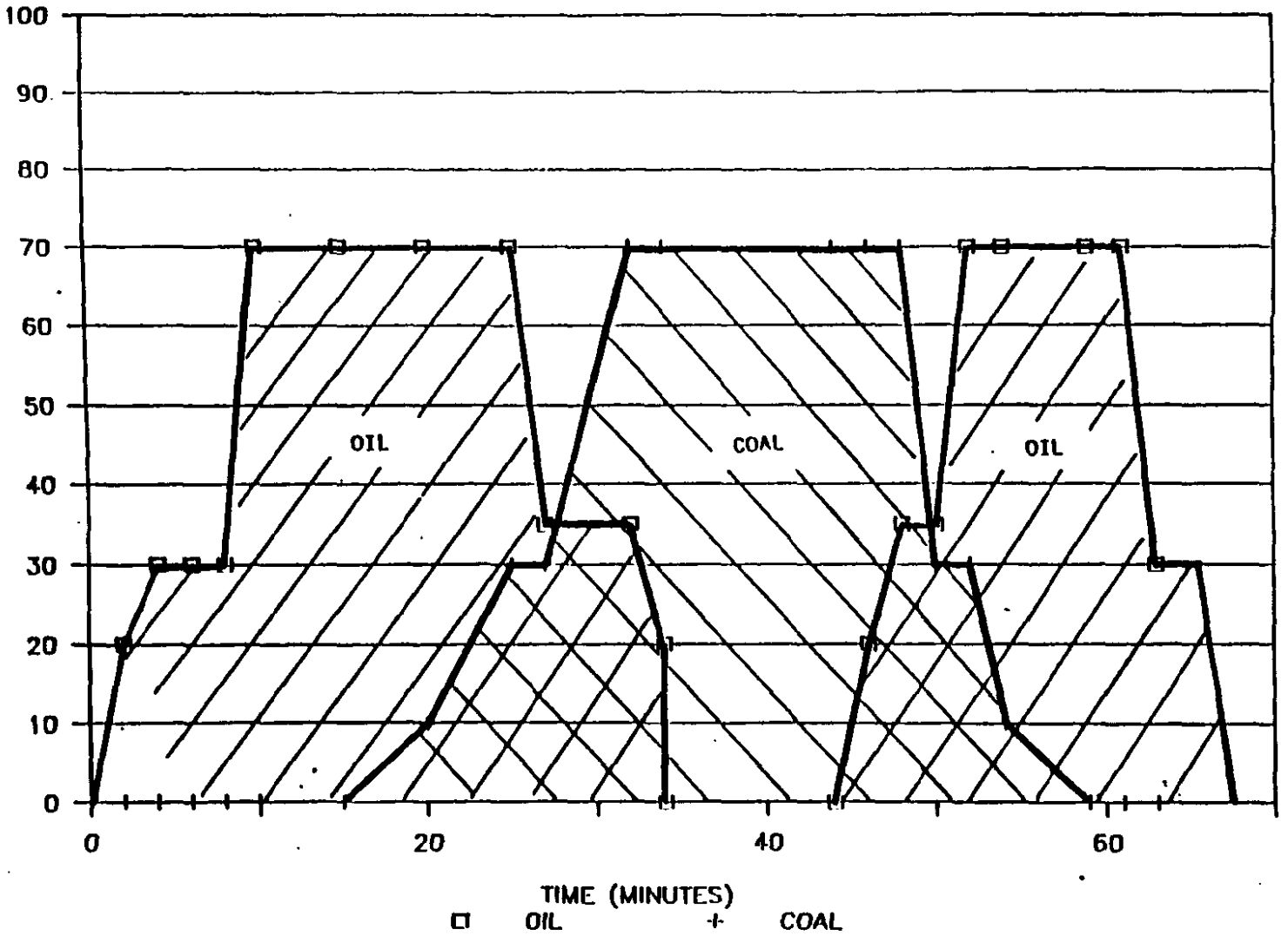

Figure 5-27 Run Conditions for Startup Simulation

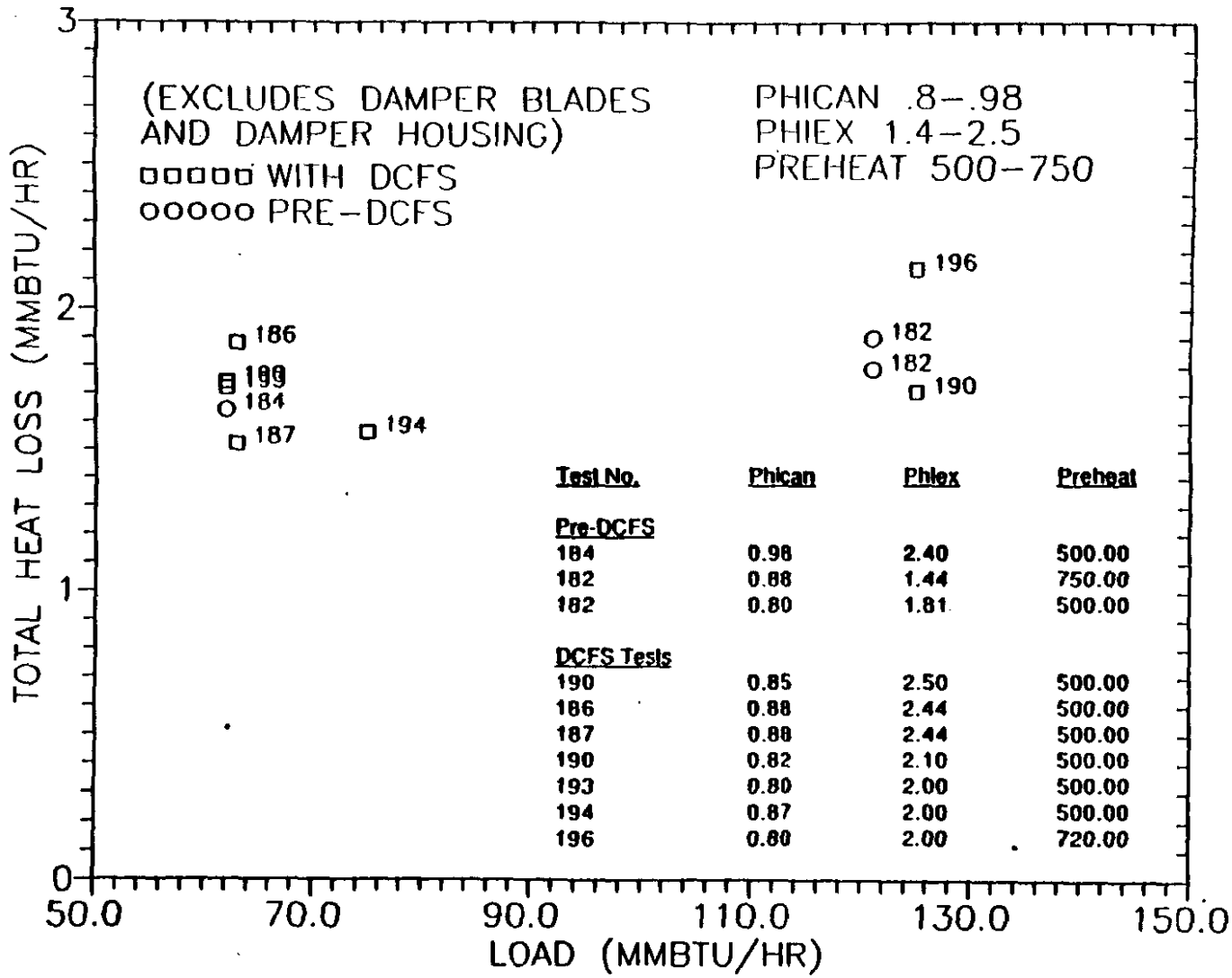

Test No.	Phican	Phiex	Preheat
Pre-DCFS			
184	0.98	2.40	500.00
182	0.88	1.44	750.00
182	0.80	1.81	500.00
DCFS Tests			
190	0.85	2.50	500.00
186	0.88	2.44	500.00
187	0.88	2.44	500.00
190	0.82	2.10	500.00
193	0.80	2.00	500.00
194	0.87	2.00	500.00
196	0.80	2.00	720.00

Figure 5-28 PC Total Heat Loss Versus Load - With and Without DCFS

6.0 Direct Coal Feed System Tests

A total of 11 tests were conducted consuming 76.4 tons of Healy performance coal during Coal Feed System tests at Capistrano to validate the new variable split direct coal feed system (DCFS) design. The coal feed system design and operation are based on scaleup from a successful cold flow model test series conducted by TRW. Figure 6-1 illustrates a schematic of this new coal feed system concept. Key CFS design and operational issues that required further investigation via design verification tests are presented in Figure 6-2. Figure 6-3 summarizes the solution or evaluation methods that have been employed to acquire the design or operational data required to complete the design of the Healy CFS. Data required from DCFS design verification tests include:

- Air flow rates
- Coal flow rates
- Coal flow splits
- Air velocities throughout the system
- Pressure drops for the overall system and each component
- Cyclone efficiency at various coal flow rates
- Sound level data
- Coal accumulation quantities (if detected)
- Normal carbon monoxide levels in the DCFS

6.1 DCFS Test Summary

The precombustor was tested first without the variable split blowdown CFS using an existing facility coal supply system which was connected to the precombustor through the transport circuit portion of the DCFS. The DCFS was installed while precombustor tests were being conducted.

After precombustor testing was concluded, emphasis was placed on DCFS testing. DCFS tests were conducted using three different hardware configurations;

- First, the common cyclone blowdown test configuration,
- Second, the split cyclone blowdown test configuration,
- Last, the long duration common blowdown test configuration

These are illustrated in the following appropriate sections. For each of these test configurations except the long duration tests, testing commenced with air flow only tests followed by coal flow tests. This safe test approach minimized risks associated with hardware damage by evaluating pressure drops, velocities, and control techniques prior to coal flow. Figure 6-4 and 6-5 summarize the logical sequence of testing, the problems encountered, modifications implemented, and primary results of the tests conducted. Table 6-1 summarizes the primary CFS design and operational issues and the conclusions reached based on the DVT.

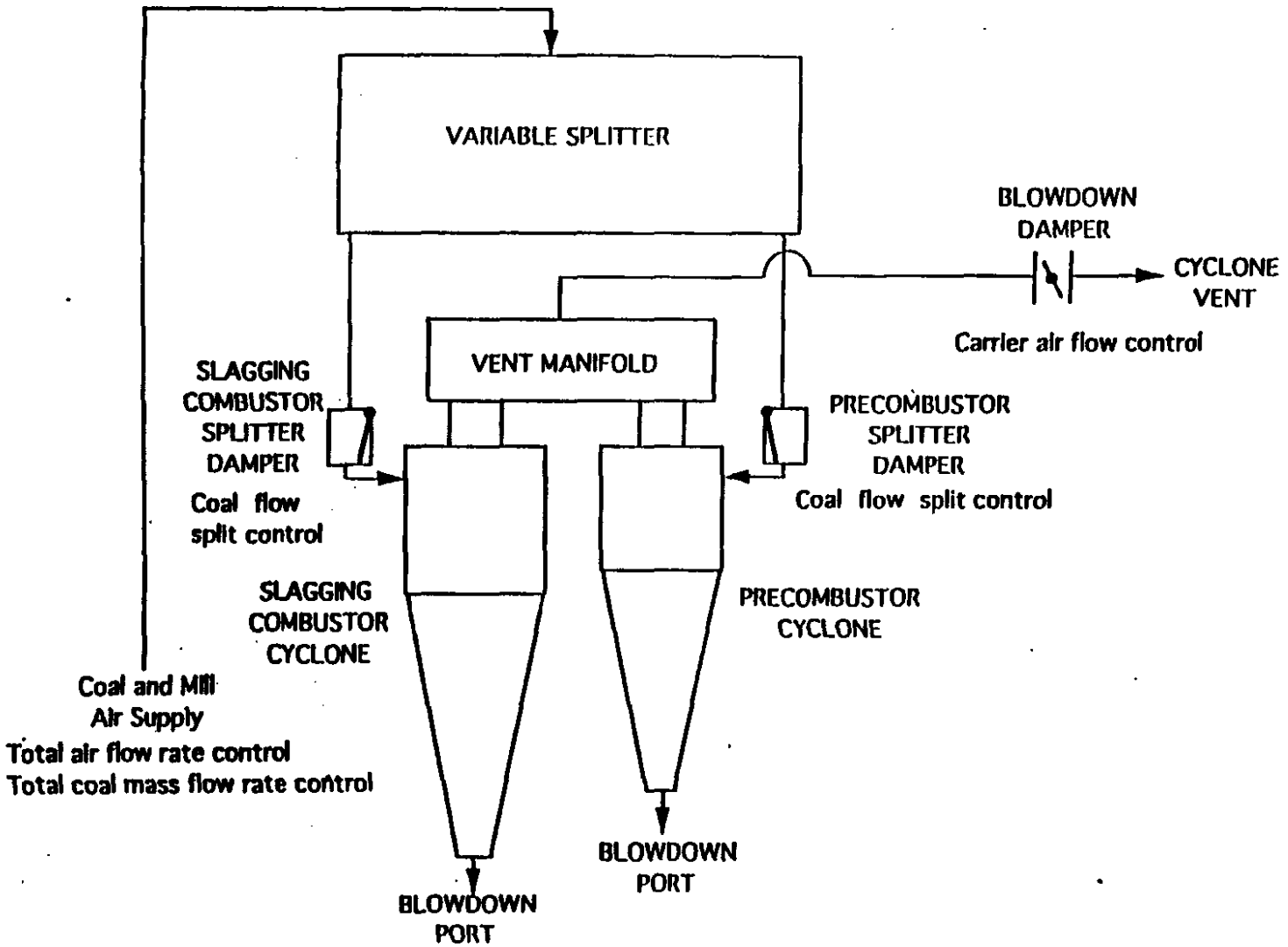

Figure 6-1 Variable Split Blowdown Coal Feed System Concept

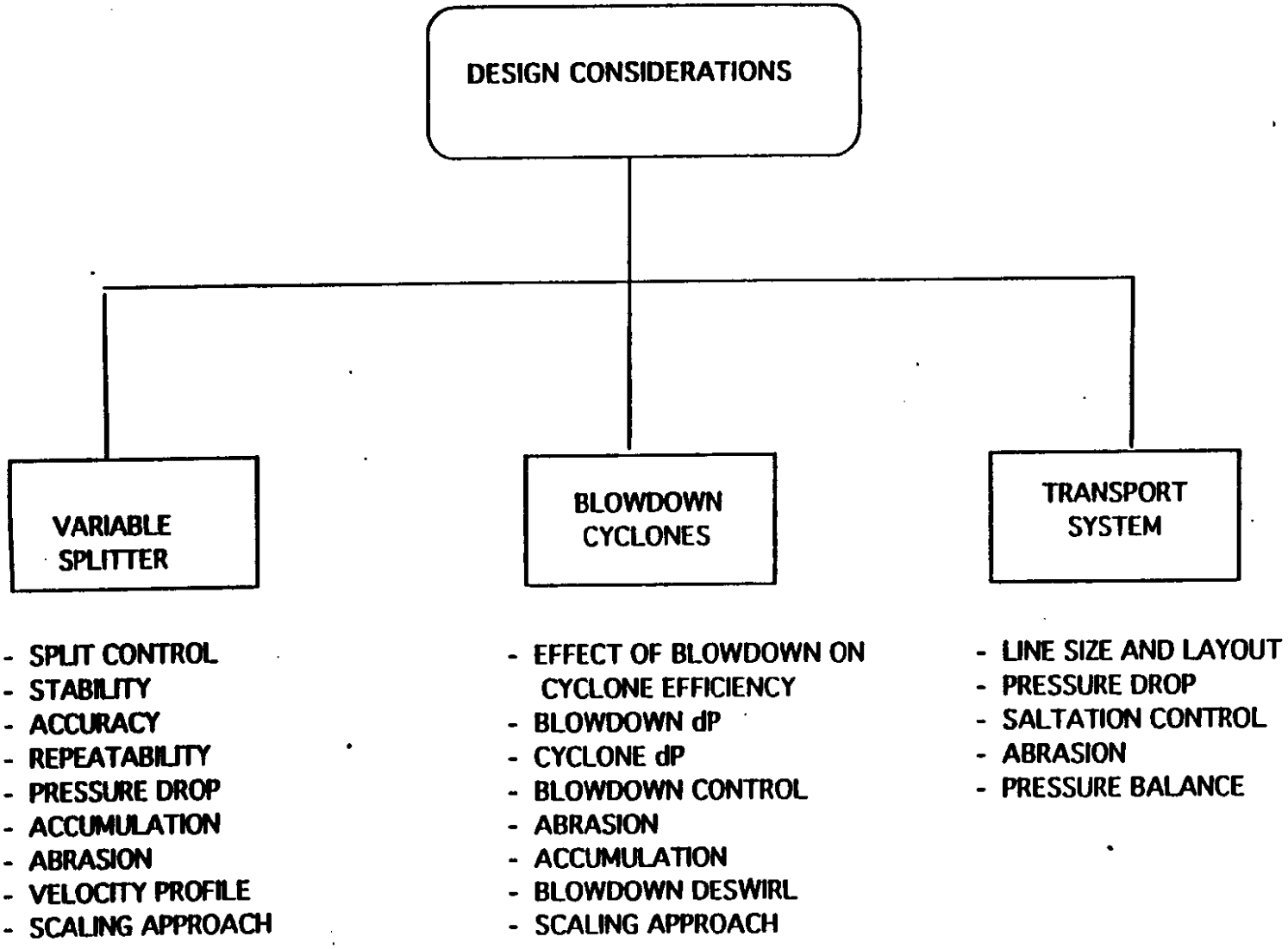

Figure 6-2 CFS Concept Design and Operational Issues

DESIGN PARAMETER	COLD FLOW MODEL	DESIGN VERIFICATION	ANALYTICAL or EXPERIENCE
VARIABLE SPLITTER			
SPLIT CONTROL	X	X	
STABILITY	X	X	
ACCURACY	X	X	
REPEATABILITY	X	X	
PRESSURE DROP	X	X	
ACCUMULATION	X	X	
ABRASION		X	X
VELOCITY PROFILE	X	X	
SCALING APPROACH	X	X	X
BLOWDOWN CYCLONES			
CYCLONE EFFICIENCY	X	X	X
BLOWDOWN dP	X	X	
CYCLONE dP	X	X	
BLOWDOWN CONTROL	X	X	
ABRASION		X	X
ACCUMULATION	X	X	
DESWIRL	X	X	
SCALING APPROACH	X	X	X
TRANSPORT SYSTEM			
LINE SIZE & LAYOUT		X	X
PRESSURE DROP		X	X
SALTATION CONTROL		X	X
ABRASION		X	X
PRESSURE BALANCE			X

Figure 6-3 Solution or Evaluation Method

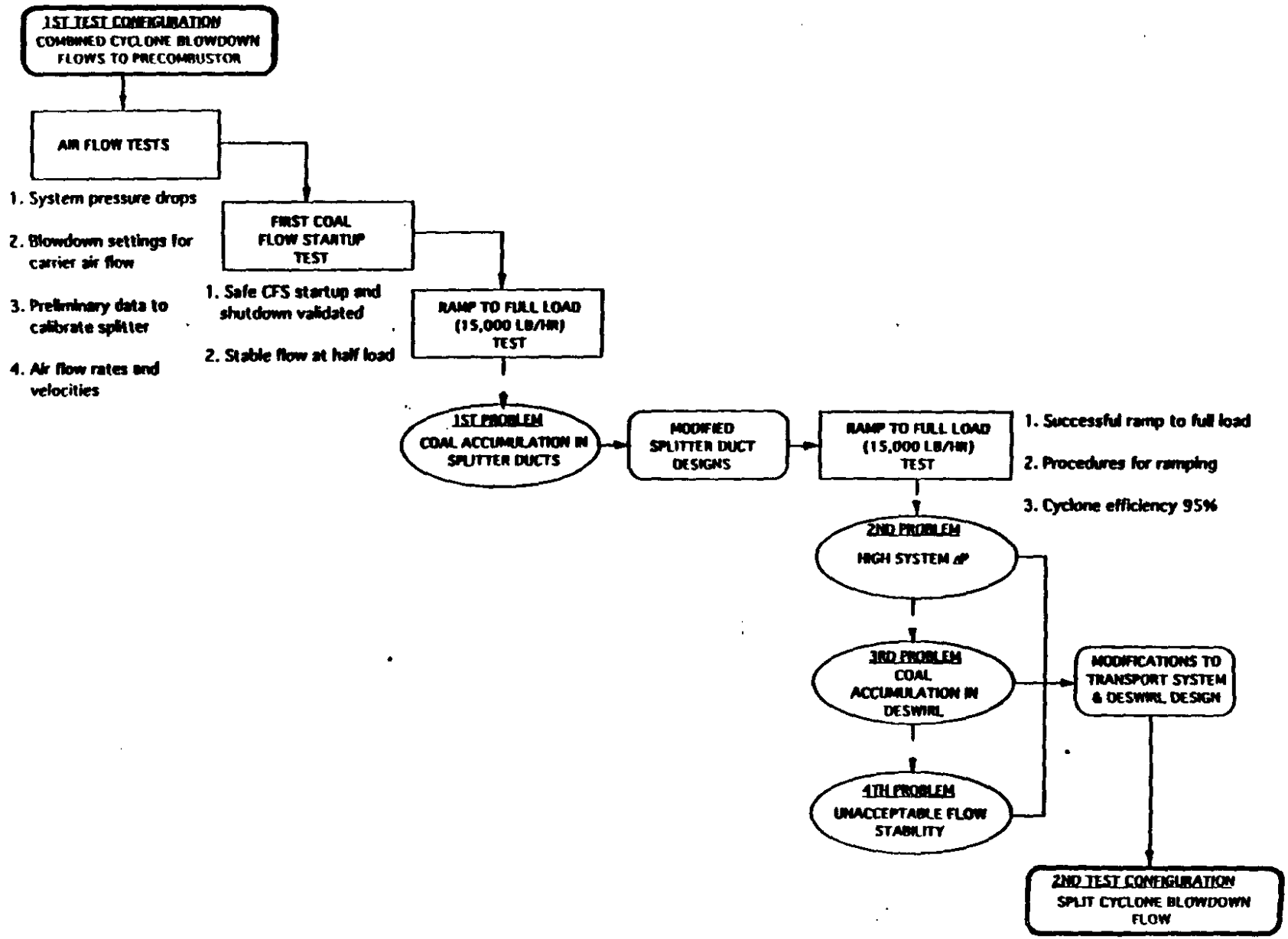

Figure 6-4 Design Verification Test Summary

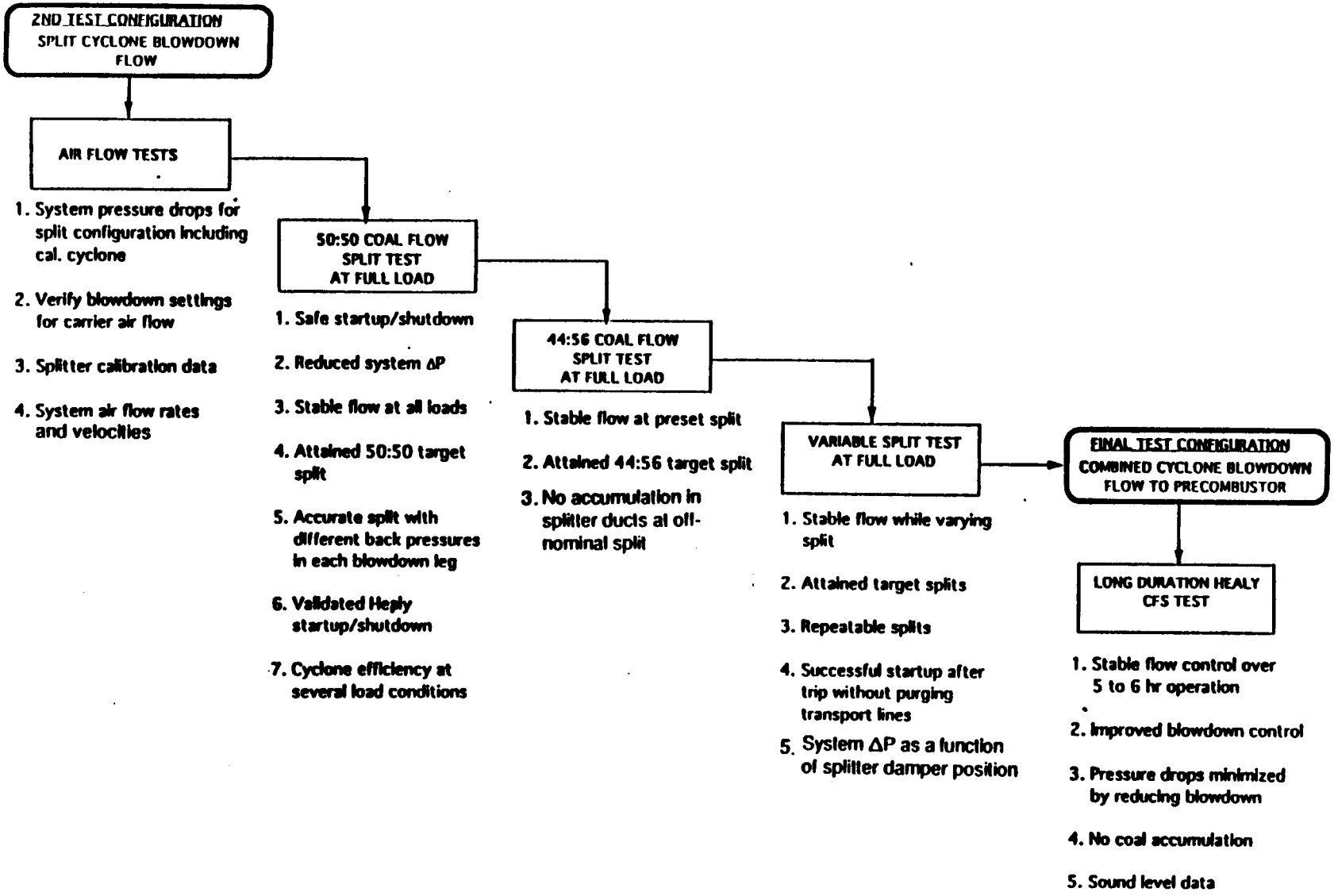

Figure 6-5 Combined DCFS-PC DVT Logic

Table 6-1 DVT Summary Conclusions for the CFS

ISSUE	RESULT
DESIGN SCALABILITY	DESIGN DEMONSTRATED SCALABLE FROM COLD FLOW TO DVT
SYSTEM PRESSURE REQUIREMENT	COAL FEED SYSTEM CAN OPERATE WITHIN 60 INCH HEALY PRESSURE REQUIREMENT. EDUCTOR/BLOWERS NOT REQUIRED
COAL FLOW SPLIT	REPEATABLE COAL FLOW SPLITS DEMONSTRATED
FLOW STABILITY	STABLE FLOW DEMONSTRATED OVER SUSTAINED PERIOD OF OPERATION AT FULL LOAD
COAL STORAGE/ ACCUMULATION	NO ACCUMULATION OR STORAGE OF COAL IN DESIGN
LINE PURGE AFTER TRIP	DEMONSTRATED STARTUP AFTER COMBUSTOR TRIP WITHOUT PURGING
SALTATION VELOCITY	CAN USE PC COAL BURNER TO MONITOR MARGIN ABOVE SALTATION
COAL STATIC CHARGE	DO NOT NEED HUMIDITY CONTROL
FLOW FLUCTUATIONS	SMOOTH FLOW FROM START-UP TO FULL LOAD AFTER MAKING HARDWARE MODIFICATIONS

6.2 Common Cyclone Blowdown Configuration Tests

The first tests conducted using the DCFS utilized cyclone blowdown (coal discharge) ports that were commonly connected using a deswirl configuration that was tested during Cold Flow Modeling. The deswirl configuration was implemented to eliminate the vortex swirl of the cyclones that could persist down through the transport system, potentially creating a wear problem in the Healy design. An objective of the test program was to demonstrate a design that did not require eductors in an effort to improve the plant energy use efficiency.

Air flow tests were conducted first as a safety precaution to characterize the DCFS without subjecting the precombustor to risk of damage. Successful conclusion of the air flow tests were then followed by coal flow tests in which all of the coal supplied through the DCFS was transported to the precombustor. This test configuration was simpler to control than the split flow configuration utilized later (since a separate coal receiving vessel was not required) and allowed evaluation of the DCFS flow stability and potential for coal accumulation.

6.2.1 Common Blowdown Air Flow Tests

Three sets of air flow tests were conducted: DCFS1, DCFS2, and DCFS3. DCFS1 air flow tests were with no blowdown but different total inlet air flow to the coal feed system. The DCFS2 set was conducted with splitter dampers 100% open but varying blowdown and total inlet air flow. The last air flow test, DCFS3, was conducted with constant total inlet, but different splitter damper positions and blowdown. The test matrix data points refer to an input test matrix submitted with a Test Plan to the Capistrano test crew. The test matrix data points acquired during testing are given in the test matrices provided in this report rather than the target data points submitted as part of the Test Plan.

Objectives of air flow tests:

- Leak checks
- Valve and damper functional checkouts
- Checkout flow, pressure, and temperature instrumentation
- Data acquisition and reduction checkout
- Characterize system and component pressure drops as a function of:

    1. blowdown ratio = (cyclone blowdown flow/inlet flow)
    2. total flow rate
    3. inlet pressure
    4. splitter damper position (cyclone inlet area)

The test matrix for the common cyclone blowdown configuration air flow tests is delineated in Table 6-2.

Table 6-2. DCFS Test Matrix For Air Flow Test

Test	Matrix Point	Configuration	Splitter Damper Position Left	Splitter Damper Position Right	Total Air Flow[a]	PC Carrier Flow[a]	Cal. Cyclone Carrier Flow[a]	Vent Flow[a]	Coal Flow to PC[a]	Coal Flow to Cal. Cyclone[a]
DCFS1 - 11/24/92 DCFS2 - 11/30/92 DCFS3 - 12/1/92	2.1-1	Common Blowdown	100	100	40	0	-	40	-	-
	2.1-2		75	75	40	0	-	40	-	-
	2.1-3		50	50	40	0	-	40	-	-
	2.1-4		100	100	30	0	-	30	-	-
	2.1-5		75	75	30	0	-	30	-	-
	2.1-6		50	50	30	0	-	30	-	-
	2.2-1		100	100	40	4	-	36	-	-
	2.2-2		100	100	40	8	-	32	-	-
	2.2-3		100	100	40	12	-	28	-	-
	2.2-4		100	100	40	16	-	24	-	-
	2.2-5		100	100	30	3	-	27	-	-
	2.2-6		100	100	30	6	-	24	-	-
	2.2-7		100	100	30	9	-	21	-	-
	2.2-8		100	100	30	12	-	18	-	-
	2.2-9		100	100	30	15	-	15	-	-
	2.3-1		100	100	40	4	-	36	-	-
	2.3-2		80	80	40	4	-	36	-	-
	2.3-3		70	70	40	4	-	36	-	-
	2.3-4		50	50	40	4	-	36	-	-
	2.3-5		100	100	40	8	-	32	-	-
	2.3-6		80	80	40	8	-	32	-	-
	2.3-7		70	70	40	8	-	32	-	-
	2.3-8		50	50	40	8	-	32	-	-
	2.3-9		100	100	40	12	-	28	-	-
	2.3-10		80	80	40	12	-	28	-	-
	2.3-11		70	70	40	12	-	28	-	-
	2.3-12		50	50	40	12	-	28	-	-
	2.3-13		100	100	40	16	-	24	-	-
	2.3-14		80	80	40	16	-	24	-	-
	2.3-15		70	70	40	16	-	24	-	-
	2.3-16		50	50	40	16	-	24	-	-
	2.3-17		100	100	40	18	-	22	-	-
	2.3-18		80	80	40	18	-	22	-	-
	2.3-19		70	70	40	18	-	22	-	-
	2.3-20		50	50	40	18	-	22	-	-

[a] Flow rates in 1000 lb/hr.

6.2.2 Common Blowdown Coal Flow Tests

This is the first set of tests utilizing the variable split blowdown DCFS. The common deswirl configuration and used for the air flow tests, was utilized for these coal flow tests (186 through 190).

Objectives:

- Characterize DCFS steadiness
- Verify DCFS flow rate capacity
- Determine overall DCFS and component pressure drops as a function of carrier air and coal flow rates
- Provide basis for selection of line velocities
- Verify overall CFS pressure drop within budget
- Verify coal accumulation-free operation
- Verify method of blowdown control
- Evaluate cyclone efficiency
- Investigate methods for monitoring system operation

The test matrix for the common cyclone blowdown configuration coal flow tests is shown in Table 6-3.

6.3 Split Cyclone Blowdown Configuration

The accumulation and fluctuation problems encountered during Test 189 and 190 were believed attributable primarily to the cyclone deswirl configuration. Split capability had not yet been evaluated. Therefore, the decision was made to change to the split blowdown configuration. Deswirl elbows in the cyclone blowdown legs, originally planned for this configuration, were not installed. Eductors were also not installed even though the overall system pressure drop appeared to be high. Hardware modifications and operational changes would be implemented to try and reduce the overall pressure drop instead.

In this configuration, one cyclone feeds the precombustor and the other cyclone feeds a calibration cyclone which discharges coal to a collection tank. The collection tank is weighed to ascertain coal split. The reducing elbow in the precombustor transport line was also replaced with an impact elbow to minimize swirl in the transport line and evaluate its pressure drop. An off-center orifice plate was also installed at outlet of the cyclone vent manifold to increase the pressure drop in the vent line and thus allow the blowdown damper to control over a more stable regime. Again, air flow tests were conducted first to characterize the new configuration and obtain calibration data for predicting coal splits with air only.

6.3.1 Split Blowdown Air Flow Test

Objectives:

Table 6-3 DCFS Test Matrix (Hot Fire)

Test	Date	Matrix Point	Configuration	Cyclone Inlet Damper Position Left	Right	Total Air Flow[a]	PC Carrier Flow[a]	Cal. Cyclone Carrier Flow[a]	Vent Flow[a]	Coal Flow to PC[a]	Coal Flow to Cal. Cyclone[a]
186	12/31/92	3.1-1	Common Blowdown	100	100	40	11	-	29	7.5	-
187	12/8/92	3.1-1	Common Blowdown	100	100	40	11	-	29	7.5	-
187	12/8/92	3.1-1'	Common Blowdown	100	100	40	11	-	29	12	-
188	12/11/92	3.1-1	Common Blowdown	100	100	47	12	-	35	7.5	-
188	12/11/93	3.1-1	Common Blowdown	100	100	47	12	-	35	12	-
189	12/16/92	3.1-1	Splitter Ducts Modified	100	100	40	12	-	28	7.5	-
189	12/16/92	3.1-2		100	100	40	12	-	28	15	-
190	12/23/92	3.1-1	Transport Line Modified More Pressure Trans-ducers	100	100	40	10	-	30	7.5	-
190	12/23/92	3.1-2		100	100	40	10	-	30	15	-
190	12/23/92			100	100	40	10	-	30	12	-

[a] Flow rates in 1000 lb/hr

- o Checkout new flow, temperature, and pressure instrumentation
- o Determine calibration cyclone flow characteristics
- o Characterize system and component pressure drops as a function of blowdown ratio and cyclone inlet area (damper position)
- o Characterize variable splitter air split for different back pressures

The test matrix for the split cyclone blowdown configuration air flow tests is shown in Table 6-4.

6.3.2 Split Blowdown Coal Flow, Hot Fire, Tests

Test 191 through 194 were conducted primarily to evaluate the coal flow split capabilities of the variable splitter.

Objectives:

- o Characterize feed system steadiness in split configuration
- o Verify ability of feed system to deliver coal to two different locations at two different back pressures (pressure balance)
- o Verify method of blowdown control
- o Determine feed system and component pressure drops as a function of carrier and coal flow rates
- o Verify mill startup conditions
- o Verify accumulation-free operation over complete splitter operating window
- o Evaluate cyclone efficiency
- o Verify flow split control accuracy and measurement
- o Demonstrate flow split changes during coal-fired operation
- o Characterize feed system operation during combustor upsets (i.e., loss of oil flow)

The test matrix for the split cyclone blowdown configuration coal flow tests is shown in Table 6-5.

The first 50:50 split test, Test 191, was shutdown prematurely due to problems encountered with the collection tank weight monitoring device and elevated pressures in the collection tank which effected calibration cyclone coal discharge flow. The collection tank pressurization was caused by a particle filtration unit used for the collection tank vent.

With instrumentation problems fixed and the collection tank vent routed to a scrubber system rather than the cartridge filter, the successful completion of three split tests, Tests 192, 193, and 194, was achieved. During these three tests, the following Healy simulated startup and shutdown were demonstrated: lower mill air flow during startup, and a sequence of air flow adjustments followed by coal flow for startup, and a sequence of coal flow

Table 6-4 Split Blowdown Configuration Air Only Test Matrix

Test	Date	Matrix Point	Configuration	Cyclone Inlet Damper Left	Right	Total Air Flow[a]	PC Carrier Flow[a]	Cal. Cyclone Carrier Flow[a]	Vent Flow[a]	Coal Flow to PC[a]	Coal Flow to Cal. Cyclone[a]
DCFS4	1/14/93	4.1-1	Split Blowdown	100	100	40	0	0	40	-	-
		4.1-6		83	83	40	0	0	40	-	-
		4.1-7		83	83	40	10	3.3	26.7	-	-
		4.1-8		83	83	40	12	5.5	22.5	-	-
		4.1-9		67	67	40	0	0	40	-	-
		4.1-10		67	67	40	10	3.4	26.6	-	-
		4.1-11		67	67	40	12	5.5	22.5	-	-
		4.1-12		50	50	40	0	0	40	-	-
		4.1-13		50	50	40	10	3.4	26.6	-	-
		4.1-14		50	50	40	12	5.5	22.5	-	-
		4.1-15		100	100	29	10	5.3	13.7	-	-
		4.1-16		100	100	35	10	4.2	20.8	-	-
		4.1-17		100	100	37.5	10	3.8	23.7	-	-
		4.1-18		100	100	40	10	2.9	27.1	-	-
		4.1-19		100	100	27	5	0	22	-	-
		4.1-20		100	100	40	8	0	32	-	-
		4.1-21		100	100	40	10	0	30	-	-
		4.1-22		100	100	40	12	0	28	-	-
		4.1-23		100	100	40	14	0	26	-	-
		4.1-24		100	100	40	14	6	20	-	-
		4.1-25		100	100	40	12	4	24	-	-
		4.1-26		100	100	40	10	0	30	-	-
		4.1-27		100	100	40	8	0	32	-	-
		4.1-28		100	100	40	8	0	32	-	-
DCFS5	1/14/93	4.2-1	Split Blowdown	83	100	40	0	0	40	-	-
		4.2-2		83	100	40	10	3.7	26.3	-	-
		4.2-3		83	100	40	12	5.4	22.6	-	-
		4.2-4		67	100	40	0	0	40	-	-
		4.2-5		67	100	40	10	3.6	26.4	-	-
		4.2-6		67	100	40	12	5.5	22.5	-	-
		4.2-7		67	100	40	0	0	40	-	-
		4.2-8		50	100	40	10	3.3	26.7	-	-
		4.2-9		50	100	40	12	5.4	22.6	-	-
		4.2-10		50	100	40	14	3.3	22.7	-	-
		4.2-12		100	100	40	10	1.0	29.0	-	-

[a] Flow rates in 1000 lb/hr

Table 6-5 DCFS Test Matrix for Coal Flow Hot Fire Tests

Test	Date	Matrix Point	Configuration	Cyclone Inlet Damper Position Left	Right	Total Air Flow[a]	PC Carrier Flow[a]	Cal. Cyclone Carrier Flow[a]	Vent Flow[a]	Coal Flow to PC[a]	Coal Flow to Cal. Cyclone[a]
191	1/15/93	4.3-1	Split Blowdown	100	100	29	11	6	12	1.0	1.0
192	1/20/93	4.3-1		100	100	29	13	5	11	1.2	1.2
192	1/20/93	4.3-2		100	100	29	13	7	9	2.5	2.5
192	1/20/93	4.3-3		100	100	34.5	13	9	12.5	4.2	4.2
192	1/20/93	4.3-3		100	100	34.5	10	3.5	21	4.2	4.2
192	1/20/93	4.3-4		100	100	37.5	10	3.5	24	5.8	5.8
192	1/20/93	4.3-5		100	100	40	10	3.5	26.5	7.5	7.5
193	1/20/93	4.4-1		50	100	40	12	3.0	25	1.4	1.1
193	1/20/93	4.4-2		50	100	40	14	4.5	21.5	2.5	2.0
193	1/20/93	4.4-3		50	100	40	10	3.5	26.5	4.2	3.4
193	1/20/93	4.4-4		50	100	40	10	4.0	26.0	5.8	4.5
193	1/20/93	4.4-5		50	100	40	10	4.0	26.0	7.5	5.9
194	1/25/93	4.5-1		100	100	40	10	3	27	7.5	7.5
194	1/25/93	4.5-2		75	75	40	10	3	27	7.5	7.5
194	1/25/93	4.5-3		50	50	40	10	3	27	7.5	7.5
194	1/25/93	4.5-4		100	100	40	10	3	27	7.5	7.5
194	1/25/93	4.5-5		83	100	40	10	3	27	7.8	7.2
194	1/25/93	4.5-6		67	100	40	10	3	27	8.1	6.9
194	1/25/93	4.5-7		50	100	40	10	3	27	8.4	6.6

[a] Flow rtes in 1000 lb/hr

adjustments followed by air flow adjustments for shutdown. The split objectives for the three tests were:

- o Test 192 - 50:50 coal split,
- o Test 193 - 44:56 split,
- o Test 194 - variable split

Table 6-6 summarizes the results of the three coal split tests.

During Test 193, isokinetic samples of the cyclone vent line were taken at half load and at about 3/4 load to determine cyclone efficiencies. Efficiencies of 97% at half load and 95% at 3/4 load were obtained.

Test 194 demonstrated a successful start after an abort shutdown of Test 193. This demonstrated that a startup could safely be implemented without the requirement to purge the transport line of residual coal after a trip.

6.4 Long Duration Common Blowdown Configuration Tests

The DCFS coal flow tests, 186 through 194, had a duration of less than 2 hours of operation on coal flow. A longer duration test of about 5 hours was required to evaluate flow steadiness and the effects of sustained operation of the DCFS with the precombustor.

Test 195 and 196 were both conducted with the cyclone blowdown legs commonly connected, to allow complete combustion of all remaining coal. Test 195 would have been the final long duration test, however, time-consuming mill air fan repairs prevented extended operation. Therefore, Test 196 was conducted to obtain the 4 to 5 hour coal operation data. Blowdown flow control was modified in Test 196. It was postulated that more stable blowdown flow control could be accomplished using flow input from the vent line orifice rather than the annubar flow meter.

Objectives:

- o Verify stability of CFS and precombustor over longer operating period (5 hours)
- o Verify CFS overall pressure drop is within required budget
- o Verify that no coal accumulation occurs during longer operating period
- o Verify blowdown flow control based on orifice pressure drop
- o Provide data for CFS pressure drop correlations

The test matrix for the long duration common blowdown configuration coal flow tests is shown in Table 6-7. Table 6-8 summarizes the component pressure drops from all available tests for different air flows and coal flows.

Figure 6-6 illustrates one of the most accomplishments resulting

Table 6-6 Cold Flow Mass Split Determination

	192	193	194
Total Coal Flowed to Splitter (lb)	18,435	20,115	21,075
Total Coal Discharge through both Cyclones (lbs) (95% eff.)	17,513	19,109	20,021
Total Coal to Calibration Hopper (lbs)	8,165	8,000	8,500
Total Coal to Calibration Cyclone (lbs) (95% eff.)	8,595	8,420	8,950
Cyclone #1 Damper Setting (Feeds calibration hopper)	100	50	Variable
Cyclone #2 Damper Setting (Feeds PC)	100	100	100
Measured Coal Split	49.1/50.9	44.1/55.9	44.7/55.3
Calculated Coal Split Based on Pressure Measurements	50/50	44.0/56.0	Variable
Coal Split Based on % O2			

Table 6-7 DCFS Test Matrix for Long Duration Hot-Fire Tests

Test	Date	Matrix Point	Configuration	Cyclone Inlet Damper Position Left	Right	Total Air Flow[a]	PC Carrier Flow[a]	Cal. Cyclone Carrier Flow[a]	Vent Flow[a]	Coal Flow to PC[a]	Coal Flow to Cal. Cyclone[a]
195	2/1/93	5.1-1	Long Duration Common Blow-down	100	100	29	11	-	18	4.5	-
195	2/1/93	5.1-2	Long Duration Common Blow-down	100	100	40	11	-	29	4.5	-
195	2/1/93	5.1-3	Long Duration Common Blow-down	100	100	40	10	-	30	7.5	-
195	2/1/93	5.1-4	Long Duration Common Blow-down	100	100	40	10	-	30	10.0	-
195	2/1/93	5.1-5	Long Duration Common Blow-down	100	100	40	10	-	30	15.0	-
196	2/2/93	5.1-6	Long Duration Common Blow-down	100	100	40	10	-	30	8.0	-
196	2/2/93	5.1-7	Long Duration Common Blow-down	100	100	40	10	-	30	13.0	-

[a] Flow rates in 1000 lb/hr

Table 6-8 DCFS COMPONENT PRESSURE DROPS

	AIR ONLY	HALF LOAD 50/50 SPLIT	FULL LOAD 50/50 SPLIT
Air Flow	10,000	10,000	10,000
Coal Flow	0	7,500	15,000
Splitter ΔP	2.2	2.8	3.0
Cyclone Blowdown ΔP	12.0	7.9	8.2
Elbow ΔP	4.9	6.3	8.5
Line ΔP	0.7	1.0	1.3
Miter Elbow & Line ΔP*	1.2	2.8	4.5
Tee, Hose ΔP*	0.9	1.9	2.8
Fire Valve ΔP	0.8	1.0	1.2
Burner ΔP	4.9	5.4	5.8
CTS Total ΔP	27.6	29.1	35.3
Predicted Healy Total ΔP	25.5	24.4	28.0

* DVT - Unique component pressure drops

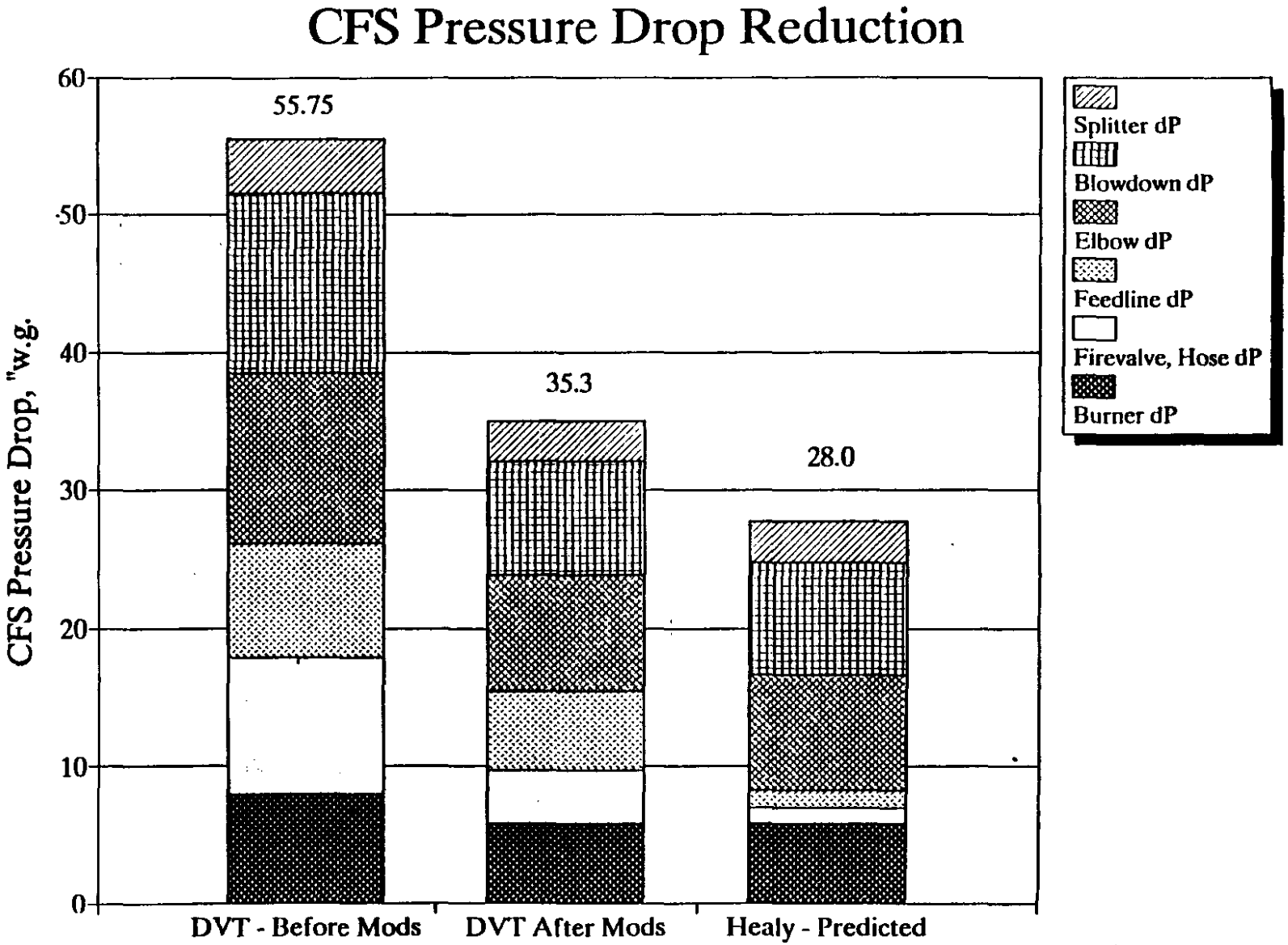

Figure 6-6 Overall CFS Pressure Drops

from the coal feed system DVT. Shown are the overall CFS pressure drops before any modifications to the system were made, and results from the last test, 196, after all modifications were implemented. System pressure drops were reduced about 20 inch WG. After eliminating pressure drops unique to the DVT setup results in a Healy CFS pressure drop of 28 inch WG. Add that to a precombustor back pressure of 23 inch WG results in a requirement of 51 inches WG at the CFS inlet based on performance coal. As a result, the requirement for eductors to boost the transport system pressure is not required for the Healy design. Note that for waste coal at maximum flow rate, this translates into a delta-P of 55 inches WG, which is within the 60 inches WG requirement.

Sound level data was also acquired during Test 195 and 196. Since there is no need for an eductor/blower system for the Healy coal feed system, noise levels of less than 85 dB may be inferred from the data. Most of noise for the DVT was attributed to the secondary, primary, and mill air fans. The sound level data are summarized in Appendix C.

6.5 Startup and Shutdown Safety Issues

After the completion of hardware modifications, and ensuring that the coal flow fluctuations were within acceptable levels, it was decided to perform the following tests.

Instead of ramping down the coal prior to shutdown, an emergency shutdown was manually enforced thereby shutting down all systems simultaneously. The goal was to shutdown the DCFS instantly and let any coal in the lines reside and settle down in the lines and components of the DCFS, and then see if this coal would have any adverse impact during the startup of the next test. Therefore no attempt was made to clear the lines of coal, and the next test was started up with the coal from the previous test remaining in the system. It was observed that the startup was without any observable abnormal peaks, and was achieved without any incident. Several such shutdown and startup tests were performed while maintaining the test matrix as planned. These tests proved the safety and reliability of the system.

Carbon monoxide levels in the DCFS were also measured during testing. The levels of CO measured in the DCFS were always less than 10 PPM, indicating no evidence of burning or smoldering of the coal in the DCFS throughout the test program.

7.0 Impact of DVT on Healy Precombustor Design

As a general statement, the results of the precombustor DVT had no major impact on the Healy precombustor design. The tests validated the basic sizing, geometry and operation of the precombustor. The mix annulus windbox design was validated, as was the approach for injecting and burning coal fines in the cyclone vent exhaust. Both of these represented significant departures from the Cleveland PC design. Furthermore, the use of the Foster Wheeler coal burner, which was a departure from the Cleveland design, was also successfully validated.

Near the conclusion of the test series a nominal accumulation of slag was noted on the lower edge of the water cooled combustion chamber and on adjacent hardware. The last 3 feet of the chamber had a wet slag appearance 360 degrees around but no significant buildup. An analysis of the Performance Coal used throughout the test program indicated a T_{250} which is nearly 300°F less than the Healy specification.

Still, concerns were raised that over long operating periods, a significant buildup of slag may interfere with the lower coal fines injection ports. The coal fines injection arrangement was reconfigured for the Combined DCFS-Precombustor tests, discussed in the following sections. The new arrangement included the top six injectors and blocked off the bottom two injectors. A review of the design of the exit transition indicated that even if slag buildup occurred, the slag would escape into the Slagging Combustor if sufficient accumulation occurred to provide a flow path. This modified arrangement has been incorporated in the Healy design.

Table 7-1 summarizes the major PC issues which were addressed by the DVT, with applicable test results and impact or the PC design and/or operation. A description of two test results which have had impact on the Healy design are provided below.

Modified Cyclone Vent Air Injector Configuration

Modification of the injectors, shown in Figure 7-1, was driven by two concerns. First, tests during DVT showed that under certain conditions, slag deposits can form in the region of the injectors. If the slag deposits became significant, the lower injectors could be blocked, allowing the accumulation of coal fines in the duct.

Second, cold flow tests showed that injector legs running "uphill" with velocities of less than 40 ft/sec may experience saltation and accumulation of coal fines. Low velocities will be experienced by the injectors during normal operation (i.e. non-start-up conditions) when most of the cyclone vent air is sent to the furnace NO_x ports.

Based on the above concerns, a decision was made to rotate the

Table 7-1 Precombustor DVT Results

ISSUE	TEST RESULTS	DESIGN/OPERATION IMPACT
Coal burner performance including ignition, stability and load variation	• Demonstrated stable operation over the full load range • Demonstrated reliable coal light off • No flame failures experienced • Burner ΔP measured • Close agreement between measured and predicted stack oxygen	• High level of confidence in reliable burner operation at Healy • Adds margin to pressure budget • Good indication of high combustion efficiency
Prevention of slagging and fouling	• No significant fouling seen during test series • Portion of combustion can covered with thin (1/4-1/2") slag layer. May be due to low T250 (2400°F) • Some slag deposits seen in bottom of transition and near PC exit	None • No major impact. Will use lower ϕ for low T250 coals at Healy • Mill air injectors rotated for Healy design to avoid possible injector plugging
Combustion of cyclone vent air including coal fines	• Demonstrated burning of fines using DVT coal feed system • No adverse effects on precombustor operation • No evidence of fouling due to coal fines	• Precombustor can reliably burn fines as required during start-up at Healy
Demonstration of Healy start-up and shut-down sequences	• Successfully demonstrated Healy sequence including coal/oil exchange with oil ignitor at 70 MBtu/hr	• Validates method proposed for combustor start-up/shut-down
Validate design heat fluxes and cooling loads	• Measured heat loss slightly over target due to lack of refractory • Measured heat fluxes are within predicted range	• Healy design will include refractroy lining throughout
Operation of 70 MBtu/hr forney oil burner	• Smokeless operation demonstrated at minimum (20 MBtu/hr) and maximum (70 MBtu/hr) loads. Slight stack haze at intermediate loads • Pressures for atomization and oil significantly higher than Forney estimates, exceeding plant capability. Changed operating mode to reduce pressures to reasonable levels • Forney recommended tertiary air flow causes oil flame failure at low loads	• Haze can be eliminated at Healy with tighter air flow controls • Required pressures for Healy Atomization: 95 psig Oil: 150 psig • Reduce tertiary air flow for Healy

Table 7-1 Precombustor DVT Results - Continued

ISSUE	TEST RESULTS	DESIGN/OPERATION IMPACT
Verify pressure budget for Healy design	• Measured ΔP's in relatively good agreement with predictions	• Pressure budget leaves sufficient margin for flow control at Healy
Reliable operation of flame scanner system	• Not able to discriminate between oil and coal flames using Forney supplied system • Forney has indicated that this problem is common to all of their installations • Flame scanner on burner periphery provides a strong signal whether firing oil only, coal only or oil and coal • Repeatable coal ignition was obtained with oil burner firing at 70 MBtu/hr	• DVT experience suggests that oil/coal flame discrimination may not be required for safe operation at Healy • Working to obtain resolution through NFPA and/or industry experience
Thermal effects, thermal mistmatches	• Small cracks appeared on joint with high thermal stresses (ΔT = 600°F) • Measured high temperature on mix annulus windbox coupons due to back radiation	• Redesigned for Healy ΔT limited to 300°F • "Shield tubes" required for Healy design

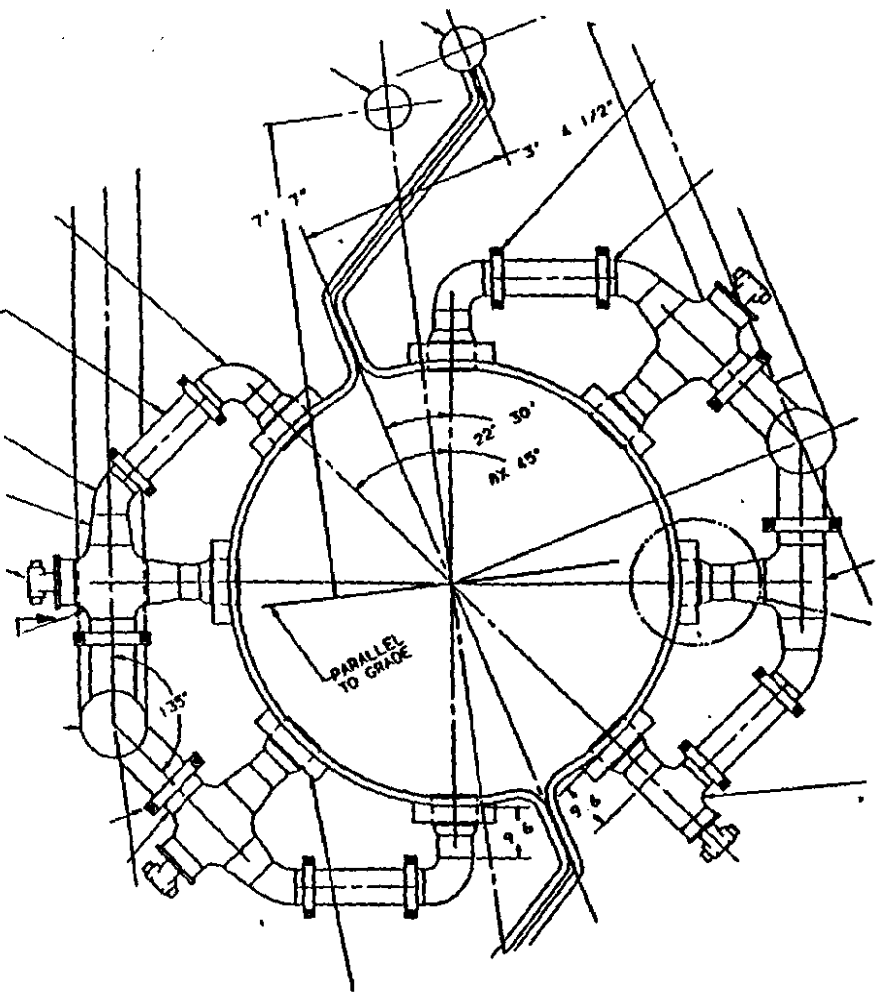

PRE-DVT

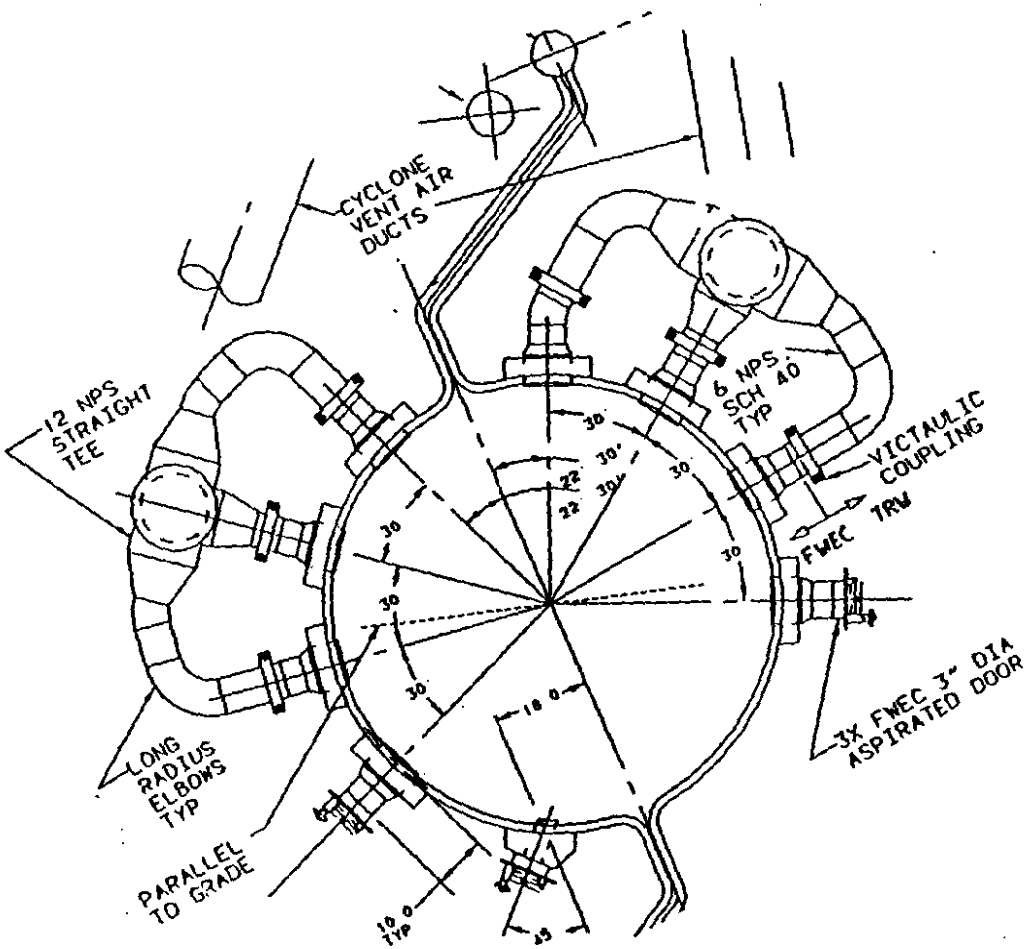

POST-DVT

Figure 7-1 Changes to Cyclone Vent Air Injector Configuration

injectors to orientations of horizontal or above (Figure 7-1). Due to space constraints, the number of injectors was reduced from 8 to 6. The I.D. of the injectors will be slightly larger, so that the injection velocities at Healy will be nearly the same as for DVT.

Damper Blade Heat Loss

Heat loss to the damper blades reduces the plant efficiency at Healy since the heat is rejected to low temperature water (condensate). The DVT results indicated that the heat loss is strongly driven by convection, which can be significantly reduced by providing a thin refractory (e.g., plasma spray) coating on the surface of the blades. TRW has used plasma spray coatings (alumina) in some areas of the MHD combustor, however, the coatings have been found to spall under certain conditions.

TRW will investigate the viability of thin refractory coatings for the Healy damper blades. Because the coatings are thin (approximately 0.050-0.100"), they can be applied during the manufacturing process and have no effect on the dimensions of the present damper blade design.

8.0 Impact of DVT on Direct Coal Feed System Design

The DVT proved that the total system pressure drop was within the 60 inches water pressure budget requirement. Utilizing the DVT data, we can now calculate that the predicted overall operating pressure drop for the Healy design will be about 50 to 52 inch WG for performance coal at full load. This is 8 inch WG below the required maximum limit of 60 inch WG. For waste coal, overall pressure drop is predicted to be 57 to 58 inch WG. Figure 8-1 illustrates the required CFS inlet pressure as a function of load. Because the variable split blowdown coal feed system complies with the 60 inch WG limitation without the application of eductors to boost the transport system pressure, the plant overall efficiency increases due to the elimination of the blowers that would furnish the motive air required for the eductor boost.

Coal accumulations in the original variable splitter discharge ducts, occurred during initial attempts to achieve full load. After evaluating corrective solutions both analytically and via cold flow modeling, a relatively simple modification to the splitter discharge duct design eliminated the coal accumulations in the splitter with only a 3 inch WG increase in pressure drop. The splitter discharge duct design change to the Healy CFS design was also incorporated. Velocities, pressure drops, geometry are preserved in the Healy design. An added feature to the Healy design is a manual damper in the top of the splitter discharge duct which may be lowered to increase velocities in critical areas to prevent coal accumulation. The system is designed in an effort to minimize velocities in this section to minimize pressure drop as well as wear. If it is necessary to utilize these discharge dampers, they must be positioned symmetrically to prevent coal split bias.

Flow stability was also improved during the DVT through hardware as well as operational modifications. Figure 8-2 illustrates the improvements made with modifications to the transport system. Peak to peak precombustor and burner pressure variations of 4 inch WG were reduced to peak to peak variations of less than 2 inch WG after transport line modifications were implemented.

Cyclone blowdown port size and blowdown leg diameter effects were also evaluated during testing. Minimum sizes were established based on pressure drop measurements and total flow rates of air and coal per cross sectional area. Cyclone blowdown port sizes and blowdown pipe sizes were established for the Healy CFS in which the precombustor and slagging combustor cyclones are sized in proportion to the total flow received by each cyclone.

Flow control was also improved during the DVT. Controlling blowdown based on input from the annubar flow meter proved to be difficult to tune. The blowdown damper was either overdamped or underdamped in response to fluctuations in CFS input flow emanating from the mill air fan and lock hopper facility coal supply system. Therefore, an orifice plate was added upstream of the blowdown

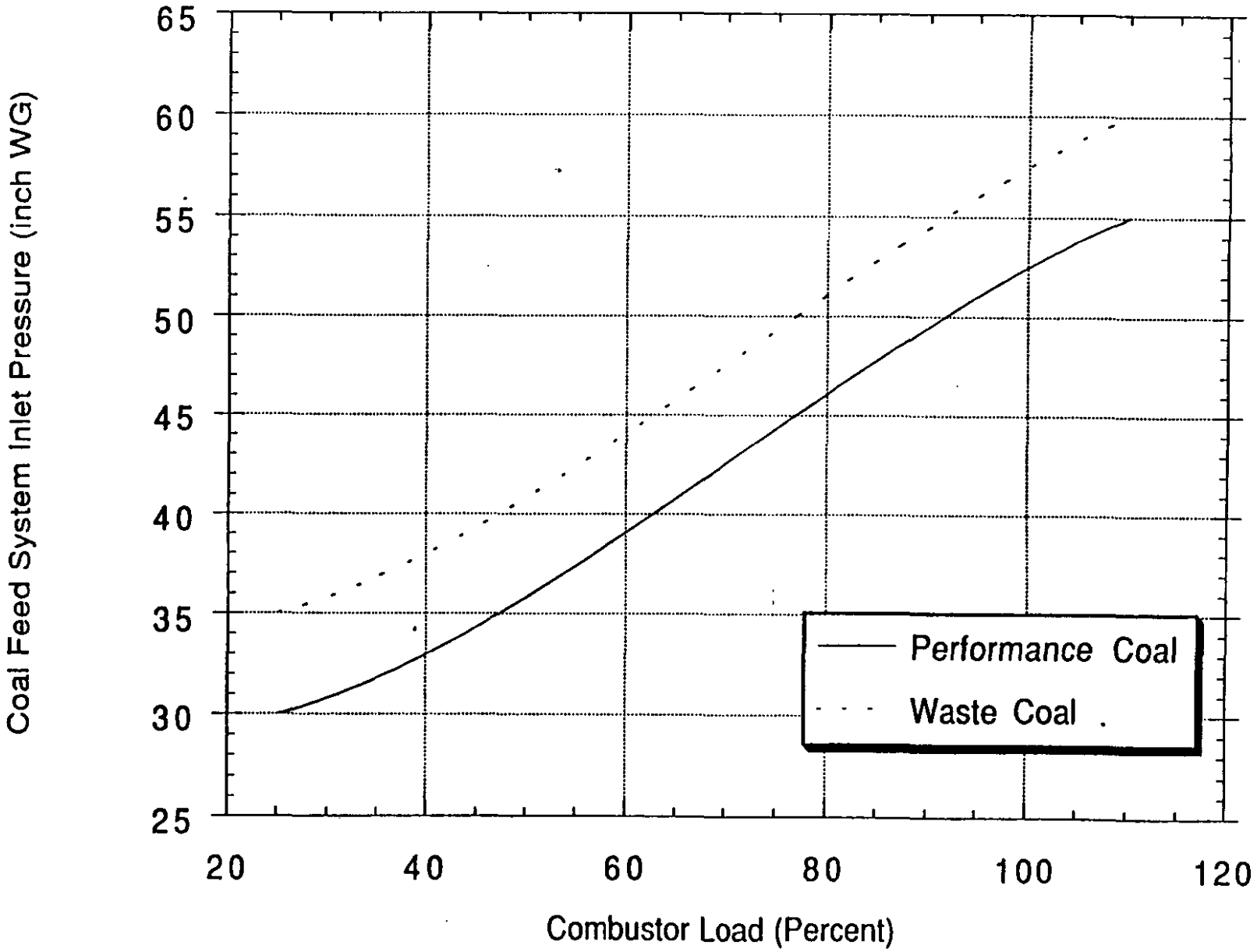

Figure 8-1 CFS Inlet Pressure as a Function of Combustor Load

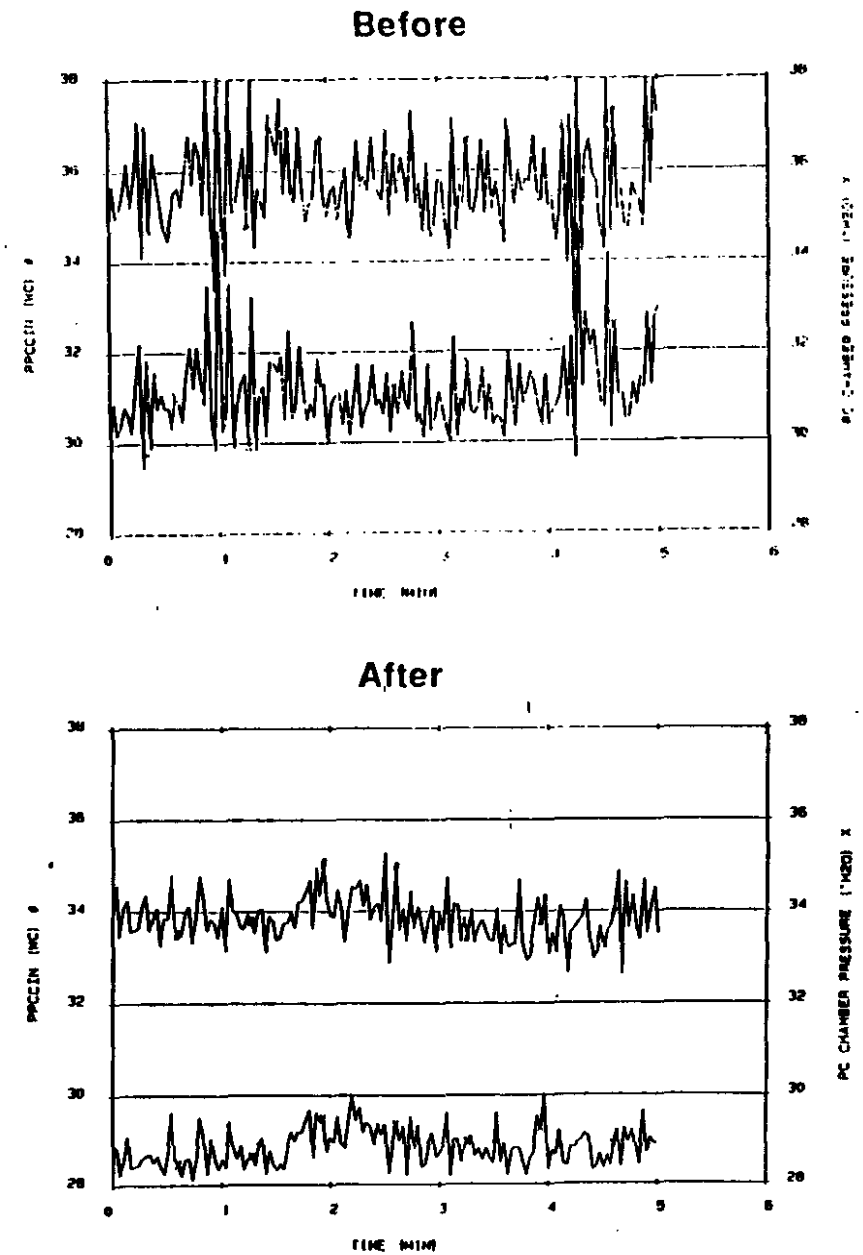

Figure 8-2 Flow Fluctuations Before and After Transport Line Modification

damper which enabled the damper to control in a more stable regime and be less responsive to fluctuations in total inlet flow. Figure 8-7 illustrates stable precombustor and burner pressures even though flow from the facility coal supply system experienced periodic fluctuations due to coal transfers. To a degree, the CFS tends to dampen fluctuations in supply pressure, important in the Healy design with exhauster fans located upstream of the CFS.

A method for ascertaining velocity and margin above saltation was also determined during DVT. The precombustor burner pressure drop proved to be a reliable means for predicting velocity during the DVT. Lower trip limits were established for velocity based on test experience which indicated that burner pressure drops of less than 4 inch WG were indicative of saltation. Therefore, blowdown ratios were established to maintain burner pressure drops of 6 inch WG on average. A lower trip limit of 4.5 inch WG was used effectively during the DVT as illustrated in Figure 8-3. For Healy lower trip limits will be established based on air flow test results. TRW is planning on using the slagging combustor splitter pressure drop as a means of predicting slagging combustor transport line velocity and margin above saltation.

Acceptable instrumentation locations, orientation, and port sizes were also determined from DVT testing. At first some ports were found susceptible to plugging. Plugging problems diminished after resizing and relocating instrumentation ports. For Healy, ports susceptible to plugging will have purges which shall be activated intermittently.

The DVT demonstrated that the hardware design could be scaled. The DVT hardware design was based on scaling from the cold flow model design. Cyclone efficiencies and pressure drops indicated that blowdown cyclones could be designed using conventional cyclone design techniques. Blowdown port size, however, is determined using nonconventional means based on pressure drop and total air and coal flow. The variable splitter also proved to be scalable. Results were illustrated to be repeatable and scalable from cold flow modeling data.

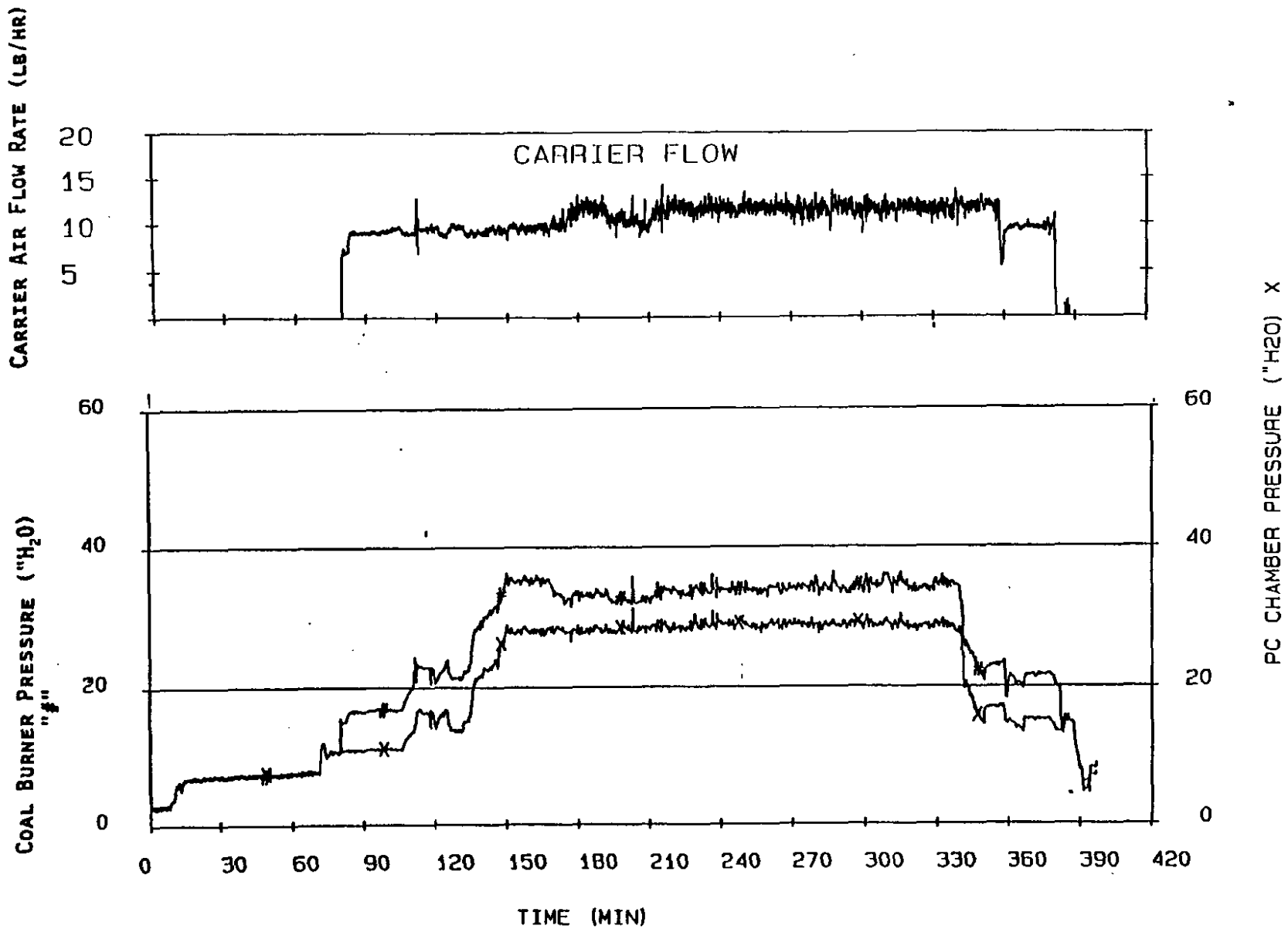

Figure 8-3 Stable Flow After Design Modifications Were Implemented

9.0 Post-Test Hardware Condition

The overall condition of the precombustor at the conclusion of the DVT Program was very satisfactory. Judging from the appearance of the hardware and the test data obtained, the precombustor as is could continue to be fired indefinitely.

The Foster Wheeler burner did have minor coal and oil deposits in the oil burner cavity and on the oil gun tip. These did not interfere with operation and probably would not have occurred if a purge had been present. Post firing examinations did not reveal these deposits before modification of the tertiary air fan setup. The appearance of the HESI never changed. It sparked without problem throughout the program. The coal passages internal to the burner, as viewed from inside the PC, did not appear to contain any coal deposits.

The chamber refractory was in excellent shape except for a small bare spot (about 6 square inches) near the edge between the baffle throat and the chamber face as shown in Figure 9-1. Minor cracks in the chamber refractory were also noted, however, most of these appeared during curing. Molten slag about 1/4 thick coated the full circumference of the last three feet of the chamber wall. Approximately 50 pounds total of molten slag accumulated at the lower edge of the chamber and on adjacent downstream surfaces.

A crack appeared at the weld junction between the water cooled chamber and surrounding windbox wall was noted. Further details are provided below. The first sign of gas leakage out these cracks occurred early in the DVT Program. The problem did not appear to get worse and never interfered with operation. This zone was known to be affected by thermal stresses and an improved arrangement will be provided for Healy. No other structural design problems were noted. The flex lines used to connect the coal fines injectors to the splitter never overheated during testing. A problem with coal smoldering did occur when oxygen was applied to a cutting torch to modify some attachment fittings. The lines in which smoldering occurred were replaced.

9.1 Precombustor Condition

1. The precombustor installation was left intact with the exception of the damper blades, which were removed and stored. Inspection of the blades indicated no heat-induced warpage. Both blades had a scraped surface along the bottom edge (1/8" x 12") due to interference with swirl housing duct. Both blades were removed from PC assembly, drained of water and purged with nitrogen. Afterwards the water circuits were capped, and both blades were placed in storage. Figure 9-2 shows the transition exit section condition.

2. Several small cracks were found in the secondary air windbox reinforcing gussets. A preliminary inspection indicated

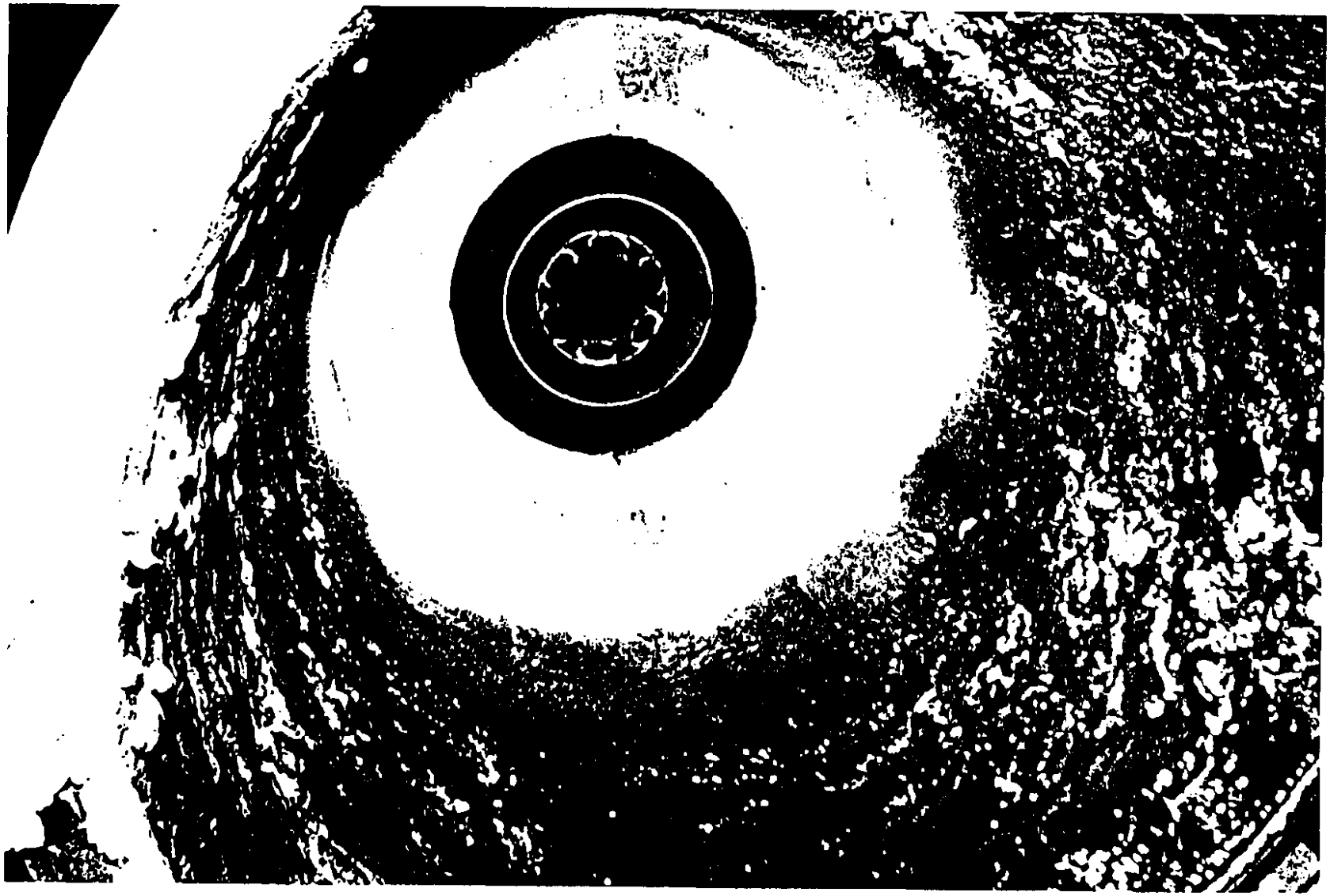

Figure 9-1 Combustion Chamber Condition - Post Test (View Looking Upstream)

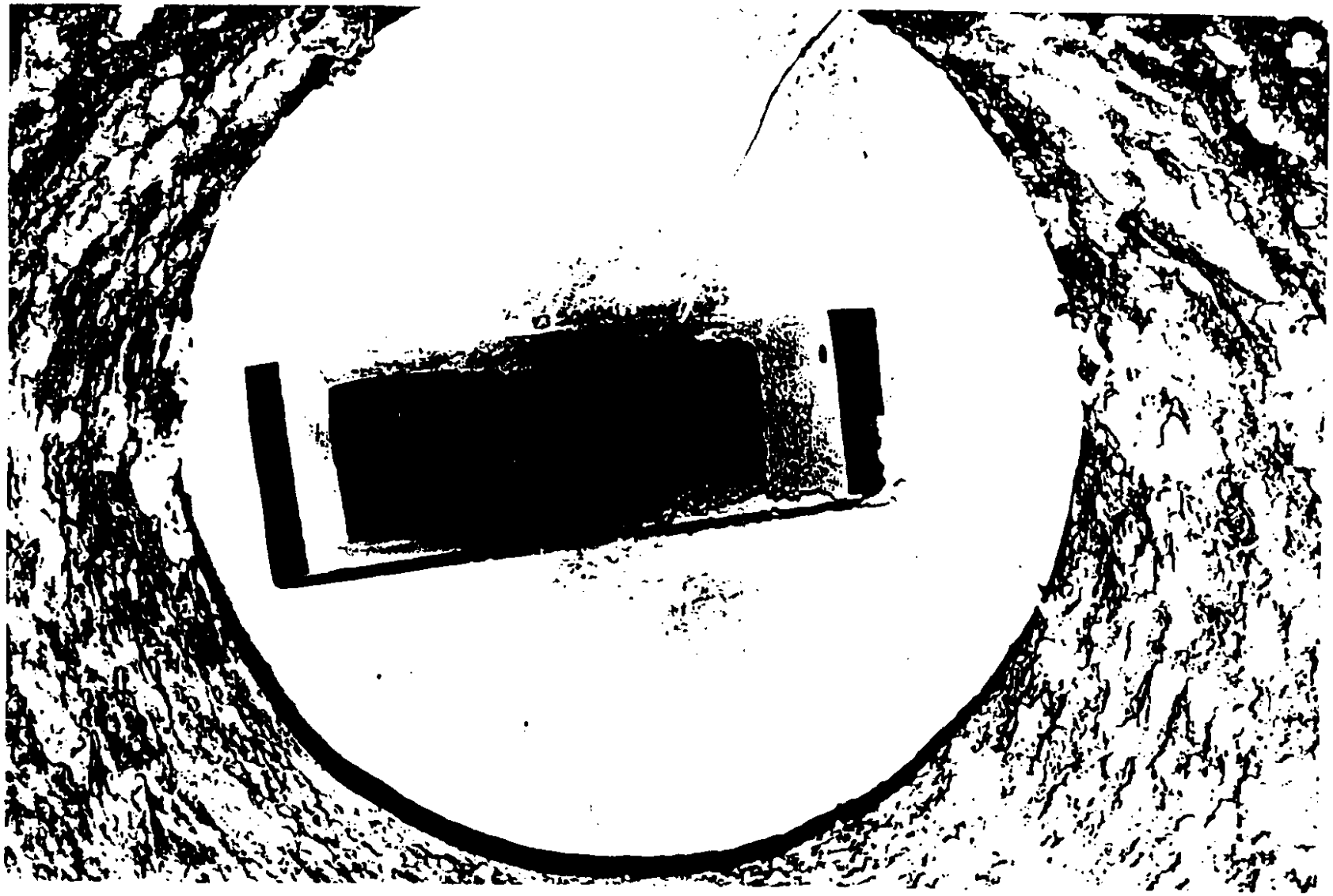

Figure 9-2 Transition Exit Section Condition - Post Test (View Looking Downstream)

cracks present in structural welds and parent material. The cracks were in the structural attachment of gussets to shell near windbox downstream edge. At no time did the cracks compromise the structural integrity of the precombustor.

The total number of thermal cycles (i.e. ambient to 700°F, back to ambient) was approximately 50. Figure 9-3 shows the location of the cracks. The cracks developed because of thermal cycling over high temperature swings (over 500°F). Because of this experience, the design of the Healy precombustor has been improved to accommodate such thermal cycling and eliminate the possibility of such cracks from occurring.

The hot gas leakage discovered at the upstream end of the secondary windbox during test 3A189 was traced to the combustion chamber/windbox weld joint at the downstream end of the combustion chamber. At least 3 cracks were discovered along the trailing edge of chamber between the water-cooled tubes and outer shell. These cracks created a path for hot gases to back-up and vent through the expansion joint of the secondary windbox. Figures 9-4 and 9-5 show the gas leakage path.

3. Inner and outer dual air registers remained set at nominal open values of 25% and 30%, clockwise, respectively.

4. There were no signs of coking or char buildup in the coal burner injector passages after 43.1 hours of service.

5. There was no visible sign of damage to the oil gun HESI or swirler head assemblies. The HESI position switch was inoperative, but was not used, except for a sequence program.

6. The Forney oil gun complete with flame scanners and electrical cabinets remained installed. Both flame detectors and oil gun control panel were functioning properly prior to shutdown.

7. A small amount of material which appeared to be oil-soaked coal dust continued to accumulate in air duct surrounding the oil gun. Figure 9-6 shows the location of coal accumulation.

8. The face of oil nozzle tip had the usual signs of oil char, but no signs of injector holes being blocked.

9. A section of the 2" thick refractory at baffle throat was missing. Located approximately at 12 o'clock position, the affected area was about 4" wide and 10" long. The affected refractory was at the interface between Foster Wheeler supplied refractory for the burner throat and TRW-supplied refractory for the combustion can. Figure 9-7 shows the condition which worsened since 3A193. It has been suggested that larger refractory clips may solve this problem.

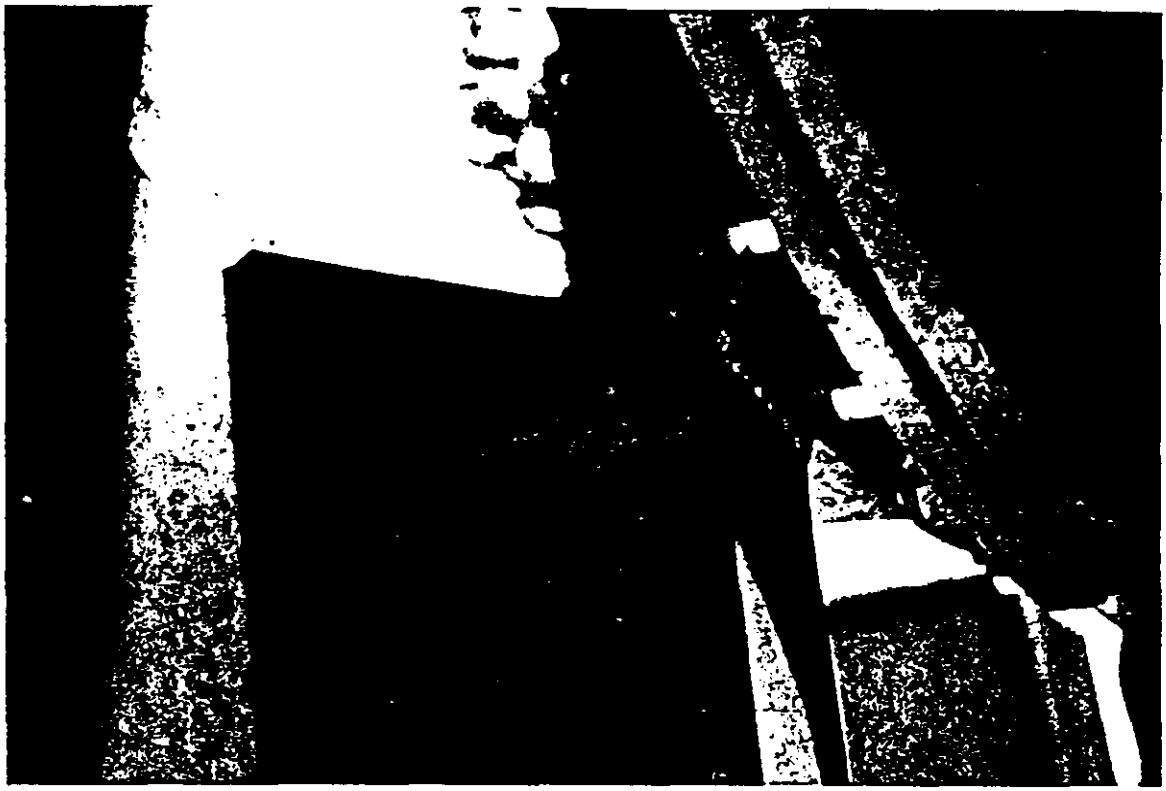

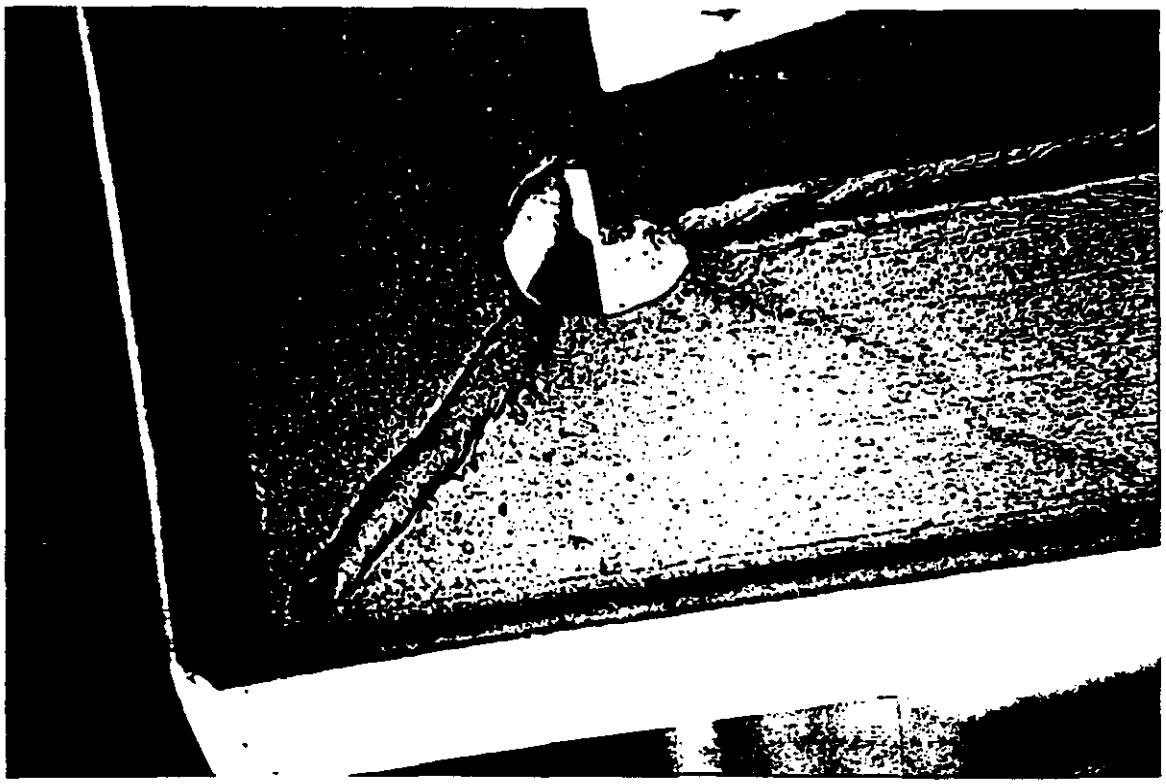

Figure 9-3 Secondary Windbox Cracks

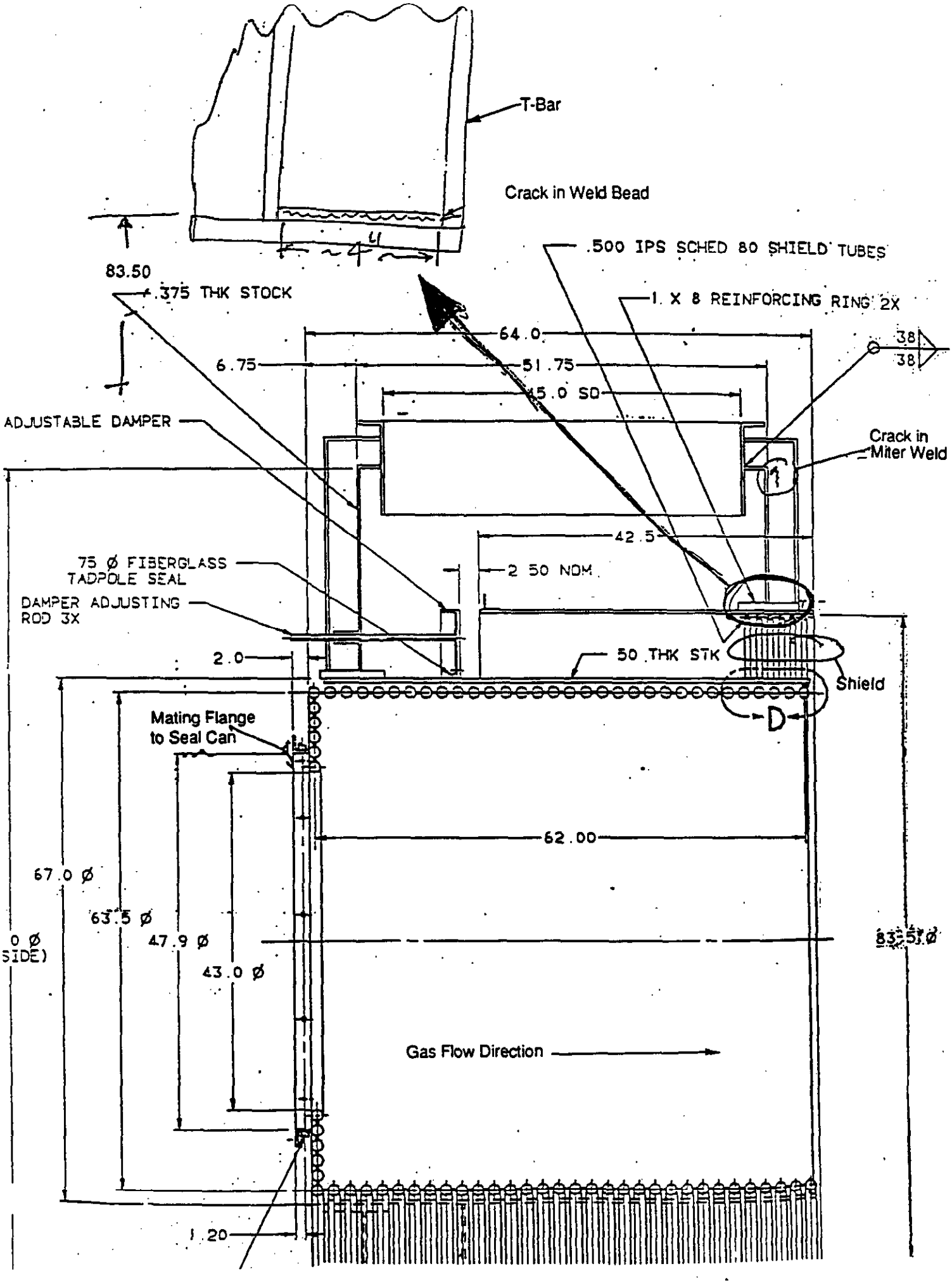

Figure 9-4 PC Gas Leakage

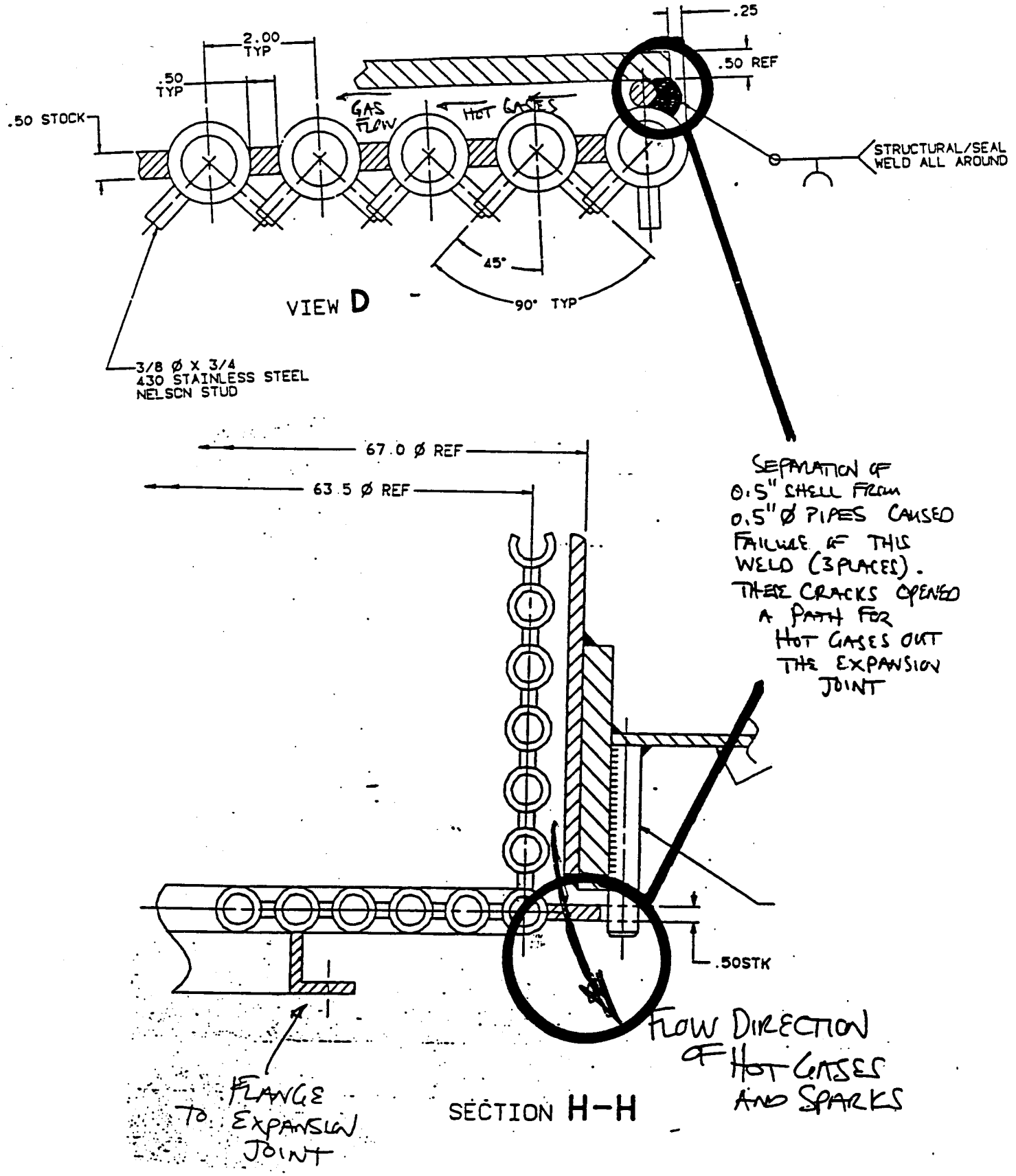

Figure 9-5 PC Gas Leakage

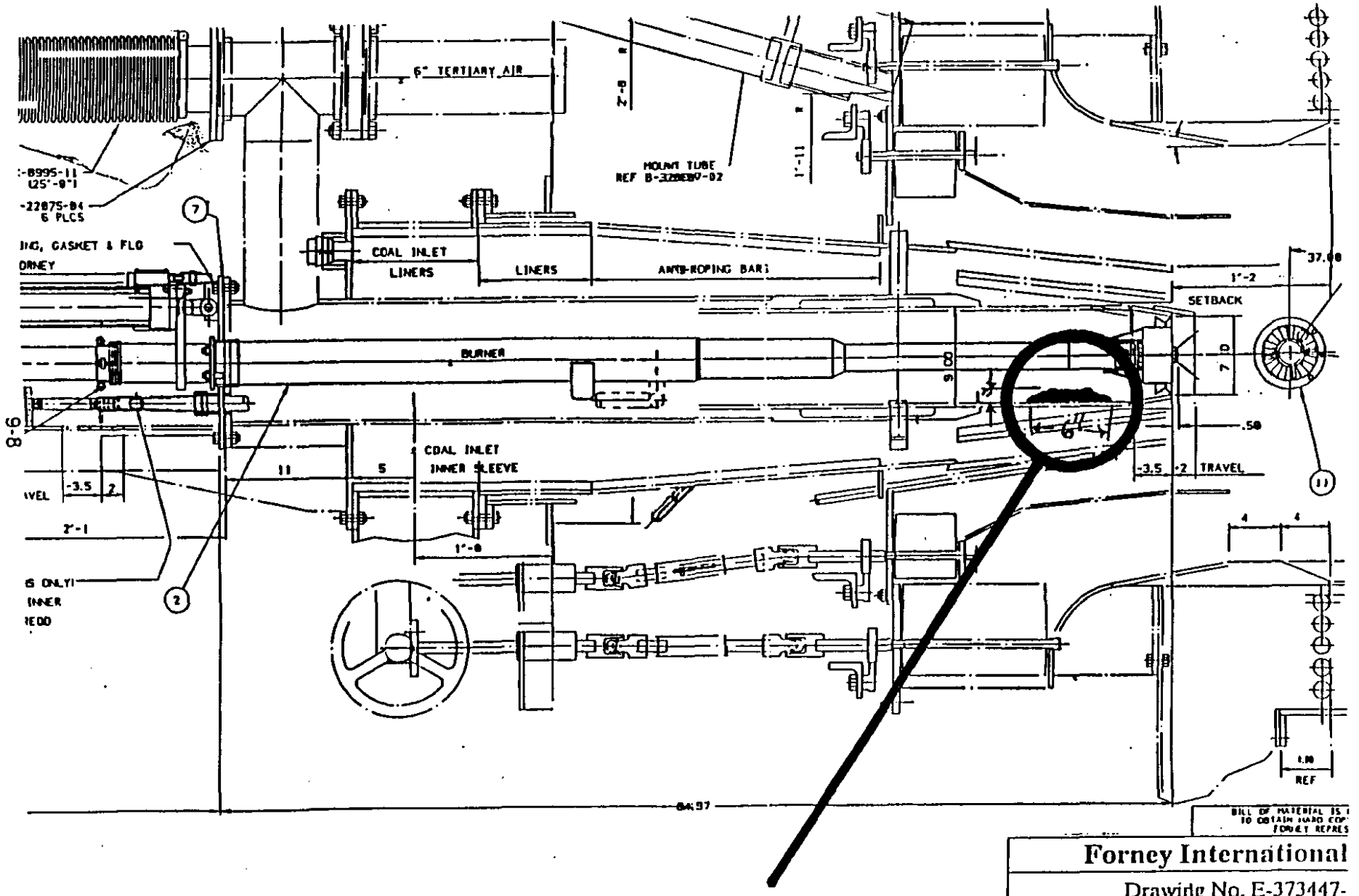

Figure 9-6 Coal Dust Accumulation

Forney International

Drawing No. E-373447-

Light Up Burner (LUF

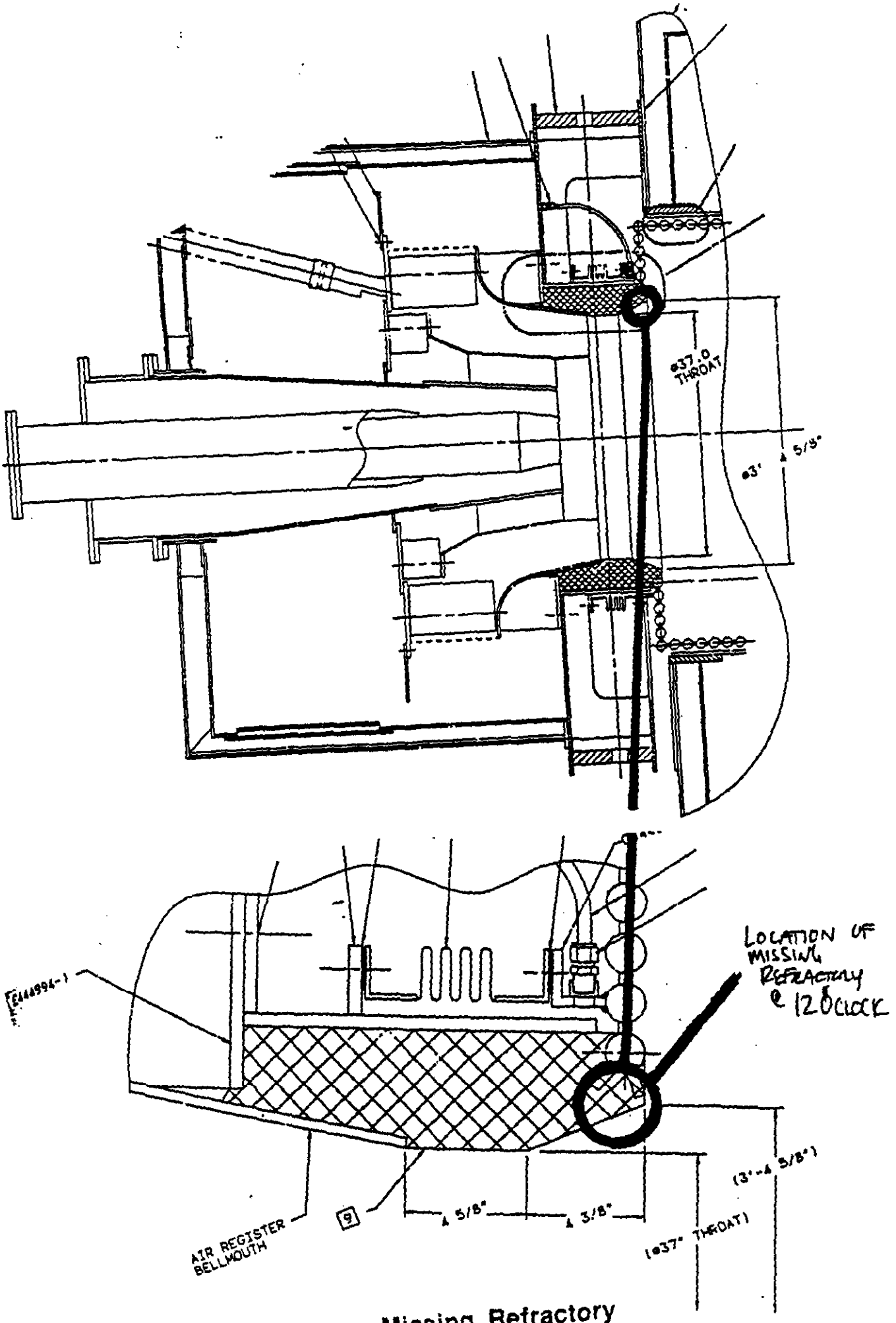

Figure 9-7 Missing Refractory

10. A patch of non-molten ash was found at the forward end of combustion chamber near top-dead-center location. This patch was only about 4" x 6" in size in an otherwise bare refractory surface. Figure 9-8 shows this condition.

11. Two oil char splotches were seen on combustion chamber surface about halfway down the length of chamber. Each splotch was about 6" in diameter and located on the "headend" side of the chamber. Figure 9-8 shows this condition.

12. A greenish/black molten layer of ash, typically 0.25" thick covered the combustion chamber over approximately 50% of its surface. Slag extended upstream about 36" from trailing edge. A clockwise swirl was apparent in the coating. This condition, shown in Figure 9-9 had been continuing for several tests.

13. Greenish/black molten ash was found on the downstream edge of the combustion chamber between 5 o'clock and 7 o'clock positions. This growth had not "bridged" with the refractory-coated transition assembly. Figure 9-9 shows this condition.

14. Ash deposits within the transition section were heaviest on the "exit end" side. The "head end" side was again free of ash. Typically, the lower half of the transition section had more ash attachment than the upper half.

15. All bare metal surfaces of the swirl damper housing and swirl blades were free of ash attachment. The water-cooled surfaces were coated with coal dust.

16. The uncooled material coupons placed near the shield tubes continued to exhibit reddish/grey heat staining. This condition started during test 3A190 as a sign of heat input from coal fines in mill air hoses.

17. The refractory which was installed to block unused mill air ports was intact.

9.2 DCFS Condition

1. Post test 3A196 inspection revealed no significant coal accumulation in splitter, cyclone inlets or cyclone exhaust manifold. Coal coverage was limited to non-uniform dusting, with no preference to top, bottom or sidewalls.

2. Coal accumulation was found in the 24" diameter mill air pipe upstream of the mill air manifold. Although the exact depth and coverage was not possible to determine due to a lack of available inspection ports, approx. 3" layer of coal fines existed in the bottom of 24" diameter pipe. This coal accumulation existed after we had purged the pipe with 25-30 K#/HR of air for several minutes. Figure 9-10 illustrates the coal accumulation.

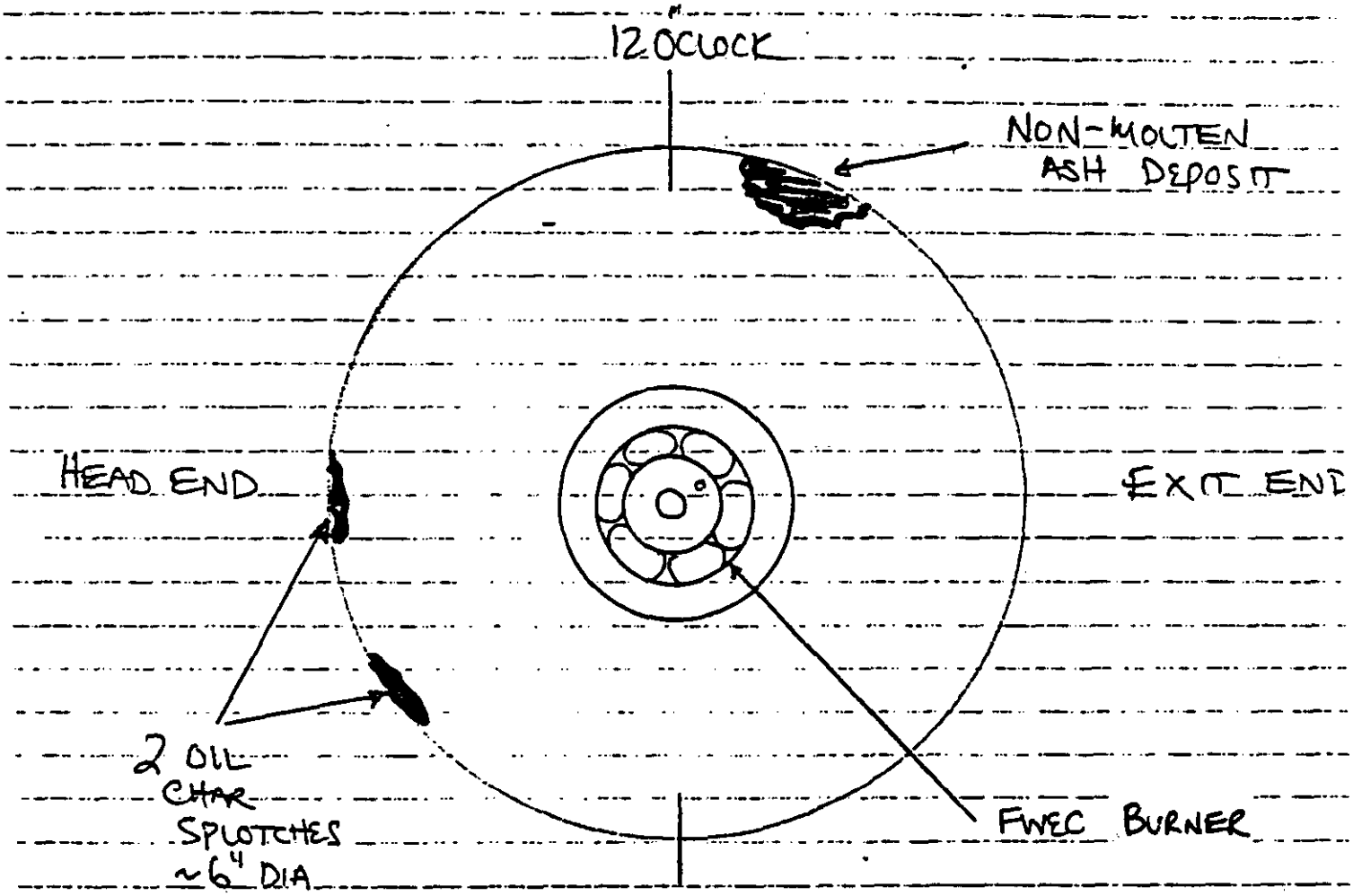

Figure 9-8 Chamber Deposits

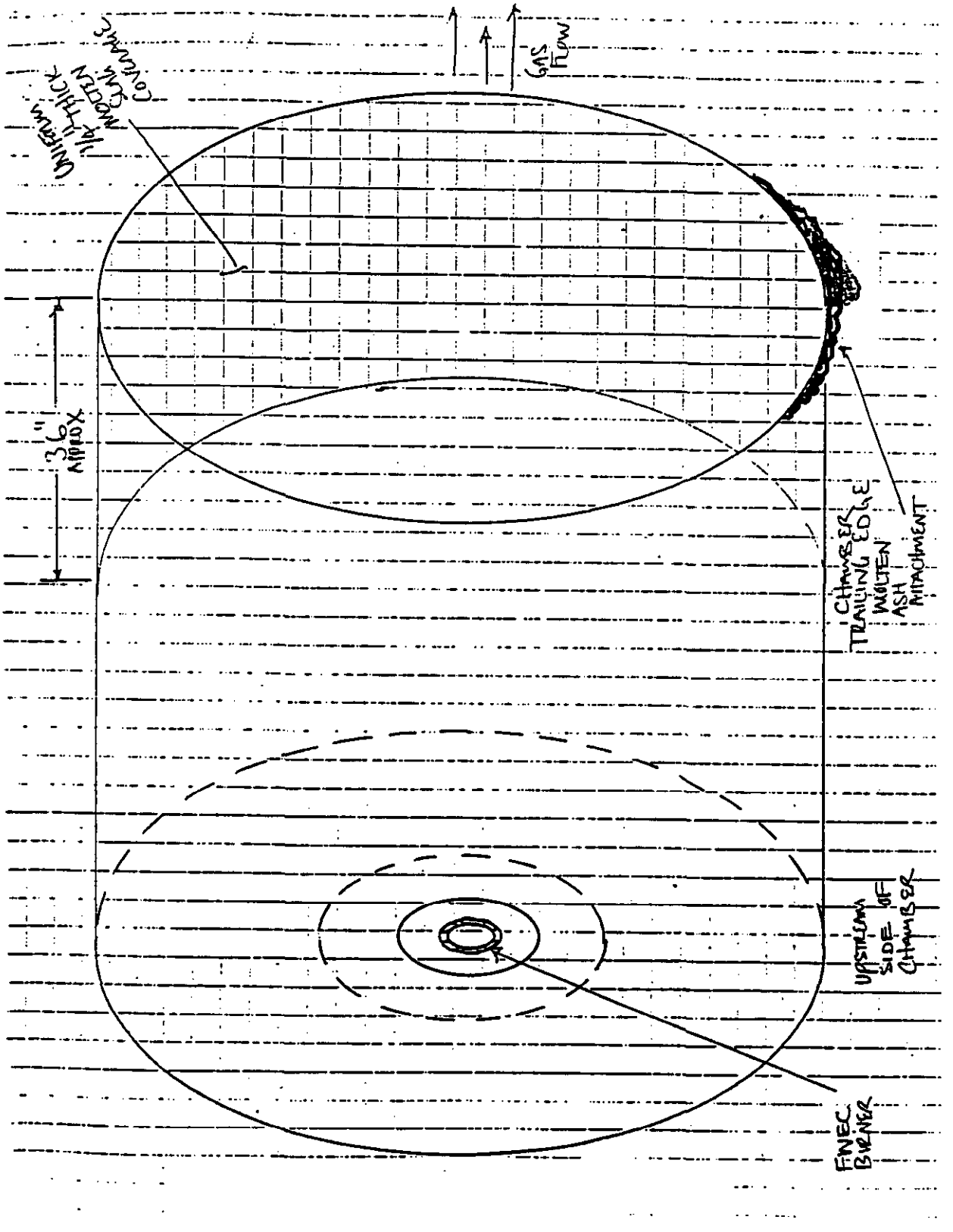

Figure 9-9 Chamber Slag Conditions

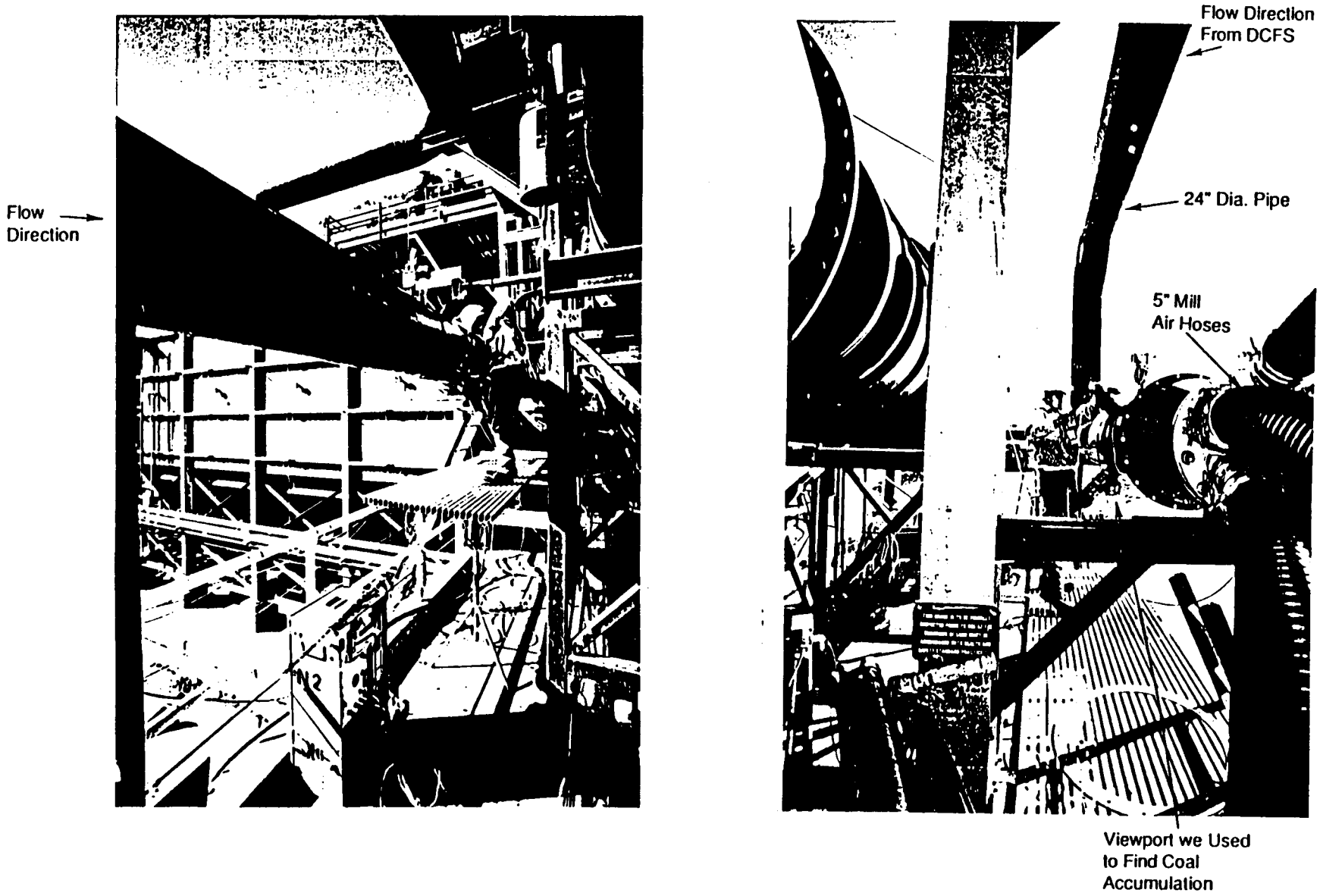

Figure 9-10 DCFS Coal Dust Accumulation

3. Flow annubars and cyclone vane actuators remain installed.

4. Coal samples from various shipments and a sample of fines removed from 24" diameter mill air pipe following 3A196 have been taken and stored in the fire locker at FETS.

9.3 General Facility Condition

1. The boiler simulator had an ash layer height reaching to within 2-3" of top of manway door. Ash along the walls and roof was non-molten, and beige-colored along the floor. Access to the boiler simulator required technicians to chisel and remove slag from entrance.

2. The scrubber was free from blockage at the drain, at the overhead mesh screen and at the nozzle interface duct. There were no signs of ash deposits remaining in scrubber.

3. All pressure transducers and thermocouples remained in place.

4. All cooling water flowmeters were replaced with spool pieces to allow circulation of cooling water as needed in the future.

5. Two J.B. Kelly coal guppies and 1 pup were washed out with water and inspected from top hatch. A vendor removed all material.

6. All Healy coal was consumed and hence none remained.

7. Ambient PM10 samples remained in satellite room #2. The SCAQMD records and other test documents are in FETS 46A engineering office.

8. Spare valves of the DCFS piping replaced during various modifications are located on first level of the DCFS structure. A few pieces of spare piping are in FETS storage yard.

APPENDIX A

COAL ANALYSES

A. COAL ANALYSES

Attachments A-1 and A-2 are the proximate and ultimate analysis for two different coal deliveries to CTS. Attachment A-3 is a representative ash content analysis performed on the coal that was consumed during testing at CTS.

Table A-1 summarizes the coal delivery dates and quantities as well as the results of the sieve analysis and moisture content tests that were performed on a sample from each delivery. Certification sheets from the sieve and moisture analyses tests are attached as Attachments A-4 through A-18.

TABLE A-1 COAL PARTICLE SIZE/MOISTURE ANALYSIS RESULTS

DELIVERY NUMBER	DELIVERY DATE	TONS DELIVERED	% THROUGH 200 MESH	MOISTURE CONTENT (%)
1	3 Aug 92	5.74	61.50	10.40
2	5 Aug 92	22.92	57.50	10.22
3	18 Aug 92	23.27	60.41	9.99
4	21 Aug 92	22.49	60.97	10.37
5	23 Oct 92	26.26	54.71	10.98
6	2 Nov 92	23.55	53.61	11.64
7	13 Nov 92	33.21	53.70	9.90
8	18 Jan 93	22.7	56.41	8.55

COMMERCIAL TESTING & ENGINEERING CO.
GENERAL OFFICES: 1919 SOUTH HIGHLAND AVE., SUITE 210-B, LOMBARD, ILLINOIS 60148 • (708) 953-9300
SINCE 1908
Member of the SGS Group (Société Générale de Surveillance)

PLEASE ADDRESS ALL CORRESPONDENCE
1921 N. GAFFEY STREET, SUITE B, SAN PEDRO, CA 9
TELEPHONE: (213) 831-133
FAX: (213) 831-189

September 1, 1992

ENERGY & ENVIRON. RESEARCH CRP
18 MASON
IRVINE CA 92718

Sample identification by EER

SAMPLE IDENTIFICATION
8-13-92
TRUCK #3 P003
SITE: EER TEST SITE
LOCATION: LARGE MILL
SAMPLE DESCRIPTION: TRW COAL NO. 136996

Kind of sample reported to us COAL

Sample taken at ------

Sample taken by ------

Date sampled ------

Date received August 14, 1992

Analysis Report No. 04-68442

PROXIMATE ANALYSIS	As Received	Dry Basis
% Moisture	9.90	xxxxx
% Ash	17.85	19.81
% Volatile	39.86	44.24
% Fixed Carbon	32.39	35.95
	100.00	100.00
Btu/lb	8405	9328
% Sulfur	0.16	0.18
MAF Btu		11632

ULTIMATE ANALYSIS	As Received	Dry Ba
% Moisture	9.90	xxxxx
% Carbon	49.92	55.40
% Hydrogen	3.67	4.07
% Nitrogen	0.69	0.77
% Sulfur	0.16	0.18
% Ash	17.85	19.81
% Oxygen(diff)	17.81	19.77
	100.00	100.00

Respectfully submitted,
COMMERCIAL TESTING & ENGINEERING CO.

Manager, San Pedro Laboratory

COMMERCIAL TESTING & ENGINEERING CO.
GENERAL OFFICES: 1919 SOUTH HIGHLAND AVE., SUITE 216 B, LOMBARD, ILLINOIS 60148 • (708) 953-9300
SINCE 1908
Member of the SGS Group (Société Générale de Surveillance)

PLEASE ADDRESS ALL CORRESPONDENCE TO
1921 N. GAFFEY STREET, SUITE B, SAN PEDRO, CA 9073
TELEPHONE: (213) 831-133
FAX: (213) 831-189

November 18, 1992

ENERGY & ENVIRON. RESEARCH CRP
8001 IRVINE BLVD
SANTA ANA CA 92705

Sample identification by
EER

SAMPLE IDENTIFICATION
SAMPLE #108934
11-2-92
7:30 A.M.
TRUCK #6
EER
LARGE MILL
COAL

Kind of sample reported to us COAL

Sample taken at ------

Sample taken by ------

Date sampled ------

Date received November 4, 1992

Analysis Report No. 04-68510

PROXIMATE ANALYSIS	As Received	Dry Basis
% Moisture	11.64	xxxxx
% Ash	17.15	19.41
% Volatile	39.59	44.80
% Fixed Carbon	31.62	35.79
	100.00	100.00
Btu/lb	8292	9384
% Sulfur	0.14	0.16
MAF Btu		11644

ULTIMATE ANALYSIS	As Received	Dry Basis
% Moisture	11.64	xxxxx
% Carbon	49.83	56.39
% Hydrogen	3.46	3.92
% Nitrogen	0.66	0.75
% Sulfur	0.14	0.16
% Ash	17.15	19.41
% Oxygen(diff)	17.12	19.37
	100.00	100.00

Respectfully submitted,
COMMERCIAL TESTING & ENGINEERING CO.

Manager, San Pedro Laboratory

COMMERCIAL TESTING & ENGINEERING CO.
GENERAL OFFICES: 1919 SOUTH HIGHLAND AVE., SUITE 210-B, LOMBARD, ILLINOIS 60148 • (708) 953-9300
SINCE 1908
Member of the SGS Group (Societe Generale de Surveillance)

PLEASE ADDRESS ALL CORRESPONDENCE
1921 N. GAFFEY STREET, SUITE B, SAN PEDRO, CA 9
TELEPHONE: (213) 831-13
FAX: (213) 831-1892

January 21, 1993

TRW
33000 PICO AVENUE
SAN CLEMENTE CA 92672

Sample identification by
TRW

SAMPLE IDENTIFICATION
TRW HEALY COAL
DALE SICHER
(714) 361-7172

Kind of sample reported to us: COAL

Sample taken at: ------

Sample taken by: ------

Date sampled: ------

Date received: January 18, 1993

Analysis Report No. 04-68558

ANALYSIS OF ASH	WEIGHT %, IGNITED BASIS
Silicon dioxide	55.68
Aluminum oxide	12.81
Titanium dioxide	0.54
Iron oxide	4.71
Calcium oxide	14.75
Magnesium oxide	2.25
Potassium oxide	2.84
Sodium oxide	1.84
Sulfur trioxide	3.67
Phosphorus pentoxide	0.16
Strontium oxide	0.19
Barium oxide	0.43
Manganese oxide	0.13
Undetermined	0.00
	100.00

Silica Value = 71.95
Base:Acid Ratio = 0.38
T_{250} Temperature = 2433 °F

Respectfully submitted,
COMMERCIAL TESTING & ENGINEERING CO

Manager, San Pedro Laboratory

COMMERCIAL TESTING & ENGINEERING CO.
GENERAL OFFICES: 1919 SOUTH HIGHLAND AVE., SUITE 210-B, LOMBARD, ILLINOIS 60148 • (708) 953-9300
SINCE 1908
Member of the SGS Group (Société Générale de Surveillance)

PLEASE ADDRESS ALL CORRESPONDENCE TO
1921 N. GAFFEY STREET, SUITE B, SAN PEDRO, CA 9073
TELEPHONE: (213) 831-133
FAX: (213) 831-189

August 5, 1992

ENERGY & ENVIRON. RESEARCH CRP
18 MASON
IRVINE CA 92718

Sample identification by
EER

SAMPLE IDENTIFICATION
7-30-92
TEST #TRW001
NO. 108792

Kind of sample reported to us: COAL

Sample taken at: ------

Sample taken by: ------

Date sampled: ------

Date received: July 4, 1992

P.O. NUMBER 48912

SAMPLE NOT DRIED BEFORE SCREENING

Analysis Report No. 04-68430

SIEVE ANALYSIS

Passing	Retained On	% Weight	CUMULATIVE RESULTS % Retained	% Passing
-----	NO. 100	8.10	8.10	91.90
NO. 100	NO. 200	30.40	38.50	61.50
NO. 200	NO. 325	28.80	67.30	32.70
NO. 325	0	32.70	100.00	0.00

Respectfully submitted,
COMMERCIAL TESTING & ENGINEERING CO.

Manager, San Pedro Laboratory

COMMERCIAL TESTING & ENGINEERING CO.
GENERAL OFFICES: 1919 SOUTH HIGHLAND AVE., SUITE 210-B, LOMBARD, ILLINOIS 60148 • (708) 953-9300
SINCE 1908
Member of the SGS Group (Societe' Generale de Surveillance)

PLEASE ADDRESS ALL CORRESPONDENCE ,
1921 N. GAFFEY STREET, SUITE B, SAN PEDRO, CA 90731
TELEPHONE: (213) 831-1331
FAX: (213) 831-1892

August 5, 1992

ENERGY & ENVIRON. RESEARCH CRP
18 MASON
IRVINE CA 92718

Sample identification by
EER

SAMPLE IDENTIFICATION
7-30-92
TEST #TRW001
NO. 108792

Kind of sample reported to us COAL

Sample taken at ------

Sample taken by ------

Date sampled ------

Date received July 4, 1992

P.O. NUMBER 48912

SAMPLE NOT DRIED BEFORE SCREENING

Analysis report no. 04-68430

MOISTURE..... 10.40 %

Respectfully submitted,
COMMERCIAL TESTING & ENGINEERING CO.

Manager, San Pedro Laboratory

COMMERCIAL TESTING & ENGINEERING CO.
GENERAL OFFICES: 1919 SOUTH HIGHLAND AVE., SUITE 210-B, LOMBARD, ILLINOIS 60148 • (708) 953-9300
Member of the SGS Group (Société Générale de Surveillance)

PLEASE ADDRESS ALL CORRESPONDENCE TO
1921 N. GAFFEY STREET, SUITE B, SAN PEDRO, CA 90731
TELEPHONE: (213) 831-1331
FAX: (213) 831-1692

August 7, 1992

ENERGY & ENVIRON. RESEARCH CRP
18 MASON
IRVINE CA 92718

Sample identification by
EER

SAMPLE IDENTIFICATION
6-5-92
TEST # TRW 002
SITE: TRW SAMPLE
LOCATION: TRUCK #2
NO. 108837

Kind of sample reported to us: COAL

Sample taken at: ------

Sample taken by: ------

Date sampled: ------

Date received: August 6, 1992

Analysis Report No. 04-68434

SIEVE ANALYSIS

Passing	Retained On	% Weight	CUMULATIVE RESULTS % Retained	% Passing
-----	No. 100	9.20	9.20	90.80
No. 100	No. 200	33.30	42.50	57.50
No. 200	No. 325	28.50	71.00	29.00
No. 325	0	29.00	100.00	0.00

Respectfully submitted,
COMMERCIAL TESTING & ENGINEERING CO.

[signature]

Authorized Agent (Laboratory)

COMMERCIAL TESTING & ENGINEERING
GENERAL OFFICES: 1919 SOUTH HIGHLAND AVE., SUITE 210-B, LOMBARD, ILLINOIS
SINCE 1919
Member of the SGS Group (Société Générale de Surveillance)

PLEASE ADDRESS ALL
1921 N. GAFFEY STREET, SUITE B, SA
TELEPHONE
FAX (2

August 7, 1992

ENERGY & ENVIRON. RESEARCH CRP
18 MASON
IRVINE CA 92718

Sample identification by
EER

SAMPLE IDENTIFICATION
8-5-92
TEST # TRW 002
SITE: TRW SAMPLE
LOCATION: TRUCK #2
NO. 108637

Kind of sample reported to us: COAL
Sample taken at: ------
Sample taken by: ------
Date sampled: ------
Date received: August 6, 1992

Analysis report no. 04-68434

MOISTURE..... 10.22 %

Respectfully submitted,
COMMERCIAL TESTING & ENGINEERING CO

COMMERCIAL TESTING & ENGINEERING CO.
GENERAL OFFICES: 1919 SOUTH HIGHLAND AVE., SUITE 210-B, LOMBARD, ILLINOIS 60148 • (708) 953-9300
SINCE 1908
Member of the SGS Group (Société Générale de Surveillance)

PLEASE ADDRESS ALL CORRESPONDENCE
1921 N. GAFFEY STREET, SUITE B, SAN PEDRO, CA 90
TELEPHONE. (213) 831-1
FAX: (213) 831-1

August 18, 1992

ENERGY & ENVIRON. RESEARCH CRP
18 MASON
IRVINE CA 92718

Sample identification by EER

SAMPLE IDENTIFICATION
8-13-92
TRUCK #3 P003
SITE: EER TEST SITE
LOCATION: LARGE MILL
SAMPLE DESCRIPTION: TRW COAL
NO. 136996

Kind of sample reported to us COAL

Sample taken at ------

Sample taken by ------

Date sampled ------

Date received August 14, 1992

Analysis Report No. 04-68442

SIEVE ANALYSIS

Passing	Retained On	% Weight	CUMULATIVE RESULTS % Retained	% Passing
-----	NO. 100	9.69	9.69	90.31
NO. 100	NO. 200	29.90	39.59	60.41
NO. 200	NO. 325	23.33	62.92	37.08
NO. 325	0	37.08	100.00	0.00

Respectfully submitted,
COMMERCIAL TESTING & ENGINEERING CO.

Manager, San Pedro Laboratory

COMMERCIAL TESTING & ENGINEERING CO.
GENERAL OFFICES: 1919 SOUTH HIGHLAND AVE., SUITE 210-B, LOMBARD, ILLINOIS 60148 • (708) 953-9300
SINCE 1908
Member of the SGS Group (Societe Generale de Surveillance)

PLEASE ADDRESS ALL CORRESPONDENCE
1921 N. GAFFEY STREET, SUITE B, SAN PEDRO, CA 90
TELEPHONE: (213) 831-1
FAX: (213) 831-1

August 18, 1992

ENERGY & ENVIRON. RESEARCH CRP
18 MASON
IRVINE CA 92718

Sample identification by EER

SAMPLE IDENTIFICATION
8-13-92
TRUCK #3 P003
SITE: EER TEST SITE
LOCATION: LARGE MILL
SAMPLE DESCRIPTION: TRW COAL
NO. 136996

Kind of sample reported to us COAL

Sample taken at ------

Sample taken by ------

Date sampled ------

Date received August 14, 1992

Analysis report no. 04-68442

MOISTURE ..... 9.99 %

Respectfully submitted,
COMMERCIAL TESTING & ENGINEERING CO.

Manager, San Pedro Laboratory

COMMERCIAL TESTING & ENGINEERING CO.
GENERAL OFFICES: 1919 SOUTH HIGHLAND AVE., SUITE 210-B, LOMBARD, ILLINOIS 60148 • (708) 953-9300
SINCE 1908
Member of the SGS Group (Société Générale de Surveillance)

PLEASE ADDRESS ALL CORRESPONDENCE TO:
1921 N. GAFFEY STREET, SUITE B, SAN PEDRO, CA 90731
TELEPHONE. (213) 831-1331
FAX: (213) 831-1892

August 28, 1992

ENERGY & ENVIRON. RESEARCH CRP
18 MASON
IRVINE CA 92718

Sample identification by EER

SAMPLE IDENTIFICATION
8-20-92
TRUCK #4 P049
NO. 136987

Kind of sample reported to us COAL

Sample taken at ------

Sample taken by ------

Date sampled ------

Date received August 26, 1992

P.O. NUMBER 49135

Analysis Report No. 04-68447

SIEVE ANALYSIS

			CUMULATIVE RESULTS	
Passing	Retained On	% Weight	% Retained	% Passing
-----	NO. 100	8.84	8.84	91.16
NO. 100	NO. 200	30.19	39.03	60.97
NO. 200	NO. 325	24.23	63.26	36.74
NO. 325	0	36.74	100.00	0.00

Respectfully submitted,
COMMERCIAL TESTING & ENGINEERING CO

Manager, San Pedro Laboratory

COMMERCIAL TESTING & ENGINEERING CO.
GENERAL OFFICES: 1919 SOUTH HIGHLAND AVE., SUITE 210-B, LOMBARD, ILLINOIS 60148 • (708) 953-9300
SINCE 1908
Member of the SGS Group (Societe Generale de Surveillance)

PLEASE ADDRESS ALL CORRESPONDENCE
1921 N. GAFFEY STREET, SUITE B, SAN PEDRO, CA 9(
TELEPHONE: (213) 831-1
FAX: (213) 831-189

August 28, 1992

ENERGY & ENVIRON. RESEARCH CRP
18 MASON
IRVINE CA 92718

Sample identification by
EER

SAMPLE IDENTIFICATION
8-20-92
TRUCK #4 P049
NO. 136987

Kind of sample reported to us COAL

Sample taken at ------

Sample taken by ------

Date sampled ------

Date received August 26, 1992

P.O. NUMBER 49135

Analysis report no. 04-68447

MOISTURE..... 10.37 %

Respectfully submitted,
COMMERCIAL TESTING & ENGINEERING CO.

Manager, San Pedro Laboratory

COMMERCIAL TESTING & ENGINEERING CO.
GENERAL OFFICES: 1919 SOUTH HIGHLAND AVE., SUITE 210-B, LOMBARD, ILLINOIS 60148 • (708) 953-9300
SINCE 1908
Member of the SGS Group (Société Générale de Surveillance)

PLEASE ADDRESS ALL CORRESPONDENCE TO
1921 N. GAFFEY STREET, SUITE B, SAN PEDRO, CA 90731
TELEPHONE (213) 831-1331
FAX: (213) 831-1892

November 2, 1992

ENERGY & ENVIRON. RESEARCH CRP
8001 IRVINE BLVD
SANTA ANA CA 92705

Kind of sample reported to us	COAL
Sample taken at	------
Sample taken by	------
Date sampled	------
Date received	October 26, 1992

Sample identification by
EER

SAMPLE IDENTIFICATION
SAMPLE #108801
10-23-92
3:30 P.M.
TRUCK #5 PO49
EER
LARGE MILL
COAL

Analysis Report No. 04-68499

SIEVE ANALYSIS

Passing	Retained On	% Weight	CUMULATIVE RESULTS % Retained	% Passing
-----	NO. 100	12.33	12.33	87.67
NO. 100	NO. 200	32.96	45.29	54.71
NO. 200	NO. 325	31.03	76.32	23.68
NO. 325	0	23.68	100.00	0.00

Respectfully submitted,
COMMERCIAL TESTING & ENGINEERING CO.

Manager, San Pedro Laboratory

COMMERCIAL TESTING & ENGINEERING CO.
GENERAL OFFICES: 1919 SOUTH HIGHLAND AVE., SUITE 210-B, LOMBARD, ILLINOIS 60148 • (708) 953-9300

SINCE 1908

Member of the SGS Group (Société Générale de Surveillance)

PLEASE ADDRESS ALL CORRESPONDENCE T
1921 N. GAFFEY STREET, SUITE B, SAN PEDRO, CA 9(
TELEPHONE: (213) 831-1
FAX: (213) 831-189

November 2, 1992

ENERGY & ENVIRON. RESEARCH CRP
8001 IRVINE BLVD
SANTA ANA CA 92705

		Sample identification by EER
		SAMPLE IDENTIFICATION
		SAMPLE #108801
Kind of sample reported to us	COAL	10-23-92
		3:30 P.M.
		TRUCK #5 PO49
Sample taken at	------	EER
		LARGE MILL
Sample taken by	------	COAL
Date sampled	------	
Date received	October 26, 1992	

Analysis report no. 04-68499

MOISTURE..... 10.98 %

Respectfully submitted,
COMMERCIAL TESTING & ENGINEERING CO.

Manager, San Pedro Laboratory

COMMERCIAL TESTING & ENGINEERING CO.
GENERAL OFFICES: 1919 SOUTH HIGHLAND AVE., SUITE 210-B, LOMBARD, ILLINOIS 60148 • (708) 953-9300
SINCE 1908
Member of the SGS Group (Société Générale de Surveillance)

PLEASE ADDRESS ALL CORRESPONDENCE TO:
1921 N. GAFFEY STREET, SUITE B, SAN PEDRO, CA 90731
TELEPHONE: (213) 831-1331
FAX: (213) 831-1892

November 18, 1992

ENERGY & ENVIRON. RESEARCH CRP
8001 IRVINE BLVD
SANTA ANA CA 92705

		Sample identification by EER
		SAMPLE IDENTIFICATION
		SAMPLE #108934
Kind of sample reported to us	COAL	11-2-92
		7:30 A.M.
		TRUCK #6
Sample taken at	------	EER
		LARGE MILL
Sample taken by	------	COAL
Date sampled	------	
Date received	November 4, 1992	

Analysis Report No. 04-68510

SIEVE ANALYSIS

Passing	Retained On	% Weight	CUMULATIVE RESULTS % Retained	% Passing
-----	NO. 100	12.07	12.07	87.93
NO. 100	NO. 200	34.32	46.39	53.61
NO. 200	NO. 325	34.05	80.44	19.56
NO. 325	0	19.56	100.00	0.00

Respectfully submitted,
COMMERCIAL TESTING & ENGINEERING CO.

Manager, San Pedro Laboratory

COMMERCIAL TESTING & ENGINEERING CO.
GENERAL OFFICES: 1919 SOUTH HIGHLAND AVE., SUITE 210-B, LOMBARD, ILLINOIS 60148 • (708) 953-9300
SINCE 1908
Member of the SGS Group (Societe Generale de Surveillance)

PLEASE ADDRESS ALL CORRESPONDENCE T
1921 N. GAFFEY STREET, SUITE B, SAN PEDRO, CA 90
TELEPHONE: (213) 831-1
FAX: (213) 831-1892

January 4, 1993

ENERGY & ENVIRON. RESEARCH CRP
8001 IRVINE BLVD
SANTA ANA CA 92705

Sample identification by
EER

SAMPLE IDENTIFICATION
SAMPLE #136982
11-11-92
2:30 P.M.
TRUCK #7
EER
LARGE MILL
COAL

AMENDED REPORT
RE-RUN ANALYSES

Kind of sample reported to us	COAL
Sample taken at	------
Sample taken by	------
Date sampled	------
Date received	December 14, 1992

Analysis Report No. 04-68539

SIEVE ANALYSIS

Passing	Retained On	% Weight	CUMULATIVE RESULTS % Retained	% Passing
-----	NO. 100	14.13	14.13	85.87
NO. 100	NO. 200	32.17	46.30	53.70
NO. 200	NO. 325	27.09	73.39	26.61
NO. 325	0	26.61	100.00	0.00

Respectfully submitted,
COMMERCIAL TESTING & ENGINEERING CO.

Manager, San Pedro Laboratory

COMMERCIAL TESTING & ENGINEERING CO.
GENERAL OFFICES: 1919 SOUTH HIGHLAND AVE., SUITE 210-B, LOMBARD, ILLINOIS 60148 • (708) 953-9300
SINCE 1908
Member of the SGS Group (Société Générale de Surveillance)

PLEASE ADDRESS ALL CORRESPONDENCE TO:
1921 N. GAFFEY STREET, SUITE B, SAN PEDRO, CA 90731
TELEPHONE: (213) 831-1331
FAX: (213) 831-1892

December 22, 1992

ENERGY & ENVIRON. RESEARCH CRP
8001 IRVINE BLVD
SANTA ANA CA 92705

Kind of sample reported to us	COAL
Sample taken at	------
Sample taken by	------
Date sampled	------
Date received	December 14, 1992

Sample identification by EER

SAMPLE IDENTIFICATION
SAMPLE #136982
11-11-92
2:30 P.M.
TRUCK #7
EER
LARGE MILL
COAL

Analysis report no. 04-68539

MOISTURE..... 9.90 %

Respectfully submitted,
COMMERCIAL TESTING & ENGINEERING CO.

Manager, San Pedro Laboratory

COMMERCIAL TESTING & ENGINEERING CO.
GENERAL OFFICES: 1919 SOUTH HIGHLAND AVE., SUITE 210-B, LOMBARD, ILLINOIS 60148 • (708) 953-9300
SINCE 1908
Member of the SGS Group (Société Générale de Surveillance)

PLEASE ADDRESS ALL CORRESPONDENCE
1921 N. GAFFEY STREET, SUITE B, SAN PEDRO, CA 90
TELEPHONE: (213) 831-13
FAX: (213) 831-1892

February 5, 1993

ENERGY & ENVIRON. RESEARCH CRP
8001 IRVINE BLVD
SANTA ANA CA 92705

Sample identification by EER

SAMPLE IDENTIFICATION
SAMPLE #148105
JAN. 18, 1993
8:00 A.M.
EER TEST SITE
TRUCK #9
COMPOSITE SAMPLE #148109

Kind of sample reported to us COAL

Sample taken at ------

Sample taken by ------

Date sampled ------

Date received January 21, 1993

Analysis Report No. 04-68563

SIEVE ANALYSIS

Passing	Retained On	% Weight	CUMULATIVE RESULTS % Retained	% Passing
-----	NO. 100	9.92	9.92	90.08
NO. 100	NO. 200	33.67	43.59	56.41
NO. 200	NO. 325	40.32	83.91	16.09
NO. 325	0	16.09	100.00	0.00

Respectfully submitted,
COMMERCIAL TESTING & ENGINEERING CO

Manager, San Pedro Laboratory

COMMERCIAL TESTING & ENGINEERING CO.
GENERAL OFFICES: 1919 SOUTH HIGHLAND AVE., SUITE 210-B, LOMBARD, ILLINOIS 60148 • (708) 953-9300
SINCE 1908
Member of the SGS Group (Société Générale de Surveillance)

PLEASE ADDRESS ALL CORRESPONDENCE TO
1921 N. GAFFEY STREET, SUITE B, SAN PEDRO, CA 90731
TELEPHONE: (213) 831-1331
FAX: (213) 831-1892

February 5, 1993

ENERGY & ENVIRON. RESEARCH CRP
8001 IRVINE BLVD
SANTA ANA CA 92705

Sample identification by EER

SAMPLE IDENTIFICATION
SAMPLE #148105
JAN. 18, 1993
8:00 A.M.
EER TEST SITE
TRUCK #8
COMPOSITE SAMPLE #148109

Kind of sample reported to us	COAL
Sample taken at	------
Sample taken by	------
Date sampled	------
Date received	January 21, 1993

Analysis report no. 04-68563

MOISTURE..... 8.55 %

Respectfully submitted,
COMMERCIAL TESTING & ENGINEERING CO.

Manager, San Pedro Laboratory

APPENDIX B

TEST DATA SUMMARY TABLES

B. TEST DATA SUMMARY TABLES

On February 2, 1993, the Design Verification Test (DVT) series was completed with a successful duration run. Overall, 43.1 hot-fire hours were accumulated on the precombustor and the DCFS was run for 22 hours. These hours were accumulated over 28 tests utilizing 160 tons of performance coal.

Table B.1 is a listing of the tests that were conducted, their objectives, and the conditions at which they were run. The first Healy test is designated as CTS test no 3A169 because it was the 169th test run in Cell 3A. The precombustor was run utilizing the CTS facility coal feed system through test 3A185. Between tests 3A185 and 3A186, the DCFS installation was completed and a series of air flow tests were performed. Table B.2 is a listing of the major precombustor data taken during each test. Table B.3 shows the major DCFS data taken starting with test 3A186. Table B.4 shows the conditions and measurements taken during the initial DCFS air flow tests.

The emissions data shown on these tables was taken as a reference and diagnostic for use during the DVT series. This emissions data has no relevance to the Healy Plant since at Healy the total precombustor/slagging combustor system will be operated. Firing only the precombustor produces higher NO_x and CO than when it is coupled to the slagging combustor. However, the CO measurements provide a good diagnostic for assessing the combustion performance of the precombustor.

Table Test Summary

Healy Clean Coal Project
Test Summary:
Precombustor DVT Series at CTS/ETS Cell 3A

CTS Test No.	Test Date	Test Objective	Hardware Config	Run Duration, Minutes			Preheat, Deg. F		Equivalence Ratio		Load, MMBtu/Hr			Results/Observations
				Duct Heater	Oil Gun	Coal PC	Oil	PC	Can	Ext	Oil	Coal	Total	
3A169	9/24/92	Coal ignition at 30 MMBtu/Hr	No Sec. Duct Htr., no ox. flows, direct coal	37	37	7	500	2000/ 2100	0.6/1.	2.8/3.7	35	35	35- 70	Stable coal ignition at 4 MMBtu/Hr hardware boks ok, oil on all time
3A170	9/25/92	Tune Coal Burner Air Register	Same As Before	N/A	117	27	500	2000/ 2100	0.8/1.2	2.8/3.3	35	85	35- 60	Good coal operation, clean slack Oil on for test duration
3A171	9/30/92	Operate Coal Burner without Oil Gun	Same As Before	N/A	82	28	500	2000/ 2100	1.0/1.2	N/A	35	30	30- 65	Test Aborted. Unsteady Test.
3A172	9/30/92	Same As Before	Delta P Coal On. No O2, Sec. Duct Htr.	N/A	84	52	500	2000/ 2100	1.0/1.2	1.7/2.8	10- 65	33- 75	35- 110	Good test. Stable coal flame. No O2 used. No Sec. Duct Htr.
3A173	10/6/92	Coal at 120 MMBtu/Hr w/o Oil	Tert. Orifices installed O2 Funct., Sec. Duct ok	7	101	84 5.0-*	500	2000/ 2100	1.0/1.2 1.0-*	3.0/4.9 2.0-*	30	120 120-*	30- 120	Great test! Everything Operational 120 mmBtu/hr coal, No oil
3A174	10/7/92	Reduce delta P on burner - coal at 120 MMBtu/HR	Coal burner retracted	N/A	84	42	500	2000/ 2100	1.0/1.5 1.2-*	2.4/3.7 3.0-*	30	37- 75 75-*	37- 105	Coal burner delta P dropped by 1- 2" H2O, Burner face temp same
3A175	10/8/92	Operate coal at 120 MMBtu/HR	Coal burner retracted	N/A	170	124	500	2000/ 2100	0.8/1.0	1.7/2.4	30	37- 134 134-*	35- 134	Great Test! Coal flow stable - primary at at 500- 700 deg F
3A176	10/13/92	Begin test matrix, C-series-coal Burner tuning	Coal burner retracted Register vanes adjusted	N/A	76	31	500	2230	0.85	2.5	30	70	30- 100	Computer locked up - test aborted
3A177	10/15/92	80% MCR D-series, Damper Checkout E-series, Load/phi sweep	Same as before	N/A	157	129	500/ 700	2300	0.85	2.1	30	84-*	30- 110	Great test! PC blade operate well. Coal stable, ductheater fire.
3A178	10/20/92	80% MCR C-series - try again E-series-repeat F-series-preheat sweep	Adjust Inner/Outer Vanes	N/A	102	105	700/ 750	2700	0.7, 0.85, 1.0	1.7/2.0	30	84	30- 84	Coal burner operate best with higher swirl (Inner vanes 25% open, outer vanes 30% open)
3A179	10/21/92	80% MCR E-series-continue F-series-continue	No changes	N/A	82	98	400/ 700	2700	0.85	1.5/2.4	30	84	30- 84	Coal burner stable at 80% MCR, 400 deg F preheat
3A180	10/22/92	80% MCR E-series-continue F-series-continue H-series-damper test	Thermocouple at PC Ext installed 3.6" 3" coal line moved	N/A	67	133	400/ 700	2550	0.85	1.9	30	105	30- 105	Coal burner stable at 80% MCR, 400 deg F preheat
3A181	10/28/92	100% MCR E-series-continue F-series-continue	Accelerometer installed Scrubber sampler Blades at 375 Rb	N/A	27	76	600/ 700	2800	0.85/1.0	2.12	30	118	30- 118	At fans limit phi ext to 1.9 at 100% MCR - Steady test
3A182	10/30/92	100% MCR E-series-continue F-series-continue	Blades at 375 Rb	N/A	155	112	500/ 700	2900	0.70/0.85	1.5/2.1	30	118	30- 118	Pressure spikes observed. Another steady test
3A183	11/03/92	Repeat conditions E3 and F3, Flame scanner checkout	Same as before	N/A	57	74	500/ 700	2000/ 2400	0.85/1.0	1.83/3.	30	85	30- 105	Great test at conditions. 27 psi Atomization pres. solves lift off prob. 82 MMBtu/hr max for oil gun
3A184	11/04/92	Flame scanner checkout cont.	Coal scanner online	N/A	68	84	500/ Ambient	2300	1.0	2.5	30	60	30- 85	Flame scanner at Forney port - Lose signal when carb turned on. Flame may move outbound of view port.
3A185	11/16/92	Healy Start Up Simulation	No tertiary air, low oil atomization pressure	N/A	137	88	300	2150	0.78/1.3	1.7/2.8	30	70	30- 100	Good start up simulation, oil gun does not atomize well at low pressure
				Totals...	2868 lbs.	2114 lbs.								

* - At maximum coal only load

Table Test Summary - Continued

Healy Clean Coal Project
Test Summary:
Direct Coal Feed System (DCFS) DVT Series at CTS/FETS Cell 3A

CTS Test No.	Test Date	Test Objective	Hardware Config.	Run Duration, Minutes			Preheat, Deg. F		Equivalence Ratio		Load, MMBtu/Hr			Results/Observations
				Duct Heater	Oil Gun	Coal PC	Oil	PC	Can	Ext	Oil	Coal	Total	
DCFS1 to DCFS3	11/24/92 to 12/01/92	Air flow only tests DCFS Matrix tests 2.1's, 2.2's and 2.3's	---	-----	---	---	---	---	---	---	---	---	---	Good air flow test data obtained
3A186	12/03/92	First PC Hot-fire using DCFS	Nominal PC Config. New shielded TC installed	---	137	40	350/ 500	---	0.85	---	70	63	20- 70	Oil gun clean life at 20. Dirty between 30- 60. Clean after 60. On coal only at 63 for 6 mnh. Abort on minor puff.
3A187	12/08/92	PC Hot Fire tests DCFS Matrix tests 3.1- 1 and 3.2- 1	Same as before	---	123	108	350/ 500	2250	0.85	2.4	70	100	20- 100	Clean oil life with no preheat. Good condition at 3.1- 1. Abort on high coal feed line delta P during ramp up to 3.2- 1- Coal accumulation observed post test in connect duct.
3A188	12/11/92	DCFS Matrix Tests 3.2- 1	Same as before	---	84	78	350/ 500	2393	0.85	2.4	70	100	20- 100	Fairly clean oil at 30/50. Good 3.1- 1. Coal accumulation experienced again during ramp up.
3A189	12/16/92	DCFS Matrix test 3.2- 1 - AIDEA visit -	Modified cyclone inlet connecting ducts for 100 f/s	---	65	104	350/ 500	2383	0.85	2.4	70	126	20- 126	Good test burn. However, cyclone inlet pressure too high at full load
3A190	12/23/92	backhalls Test, Adjust Outer register valves, lower carrier flow	Instrument downstream coal feed line components, add reducing elbow, add vent P transducer	---	90	170	350/ 500	2425	0.80	2.2/ 2.4	70	125	30- 125	Rough coal burn. backhalls samples taken, large oscillation with secondary air. Cyclone inlet pressure still high.
3A191	1/16/93	1BT test with split DCFS cyclones	#1 cyclone Pvp #2 cyclone - PC See notes	---	113	38	350	2430	0.75	2.1	10			Coal flow steady in 6 seconds. PC flame stable entire test. DCFS pressure stable. Coal pup says we sent all coal to PC. Oil gun still dirty for 30- 50 MBtu/hr at 0 = 1.3 - 1.6. No blockage in calib cyclone
3A192	1/20/93	2nd test with split cyclones	100% open on both cyclone vanes	500°F not 350°F	230	165	500TAPPC 78°TASPC	2300	0.62- 0.80	2.1/ 2.4	10	63		A good overall test confirming desired controllable coal split. Although we lost pup scales and calib cyclone carrier flow rates during test. See notes No significant coal accum in DCFS Abort S/D
3A193	1/22/93	backhalls tests	Split cyclones	---	187	1176	350/ 500	2300	0.82	2.1	0	60		O2% measurements high 3% until 17:05. Pup scales not working on site. Precombustor flame/stack stable. No coal accumulation in DCFS. Oil gun dirty at 30- 50MBtu/hr still.
3A194	1/25/93	Symmetric and unsymetric cyclones	Split cyclones	---	108	116	350/ 500	2300	0.82	2.1	10	70		Good test in terms of info learned. Pup coal flow titration was after 27 minutes we still don't understand what prevents coal flow. This test assumed 40:60CPO split. Abort to bp.
3A195	2/1/93 (n/a)	Duration checkout test	Y- connected DCFS reconfig millhouse.	---	104	82	350/ 500	2300	0.83	2.1	10	120		First test with carrier fan repaired wheel and starter. Test delayed to fix starter. Ran 30 mh @100% MCR to checkout new DCFS connection. DCFS and PC stable.
3A196	2/2/93 (n/a)	Duration test @100% MCR	Same as 3A195	---	150	273	350/ 740	2300	0.83	2.1	10	120		DCFS and PC operating very smooth @100% MCR using "2nd generation" coal. We could have continued, but no coal. PC blades not in to keep air flow unrestricted. Emissions good.

Table 2 Major PC Data

Healy Clean Coal Project
Test Summary:
Precombustor DVT Series at CTS/FETS Cell 3A

DVT Test No.	CTS Test No.	Test Date	PC Heat Fluxes, Btu/S/Ft2							PC Heat Loss, MMBtu/HR	Emissions Data				Results/Observations
			Baffle	Can	Trans.	Mill Air Spool	Swirl Housing	HE Damper	Exit Damper		O2, %	CO PPM	NOx@3%O2 PPM	CO2, %	
1	3A169	9/24/92	2	3	1.25	1.25	7.5/12–a	15	18/30–a	2.0	13–16	100–750	225–850	3–7	Stable coal ignition at 4 MMBtu/Hr hardware looks ok, oil on all time
2	3A170	9/25/92	1.5	3	1.4	1.25	7.5/12–a	15	23/30–a	1.9	N/A	200	N/A	1.5	Good coal operation, clean stack Oil on for test duration
3	3A171	9/30/92	N/A	N/A	N/A	N/A	N/A	N/A	N/A	N/A	N/A	N/A	N/A	N/A	Test Aborted. Unsteady Test.
4	3A172	9/30/92	1.5	3	1.25	1	10	15	18/30–a	2.5	11–16	200–750	200–600	3–8	Good test. Stable coal flame. No O2 used. No Sec. Duct Htr.
5	3A173	10/6/92	1.8	3	1.25	1.5	6/11–a	10/22–a	18/30–a 24–b	2.5	9–16 9–b	180–1500 180–b	300–800 800–b	3–12 12–b	Great test Everything Operational 129 mm Btu/hr coal, No oil
6	3A174	10/7/92	1.8/1.8–a 2–b	3/3.6–a 3.9–b	1.25	1.5	6.5/11.2–a	11/19–a	18/30–a	2.5	11.2–16.5 13–b	160 – 1500 180–b	100–400 400–b	3.6–9 7.8–b	Coal burner delta P dropped by 1–2" H2O. Burner face temp. same
7	3A175	10/8/92	1.2/2.5–a 1.8–b	2.5/4.4–a 3.1–b	.8/1.8–a 1.2–b	1.25/2.2–a 1.25–b	6.6/12.5–a 12.5–b	11/24–a 24–b	18/30–a 26–b	2.5	8.2–16 8.2–b	150–1500 180–b	80 – 550 480–b	3.3–12 12.–b	Great Test! Coal flow stable – primary air at 600–700 deg F
8	3A176	10/13/92	1.5/2–a	2.5/3.8–a	0.8/1.25–a	1.25/1.8–a	5.8/11–a	13/22–a	38/62–a	2.5	12–16	188–975	80–450	3–6.5	Computer locked up – test aborted
9	3A177	10/15/92	1.25/1.8–c	2.5/3.7–c	1.25	1.25/1.8–c	12	18	25	2.5/3.1–c	11	140	550	10.5	Great test! PC blade operate well. Coal stable, duct heaters lite.

a – Heat Fluxes – 1st Number Oil On, 2nd Number, Coal or Oil+Coal On

b – At maximum coal only load

c – 1st number at 500 F preheat
2nd number at 700 F preheat

Table 2 Major PC Data - Continued

STEADY STATE CONDITION SUMMARY (Coal only conditions)

Test	Condition	Coal (MM Btu/hr)	Phi Can	Phi Exit	Preheat (F) PA/SA	Emissions			Heat Loss (MM Btu/hr)	Heat Fluxes (Btu/s/ft^2)						
						CO (ppm)	NO_x at 3% O_2 (ppm)	O_2 (%)		PC Baffle	PC Can	PC Mill Air	PC Trans.	PC Damper Housing	Headend Damper	Exit Damper
178	E1 16:25:00 to 17:00:00	85	0.8	1.8	700/700	150	550	9	3.0	2.5	3.7	2	1.25	10	9.4	16
	E3 17:04:00 to 17:11:00	85	0.95	1.88	700/700	135	550	10	3.7	2.5	3.7	2	1.3	13.8	22	32
	E2 17:13:00 to 17:18:00	85	0.65	1.6	700/700	150	550	8	3.2	2.5	3.7	2	1.3	10	18	23
	F4 17:24:00 to 17:30:00	85	0.8	1.75	750/750	145	550	8	3.2	2.5	3.7	2	1.3	10	20	22
	F3 17:32:00 to End	85	0.8	1.75	700/700	138	575	9.5	2.9	2.5	3.7	2	1.3	9.4	18	19
179	E8 18:04:00 to 18:11:00	86	0.8	1.44	700/700	140	500	7.5	3.0	2.2	3.7	2	1.3	9.4	18	19
	E9 18:13:00 to 18:22:00	86	0.8	2.31[1]	700/700	115	500	10[7]	3.2	2	3.7	2	1.3	10	20	22
	E1 18:25:00 to 18:31:00	86	0.8	1.75	700/700	138	550	9	3.0	2	3.7	2	1.3	10	19	21
	F2 18:33:00 to 18:38:00	86	0.8	1.75	500/500	1387	525	8	2.7	2	3.1	2	1.2	8.8	15.6	17.5
	F1 18:40:00 to 18:51:00	86	0.8	1.75	400/400	130	525	9	2.5	2	3.1	2	1.2	8.1	14.4	16
	F1 18:52:00 to 18:55:00	86	0.8	1.75	400/400	130	525	9	2.3	2	2.5	2	1.2	7.5	13.8	16

Table 2 Major PC Data - Continued

STEADY STATE CONDITION SUMMARY (Coal only conditions)

Test	Condition	Coal (MM Btu/hr)	Phi Can	Phi Exit	Preheat (F) PA/ SA	Emissions			Heat Loss (MM Btu/hr)	Heat Fluxes (Btu/s/ft^2)						
						Co (ppm)	NO_x at 3% O_2 (ppm)	O_2 (%)		PC Baffle	PC Can	PC Mill Air	PC Trans.	PC Damper Housing	Headend Damper	Exit Damper
180	E7 12:24:00 to 12:45:00	105	0.8	1.94	725/ 725	150	600	9.5	3.25	3	3.8	2	1.2	11	22.5	24
	F6 12:47:00 to 12:57:00	105	0.8	1.94	750/ 750	155	625	9.5	3.3	3	3.8	2	1.2	11	23	24
	F5 12:58:00 to 13:10:00	105	0.8	1.94	400/ 400	145	600	10	2.6	2.5	3	1.8	1.2	9	16	19.5
	H1 13:13:00 to 13:26:00	105	0.8	1.94	750/ 750	155	600	10	3.5	2.5	3.8	1.8	1.2	13	23	31
181	E4 16:41:00 to 16:53:00	118	0.8	1.81	750/ 750	135	575	9.5	5.4	3	5	2.5	1.9	22	54	57
	F8 16:59:00 to 17:08:00	118	0.8	1.81	600/ 600	135	575	9.5	4.8	2.5	4.4	2.4	1.9	19.4	51	48
	E6 17:10:00 to 17:20:00	118	0.9	1.81	750/ 750	145	625	9.2	5.4	2.5	4.4	2.5	1.9	24	60	53
182	E10 09:54:30 to 10:04:00	121	0.8	1.44	750/ 750	1627	400	6	3.9	3.1	4.3	1.9	1.2	13	24	33
	F7 11:38:00 to 11:45:00	121	0.8	1.81	500/ 500	148	450	9	3.2	3.1	3.8	1.9	1.2	10	17	24
	E5 11:49:00 to 11:58:00	121	0.67	1.68	750/ 750	165	450	8.2	4.0	3.0	4.4	1.8	1.2	11	21	29
	10:16:00 to 10:22:00	121	0.8	1.81	500/ 1507	135	450	9.8	2.3	2.5	2.5	1.2	1.2	7.5	12	16

Table 2 Major PC Data - Continued

STEADY STATE CONDITION SUMMARY (Coal only conditions)

Test	Condition	Coal (MM Btu/hr)	Phi Can	Phi Exit	Preheat (F) PA/ SA	Emissions			Heat Loss (MM Btu/hr)	Heat Fluxes (Btu/s/ft^2)						
						CO (ppm)	NO_x at 3% O_2 (ppm)	O_2 (%)		PC Baffle	PC Can	PC Mill Air	PC Trans.	PC Damper Housing	Headend Damper	Exit Damper
183	F3 16:53:00 to 17:03:00	88	0.75	1.69	600/ 600	155	525	8	2.8	1.8	3.1	1.9	1.2	10	16	24
	E3 17:05:00 to 17:15:00	88	0.95	1.7	700/ 700	150	525	9	2.8	1.9	3.1	1.9	1.2	9.4	17.5	19
184	15:01:00 to 15:10:00	62	0.98	2.4	500/ 500	105	500	12.5	2.4	1.9	3.7	1.4	1.2	11	*	*

* - Dampers not inserted

Table 2 Major PC Data - Continued

CONDITION SUMMARY

Test	Condition	Oil (MMBtu/hr)	Coal (MMBtu/hr)	Phi Can	Phi Exit	Preheat PA/SA (F)	Coal Carrier * (KPPH)		Emissions (ppm)		Exit Temps (F)		Delta P's (H_2O) ****	
							Air	N_2	CO	NOx @ 3% O_2	Calc'd	Meas'd ***	Coal Feed Line	Coal Burner
1	15:42:00 to 15:47:00	70	0	1.13	2.5	300/ 300	0	0	100	125	**	2320	2	0
	15:52:15 to 15:57:00	70	0	1.10	2.5	300/ 300	9	1.6	100	125	**	2080	2.5	4.25
	16:09:30 to 16:19:00	70	34	0.80	1.75	300/ 300	12	1.6	110	275	**	2200	5.0	7.0
1BS	16:35:00 to 16:40:00	36	70	0.78	1.75	300/ 300	12	1.6	125	350	**	2200	7.25	7.75
	16:48:00 to 17:00:00	0	71	1.2	2.69	300/ 300	12	1.6	160-220	450	2160	1920	7.25	8.0
	17:05:00 to 17:10:00	36	68	0.80	1.75	300/ 300	12	1.6	110	350	**	2320	6.75	7.6
	17:27:30 to 17:34:00	0	71	1.18	2.62	300/ 300	12	1.6	90	125	**	2160	3.5	6.1

* No tertiary air on during test

** Based on coal only conditions

*** Type S thermocouple, 3.5" insertion depth

**** No signs of plugging during test

Table 2 Major PC Data - Continued

Test	Condition Summary	Coal (MMBtu/Hr)	Phi		Preheat IA/SA	Emissions			Heat Loss (MMBtu/Hr)	Heat Fluxes (Btu/Hr/ft^2)							PC Chamber Pressure (H_2O)	PC Exit Temp. (°F)
			Can	Exit		Co (ppm)	NO_x@3% (ppm)	O_2 (%)		PC Baffle	PC Can	PC Mill Air	PC Trans.	Damper Housing	Headend Damper	Exit Damper		
186	3.1-1 15:36:00 to 15:44:00	63	0.88	2.44	500/ 500	150	500	12.5	3.0	2.5	3.75	1.8	1.9	14.	---	---	9.4	1920
187	3.1-1 14:40:00 to 14:50:00	63	0.88	2.44	500/ 500	180	550	12.5	2.45	1.9	3.1	1.25	1.9	11	---	---	8.3	2240
188	3.1-1 14:40:30 to 14:43:30	68	0.80	2.38	500/ 130	140	475	12	2.8	1.9	2.5	1.3	1.9	10	---	---	8.3	2200
189	3.1-1 14:48:30 to 14:51:30	63	0.90	2.44	500/ 80	200	480	12	2.3	1.9	3.2	1.3	1.3	10	---	---	6.8	1920
	3.2-1 15:40:00 to 15:50:00	124	0.90	2.2	500/ 80	140	480	11.8	1.6	1.3	1.9	0.6	1.2	8.1	---	---	27	1440
190	3.1-1 16:52:00 to 16:57:00	62	0.85	2.5	500/ 500	95	525	12.8	2.8	1.9	3.75	1.9	1.9	13.1	---	---	8.8	2200
	3.2-1 17:47:00 to 17:52:00	125	0.82	2.1	500/ 530	115	525	10.2	2.6	1.9	3.75	1.3	1.25	11.9	---	---	31	1520
192	4.3-5 18:32:00 to 18:37:45	60	0.86	2.1	350/ 70	150	577	10.8	5.8	2.5	2.7	1.0	1.5	13.3	---	---	8.7	2160
193	4.4-5 18:57:00 to 19:12:00	62	0.80	2.0	500/ 500	100	465	10.8	2.8	2.3	3.5	1.3	1.6	15.0	---	---	9.3	2330
194	4.5-1 17:43:00 to 18:00:00	75	0.87	2.0	500/ 500	125	334	10.8	2.3	1.9	3.3	1.3	1.3	11.7	---	---	11.3	2220
195	E4 23:58:00 to 00:06:00	125	0.78	1.8	720/ 500	175	549	8.75	2.7	2.2	3.7	1.7	1.4	11.7	---	---	22.7	1750
196	E4 22:30:00 to 22:46:00	125	0.80	2.0	720/ 720	150	620	11.2	3.3	2.5	5.0	1.7	1.3	16.7	---	---	28.3	1750

Table 2 Major PC Data - Continued

Test	Condition Summary	Cool (MMBtu/Hr)	Phi		Preheat PA/SA	Emissions			Heat Loss (MMBtu/Hr)	Heat Fluxes (Btu/S/ft^2)							PC Chamber Pressure (H_2O)	PC Exit Temp. (°F)
			Can	Exit		Co (ppm)	NO_x@3 % (ppm)	O_2 (%)		PC Baffle	PC Can	PC Mix Air	PC Trans.	Damper Housing	Headend Damper	Exit Damper		
186	3.1-1 15:36:00 to 15:44:00	63	0.88	2.44	500/ 500	150	500	12.5	3.8	2.5	3.75	1.8	1.9	14	---	---	9.4	1920
187	3.1-1 14:40:00 to 14:50:00	63	0.88	2.44	500/ 500	180	550	12.5	2.65	1.9	3.1	1.25	1.9	11	---	---	8.3	2240
188	3.1-1 14:40:30 to 14:43:30	60	0.80	2.38	500/ 130	148	475	12	2.8	1.9	2.5	1.3	1.9	10	---	---	8.3	2200
189	3.1-1 14:48:30 to 14:51:30	63	0.90	2.44	500/ 80	200	480	12	2.3	1.9	3.2	1.3	1.3	10	---	---	6.8	1920
	3.2-1 15:60:00 to 15:50:00	124	0.90	2.2	500/ 80	148	480	11.0	1.6	1.3	1.9	0.6	1.2	8.1	---	---	27	1440
190	3.1-1 16:52:00 to 16:57:00	62	0.85	2.5	500/ 500	95	525	12.8	2.8	1.9	3.75	1.9	1.9	13.1	---	---	8.8	2200
	3.2-1 17:47:00 to 17:52:00	125	0.82	2.1	500/ 530	115	525	10.2	2.6	1.9	3.75	1.3	1.25	11.9	---	---	31	1520

Table 3 Major DCFS Data

Test	Condition Summary	Blow Down Ratio	Flows (KPPH)				Cyclone Inlet Pressure (H_2O)	Splitter Delta P (H_2O)		Cyclone Delta P (H_2O)		Bloudown Delta P (H_2O)	
			Cyclone Inlet	Cyclone Vent	Bloudown	Carrier H_2		Left	Right	Left	Right	Left	Right
186	3.1-1 15:36:00 to 15:44:00	28	41.6	30	11.6	1.6	42.5	1.25	1.25	3.8	3.8	9.4	9.4
187	3.1-1 14:40:00 to 14:50:00	30.4	40.6	28.1	12.3	1.6	40	1.5	1.8	3.8	4.1	---	10
188	3.1-1 14:40:30 to 14:43:30	24.8	49.1	36.9	12.2	1.6	50	1.6	1.6	4.9	4.9	11.9	11.9
189	3.1-1 14:48:30 to 14:51:30	30.4	40.6	28.1	12.3	1.6	47.5	2.75	2.75	3.0	3.0	10	10
	3.2-1 15:40:00 to 15:50:00	30.4	40.6	28.1	12.3	1.6	80	3.9	3.9	5.25	5.25	12.5	12.5
190	3.1-1 16:52:00 to 16:57:00	25.0	40.1	30	10.0	1.6	45	2.75	2.9	3.1	3.1	8.75	9.0
	3.2-1 17:47:00 to 17:52:00	24.0	39.6	30	9.6	1.6	82	3.5	3.5	4.25	4.25	10.8	11.0
192	4.3-5 18:32:00 to 18:37:45	25.8	38.7	28.7	10.0	1.6	40.0	3.3	3.5	4.0	4.2	9.6	9.6
193	4.4-5 18:57:00 to 19:12:00	21.6	38.4	30.1	8.3	1.6	48	2.3	3.8	4.6	4.0	12.7	11.6
194	4.5-1 17:43:00 to 18:00:00	32	38.0	25.8	12.2	1.6	44	3.3	3.3	3.6	3.6	8.9	8.9
195	E4 23:58:00 to 00:06:00	21	37.0	29.2	7.8	1.6	59.2	3.4	2.8	3.1	3.8	8.1	8.8
196	E4 22:30:00 to 22:46:00	30.3	38.6	26.9	11.7	1.6	60.7	3.2	3.0	8.0	8.0	8.6	8.1

Table 4 DCFS Air Flow Test Data

Test	Sym. Damper Setting	Flow In (kpph)	Flow Vent (kpph)	Flow Bd (kpph)	Mat. Bal. (%)	#1 Blow Down Ratio	#2 Blow Down Ratio	Inlet Press ("h2o)	Avg. Split DP	Avg. DP cyc ("h2o)	Avg. DP bd ("h2o)	Rho In (#/ft3)	Splitter Inlet Vel. (ft/s)	"Q Splitter ("h2o)	Cyclone Inlet Vel. (ft/s)	Q Cyclone ("h2o)	DP/Q Splitter	DP/Q Cyclone	DP/Q Blowdown
2.1-1	100	39.98	41.07	0.00	102.73	-2.7	0.0	12.75	0.95	5.96	0.00	0.0729	48.99	0.52	53.9	0.633	1.82	7.99	0.00
2.1-1	100	39.92	41.02	0.00	102.76	-2.8	0.0	31.72	0.88	4.95	0.00	0.0762	46.79	0.50	51.5	0.604	1.77	8.20	0.00
2.1-1	100	40.03	41.25	0.00	103.05	-3.0	0.0	56.26	0.85	4.71	0.00	0.0805	44.42	0.47	48.9	0.575	1.79	8.19	0.00
2.1-1	100	40.12	40.75	1.18	104.51	-1.6	2.9	80.16	0.83	4.51	0.00	0.0811	44.15	0.47	48.6	0.573	1.76	7.87	0.00
2.1-2	75	40.12	40.57	0.77	103.84	-1.1	1.9	59.73	0.81	5.12	0.00	0.0811	44.19	0.47	64.9	1.019	1.71	6.01	0.00
2.1-3	50	40.00	40.79	0.44	103.08	-2.0	1.1	59.74	0.81	8.93	0.00	0.0811	44.06	0.47	87.0	2.278	1.72	3.92	0.00
2.1-4	100	29.43	31.29	0.00	106.32	-6.3	0.0	7.20	0.57	2.92	0.00	0.0720	36.51	0.21	48.2	0.347	1.99	8.41	0.00
2.1-4	100	29.84	30.80	0.00	106.80	-6.8	0.0	61.29	0.47	2.48	0.00	0.0814	31.64	0.24	34.8	0.295	1.93	8.41	0.00
2.1-5	75	29.94	31.21	0.63	106.35	-4.2	2.1	59.78	0.48	3.63	0.00	0.0811	32.95	0.26	48.4	0.567	1.82	6.39	0.00
2.1-6	50	29.85	30.93	0.47	105.19	-3.6	1.6	60.75	0.47	4.99	0.00	0.0813	32.78	0.26	72.2	1.265	1.80	3.94	0.00
2.1-7	100	40.20	40.93	0.15	102.19	-1.8	0.4	41.27	0.89	4.68	0.00	0.0778	46.11	0.49	50.8	0.599	1.80	7.78	0.00
2.1-7	100	39.96	40.48	0.44	102.48	-1.3	1.1	13.48	0.89	4.95	0.00	0.0730	48.87	0.52	53.8	0.631	1.71	7.84	0.00
2.1-8	100	40.01	41.39	0.31	104.23	-3.4	0.8	58.62	0.85	4.56	0.00	0.0809	44.18	0.47	48.6	0.571	1.80	7.98	0.00
2.1-8	100	39.98	40.92	0.35	103.23	-2.4	0.9	61.29	0.88	4.75	0.00	0.0778	45.86	0.49	50.5	0.593	1.80	8.02	0.00
2.2-1	100	39.46	36.07	3.99	101.52	8.6	10.1	11.12	0.80	4.93	8.12	0.0726	48.53	0.51	53.4	0.619	1.76	7.96	13.12
2.2-2	100	40.10	32.77	7.80	101.17	18.3	18.5	17.47	0.92	5.00	9.37	0.0737	48.58	0.52	53.5	0.630	1.77	8.08	14.88
2.2-3	100	40.12	28.27	11.76	99.78	29.5	29.3	21.12	0.91	5.01	10.90	0.0754	47.52	0.51	52.3	0.616	1.79	8.13	17.56
2.2-4	100	39.98	23.91	16.29	100.55	40.2	40.7	41.45	0.88	5.05	12.17	0.0779	45.84	0.49	50.5	0.592	1.80	8.52	20.54
2.2-5	100	29.78	28.09	3.33	105.19	5.4	11.2	5.75	0.56	2.80	4.72	0.0719	36.88	0.28	48.6	0.354	1.92	8.19	13.33
2.2-6	100	30.04	25.49	5.97	104.73	15.1	19.9	10.13	0.57	2.99	5.40	0.0725	37.01	0.30	48.7	0.359	1.92	8.32	15
2.2-7	100	30.21	21.96	9.21	103.18	27.3	30.5	16.48	0.56	2.93	6.39	0.0736	36.66	0.30	48.3	0.358	1.90	8.19	17..
2.2-8	100	29.78	19.18	11.75	104.14	35.4	39.6	22.50	0.54	2.87	6.68	0.0746	35.53	0.28	39.1	0.341	1.92	8.41	19.61
2.2-9	100	30.19	16.62	14.46	102.95	44.9	47.9	38.71	0.54	2.92	7.63	0.0761	35.44	0.29	39.8	0.346	1.89	8.44	22.86
2.3-1	100	40.39	36.09	4.71	101.82	10.6	11.7	12.18	0.93	5.03	8.87	0.0728	49.56	0.53	54.6	0.647	1.74	7.77	13.71
2.3-2	80	39.83	35.98	4.85	101.75	9.9	11.6	14.98	0.93	5.51	11.40	0.0732	48.67	0.52	67.0	0.982	1.79	8.03	11.61
2.3-3	70	39.79	35.96	4.78	102.19	9.6	11.8	16.00	0.91	7.11	12.46	0.0734	48.37	0.51	76.1	1.270	1.77	5.60	9.81
2.3-4	50	40.02	36.18	4.84	102.75	9.6	12.3	29.10	0.84	9.87	16.21	0.0741	48.19	0.51	106.1	2.493	1.83	3.96	8.50
2.3-5	100	39.81	31.98	8.38	101.38	19.7	21.8	18.52	0.88	4.98	9.81	0.0738	48.11	0.51	53.8	0.619	1.76	8.04	15.84
2.3-6	80	39.79	31.71	8.38	100.75	20.3	21.1	21.15	0.88	6.56	12.34	0.0743	47.79	0.51	65.8	0.968	1.77	6.83	12.85
2.3-7	70	39.74	31.89	8.47	101.56	19.8	21.3	22.87	0.90	7.40	13.30	0.0746	47.54	0.50	74.8	1.246	1.79	5.94	11.87
2.3-8	50	40.19	32.18	8.69	101.59	19.9	21.6	27.33	0.93	19.15	17.96	0.0754	47.59	0.51	104.8	2.473	1.82	4.10	7.27
2.3-9	100	40.01	28.06	12.14	100.47	29.9	30.3	27.87	0.90	4.89	11.10	0.0755	47.31	0.50	52.1	0.612	1.78	7.99	18.14
2.3-10	80	39.76	28.02	12.53	101.99	29.5	31.5	31.68	0.88	6.73	14.96	0.0762	46.60	0.49	64.1	0.936	1.78	7.19	15.92
2.3-11	70	40.02	28.11	12.79	102.20	29.8	32.0	34.04	0.92	7.64	15.71	0.0766	46.66	0.50	73.4	1.232	1.85	6.20	12.75
2.3-12	50	39.62	28.01	12.54	102.35	29.3	31.7	36.28	0.89	9.74	18.68	0.0770	45.96	0.49	101.2	2.354	1.83	4.14	7.93
2.3-13	100	40.13	23.91	16.36	100.35	40.4	40.8	41.67	0.88	5.03	12.44	0.0779	45.99	0.49	58.6	0.597	1.78	8.42	20.85
2.3-14	80	40.10	24.36	16.05	100.77	39.3	40.8	43.77	0.90	6.59	15.45	0.0783	45.74	0.49	82.9	0.826	1.84	7.11	16.68
2.3-15	70	40.21	23.85	16.63	100.87	40.7	41.4	47.00	0.89	7.35	16.72	0.0788	45.54	0.49	71.6	1.208	1.81	6.00	13.84
2.3-16	50	40.48	24.56	15.98	100.15	39.6	39.1	47.56	0.85	9.45	19.97	0.0796	45.69	0.49	100.5	2.363	1.81	3.96	8.33
2.3-17	100	40.02	21.33	18.21	98.80	46.7	45.5	51.00	0.86	4.80	12.88	0.0795	44.03	0.48	48.5	0.581	1.79	8.40	22.18
2.3-17	100	39.96	19.87	18.32	95.57	50.3	45.8	56.91	0.84	4.85	13.70	0.0806	44.28	0.47	48.7	0.572	1.78	8.48	23.95
2.3-18	80	39.83	20.17	18.31	96.61	49.4	46.0	60.16	0.85	6.48	16.44	0.0811	43.83	0.47	60.3	0.882	1.82	7.26	19.64
2.3-19	70	39.92	20.10	18.36	96.34	48.6	46.0	60.16	0.83	7.83	17.35	0.0811	43.93	0.47	69.1	1.157	1.77	6.88	14.99
2.3-20	50	40.06	20.05	18.35	95.86	50.0	45.8	63.46	0.84	9.12	20.84	0.0817	43.78	0.47	96.4	2.267	1.80	4.02	9.19

#1 Blowdown - (Inlet-Vent)/Inlet
#2 Blowdown - Bottom/Inlet

APPENDIX C

SOUND LEVEL DATA

C. SOUND LEVEL DATA

Sound level measurements were taken during the last two Healy DVT hot-fire tests at CTS. As various systems (air, water, fuel) were successively activated, the decibel level at each condition was determined at the precombustor head end. The sound meter was held approximately 1 to 2 feet from, and pointed directly at, the PC. Unless noted, the acoustic level given for each particular condition includes all of the previously listed conditions.

Activation Sequence	Sound Level
PC main cooling water and scrubber/quench pumps on	84 dB
Secondary air fan on	85 dB
Primary air fans on	89 dB
Duct heaters on	92 dB
Oil gun on	93 dB
Carrier air fan on	97 dB
Oil gun off & coal at half load	98 dB
Oil gun off & coal at full load	99 dB
Oil gun on & coal at half load	104 dB

1. EXECUTIVE SUMMARY

This report describes cold flow tests that were conducted at TRW in support of the Healy combustor design. The primary purpose of the combustor cold flow model testing was to determine the effect of proposed combustor design modifications on combustor flow patterns and mixing performance. These design modifications include a new precombustor secondary mixing section to accommodate higher temperature air as well as the addition of mill air, multiple coal injectors in the slagging stage, a modified combustor exit geometry to accommodate firing into the bottom of the furnace, and limestone injector location and geometry in the slag recovery section.

The main focus of cold flow testing is on the following areas:

- Precombustor secondary and mill air mixing
- Multiple coal injector positioning
- Slag recovery section flow patterns
- Limestone injector positioning and geometry

Tests were performed using a transparent, 1/10 scale model of the Healy combustor and included qualitative flow visualization as well as detailed measurements of concentration and velocity profiles at selected locations. Key combustor flow parameters such as the swirl number and injector-to-freestream momentum ratios were maintained during testing in order to preserve the major flow and mixing patterns within the combustor.

Based on a comparison between the baseline Cleveland secondary air mixing section and the new Healy configuration, the new arrangement allows for significantly improved mixing between the precombustor burner exhaust and the secondary air for the same level of burner swirl. This improved mixing was achieved by introducing the secondary air at the inlet to the round-to-rectangle transition section, rather than through a slotted mix bustle used during Cleveland testing. This should reduce the fouling risk in the rectangular connection duct leading to the slagging stage as well as in the oxidizer footprint region in the slagging stage.

The key parameter which affects secondary air mixing is the burner swirl number. Mixing performance was also found to be relatively insensitive to the ratio of burner to secondary air flows, which implies that mixing performance should be preserved at off-nominal coal splits and loads, provided the level of swirl in the burner is preserved. The azimuthal location of the secondary air windbox inlet was found to have only a secondary effect on mixing performance.

Tests were also performed to characterize the degree in which mill air mixes with both the primary and secondary flows. The mill air injection arrangement, with 16 individual injection ports located around the circumference of the precombustor, was found to produce very good mixing between the mill air and the primary and secondary flows. Mixing performance was observed to be rather insensitive to mill air-to-burner mass (or momentum) ratios, and was instead primarily a function of the degree of burner swirl. Parametric tests also showed that mixing performance was relatively insensitive to the number of mill air injection ports in the range of 8 to 16, provided the total injection flow area was held constant. This indicates that it may be possible to reduce the number

of mill air ports without significantly affecting precombustor secondary mixing or fouling risk.

Slagging stage multiple coal injector mixing tests were performed using carbon dioxide, powder, and water as injection materials. The tests were performed to characterize mixing of the flow from the coal injectors with the swirling flow in the slagging stage. Of primary interest was the interaction between the flow from the injectors and the off-axis vortex which exists in the headend due to a single tangential air inlet. Based upon the cold flow model tests, it was observed that the injectors placed at the out-board location (74" full scale) were found to be less affected by the vortex in the headend than injectors placed at the in-board location (52.5" full scale). Furthermore, the injector at the 9:00 location (looking downstream) was found to interact with the vortex more than the other injectors. The adjacent injectors at the 8:00 and 10:00 locations, together, interacted similarly to the single injector at the 9:00 location.

Tests were also performed to characterize flow in the slag recovery section (SRS). Parameters investigated included a jet trap located at the back wall of the SRS, angle of exhaust, slag recovery section height, and swirl number. The flow velocity in the slag recovery section was observed to be highest along the back face of the slag recovery section with a slight bias toward the right side (away from the precombustor). The flow velocity was highest along the back face because the flow impinges on the back face while making the 90 degree turn from the baffle into the slag recovery section. The flow slightly biases the right side because of the swirl direction (for the left-handed combustor). Tests with and without the jet trap were not observed to change the flow distribution significantly. Also, in the range of exhaust angles tested (vertical and orthogonal with respect to the combustor), the flow distribution was not observed to change significantly.

Lastly, tests were performed to determine an appropriate location and geometry for the limestone injector in the slag recovery section. Combustor testing at Cleveland has shown that the best location for the limestone flow is in the middle of the slag recovery section flow, in order to minimize limestone losses due to deposition on the combustor walls. The limestone injector configuration which best accomplishes this is injection at the wall, with a reduced injector diameter (2.1" full scale) to increase the penetration of the limestone flow so that the limestone flow reaches the center of the slag recovery section flow.

2. INTRODUCTION

This document presents the objectives, modeling guidelines, test configurations, test results and conclusions of sub-scale cold flow model tests that were conducted at TRW in support of Healy combustor design.

The Healy slagging coal combustor is a scale-up from TRW's 34 inch diameter combustor successfully fired on Healy coal at TRW's Cleveland test facility. In order to meet Healy performance and operational requirements, several combustor modifications are required, including a precombustor secondary mixing section compatible with both high temperature secondary air (730°F) and mill air exhaust, multiple coal injectors in the slagging stage, a modified slag recovery section for firing into the bottom of the furnace, and a limestone injector in the slag recovery section.

Cold flow modeling has been successfully used by TRW in the past to provide valuable information on combustor flow and mixing patterns, particle trajectories, and flow uniformity. Cold flow modeling is useful during the design phase as it allows several promising combustor configurations to be evaluated in a convenient and expeditious manner, prior to hot-fired design verification testing. A cold flow model can also serve as a diagnostic tool during hot-fire testing in two ways: first, by confirming a problem identified during testing, and second, by quickly evaluating possible design modifications.

In order to minimize the risk associated with these design modifications, cold flow model tests were conducted to provide information on combustor flow and mixing performance. Tests were performed with a 1/10 scale, transparent model of the Healy coal combustor with atmospheric, room-temperature air as the primary fluid. A photograph of the cold flow set-up is shown in Figure 1.

Figure 2 shows the relationship between cold flow testing and Healy combustor design and Design Verification Testing (DVT) activities. The precombustor cold flow tests were defined based on issues identified during performance assessment and engineering analysis activities. These tests were then used to help evaluate and confirm DVT precombustor design choices. As shown in Figure 2, additional precombustor cold flow tests may be conducted, if necessary, during DVT precombustor testing to support troubleshooting.

Cold flow testing related to the multiple coal injectors and the slag recovery section were performed to evaluate various aspects in the Healy combustor design (i.e. jet trap, exit angle, coal injector positioning, limestone injector positioning). The results of this testing will be fed into the preliminary design of the Healy combustor slagging stage and slag recovery section.

The next section of this report (Section 3) covers the design issues addressed in the cold flow model testing. The modelling approach and the guidelines utilized are described next in Sections 4 and 5, respectively. Section 6 covers the test results and Section 7 covers a discussion of the major finds. Lastly, in Section 8, major findings and conclusions are given.

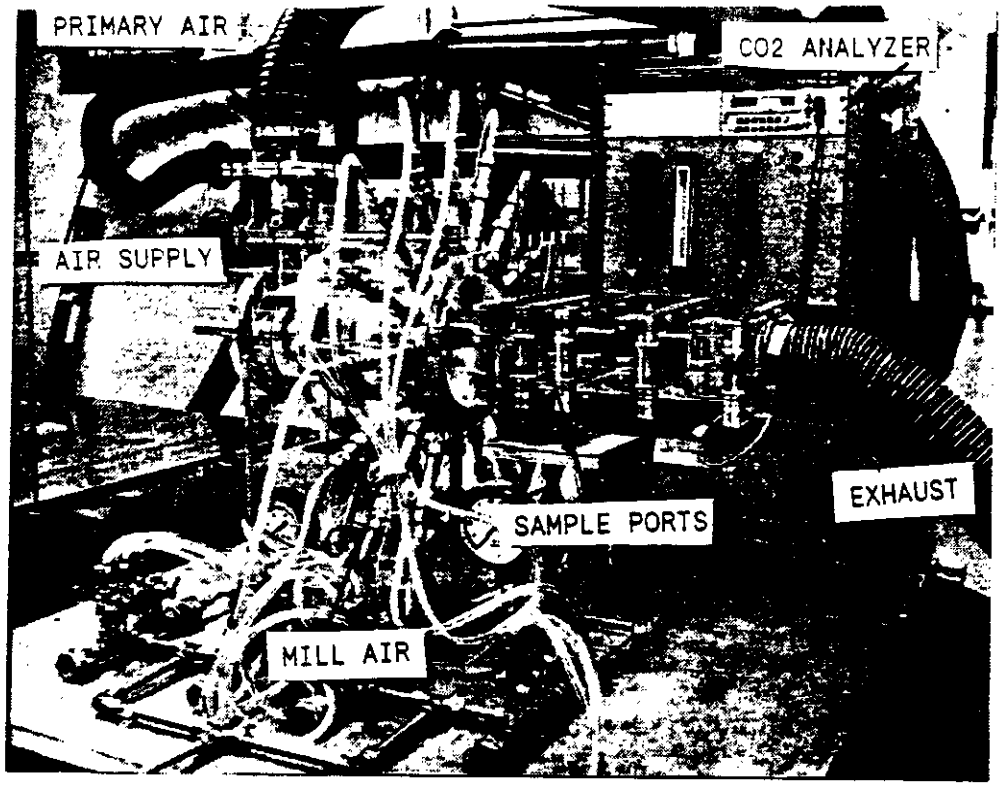

HEALY PRECOMBUSTOR TEST SET UP

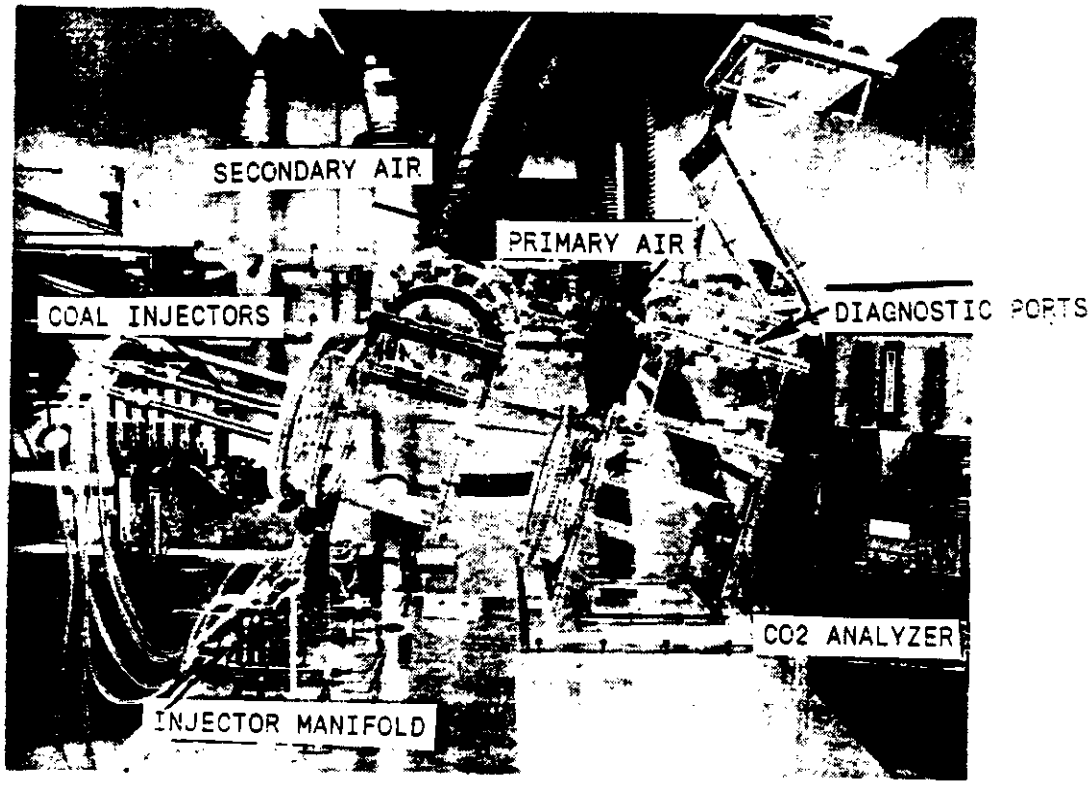

HEALY SLAGGING COMBUSTOR AND
SLAG RECOVERY SECTION TEST SET UP

FIGURE 1. SET UP OF COLD FLOW EXPERIMENT

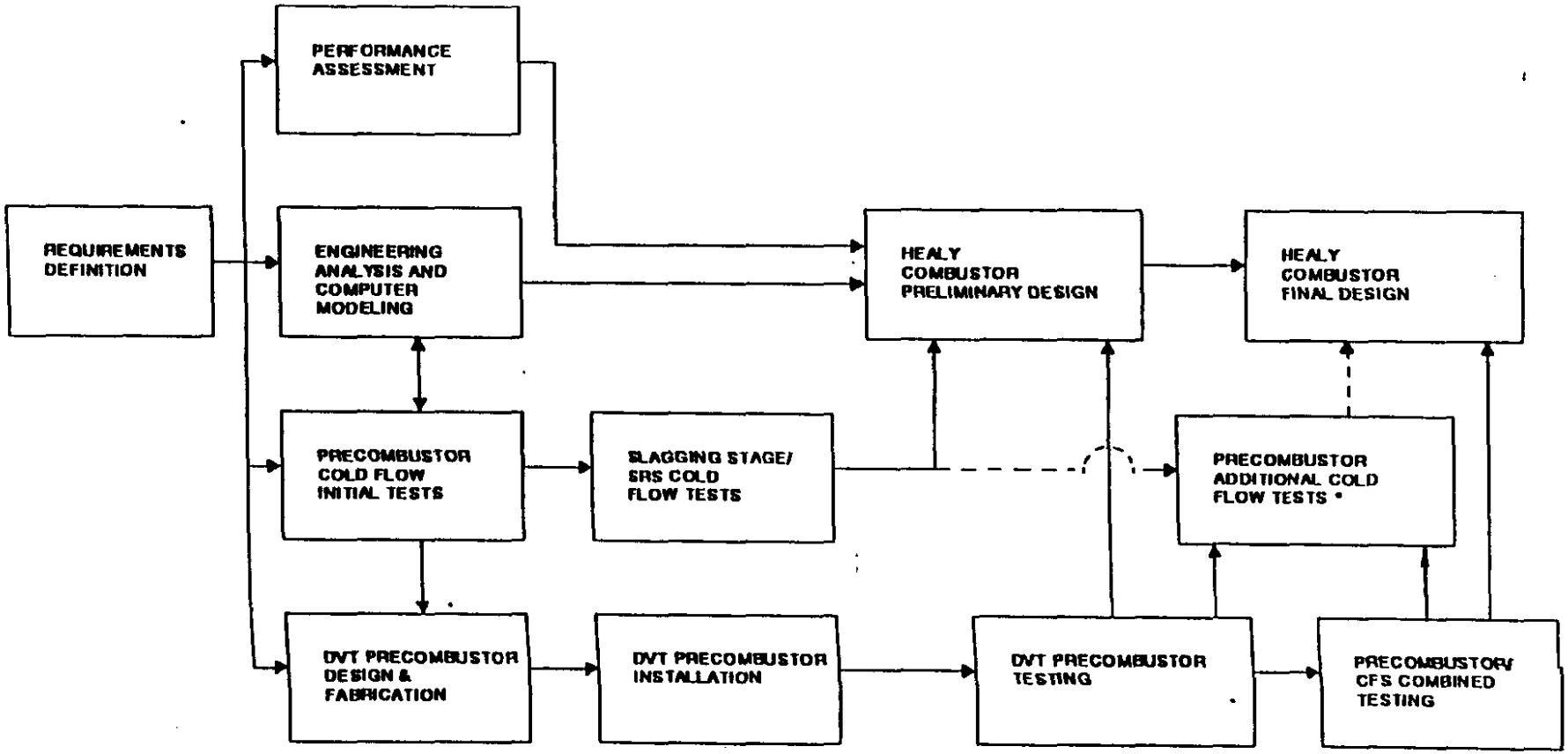

FIGURE 2 RELATIONSHIP BETWEEN COLD FLOW TESTING AND HEALY DESIGN/DVT ACTIVITIES

3. COMBUSTOR DESIGN ISSUES

As mentioned in the introduction, several combustor design modifications have been proposed in order to accommodate specific Healy operational and configurational requirements, including secondary air preheat temperatures of up to 730°F, the introduction of some, or all of the mill air into the precombustor, and a vertical combustor exhaust into the furnace. In addition, the Healy combustor will be equipped with multiple injectors in the slagging stage in order to preserve slag recovery and coal/air mixing at the larger combustor size. The main purpose of the combustor cold flow modeling activities was to provide information on the effect of these design modifications on combustor flow and mixing patterns. This was accomplished through both qualitative flow visualization as well as quantitative pressure drop, velocity, and mixing measurements.

Table 1 lists specific combustor design issues that have been addressed through cold flow model tests. These issues include precombustor secondary air mixing, multiple coal injector positioning in the slagging stage, slag recovery section flow patterns, and limestone injector positioning in the slag recovery section.

3.1 Precombustor Secondary Mixing

In the precombustor, coal is burned with primary air in the head end at a stoichiometry in the range of 0.85 to 1.0 as indicated in Figure 3. Secondary air is added downstream of the primary combustion zone to achieve the required stoichiometry in the slagging stage. During Cleveland testing, the secondary air temperature was approximately 350°F. An uncooled mix bustle, shown in Figure 4, was used to mix the primary and secondary flow prior to injection into the slagging stage.

For the Healy combustor, secondary air temperatures are expected to reach 730°F. In addition, the precombustor must be designed to accommodate a portion of the mill air exhausted from the coal feed system, at a nominal temperature of 135°F. Coal fines that are not captured by the coal feed system cyclones are included with the mill air, at an approximate particulate loading of 6 pounds coal for every 1000 pounds of mill air.

Following a preliminary assessment, it was concluded that design modifications to the precombustor were necessary to accommodate these new requirements. The baseline Healy precombustor design is shown in Figure 5. The primary combustion air and precombustor coal are delivered to a Foster Wheeler-designed swirl burner in the head-end of the precombustor. Clean, high temperature secondary air enters the precombustor through a windbox and is injected in an annular region at the downstream end of the combustion chamber. An adjustable orifice plate is located at the upstream end of the annulus to distribute the secondary air uniformly in the circumferential direction. The mill air is injected through 8-16 ports just downstream of the combustion chamber. In the transition region, the secondary air and mill air mix with the swirling combustion products from the precombustor burner in order to achieve a mix temperature in the range of 2000-2500°F.

A key operational issue related to the design of the precombustor secondary mixing section is slag accumulation in the mixing section or in downstream

TABLE 1. COLD FLOW COMBUSTOR DESIGN ISSUES AND DESIGN IMPACTS

COMBUSTOR DESIGN ISSUE	COMBUSTOR DESIGN IMPACTS
1. Precombustor Secondary Mixing and Fouling	• Secondary mixing section configuration • Secondary windbox geometry • Secondary windbox air inlet location • Number and size of mill air injection ports
2. Miltiple Coal Injector Positioning	• Injector clocking relative to air inlet • Injector circle diameter
3. Slag Recovery Section Flow Patterns	• Provision for "back wall pocket" • Length of exit section • Angle of combustor exhaust
4. Limestone Injector Positioning	• Injector location in slag recovery section • Injector geometry

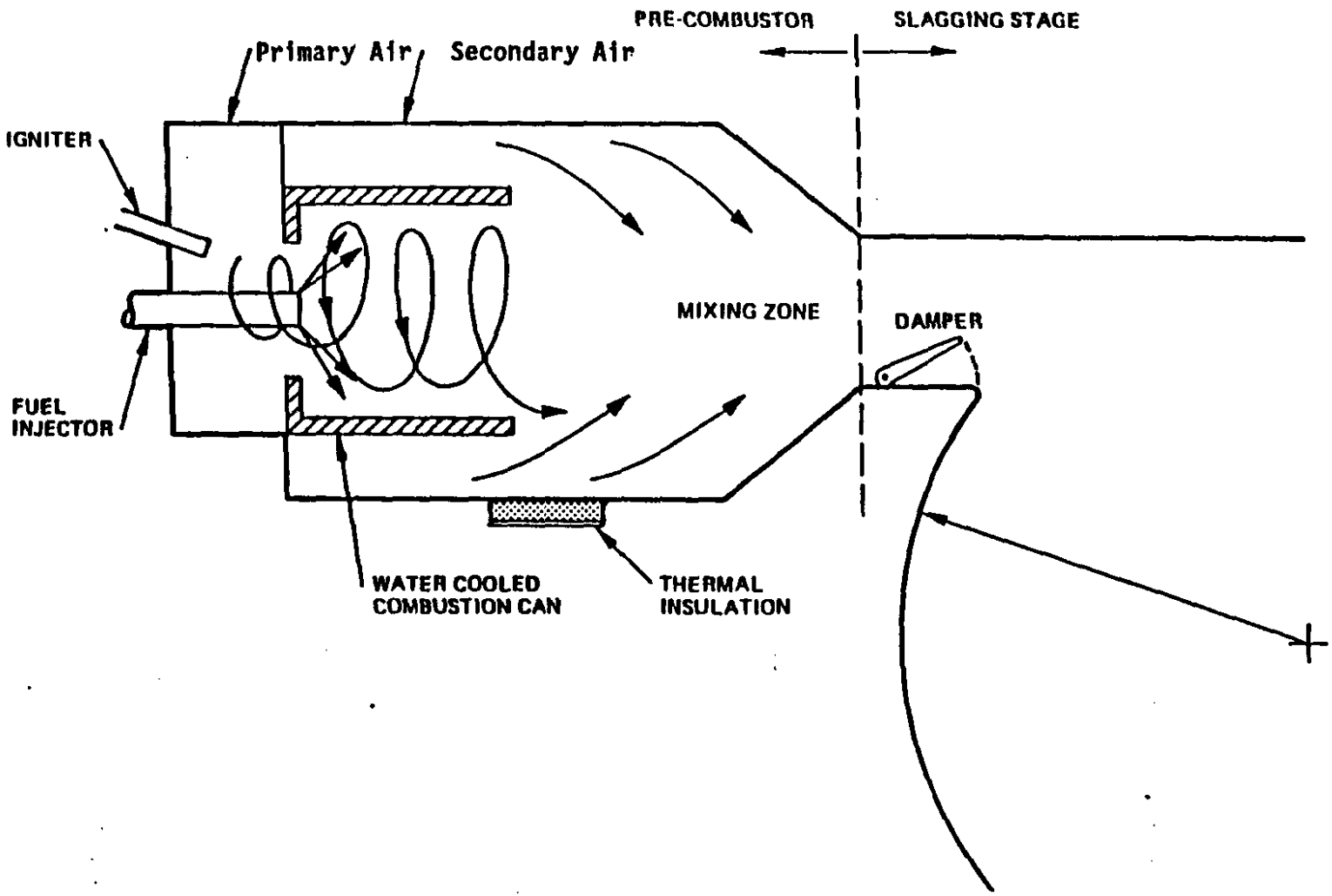

FIGURE 3. PRECOMBUSTOR SCHEMATIC

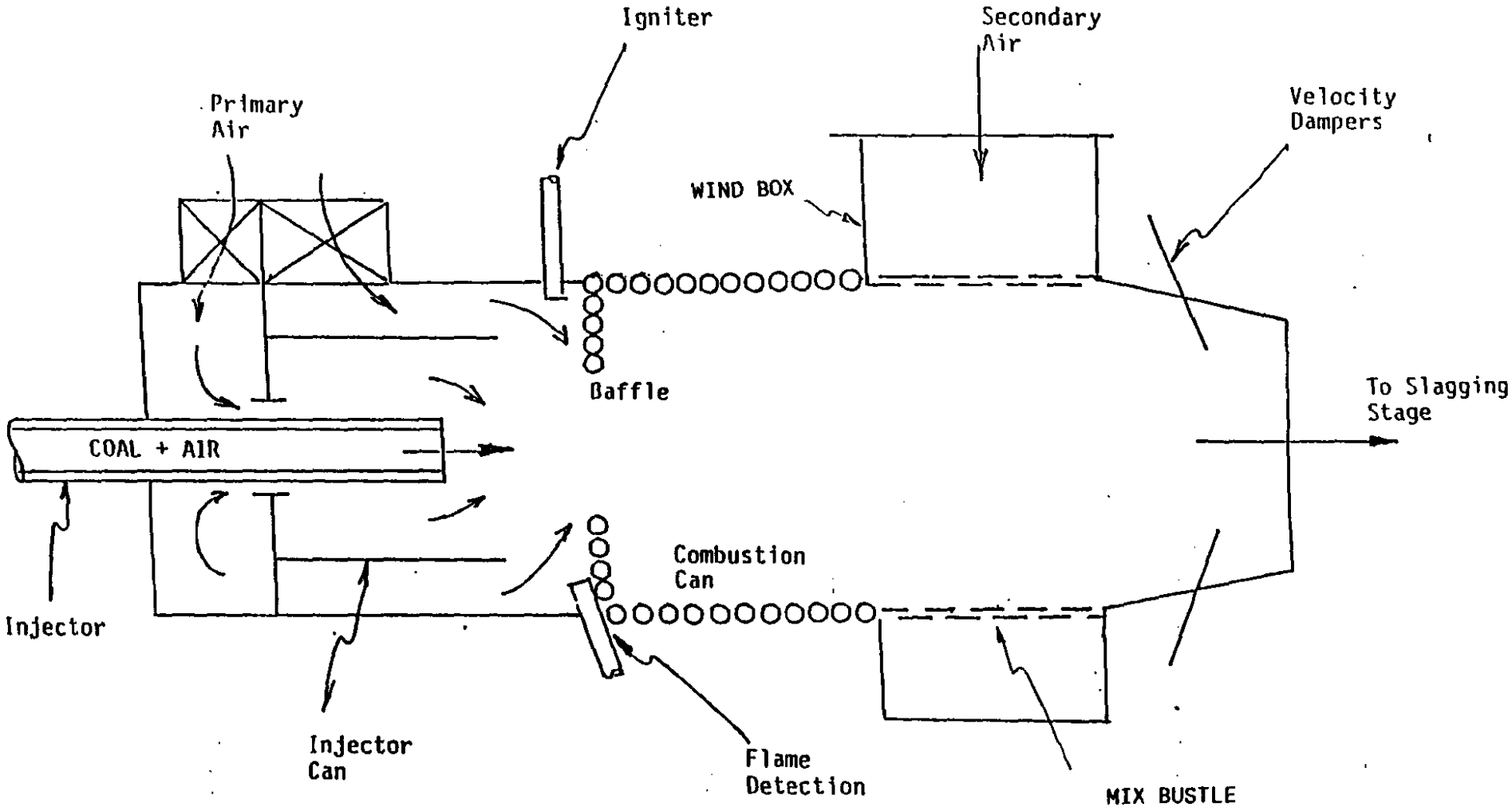

FIGURE 4. PRECOMBUSTOR SCHEMATIC (CLEVELAND CONFIGURATION)

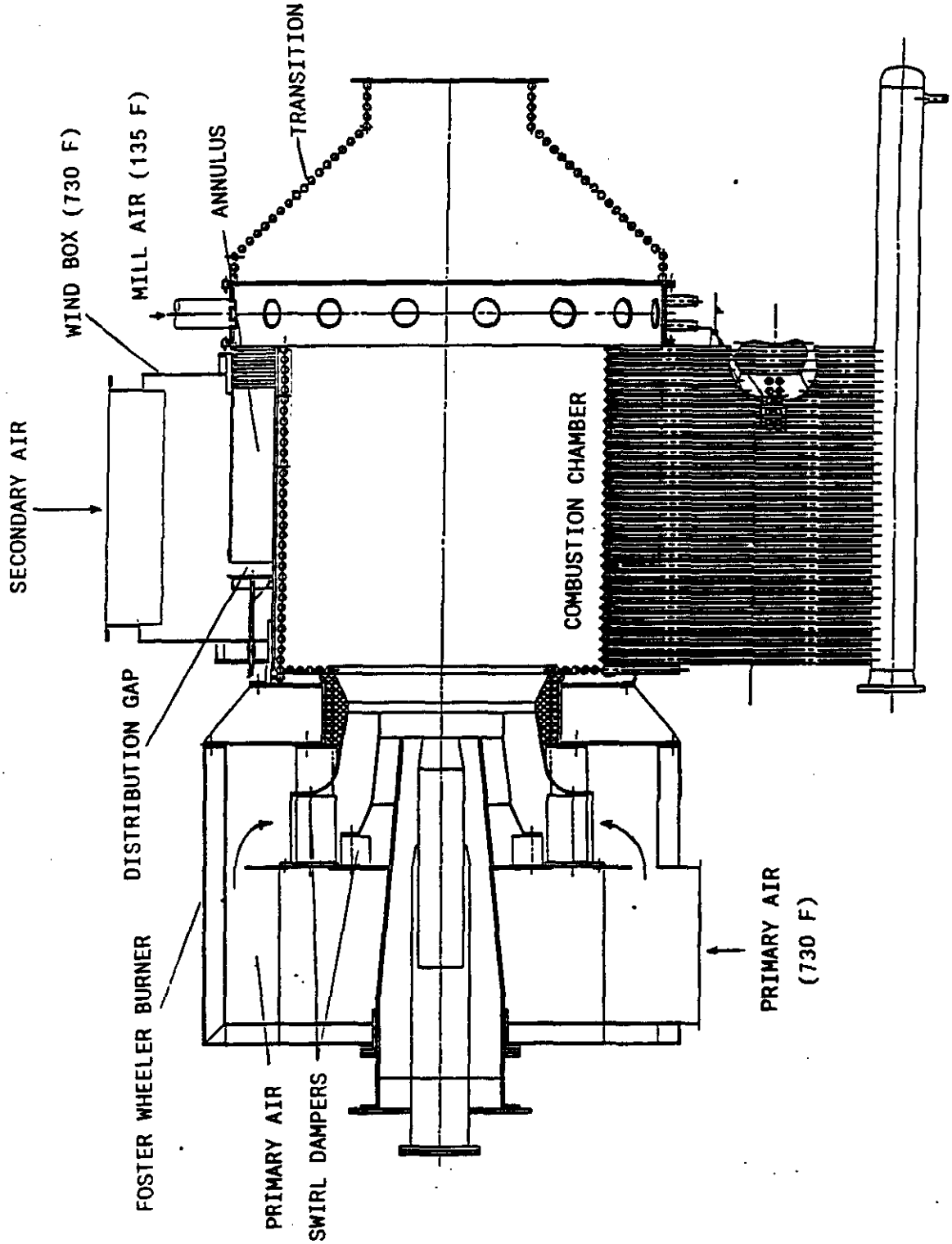

FIGURE 5. PRECOMBUSTOR SCHEMATIC (HEALY CONFIGURATION)

components. Porous slag growths can occur along relatively hot, rough surfaces that do not receive adequate radiative or convective heating. For example, if mixing between the primary combustion products and secondary air is poor, a relatively cold layer of air may be present along the outer walls of the air inlet section, which may in turn promote porous slag growths through convective cooling. These slag growths may eventually reduce the flow area significantly, and cause an unacceptable pressure loss in the combustor. If this relatively cold layer of gas persists into the slagging stage, fouling may also occur within the oxidizer footprint region, which may in turn adversely affect slagging stage performance. The precombustor secondary mixing section should thus be designed to promote rapid mixing of the primary, secondary and mill air flows.

3.2 Multiple Coal Injector Positioning

After mixing in the precombustor, the flow enters the main, or slagging stage through a tangential inlet, creating a highly turbulent, confined vortex flow field. The remainder of the coal is injected in the head-end of the combustor through multiple coal injector ports, as shown in Figure 6. The overall stoichiometry in the slagging stage is nominally 0.87 for Healy performance coal.

One of the important combustor design issues addressed during cold flow modeling was the positioning and location of the multiple coal injectors in the head-end of the combustor. Typically, six injector are evenly spaced around the circumference of an injector circle. As the injector circle diameter is increased, ash particle confinement in the slagging stage is expected to improve, however the mean particle in-flight residence time may decrease, which may lead to lower carbon burnout. Two injector circles are being built into the Healy combustor design, one with a 52.5 inch diameter (half the combustor diameter), and one with a 74 inch diameter. Cold flow model tests have been conducted to characterize particle trajectories and fuel/oxidizer mixing for each injector case.

Another important consideration is the clocking of the coal injectors relative to the air inlet. Due to the use of a single air inlet, the flow along the head endplate is not symmetric about the main axis. Instead, the center of the vortex is shifted slightly to the air inlet side. As a result of this asymmetry, initial coal particle trajectories depend in part on the positioning of the coal injector relative to the air inlet. Cold flow model tests have been performed to determine the best clocking of the injectors for the Healy combustor.

3.3 Slag Recovery Section Flow Patterns

After leaving the slagging stage, the flow enters the slag recovery section, where slag is tapped along the bottom of the combustor and the gas flow is directed upwards towards the furnace. In previous installations, the combustor was designed for sidewall firing into the furnace, as shown in Figure 7. At Healy, the combustors will fire directly into the bottom of the furnace, as shown in Figure 6.

One objective of cold flow testing the slag recovery section was to characterize the flow uniformity at the exit. The results will be utilized in combustor design and furnace design efforts. Slag recovery section parameters which may affect flow uniformity at the exit are the presence or absence of the "back wall pocket" or jet trap, the angle of exhaust, and the height of the slag

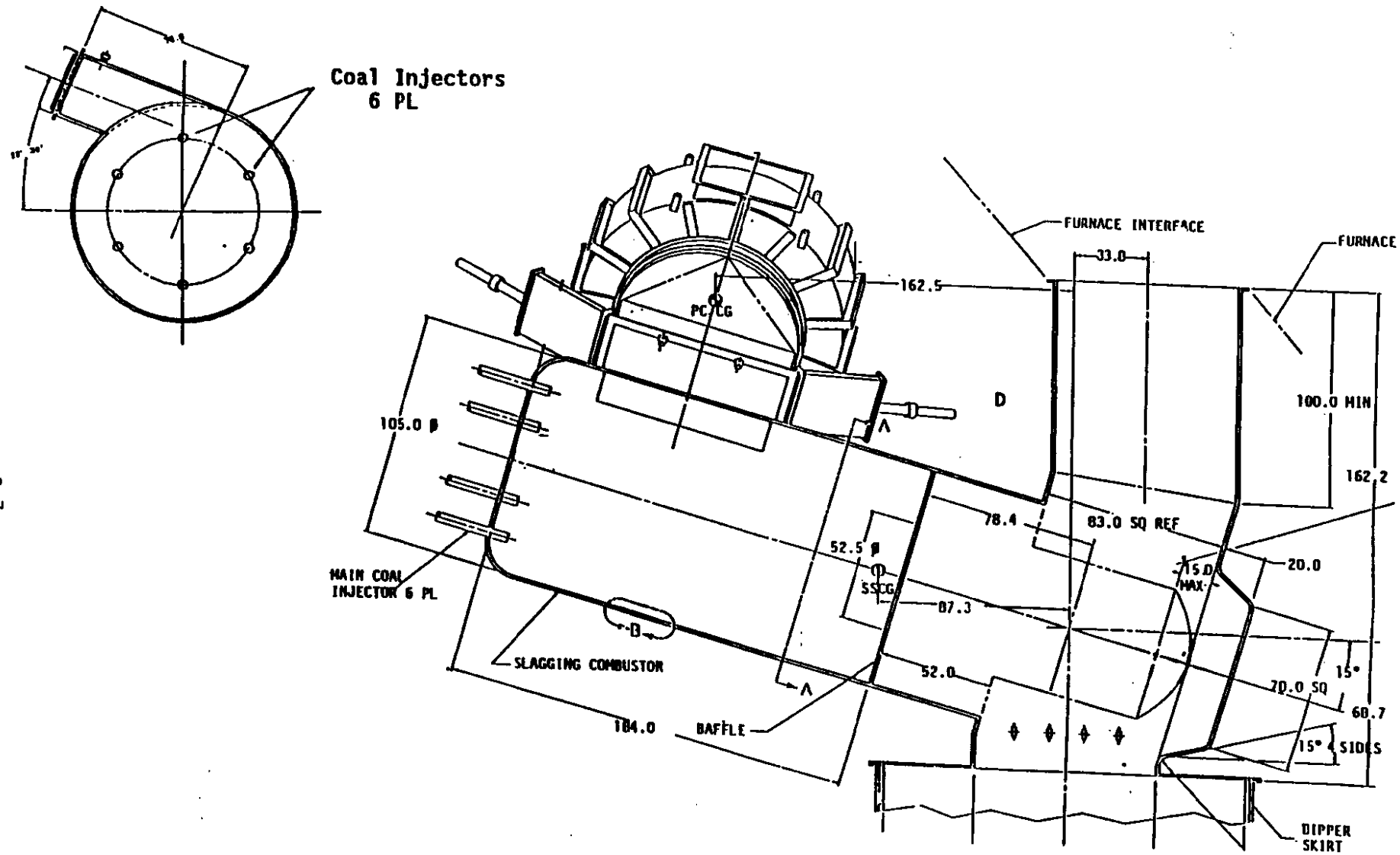

FIGURE 6. HEALY COMBUSTOR SIDE ELEVATION

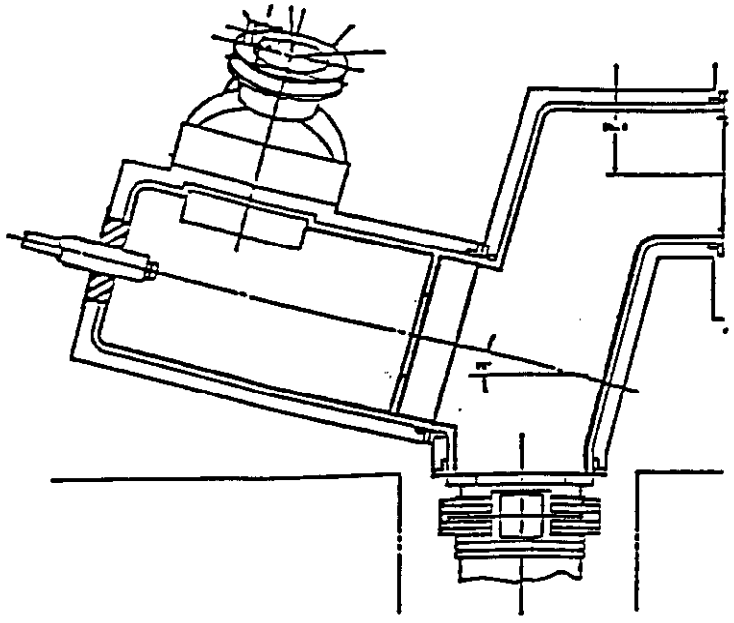

FIGURE 7A. CLEVELAND COMBUSTOR CONFIGURATION

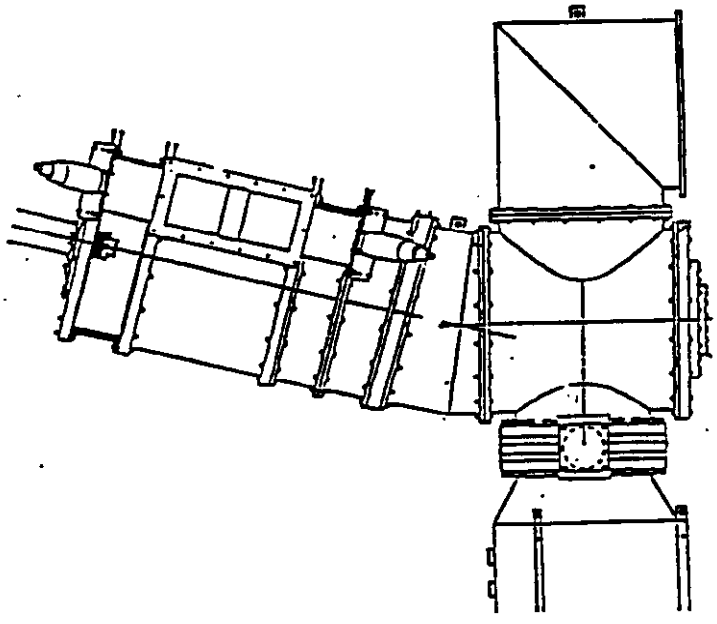

FIGURE 7B. CTS COMBUSTOR CONFIGURATION

recovery section. These design parameters have been investigated in the cold flow model.

3.4 Limestone Injector Positioning

In the slag recovery section, limestone is injected into the exiting combustion gases and is carried into the furnace where it undergoes calcination. The preferred injection location is such that the limestone is centrally located in the main stream of the SRS. This is to minimize limestone losses due to deposition on the combustor walls. It is also important to locate the injector as close as possible to the SRS exit, to minimize potential dead burning.

In the cold flow model, limestone injector depth, injection height (along the SRS), and injection face (SRS face) were varied. Furthermore, the momentum flux of the limestone simulated flow was varied relative to the freestream momentum flux to see the effect on limestone penetration and mixing.

4. MODELING APPROACH

4.1 Precombustor Secondary Mixing Tests

The general approach adopted for the precombustor secondary mixing tests was to first characterize the mixing and flow patterns of the secondary air mix bustle used during Cleveland testing, since there exists a large amount of operational experience with this configuration. Testing involved qualitative flow visualization using flow tufts, and quantitative mixing experiments. The degree of mixing between the primary and secondary flow streams was determined by introducing a tracer gas into either the primary or secondary flow and measuring tracer concentrations downstream of the mixing section. Details of the testing method are provided in Section 6 (Test Configurations and Results).

Once the flow and mixing patterns in the Cleveland mix bustle were characterized, similar tests were conducted with the proposed Healy secondary mixing section and compared against the Cleveland results. In addition, a number of parametric tests were conducted with the Healy configuration to assess the flow distribution in the secondary windbox and to identify the parameters which affect the precombustor secondary mixing process.

The specific test objectives of the precombustor secondary air mixing tests were to:

- Characterize the flow and mixing patterns of the Cleveland mix bustle.
- Evaluate flow distribution and uniformity in the Cleveland secondary air windbox.
- Characterize the flow and mixing patterns of the Healy secondary mixing section to be tested at CTS.
- Evaluate flow distribution and uniformity in the Healy secondary air windbox.
- Characterize mixing patterns of mill air injected in precombustor as a function of jet-to-freestream momentum ratio and the number and size of injection ports.

4.2 Multiple Coal Injector Tests

For the multiple coal injector characterization testing, both qualitative and quantitative mixing measurements were performed to characterize the flow patterns and particle trajectories in the headend of the combustor. Mixing measurements down the length of the combustor were also performed.

Specific cold flow test objectives were to:

- Characterize the flow patterns, particle trajectories, and mixing as a function of the injector clocking, injector circle diameter, and number of injectors.

- Characterize fuel and oxidizer mixing patterns in the head-end, air inlet, and baffle regions of the slagging stage as a function of coal injector configuration.

4.3 Slag Recovery Section Flow Tests

The slag recovery section tests focused on the flow patterns and velocity profiles from the slagging stage baffle to the furnace entrance.

The specific test objectives of the slag recovery section flow characterization tests were to:

- Characterize the flow patterns in the slag recovery section through flow visualization.
- Determine velocity profiles at the combustor exit for the Healy baseline configuration.
- Determine the effect of exit section length on the combustor exit velocity profile.
- Investigate effect of the jet trap on the flow uniformity at the combustor exit.
- Investigate the effect of combustor exhaust angle on combustor exit velocity profile.

4.4 Limestone Injector Tests

The limestone injector tests focused on penetration and mixing patterns of the limestone-simulated flow in the SRS flow. Quantitative mixing measurements were performed.

The specific test objectives were to:

- Determine the effect of injector insertion depth on limestone penetration and mixing.
- Determine the effect of injection location in the SRS on limestone penetration and mixing.
- Determine the effect of limestone momentum flux on penetration and mixing.

5. MODELING GUIDELINES

A number of modeling guidelines were developed for the Healy cold flow experiments for the purpose of ensuring that the major flow and mixing patterns within the combustor were preserved. These modeling guidelines were then used to size the model hardware and to select cold flow test conditions. Each modeling guideline is discussed briefly below:

(1) Preserve geometrical similarity.

This guideline is one of several necessary to preserve the macro flow patterns within the combustor. In order to keep the model at a workable size, all internal dimensions of the Healy combustor were scaled down by a factor of 10.3.

(2) Preserve swirl number (in both PC burner and slagging stage).

The swirl number, or the ratio of tangential to axial velocity, is an important parameter in determining the flow patterns, recirculation zones, mixing, turbulence levels and pressure drop within the combustor.

(3) For experiments in which the mixing of two or more flows is being studied, preserve the momentum flux ratio of the two streams.

In addition to preserving geometrical similarity and swirl number, matching the momentum flux ratio of the two stream being mixed is important in order to preserve the degree of penetration or diffusion of one fluid into the other. The momentum ratio is defined as

$$R^2 = \frac{\rho_2 V_2^2}{\rho_1 V_1^2}$$

where the density, ρ, and the velocity, U, of each stream (1 and 2) corresponds to values just upstream of the mixing section.

(4) For experiments in which particle trajectories are being studied, preserve the ratio of particle accommodation length to combustor diameter.

Particle aeroballistics and dynamics are determined by the combustor diameter, the swirl in the flow and by the ratio of the particle accommodation length, ℓ, to the combustion chamber diameter, D, is defined as

$$\ell = \frac{4}{3C_D} \frac{\rho_p}{\rho_g} \cdot d$$

where ρ_p and ρ_g are the particle and gas density, d the particle diameter and C the drag coefficient.

(5) Select cold flow model size such that model Reynolds numbers are in fully turbulent regime and in the same approximate range as actual combustor.

In addition to the above modeling guidelines, there were a number of other considerations and constraints which factored into the selection of model size and operating conditions. These include:

- Use existing blower (0.4-0.5 lb/s max capacity).
- Install model in existing combustor cold flow model lab.
- Model should be large enough to allow access for flow tufts, hand-held probes, etc.
- Model should be small enough to be conveniently located in cold flow model lab and to accommodate existing air supply.
- Model should not have excessive pressure drop since overall air system pressure drop is limited. Model pressure drop should be limited to approximately 5 inches of water.
- Majority of model should be transparent to allow for visual observations.
- Model should be of modular construction to allow for investigation of alternate geometries and injector configurations.
- Cold flow investigations should take full advantage of existing diagnostic equipment.
- Model design should emphasize simplicity and ease of manufacture. Use standard plexiglas tube sizes and plate thicknesses whenever possible.

The selection of the model size was based primarily on existing blower limitations, the use of flow tufts for flow visualization, and Reynolds number considerations. A plot of model flow velocities at selected locations is shown in Figure 8 for a air flow rate of Q.4 lb/s. Flow tufts in the slagging stage are usually not very effective below tangential velocities of about 40 ft/s (27 mph), which limits the slagging stage diameter to approximately 10 inches or less given the present capacity of the air blower. It is also necessary to keep flow velocities in the slag recovery section above approximately 10 ft/sec to ensure accurate measurement of velocity profiles. Finally, it should be noted that model Reynolds numbers decrease with increasing model size, for a constant air flow rate. This relationship is shown in Figure 9, where the ratio of cold flow model Reynolds number to hot-fired combustor Reynolds number is plotted as a function of model diameter. At a model combustor diameter of 10 inches, model Reynolds numbers (based on combustor diameter) are 15-20% of the corresponding hot-fired values, or approximately 33,000 to 90,000 (depending on combustor location). As the cold flow combustor diameter is increased to 20 inches, this ratio drops off to 0.10, which is on the lower end of the fully turbulent flow regime.

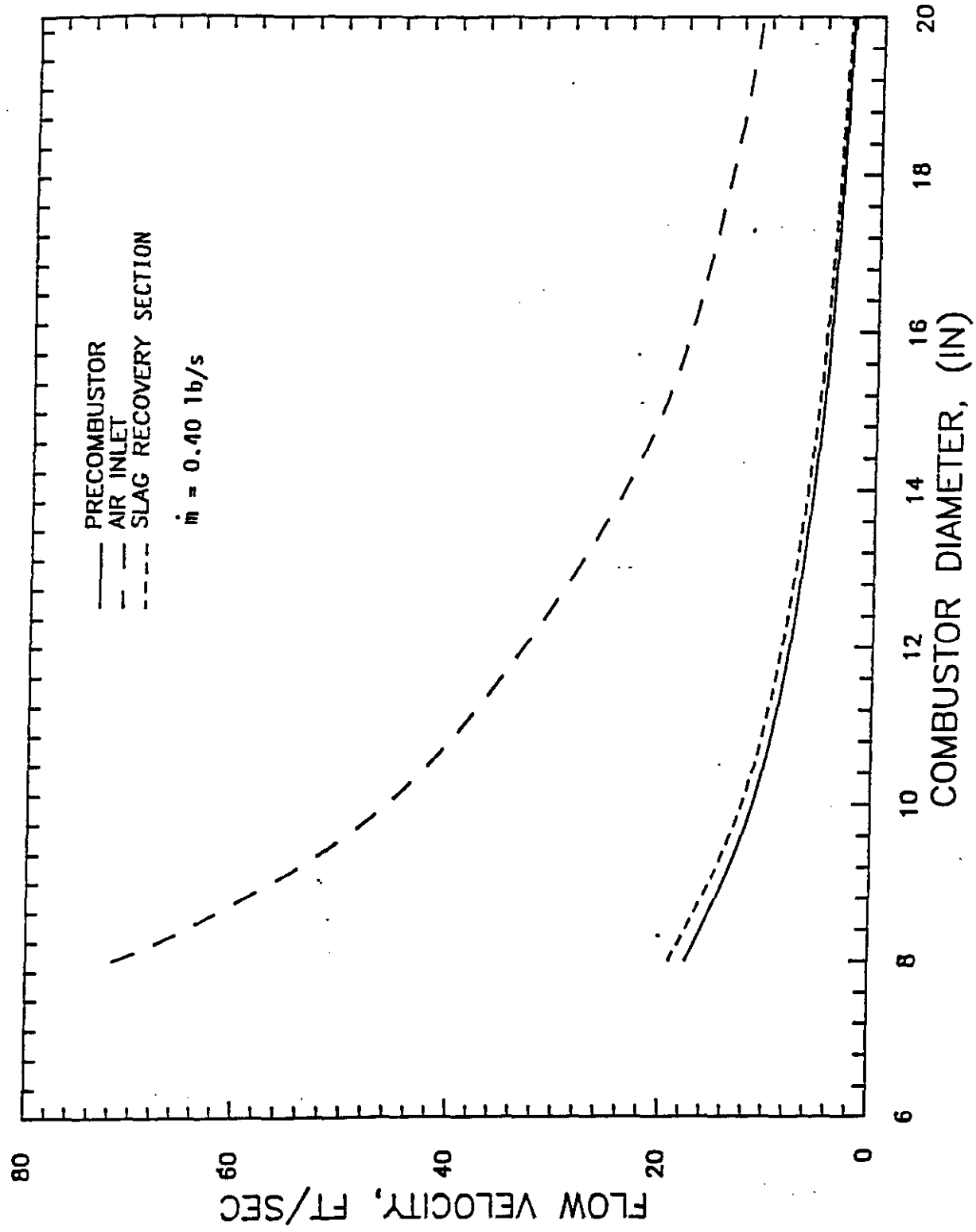

FIGURE 8. MODEL PLUG FLOW VELOCITIES AS A FUNCTION OF MODEL MAIN STAGE DIAMETER

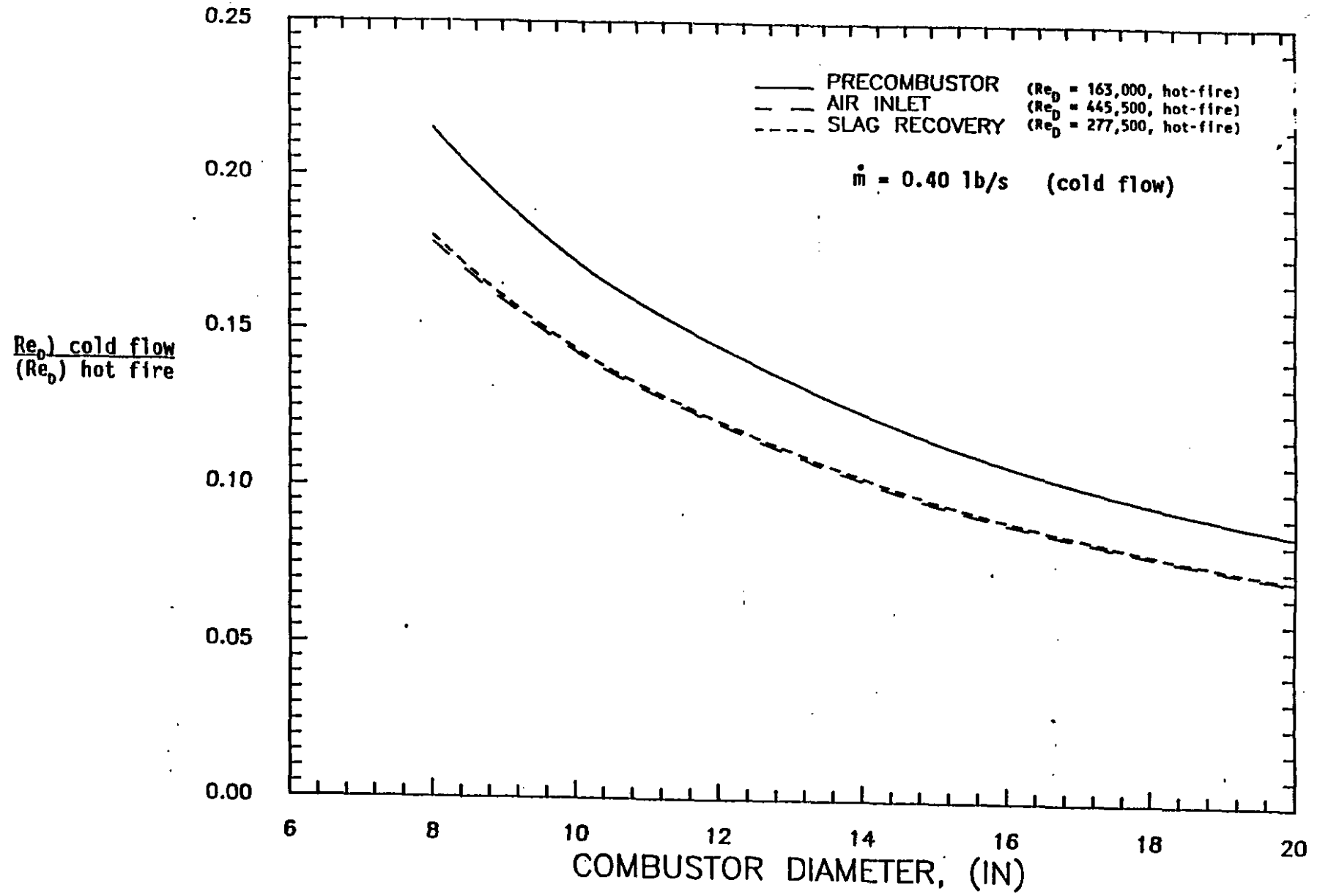

FIGURE 9. RATIO OF MODEL REYNOLDS NUMBER TO ACTUAL REYNOLDS NUMBER AS A FUNCTION OF MODEL MAIN STAGE DIAMETER

Therefore, based on the above considerations, a cold flow combustor internal diameter of 10 inches was selected. This is a large enough size to allow for convenient flow visualization, while small enough to ensure turbulent flow with the existing blower air supply. The resulting modeling scaling factor assuming a Healy combustor diameter of 105 inches and a 1 inch slag layer is thus 1 : 10.3.

6. TEST CONFIGURATIONS AND RESULTS

6.1 Cleveland Precombustor Secondary Mixing Testing

6.1.1 Test Configuration

The first configuration tested, shown in Figure 10, simulates the Cleveland mix bustle. Cold flow mixing tests were performed to establish a baseline prior to evaluation of the proposed Healy secondary mixing section. Primary air enters tangentially in the head end of the precombustor, creating a swirling flow. Secondary air is introduced at the mixing bustle. Flow tufts (both wall-mounted and probe-mounted) were used for qualitative flow visualization. Mixing patterns were determined by introducing CO_2 tracer into one of the flows and measuring CO_2 concentrations at subsequent positions downstream of the injection point. A diagnostic section is located in the rectangular duct section downstream of the secondary mixing zone to allow for CO_2 measurements with a 1/8" gas sampling probe. Measurements were taken throughout the flow cross-section and converted to concentration and/or temperature profiles. Figure 11 defines the duct coordinate system (X,Y,Z) used for plotting the results, as well as the corresponding hardware dimensions H, W, and L. The same coordinate system is used for describing the results from Healy secondary mixing tests. (Section 6.2.2)

It should be noted that the cold flow model head-end geometry was fabricated to match that of the backup Healy precombustor burner, with primary air entering through a single tangential inlet as shown in Figure 10. A single coal injector is located on-axis within a combustion can which serves as a flame holder. (A more detailed sketch of the internals is given in Figure 15). This configuration was used for both the Cleveland and Healy secondary mixing tests. Recently, a decision has been made to use a split flame swirl burner supplied by Foster Wheeler Energy Corporation, shown in Figure 5, during DVT. While the two burners are similar in that coal is injected in the center of a swirling air flow just upstream of a flow baffle, there may be some differences in the degree of swirl at the inlet to the secondary mixing section. The actual swirl numbers at the exit of the Foster Wheeler burner will be determined during DVT. At the time of this submittal, the need to conduct additional cold flow experiments simulating the exhaust conditions of the Foster Wheeler burner is being assessed.

6.1.2 Test Results

Table 2 lists the test matrix followed for the Cleveland mix bustle testing. A total of ten tests were performed, with the key parameters of interest being axial distance downstream of the transition section, precombustor burner swirl number, and the momentum flux ratio between the secondary and primary air streams. The swirl number is defined as the ratio of the maximum tangential to axial velocity at the precombustor baffle.

The momentum flux ratio is defined as

$$R^2 = \frac{\rho_2 V_2^2}{\rho_1 V_1^2}$$

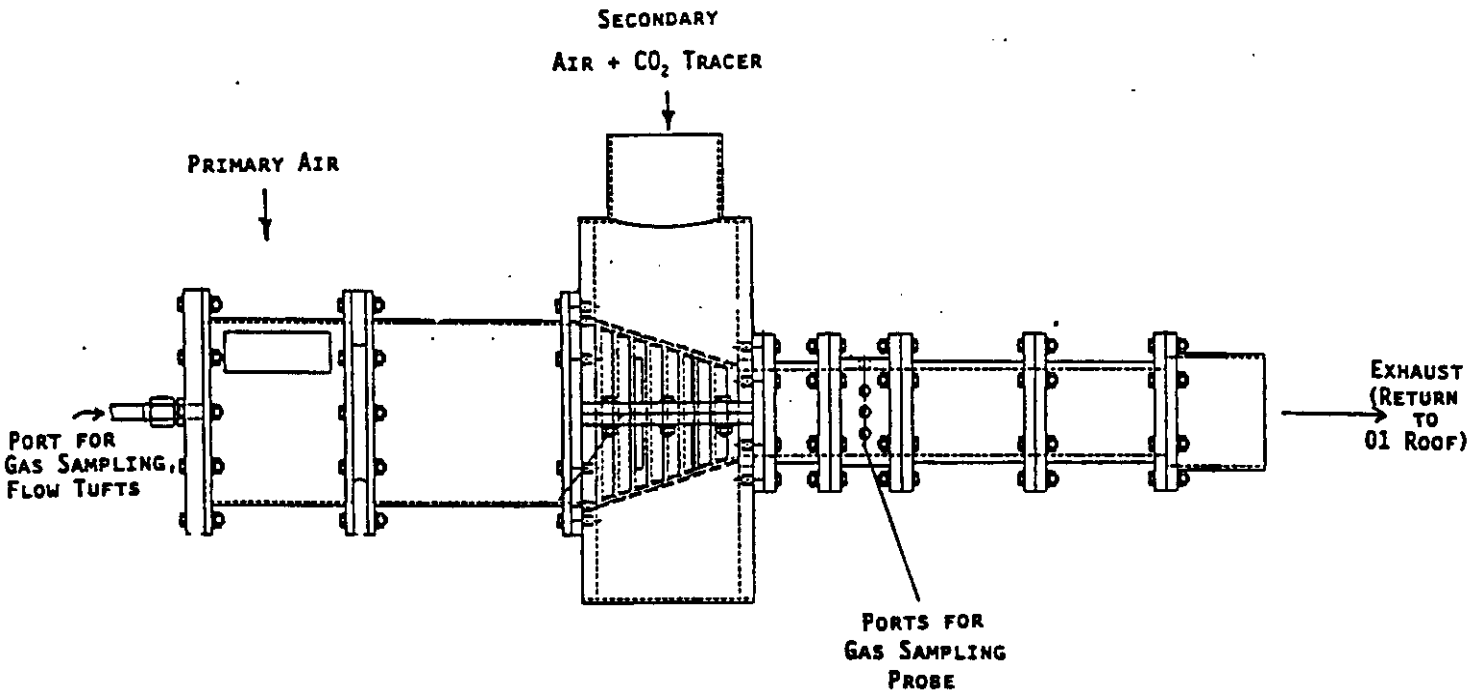

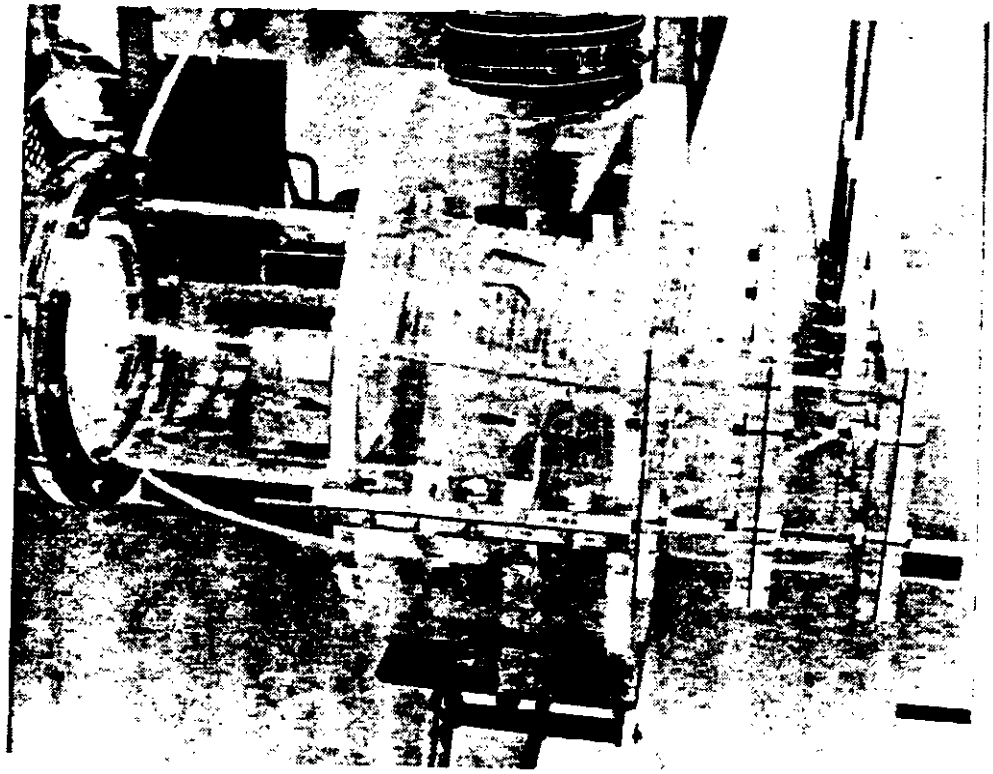

FIGURE 10. CLEVELAND MIX BUSTLE TEST SET-UP

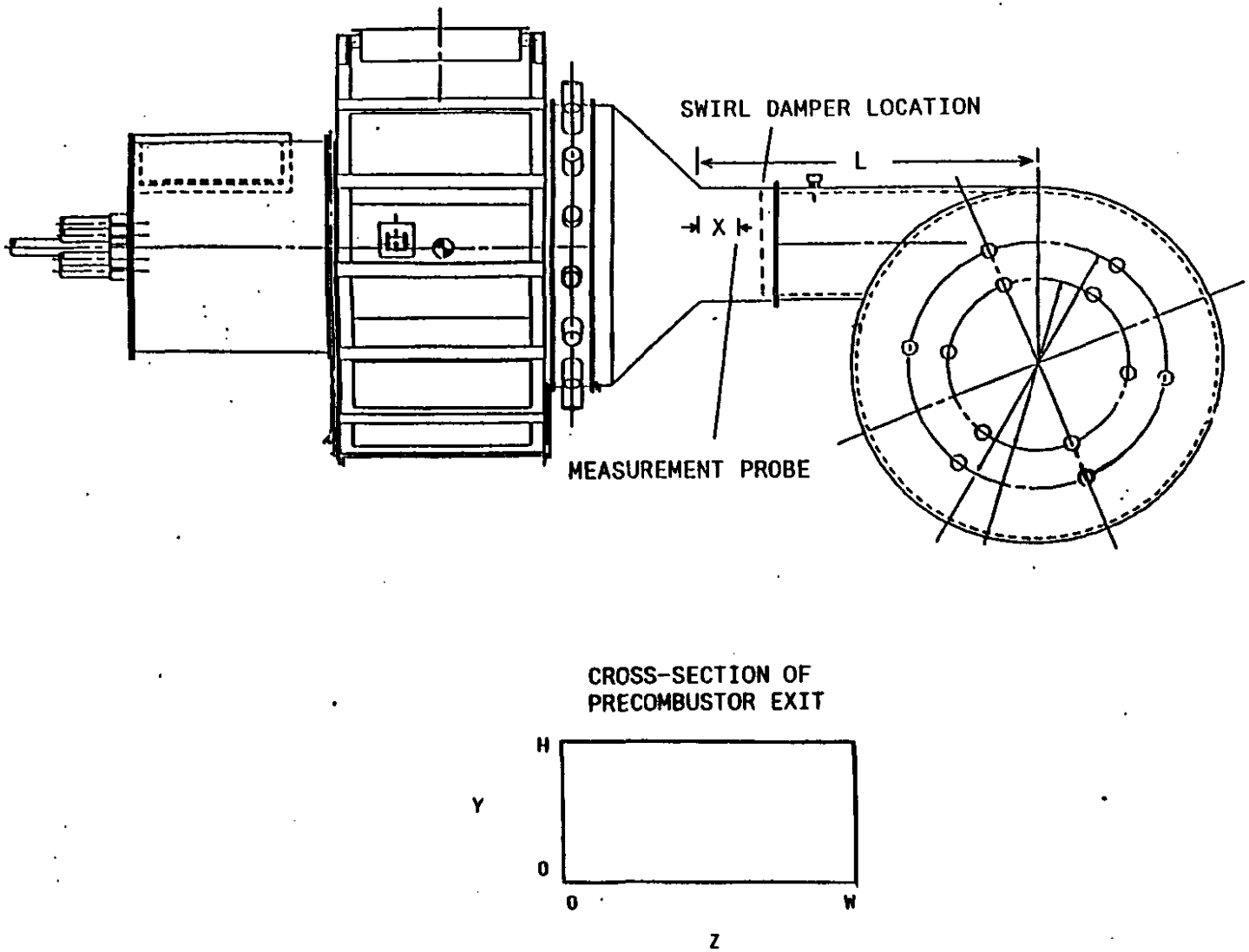

FIGURE 11. PRECOMBUSTOR EXIT COORDINATE SYSTEM FOR COLD FLOW MEASUREMENTS

- (X/L=0.3 FOR SWIRL DAMPER POSITION)

TABLE 2. COLD FLOW TEST MATRIX - CLEVELAND PRECOMBUSTOR CONFIGURATION

	AXIAL STATION X/L			SWIRL NUMBER		SECONDARY AIR MOMENTUM RATIO (R^2)			
CASE	0.05	0.3	0.55	0	3.5	0.05	0.21	0.85	COMMENTS
CLEVE1		X		X			X		CO2 TRACER WITH SECONDARY AIR
CLEVE2		X		X				X	CO2 TRACER WITH SECONDARY AIR
CLEVE3			X	X			X		CO2 TRACER WITH SECONDARY AIR
CLEVE4			X		X		X		CO2 TRACER WITH SECONDARY AIR
CLEVE5		X			X		X		CO2 TRACER WITH SECONDARY AIR
CLEVE6		X			X			X	CO2 TRACER WITH SECONDARY AIR
CLEVE7		X			X		X		CO2 TRACER WITH PRIMARY AIR
CLEVE8	X				X		X		CO2 TRACER WITH SECONDARY AIR
CLEVE9	X				X			X	CO2 TRACER WITH SECONDARY AIR
CLEVE10	X				X	X			CO2 TRACER WITH SECONDARY AIR

where ρ_1 = density of PC burner exhaust stream
V_1 = plug flow velocity at PC combustion chamber exit
ρ_2 = density of secondary air
V_2 = effective flow velocity through mix bustle slots (based on effective flow area)

For cold flow testing, the densities of the two streams were essentially equal (except for the effect of the CO_2 tracer). The correct momentum ratio was thus obtained by adjusting the velocity ratio, or the mass flow ratio, of the two streams. In most gas-gas mixing situations, density differences usually have only a secondary role on mixing, provided the momentum ratio of the two streams is preserved. In order to verify this, the density of the mill air gas stream was varied during parametric Healy cold flow tests (see Section 6.2.2.5).

Figure 12 presents isotherm plots for the baseline Cleveland configuration, both with and without burner swirl. These plots are based on CO_2 concentration measurements taken over the flow cross-section at X/L= 0.3, which roughly corresponds to the location of the air inlet dampers just downstream of the mix bustle in the rectangular duct leading to the slagging stage. The view is looking downstream towards the slagging stage from the PC burner. To generate these plots, the temperature distribution in the primary flow upstream of the mixing section was assumed to be uniform at a temperature of 3620°F, which is consistent with rapid devolatilization of coal in the burner at a stoichiometry of approximately 1.0. The secondary air temperature was assumed to be 350°F, consistent with Cleveland air preheat conditions. If both streams were perfectly mixed, the resulting temperature would be 2440°F.

For the case with no primary swirl, the mixing of the primary and secondary flows is far from complete, with a temperature difference of approximately 1500°F between the coldest areas near the lower corners and the hottest region in the center of the rectangular duct. With swirl, mixing is significantly improved, with a maximum temperature difference of approximately 600°F. Note also that while the temperature contours in the no swirl case are fairly symmetric, the swirl case has a distinct asymmetric mixing pattern. The center, upper right, and lower left regions are fairly well-mixed, while the upper left and lower right corners have higher temperatures (less than average amounts of secondary air in these regions). This effect is attributed to the combination of a single air inlet to the secondary air windbox coupled with a swirling primary flow. A more detailed explanation of this mixing pattern is provided in Section 7.1.

Figure 13 shows the effect of secondary air momentum ratio on overall mixing performance for X/L=0.05. In each case, the perfectly mixed temperature was set to 2440°F in order to isolate any mixing differences. Note that the overall mixing patterns are similar in all three cases, with a fairly well mixed core region. Higher than average temperatures were observed in the upper left and lower right corners, while lower than average temperatures were observed in the lower right and upper left corners. In each case, the maximum temperature difference is on the order of 1000-1100°F. Thus it appears that the secondary air momentum ratio, or alternately the ratio of secondary flow to primary flow, has at most a secondary effect on overall mixing performance.

Cold flow tests were also run to characterize mixing changes as the flow proceeds down the rectangular duct connecting the precombustor and the slagging stage. The results are plotted in Figure 14 for various mixing lengths. As

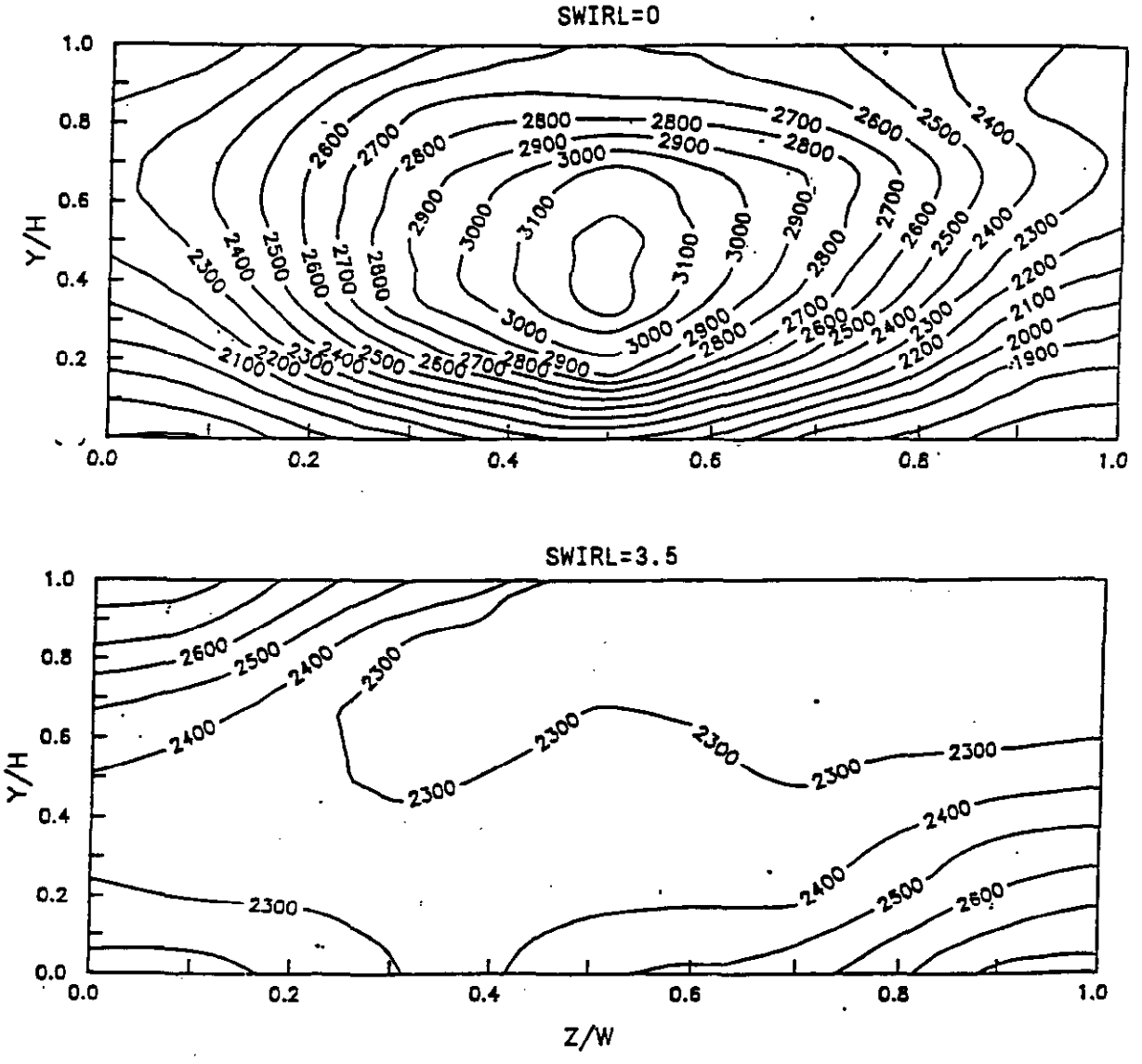

FIGURE 12. TEMPERATURE DISTRIBUTION AT PRECOMBUSTOR EXIT BASED ON COLD FLOW CONCENTRATION MEASUREMENTS - EFFECT OF PRIMARY AIR SWIRL (CLEVE 1 VS CLEVE 5)

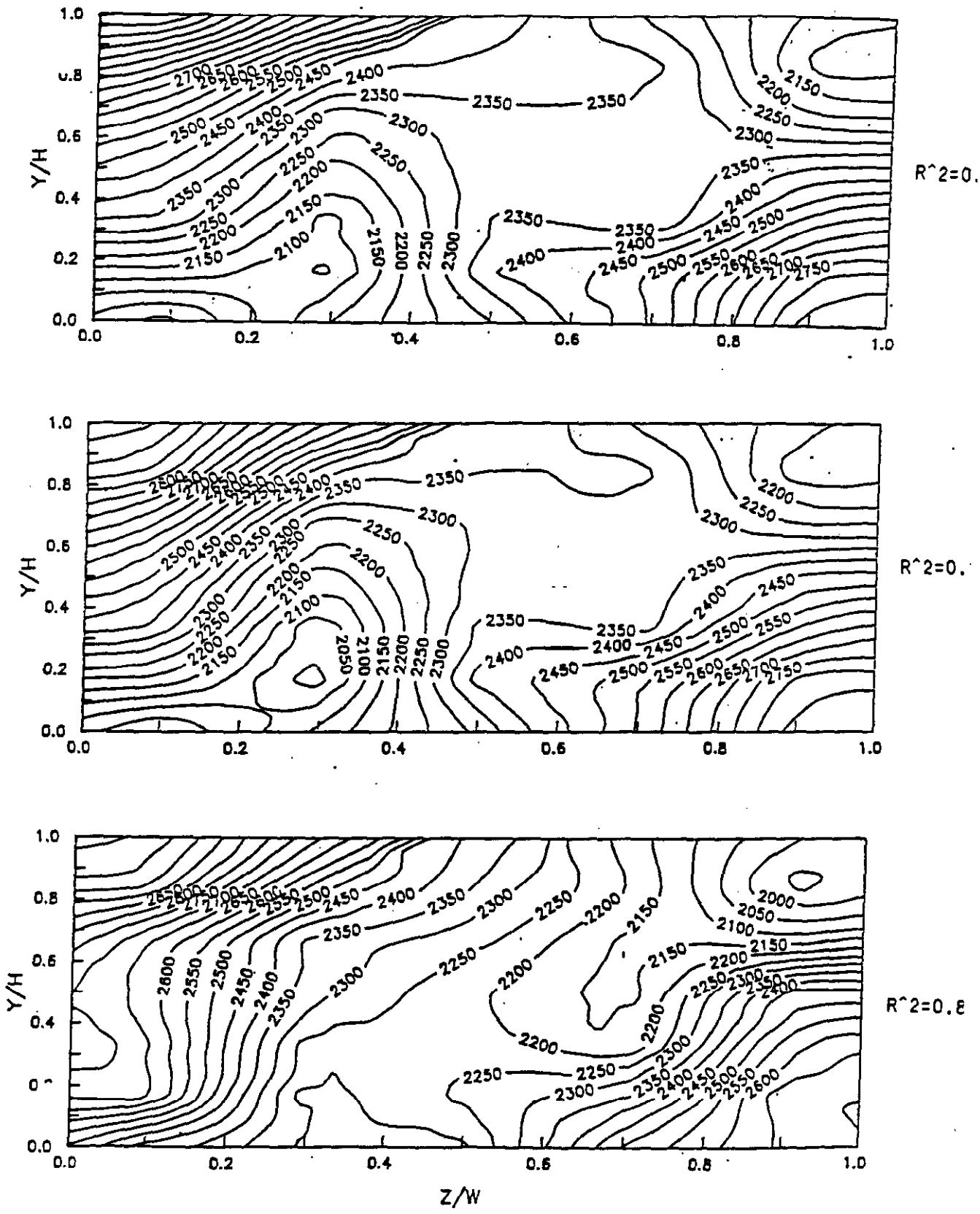

FIGURE 13. TEMPERATURE DISTRIBUTION AT PRECOMBUSTOR EXIT BASED ON COLD FLOW CONCENTRATION MEASUREMENTS - EFFECT OF SECONDARY AIR MOMENTUM RATIO (CLEVE 10, CLEVE 8, CLEVE 9)

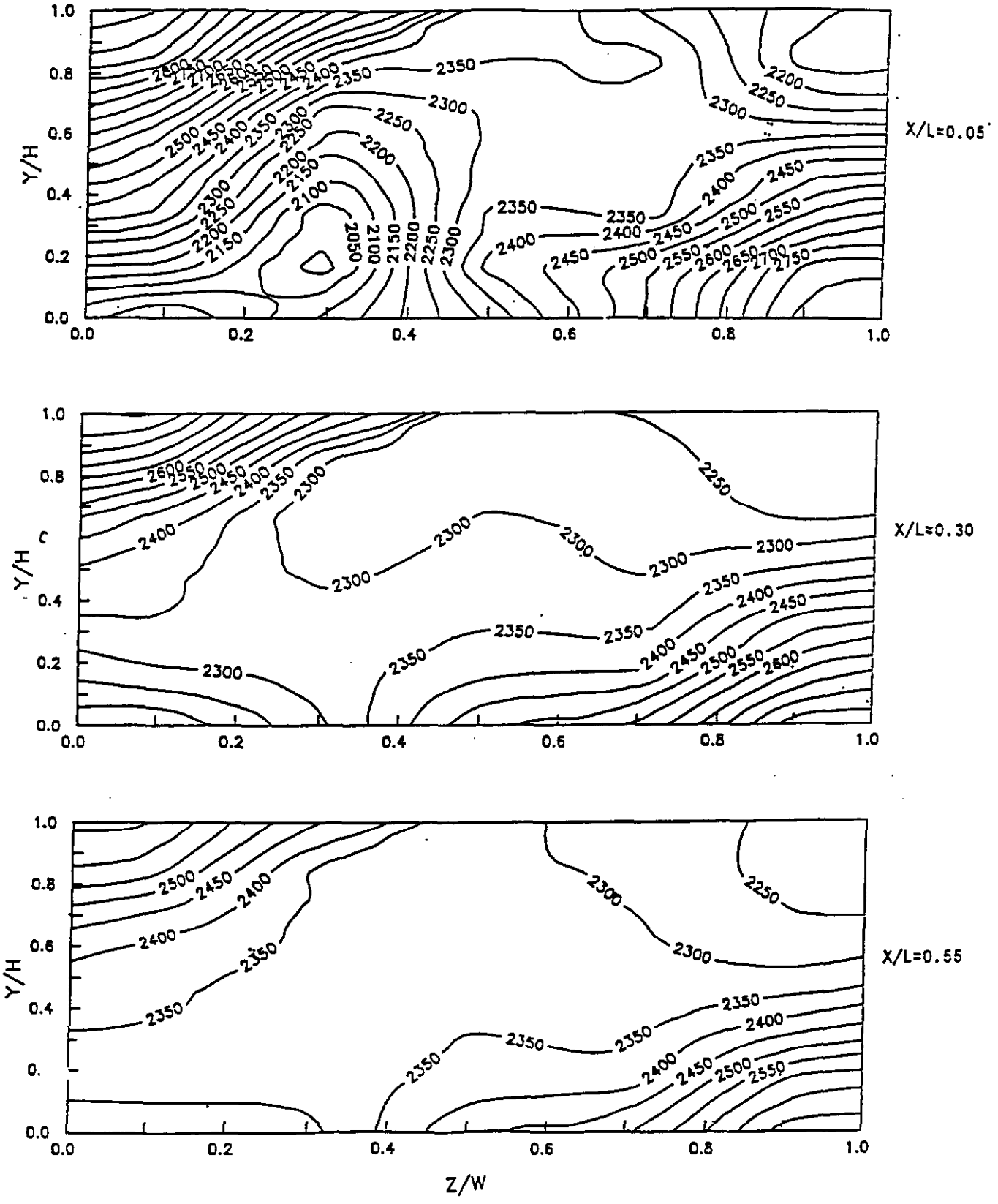

FIGURE 14. TEMPERATURE AT PRECOMBUSTOR EXIT BASED ON COLD FLOW CONCENTRATION MEASUREMENTS - EFFECT OF MIXING LENGTH (CLEVE 8, CLEVE 5, CLEVE 4)

expected, mixing improves as the flow moves downstream, with maximum temperature differences of 1000, 600, and 450°F for X/L= 0.05, 0.30, and 0.55, respectively. Note, however, that while the temperature differences decrease with an increase in mixing length, the same distinct mixing pattern is present in each case. This is consistent with visual observations, which indicated that the swirl portion of the flow is confined to the center region of the duct, while the flow along the side walls and in the corners is primarily axial with little swirl. Additional mixing is expected as the flow passes through the air inlet dampers, since the sidewall flows are then directed back into the swirling core flow.

6.2 Healy Precombustor Secondary Mixing Testing

6.2.1 Test Configuration

Following the evaluation of the Cleveland mix bustle performance, a model of the Healy secondary mixing section, shown in Figure 15, was installed and tested. As mentioned previously, the same precombustor head-end geometry was used for both configurations in order to isolate the mixing differences. In addition to the primary and secondary air streams used above, a third air stream was introduced to simulate injection of mill air. Flow visualization and mixing studies were conducted similar to those described above. CO_2 tracer was introduced into either the secondary or mill air flow during individual runs to characterize mixing performance. Parametric tests were run for different momentum ratios, windbox gap settings, and number of mill air injection ports to determine mixing sensitivity.

6.2.2 Test Results

Table 3 lists the test matrix followed during the Healy secondary air mixing test phase. The first series of tests focused on mixing between the primary burner flow and secondary air. Key parameters of interest were the precombustor burner swirl number, the location of the secondary air inlet, the secondary windbox gap opening, and the momentum ratio between the primary and secondary air. In order to determine mixing performance, CO_2 tracer was introduced with the secondary air.

The second series of tests focused on the mixing of the mill air with both the primary and secondary flows. The key parameters for this testing were the momentum ratio between the mill air and primary flows, the number of mill air ports, and the mill air injection port diameter. A CO_2 tracer gas was introduced with the flow simulating mill air. Several tests were also dedicated to assessing the impact of density differences on mixing performance, with either argon gas or carbon dioxide gas used to simulate the colder, higher density mill air.

Table 4 lists the range of primary, secondary, and mill air flows expected during start-up and steady state operation of the Healy combustor. The range of secondary air-to-PC burner flow momentum ratio, R_1^2 , ranges from 0.01 (during start-up) to 0.85 (35% MCR firing waste coal), with a nominal value of 0.55 for performance coal at 100% MCR. The range of mill air-to-PC burner flow momentum ratio, R_2^2 , ranges from 0.0 (no mill air injection to 17.9 (during start-up), with a nominal value of 0.64 for performance coal at 100% MCR. Figure 16 shows the expected operating map for both secondary air momentum ratio and mill air momentum ratio, along with cold flow test conditions. Note that in both cases,

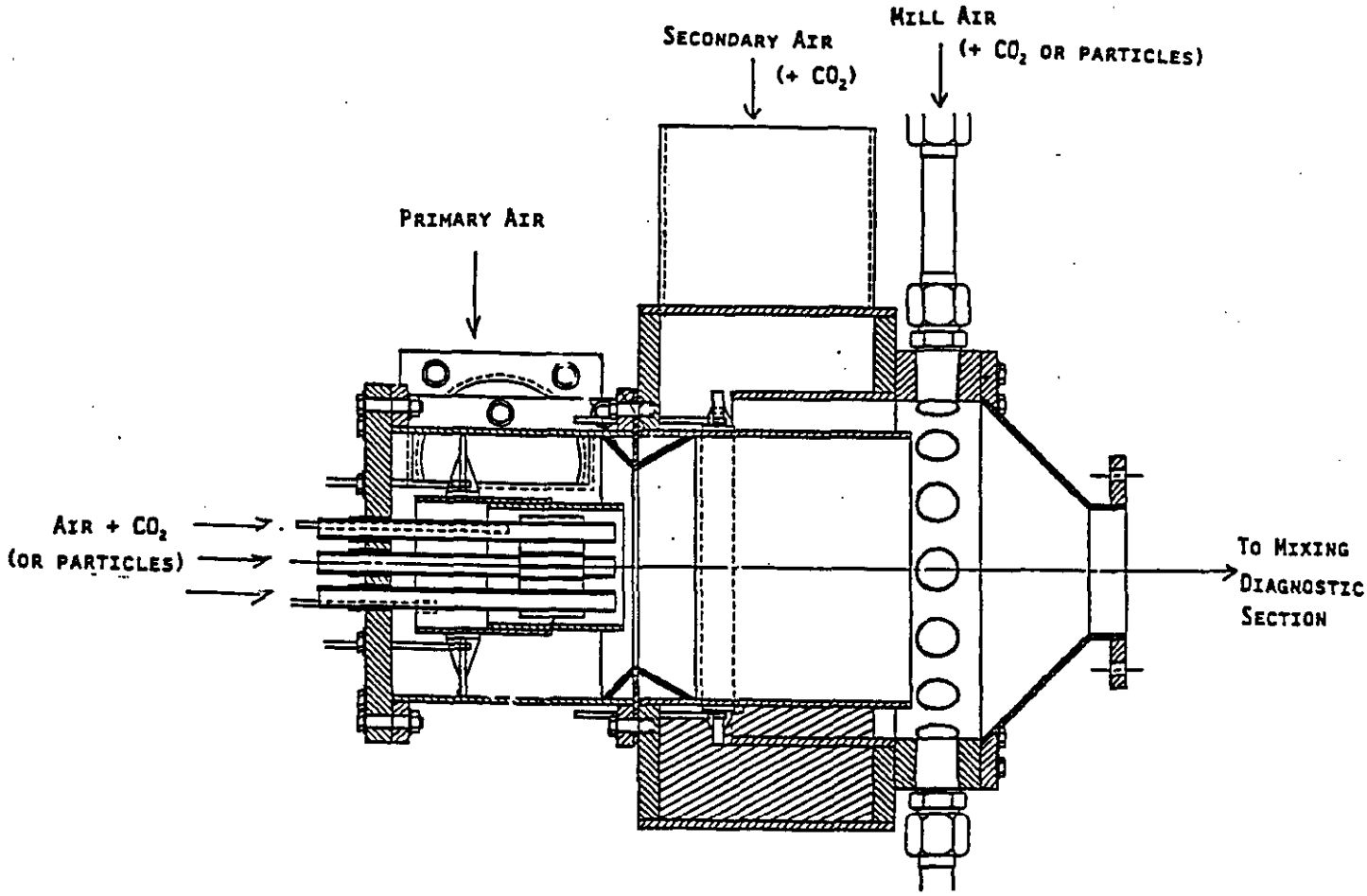

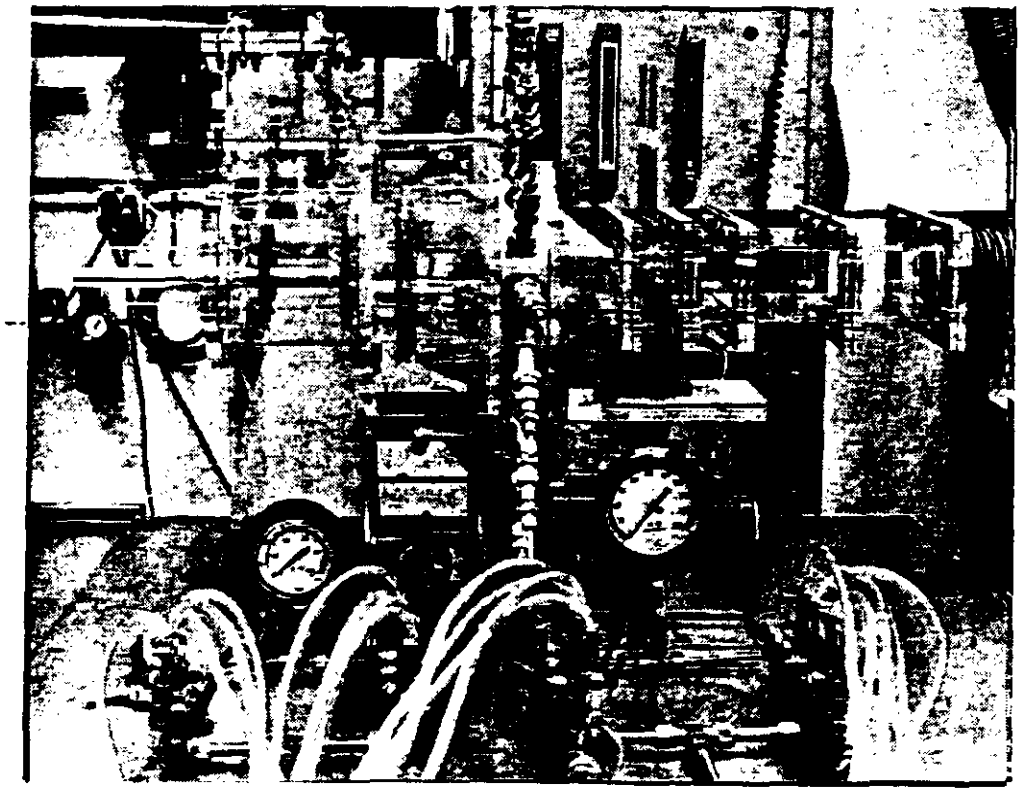

Figure 15. Healy Precombustor Test Set-Up

TABLE 3. COLD FLOW TEST MATRIX - HEALY PRECOMBUSTOR CONFIGURATION

CASE	SWIRL NUMBER		SECONDARY WINDBOX GAP OPENING (INCHES)			SECONDARY AIR CONFIGURATION		SECONDARY AIR MOMENTUM RATIO (R1^2)			MELL AIR MOMENTUM RATIO (R2^2)	NO. OF MELL AIR PORTS				MELL AIR INJECTOR DIAMETER (INCHES)		COMMENTS
	0	3.5	0.125	0.25	0.5	TOP	SIDE	0.14	0.56	2.25		0	4	8	16	0.50	0.71	
HEALY1		X		X		X			X			X						CO2 TRACER WITH SECONDARY AIR
HEALY2		X		X		X		X				X						CO2 TRACER WITH SECONDARY AIR
HEALY3	X			X		X			X			X						CO2 TRACER WITH SECONDARY AIR
HEALY4	X			X		X				X		X						CO2 TRACER WITH SECONDARY AIR
HEALY5	X		X			X			X			X						CO2 TRACER WITH SECONDARY AIR
HEALY6	X				X	X			X			X						CO2 TRACER WITH SECONDARY AIR
HEALY7		X		X		X				X		X						CO2 TRACER WITH SECONDARY AIR
HEALY8		X	X			X			X			X						CO2 TRACER WITH SECONDARY AIR
HEALY9		X		X		X			X			X						CO2 TRACER WITH SECONDARY AIR
HEALY10		X			X	X			X			X						CO2 TRACER WITH SECONDARY AIR
HEALY11	X		X			X			X			X						CO2 TRACER WITH SECONDARY AIR
HEALY12	X			X			X		X			X						CO2 TRACER WITH SECONDARY AIR
HEALY13		X		X			X		X			X						CO2 TRACER WITH SECONDARY AIR
HEALY14		X		X			X		X		0.50				X	X		CO2 TRACER WITH MELL AIR
HEALY15		X		X			X		X		2.10				X	X		CO2 TRACER WITH MELL AIR
HEALY16	X			X			NONE		X		0.50				X	X		CO2 TRACER WITH MELL AIR
HEALY17	X			X			X		X		0.50				X	X		CO2 TRACER WITH MELL AIR
HEALY18		X		X		X			X		0.50				X	X		CO2 TRACER WITH MELL AIR
HEALY19		X		X			X		X		34.0			X		X		CO2 TRACER WITH MELL AIR
HEALY20		X		X			X		X		0.50			X			X	CO2 TRACER WITH MELL AIR
HEALY21		X		X			X		X		34.0		X				X	CO2 TRACER WITH MELL AIR
HEALY22		X		X			X		X		0.64			X			X	CO2 TRACER WITH MELL AIR
HEALY23		X		X			X		X		2.10			X			X	CO2 TRACER WITH MELL AIR
HEALY24		X		X			X		X		0.64				X	X		CO2 TRACER WITH MELL AIR
HEALY25		X		X			X		X		0.64				X	X		MELL FLOW ARGON PLUS CO2 TRACE
HEALY26		X		X			X		X		0.02				X	X		MELL FLOW IS ALL CO2

TABLE 4. RANGE OF SECONDARY AIR AND MILL AIR MOMENTUM RATIOS EXPECTED DURING START-UP AND STEADY STATE OPERATION

CASE	DESCRIPTION	BURNER FLOW LB/HR	SECONDARY FLOW LB/HR	MILL AIR LB/HR	(R_1^2)	(R_2^2)
STARTUP FLOW CONDITIONS						
A	WARM UP	27500	10000	10000	0.08	1.73
B	OIL UP	54500	10000	10000	0.02	0.44
C	MILL AIR ON	64500	10000	62000	0.02	12.1
D	COAL 20%	67500	10000	62000	0.01	11
E	OIL BACK-OUT	53000	10000	62000	0.02	17.9
F	TRANSFER AIR	58000	30000	30000	0.21	4.2
G	OIL OFF	52000	30000	30000	0.21	2.09
H	100% MCR	96800	89500	21400	0.55	0.64
STEADY STATE FLOW CONDITIONS						
1	PERFORMANCE COAL, 100% MCR	95961	89536	21288	0.55	0.64
2	PERFORMANCE COAL, 60% MCR	67258	58042	0	0.46	0
3	PERFORMANCE COAL, 35% MCR	81904	74896	0	0.53	0
4	55/45 WASTE/ROM, 100% MCR	96370	89476	29843	0.54	1.25
5	55/45 WASTE/ROM, 60% MCR	67581	62819	0	0.55	0
6	55/45 WASTE/ROM, 35% MCR	82273	80646	0	0.61	0
7	RUN OF MINE COAL, 100% MCR	80391	86574	0	0.64	0
8	RUN OF MINE COAL, 60% MCR	56987	44105	0	0.37	0
9	RUN OF MINE COAL, 35% MCR	69599	58031	0	0.44	0
10	WASTE COAL, 100% MCR	100786	102085	46843	0.56	2.43
11	WASTE COAL, 60% MCR	70864	75872	0	0.72	0
12	WASTE COAL, 35% MCR	77035	96281	0	0.85	0

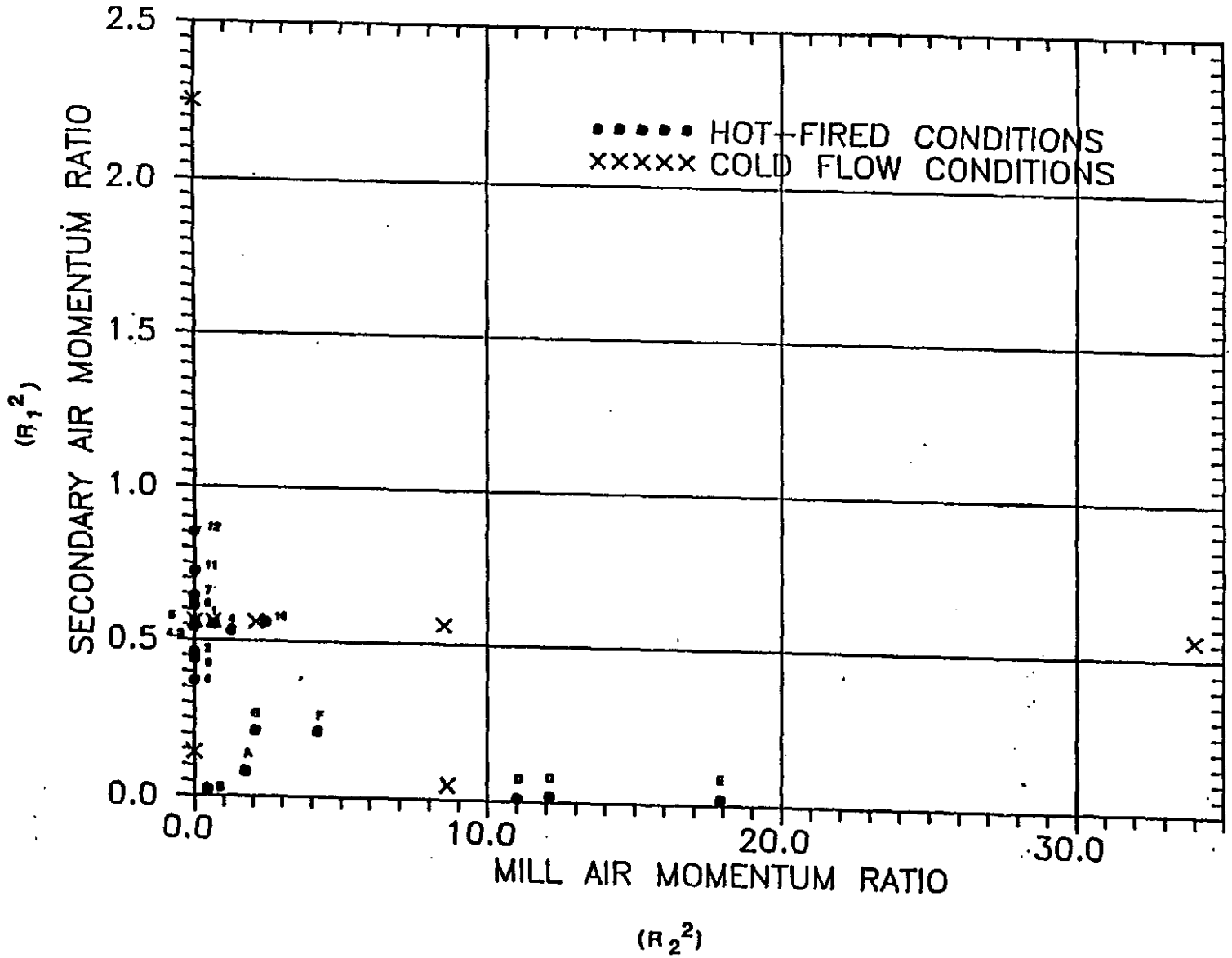

FIGURE 16. RANGE OF SECONDARY AIR AND MILL AIR MOMENTUM RATIOS EXPECTED DURING START-UP AND STEADY STATE OPERATION

cold flow momentum ratios were varied over a much larger range than that expected during hot-fired operation in order to characterize the sensitivity of mixing performance to momentum ratio.

6.2.2.1 Baseline Case - Combined Secondary and Mill Air Injection

The two baseline temperature profiles for the Healy mixing configuration are shown in Figure 17, for the secondary air inlet located on either the top and side of the secondary windbox (see Figure 18). The profiles are based on concentration measurements made just downstream of the circular-to-rectangular transition, at X/L = 0.05. These plots include both the effects of secondary air as well as mill air injection. To generate the plots, two separate measurements were made, one in which the CO_2 tracer was introduced with the secondary air, and the other in which the tracer was introduced with the mill air. Overall temperature profiles were then determined by supposition of the two measurements. For Healy conditions, the fully mixed temperature is 2500°F, which assumes rapid devolatilization of the coal in the PC burner (with no significant char oxidation), a secondary air temperature of 730°F, and a mill air temperature of 135°F.

6.2.2.2 Flow Distribution in Secondary Windbox

Note that in both cases, the level of mixing is significantly higher than that observed during testing with the Cleveland mixing configuration. Since the mass ratios and momentum ratios are similar between the two configurations, the improvement in mixing is attributed primarily to geometrical differences between the two configurations. In either case, the swirling action of the primary flow, rather than the penetration of the secondary flow, is the dominant mixing mechanism. In the Healy configuration, the secondary and mill air streams are introduced upstream of the transition section, and thus have a longer mixing time relative to the Cleveland configuration, in which the secondary flow enters through a series of slots along the transition section.

From Figure 17, it is seen that locating the air inlet on the side offers slightly better mixing performance than locating the air inlet on the top. Insight into the cause of these differences in mixing patterns can be gained by examining the corresponding cases in which the primary flow is non-swirling. These cases are plotted in Figures 19 and 20 for the side inlet and top inlet configurations, respectively.

For the side inlet case, concentration gradients are primarily in the horizontal direction, with high concentrations of secondary flow on each side and low concentrations in the center. Also note that the secondary air penetrates farther from the left side (same side as air inlet) than from the right. Also shown in Figure 19 are concentration profiles for the swirling primary flow case. Note that although the presence of swirl significantly improves mixing, there is still some evidence of a horizontal concentration gradient as well as greater penetration of secondary air on the same side as the air inlet.

For the top inlet case shown in Figure 20, the concentration of secondary air is highest along the sides and lower corners of the duct, with very little secondary air at the top. When swirl is added to the primary air, mixing again improves dramatically, although there is still more secondary air along the bottom than the top of the duct. An explanation for the difference in mixing patterns for the two air inlet locations is discussed in Section 7.3.

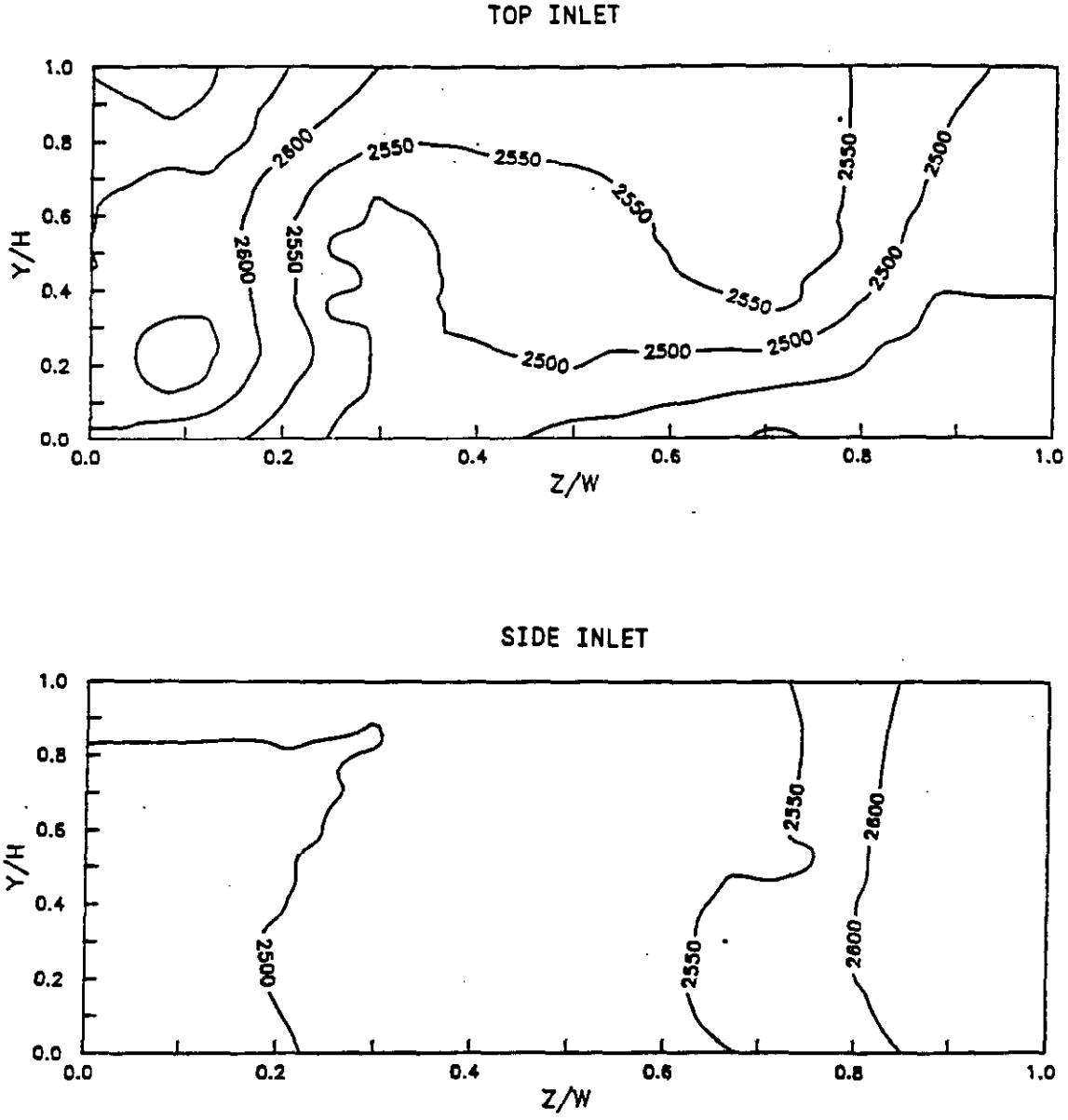

FIGURE 17. TEMPERATURE DISTRIBUTIONS AT PRECOMBUSTOR EXIT BASED ON COLD FLOW CONCENTRATION MEASUREMENTS - EFFECT OF WINDBOX AIR INLET LOCATION (HEALY 18 AND 19, HEALY 13 AND 14)

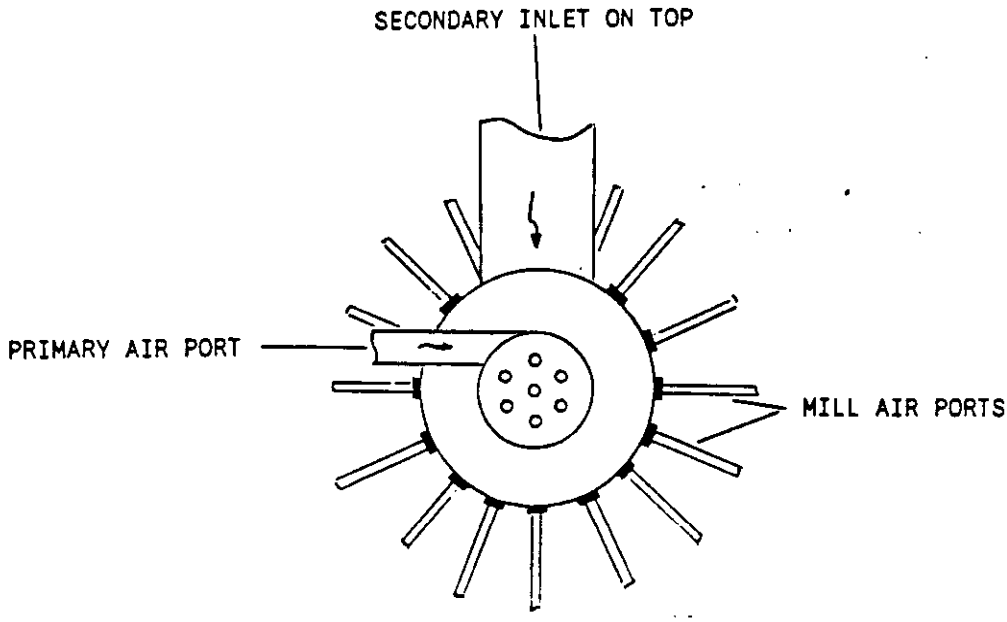

END VIEW OF PRECOMBUSTOR
(LOOKING DOWNSTREAM)

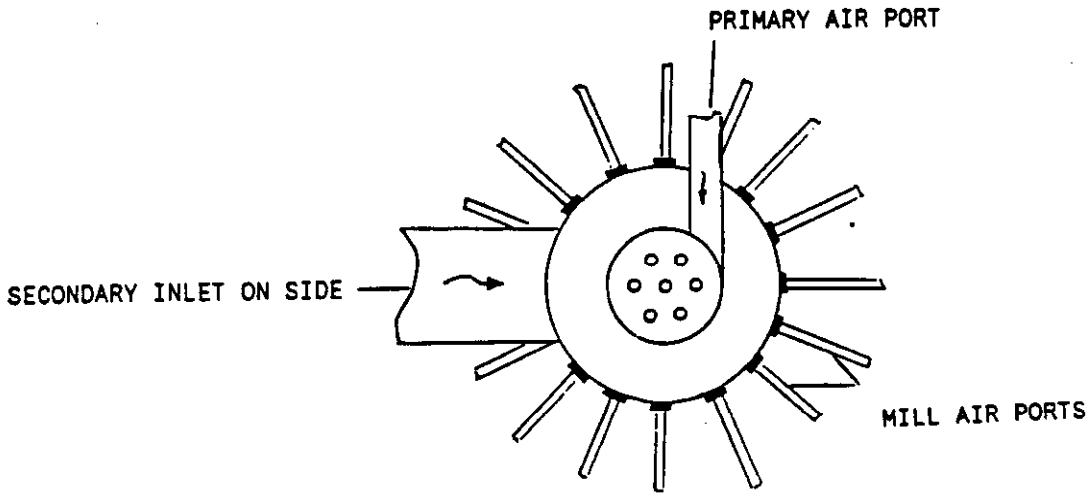

FIGURE 18. COLD FLOW PRECOMBUSTOR CONFIGURATIONS FOR SECONDARY AIR INLET ON TOP AND ON SIDE

HEALY CONFIGURATION
GAP=0.25", SIDE INLET
R1^2=0.56, R2^2=0

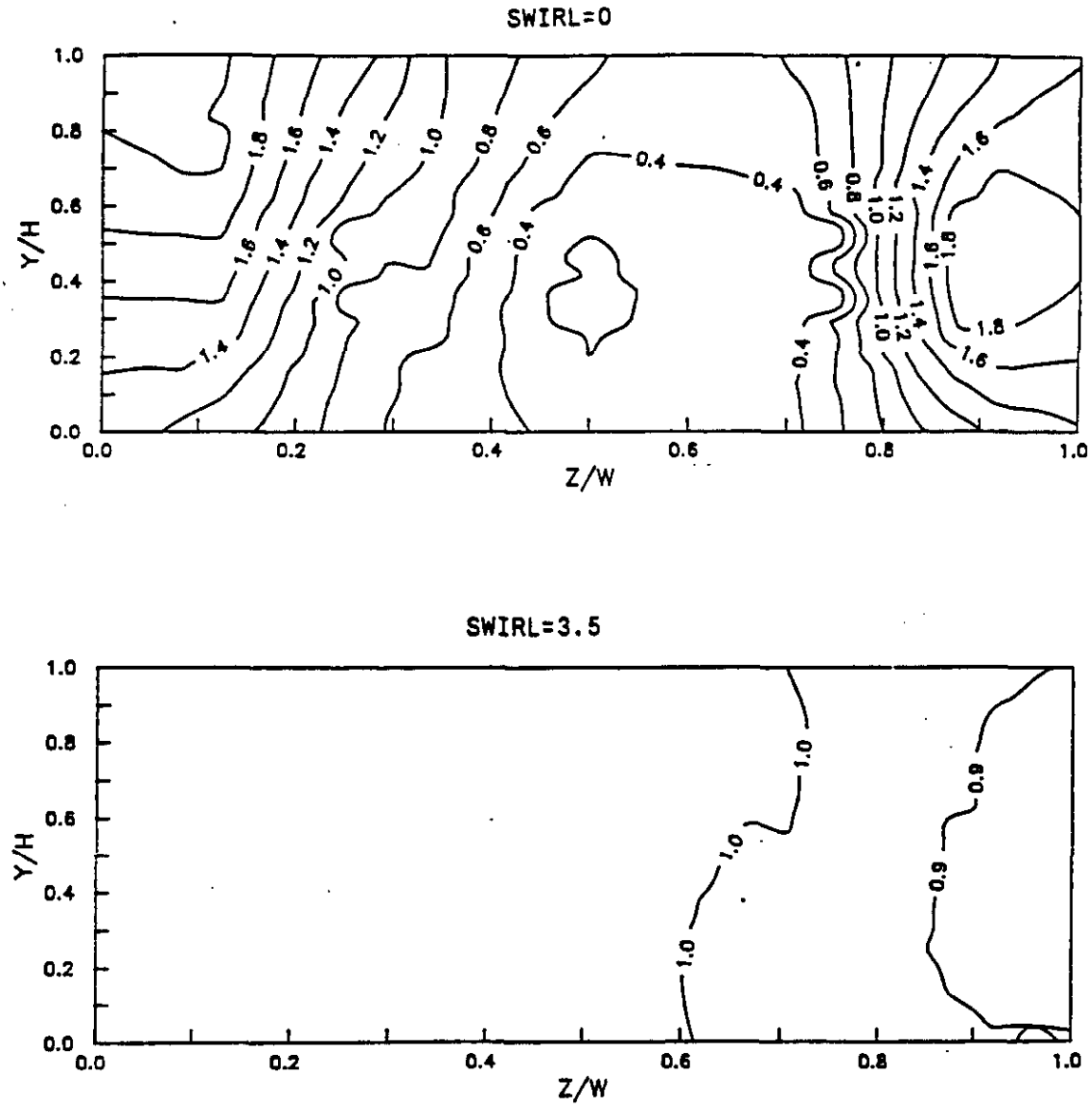

FIGURE 19. SECONDARY AIR CONCENTRATION DISTRIBUTIONS AT PRECOMBUSTOR EXIT BASED ON COLD FLOW MEASUREMENTS - EFFECT OF PRIMARY AIR SWIRL - (SIDE INLET) -(HEALY 12, HEALY 13)

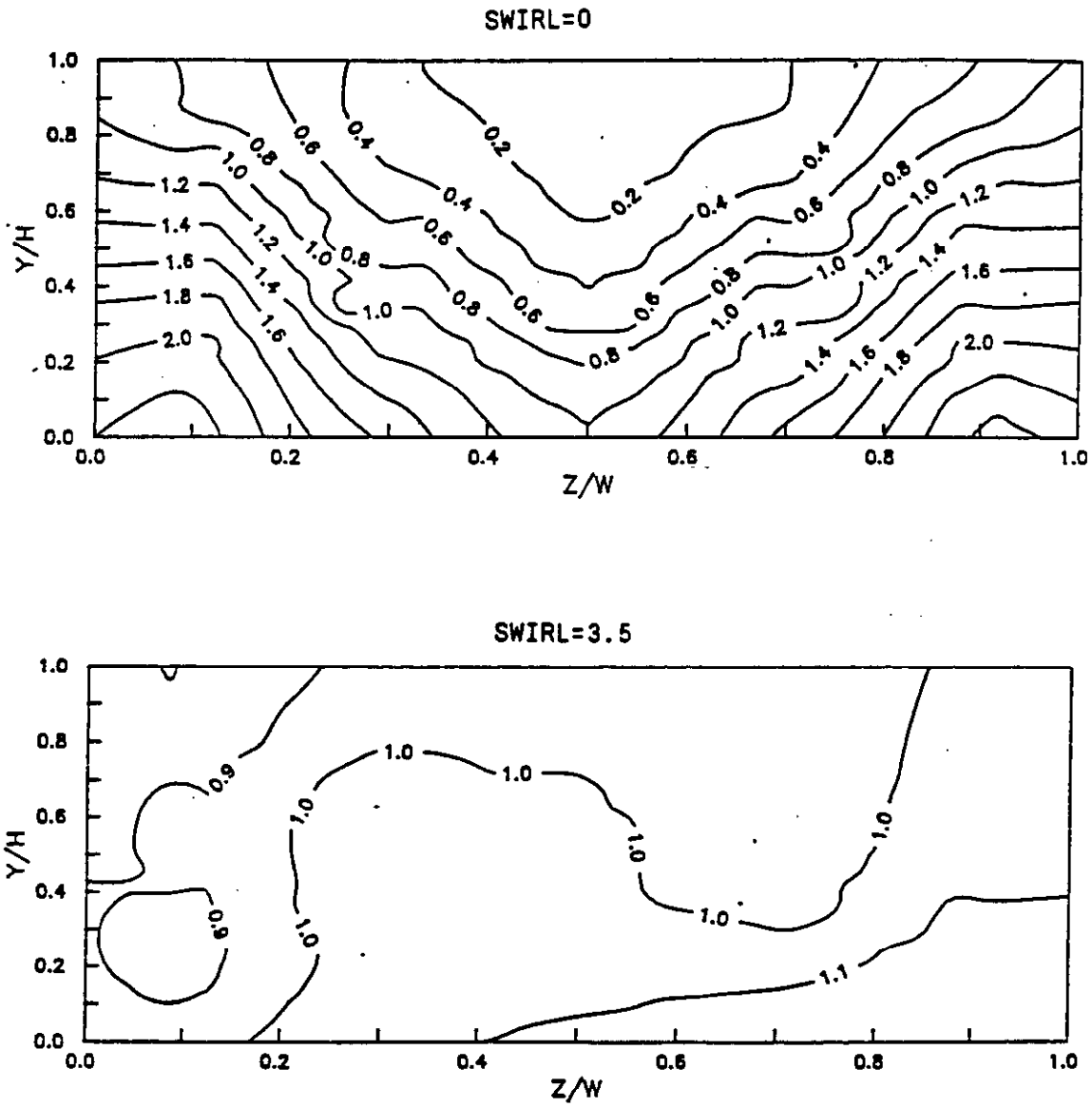

FIGURE 20. SECONDARY AIR CONCENTRATION DISTRIBUTION AT PRECOMBUSTOR EXIT BASED ON COLD FLOW MEASUREMENTS - EFFECT OF PRIMARY AIR SWIRL - (TOP INLET) - (HEALY 3, HEALY 9)

As indicated in Table 3, a series of tests were conducted to evaluate the effectiveness of the secondary windbox orifice plate in providing uniform flow distribution. Tests were run at gap openings of 0.125, 0.25 (nominal setting), and 0.50" for both a swirling and non-swirling primary flow. Figure 21 shows the results of the tests with primary swirl. From the plots, it can be seen that the gap opening has a negligible effect on the mixing patterns downstream of the transition section. At first, this was unexpected but upon further examination it was determined that most of the flow maldistribution occurs downstream of the orifice plate in the annular section due to the wall convergence on only two of the four sides. Flow patterns in the annulus were clearly flowing away from the top towards the sides and bottom corners. Similar results were obtained for the non-swirl case.

6.2.2.3 Effect of Secondary Air Momentum Ratio

A series of tests were run to assess the sensitivity of secondary air mixing to different momentum ratios, (or mass ratios) between the primary and secondary flows. The results of these tests are shown in Figure 22. Here, the ratio of secondary to primary flow momentum was varied from 0.14 to 2.25, which is a far larger range than that expected during hot-fire operation. Note that while there are noticeable differences in the mixing patterns of the three cases, the overall level of mixing is not significantly different over the range of interest. One trend that is evident is that as the momentum of the secondary flow is increased relative to the primary flow momentum, the secondary air tends to concentrate more along the sides of the duct. The distinction between a swirling core flow and primarily axial side flows also became more apparent during flow visualization as the momentum of the secondary flow was increased.

6.2.2.4 Mill Air Mixing

Figure 23 shows the concentration profiles for the case in which the CO_2 tracer was introduced with the mill air rather than with the secondary air. Without primary swirl, the mill air concentrations are higher along the walls of the duct than in the center, which indicates that the mill air does not adequately penetrate to the center of the duct in the transition section. Also note, that the mill air appears to penetrate more on the same side as the secondary air inlet, which is the same result found for the secondary air for the side inlet configuration. This appears to indicate that the primary air favors the side away from the air inlet. When swirl is added to the primary flow, mixing is improved considerably, as was observed for both Cleveland and Healy secondary air mixing. There is still, however, a slight tendency for the primary air to favor the side away from the air inlet, resulting in a slightly higher concentration of mill air on the left side of the duct. The difference, in terms of temperatures, is on the order of 50 to 100 degrees and is not considered significant.

In Figure 24, an 8-port mill air injection configuration is compared against the baseline 16-port configuration. The comparison is made for the same total injection flow area and injection-to-freestream momentum ratio. The injection flow area was held constant by increasing the injection port diameter from 0.5" to 0.71" as the number of ports were decreased from 16 to 8. In comparing the two cases, the 8-port configuration would be expected to have a slightly higher jet penetration due to the larger port diameter, while the 16-port configuration

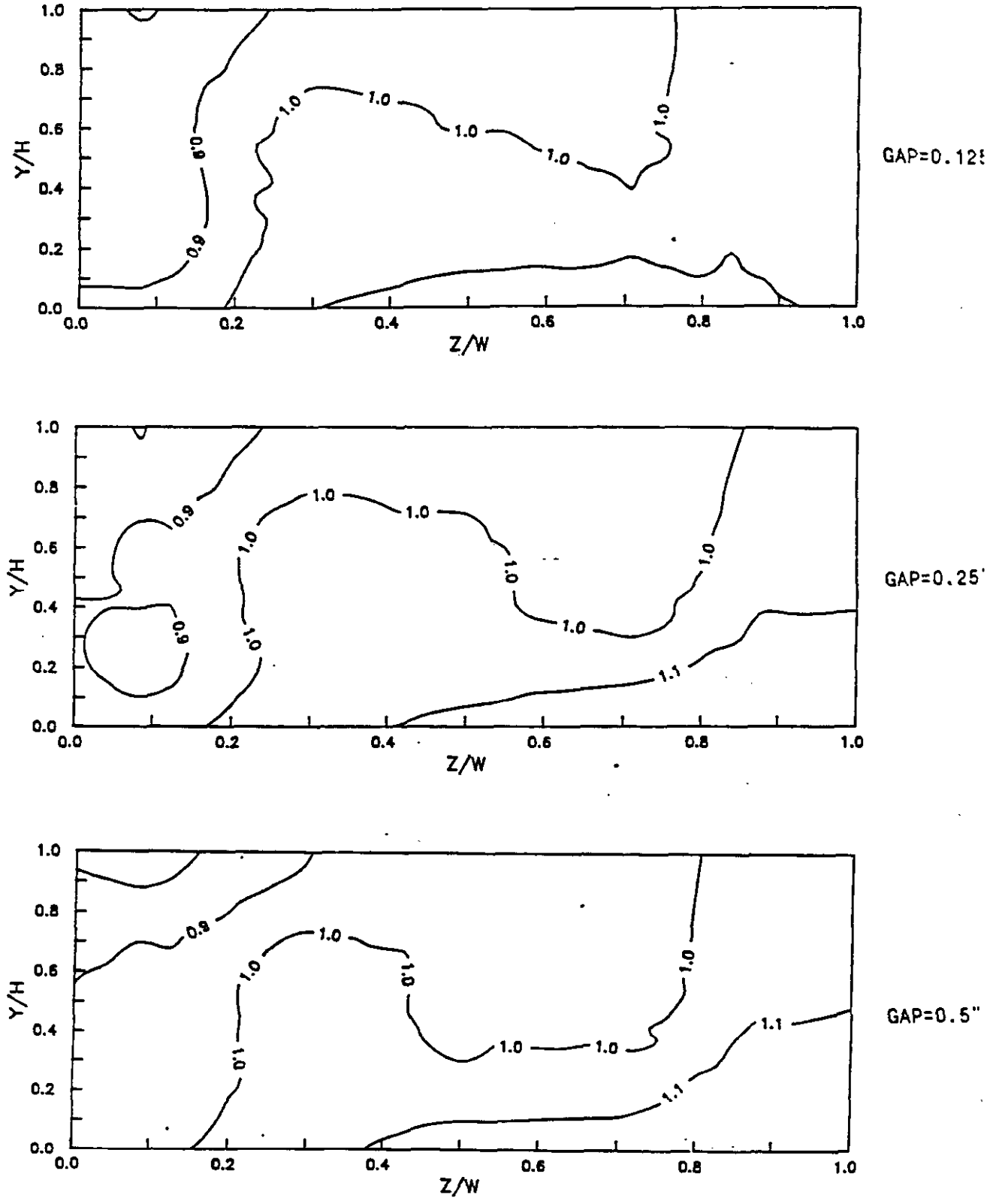

FIGURE 21. SECONDARY AIR CONCENTRATION DISTRIBUTIONS AT PRECOMBUSTOR EXIT BASED ON COLD FLOW MEASUREMENTS - EFFECT OF DISTRIBUTION GAP OPENING - (HEALY 8, HEALY 9, HEALY 10)

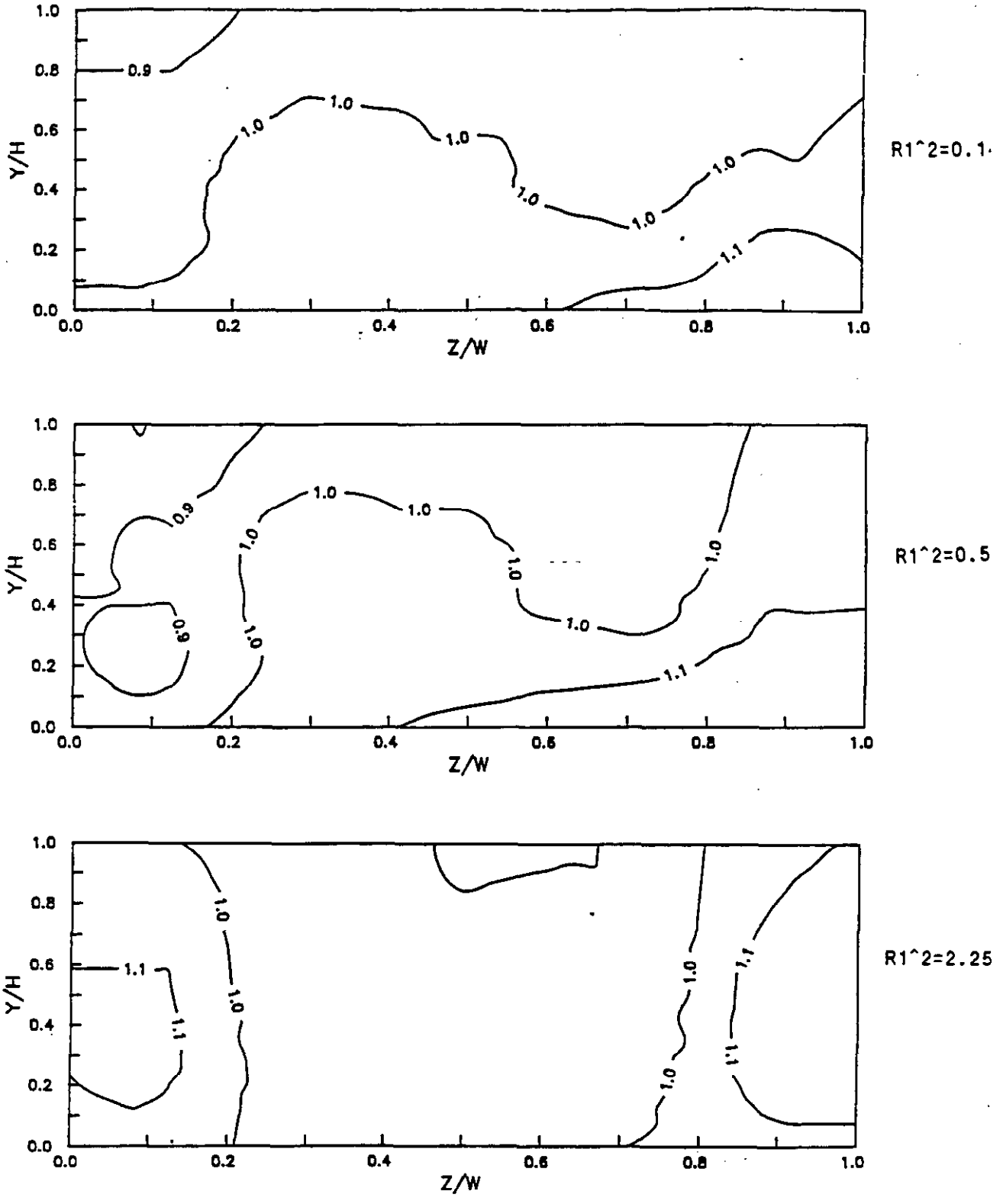

FIGURE 22. SECONDARY AIR CONCENTRATION DISTRIBUTION AT PRECOMBUSTOR EXIT BASED ON COLD FLOW MEASUREMENTS - EFFECT OF SECONDARY AIR MOMENTUM RATIO - (HEALY 2, HEALY 9, HEALY 7)

HEALY CONFIGURATION
GAP=0.25", SIDE INLET,
R1^2=0.56, R2^2=8.50,
16 PORTS, DIA=0.50"

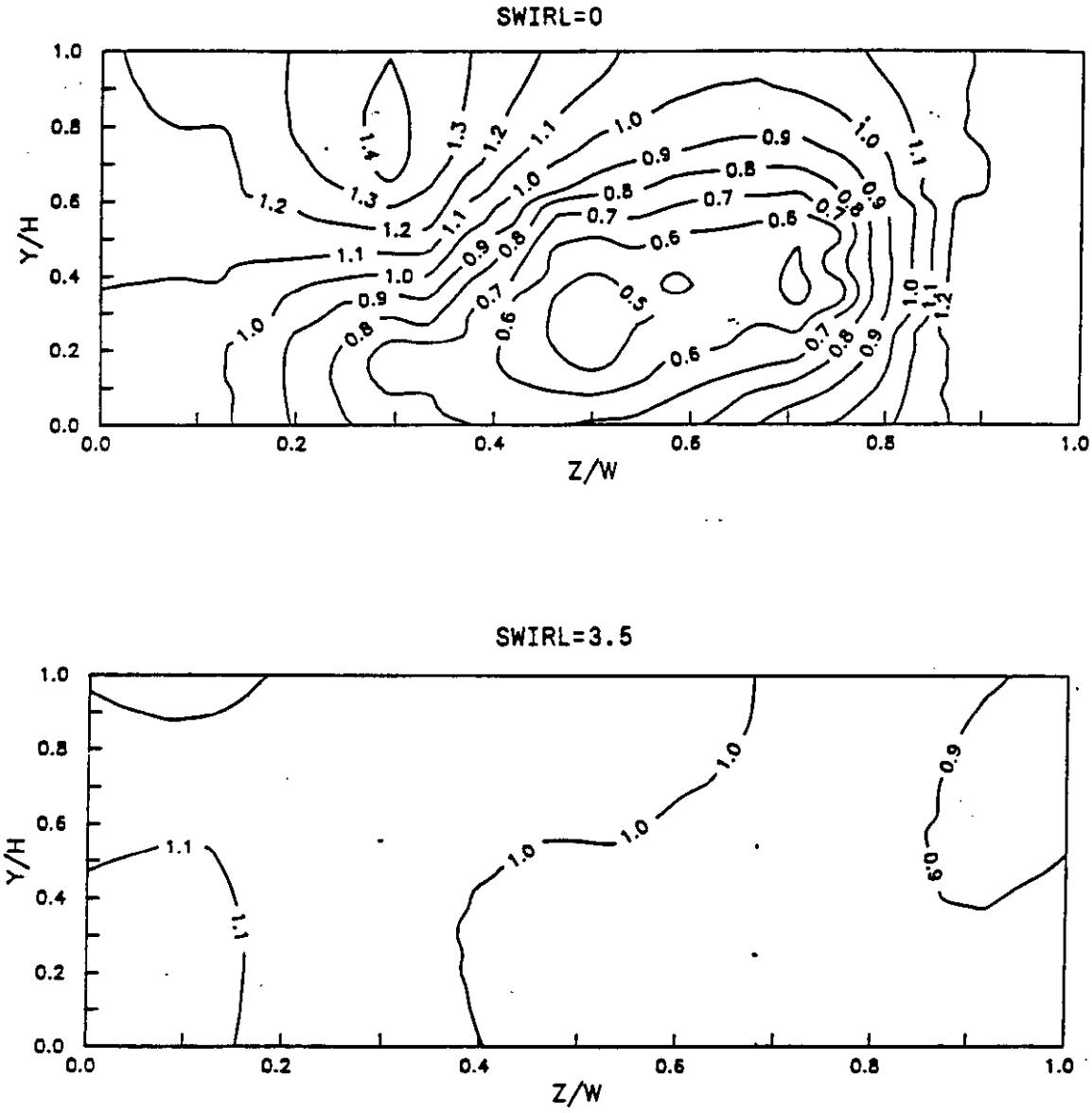

FIGURE 23. MILL AIR CONCENTRATION DISTRIBUTIONS AT PRECOMBUSTOR EXIT BASED ON COLD FLOW MEASUREMENTS - EFFECT OF PRIMARY SWIRL - (HEALY 17, HEALY 14)

HEALY CONFIGURATION
SWIRL=3.5, GAP=0.25",
R1^2=0.56, R2^2=8.50,
SIDE INLET

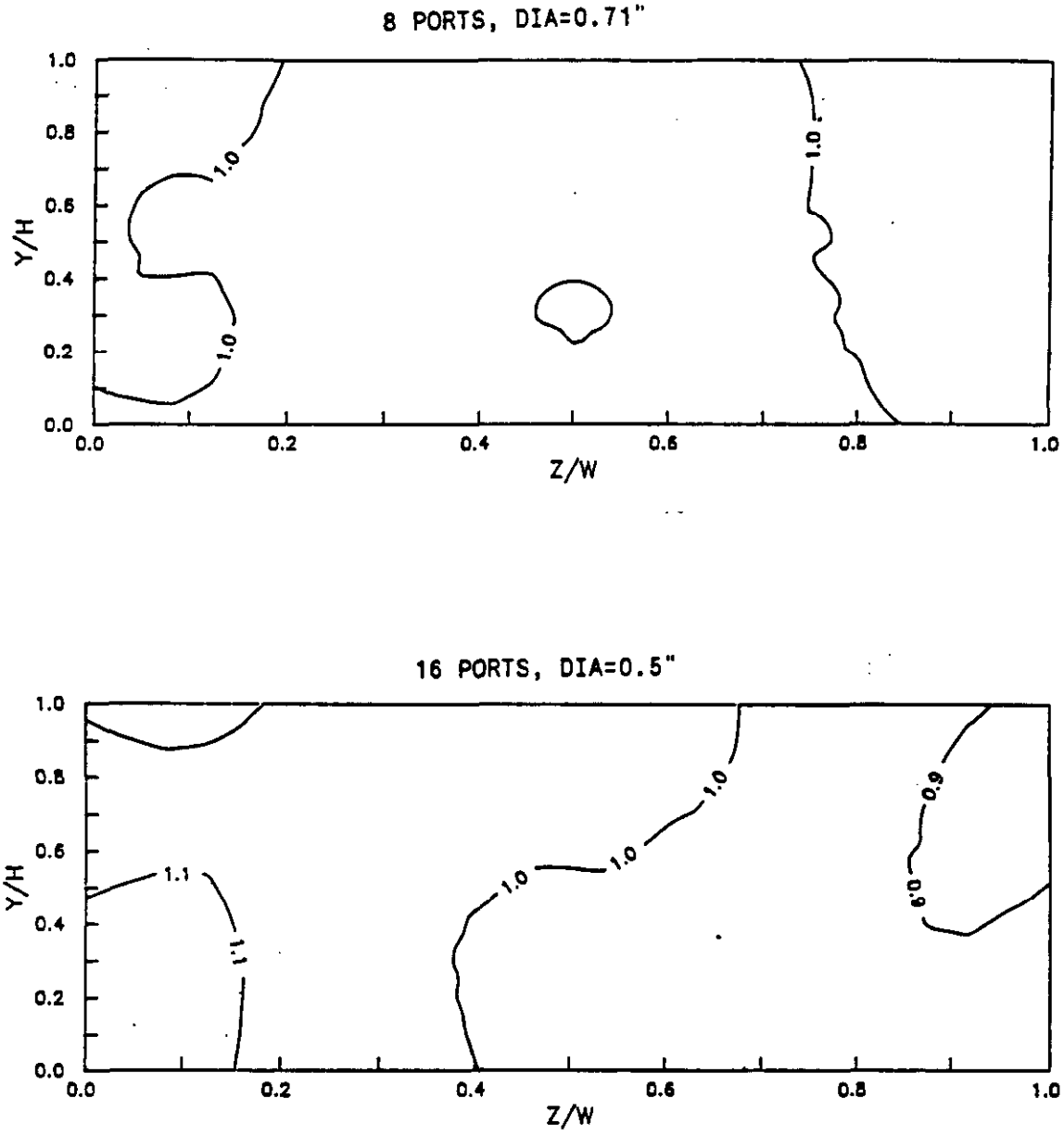

FIGURE 24. MILL AIR CONCENTRATION DISTRIBUTIONS AT PRECOMBUSTOR EXIT BASED ON COLD FLOW MEASUREMENTS - EFFECT OF NUMBER OF MILL AIR INJECTION PORTS - (HEALY 20, HEALY 14)

would be expected to achieve a somewhat more uniform mill air distribution along the periphery of the duct. As can be seen from Figure 24, the level of mixing is essentially the same in each case. Thus it appears that the two effects balance out over the range of interest, or more likely, neither jet penetration or jet distribution is a critical determinant of mixing performance. This will be further confirmed in the cases that follow.

Figures 25 and 26 show the effect of injector-to-freestream momentum ratio for the 8-port and 16-port injector configurations, respectively. Here again, it is seen that mill air momentum ratio has at most a secondary effect on mixing performance for this mixing situation. In each case, the momentum ratio was varied over the range 0.64 to 32, which is larger than the region expected during hot-fired conditions, even for the start-up scenario in which the combustor must accommodate 100% of the mill air.

6.2.2.5 Effect of Density Differences Between PC Burner Exhaust and Mill Air

Two tests were run to determine if density differences have a significant impact on mixing performance. Recall that the secondary and mill air flows have higher densities than the primary flow, at least initially, by factors of 3 and 6, respectively due to their lower temperatures. In most mixing studies, density ratios have been found to have only a secondary effect provided other important parameters, such as the momentum ratio and swirl number, are preserved. There was some concern, however, in this case, that centrifugal forces would have a negative impact on mixing as denser fluids would tend to remain near the outer wall. In order to investigate this, a worst case scenario was run in which a denser fluid, in this case CO_2, was introduced at very low momentum through the mill air ports. The results of this case are shown in Figure 27. Here, it is shown that the denser CO_2 gas, even though it is virtually dribbled along the outer walls of the transition section, mixes very thoroughly with the primary swirling flow by the time it reaches the end of the transition section. This further confirmed that the primary mixing mechanism was the swirling action of the primary precombustor flow and that secondary and mill air momentum (or mass flow) ratios have only secondary effects on the mixing process.

6.3 Slagging Stage Multiple Coal Injector Testing

6.3.1 Test Configuration

A schematic of the slagging stage multiple coal injector test set-up is shown in Figure 28. The primary air enters the slagging stage tangentially from the precombustor, while a secondary air stream is injected through the coal injectors. Flow tufts and water injection were used for flow visualization. Small particles were injected through individual coal injectors to characterize particle trajectories. Mixing patterns were determined using the CO_2 tracer method. Key parameters which were varied during testing included injector clocking and injector circle diameter.

6.3.2 Test Results

Table 5 lists the test matrix followed during the Healy multiple coal injector test phase. During this test phase, water and powder were utilized as tracer materials as well as carbon dioxide.

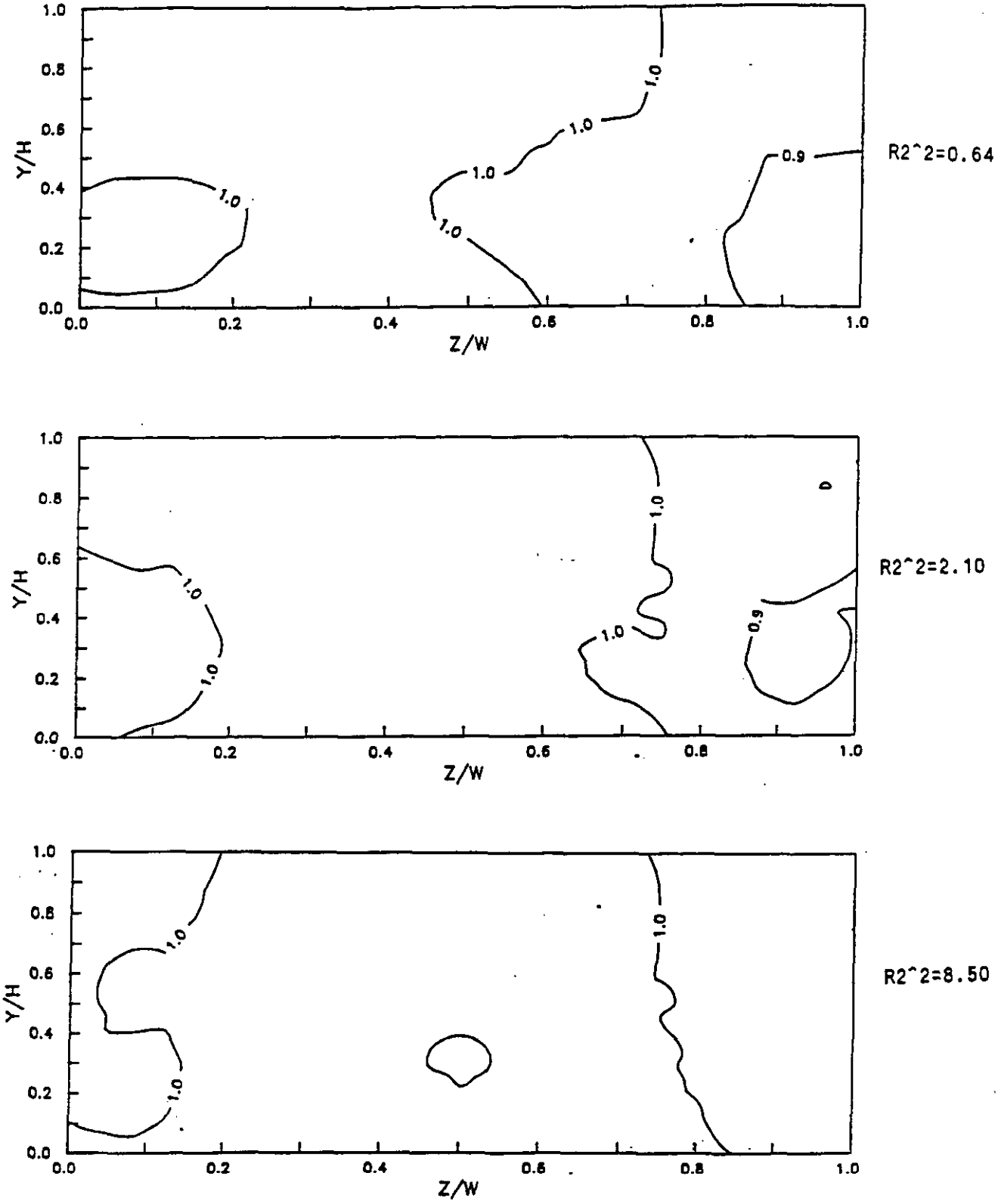

FIGURE 25. MILL AIR CONCENTRATION DISTRIBUTION AT PRECOMBUSTOR EXIT BASED ON COLD FLOW MEASUREMENTS - EFFECT OF MILL AIR MOMENTUM RATIO - (8 PORTS) - (HEALY 22, HEALY 23, HEALY 20)

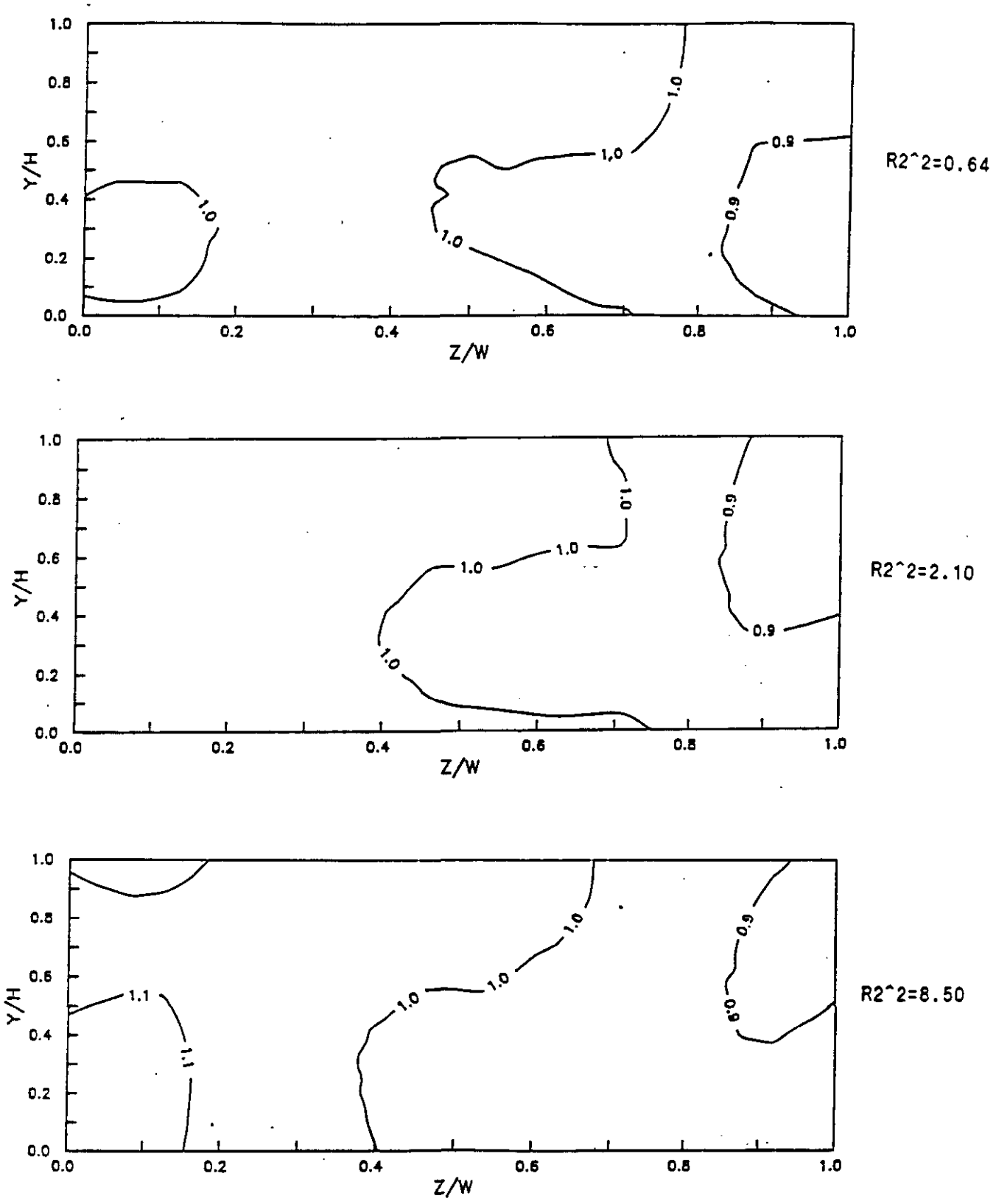

FIGURE 26. MILL AIR CONCENTRATION DISTRIBUTION AT PRECOMBUSTOR EXIT BASED ON COLD FLOW MEASUREMENTS - EFFECT OF MILL AIR MOMENTUM RATIO - (16 PORTS) - (HEALY 24, HEALY 15, HEALY 14)

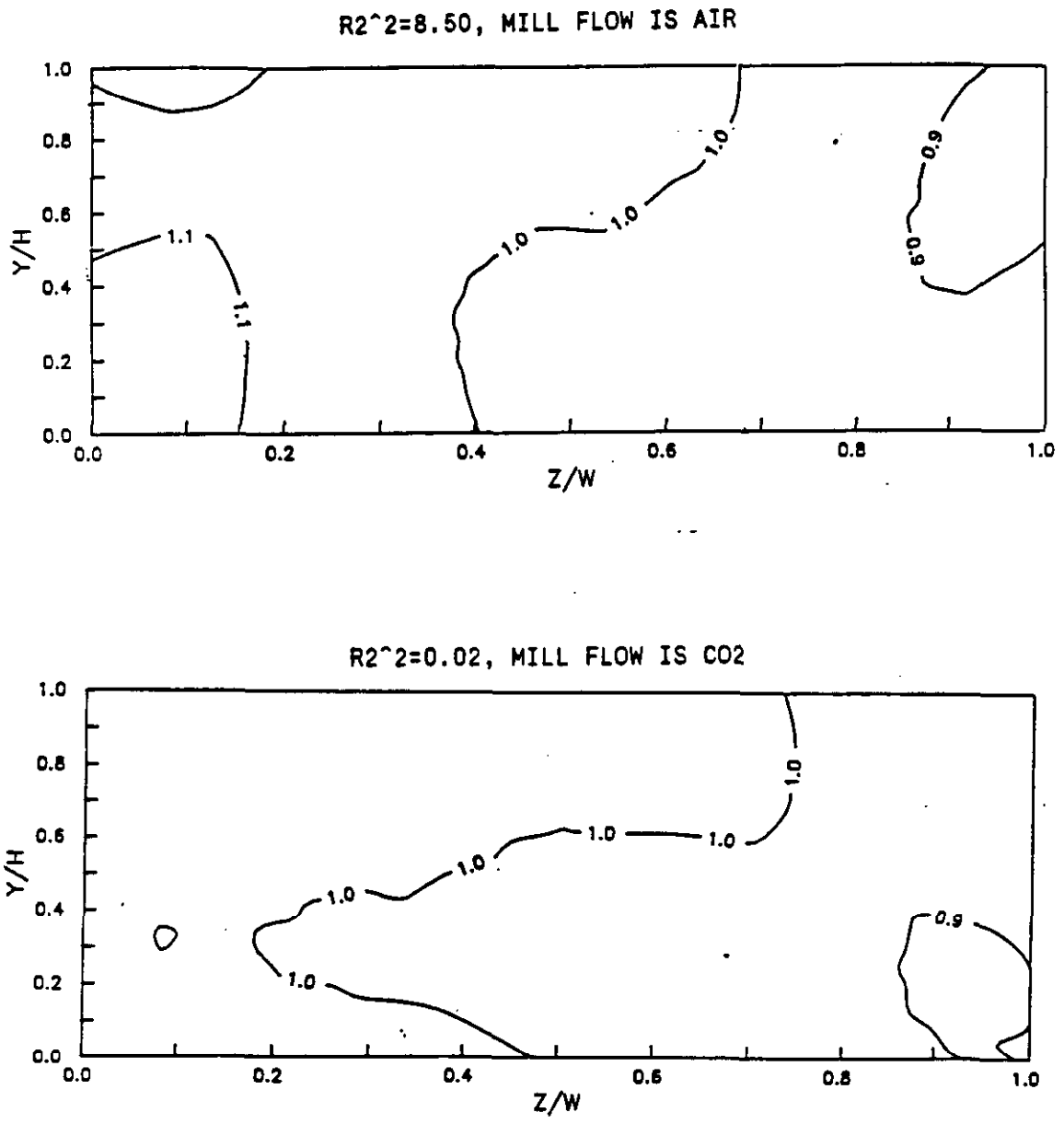

FIGURE 27. MILL AIR CONCENTRATION DISTRIBUTION AT EXIT OF PRECOMBUSTOR BASED ON COLD FLOW MEASUREMENTS - EFFECT OF MILL AIR DENSITY - (HEALY 14, HEALY 26)

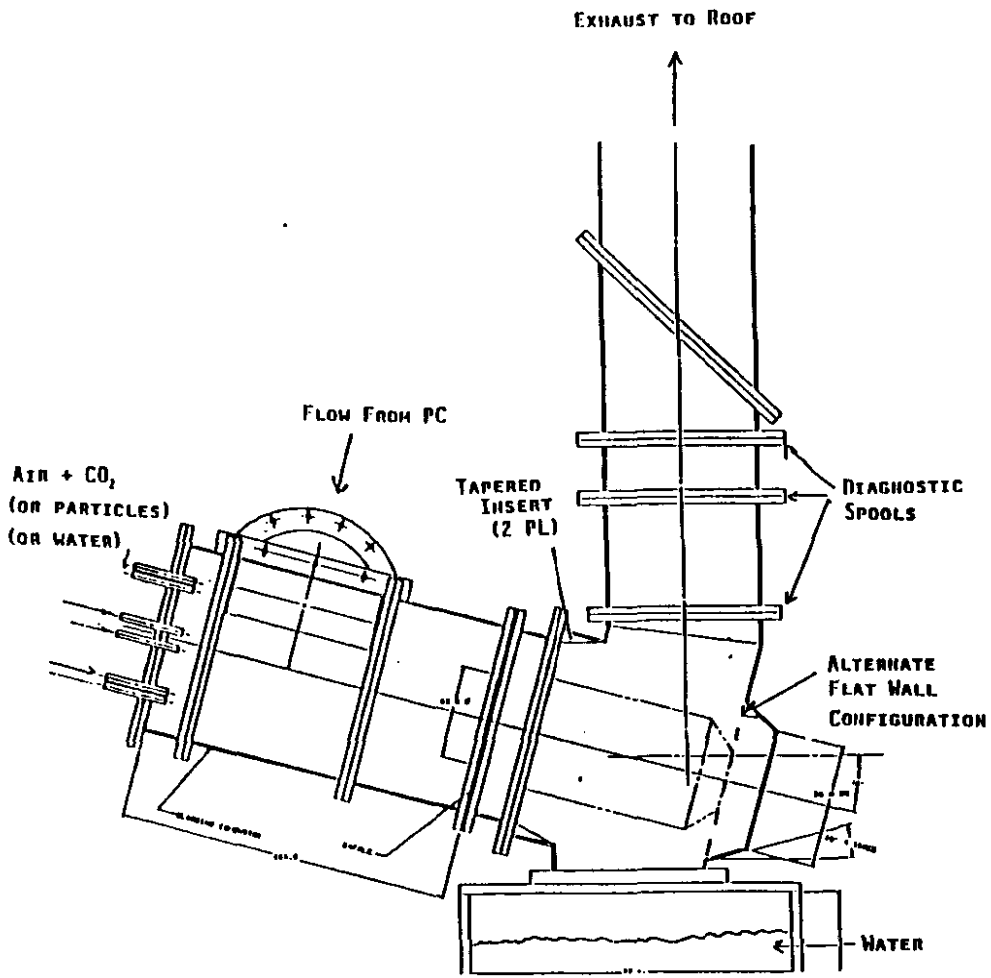

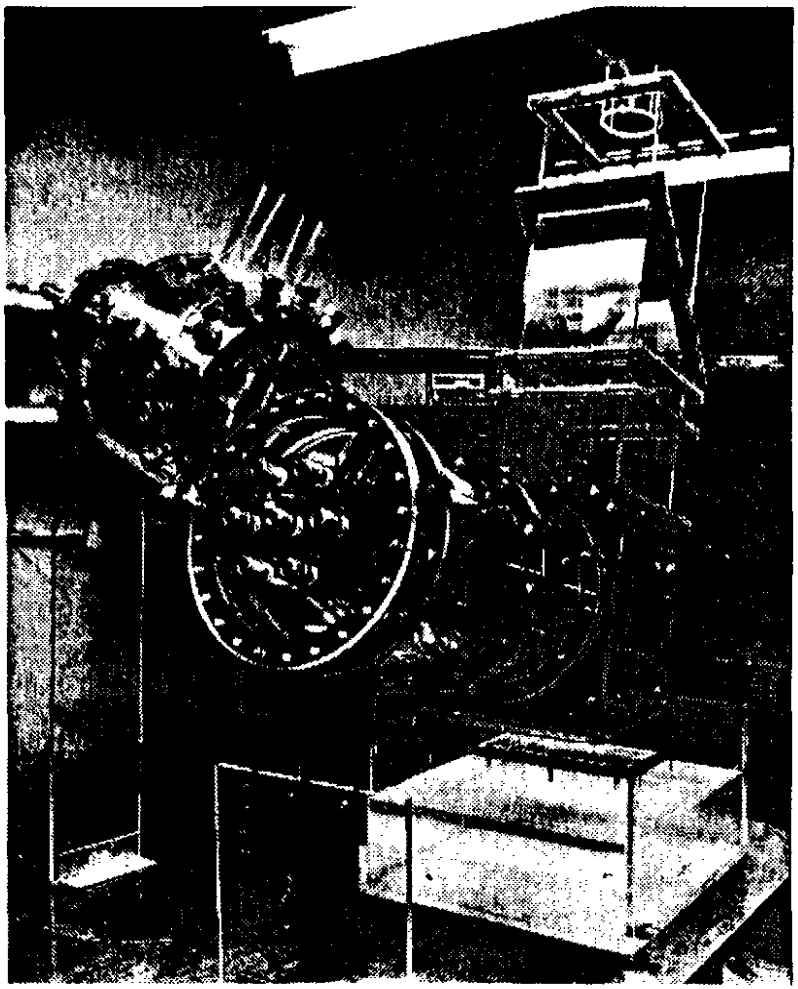

Figure 28. Healy slagging Stage and S' Recovery Section Test Set-Up

TABLE 5 . COLD FLOW MODEL TESTING OF MAIN COMBUSTOR COAL INJECTORS.

TEST CASE	INJECTOR CLOCKING	INJECTOR CIRCLE DIAMETER	INJECTORS ON	SWIRL	MOMENTUM RATIO	MOMENTUM FLUX RATIO R^2	MASS RATIO	TRACER	TRACER INJECTION LOCATION	MEASUREMENTS PERFORMED
MCI1	ODD	OUT-BOARD	ALL	4	0.06	2.16	0.04	CO2	1:00 INJECTOR	CENTERLINE MEASUREMENTS
MCI2	"	"	"	"	"	"	"	"	3:00 INJECTOR	"
MCI3	"	"	"	"	"	"	"	"	5:00 INJECTOR	"
MCI4	"	"	"	"	"	"	"	"	7:00 INJECTOR	"
MCI5	"	"	"	"	"	"	"	"	9:00 INJECTOR	"
MCI6	"	"	"	"	"	"	"	"	11:00 INJECTOR	"
MCI7	"	"	"	"	"	"	"	"	ALL INJECTORS	"
MCI8	EVEN	"	"	"	"	"	"	"	2:00 INJECTOR	"
MCI9	"	"	"	"	"	"	"	"	4:00 INJECTOR	"
MCI10	"	"	"	"	"	"	"	"	6:00 INJECTOR	"
MCI11	"	"	"	"	"	"	"	"	8:00 INJECTOR	"
MCI12	"	"	"	"	"	"	"	"	10:00 INJECTOR	"
MCI13	"	"	"	"	"	"	"	"	12:00 INJECTOR	"
MCI14	"	"	"	"	"	"	"	"	ALL INJECTORS	"
MCI15	ODD	IN-BOARD	"	"	"	"	"	"	1:00 INJECTOR	"
MCI16	"	"	"	"	"	"	"	"	3:00 INJECTOR	"
MCI17	"	"	"	"	"	"	"	"	5:00 INJECTOR	"
MCI18	"	"	"	"	"	"	"	"	7:00 INJECTOR	"
MCI19	"	"	"	"	"	"	"	"	9:00 INJECTOR	"
MCI20	"	"	"	"	"	"	"	"	11:00 INJECTOR	"
MCI21	"	"	"	"	"	"	"	"	ALL INJECTORS	"
MCI22	EVEN	"	"	"	"	"	"	"	2:00 INJECTOR	"
MCI23	"	"	"	"	"	"	"	"	4:00 INJECTOR	"
MCI24	"	"	"	"	"	"	"	"	6:00 INJECTOR	"
MCI25	"	"	"	"	"	"	"	"	8:00 INJECTOR	"
MCI26	"	"	"	"	"	"	"	"	10:00 INJECTOR	"
MCI27	"	"	"	"	"	"	"	"	12:00 INJECTOR	"
MCI28	"	"	"	"	"	"	"	"	ALL INJECTORS	"
MCI29	ODD	OUT-BOARD	"	"	"	"	"	"	"	RADIAL MEASUREMENTS, JUST UPSTREAM OF AIR INLET IN HEADER
MCI30	EVEN	"	"	"	"	"	"	"	"	"
MCI31	ODD	"	"	"	"	"	"	"	"	RADIAL MEASUREMENTS, JUST UPSTREAM OF BAFFLE
MCI32	ODD	IN-BOARD	"	"	"	"	"	"	"	RADIAL MEASUREMENTS, JUST UPSTREAM OF AIR INLET IN HEADER
MCI33	"	"	"	"	"	"	"	"	"	RADIAL MEASUREMENTS, JUST UPSTREAM OF BAFFLE
MCI34	"	"	9:00 OFF	"	0.07	3.09	"	"	ALL AVAILABLE INJECTORS	RADIAL MEASUREMENTS, JUST UPSTREAM OF AIR INLET IN HEADER
MCI35	"	"	"	"	"	"	"	"	"	RADIAL MEASUREMENTS, JUST UPSTREAM OF BAFFLE
MCI36	"	"	"	"	"	"	"	"	"	CENTERLINE MEASUREMENTS
MCI37	"	"	ALL (9:00 OUT-	"	0.06	2.16	"	"	ALL INJECTORS	CENTERLINE MEASUREMENTS

TABLE 5. COLD FLOW MODEL TESTING OF MAIN COMBUSTOR COAL INJECTORS (MCI) (CONTINUED)

TEST CASE	INJECTOR CLOCKING	INJECTOR CIRCLE DIAMETER	INJECTORS ON	SWIRL	MOMENTUM RATIO	MOMENTUM FLUX RATIO R^2	MASS RATIO	TRACER	TRACER INJECTION LOCATION	MEASUREMENTS PERFORMED
MCI38	ODD	OUT-BOARD	ALL	4	0.06	2.16	0.04	POWDER	1:00 INJECTOR	FLOW VISUALIZATION OF PARTICLE MIXING
MCI39	"	"	"	"	"	"	"	"	3:00 INJECTOR	"
MCI40	"	"	"	"	"	"	"	"	5:00 INJECTOR	"
MCI41	"	"	"	"	"	"	"	"	7:00 INJECTOR	"
MCI42	"	"	"	"	"	"	"	"	9:00 INJECTOR	"
MCI43	"	"	"	"	"	"	"	"	11:00 INJECTOR	"
MCI44	EVEN	"	"	"	"	"	"	"	2:00 INJECTOR	"
MCI45	"	"	"	"	"	"	"	"	4:00 INJECTOR	"
MCI46	"	"	"	"	"	"	"	"	6:00 INJECTOR	"
MCI47	"	"	"	"	"	"	"	"	8:00 INJECTOR	"
MCI48	"	"	"	"	"	"	"	"	10:00 INJECTOR	"
MCI49	"	"	"	"	"	"	"	"	12:00 INJECTOR	"
MCI50	ODD	IN-BOARD	"	"	"	"	"	"	1:00 INJECTOR	"
MCI51	"	"	"	"	"	"	"	"	3:00 INJECTOR	"
MCI52	"	"	"	"	"	"	"	"	5:00 INJECTOR	"
MCI53	"	"	"	"	"	"	"	"	7:00 INJECTOR	"
MCI54	"	"	"	"	"	"	"	"	9:00 INJECTOR	"
MCI55	"	"	"	"	"	"	"	"	11:00 INJECTOR	"
MCI56	EVEN	"	"	"	"	"	"	"	2:00 INJECTOR	"
MCI57	"	"	"	"	"	"	"	"	4:00 INJECTOR	"
MCI58	"	"	"	"	"	"	"	"	6:00 INJECTOR	"
MCI59	"	"	"	"	"	"	"	"	8:00 INJECTOR	"
MCI60	"	"	"	"	"	"	"	"	10:00 INJECTOR	"
MCI61	"	"	"	"	"	"	"	"	12:00 INJECTOR	"
MCI62	ODD	OUT-BOARD	"	"	"	"	"	WATER	HEAD ENDPLATE	FLOW VISUALIZATION OF VORTEX
MCI63	EVEN	"	"	"	"	"	"	"	"	"
MCI64	ODD	IN-BOARD	"	"	"	"	"	"	"	"
MCI65	EVEN	"	"	"	"	"	"	"	"	"

Water was utilized to reveal the location of the vortex on the head endplate. This location is important since the vortex is off-axis at the head endplate due to a single tangential air inlet. Tests were conducted to determine the effect of the off- axis vortex on coal particle trajectories and overall mixing.

Powder was utilized to reveal trajectories and flow paths of particles being injected through the coal injectors. In particular, the interaction between the vortex and individual coal injectors was observed.

Lastly, carbon dioxide was utilized to reveal, in a quantitative manner, the mixing behavior of flow coming from the injectors. Carbon dioxide measurements were made through the slagging combustor and in the slag recovery section transition. Both centerline measurements as well as radial measurements were performed. Mixing behavior of each individual injector was also characterized.

The multiple coal injector configurations tested are shown in Figure 29. The multiple coal injector configuration consists of setting the coal injector clocking, and the injector circle diameter.

Two coal injector clockings were utilized. The first was the "odd" clocking which refers to the injectors being placed on the odd numbered hours. The second was the "even" clocking which refers to the injectors being placed on even numbered hours. The "odd" clocking is the baseline for the Healy combustor.

Two injector circle diameters were also tested. The first was the in-board circle which refers to an injector circle diameter which matches the diameter of the baffle (52.5 inches for full scale combustor). The out- board circle refers to a calculated result geared to yield optimum hot fire slag recovery performance (74 inches). The out-board circle is the baseline for the Healy combustor.

For the majority of the tests performed, the cold flow momentum ratio was set to match hot flow conditions. The momentum ratio is defined as the ratio of the momentum of the headend flow to the precombustor flow. This preserves the global interaction between the precombustor flow and the flow from the coal injectors. The swirl number was also maintained close to hot fire conditions.

6.3.2.1 Water Injection On Head Endplate

Representative flow visualization results from water injection tests on the head endplate are shown in Figure 30. In this figure, the location of the vortex at the head endplate is observed to be off-axis, between the in-board, 9:00 injector and the combustor center.

During this series of tests, the vortex was observed to strengthen with high combustor swirl, however, the location was observed to remain essentially unchanged. The location was also the same when the out-board injector circle was used.

6.3.2.2 Baseline Mixing Test Results from Carbon Dioxide and Powder Injection

The baseline injector configuration is the six port, out-board, odd clocking case (Figure 29C). Mixing characterization results for this case are shown in Figures 31 to 35. For these tests, carbon dioxide was injected through all the injectors.

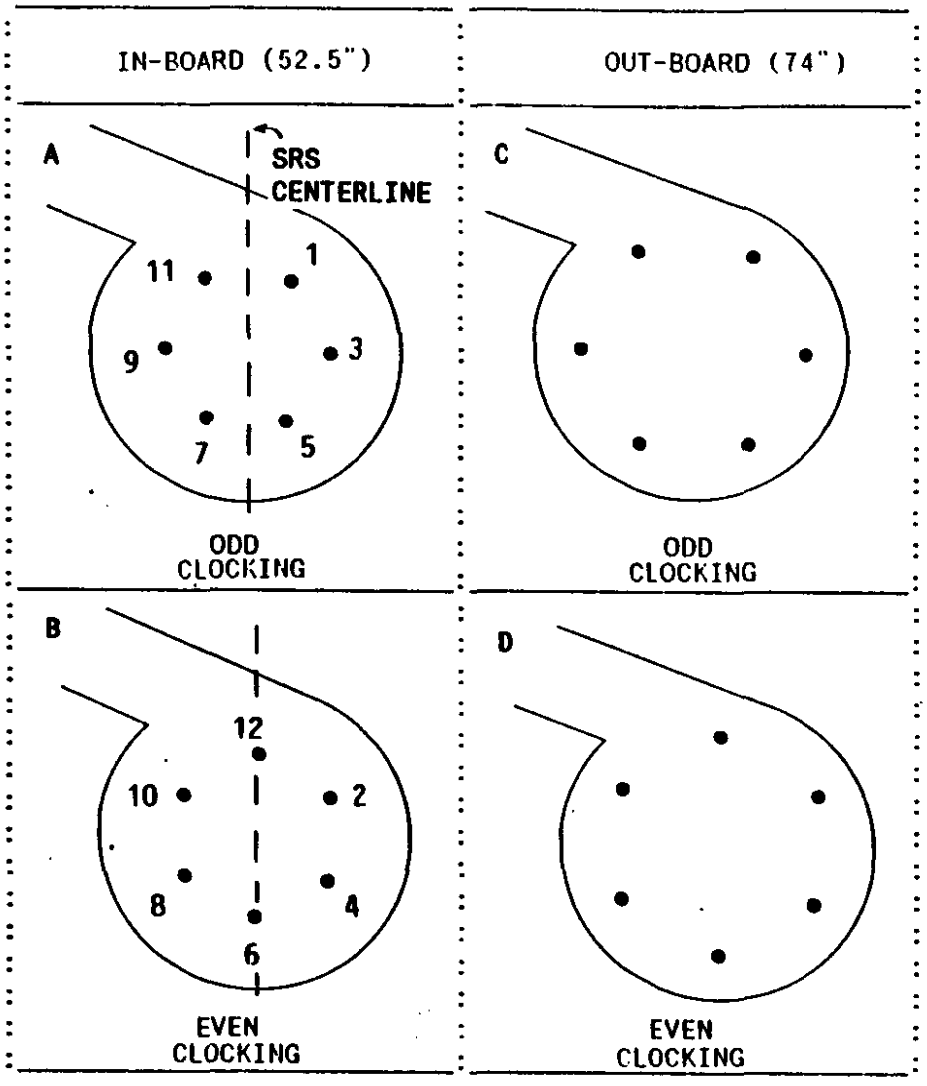

FIGURE 29. MULTIPLE COAL INJECTOR CONFIGURATION TESTED IN COLD FLOW MODEL (VIEW FOR LEFT-HANDED COMBUSTOR, LOOKING DOWNSTREAM).

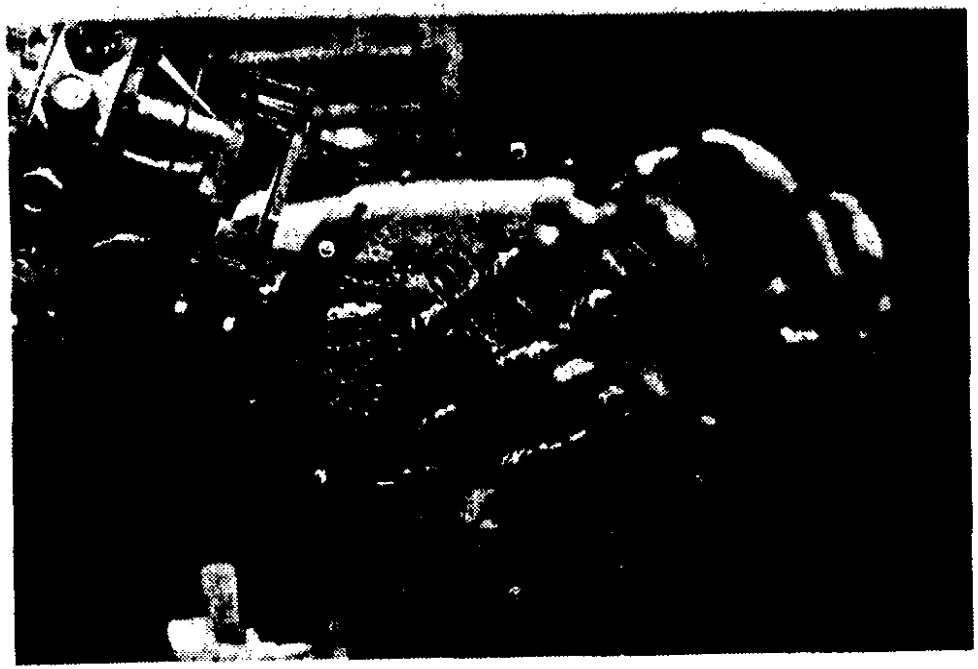

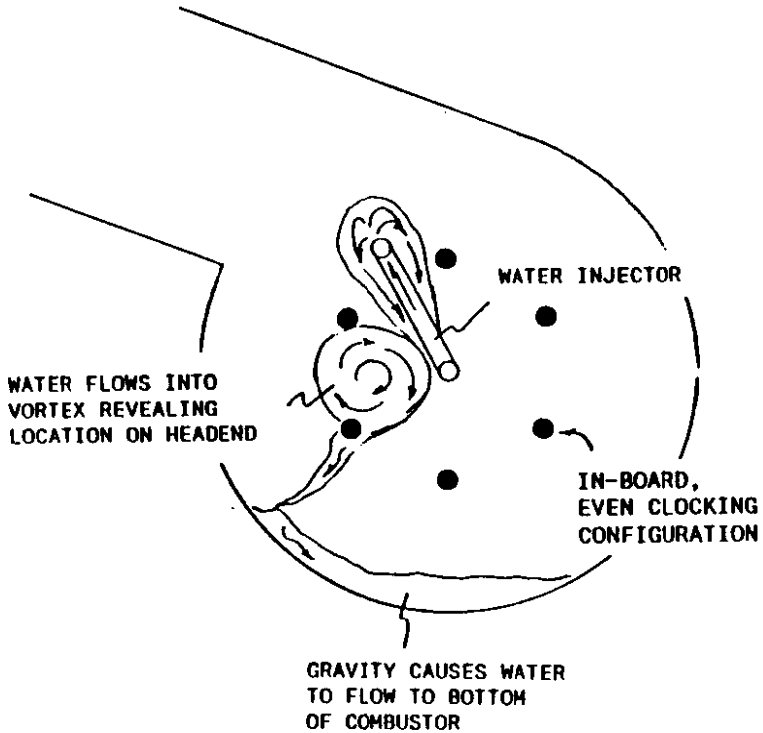

FIGURE 30. IDENTIFICATION OF VORTEX LOCATION ON HEADEND PLATE USING WATER INJECTION

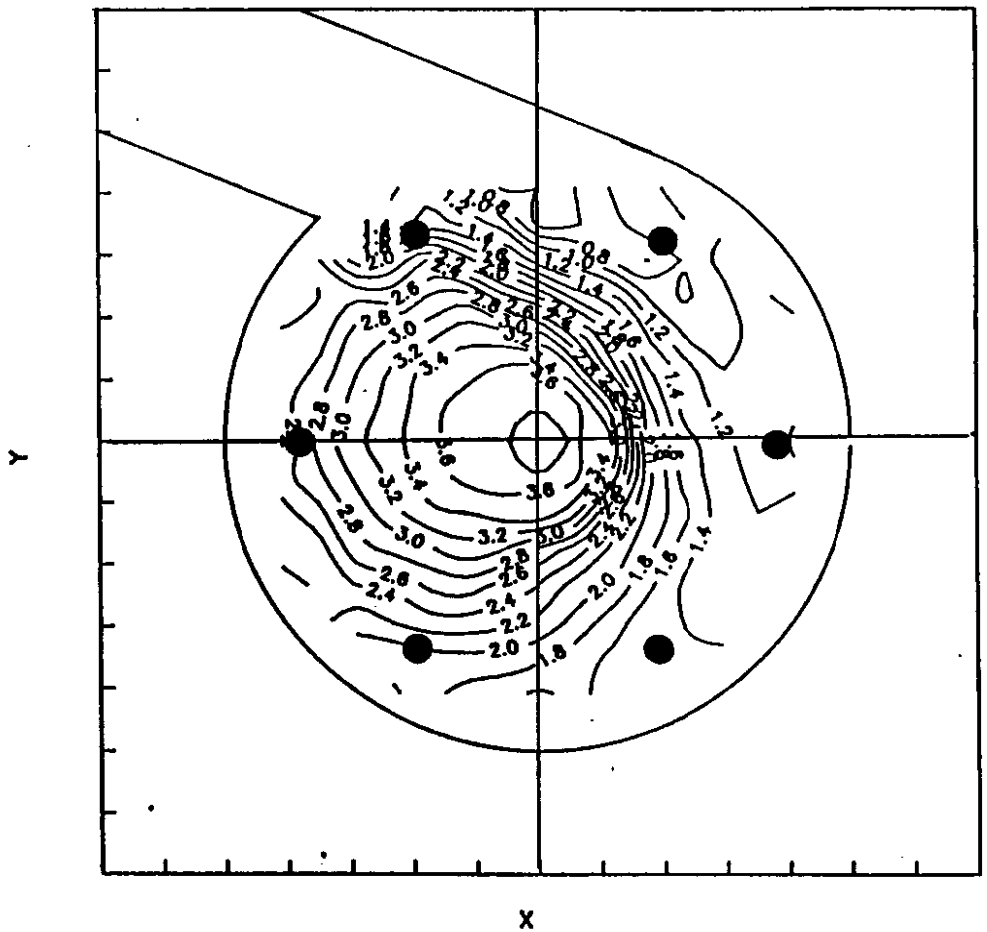

FIGURE 31. TOPOGRAPHICAL PLOT SHOWING MIXING PATTERNS IN HEADEND. INJECTOR CONFIGURATION WAS OUT-BOARD, ODD CLOCKING. TEST CASE SHOWN IS MCI29.

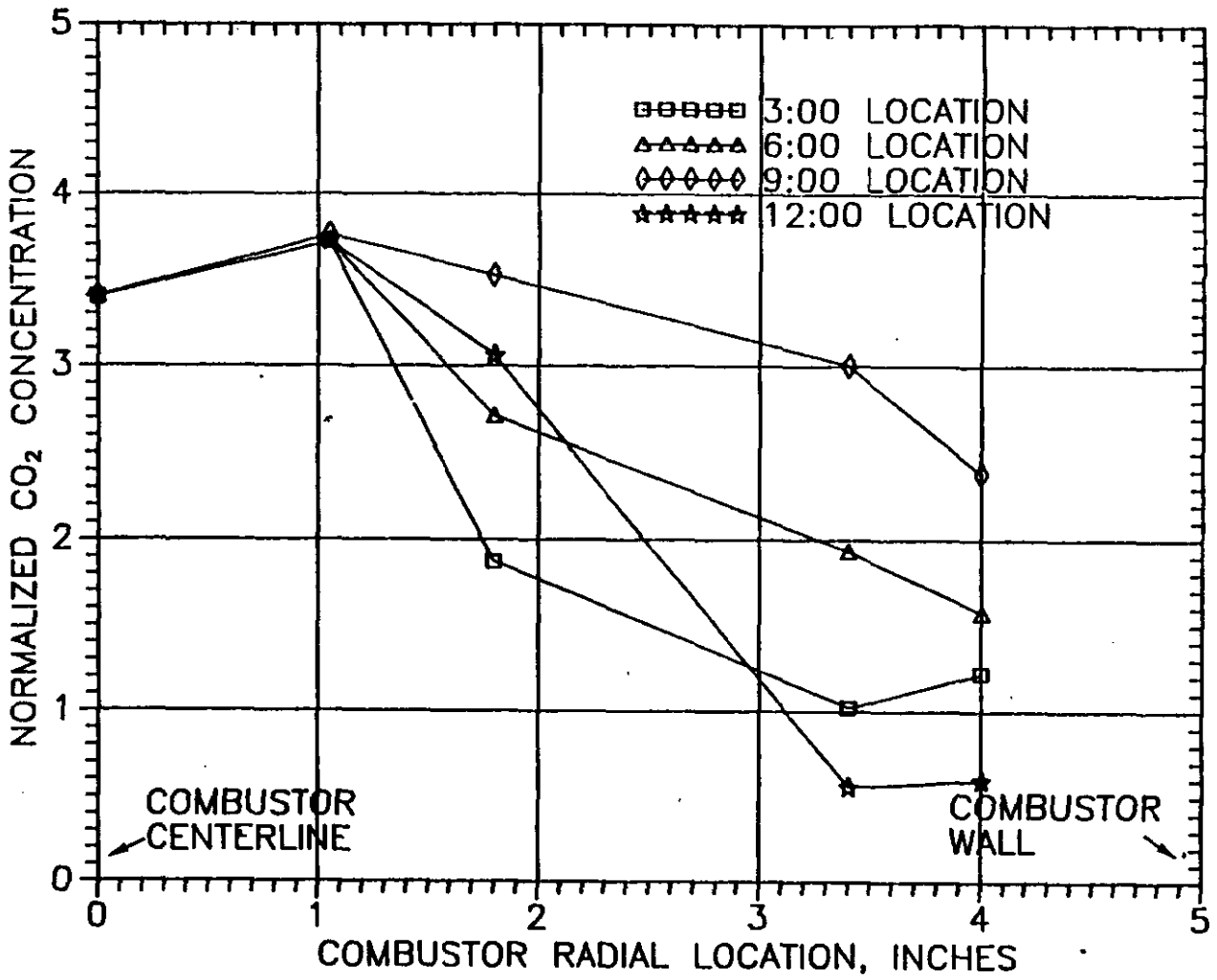

FIGURE 32. MIXING CHARACTERIZATION OF ALL INJECTORS. RADIAL MEASUREMENTS WERE PERFORMED FOR THE HEADEND LOCATION. INJECTOR CONFIGURATION WAS OUT-BOARD, ODD CLOCKING. TEST CASE SHOWN IS MCI29.

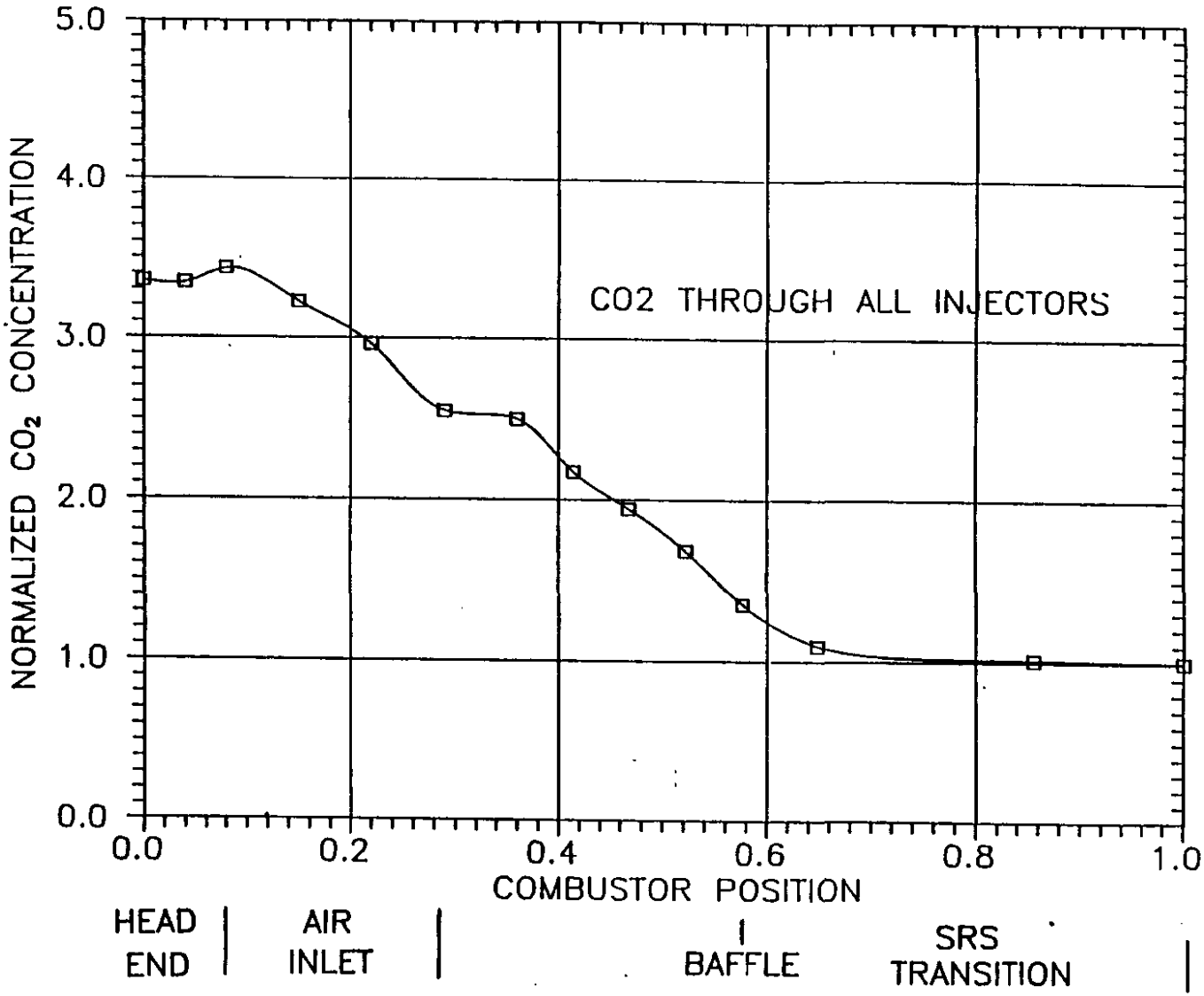

FIGURE 33. MIXING CHARACTERIZATION OF ALL INJECTORS. CENTERLINE MEASUREMENTS WERE PERFORMED DOWN COMBUSTOR LENGTH. INJECTOR CONFIGURATION WAS OUT-BOARD, ODD CLOCKING. TEST CASE SHOWN IS MCI7.

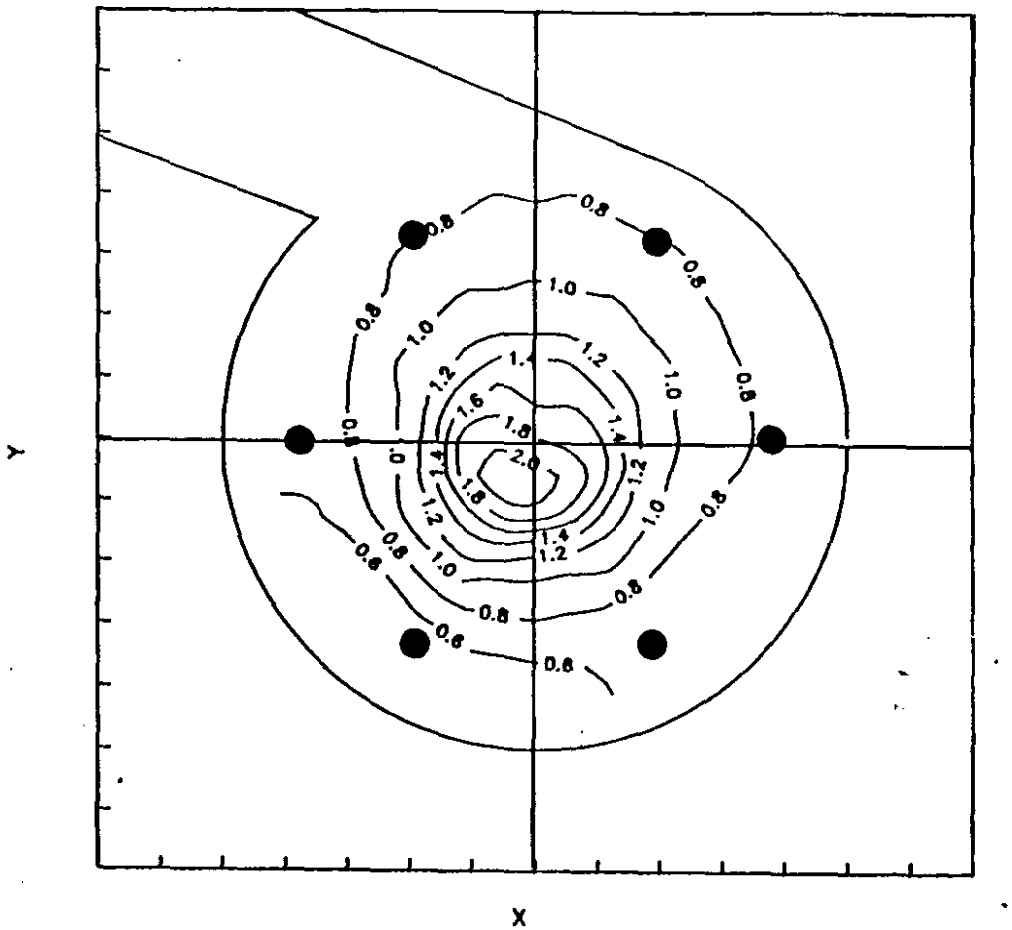

FIGURE 34. TOPOGRAPHICAL PLOT SHOWING MIXING PATTERNS IN BAFFLE REGION. INJECTOR CONFIGURATION WAS OUT-BOARD, ODD CLOCKING. TEST CASE SHOWN IS MCI31.

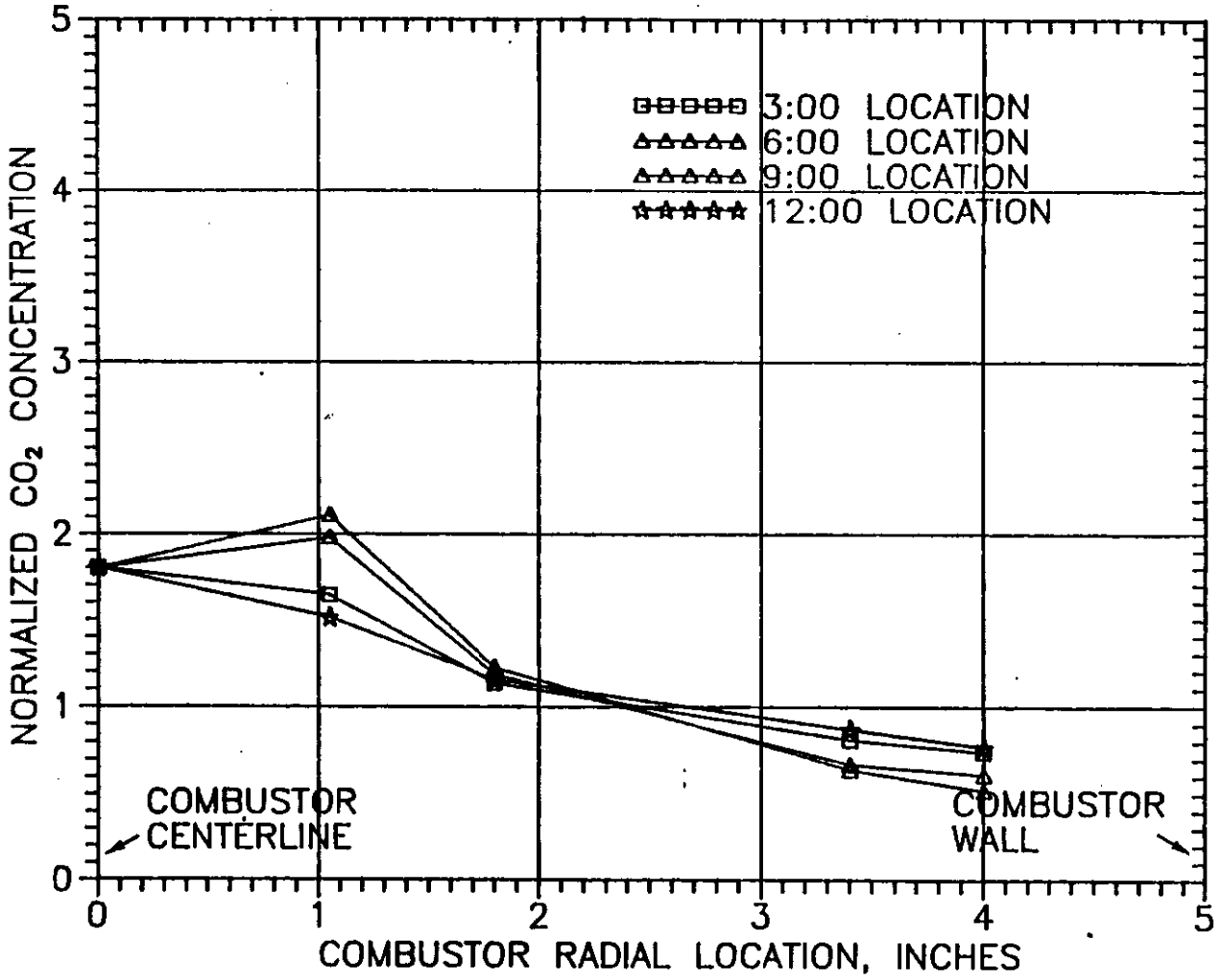

FIGURE 35. MIXING CHARACTERIZATION OF ALL INJECTORS. RADIAL MEASUREMENTS WERE PERFORMED FOR THE BAFFLE REGION. INJECTOR CONFIGURATION WAS OUT-BOARD, ODD CLOCKING. TEST CASE SHOWN IS MCI31.

Figure 31 and 32 shows mixing contours and radial carbon dioxide measurements, respectively, for the headend region. The carbon dioxide values shown are relative values, and have been normalized to the perfectly mixed carbon dioxide value. In this plot, high carbon dioxide concentrations are observed to be in the vicinity of the vortex near the 9:00 injector. Carbon dioxide concentrations are lowest nearest the air inlet. A steep gradient is thus observed between the vortex and the 12:00 and 3:00 injectors.

Figure 33 shows carbon dioxide measurements made down the center of the combustor. The profile indicates almost linear mixing from the air inlet to the baffle. Shortly after the baffle, the gases are observed to be completely mixed.

Figure 34 and 35 shows mixing contours and radial carbon dioxide measurements, respectively, for the location just upstream of the baffle. The figures are consistent with the good mixing result above. Carbon dioxide concentration values are closer to the perfectly mixed case, and more evenly distributed about the centerline as compared to the headend.

Figure 36 shows carbon dioxide measurements made down the combustor centerline. For these tests, carbon dioxide was injected, one at a time, through each injector. In this Figure, the 9:00 injector is observed to contribute more carbon dioxide to the centerline than the other injectors. The 7:00 injector also contributes more than the average, but not as much as the 9:00. Flow visualization results from powder injection can help to explain these centerline carbon dioxide measurements.

Figure 37 shows particle flow patterns observed when powder is injected through each individual injector. In these tests, the larger particles making up the powder were observed to be centrifuged to the wall, whereas the smaller particles were observed to follow paths which eventually lead to the vortex. The particles (both large and small) coming from the 9:00 injector and 7:00 injector were observed to be drawn into the vortex almost immediately. This is because of the close proximity of these injectors to the vortex. This result translates to reduced contact between these particles and the precombustor flow which results in reduced mixing in the headend. This result also explains the high carbon dioxide concentration measurements made earlier for these injectors. Powder from the other injectors travel at least a quarter turn more, allowing more time to diffuse and mix. Interestingly, these particles follow a circular path the same diameter as the injector circle. This condition may be useful in terms of start-up or light-off of the coal coming from the injectors.

6.3.2.3 Effect of Injector Clocking on Injector Performance

Mixing characterization results are shown in Figure 38 to 42 for the six port, out-board configuration with even clocking. The headend mixing contours and radial carbon dioxide measurements are shown in Figure 38 and 39, respectively. Within the measurement accuracy, these results are observed to be very similar to the baseline case (odd clocking).

Centerline carbon dioxide measurements were also performed as shown in Figure 40. The odd clocking and even clocking cases are observed to have similar centerline profiles as well.

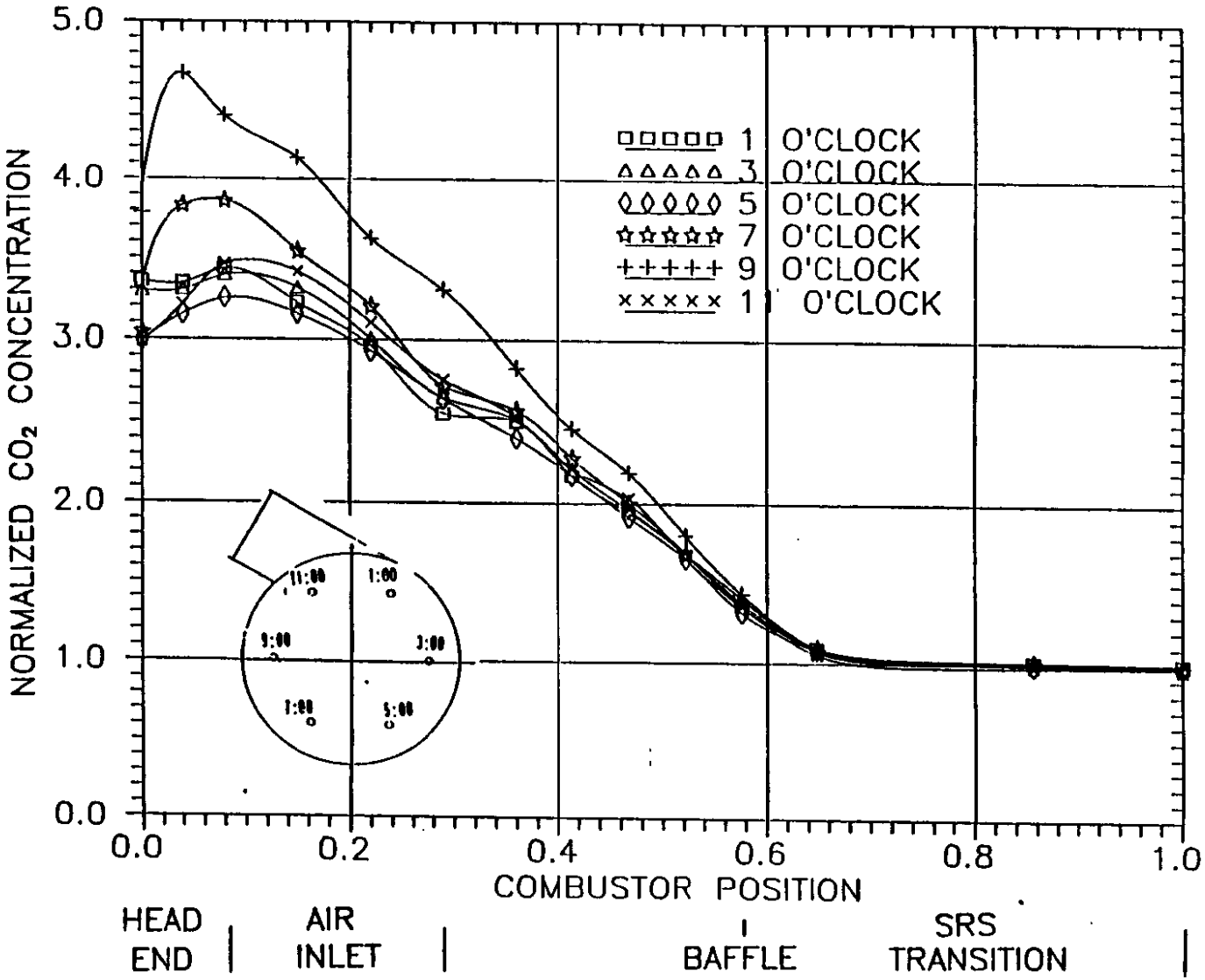

FIGURE 36. MIXING CHARACTERIZATION OF EACH INDIVIDUAL INJECTOR. CENTERLINE MEASUREMENTS WERE PERFORMED DOWN COMBUSTOR LENGTH. INJECTOR CONFIGURATION WAS OUT-BOARD, ODD CLOCKING. TEST CASES SHOWN ARE MCI1-6.

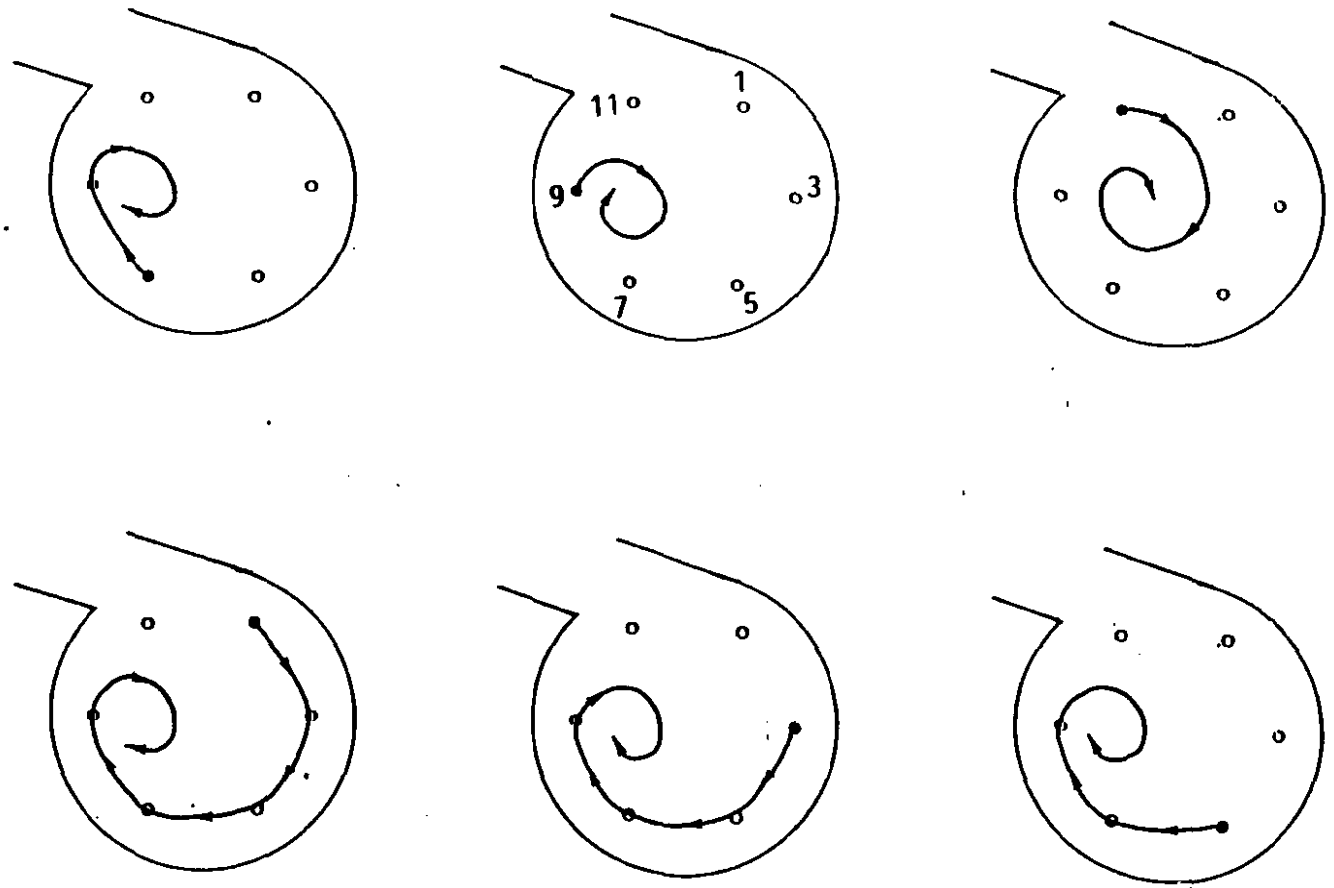

FIGURE 37. FLOW PATTERNS OBSERVED DURING PARTICLE INJECTION THROUGH EACH INDIVIDUAL INJECTOR. INJECTOR CONFIGURATION WAS OUT-BOARD, ODD CLOCKING. TEST CASES SHOWN ARE MCI38-43.

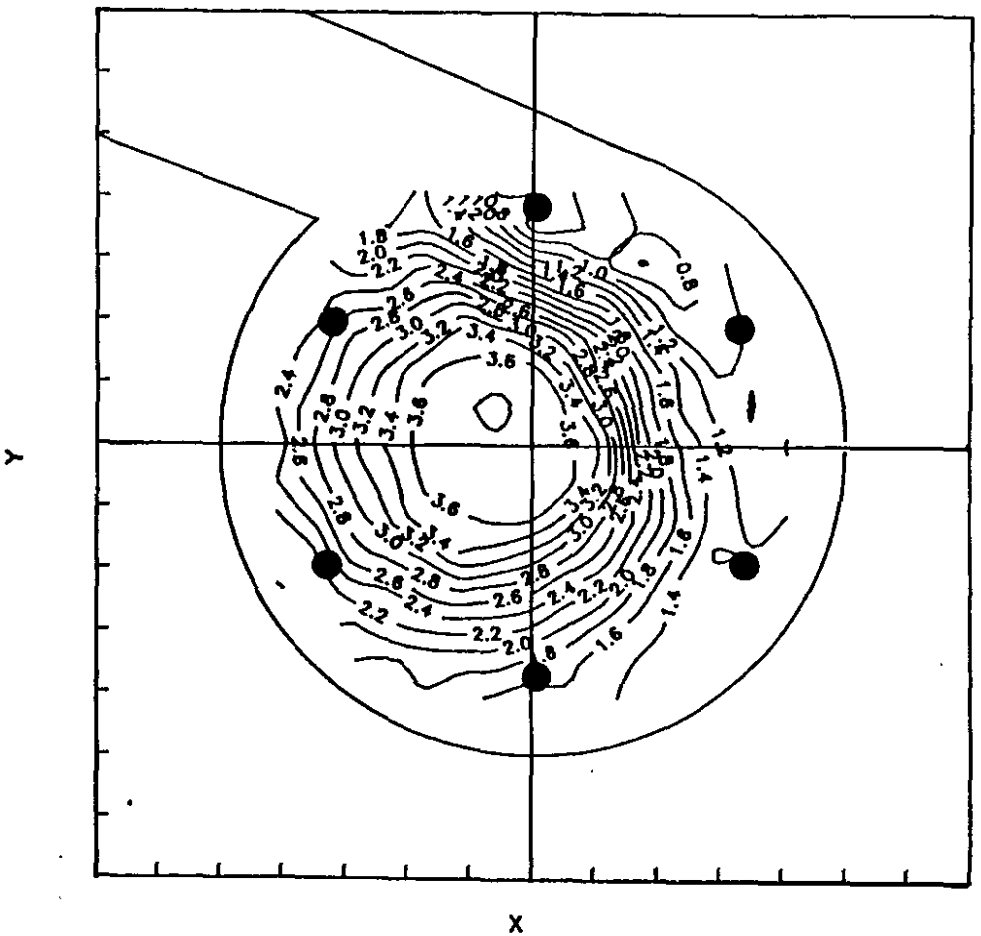

FIGURE 38. TOPOGRAPHICAL PLOT SHOWING MIXING PATTERNS IN HEADEND. INJECTOR CONFIGURATION WAS OUT-BOARD, EVEN CLOCKING. TEST CASE SHOWN IS MCI30.

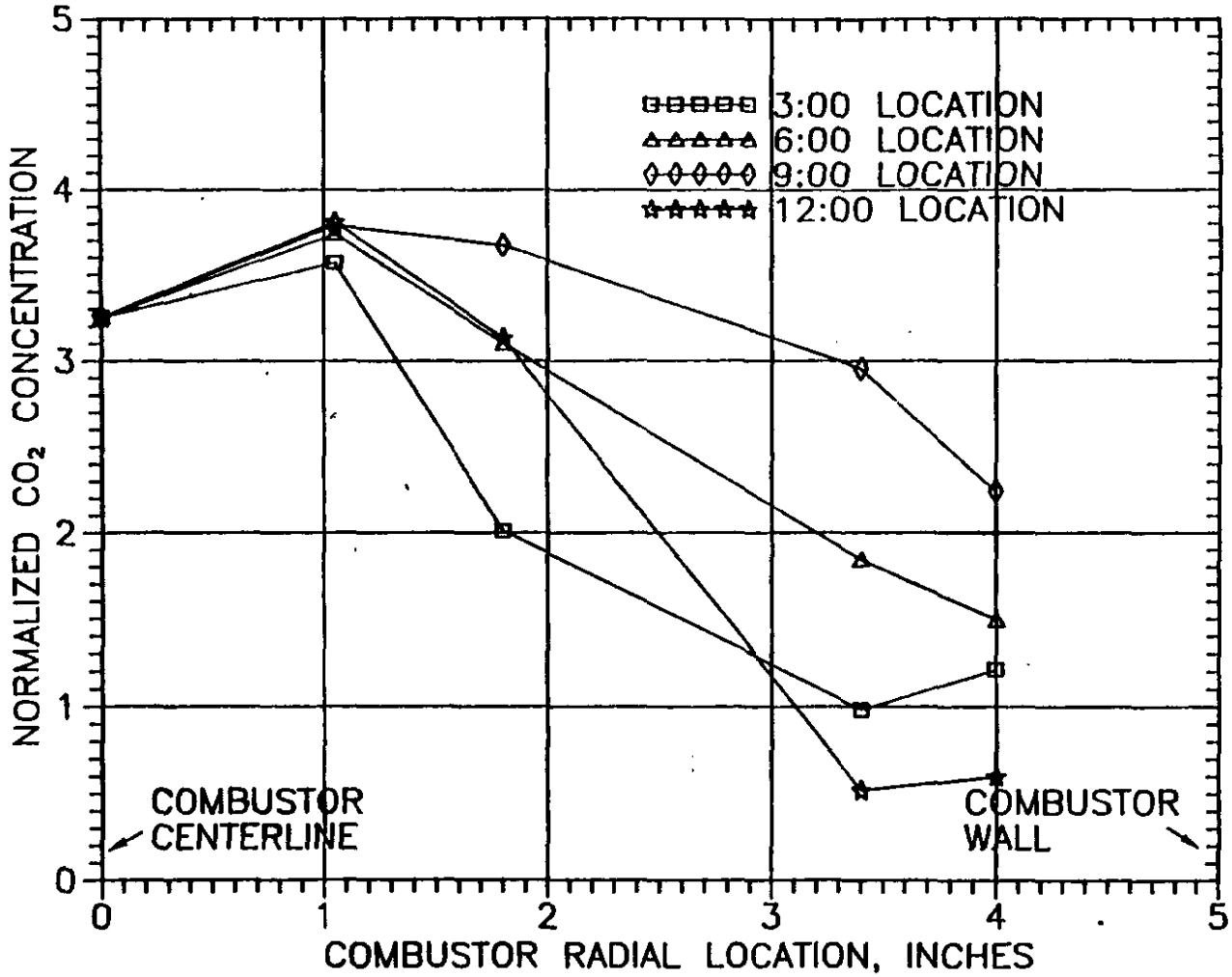

FIGURE 39. MIXING CHARACTERIZATION OF ALL INJECTORS. RADIAL MEASUREMENTS WERE PERFORMED FOR THE HEADEND LOCATION. INJECTOR CONFIGURATION WAS OUTBOARD, EVEN CLOCKING. TEST CASE SHOWN IS MCI30.

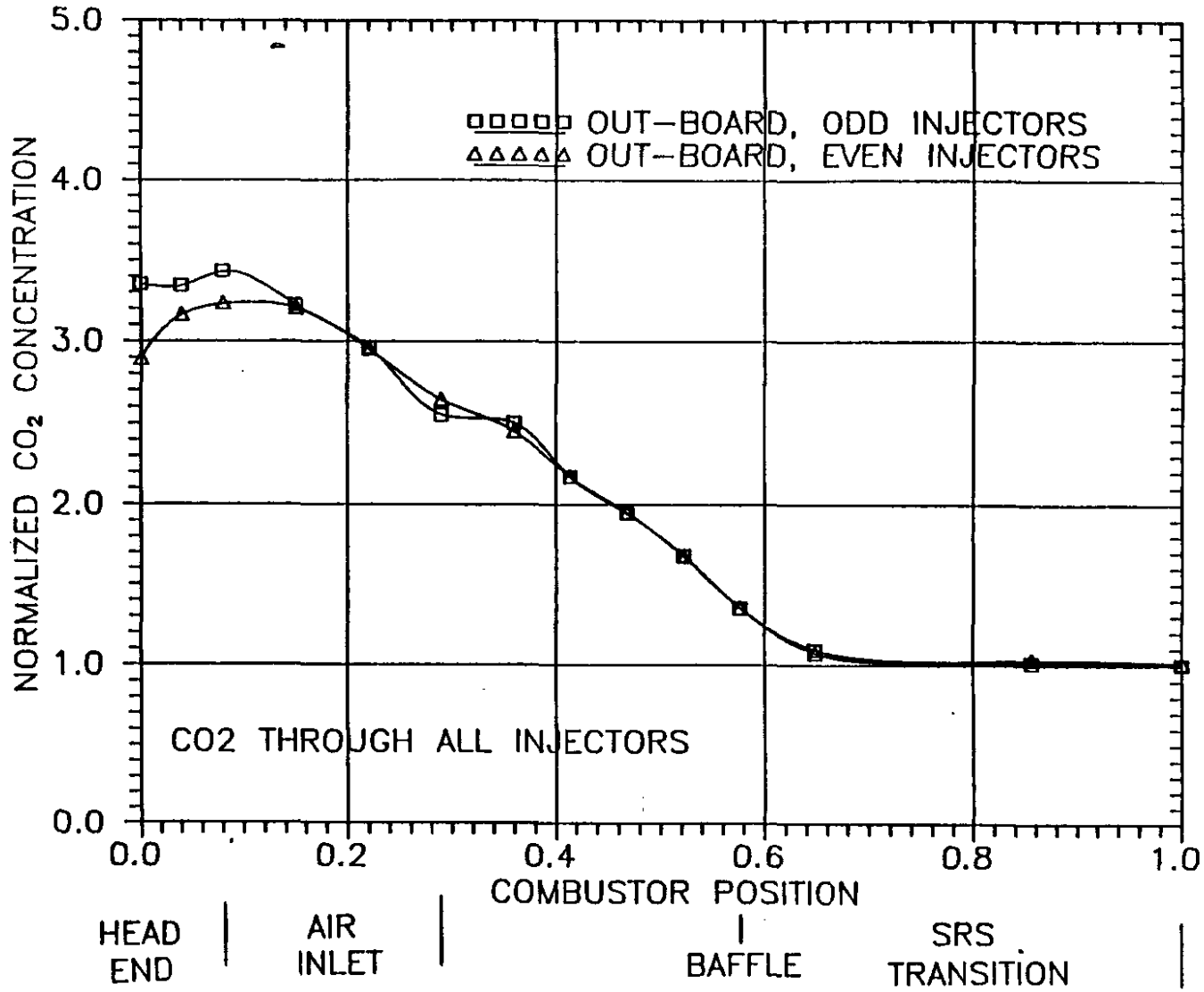

FIGURE 40. MIXING CHARACTERIZATION OF ALL INJECTORS. CENTERLINE MEASUREMENTS WERE PERFORMED DOWN COMBUSTOR LENGTH. INJECTOR CONFIGURATION WAS OUT-BOARD, EVEN CLOCKING. TEST CASE SHOWN IS MCI14.

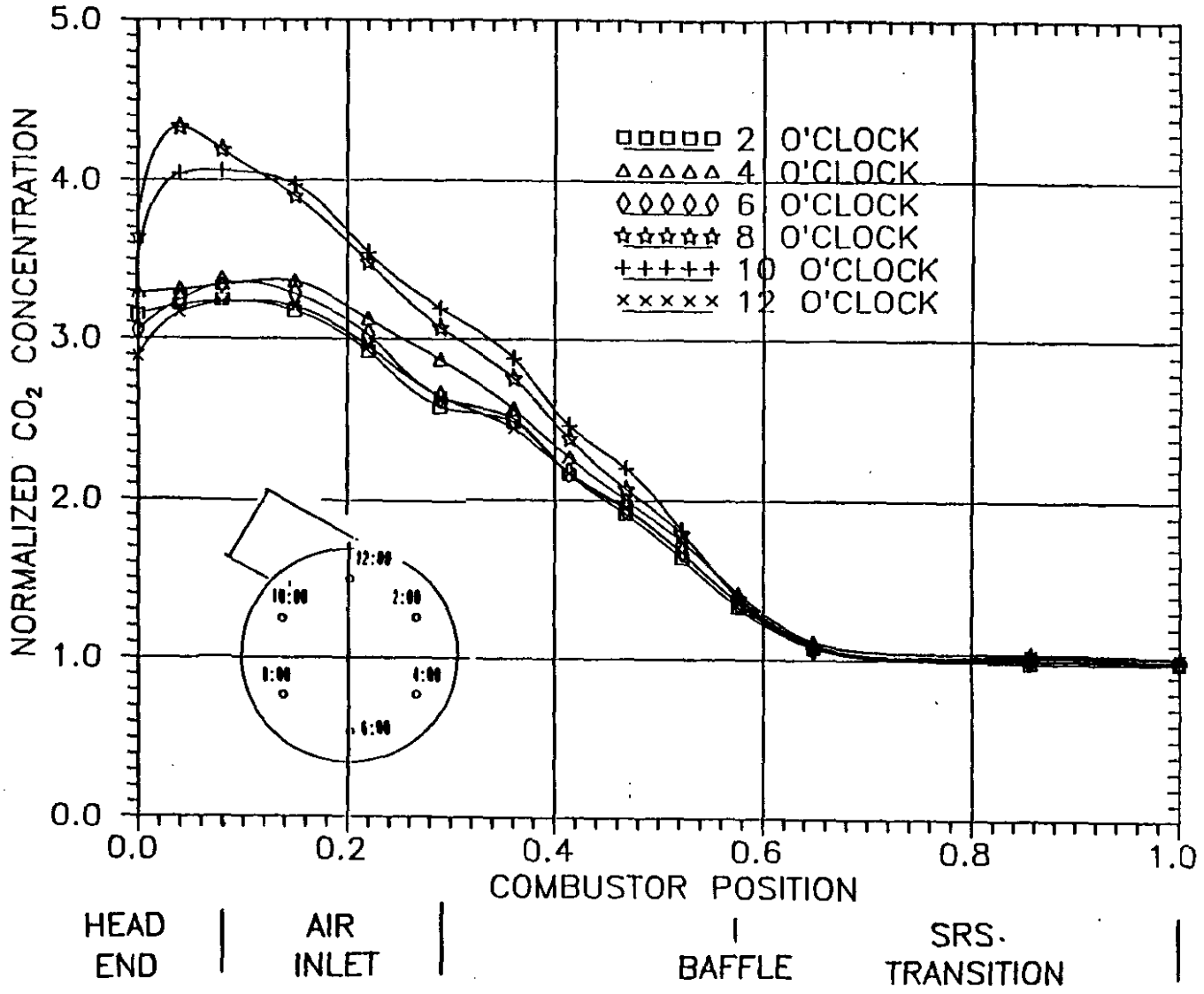

FIGURE 41. MIXING CHARACTERIZATION OF EACH INDIVIDUAL INJECTOR. CENTERLINE MEASUREMENTS WERE PERFORMED DOWN COMBUSTOR LENGTH. INJECTOR CONFIGURATION WAS OUT-BOARD, EVEN CLOCKING. TEST CASES SHOWN ARE MCI8-13.

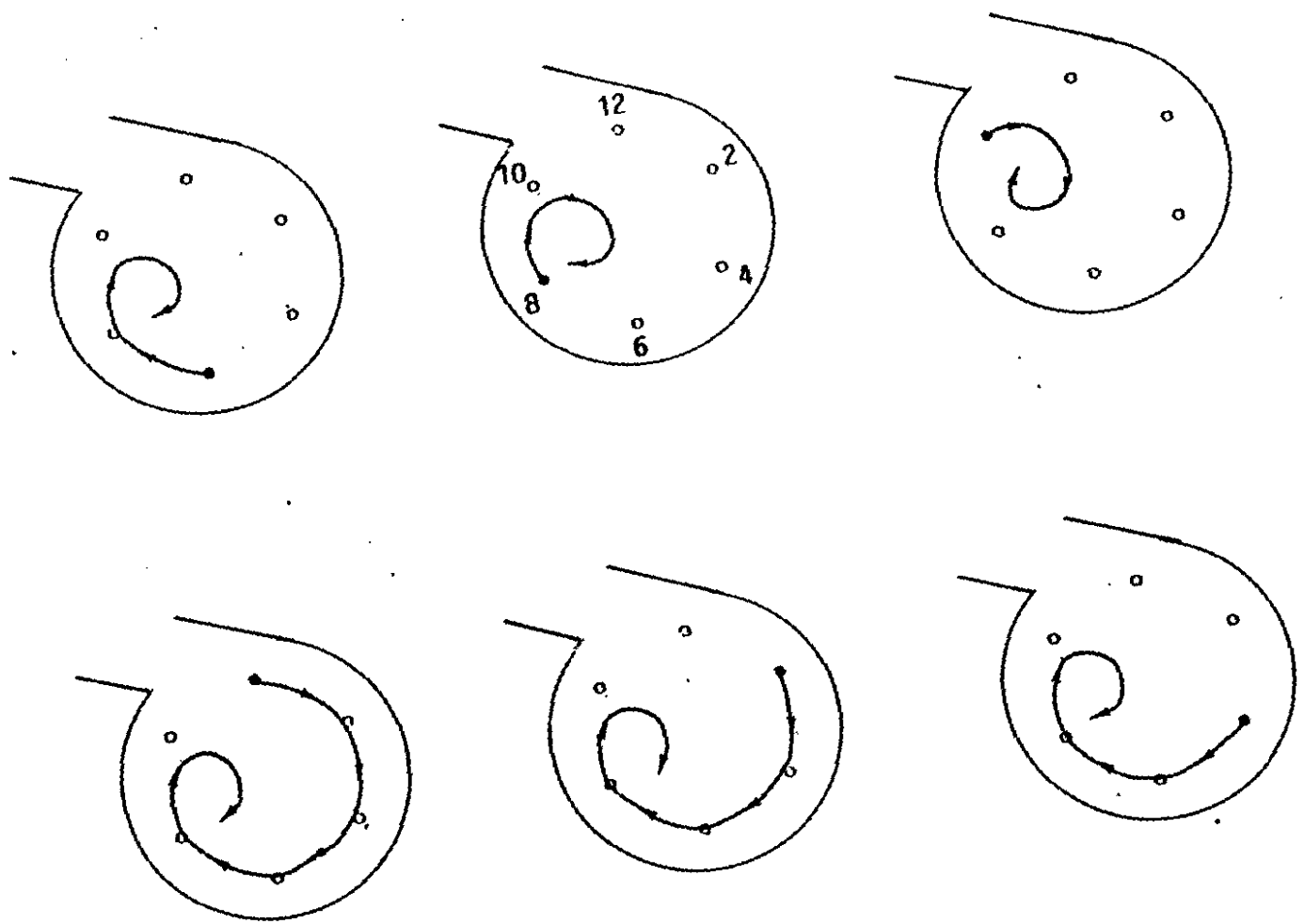

FIGURE 42. FLOW PATTERNS OBSERVED DURING PARTICLE INJECTION THROUGH EACH INDIVIDUAL INJECTOR. INJECTOR CONFIGURATION WAS OUT-BOARD, EVEN CLOCKING. TEST CASES SHOWN ARE MCI44-49.

Figure 41 shows the centerline measurements for carbon dioxide injection through each individual injector. In this case, the 8:00 and 10:00 injectors contribute more flow to the centerline than the other injectors. This result is because these injectors straddle the vortex and are closer to the center of the vortex than the other injectors. The amount of carbon dioxide contributed to the centerline from these injectors falls between those from the 9:00 injector and 7:00 injector in the odd clocking configuration. The net centerline result thus balances out for the odd clocking and even clocking cases.

Figure 42 shows the flow patterns observed from powder injection through each individual injector. For these tests, the large particles were again observed to be centrifuged to the walls, whereas the small particles were observed to be drawn into the vortex. The particles issuing from the 8:00 and 10:00 injectors were observed to flow directly into the vortex, whereas particle from the other injectors were observed to spend more travel time around the combustor periphery before entering the vortex. These results are consistent with the centerline carbon dioxide profiles observed earlier.

6.3.2.4 Effect of Injector Circle Diameter on Injector Performance

Mixing characterization results are shown in Figures 43 to 49 for the six port, in-board, odd clocking configuration. The mixing contours and radial carbon dioxide measurements for the headend region are shown in Figures 43 and 44, respectively. In these figures, the peak carbon dioxide values are again at the vortex, as in the baseline case, however, the peak values are higher. This can be observed from the centerline measurements as shown in Figure 45.

Figure 45 indicates that although the concentration gradients are more severe for the in-board injectors, near complete mixing is still achieved shortly after the baffle. The mixing contours and radial carbon dioxide measurements for just upstream of the baffle are shown in Figure 46 and 47, respectively. These results are consistent with good mixing at the baffle. Peak carbon dioxide values are observed to be closer to the completely mixed case, and the carbon dioxide values are more evenly distributed.

Figure 48 shows carbon dioxide measurements down the combustor centerline for carbon dioxide injection through each individual injector. As shown in the Figure, the 9:00 injector contributes over three times more flow than the other injectors away from the vortex (1:00 to 5:00). This is significantly higher than the out-board cases, and is the reason why the centerline measurements of carbon dioxide are higher as well.

Figure 49 shows flow patterns for powder injection through each individual injector. In this figure, powder injection from the in-board, 9:00 injector, adjacent to the vortex, is observed to flow immediately into the vortex. Powder from the 7:00 and 11:00 injectors also quickly flows into the vortex. Powder from the remaining injectors are more diffuse since they are further from the vortex.

The in-board injector configuration with even clocking is shown in Figures 50 and 51 for comparison with the above results. The results are observed to be similar to the out-board injector case in that the 8:00 and 10:00 injectors contribute more flow to the vortex than the other injectors. The contributions

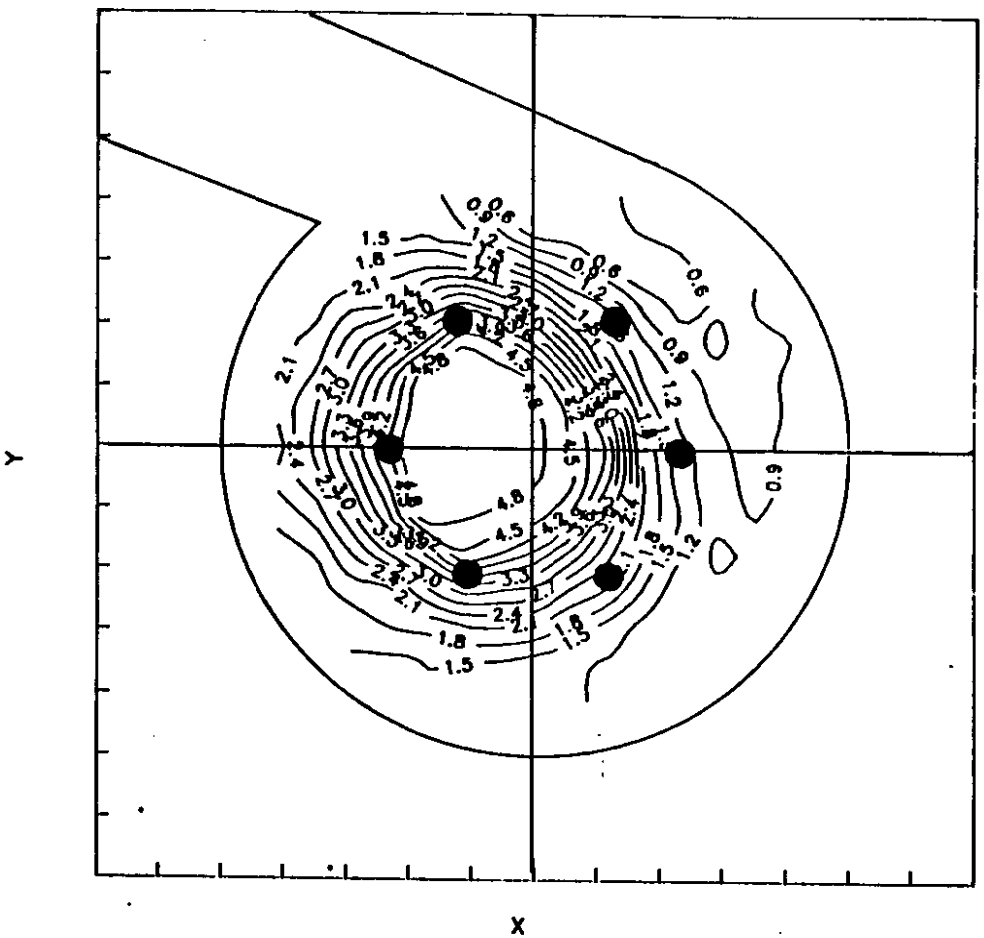

FIGURE 43. TOPOGRAPHICAL PLOT SHOWING MIXING PATTERNS IN HEADEND. INJECTOR CONFIGURATION WAS IN-BOARD, ODD CLOCKING. TEST CASE SHOWN IS MCI32.

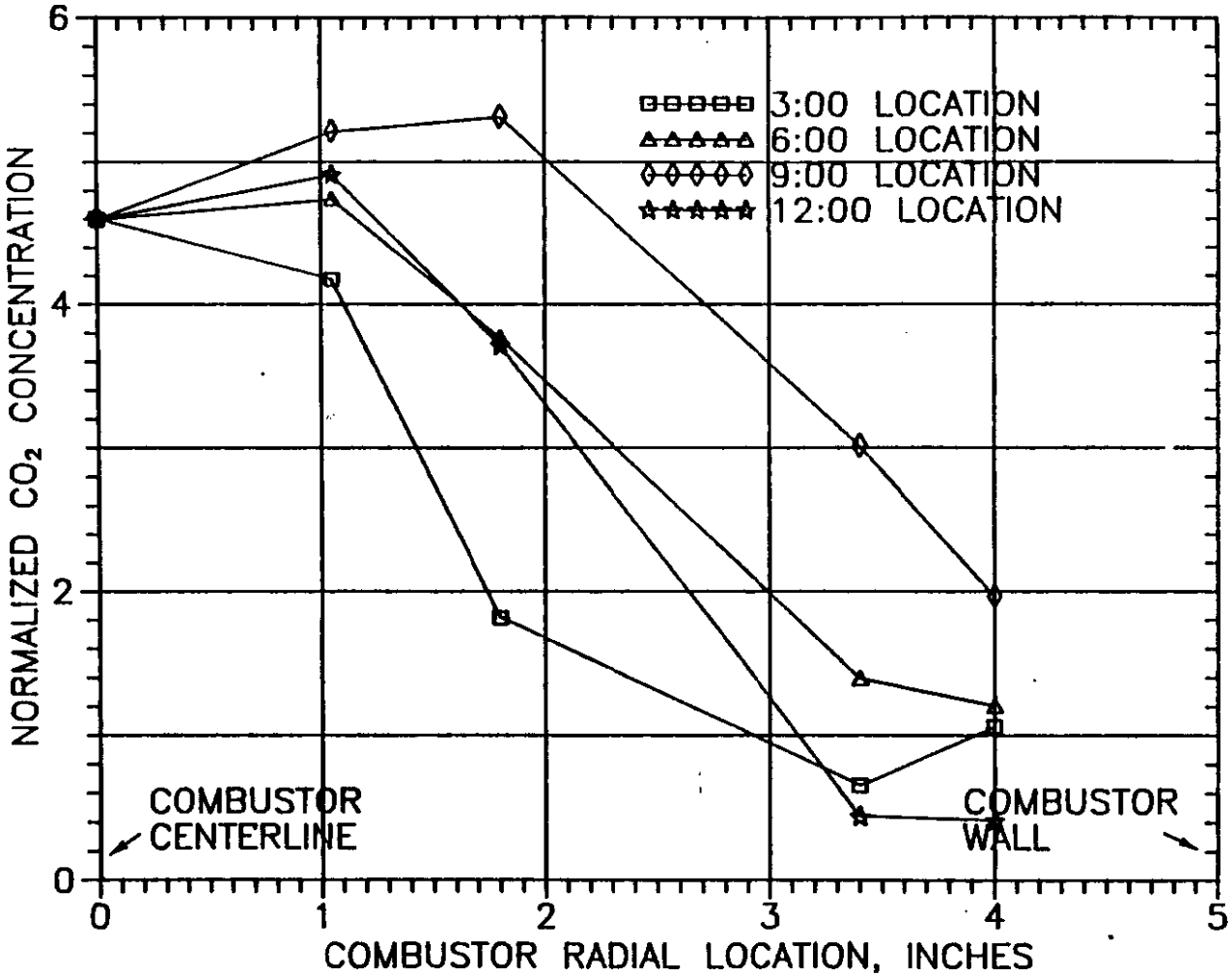

FIGURE 44. MIXING CHARACTERIZATION OF ALL INJECTORS. RADIAL MEASUREMENTS WERE PERFORMED FOR THE HEADEND LOCATION. INJECTOR CONFIGURATION WAS IN-BOARD, ODD CLOCKING. TEST CASE SHWON IS MCI32.

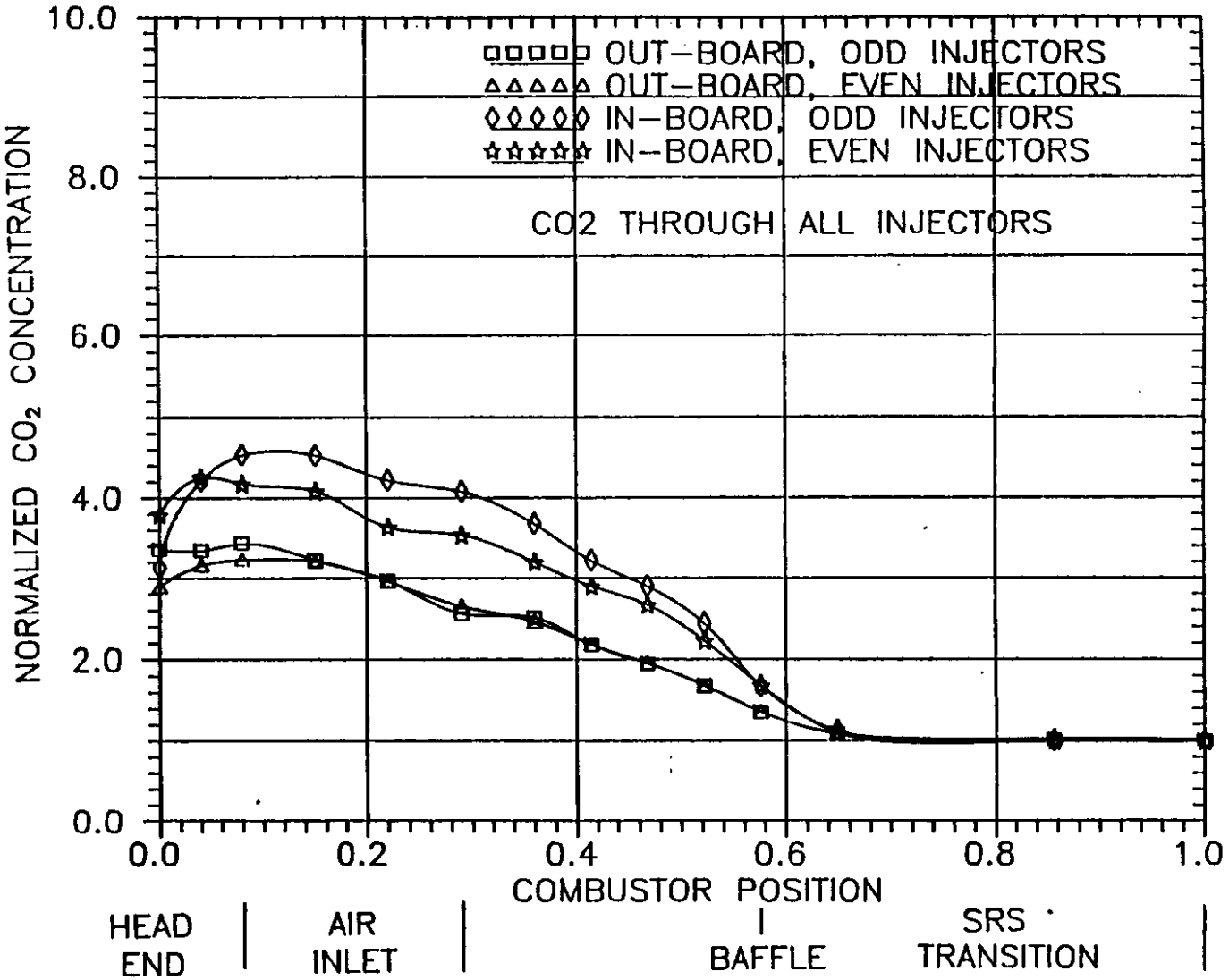

FIGURE 45. MIXING CHARACTERIZATION OF ALL INJECTORS. CENTERLINE MEASUREMENTS WERE PERFORMED DOWN COMBUSTOR LENGTH. TEST CASES SHOWN ARE MCI7,14,21, AND 28.

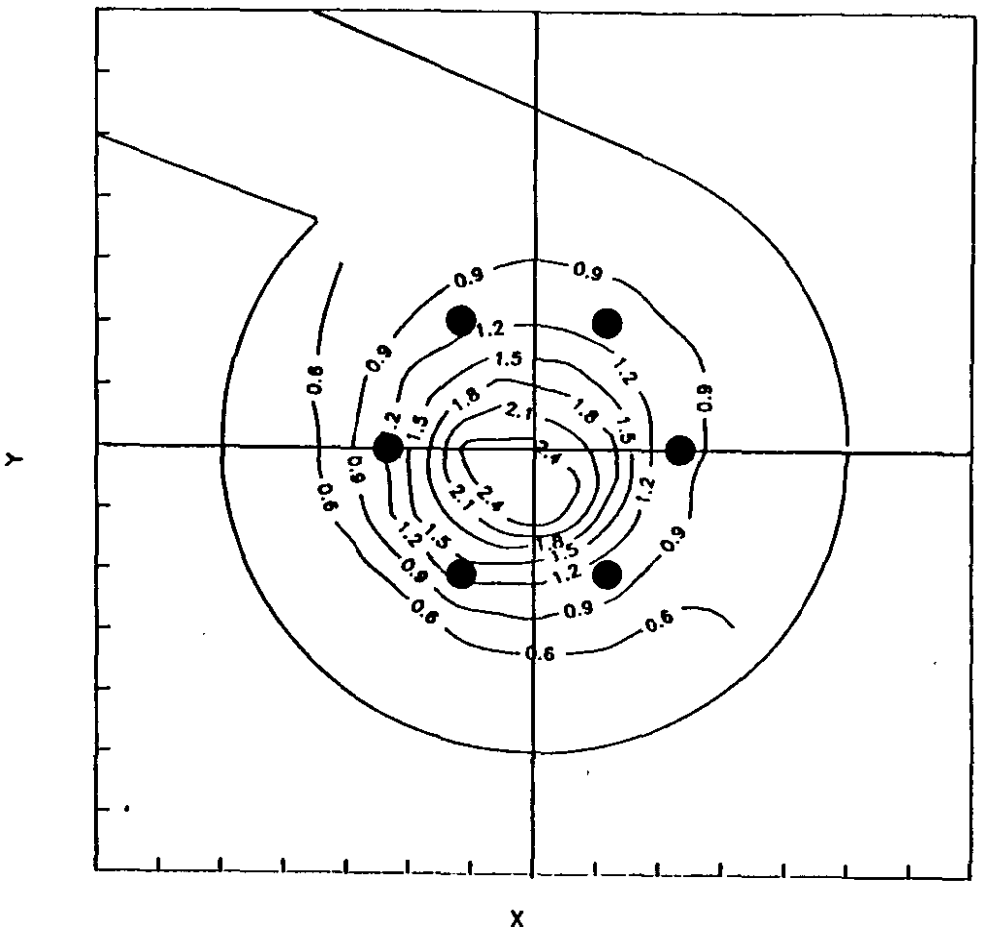

FIGURE 46. TOPOGRAPHICAL PLOT SHOWING MIXING PATTERNS IN BAFFLE REGION. INJECTOR CONFIGURATION WAS IN-BOARD, ODD CLOCKING. TEST CASE SHOWN IS MCI33.

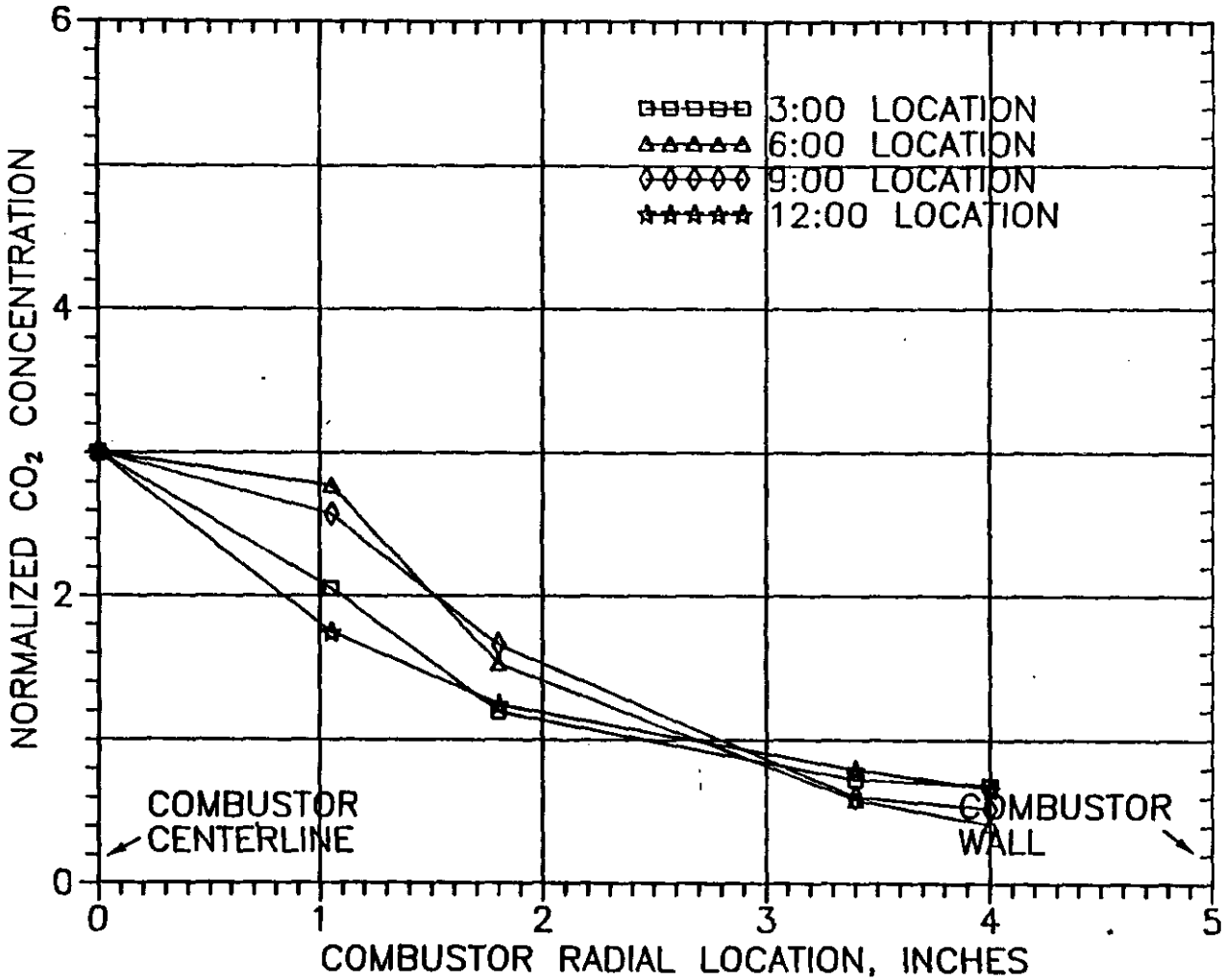

FIGURE 47. MIXING CHARACTERIZATION OF ALL INJECTORS. RADIAL MEASUREMENTS WERE PERFORMED FOR THE BAFFLE REGION. INJECTOR CONFIGURATION WAS IN-BOARD, ODD CLOCKING. TEST CASE SHOWN IS MCI33.

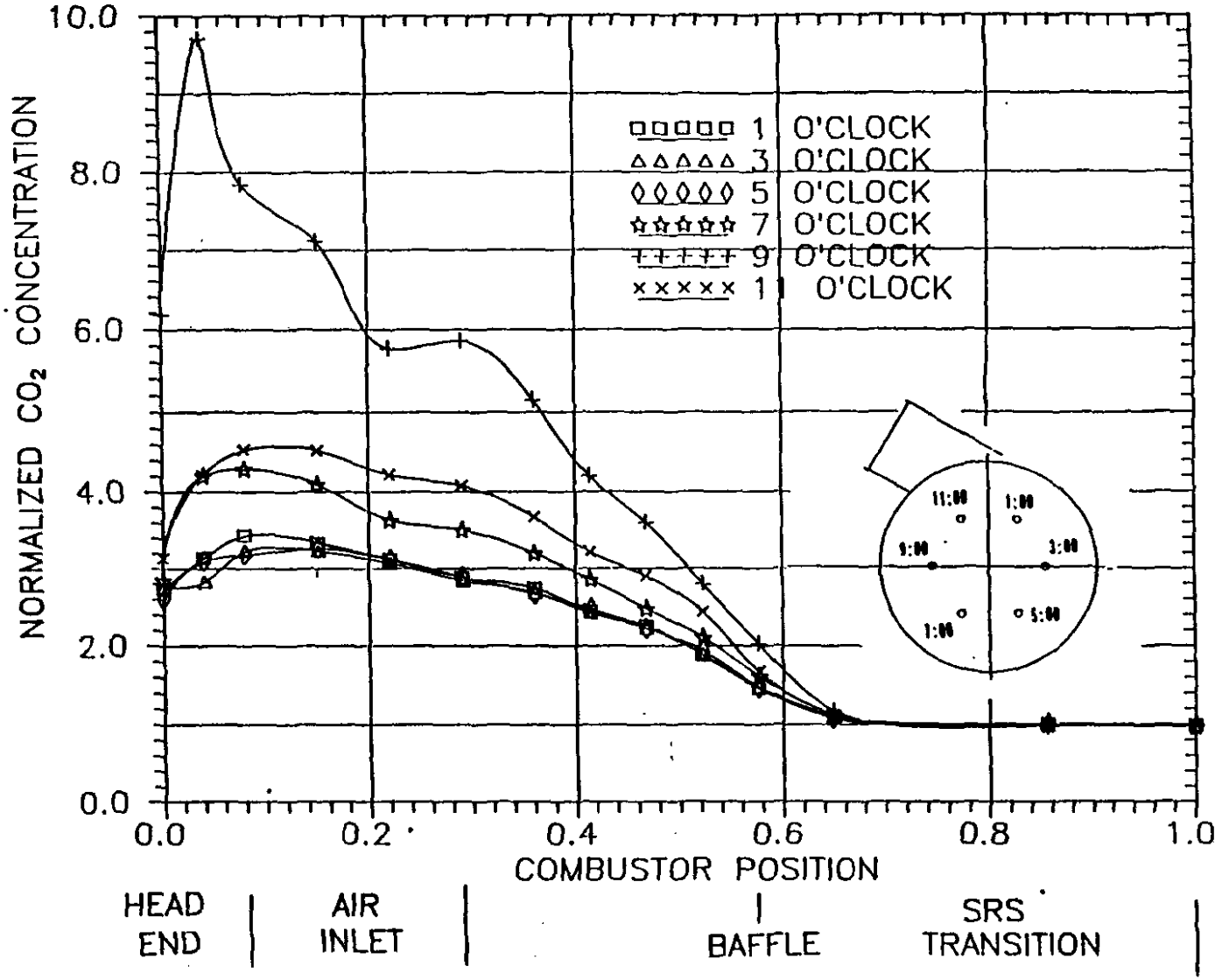

FIGURE 48. MIXING CHARACTERIZATION OF EACH INDIVIDUAL INJECTOR. CENTERLINE MEASUREMENTS WERE PERFORMED DOWN COMBUSTOR LENGTH. INJECTOR CONFIGURATION WAS IN-BOARD, ODD CLOCKING. TEST CASES SHOWN ARE MCI15-20.

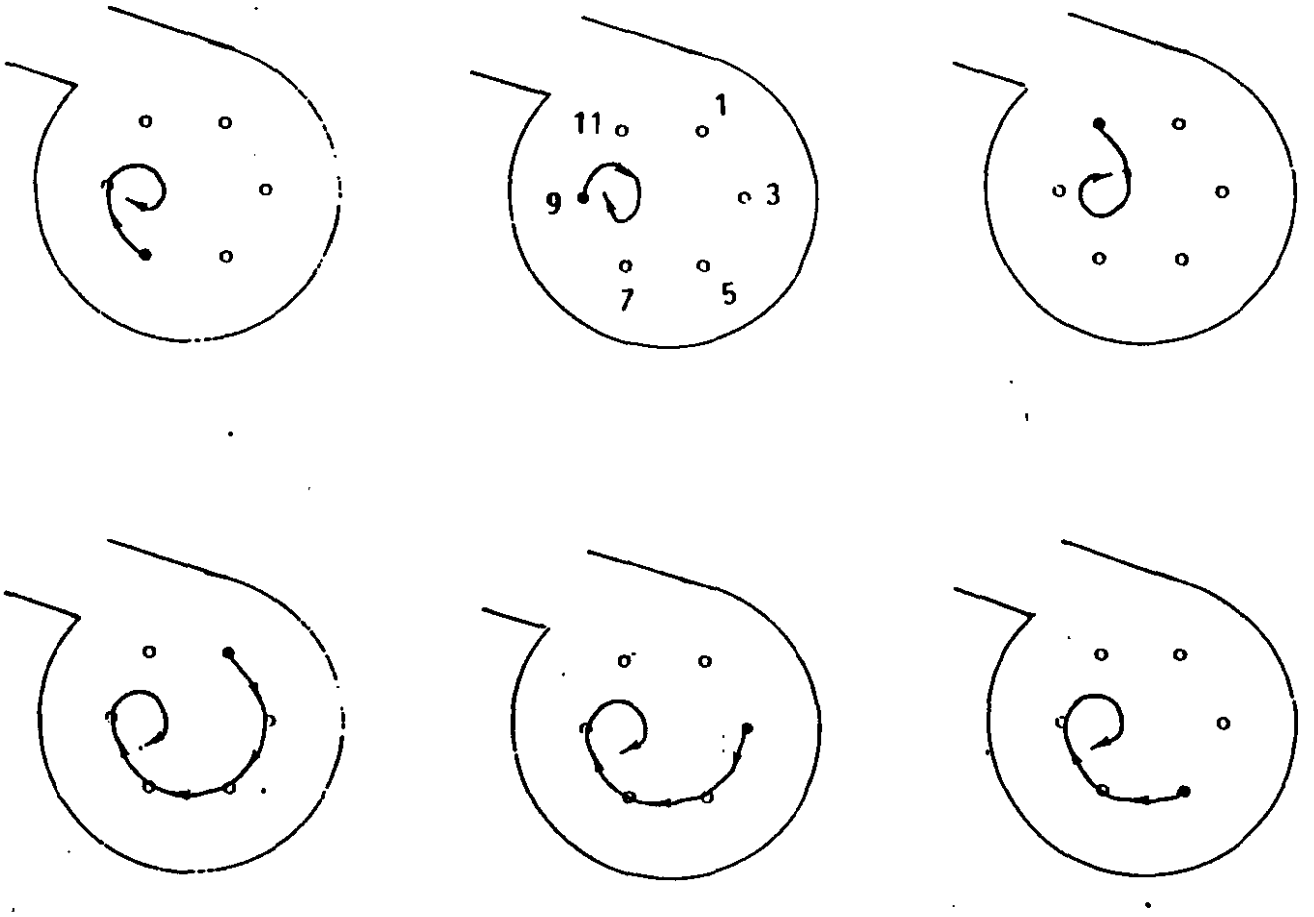

FIGURE 49. FLOW PATTERNS OBSERVED DURING PARTICLE INJECTION THROUGH EACH INDIVIDUAL INJECTOR. INJECTOR CONFIGURATION WAS IN-BOARD, ODD CLOCKING. TEST CASES SHOWN ARE MCI50-55.

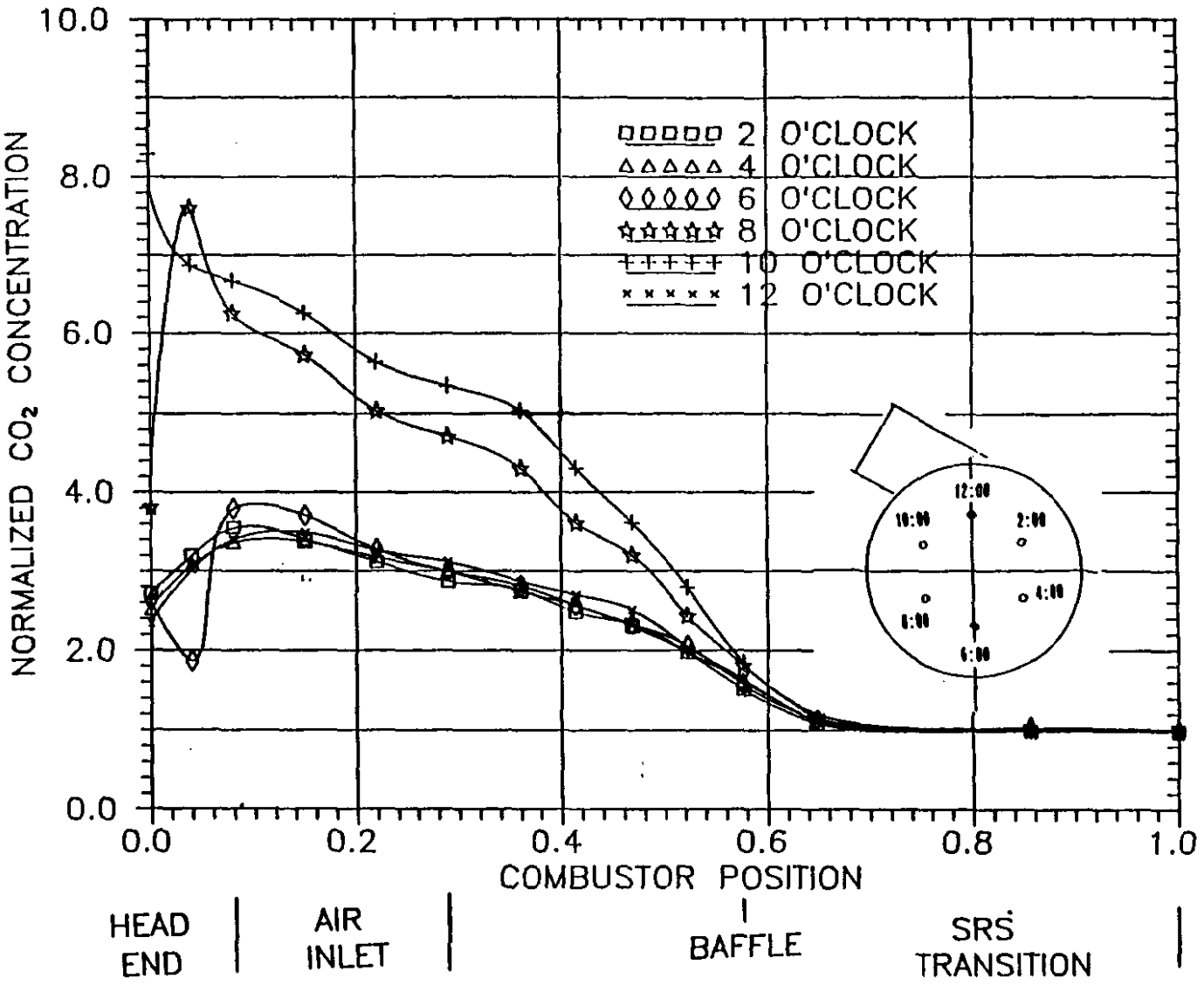

FIGURE 50. MIXING CHARACTERIZATION OF EACH INDIVIDUAL INJECTOR. CENTERLINE MEASUREMENTS WERE PERFORMED DOWN COMBUSTOR LENGTH. INJECTOR CONFIGURATION WAS IN-BOARD, EVEN CLOCKING. TEST CASES SHOWN ARE MCI22-27.

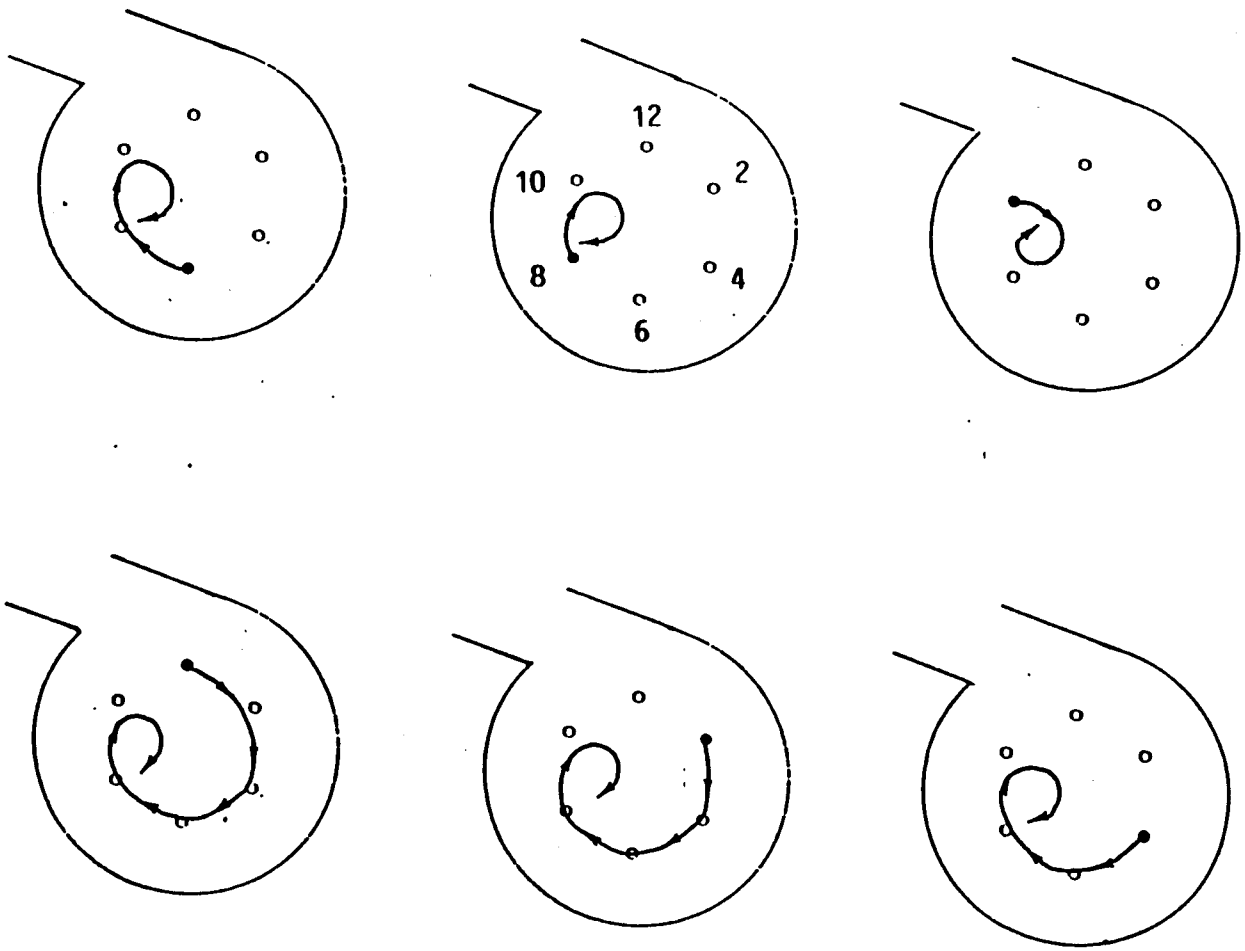

FIGURE 51. FLOW PATTERNS OBSERVED DURING PARTICLE INJECTION THROUGH EACH INDIVIDUAL INJECTOR. INJECTOR CONFIGURATION WAS IN-BOARD, EVEN CLOCKING. TEST CASES SHOWN ARE MCI56-61.

from the 8:00 and 10:00 injectors, however, are not as large as for the 9:00 injector (odd clocking).

6.4 Slag Recovery Section Testing

6.4.1 Test Configuration

A schematic of the slag recovery section test set-up is shown in Figure 28. Air flows through both the precombustor and slagging stage prior to entering the slag recovery section. Flow tufts were used for flow visualization. Velocity measurements were taken throughout the flow cross-section at selected stations, using a anemometer. Key parameters which were varied during testing included slag recovery section geometry (i.e. effect of back wall "pocket"), angle of exhaust, slag recovery section height, and swirl number.

6.4.2 Test Results

Table 6 lists the test matrix followed during cold flow testing of the Healy Slag Recovery Section (SRS). The first series of tests focused on the evaluation of the jet trap. The combustor swirl number and mass ratio between the precombustor and the main combustor flows were set similarly to Healy hot fire conditions under full load operation. Jet trap configurations tested were a flat plate or no jet trap, a regular size pocket, and an extended size pocket (3x the nominal depth) as shown in Figure 52. Velocity measurements were performed at the SRS exit for each jet trap configuration.

The second series of tests focused on the effect of the SRS exhaust angle on flow non-uniformities at the SRS exit. The previous series of tests were run at an exhaust angle orthogonal to the combustor axis (slanted with respect to the vertical) as shown in Figure 53. This series of tests focused on a vertical exhaust angle for comparison (Figure 28). Velocity measurements were again made at the SRS exit.

The last series of tests focused on the effect of SRS exit height on flow non-uniformities at the SRS exit. The SRS exit height was varied as a function of Z/Lmin where Lmin is the minimum design height for the SRS (= 100"). Details of the coordinate system used in the cold flow are shown in Figure 54.

6.4.2.1 Baseline Case Test Results

The operating conditions for the baseline test were set for a nominal swirl and mass flow ratio. A flat plate was installed in place of a jet trap (no jet trap) for the baseline case. Also, the slanted exhaust exit was utilized, with a SRS height equivalent to the minimum design height (Z/Lmin=1).

The velocity distributions are shown in Figure 55. Orientation of the velocity distribution plot with the SRS can be understood as follows. The SRS flow cross-section is in the XY plane and the velocities are in the Z direction, normalized with respect to the average plug flow velocity. The baffle face is parallel to the XZ plane. The jet trap is also parallel to the XZ plane at Y/D=0. The precombustor flow enters from the left simulating the left-handed (south) combustor. The swirl is clockwise in the XZ plane as viewed looking downstream.

TABLE 6. COLD FLOW TEST MATRIX - HEALY SLAG RECOVERY SECTION (SRS) CONFIGURATION.

CASE	COMBUSTOR CHAMBER SWIRL NO.	MASS RATIO (a)	JET TRAP CONFIG.	SRS EXIT CONFIG.	SRS EXIT LENGTH Z/Lmin (b)	VELOCITY NON-UNIFORMITY (c)	RANGE OF NORMALIZED VELOCITY MAX/MIN (d)
SRS1 (e)	3.5	.2	FLAT	SLANTED	1	32	1.5/0.4
SRS2	3.5	.2	REGULAR	SLANTED	1	26	1.4/0.6
SRS3	3.5	.2	EXTENDED	SLANTED	1	29	1.5/0.6
SRS4	3.5	.2	FLAT	VERTICAL	1	32	1.6/0.4
SRS5	3.5	.2	REGULAR	VERTICAL	1	24	1.4/0.7
SRS6	3.5	.2	EXTENDED	VERTICAL	1	29	1.4/0.7
SRS7	3.5	.2	FLAT	SLANTED	0.3	30	1.5/0.8
SRS8	3.5	.2	FLAT	SLANTED	0.6	36	1.4/0.4
SRS9	3.5	.2	FLAT	SLANTED	1.4	27	1.5/0.6
SRS10	0	.2	FLAT	SLANTED	1	48	2.2/0.4
SRS11	5.0	.2	FLAT	SLANTED	1	38	1.6/0.4

a - RATIO OF MASS FLOW FROM HEADEND TO MASS FLOW FROM PRECOMBUSTOR
b - Lmin IS THE MINIMUM SRS HEIGHT
c - RELATIVE STANDARD DEVIATION (%) ABOUT MEASUREMENTS MADE ACROSS FLOW CROSS-SECTION
d - NORMALIZED WITH RESPECT TO THE AVERAGE PLUG FLOW VELOCITY
e - BASELINE CASE

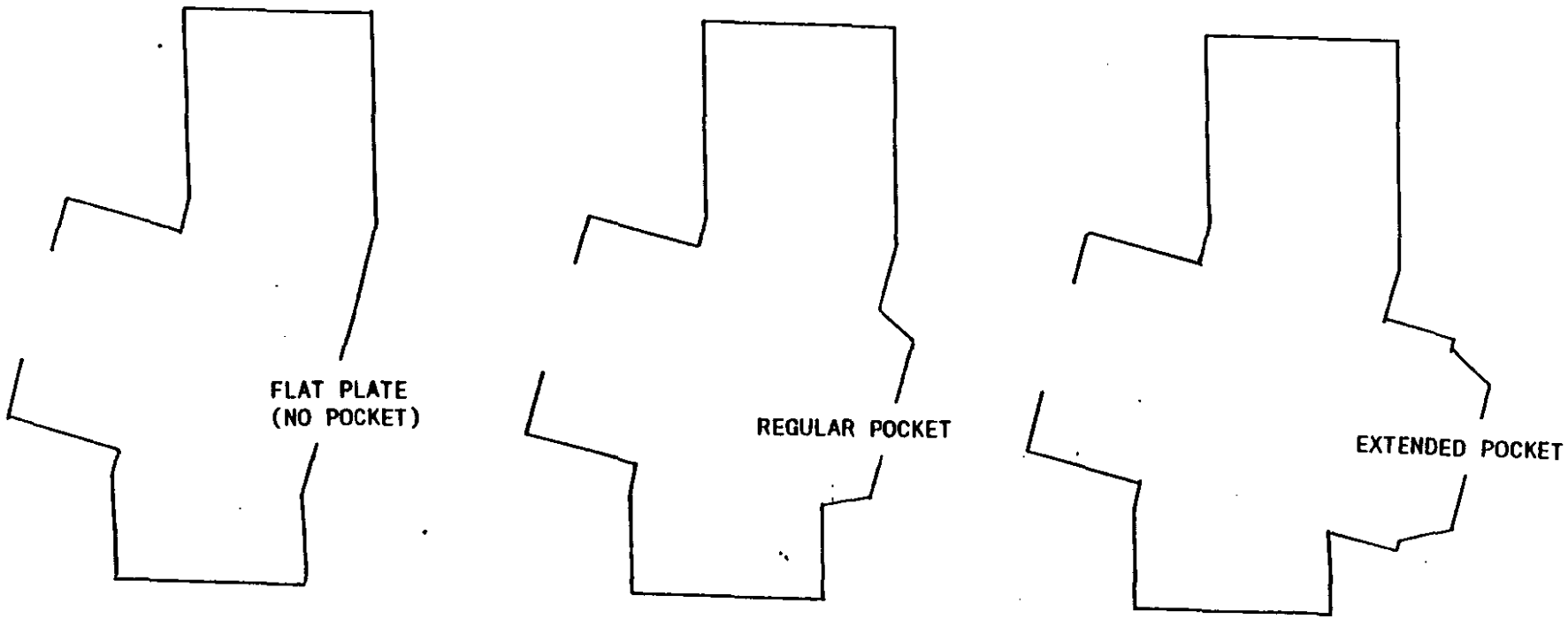

FIGURE 52. DESCRIPTION OF JET TRAPS TESTED IN COLD FLOW TESTS.

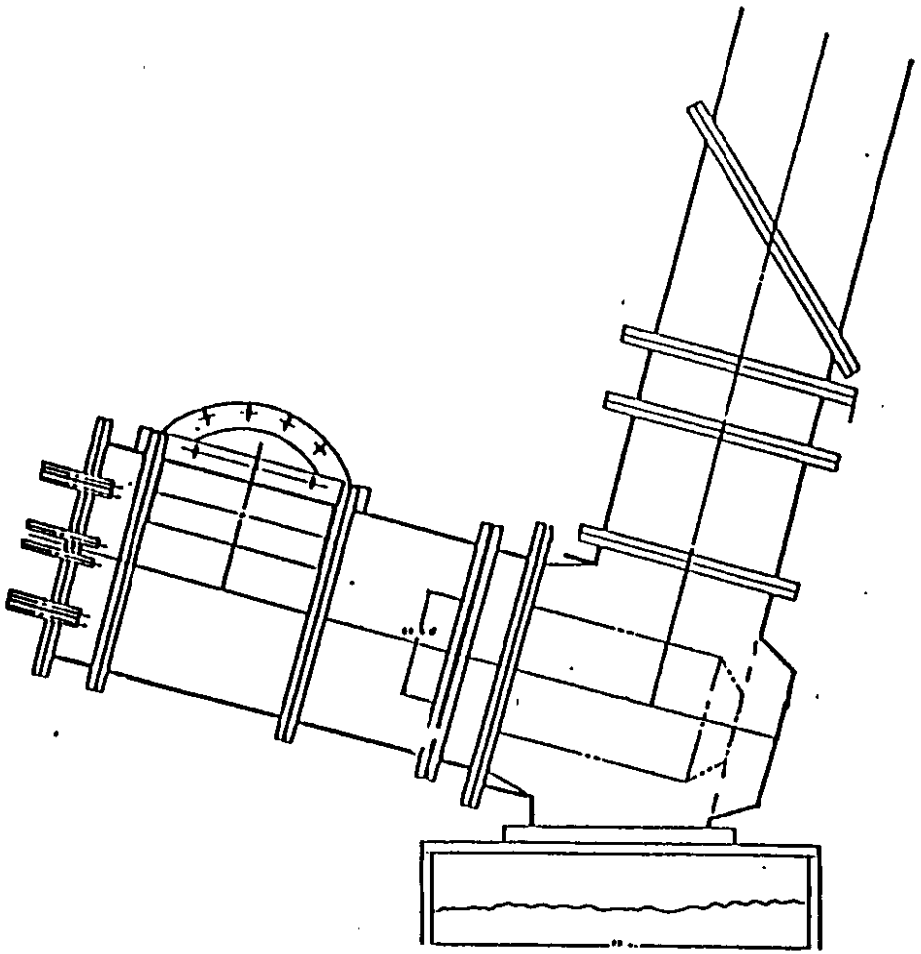

FIGURE 53. HEALY COLD FLOW SET UP WITH SLANTED EXHAUST (ORTHOGONAL CONFIGURATION).

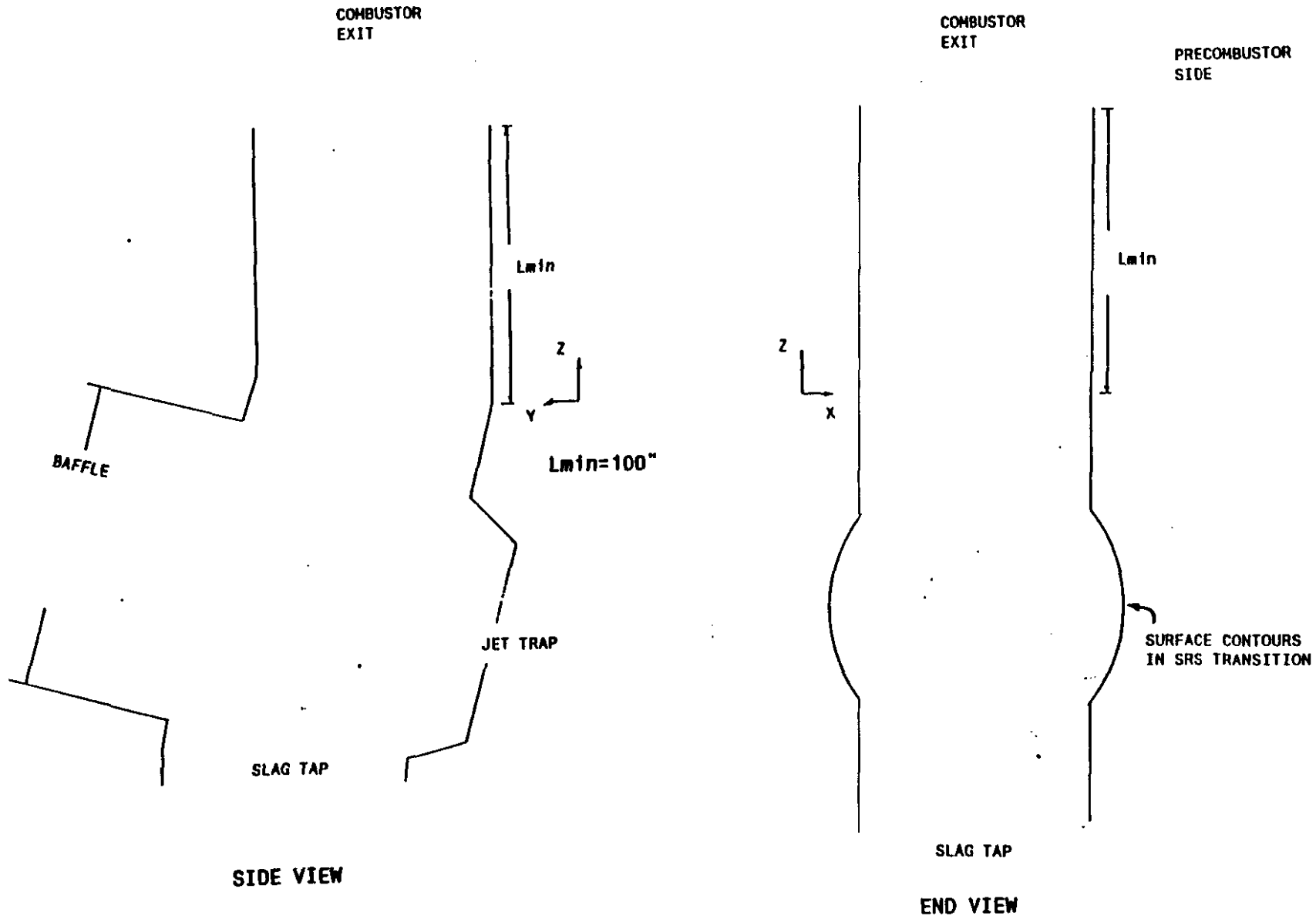

FIGURE 54. DETAILS OF SRS COORDINATE SYSTEM FOR COLD FLOW MEASUREMENTS

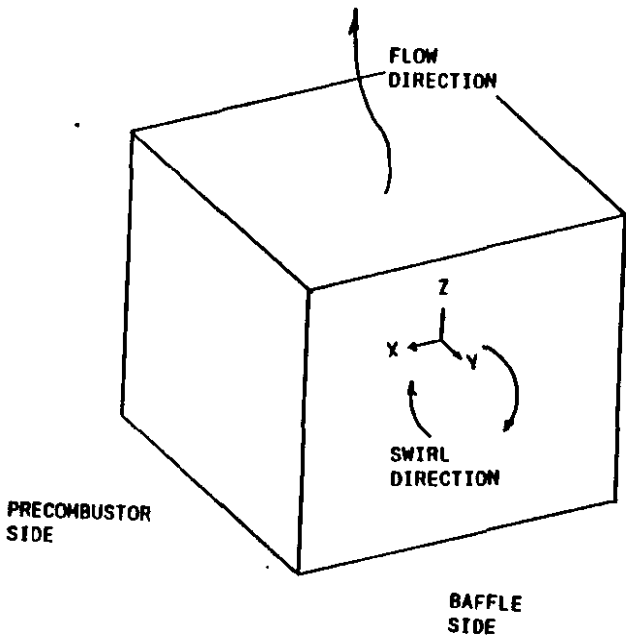

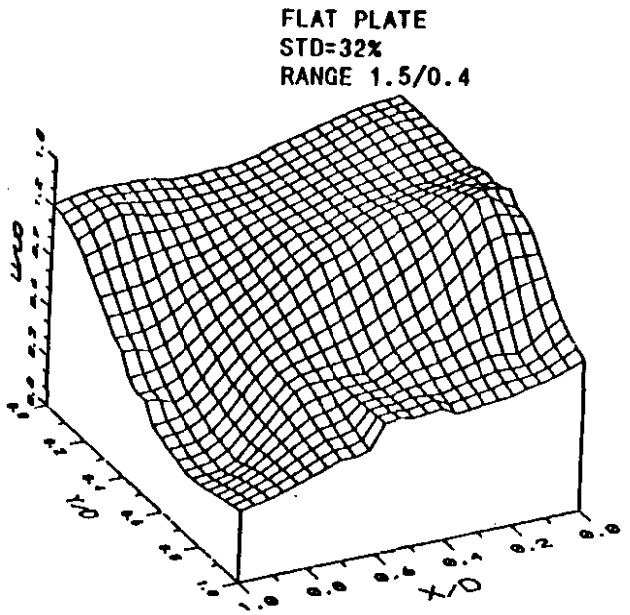

FIGURE 55. BASELINE FLOW DISTRIBUTION AT COMBUSTOR EXIT AND COLD FLOW COORDINATE SYSTEM.

The flow non-uniformity is determined by a standard deviation (std) among velocity measurements taken across the flow cross- section. For the baseline case, the non-uniformity is 32% relative to the plug flow velocity. The velocity measurements taken for the baseline case range from 0.4 to 1.5 times the average plug flow velocity. The flow is highest along the back side (flat plate), with a slight bias toward the right side. The flow is lowest along the front, left side.

6.4.2.2 Effect of Jet Trap on Velocity Distribution at the Combustor Exit

Velocity distributions at the combustor exit are shown in Figures 56 and 57 for the jet trap configurations tested. Figure 56 shows surface contour plots whereas Figure 57 shows topographical plots. In the topographical plots, the value of 1.0 represents the average or plug flow velocity case.

The operating conditions for the tests were similar to the baseline conditions. A slanted exit (Figure 53) was utilized with a SRS height equivalent to the minimum design height.

The velocity distribution for the regular pocket case showed some improvement in flow uniformity over the baseline case. The standard deviation was observed to be 26% for the regular pocket case as compared with 32% for the baseline. The flow uniformity was improved primarily due to higher velocities in the low flow zone along the front, left side. The low flow zone increased in velocity from 40% of the average plug flow velocity to 60%.

The velocity distribution for the extended pocket case showed a slight improvement in uniformity over the baseline case, however, a slight decrease in uniformity as compared with the regular pocket case. The low flow zone also changed locations moving from the front, left side to the front, right side.

6.4.2.3 Effect of Exhaust Exit Angle on Velocity Distribution at Combustor Exit

Figure 58 and 59 shows surface contour plots and topographical plots, respectively, for velocity distributions at the combustor exit for a vertical exhaust exit. Similar operating conditions as the slanted exhaust exit cases above were utilized. The same jet trap configurations were also tested.

Comparing Figures 56 and 57 with Figures 58 and 59 indicates that the flow uniformity at the combustor exit for the vertical exhaust appears to be very similar to the slanted exhaust for each jet trap configuration.

6.4.2.4 Effect of Slag Recovery Section Height on Velocity Distribution at Combustor Exit

Figure 60 and 61 shows surface contour plots and topographical plots, respectively, for velocity distributions at the combustor exit for various SRS heights. The heights are described by Z/Lmin which is the fraction of the minimum design height, Lmin, for the SRS. Diagnostic ports in the SRS were available for Z/Lmin's of .3, .6, 1 (baseline), and 1.4. A Z/Lmin of 0.3 is located just after the turn in the SRS transition.

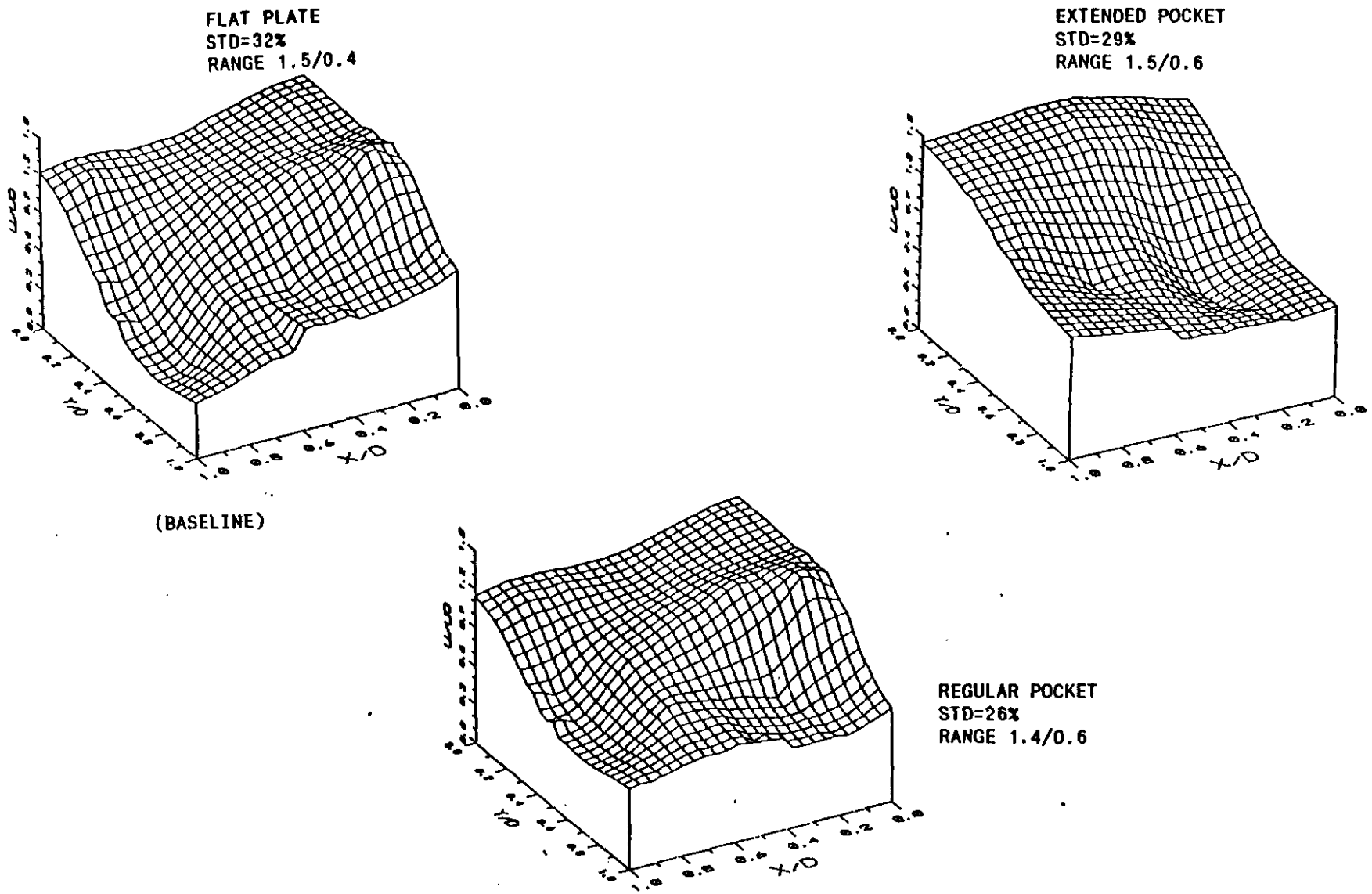

FIGURE 56. EFFECT OF JET TRAP ON VELOCITY DISTRIBUTION AT COMBUSTOR EXIT FOR A SLANTED EXIT. TEST PARAMETERS ARE SWIRL = 3.5, Z/LMIN = 1.0. TEST CASES SHOWN ARE SRS 1, 2, 3. SURFACE CONTOURS SHOWN.

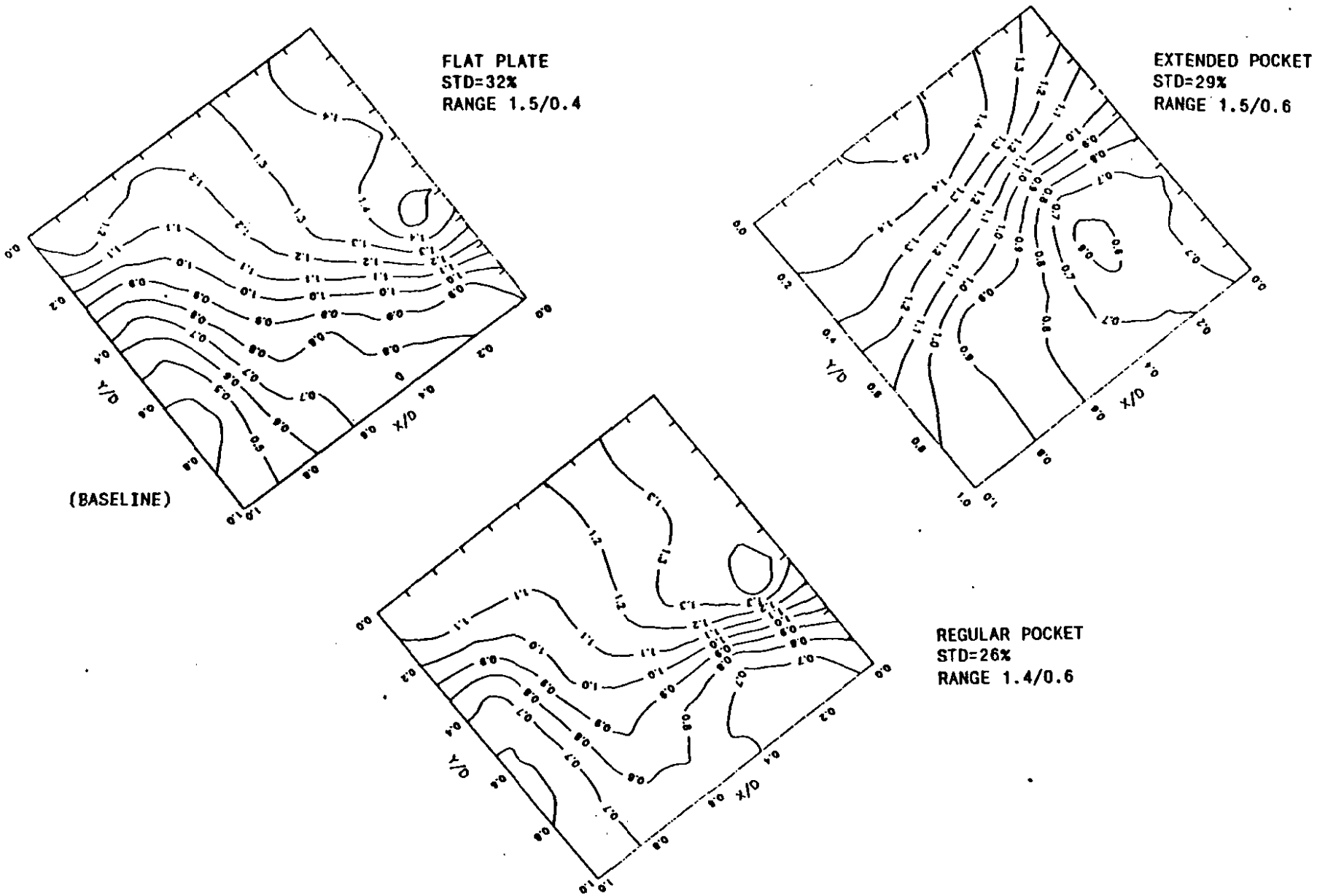

FIGURE 57. EFFECT OF JET TRAP ON VELOCITY DISTRIBUTION AT COMBUSTOR EXIT FOR A SLANTED EXIT. TEST PARAMETERS ARE SWIRL = 3.5, Z/LMIN = 1.0. TEST CASES SHOWN ARE SRS 1, 2, 3. TOPOGRAPHICAL PLOTS SHOWN.

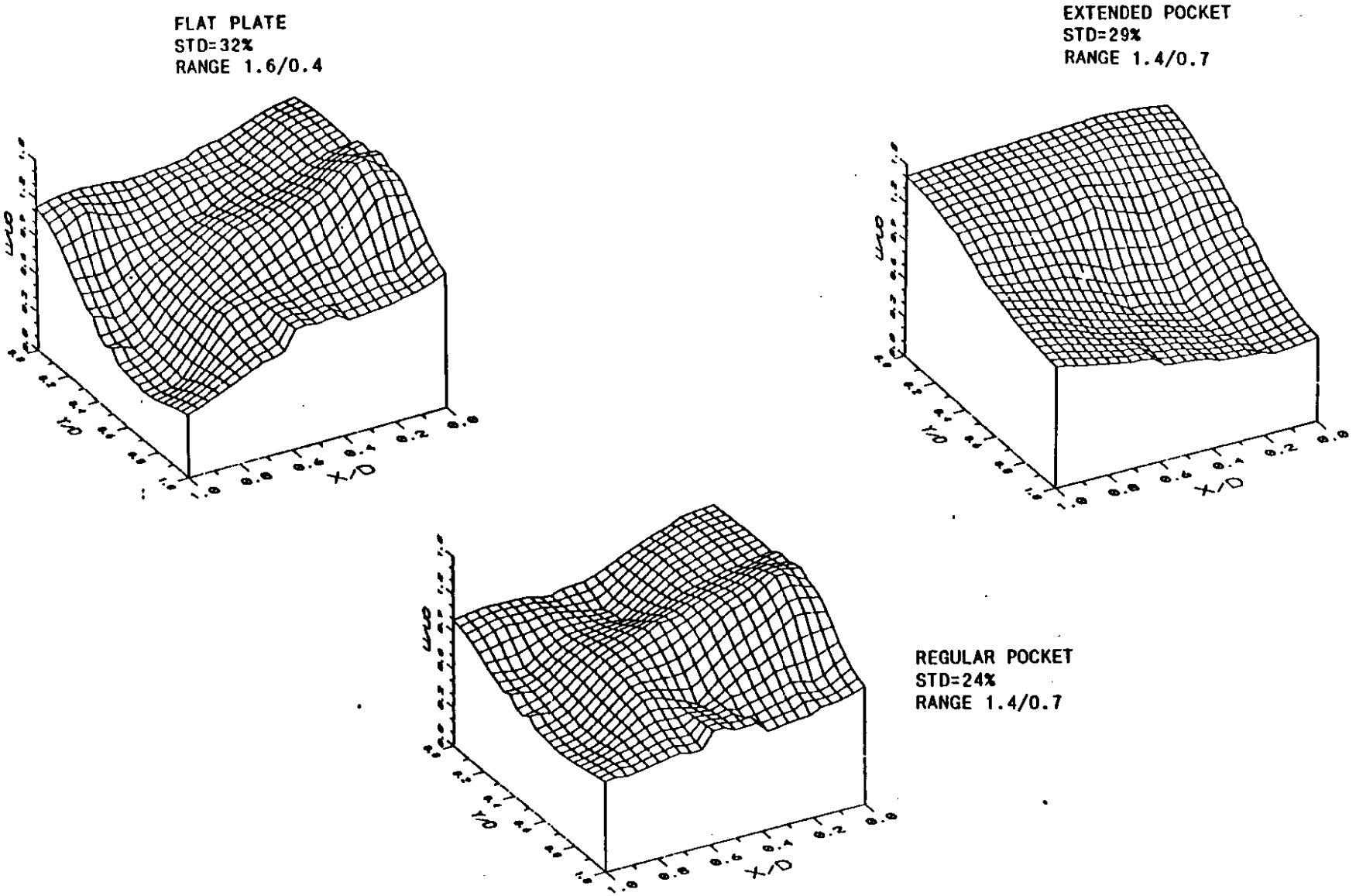

FIGURE 58. EFFECT OF JET TRAP ON VELOCITY DISTRIBUTION AT COMBUSTOR EXIT FOR A VERTICAL EXIT. TEST PARAMETERS ARE SWIRL = 3.5, Z/LMIN = 1.0. TEST CASES SHOWN ARE SRS 4, 5, 6. SURFACE CONTOURS SHOWN.

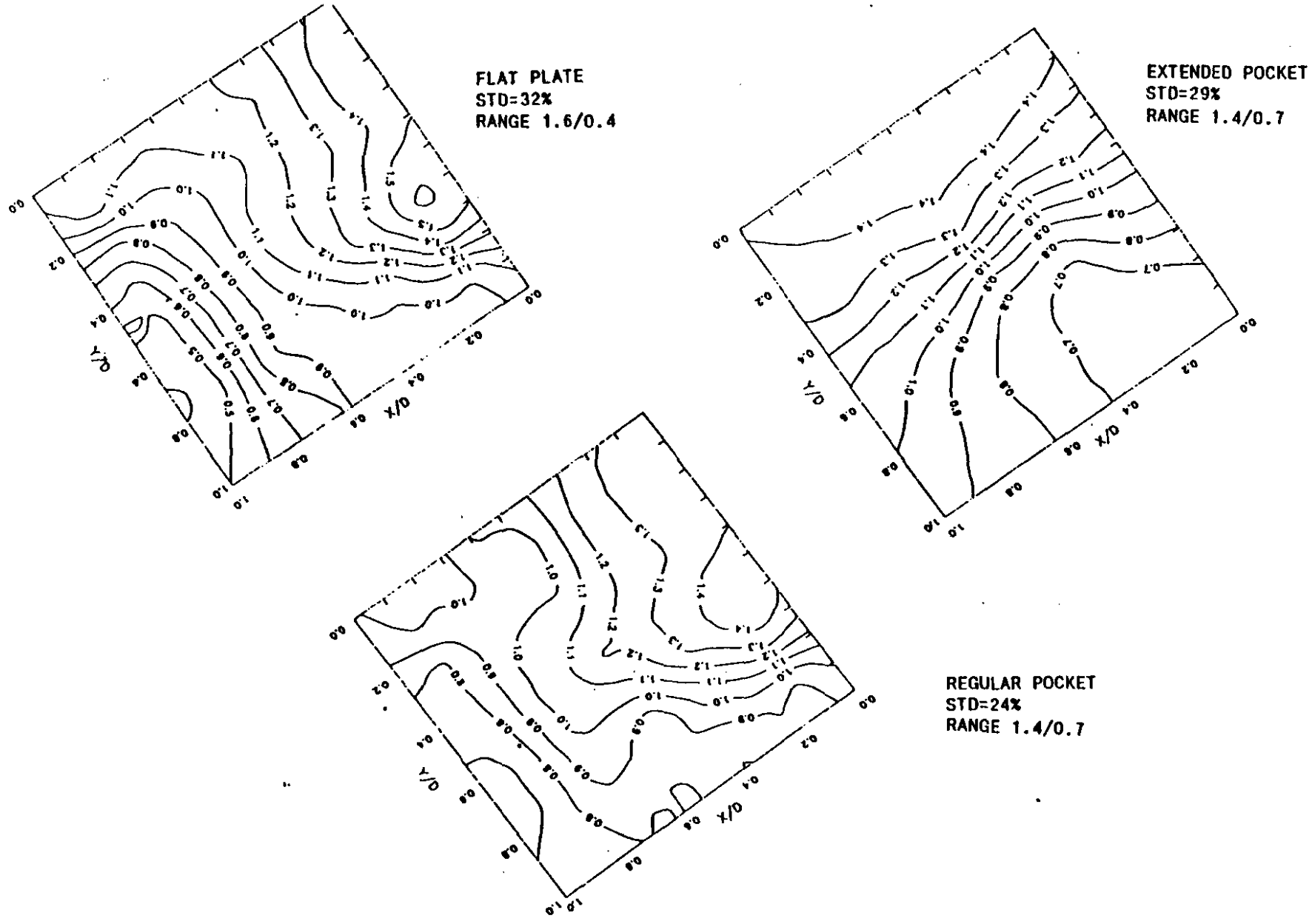

FIGURE 59. EFFECT OF JET TRAP ON VELOCITY DISTRIBUTION AT COMBUSTOR EXIT FOR A VERTICAL EXIT. TEST PARAMETERS ARE SWIRL = 3.5, Z/LMIN = 1.0. TEST CASES SHOWN ARE SRS 4, 5, 6. TOPOGRAPHICAL PLOTS SHOWN.

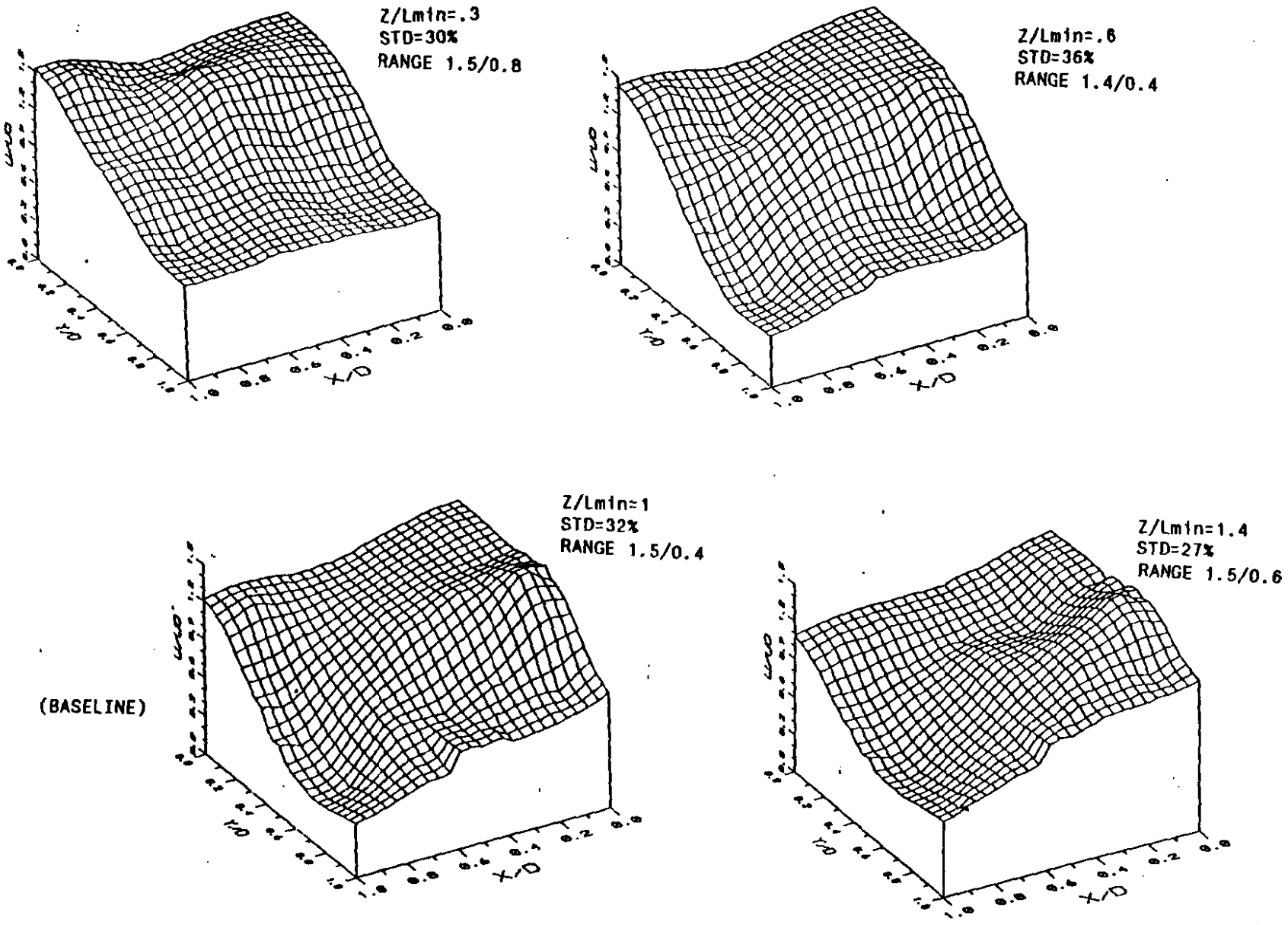

FIGURE 60. EFFECT OF SRS HEIGHT ON VELOCITY DISTRIBUTION AT COMBUSTOR EXIT. TESTS PARAMETERS ARE SWIRL = 3.5, FLAT PLATE OR NO JET TRAP, AND A SLANTED EXIT. TEST CASES SHOWN ARE SRS 7, 8, 1, 9. SURFACE CONTOURS SHOWN.

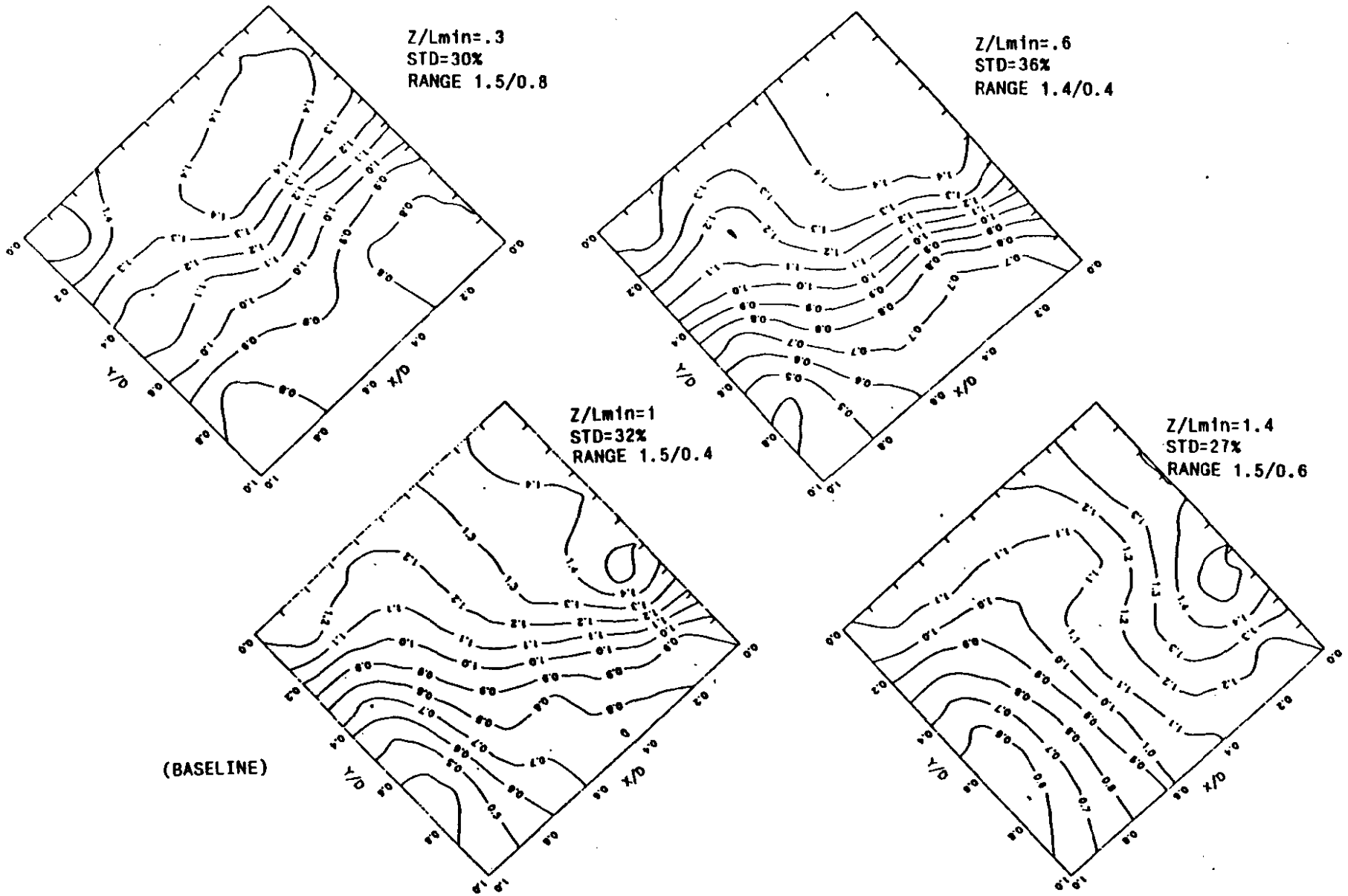

FIGURE 61. EFFECT OF SRS HEIGHT ON VELOCITY DISTRIBUTION AT COMBUSTOR EXIT. TESTS PARAMETERS ARE SWIRL = 3.5, FLAT PLATE OR NO JET TRAP, AND A SLANTED EXIT. TEST CASES SHOWN ARE SRS 7, 8, 1, 9. TOPOGRAPHICAL PLOTS SHOWN.

For these tests, no jet trap was installed. The slanted combustor exit was utilized and operating conditions were similar to the baseline conditions.

The standard deviation in the velocity distributions measured for the four diagnostic ports in order of increasing height were 30%, 36%, 32%, and 27%. The flows were initially high along the back plate (1.5 times the plug flow velocity), and low along the front (0.8 times the plug flow velocity). With increasing SRS height, the flow distribution rotated in a clockwise fashion with the higher flows moving toward the back, right, and the lower flows moving toward the front, left. The flow uniformity did not improve initially with additional height as seen from the standard deviations. The flow in the front, left corner decreased in velocity from 80% of the average velocity to only 40%. The flow in the back, right corner remained high at 1.4 times the average velocity. After the second diagnostic spool, the flow uniformity showed only slight improvement. The flow in the front, left corner increased from 40% of the average velocity up to 60%. The flow in the back, right corner remained high at 1.5 times the average plug flow velocity.

6.5 Limestone Injection Testing

6.5.1 Test Configuration

The air flow model was configured with air entering the slagging combustor tangentially from the precombustor as well as axially through the head end of the slagging combustor to obtain a combustor swirl number and mass ratio which matched hot flow conditions. Air was injected downstream of the slagging combustor in the SRS to simulate limestone injection. Key parameters which were varied during testing included injector location and the ratio of momentum flux between the limestone simulated flow and the SRS flow.

6.5.2 Test Results

Table 7 shows the test matrix followed during cold flow testing of the limestone injector. During this test phase, carbon dioxide was injected with the limestone simulated flow as a tracer material. The tracer was used to determine where the limestone goes in the SRS on injection and how well it mixes with the gas flow from the slagging combustor. Powder was not injected since the particle slip is expected to be small relative to the size of the SRS.

The first four tests investigated the effect of injector penetration depth on limestone injection performance. Limestone simulated flow was injected from the back wall of the SRS at a height of Z/Lmin of 0.6. The back wall of the SRS as well as the other injection faces of the SRS are shown in Figure 62. The SRS coordinate system used was the same one used in the velocity measurement tests performed earlier (Figure 54). Carbon dioxide measurements were made at a Z/Lmin of 1.0 which is at the exit of the SRS. Hot flow momentum flux ratio was preserved for these tests as well as injector diameter.

The next three tests investigated the effect of injector location on limestone injection performance. Tests were performed as above on the remaining three faces of the SRS.

TABLE 7. COLD FLOW MODEL TEST MATRIX - LIMESTONE INJECTION TESTS.

TEST CASE	INJECTOR LOCATION			MEASUREMENT LOCATION Z/Lmin	INJECTOR CONFIGURATION	INJECTOR DIAMETER (IN.)	MOMENTUM FLUX RATIO R^2
	SRS FACE*	HEIGHT Z/Lmin	DEPTH (IN.)				
LIME1	BACK	0.6	WALL	1	ORTHOGONAL**	0.375	5.8
LIME2	"	"	1	"	"	"	"
LIME3	"	"	2	"	"	"	"
LIME4	"	"	3	"	"	"	"
LIME5	LEFT	"	2	"	"	"	"
LIME6	FRONT	"	"	"	"	"	"
LIME7	RIGHT	"	"	"	"	"	"
LIME8	LEFT	0.3	"	"	"	"	"
LIME9	"	0.6	"	2.7	"	"	"
LIME10	BACK	"	WALL	1	"	"	22.1
LIME11	LEFT	"	"	"	"	"	"
LIME12	RIGHT	"	"	"	"	"	"
LIME13	LEFT	"	"	"	"	0.21	39.7

* - BACK FACE REFERS TO THE SIDE AWAY FROM THE HEADEND,
LEFT FACE REFERS TO THE PRECOMBUSTOR SIDE,
FRONT FACE REFERS TO THE SIDE NEAREST THE HEADEND,
AND THE RIGHT FACE REFERS TO THE SIDE AWAY FROM THE PRECOMBUSTOR

** - ORTHOGONAL MEANS PERPENDICULAR TO THE SRS WALL

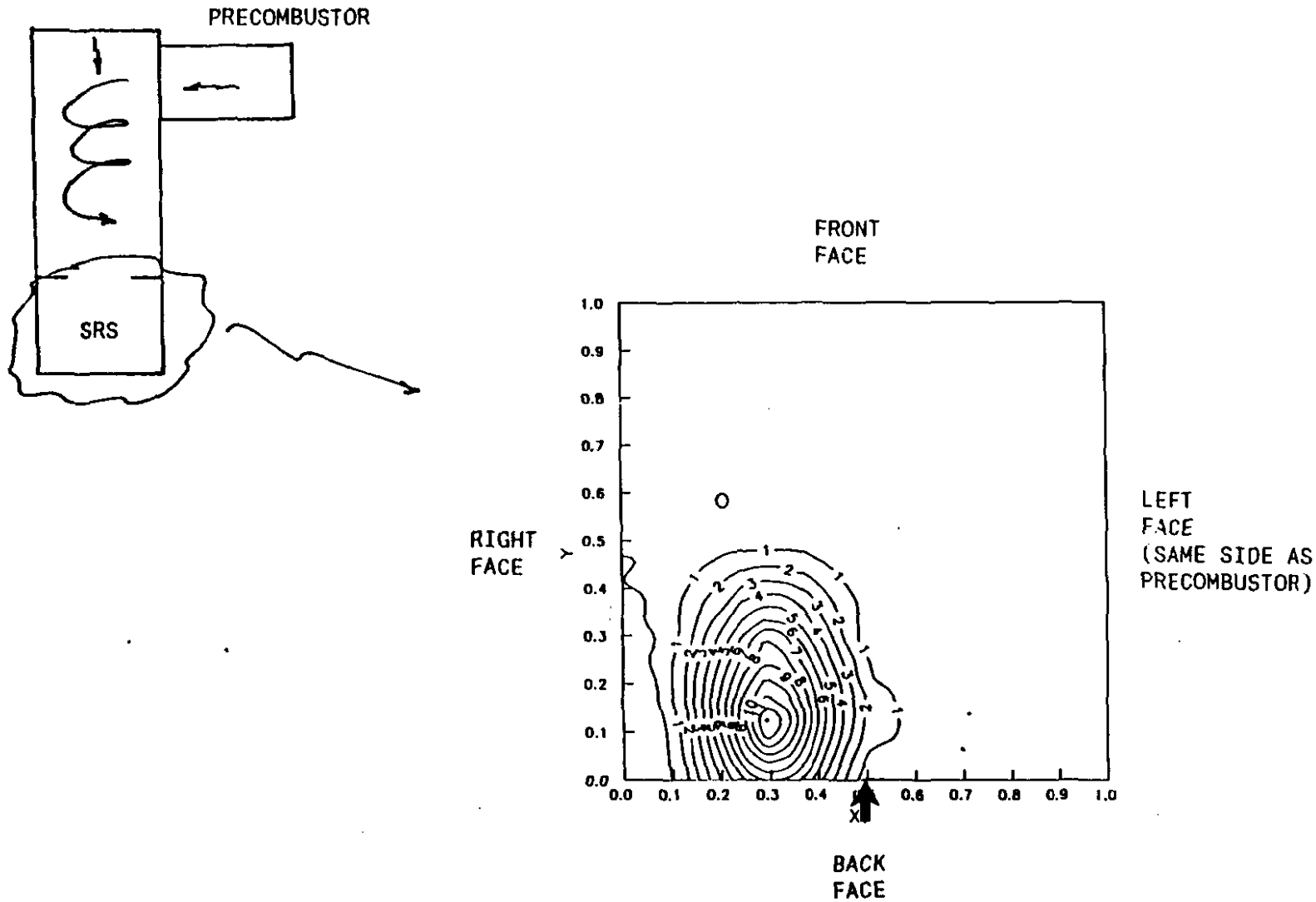

FIGURE 62. ORIENTATION OF LIMESTONE CONTOUR PLOT WITH RESPECT TO COMBUSTOR. TEST SHOWN IS LIME 1 WITH INJECTION AT THE BACK FACE AS INDICATED BY THE ARROW.

The next two tests focused on the effect of limestone injection height on limestone injection performance. The injection height was first lowered to Z/Lmin of 0.3 with carbon dioxide measurements made at the exit at Z/Lmin of 1.0. Then, the injection height was raised back to Z/Lmin of 0.6 with measurements made at Z/Lmin of 2.7. This second test determined the extent of mixing and any possible shifts in the location of the limestone downstream of the SRS exit (in the furnace).

Next, limestone injection was simulated at the wall with an increased momentum flux. The momentum flux of the limestone simulated flow was increased by increasing its mass flow. This test was performed to determine limestone penetration and mixing at the higher momentum flux.

The last test performed was similar to the previous test in that the limestone simulated flow was injected at the wall with a higher than nominal momentum flux. The difference was, however, that the momentum flux of the limestone simulated flow was increased by decreasing the diameter of the injector at constant mass flux.

6.5.2.1 Effect of Injector Penetration Depth

Figure 63 shows the effect of injector penetration depth on limestone injection performance. The limestone simulated flow was injected from the back wall of the SRS, and the arrows on the plots indicates the injection depth tested. The contour lines represent lines of constant carbon dioxide values normalized with respect to the average.

The high concentrations of carbon dioxide found in the contour plots indicates that little mixing takes place from the point of injection at Z/Lmin of 0.6 to the measurement point at Z/Lmin of 1.0.

For injection at the wall, the limestone simulated flow moved toward the right side (away from the precombustor side) and stayed along the back wall. This was consistent with the SRS flow patterns observed earlier. The 1" injector depth (10" full scale) moved the limestone further away from the back wall, however, there was still a slight bias to the right side of the SRS. The 2" injector depth (21" full scale) was observed to place the limestone close to the center of the SRS. The 3" injector depth slightly overshot the center of the SRS.

6.5.2.2 Effect of Injector Location

Figure 64 shows the effect of limestone injection from the other sides of the SRS on limestone injector performance. The tests were run at the 2" injector depth at Z/Lmin of 0.6. This case was observed previously to centrally locate the limestone for the back wall injection case. For injection on the other three faces, the limestone simulated flow was still found to be centrally located in the SRS flow at the SRS exit. Injection penetration was found to be slightly more for injection from the SRS sides versus the SRS back wall.

6.5.2.3 Effect of Injector Height

Figure 65 shows the effect of limestone injection height on limestone injection performance. Figure 65A shows the injection point as before at the 2" injector depth, from the left side, at a Z/Lmin of 0.6. Figure 65B shows the

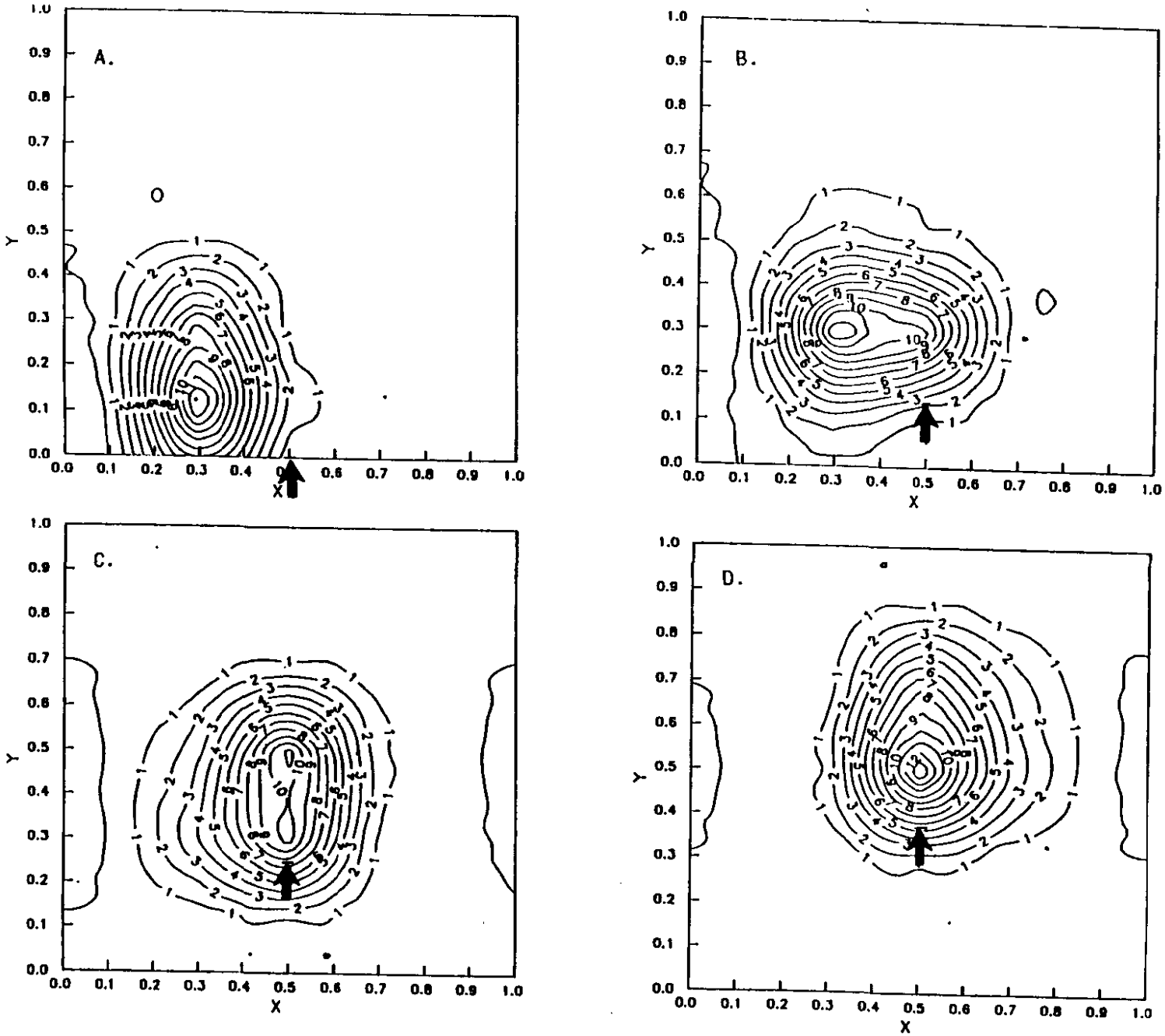

FIGURE 63. EFFECT OF LIMESTONE INJECTOR DEPTH ON INJECTION PERFORMANCE. INJECTION WAS FROM THE SRS BACK FACE, z/LMIN = 0.6 AT A). THE WALL, B). 1" DEPTH, C). 2" DEPTH, AND D). 3" D H. TESTS SHOWN ARE LIME 1-4.

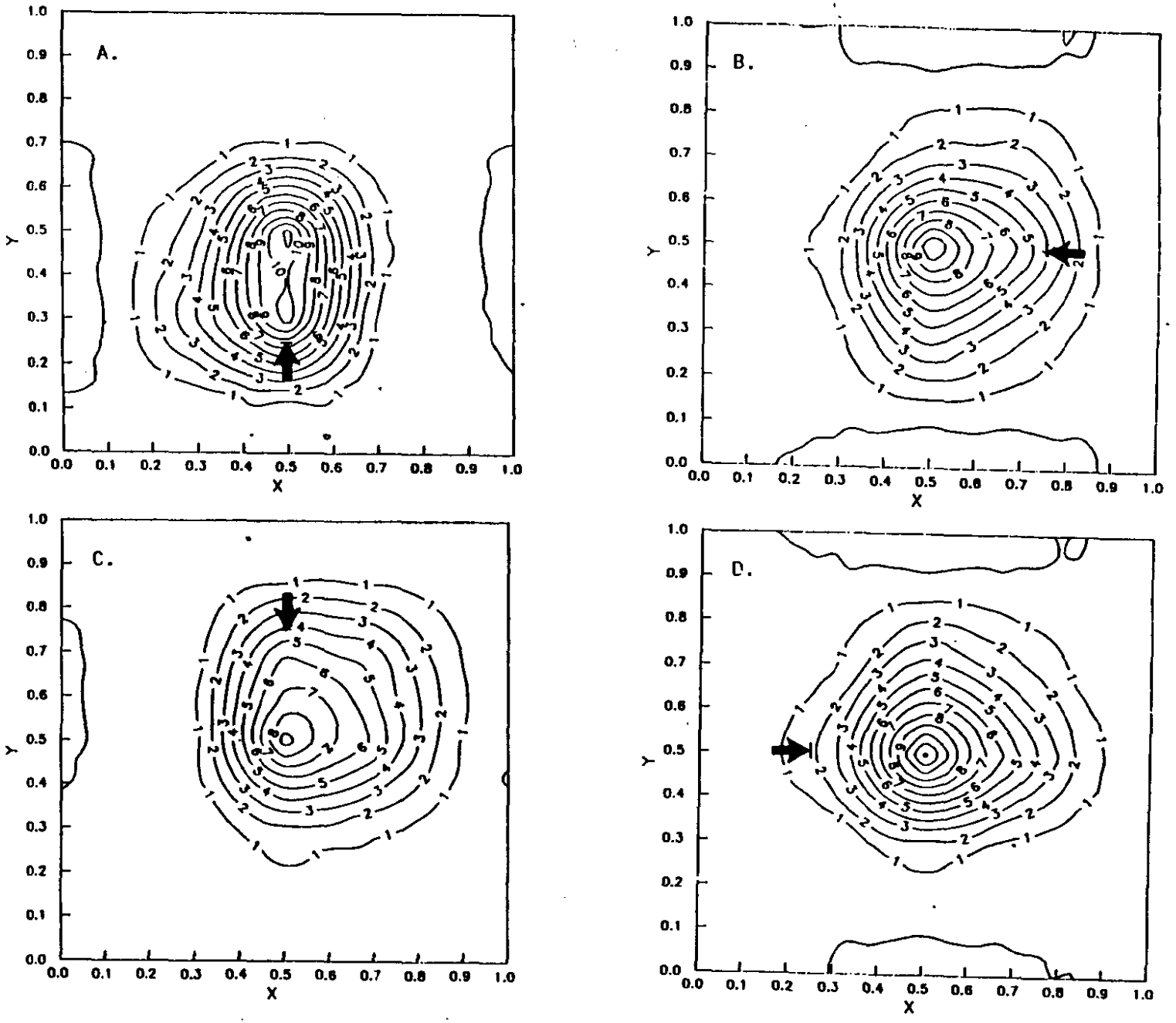

FIGURE 64. EFFECT OF LIMESTONE INJECTION LOCATION ON INJECTION PERFORMANCE. INJECTION WAS AT Z/LMIN = 0.6, 2 " DEPTH FROM A). THE BACK FACE, B). THE LEFT FACE, C). THE FRONT FACE, AND D). THE RIGHT FACE. TESTS SHOWN ARE LIME 3, LIME 5-7.

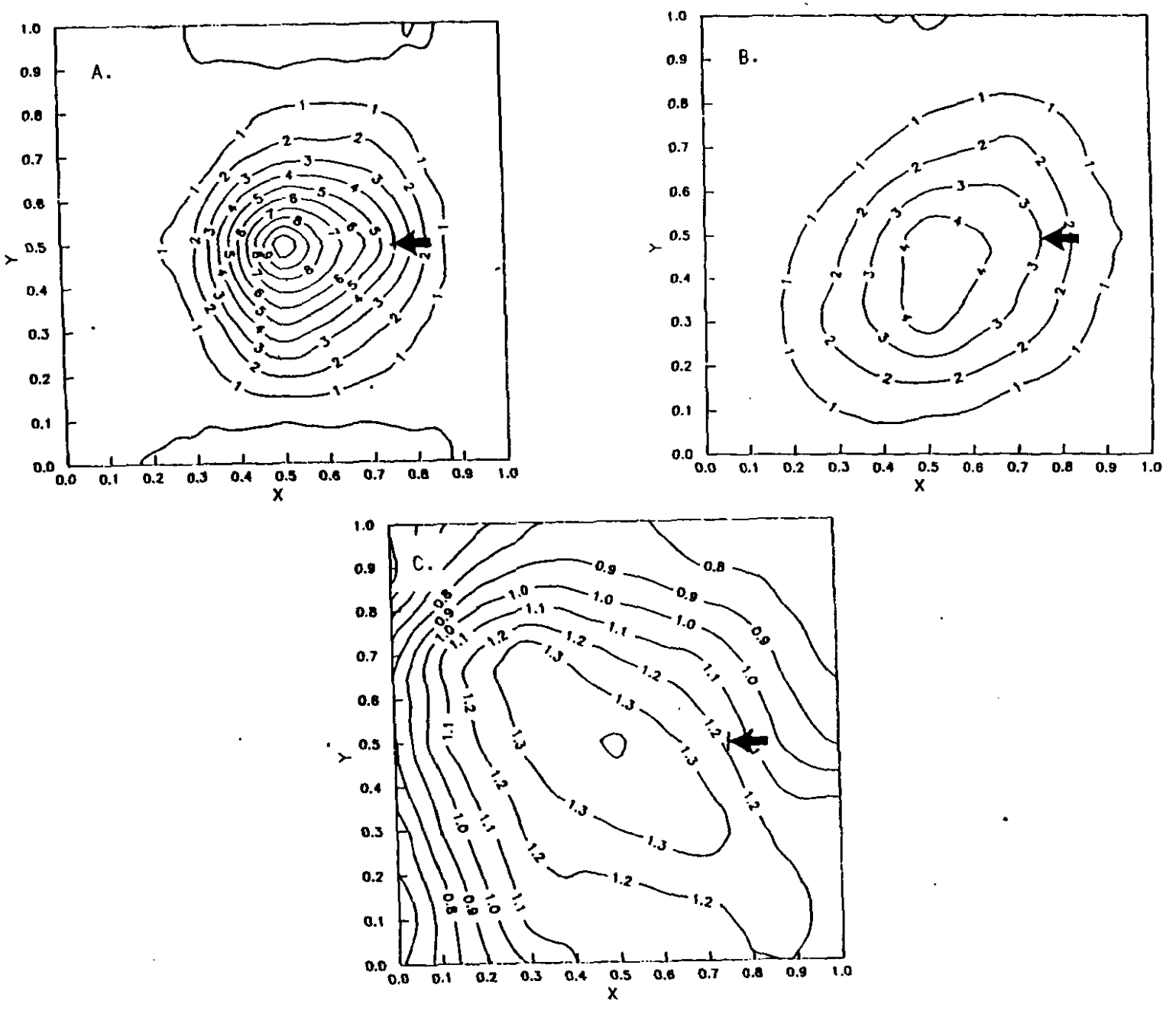

FIGURE 65. EFFECT OF LIMESTONE INJECTION HEIGHT ON INJECTION PERFORMANCE. INJECTIONS WERE AT 2" DEPTH, FROM THE LEFT FACE WITH A). Z/LMIN = 0.6, B). Z/LMIN = 0.3, AND C). Z/LMIN = 0.6 BUT WITH CO_2 MEASUREMENTS MADE AT Z/LMIN = 2.7. TEST S[illegible] ARE TIME [illegible] L[illegible] 8, [illegible]

injection point at the 2" injector depth, from the left side, but at a lower height of Z/Lmin of 0.3. For this case, the limestone was found to be still centrally located at the SRS exit, but with improved mixing.

Figure 65C shows the injection point at the same location as Figure 65A, but with the measurement point downstream of the SRS exit at a Z/Lmin of 2.7. This case was run to give a hint as to what may happen to the limestone in the furnace. The limestone was found to be still centrally located with a slight bias toward the left side, along the back wall. The mixed state of the limestone was near completion.

6.5.2.4 Effect of Injector Momentum Flux

Figure 66 shows the effect of increased momentum flux ratio on limestone injection performance. The momentum flux ratio, R^2, is the ratio of the momentum flux of the limestone flow to that of the SRS flow.

Figure 66A shows the plot for injection as before from the back wall, with a nominal momentum flux ratio of 5.8. Figure 66B shows the case with the same injection location as before, but with an increased momentum flux ratio of 22.1. For this case, the momentum flux ratio was increased by increasing the mass flow of the limestone simulated flow. Significant limestone penetration was observed with the limestone simulated flow near the center of the SRS flow. A slight bias was observed toward the right side. Mixing was slightly improved over the 2" injector depth case.

Figure 66C and Figure 66D show the plots for injection from the left face, and from the right face, respectively, for the higher momentum flux ratio of 22.1. The limestone simulated flow again appears to be centrally located in the SRS flow, with slightly more penetration for injection from the right face.

Figure 67B shows the case of injection from the left face, with an increased momentum flux ratio of 39.7. In this case, the momentum flux ratio was increased by decreasing the diameter of the injector from 0.375 inches to 0.21 inches (3.75 to 2.1 inches full scale) and keeping the mass flow through the injector the same. For this case, the limestone simulated flow was found to be centrally located in the SRS flow as before.

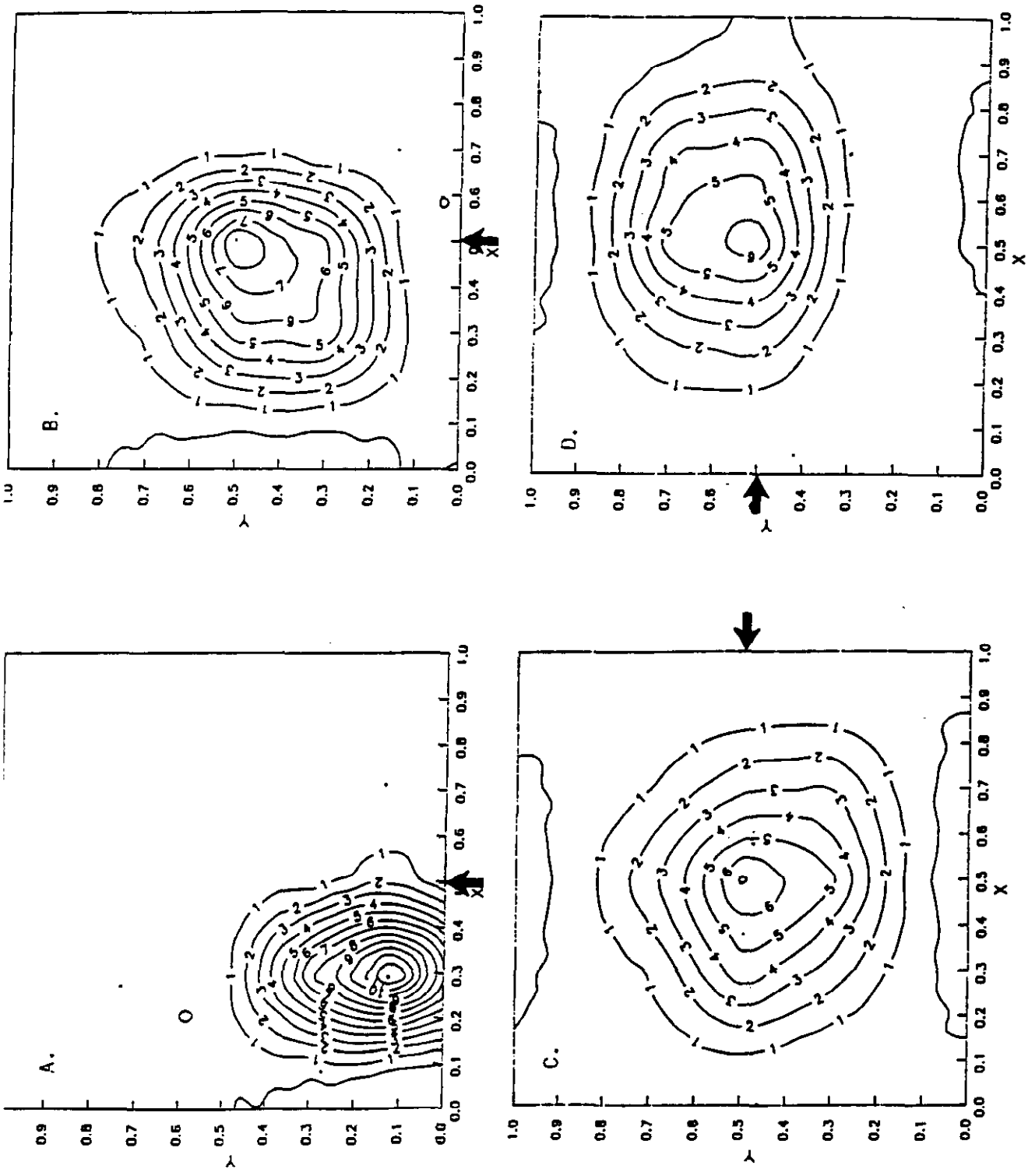

FIGURE 66. EFFECT OF LIMESTONE INJECTION MOMENTUM FLUX RATIO, R^2, ON INJECTION PERFORMANCE. INJECTIONS WERE AT Z/LMIN = 0.6, AND A). THE BACK WALL WITH R^2 = 5.8, B). AT THE BACK WALL WITH R^2 = 22.1, C). AT THE LEFT WALL WITH R^2 = 22.1, AND D). AT THE RIGHT WALL WITH R^2 = 22.1. TESTS SHOWN ARE LIME 1, LIME 10-12.

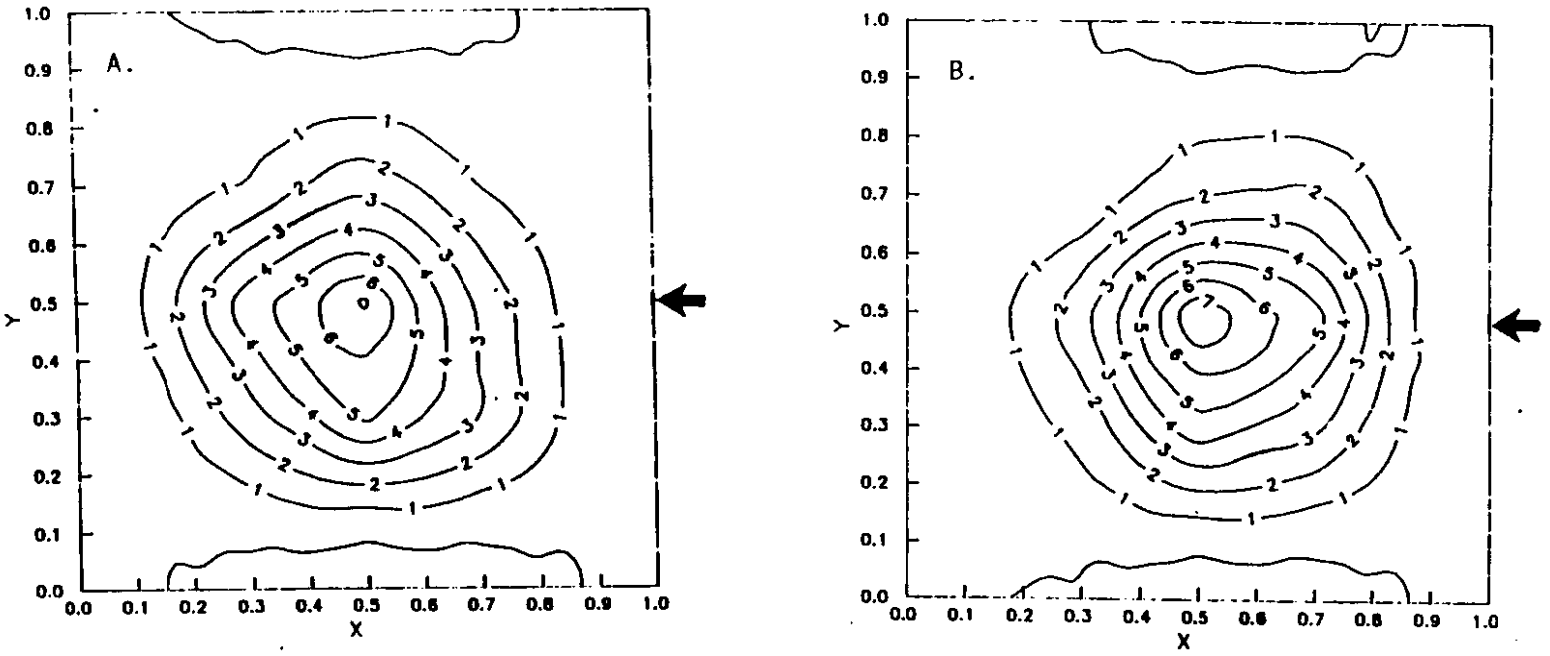

FIGURE 67. LIMESTONE INJECTION AT ELEVATED MOMENTUM FLUX RATIO. A). MOMENTUM FLUX INCREASED BY INCREASING MASS FLOW, AND B). MOMENTUM FLUX INCREASED BY DECREASING INJECTOR DIAMETER. TESTS SHOWN ARE LIME 11 AND 13.

7.0 DISCUSSION OF RESULTS

The purpose of this section is to examine some of the key results of the cold flow model testing in more detail and to discuss the implications of the cold flow results on Healy combustor design and operation.

7.1 Analysis of Asymmetric Mixing Patterns Observed With Cleveland Secondary Mix Bustle

The baseline mixing patterns for the Cleveland secondary air mix bustle are shown in Figure 12. For the swirl case, note that the center, upper right, and lower left regions are nearly isothermal, while the upper left and lower right corners have much higher temperatures. This implies that a large fraction of the colder, secondary air enters the mix bustle through the upper right and lower left corners, with a much lower fraction entering in the upper left and lower right corners.

The reason for this nonuniform distribution of secondary air can be seen from the schematic shown in Figure 68. As the secondary air enters the outer windbox, it begins to flow around the mix bustle on both sides. However, due to the orientation of the primary swirling flow, more of the secondary air should enter in the upper right corner since the swirl is moving away from the top wall and serves to aspirate the secondary air in this region. On the other hand, the swirling flow is moving towards the upper left corner, which tends to discourage secondary air entry in this region. The same argument holds for the bottom of the mix bustle, except that more secondary air should enter the lower left corner as the swirl is moving away from the bottom wall. Once the secondary flow enters the mix bustle, it appears to readily mix with the primary flow due to the strong swirling action. One of the reasons that the upper left and lower right corners remain relatively unmixed is that as the flow transitions from a circular to rectangular cross-section, the swirl primarily stays in the center of the duct while axial flow is observed near the side walls. This result can be seen in Figure 14, where one can observe that the general mixing patterns do not change significantly as the flow progresses down the rectangular duct.

It is important to note that during the Healy coal tests conducted at Cleveland, there were no signs of fouling in the precombustor upstream of the air inlet dampers. Thus, even with the marginal mixing performance inferred from cold flow modeling, the level of mixing was still high enough to prevent the persistence of relatively cold layers which can promote fouling.

7.2 Comparison of Cleveland and Healy Mixing Performance

The baseline Cleveland and Healy mixing patterns just downstream of the circular-to-rectangular transition section (X/L=0.05) are shown in Figure 69. As mentioned previously, the Healy configuration results in significantly better secondary mixing than the baseline Cleveland configuration. The primary air swirl and the secondary air momentum ratios were similar in each case. The main advantage of the Healy configuration is believed to be due to the introduction of secondary air at the inlet of the circular-to-round transition section, rather than all along the length of this transition section as is the case for the Cleveland configuration. More of the secondary air is thus exposed to the swirling primary flow for a longer length prior to entering the slagging stage

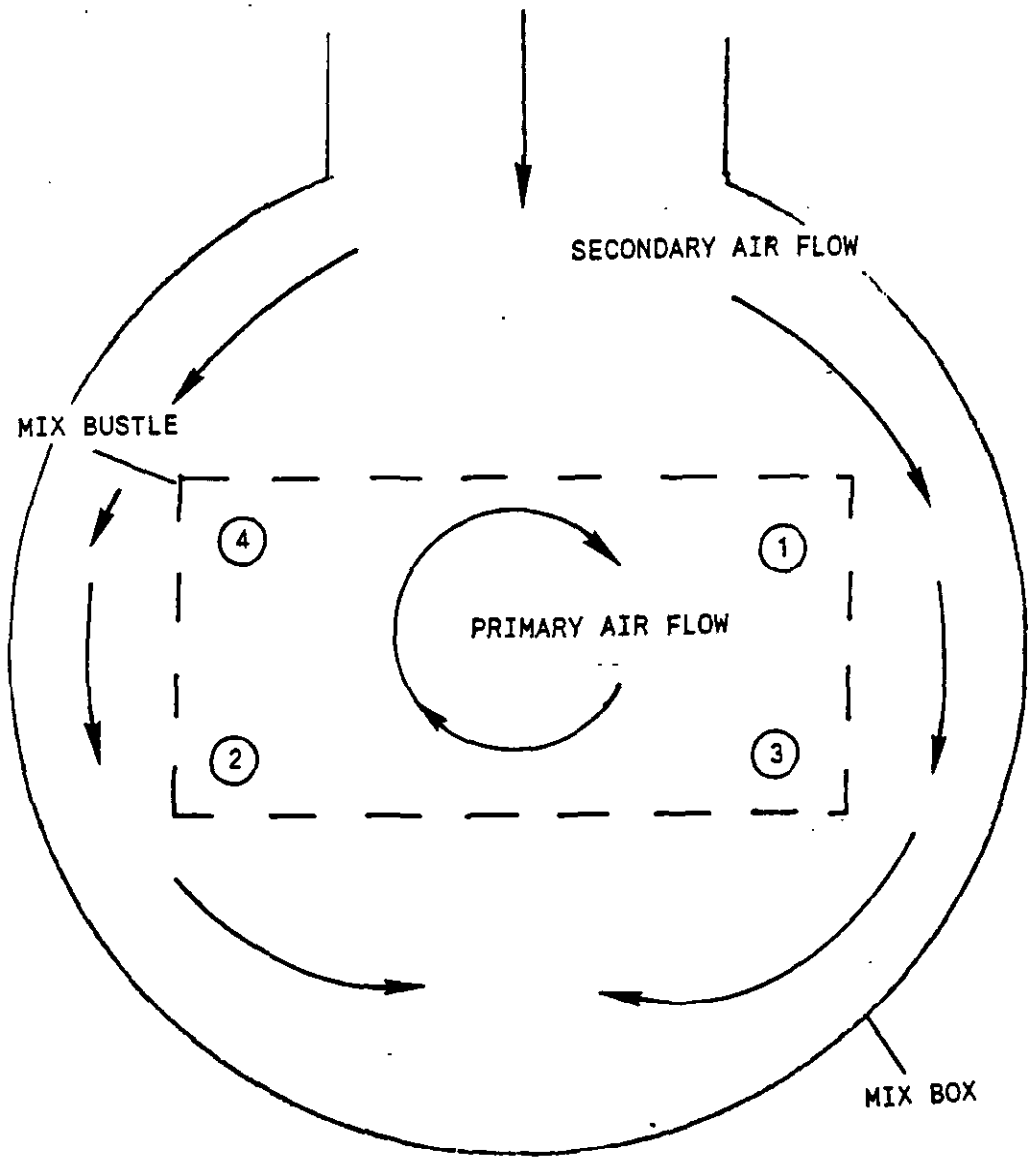

FIGURE 68. PREFERENTIAL LOCATIONS FOR SECONDARY AIR ENTRY

CLEVELAND CONFIGURATION

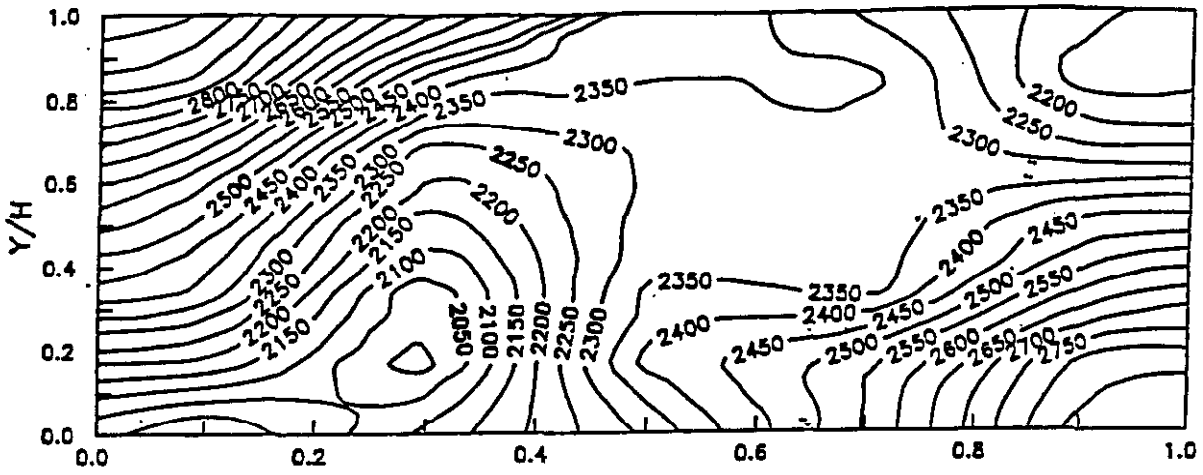

HEALY CONFIGURATION

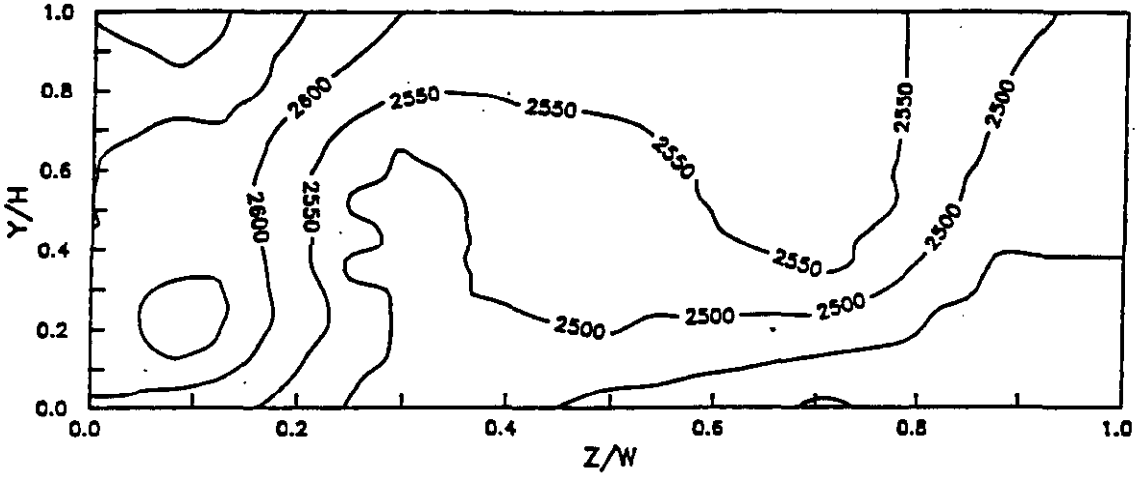

FIGURE 69. COMPARISON OF TEMPERATURE PROFILE AT PRECOMBUSTOR EXIT FOR CLEVELAND AND HEALY CONFIGURATIONS (CLEVE 8, HEALY 18, 9)

air inlet section.
the primary flow a
secondary air is e
improved mixing pe
connection duct l
footprint region
convection heat fl

7.3 Flow Distribut

The flow distri
sensitive to the
located on the sic

In the in-board configuration, the even clocking case appears to provide improved mixing relative to the odd clocking case. This is because in the odd clocking configuration, the 9:00 injector almost lies in the vortex, which causes a significant amount of the injector flow to be drawn in. In fact more flow gets entrained into the vortex when the flow originates from the 9:00 injector versus at the center of the headend as seen in Figure 70.

A test was run to see whether or not turning the in-board, 9:00 injector off improves performance. The results are shown in Figure 71. The result indicates that centerline mixing is improved. Furthermore, with the 9:00 injector off, the centerline mixing is very similar to the even clocking case with all the injectors on.

A test was also run to see whether or not moving the in-board, 9:00 injector to the out-board position improves performance. The centerline mixing result is also shown in Figure 71. The result indicates that only slight improvement in centerline mixing is obtained.

Based on the above results, odd injector clocking will allow added flexibility during combustor checkout with the least amount of impact on the other injectors. If problems with the 9:00 in-board injector are identified (i.e. fouling, reduced slag recovery), the injector can either be shut off completely or relocated to the out-board position. With even clocking, two injectors (8:00 and 10:00) would have to be either shut off or relocated, which will have a larger impact on the remaining four injectors.

7.6 Flow Distribution at Combustor Exit

The flow distribution observed at the combustor exit for the baseline case is characteristic of higher velocity along the back plate with a slight bias toward the right side, and lower velocity at the front, left corner. This flow distribution was observed not to change significantly with the change in exhaust angle or the addition of a jet trap. To help understand this flow distribution, the cold flow model was operated under zero swirl conditions. This was done to separate the effects of swirl from those related to the 90 degree turn just downstream of the baffle.

Figure 72 and 73 show surface contour plots and topographical plots, respectively, for velocity distributions at the combustor exit for the zero swirl and nominal swirl cases. The zero swirl case shows relatively high velocity at the back plate with a bias toward the corners, and low velocity at the front. This flow pattern is consistent with that observed for flow through a 90° elbow, in which the flow velocity is highest along the outside radius of the turn. In this case, the flow is also preferentially directed towards to the outside corners due to impact with the flat back plate.

The zero swirl case helps explain why the flow is high along the back plate for the baseline case. With a clockwise swirl (looking downstream for a left handed combustor) as shown in Figure 74, the flow also has a tendency to move in the direction of the right side. This explains why the flow moves in the direction of the back, right side for the baseline case. Furthermore, since the flow is moving toward the back, right side, this also explains why the flow is low toward the front, left side.

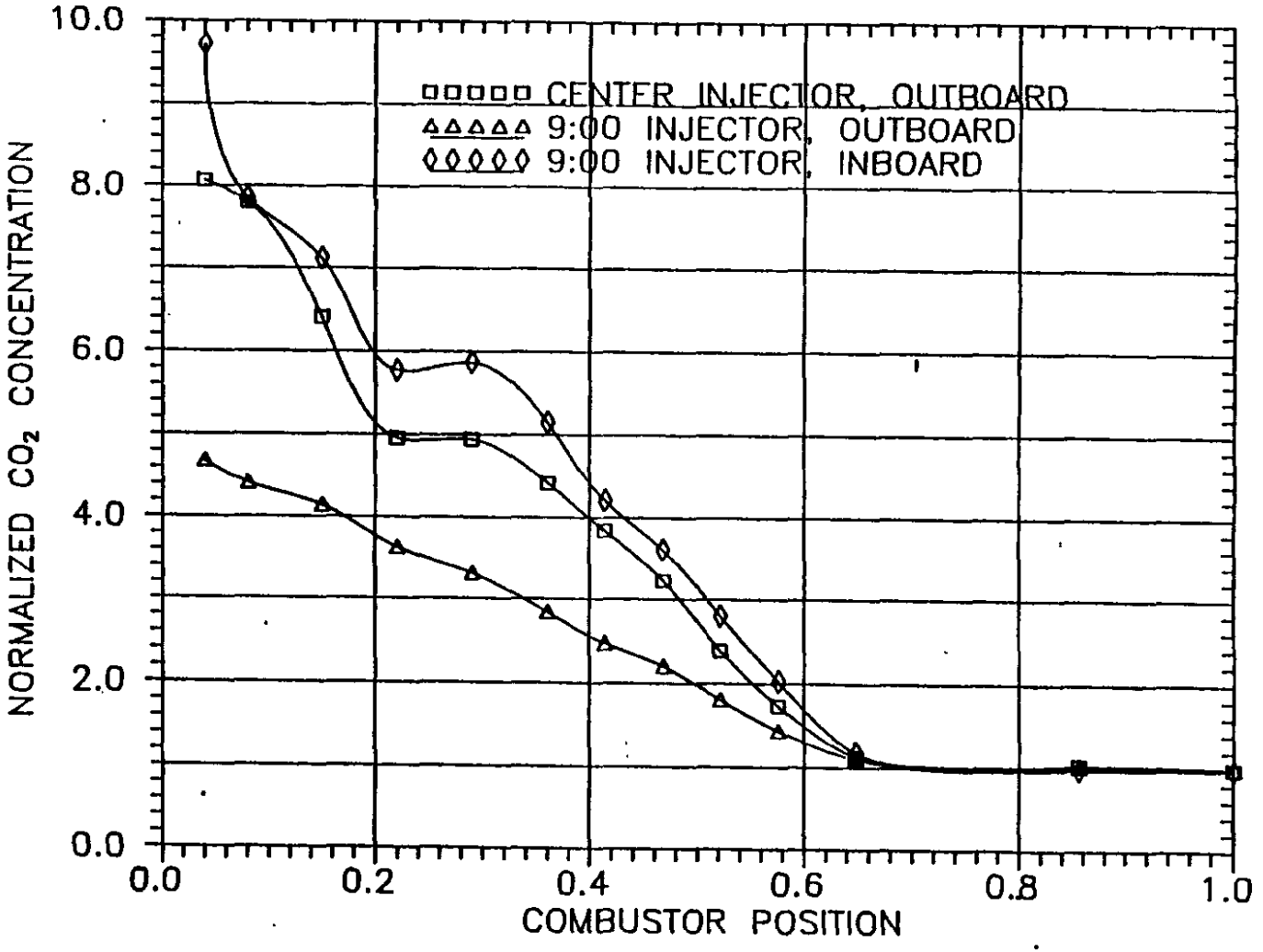

FIGURE 70. MIXING CHARACTERIZATION TESTS FOR INJECTION AT THE CENTER OF THE HEAD ENDPLATE VERSUS AT THE 9:00 LOCATION. CENTERLINE MEASUREMENTS WERE PERFORMED

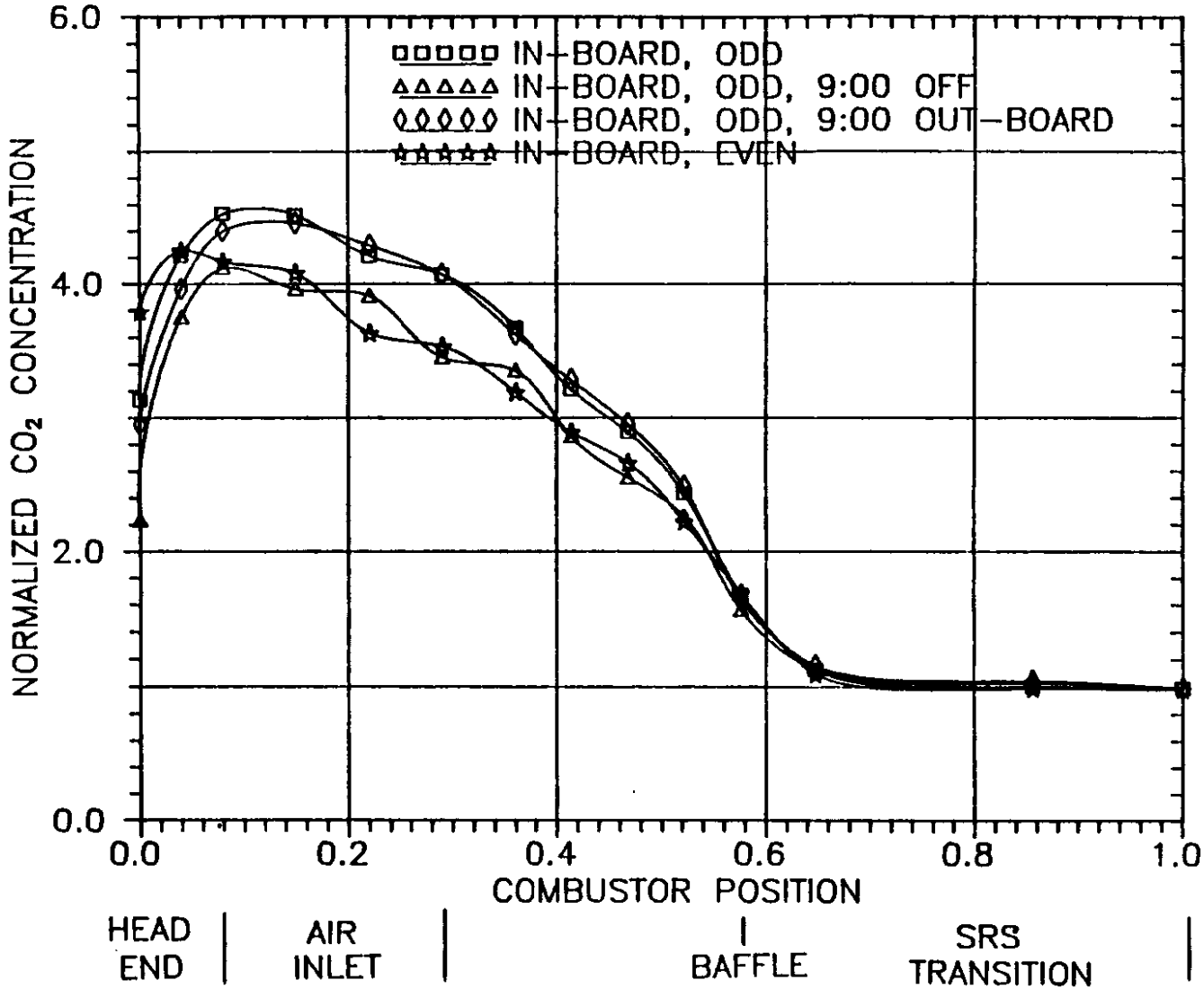

FIGURE 71. MIXING CHARACTERIZATION FOR IN-BOARD INJECTORS, ODD CLOCKING WITH THE 9 O'CLOCK INJECTOR ON, OFF, AND OUT-BOARD. CENTERLINE MEASUREMENTS WERE PERFORMED DOWN COMBUSTOR LENGTH. TEST CASES SHOWN ARE MCI21, 36, AND 37.

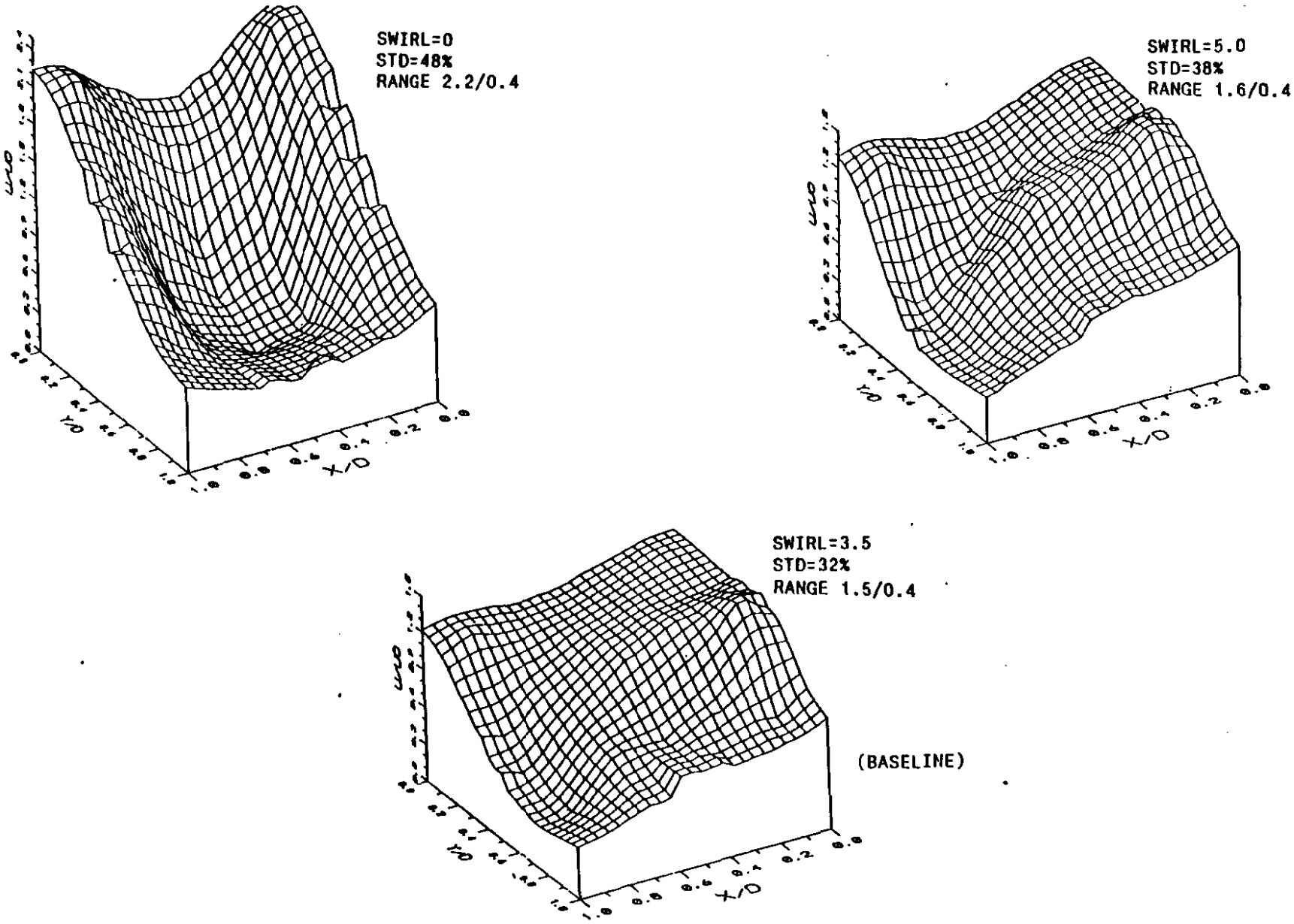

FIGURE 72. EFFECT OF COMBUSTOR CHAMBER SWIRL ON VELOCITY DISTRIBUTION AT COMBUSTOR EXIT. TEST PARAMETERS ARE Z/LMIN = 1.0, FLAT PLATE OR NO JET TRAP, AND A SLANTED EXIT. TEST CASES SHOWN ARE SRS 10, 1, 11. SURFACE CONTOURS SHOWN.

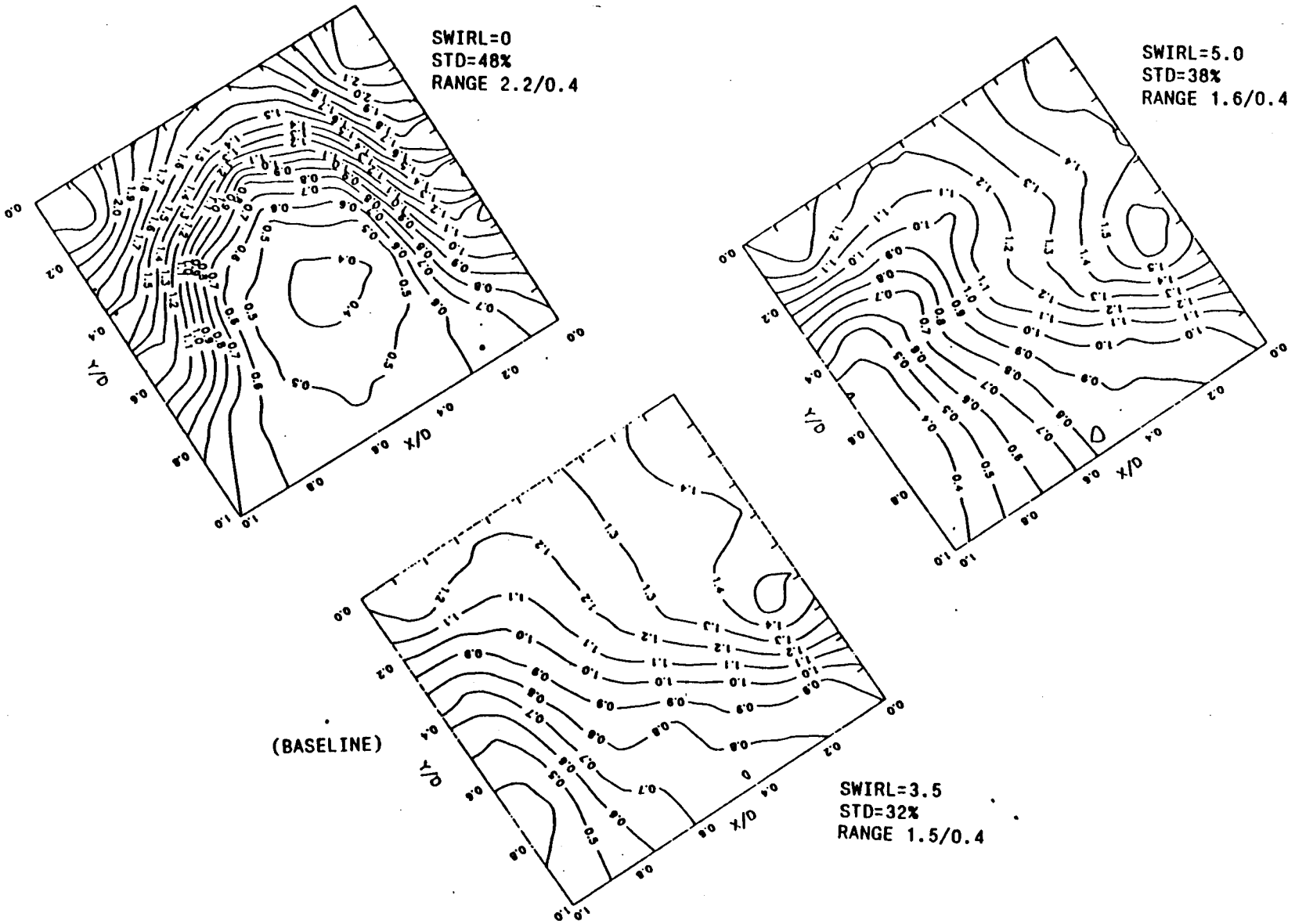

FIGURE 73. EFFECT OF COMBUSTOR CHAMBER SWIRL ON VELOCITY DISTRIBUTION AT COMBUSTOR EXIT. TEST PARAMETERS ARE Z/LMIN = 1.0, FLAT PLATE OR NO JET TRAP, AND A SLANTED EXIT. TEST CASES SHOWN ARE SRS 10, 1, 11. TOPOGRAPHICAL PLOTS SHOWN.

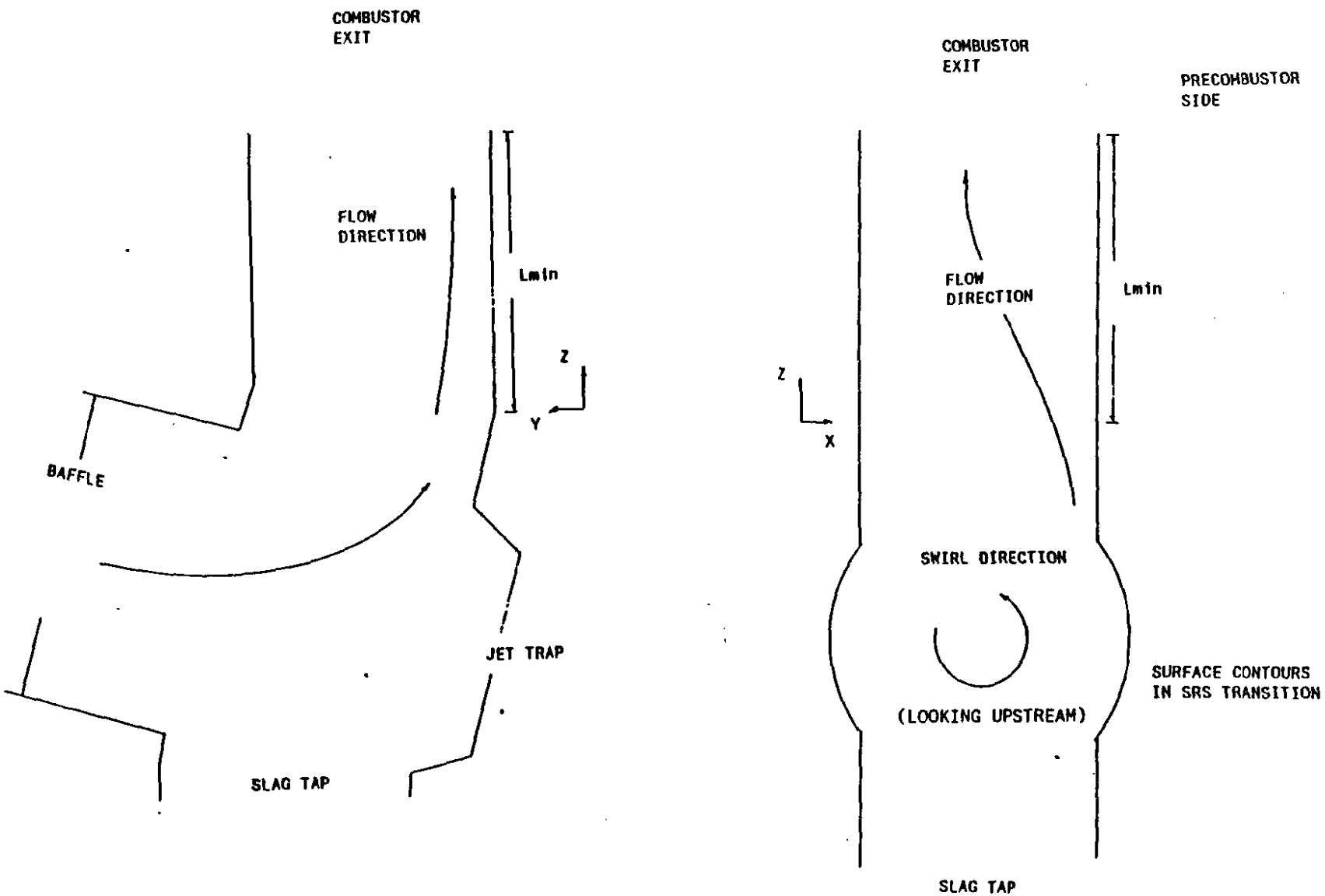

FIGURE 74. FLOW VISUALIZATION IN SRS COLD FLOW TESTS.

Figures 72 and 73 also show a case at elevated swirl conditions. This case represents swirl conditions similar to that of hot flow conditions under combustor turndown operation. The flow distribution at the combustor exit for the elevated swirl case is similar to that of the nominal swirl case. The non-uniformity, however, is slightly larger for the high swirl case (38% standard deviation) over the baseline (32%).

7.7 Limestone Injection in the Slagging Recovery Section

The preferred location for the limestone is in the center of the slag recovery section flow, away from the combustor walls. This is to prevent loss of limestone due to deposition on the combustor walls.

Limestone injector configurations tested which were observed to center the limestone in the SRS flow are given in Table 8. Of these configurations, #3 is the preferred configuration for two reasons. First, cooling requirements for the injector are not severe since injection at the wall minimizes contact with the hot combustion gases. Second, the momentum flux of the limestone is increased without having to deviate from the required flowrates (at the expense of increased delta ρ). This is accomplished instead by decreasing the injector diameter.

TABLE 8. PREFERRED LIMESTONE INJECTOR CONFIGURATIONS

Test Parameters	Configurations		
	#1	#2	#3
Injector Depth, inches	2"	At wall	At wall
Injection Face*	Any	b, l, r	l
Z/Lmin	0.6	0.6	0.6
Momentum Flux Ration, R^2	5.8	22.1	39.7
Injector Diameter, inches	0.375	0.375	0.21

* l = left face, r = right race, b = back face of SRS

8.0 CONCLUSIONS

1. Based on a comparison between the baseline Cleveland secondary air mixing section and the new Healy configuration, the new arrangement allows for significantly improved mixing between the precombustor burner exhaust and the secondary air for the same level of burner swirl. This improved mixing was achieved by introducing the secondary air at the inlet to the transition section, rather than all along the length of the transition as in the case with the mix bustle.

2. The improved mixing provided by the Healy configuration should serve to reduce the risk of fouling in the air inlet region as higher temperature air will be present near the walls of the air inlet.

3. The key parameter which affects secondary air mixing is the precombustor burner swirl number, or ratio of tangential to axial velocity at the burner exit.

4. Mixing performance was found to be relatively insensitive to the ratio of burner to secondary air flows, which suggests that mixing performance should be preserved at off-nominal precombustor coal splits and combustor loading, provided the level of swirl in the burner is maintained.

5. Mixing patterns at the precombustor exit were found to be dependent on the location of the secondary air inlet, however the overall level of mixing was similar for both the top inlet and side inlet cases.

6. The baseline mill air injection configuration was found to promote excellent mixing between the mill air and the primary and secondary flows.

7. The degree in which the mill air mixes with the primary and secondary flows was found to be relatively insensitive to injection-to-freestream momentum ratio. As in the case of secondary air mixing, the main mixing mechanism is the primary air swirl.

8. Mill air mixing performance was also relatively insensitive to the number of mill air injection ports in the range of 8 to 16, provided the total injection area was held constant. This indicates that it may be possible to reduce the number of mill air ports without significantly affecting precombustor secondary mixing or fouling risk.

9. The location of the vortex in the headend is between the in- board, 9:00 injector and the center of the combustor. The vortex is adjacent to the 9:00 injector.

10. The out-board multiple coal injector configuration yields improved headend mixing results over the in-board configuration. This is because injector flow from the out- board configuration is not as readily drawn into the vortex as the in-board configuration. Complete mixing, however, is still achieved for both cases by the time the flow passes past the baffle.

11. For the out-board configuration, odd and even clocking yield similar headend mixing results. This is because the combined contributions of the 8:00 and 10:00 injectors in the even clocking are similar to the single contribution of the 9:00 injector in the odd clocking.

12. The out-board odd-clocking injector configuration is recommended as the baseline for the Healy combustor. An in-board odd-clocking injector ring should also be included in the Healy design to allow for greater flexibility during combustor check-out.

13. The jet trap was observed to have an insignificant effect on the velocity distribution uniformity at the combustor exit. The velocity distribution at the combustor exit is determined mainly by the 90 degree turn at the SRS transition and the combustor swirl.

14. The angle of exhaust was also observed to have an insignificant effect on the velocity distribution at the combustor exit.

15. Limestone injection at the wall is preferred to minimize cooling requirements. Adequate limestone penetration to the center of the SRS can be achieved, without increasing the limestone carrier flow, by decreasing the injector diameter from 0.375" to 0.21" (3.75" to 2.1" full scale).

Part 3

Direct Coal Feed System
Cold Flow Model Report

Table of Contents: Part 3
Direct Coal Feed System
Cold Flow Modeling Report

1.0 EXECUTIVE SUMMARY

This report describes the cold flow model tests that were conducted in support of the design of a direct coal feed system for the Healy Clean Coal Project.

In conventional pulverized coal-fired boilers, the total output from the mill is directly fired into the furnace using conventional burners. For Healy coals, this mill output has an air-to-coal ratio of approximately 3 at full load. If this were to be fired directly into the TRW coal combustion system, the temperatures in the slagging stage would be low enough to cause slag freezing, since the mill air is at only about 130°F. Therefore, in order to prevent slag freezing, it is necessary to reduce the carrier air per pound of coal fired, that is, reduce the air-to-coal ratio to less than 1. This poses the following unique requirement on the direct coal feed system: Concentrate the mill output such that the combustor receives all (or most) of the coal but only about one-third of the mill air (the balance of the air and any remaining coal is bypassed to the furnace directly) and split this concentrated stream to the precombustor and the slagging combustor.

A direct coal feed system (DCFS) was selected over an indirect storage-type system as it offers advantages in terms of safety, simplicity, and cost. The proposed system features an upstream cylindrical splitter, a pair of cyclones, and individual feed lines which deliver coal separately to the precombustor and slagging stage of the TRW combustor. Both cyclones are operated in a unique blowdown mode to furnish the carrier air required to transport the coal to the combustor. The remaining air and fines from the pulverizing mill are vented through the top of the cyclones and are subsequently injected into the precombustor or furnace NO_x ports.

Due to the unique operation of the proposed system, cold flow tests were required to provide key information to guide system design and operation. Of primary concern were issues related to system pressure budget, blowdown cyclone characteristics and coal splitter design and operation. Results of cold flow tests were then used to help define the design criteria for the full-scale Healy system, as well as a sub-scale coal feed system that will be tested during precombustor tests at TRW's Capistrano Test Site (CTS).

The cold flow test hardware was designed to simulate the key aspects of DCFS operation while maintaining flexibility to investigate alternate concepts if necessary. The model was constructed primary from a transparent material to allow for flow visualization. Key modeling guidelines to ensure a realistic simulation included preserving geometrical similarity, cyclone efficiency, solids-to-gas ratio, and saltation velocity margin. Talcum powder was used to simulate pulverized coal. The model was installed and tested in the existing cold flow laboratory at TRW.

The cold flow test program was divided into 4 phases: twin cyclone characterization, splitter evaluation, eductor evaluation, and transport line/slagging combustor splitter evaluation. This sequencing allowed for cyclone-specific issues to be addressed independently of the type of splitter selected. Once twin cyclone operation was adequately characterized, tests were conducted to evaluate the most promising splitter configurations. Tests focused on splitter geometrical arrangement, splitter accuracy, flow split control range, and sensitivity to inlet coal distribution. Following the splitter evaluation, tests were conducted to evaluate the performance and overall effect of a single eductor system installed in the precombustor leg, in the event that such an eductor may be required at Healy to provide additional pressure boost. Finally, tests were performed to evaluate several different slagging combustor splitter configurations, and to obtain pressure drop data for the splitter and injector feed lines.

Twin Cyclone Characterization Testing

The primary objective of the twin cyclone tests was to characterize twin blowdown cyclone operation in terms of pressure drop, flow stability, powder loading, and blowdown control. Cyclone pressure drop, measured from cyclone inlet to cyclone vent, was found to be independent of blowdown ratio in the range of interest (20-40%).

Both the cyclone and blowdown pressure drops were confirmed to be proportional to the square of the cyclone inlet velocity, for a given cyclone inlet area. In addition, both pressure drops were found to decrease as the cyclone area was reduced, for a constant inlet velocity. This revealed that the cyclone pressure drop was not only dependent on cyclone inlet velocity, but on inlet mass flow as well. This result has implications on the control and measurement of flow split, as is discussed in the splitter evaluation section.

The cyclone and blowdown pressure drops were also found to decrease proportionately when powder was injected into the air stream upstream of the cyclone. This decrease in pressure drop is attributed to an increase in effective wall roughness, which in turn reduces the average tangential velocity in the cyclone and subsequently the overall pressure drop.

Finally, cold flow tests confirmed the initial configuration for CTS testing, in which the twin cyclones are connected at the blowdown end to feed a single precombustor. The baseline U-shaped connection was shown to effectively de-swirl the blowdown flow from the cyclones without powder accumulation.

Splitter Evaluation

The primary objective of the splitter tests was to evaluate the most promising splitter concepts and select a configuration for

CTS testing based on split control range and accuracy, flow stability, and pressure drop considerations. The first, a 360° upstream cylindrical splitter was rejected due to unacceptable powder accumulations in the splitter drum. The second, a 135° upstream cylindrical splitter, was found to effectively minimize solids storage while promoting a continuous flow of powder through the splitter and cyclone components. In addition, splitter pressure drop was found to be small relative to cyclone pressure drop (on the order of 10%).

In general, the flow of powder and air through the splitter and cyclone hardware was observed to be very stable, with little or no solids storage in the system. The nominal flow split was found to be slightly dependent on the powder distribution upstream at the inlet, however for a given powder injection method, the powder split was very repeatable, with a relative standard deviation of 1.3%. Another promising aspect of the system was the tendency of the splitter and cyclone to dampen, to some extent, inlet powder flow fluctuations, apparently as a result of recirculation zones that exist in the splitter and upper region of the cyclones. This indeed is an encouraging result, since the combustor operates best when a continuous, steady coal stream is supplied from the coal feed system.

The powder split was found to be primarily controlled by the positioning of the cyclone inlet dampers. As one damper is closed down, the air and powder flow to that cyclone decreases, with a corresponding increase of air and powder to the other cyclone. The change in flow split lags the change in cyclone inlet area, due to the coupled nature of the two cyclones and the fact that the cyclone pressure drop depends on both inlet velocity and inlet mass flow. This, however, does not prevent the splitter from operating reliably over the required flow split range (± 15%), which was demonstrated during cold flow tests. Tests also confirmed that the powder splits in the same proportion as the air (no phase segregation), as a result of the long entrance region upstream of the splitter. This simplifies flow split measurement.

Tests also demonstrated that the position of the splitter plate (within the splitter drum) plays only a secondary role on flow split for splitter plate positions between 40 and 60%. As a result, most tests were conducted with the splitter plate in its nominal 50/50 position.

During the splitter evaluation, several important features of the DCFS were verified. First, the overall cyclone blowdown, or total carrier air, was found to be independent of the air and powder split to the two cyclones. This verified the baseline control approach in which the cyclone vent dampers control the total carrier flow to the combustor, while the cyclone inlet dampers control the air and powder split to the precombustor and slagging stage.

Second, the pressures at the bottom of each cyclone were found to be equal over the expected range of flow split. Since total carrier air also remains constant, this suggests that the individual carrier flows will automatically adjust with coal flow split in order to maintain this pressure balance.

Third, total cyclone efficiency was found to remain effectively constant over the full range of the flow split. This verified that the position of the inlet damper does not adversely affect cyclone efficiency.

Finally, a method was developed for determining coal split indirectly through measurement of cyclone pressure drop and inlet damper position. Very good agreement was found between this method and post-test powder splits. Preferably, calibration of cyclone pressure drop in the field should be performed at the nominal solids-to-gas ratio, however, if this is not feasible, then cold flow data can be used to correct calibration curves obtained during air-only checkout.

Eductor Evaluation

The primary objective of the eductor tests was to characterize eductor operation in terms of flow requirements, coal/gas outflow uniformity, and impact of other DCFS components. In general, good agreement was found between measured and calculated eductor performance for tests with and without powder flow. The flow through the eductor was observed to be steady at the nominal eductor conditions. A slight swirl pattern was observed both upstream and downstream of the eductor (left over from the cyclones), however, the presence of swirl does not appear to significantly affect eductor performance. Finally, the presence of the eductor in the system did not appear to adversely affect the operation of either the splitter or the cyclones.

Slagging Combustor Splitter and Transport Line Evaluation

The primary objective of the slagging combustor splitter tests was to help select a configuration for the Healy DCFS that could reliably and stably split the slagging combustor coal flow into six individual stream feeding the six coal injectors located at the head end of the combustor. This test phase was particularly important since the slagging stage coal feed line and splitter will not be verified with hot-fired tests at CTS prior to installation at Healy.

The most successful splitter tested was a cone-like splitter located in a vertical line section just upstream of the combustor. A similar splitter was successfully operated during Healy tests at TRW's Cleveland facility. The splitter pressure drop was determined to be within the allowable pressure budget for the Healy DCFS.

A unique "cobra" splitter, similar in concept to the main DCFS

splitter, was also evaluated. This splitter was found to be susceptible to solids accumulation in the horizontal transition section just upstream of the splitter. Several different modifications were attempted to eliminate this problem, however some temporary accumulation remained. As a result, this splitter type was removed from consideration.

In conclusion, the cold flow tests described herein verified the feasibility of the proposed direct coal feed system. Flow through the system was found to be inherently stable, with continuous movement of both air and powder. The cyclone inlet flow dampers were found to be an effective and reliable means of controlling the split over the required range. The total coal carrier flow can be controlled independently by the cyclone exhaust damper. The overall pressure drop appears to be within allowable limits. Finally, design verification tests at CTS have now verified the overall design and operation of the direct coal feed system.

2.0 INTRODUCTION

2.1 Background

Starting in September 1991 under the Phase I Healy Clean Coal Project, TRW had been proceeding with the design of an indirect pulverized coal feed system which would supply a steady, metered flow of coal to the TRW slagging combustor. TRW's on-going efforts to design an indirect coal feed system for application on Healy were suspended by AIDEA on January 21, 1992 due to concerns pertaining to the safety of coal storage systems for high volatile sub-bituminous coals. TRW's experience when firing slagging combustors had been with indirect coal feed systems which depend on the temporary storage of coal. Non-storage systems, and direct systems in particular, tend to be safer and less complicated and consequently, AIDEA directed TRW to perform an evaluation of such systems for application to the Healy Project. As an alternative to indirect coal feed systems, TRW submitted a proposal on February 17, 1992 for a direct coal feed system design concept. The proposed system featured a pair of counter-rotating flow twin cyclones, a single fire valve, and a variable splitter as. The logic that led to the proposal of this direct CFS design approach is outlined in Figure 2-1.

The proposed system depends on the pressurization of the mill or the coal-laden air leaving the mill to yield a favorable pressure gradient. TRW predicted that 60 inches W.G. would be required. As illustrated in Figure 2-2, the proposed direct coal feed system would control blowdown and coal split. Coal flow rate control to the combustor, which in the indirect system had been controlled by the CFS mass weigh feeder, would now be regulated by the stock feeder upstream of the pulverizer.

Both cyclones are operated in a unique blowdown mode to furnish the carrier air required to transport the coal to the combustor. Approximately 25 to 30% of the inlet mill air from the pulverizer is required for this purpose. This configuration complies with slagging combustor restrictions for maximum carrier air flow rate.

Blowdown is controlled by a damper in the cyclone common vent stream positioned to provide back pressures to promote air flow through both cyclone blowdown "coal discharge" ports. A common vent pipe and single blowdown damper ensures that the cyclones will be maintained at about the same pressure over the specified load range. TRW believed this would enable the whole process to function predictably. Vent air containing coal fines exiting the blowdown damper is transferred to either the precombustor mill air ports or to the boiler furnace NO_x ports.

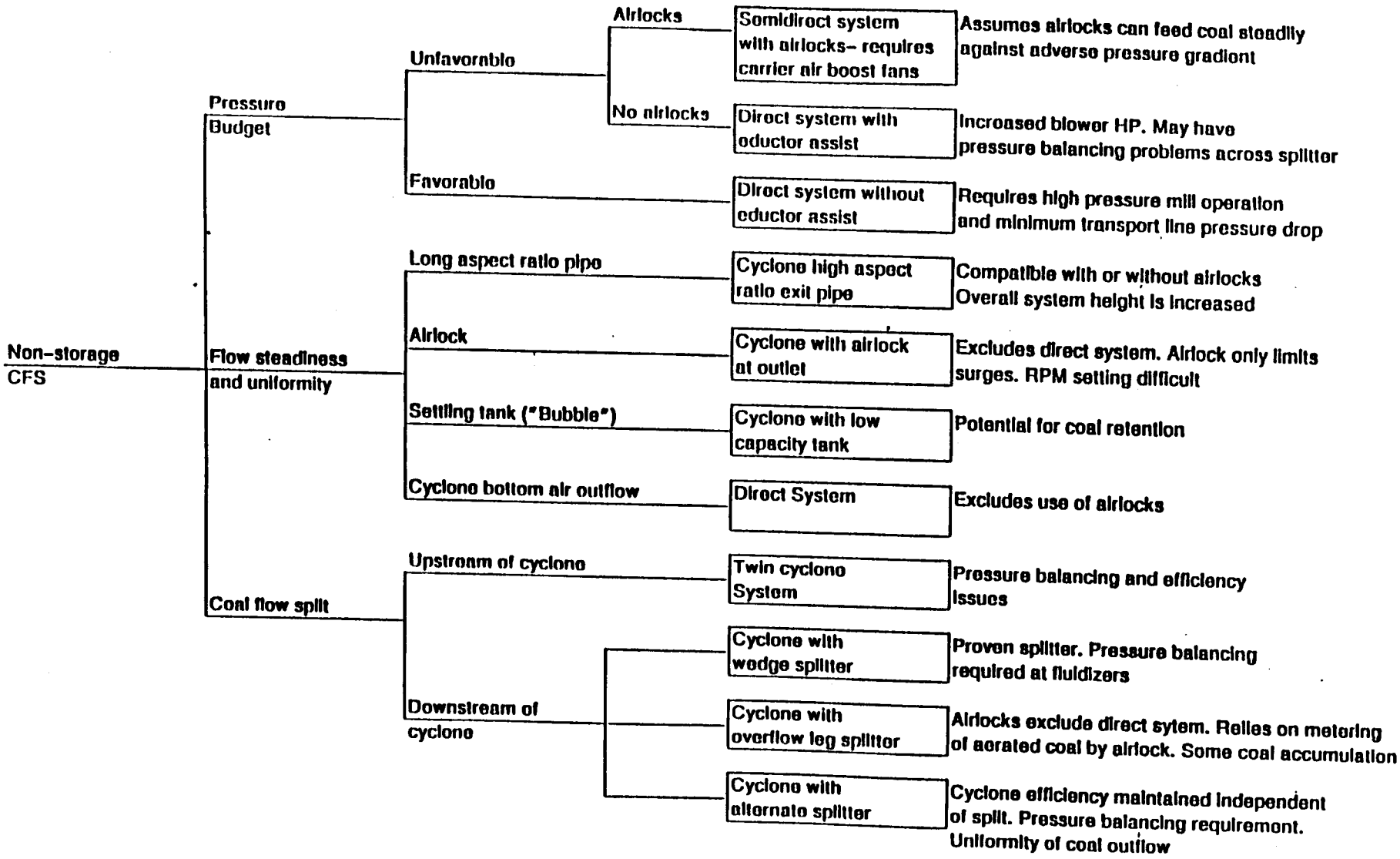

Figure 2-1 Direct CFS Design Factors and Trade-Offs

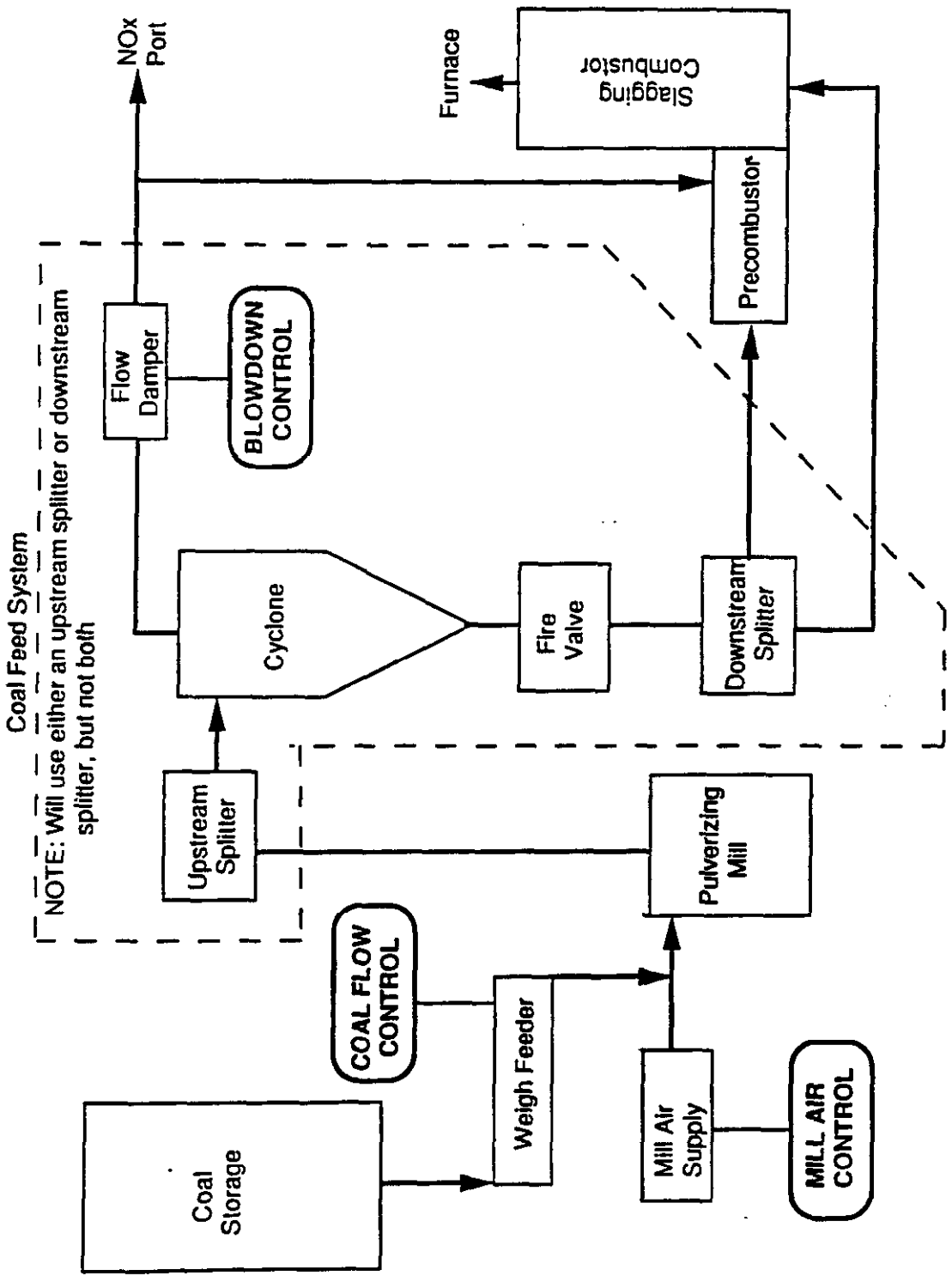

Figure 2-2 Direct Coal Feed System

A variable flow split between the precombustor and slagging combustor was proposed utilizing an "in-line" isokinetic splitter located downstream of the cyclones in the vertical flow leg, to minimize pressure drop. This splitter relied on a common cyclone discharge configuration to provide a non-swirling, uniform flow across the cross-section without hindering the cyclone vortex motion.

2.2. Concept Evaluation

In addition to the proposed downstream isokinetic splitter, other concepts utilizing the proposed direct coal feed system with blowdown cyclone operation were hypothesized after receipt of notice to proceed. The three primary alternative concepts investigated included:

1. Downstream proportioner splitter
2. Upstream splash plate splitter
3. Upstream "cylindrical" splitter

The splitters can be categorized into two basic configurations relative to the cyclones: upstream splitters or downstream splitter, as illustrated in Figure 2-3. The general Capistrano DVT test configuration for the coal feed system was established to accommodate either splitter configuration readily. Attributes of the four splitters are presented in Table 2-1. The upstream splitters were determined to be more attractive concepts because the split occurs in a dilute coal in air stream which results in less pressure drop, a key Healy design constraint.

2.2.1 Downstream Isokinetic Splitter

The isokinetic splitter divides the coal flow as the particles move vertically down the pipe.

To yield a reliable split, the splitter requires a uniform distribution of coal at the inlet. Any significant variations in uniformity could potentially result in coal split errors. The splitter also requires a significant amount of balance air to achieve a reasonable coal split range. Adding large quantities of balance air to obtain a wide split range would result in increased blower and operating costs. Also, the inner assembly leading edge and side walls, and the interior walls of the exterior assembly are subject to erosion. Changes in the cross-sectional area due to erosion would result in split errors since the split is a function of geometry.

The following is a summary of the attributes and deficiencies of the downstream isokinetic splitter concept.

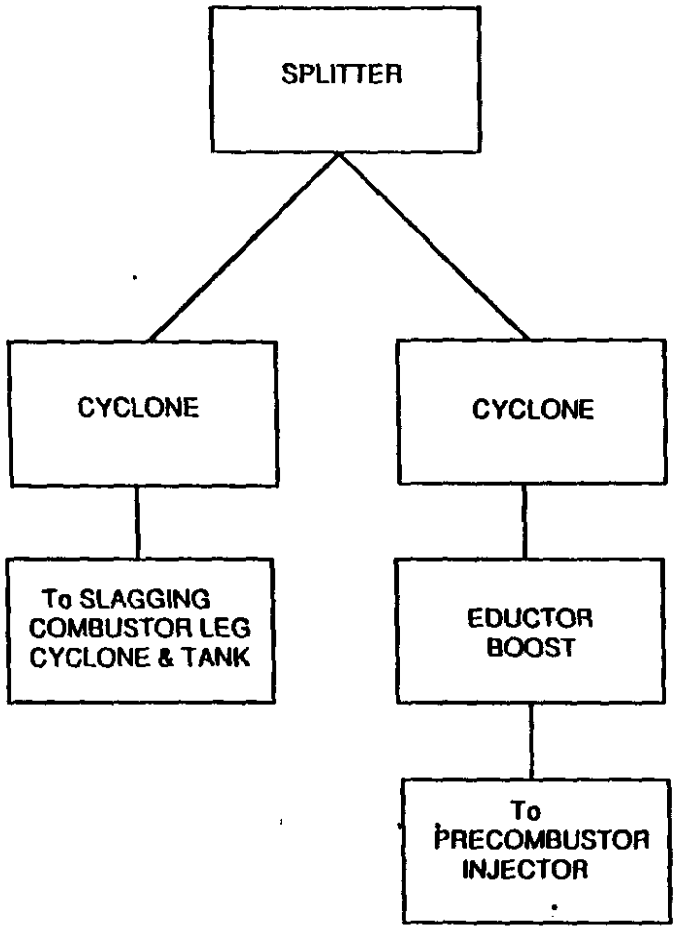

FLOW SPLIT UPSTREAM OF CYCLONE

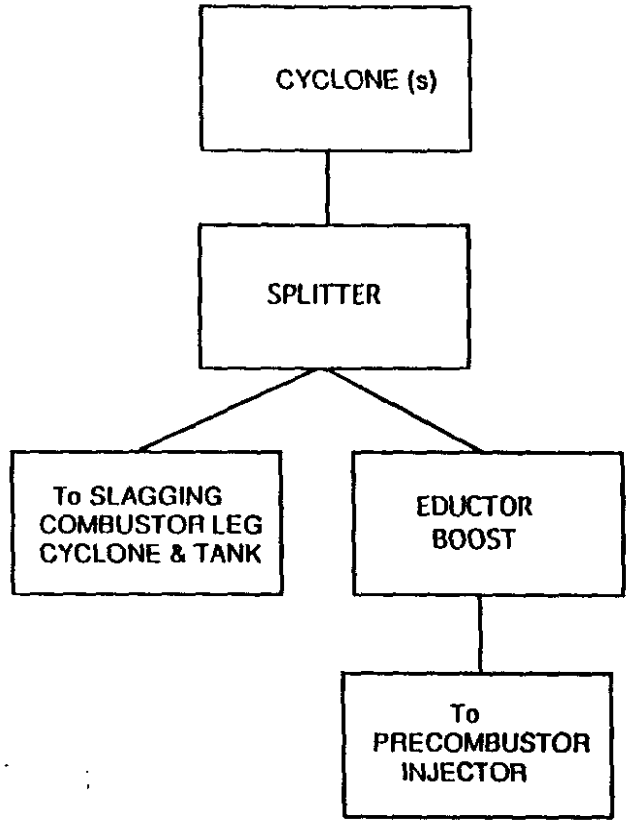

FLOW SPLIT DOWNSTREAM OF CYCLONE

Figure 2-3 Two Basic Direct CFS Configurations

TABLE 2-1. ATTRIBUTES OF SPLITTER CONCEPTS

Splitter Concept	Requires Twin Cyclone	Split By Area Ratio	Compatible w/Precomb. Boost	ΔP	Insensitive to Flow non-uniformity	Insensitive to load & Comb. Swirl Setting	Self Pressure Balancing
Upstream Splash Plate Splitter	Yes	Yes	Yes	Low	?	Yes	Yes
Upstream Cylindrical Splitter	Yes	Yes	Yes	Low	Somewhat	Yes	Yes
Downstream Scoop Splitter	?	Yes	Yes With pres. balance boost limit	Medium	No	Yes	No
Downstream Proportioner Splitter	No	No	Yes But will affect split	High	Yes	No	No

Attributes:

- Provides split to multiple injectors
- Isokinetic split if pressure balanced
- Low pressure drop for a downstream splitter

Deficiencies:

- Limited split range
- Requires pressure balancing which would be difficult to control over a large split
- Wear effects split
- Requires uniform cross-sectional distribution of coal
- Precombustor eductor boost would affect split

2.2.2 Downstream Proportioner Splitter

The downstream proportioner splitter is a commercially available device presently used to obtain 50:50 splits. It has an adjustable diverter shoe to balance the discharge flows. Inlet flow uniformity is not a prerequisite for effective flow splitting due to the inlet conditioning geometry of the splitter. Control of the air stream split is accomplished by adjusting the shoe which acts like an orifice to the air flow. A decrease in discharge area in one leg results in a corresponding increase in discharge area in the other leg. A split other than 50:50 could be obtained by adjusting the shoe to control coal flow rates in each discharge leg, although this would require demonstration tests. To achieve the require range of flow split control, the splitter must have a pressure drop of the same order as the downstream feed lines. Some of the attributes and deficiencies of the downstream proportioner splitter are listed below.

Attributes:

- Wear resistant
- Commercially available hardware
- Less sensitive to coal flow uniformity at inlet
- No pressure balancing required
- Compact design

Deficiencies:

- Limited split range
- High pressure drop necessary to obtain required splits
- May cause coal classification between split streams
- Precombustor eductor boost affects split

2.2.3 Upstream Splash Plate

The upstream splash plate impacts coal on a plate located near the inlet to the cyclones and then re-entrains the coal in the air stream. The air flow rates to each cyclone are controlled by flow

dampers located at the inlets to the cyclones. The premise to successful operation of this concept is that the coal splits in proportion to the air split upon re-entrainment. This splitter may be sensitive to inlet flow nonuniformity and requires inlet flow conditioning. The main concern with this device pertains to whether the coal splits in proportion to the air split since the particles of coal have an established inlet momentum that must be overcome by the shear forces of the air stream. The primary attributes and deficiencies of the upstream splash plate splitter are listed below.

Attributes:

- Wear resistant
- Low pressure drop
- Self pressure balancing
- Simplicity
- Wide split range

Deficiencies:

- Unproven technology
- Relies on coal to split in proportion to air split
- Potential for coal accumulation

2.2.4 Upstream Cylindrical Splitter

Of the two upstream splitter concepts considered, the cylindrical splitter appeared to be the most promising. The cylindrical splitter concept keeps the coal flow moving on the interior housing of the splitter. This minimizes the pressure drop associated with coal re-entrainment into the air stream. The splash plate concept, on the other hand, relies on the pressure drop associated with the stagnation of coal particles and subsequent re-entrainment into the air stream. The cylindrical splitter also provides a convenient means for transitioning from the circular mill duct to the rectangular cyclone inlet ducts without significant flow separation. The cylindrical splitter can also be designed to minimize coal accumulation, whereas the splash plate would inherently have some accumulation of coal. The primary attributes and deficiencies of the upstream cylindrical splitter are given below.

Attributes:

- Low pressure drop, keeps coal moving
- Provides means to transition from circular duct to cyclone rectangular inlets without flow separation or coal accumulation
- Self pressure balancing
- Splitter disc feature improves splitter damper control to ensure more reliable split than splash plate splitter
- Based on commercial experience with similar hardware

- Recommended by experienced CFS engineering firm

Deficiencies:

- None

After a detailed evaluation of all four splitter concepts, TRW selected the cylindrical splitter operating in conjunction with the blowdown cyclones as the baseline configuration for cold flow testing. The downstream isokinetic splitter and the proportioner splitter were considered primary backups to be tested if the results with the upstream cyclindrical splitter were not promising.

3. BASELINE DIRECT COAL FEED SYSTEM DESCRIPTION

The Healy CFS components, from the inlet elbow, which receives coal and primary air from the exhauster fan, to the injector interfaces on the combustor, define the extent of equipment comprising the coal feed system.

The coal feed system splits and transports pulverized coal and primary air received from the exhauster fan, to the TRW two-staged combustor. The first stage, known as the precombustor, nominally receives 30 to 45% of the total pulverized coal feed to the combustor. The rest of the coal is directed into the second stage, known as the slagging combustor. The design requirements pertaining to the Healy CFS are delineated in Table 3-1.

The physical details of the coal feed system are TRW proprietary and are excluded from this report.

3.1 Pressure Budget

The available pulverizer mill system pressure level, above the pressure required at the precombustor and slagging combustor coal injectors, determines the pressure budget available for operation of the coal feed system. CFS pressure drops include the drop in the cyclones required for separation of the mill air, the pulverized coal and carrier air exiting the blowdown port of the cyclone and the vent air with fines exiting the top of the cyclone. The pressure drops of the variable flow splitter, transport lines, and slagging combustor injector splitter are also included. The pressure must be sufficient for the overall system to achieve full load.

Implementing the proposed TRW direct coal feed system, requires that the mill system be pressurized and that coal transport line pressure drops be minimized. Transport line pressure drops are minimized for the Healy design by minimizing the number of bends and line lengths, and selecting appropriate transport pipe diameters that provide a margin above saltation yet minimize pressure drop over the range of loads and splits. Figure 3-1 illustrates the mill pressure required at the inlet to the coal feed system for various loads.

If the available pressure budget is insufficient and a small boost pressure is required, the addition of an eductor in the precombustor leg, which has a higher back pressure, may be incorporated. If the pressure boost requirement is large, the amount of eductor air and subsequent blower power demand will become a issue.

3.2 Cyclone Characteristics

The use of two smaller cyclones as opposed to one larger cyclone offers the advantage of reduced pressure drop for a given

TABLE 3-1. COAL FEED SYSTEM REQUIREMENTS FOR DVT

1.	Coal Feed System Type:	Nonstorage system (contractual)
2.	Nominal Capacity:	49,240 lb/hr coal
3.	Facility "Mill" Air Flow Rate:	122,860 lb/hr air nominal
4.	Carrier Flow Rate:	28,000 lb/hr air total
5.	Carrier Air Temperature:	135°F (150°F max)
6.	Coal Type:	Performance, blend, ROM, waste
7.	Coal Grind:	50 to 70% through 200 mesh
8.	Coal Moisture:	9 to 13%
9.	Coal Feed System Inlet Pressure:	60 inch W.G.
10.	Cyclone Separation Efficiency:	> = 93%
11.	Combustor Interface Pressures:	24 inch W.G. at precombustor 11 inch W.G. at slagging combustor
12.	Coal Flow Split:	30 to 45% (38% nominal)
13.	Coal Flow Accuracy Input:	Input to DCFS must be better than +/- 1.0%
	Output:	Output of DCFS must be better than +/- 2.5%
14.	Standards:	Compliance with NFPA 85F

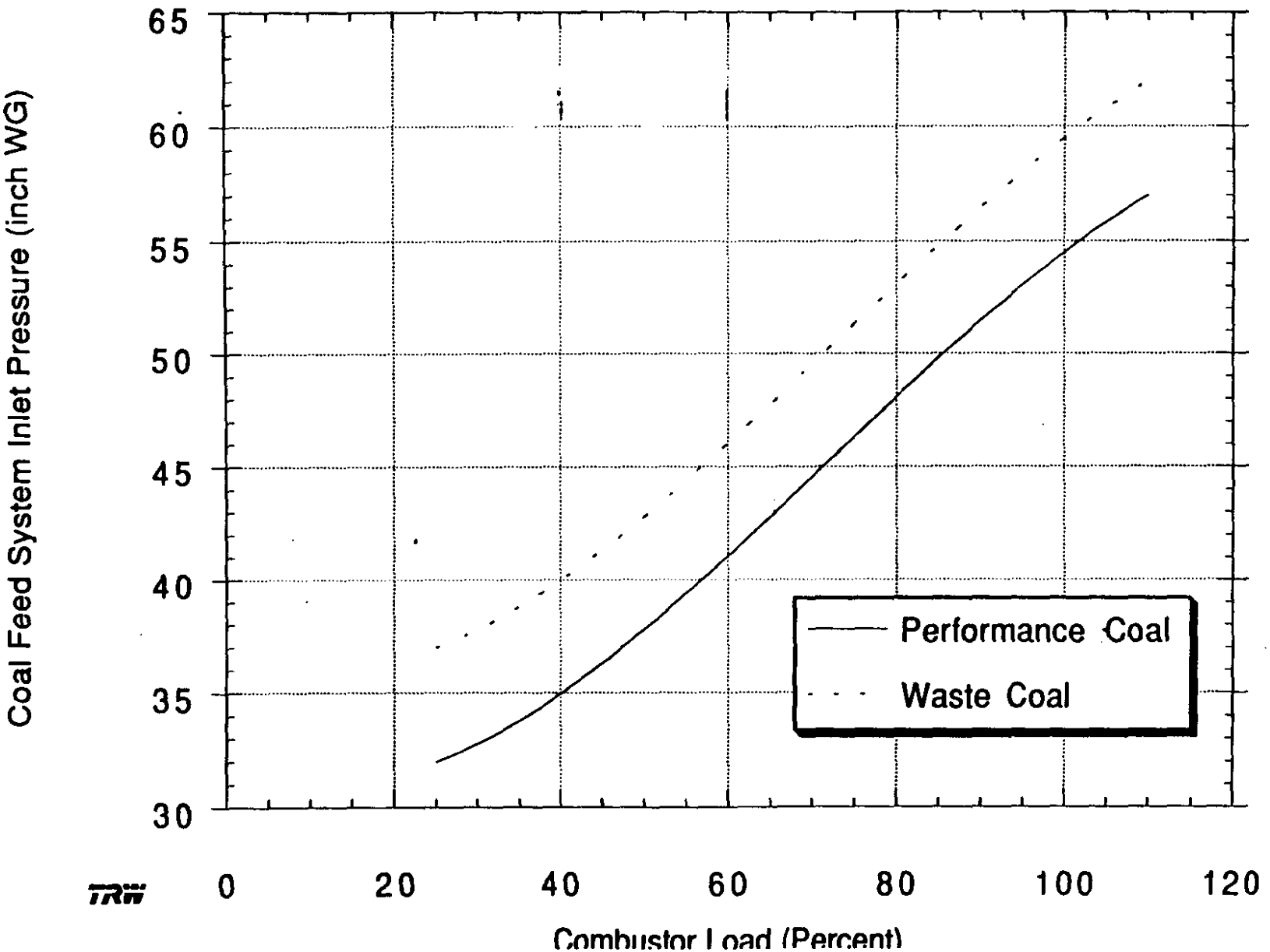

Figure 3-1 CFS Inlet Pressure as Function of Combustor Load

separation efficiency. If the cyclonic flow field within the cyclone is not affected, blowdown should provide increased performance at the same pressure drop due to more effective removal of the smaller particles near the bottom of the cyclone. these fines would normally be entrained with the vent air stream. A configuration employing two cyclones allows application of either an upstream or downstream variable flow splitter configuration, whereas a single cyclone allows only a downstream splitter configuration. The downstream configuration is compatible with a simple flow deswirl design which provides a uniform flow to a downstream splitter, without affecting the strength of the cyclonic vortex.

3.3 Coal Flow Split

The best configuration, upstream or downstream, for obtaining flow split cannot be resolved solely by analytical methods only. An economical approach to obtaining splitter design and performance data is to conduct cold flow tests using a bench scale model. Trying to resolve design issues and implement design modifications in a DVT size coal feed system or Healy coal feed system is not practical. The cold flow test results are used to obtain the required design criteria and performance characteristics to minimize the risk associated with fabricating the DVT and Healy CFS.

4.0 DCFS DESIGN ISSUES

Because the proposed direct coal feed system was a new concept that had never been operated before, there was a need to resolve both analytically and experimentally, technical issues pertaining to the design and operation of this system.

4.1 Blowdown Cyclone Design Issues

Cyclone characterization analyses and cold flow tests were required to resolve the following issues:

1. Pressure drop during blowdown operation as compared to normal cyclone, zero blowdown, operation.

2. Cyclone pressure drop, from inlet to vent and from inlet to blowdown port, variations as a function of blowdown air flow rate.

3. Flow uniformity across the cross-section of the cyclone blowdown port leg.

4. Effect of cyclone blowdown mode operation on flow split, cyclone efficiency.

5. An upstream splitter, blowdown cyclone configuration relies on balanced pressures between the precombustor cyclone and slagging combustor cyclone. Is balanced pressure maintained over all operating conditions?

6. Blowdown control sensitivity.

7. Range limitation of blowdown operation.

4.2 Variable Flow Splitter Design Issues

Variable flow splitter characterization analyses and cold flow tests were required to resolve the following issues:

1. Influence on blowdown cyclone operation.

2. Effect of particle distribution flow uniformity in splitter inlet duct cross section.

3. Range of flow split control.

4. Pressure drop across splitter.

5. Sluggishness of splitter control and method for split control feedback.

6. Influence of inlet flow swirl on splitter.

7. Susceptibility to coal accumulation and wear.

8. Sensitivity to coal to air ratio.

9. Impact on performance if application of eductor boost is required

4.3 Overall CFS Design Issues

Tests incorporating both the cyclones and variable splitter were required to obtain the following information or resolve the following issues:

1. Provide scaling criteria and relationships for DVT and Healy design.

2. Provide data inputs to analytical models.

3. Confirm eductor configuration and pressure boost.

4. Investigate eductor influence on other CFS hardware performance.

5. Ascertain method to achieve slagging combustor and precombustor interface pressures with limited pressure budget and provide data to predict overall pressure drop of CFS.

6. Validate overall Healy design configuration.

5.0 COLD FLOW MODEL TEST APPROACH

The overall approach was to divide the cold flow study into three distinct phases:

(1) Twin Cyclone Characterization Testing
(2) Splitter Evaluation
(3) Eductor Evaluation
(4) Slagging Combustor Splitter and Transport Line Evaluation

This four phase test program allowed for specific cyclone issues like pressure drop, efficiency, blowdown control, particle loading, and flow uniformity to be investigated without complicating the system with the addition of a flow splitter. Once these issues were adequately addressed, tests were conducted to evaluate the most promising splitter arrangements. Then, additional tests were conducted to more fully characterize splitter flow control range, split accuracy, the effect of powder loading, system pressure drop and pressure balancing, and sensitivity to inlet powder distribution. Next, an eductor was installed in one of the coal feed lines to assess eductor performance as well as the impact of the eductor on DCFS operation. Finally, several different slagging combustor splitter configurations were evaluated in terms of flow patterns, split distribution, and pressure drop characteristics.

6.0 MODELING GUIDELINES

A number of modeling guidelines were developed for the Healy DCFS cold flow experiments for the purpose of ensuring that the results of the experiments could be reliably transferred to the design and operation of the CTS design verification tests as well as to the actual Healy system. These modeling guidelines were then used to size the model hardware and to select cold flow test conditions. Each modeling guideline is discussed briefly below:

(1) Preserve geometrical similarity.

Preserving geometrical similarity means that all critical DCFS component dimensions are geometrically scaled by the same factor. This is necessary to preserve the macro flow patterns of the gas and particle trajectories. In order to keep the model at a workable size, internal dimensions of the splitter and blowdown cyclones were scaled down by a factor of 4 from the CTS hardware.

(2) Preserve cyclone efficiency.

The cold flow cyclones were designed to yield cyclone efficiencies comparable to values expected for CTS tests as well as for the Healy system. This was important since one of the major objectives of the test was to determine whether cyclone efficiency varies over the flow split range, or as a function of mill air flow rate. To reasonably address this issue, the cyclone efficiency should be in approximately the same range, i.e 90-98%.

(3) Preserve solids-to-gas ratio.

The solids-to-gas ratio is an important parameter in the feed system as it affects the minimum allowable velocity in the splitter drum-to-cyclone connecting ducts, the cyclone pressure drops, eductor performance and the pressure drops in the feed lines to the combustor.

(4) Preserve ratio of transport velocity to saltation velocity.

The saltation velocity is the minimum velocity in which particles are fully entrained in the gas. It is most important in horizontal runs of pipe. Cold flow transport lines and flow rates were selected in order to preserve the margin above saltation velocity that is expected at CTS and Healy in order to preserve transport line gas and particle dynamics.

(5) Allow for flow split control in the range 42.5-57.5%.

The Healy coal splitter must be capable of controlling the split over a precombustor fuel split range of 30-45%, or 15 percentage points. To simplify testing, both the cold flow splitter and the CTS splitter were designed to be symmetric splitters, with a required flow control range of 42.5-57.5%, or 15

percentage points.

In addition to the above modeling guidelines, there were a number of other considerations and constraints which factored into the selection of model size and operating conditions. These included:

- Use existing blower - (maximum flow capacity = 0.6 lb/s) (maximum pressure = 20 " H_2O)
- Maximum particulate feed system capability = 10 lb/min.
- Install model in existing cold flow lab - (maximum lab height available for model installation = 12 feet.)
- Model should be large enough to allow access for flow tufts, hand-held probes - (minimum cyclone diameter = 6".)
- Majority of model should be transparent to allow for visual observations.
- Model should be of modular construction to allow for investigation of alternate DCFS arrangements.
- Cold flow investigations should take full advantage of existing diagnostic equipment.
- Model design should emphasize simplicity and ease of manufacture. Use standard plexiglas tube sizes and plate thicknesses whenever possible.

The selection of model size was based primarily on existing blower limitations, flow visualization considerations, and room height limitation. As mentioned previously, the minimum cyclone diameter was determined to be six inches in order to allow for meaningful flow visualization, while the maximum cyclone diameter was determined to be 12 inches based on the limited room height available as well as the fact that both upstream and downstream splitters were being considered at the time of model design.

The other important sizing issue is the diameter of the various feed lines downstream of the blowdown cyclones. Here, the modeling guideline was to preserve the margin above saltation velocity.

7.0 TWIN CYCLONE CHARACTERIZATION TESTING

7.1 Test Objectives

The primary objective of the twin cyclone tests was to characterize twin blowdown cyclone operation in terms of pressure drop, flow stability, particulate loading, and blowdown control.

During the preliminary evaluation of non-storage coal feed systems performed as part of the DCFS proposal activities, very little information was found in the open literature related to the fluid dynamic characteristics of blowdown cyclones. Some of the important questions to be answered as part of this study were:

- o What are the pressure drop characteristics of blowdown cyclones (relative to standard zero blowdown cyclones)?
- o How does cyclone pressure drop (from cyclone inlet to cyclone top) and blowdown pressure drop (from cyclone inlet to cyclone bottom) vary as a function of the ratio of blowdown flow to total cyclone flow?
- o How stable is the gas and coal flow at the cyclone exits?
- o What is the effect of particulate loading on blowdown cyclone pressure drop and flow stability?
- o Over what range of blowdown can the cyclone be reliably and stably operated?

A second overall objective of the tests was to evaluate twin cyclone exit manifold options and select a configuration for CTS testing based on pressure drop, flow stability, and flow uniformity considerations.

The first configuration proposed for CTS testing consisted of two blowdown cyclones feeding a single precombustor. The coal and carrier air enters the twin cyclone arrangement, with approximately 25% of the air discharged through the bottom of the twin cyclones along with nearly all of the coal. At the bottom of the two cyclones, the two discharge streams are combined together prior to feeding a full-scale Healy precombustor. This configuration was selected since it allows for an evaluation of twin blowdown cyclone operation without employing a coal splitter.

Some of the key questions that needed to be answered prior to proceeding with the detail design of the CTS hardware were:

- o How should the two cyclone blowdown exits be configured, i.e u-shaped manifold, settling tank, v-shaped?
- o What should be the size of the blowdown cyclone exits so as to limit the blowdown pressure drop, and allow non-inhibited

flow?

- What should be the size of the common exit line?

- How uniform is the flow in the common exit line?

7.2 Test Configuration

A photograph of the cold flow model installed in the lab is shown in the original proprietary version of this report. Primary air was supplied to the cold flow model by a 10 hp blower through existing ductwork located in the lab. Air flow was measured with a sharp edge orifice plate that had previously been calibrated with a laser doppler anemometer (LDV) system. For the air and powder tests, talcum powder was pneumatically fed from a particulate feed tank at a nominal flow of 6 lb/min. The pressure and flow of the particle carrier air was also measured with a sonic venturi. The particulate was injected into the primary air stream far upstream of the twin cyclones (approximately 20 duct diameters) to achieve a well-mixed flow stream at the cyclone inlets.

The twin cyclones were configured with a single Y-shaped inlet in order to evaluate the cyclone characteristics independent of the splitter arrangement. A portion of the total air (nominally 25%) is "blown down" through the bottom of the cyclones, along with 90-98% of the powder. The remaining air and powder fines were vented through the top of the cyclones. The bottom of the cyclones were joined together into a single blowdown exit through the use of two 90 degree elbows and a tee. For several of the tests, a flow straightening cross was located just downstream of the tee. For powder tests, the blowdown air and powder was driven through a particulate collection tank and filter. The particulate collection tank was bypassed during air-only testing. A butterfly valve was located downstream of the collection tank for the purpose of controlling the hydraulic impedance of the blowdown lines. The clean air flow was measured with a sharp-edge orifice plate and exhausted to the roof of the building.

The cyclones were also coupled together with a single exhaust manifold located at the top of the twin cyclone assembly. A control damper was located in this exhaust line for the purpose of controlling the cyclone pressure and thus the amount of air blown down through the bottom of the cyclones. The cyclone exhaust stream was also measured with an orifice plate prior to being exhausted to the roof of the building.

Pressure measurements were made in the air supply line just upstream of the Y-shaped inlet, in the top exhaust manifold, and in the single blowdown line. During powder tests, these pressure measurements were recorded by a video camera along with the air flow measurements for post-test data reduction. Initial and final powder weights were also recorded for the purpose of determining cyclone efficiency and individual cyclone powder splits.

7.3 Test Results

A total of 12 cold flow tests were conducted during this test phase, including 7 air-only tests and 5 powder tests. A test matrix highlighting the important test parameters is shown in Table 7-1. Key test parameters were cyclone blowdown ratio, cyclone air flow rate, cyclone inlet area, cyclone exit pipe diameter, and particulate loading. Tests were also conducted to investigate the effect of a flow straightening cross on cyclone operation and flow uniformity and steadiness.

Tests are listed in Table 7-1 in chronological order. The first twin blowdown cyclone set-up was configured with 2" cyclone exits (8" - CTS scale). This exit pipe size was determined to have a relatively high pressure loss and thus the pipe size was increased to 2.5" for subsequent tests. Tests were run to assess the effect of particulate loading, blowdown ratio and cyclone inlet velocity for each configuration. Following these tests, several tests were conducted with a reduced cyclone inlet area to determine the effect of cyclone pressure drop.

The other details of test results are TRW proprietary and are excluded in this report. These results include the effect of the following parameters:

- Blowdown Ratio
- Cyclone Inlet Velocity
- Blowdown Pipe Diameter
- Powder Loading
- Cyclone Inlet Area

TABLE 7-1. TWIN CYCLONE CHARACTERIZATION TEST MATRIX.

TEST NAME	TEST OBJECTIVE	POWDER	CYCLONE INLET AREA	CYCLONE OUTLET DIAMETER	INLET VELOCITY (FT/SEC)	BLOWDOWN RATIO
DCFS1	Effect of blowdown	No	100%	2"	28	0.0–0.46
DCFS3	Effect of inlet velocity	No	100%	2"	44	0.0–0.44
DCFS4	Effect of powder addition	Yes	100%	2"	44	0.18–0.40
DCFS5	Effect of cyclone outlet pipe diameter w/powder	Yes	100%	2.5"	44	0.22
DCFS6	Effect of cyclone outlet pipe diameter w/o powder	No	100%	2.5"	44	0.0–0.46
DCFS7	Effect of cyclone outlet pipe diameter w/powder	Yes	100%	2.5"	28	0.2
DCFS8	Effect of zero blowdown w/powder	Yes	100%	2.5"	28	0
DCFS9	Effect of blowdown w/powder	Yes	100%	2.5"	28	0.10–0.30
DCFS10	Effect of inlet area	No	80%	2.5"	28	0.0–0.45
DCFS11	Effect of inlet area	No	60%	2.5"	44	0.0–0.45
DCFS12	Repeat of DCFS11	No	60%	2.5"	44	0.0–0.45

8.0 SPLITTER EVALUATION

8.1 Test Objectives

The primary objective of the splitter tests was to evaluate viable splitter concepts and select a configuration for CTS testing based on split control range and accuracy, flow stability, and pressure drop considerations.

This test phase was perhaps the most critical part of the cold flow study. Initially, four different splitter concepts were selected for possible cold flow investigation: an upstream cylindrical splitter, an upstream splash plate, a downstream isokinetic scoop splitter, and a downstream proportioner splitter. The attributes and disadvantages of each splitter concept were discussed in Section 2.2. The baseline splitter going into cold flow testing was the upstream cylindrical splitter, with the downstream isokinetic splitter and the downstream proportioner splitter as alternates. As the evaluation of the upstream cylindrical splitter proceeded, it became apparent that this splitter was by far the most promising candidate due to its simple operation. Thus, the entire splitter evaluation test phase was dedicated to a thorough examination of upstream splitter operation and control.

The major questions for the upstream splitter were as follows:

- How sensitive is splitter operation to the powder distribution at the splitter inlet?
- How effective are the cyclone inlet dampers in controlling the air and powder split?
- Does the powder split in the same proportion as the air?
- How does cyclone and blowdown pressure drop vary with damper position?
- What is the effect of powder addition on cyclone and blowdown pressure drop?
- What is the effect of splitter plate position on flow split?
- Can coal split and total carrier flow be independently controlled?
- Is the flow split stable and repeatable?
- Can the flow split be accurately determined?

8.2 Test Configuration

The test configuration is TRW proprietary and is excluded in

this report.

8.3 Test Results

Table 8-1 lists the overall test matrix for the splitter characterization tests. In all, a total of 69 tests were conducted, including 3 air-only calibration tests, 9 powder calibration tests, and 57 parametric powder runs. The majority of the tests were operated in the zero blowdown mode, in which powder collection pipes were installed at the bottom of each cyclone. This test mode was inherently simpler to operate and thus allowed a variety of parameters to be investigated in a expeditious manner. The key results of the zero blowdown tests, however, were confirmed during blowdown testing.

As shown in Table 8-1, the initial tests were dedicated to investigating basic splitter geometry. The 360° splitter was evaluated first, however it was determined that the tangential velocity in the splitter drum was insufficient to lift all of the powder up the splitter drum wall, thus resulting in significant powder storage in the bottom of the drum. The splitter drum was then reconfigured for a 135° turn, which eliminated the need to transport the solids up the wall of the splitter drum. Rectangular 45° elbows were installed downstream of the splitter drum to minimize the horizontal portion of the connecting duct. This arrangement eliminated particle accumulation in the splitter drum.

Tests were also run to assess the impact of inlet powder uniformity on solid split. The results of these tests, discussed in more detail in subsequent sections, indicated that the nominal split varied somewhat, from 45 to 55%, for different powder injector positions. However, for a given powder injector configuration, the flow split was very consistent from test to test, with a relative standard deviation of 1.3%.

A series of tests was also conducted to assess the effect of cyclone damper and splitter plate positions on cyclone air and solids split. During these tests it was determined that cyclone air and solids splits were primarily controlled by cyclone inlet damper position, with the splitter plate having only a secondary effect.

The next series of tests focused on accurate control and measurement of the solids and air split through changes in inlet damper positioning. Tests were run in both the blowdown and zero blowdown mode and compared with flow split predictions based on symmetric damper test data (CALIB1-9). The agreement between the experimental data and predictions was very good, demonstrating that the coal flow split can be accurately controlled through cyclone inlet damper positioning and determined indirectly through measurements of cyclone pressure drop and damper position.

TABLE 8-1. OVERALL TEST MATRIX FOR THE SPLITTER CHARACTERIZATION TESTS.

Test Parameter/Test Description	Number of Tests	Test Names
Baseline 360° Splitter Checkout	1	DCFS14
Baseline 135° Splitter Checkout	4	DCFS15-18
Effect of Inlet Powder Uniformity	16	DCF24-27,46-57
Effect of Inlet Damper Position (Air Only) (Air & Powder	 3 26	 DCFS35-37 DCFS19-21, 38-41, 43-45, 58-71, 74-75
Effect of Splitter Plate Position (Air Only) (Air & Powder)	 1 10	 DCFS37 DCFS22-23, 28-31, 33, 42, 72-73
Effect of Blowdown	5	DCFS38-42
Powder Calibration Tests	9	CALB1-9
Effect of Particulate Loading	3	DCFS48-50

A number of miscellaneous tests were also conducted to assess the impact of splitter design modifications on DCFS operation. These design modifications included lengthening the horizontal connecting duct sections just upstream of the cyclone inlet dampers, reducing the effective width of the connecting ducts, and providing a gap along the bottom of the damper blades to allow a small amount of air behind the damper to prevent powder storage. In addition, tests were also run to confirm instrumentation and diagnostic equipment locations for testing at CTS.

In general, the flow of powder and air through the splitter and cyclones hardware was observed to be very stable, with a minimal amount of solids storage in the system.

The tests were designed to observe and record the effect of the following parameters:

- Inlet Powder Distribution
- Cyclone Inlet Damper Position
- Effect of Splitter Plate Position
- Effect of Powder Addition on Cyclone Pressure Drop

8.4 Discussion

The baseline direct coal feed system (DCFS) concept demonstrated during cold flow model tests is a simple, inherently stable system that requires a minimum amount of control and instrumentation equipment to operate. The total coal flow rate is controlled by a weigh feeder upstream of the pulverizing mill. The total mill air flow is also controlled at the inlet of the mill. The basic function of the DCFS is to obtain the desired coal split between the precombustor and slagging combustor while controlling the amount of mill air to be used as carrier gas.

The DCFS is designed in a manner such that the functions of coal split control and total carrier air control are independent of each other. Coal split is controlled by the relative positions of the cyclone inlet dampers. Total carrier flow, on the other hand, is controlled by a single cyclone exhaust damper. Due to the coupled nature of the twin cyclone system, individual coal-to-carrier ratios will vary as a function of coal split in an unique manner such that the cyclone pressures are balanced.

A discussion on the mechanics of DCFS flow control and measurement based on the information obtained from cold flow testing is provided below.

The basic principle of splitter operation is to control the coal split through control of the air flow to each cyclone. This is accomplished by ensuring that essentially all coal particles are

fully entrained at the splitter inlet and thus travel along flow streamlines. The splitter inlet region is designed to minimize streamline curvature over the split control range of interest (± 15%), in order to minimize phase segregation, or particle "slippage" effects. The air flow to each cyclone is controlled by the relative position of the cyclone inlet dampers.

There are essentially four different ways to determine the coal flow split to the precombustor and slagging combustor. They are (1) measure coal flow directly in the individual feedlines, (2) infer coal split from direct measurement of the air flow to each individual cyclone, (3) infer coal split from indirect measurement of the air flow to each individual cyclone, and (4) infer the coal split based on precombustor and combustor operational characteristics. While all four methods above are still considered viable options, cold flow testing focused on item (3) above.

Two different indirect air flow measurement schemes were considered. The first method allows one to infer cyclone inlet velocity and mass split based on cyclone pressure drop and inlet damper position. The second method relies on direct measurement of flow velocity in the region just upstream of the cyclone inlet dampers. In both cases, the actual powder split is determined by assuming that no phase segregation occurs upstream of the splitter, i.e. the powder is fully entrained and uniformly distributed throughout the flow, and travels along flow streamlines. Comparisons between actual and calculated flow splits were then made to determine the validity of this assumption.

In the first method, cyclone pressure drop must first be characterized as a function of damper position. This was accomplished by conducting a series of tests at different inlet damper positions. For each test, the relative damper position of each cyclone was the same so that the cyclone inlet velocity and inlet mass flow rate should also be the same. As powder was added, the cyclone pressure drop was observed to decrease, due to changes in the effective wall friction coefficient.

One of the objectives of the cold flow test program was to develop recommendations on DCFS instrumention for CTS testing. To this end, a number of different pressure tap locations were evaluated during cold flow testing. Table 8-2 lists the recommended locations for CTS testing. All pressures correspond to static conditions with the exception of the cyclone exhaust manifold, where the pressure tap is located at a stagnation point. The splitter inlet pressure tap should be located 1 duct diameter upstream of transition section. The cyclone inlet pressure taps should be located on the top wall of the connecting ducts just upstream of the inlet dampers, in order to keep the pressure taps relatively clean. Likewise, the pressure taps in each of the blowdown legs should also be located along the top of the pipe, downstream of the 90° elbows. Pressure measurement upstream of the elbows should be avoided as significant circumferential variations

Table 8-2 Recommended Pressure Tap Locations for CTS Testing

Location	Description
Splitter Inlet	• Locate 1 duct diametr upstream of transition section, with 90° rotation away from powder injection line
Cyclone Inlets	• Locate half-way between 45° elbow outlet and damper shaft in the center of top wall
Cyclone Vent Manifold	• Locate directly opposite center line of single exit pipe
Cyclone Blowdown Line	• Locate approximately 3-5 line diameters downstream of 90° elbow along top of pipe.

in pressure were observed due to the swirl in the pipe.

A number of tests were conducted to ensure that the DCFS was designed to minimize the temporary and/or permanent storage of coal within the various DCFS components. Temporary storage is defined as accumulation of powder during operation which does not remain when powder flow to the system is shut off. Permanent solids storage persists after shutdown and thus may be considered in some circumstances to be a safety hazard. During initial splitter testing, both types of storage were observed in the system. Subsequent to this observation, design modifications were made to minimize solids storage.

The first area of concern was the splitter drum. With a flat splitter plate, the axial velocity within the drum was not high enough to direct the powder to the splitter exit within the first half turn. To correct this, a contoured splitter plate, was designed and installed in the cold flow model. The contoured plate was observed to effectively direct both the air and powder towards the spliiter exits while minimizing powder accumulation within the drum.

Temporary solids storage was also observed in the connecting ducts between the splitter and the two cyclones, particularly for duct velocities below 40 ft/s. At first, an attempt was made to locally increase the velocity in the critical region of the duct by adding ramp-like inserts. This approach proved to be unsuccessful as powder accumulation was still present downstream of the ramp inserts where the velocity fell below 40 ft/s. The next approach was to reduce the width of the connecting duct along its entire length. This was accomplished in the cold flow model by installing 3/8" inserts along the inside wall of each duct. This increased the average velocity along the entire duct and effectively eliminated the solid storage problem in the cold flow model.

During DCFS Design Verification Tests at CTS, coal accumulation in the connecting ducts was observed. In response to this problem, the DCFS cold flow model was reactivated and used for trouble shouting. A new insert was designed and verified through cold flow testing. This insert was subsequently scaled to DVT size and then successfully tested at CTS. The connecting ducts for the Healy DCFS are based on this modified design.

The powder storage was also observed behind each damper at the inlet of the cyclones, which was believed to be caused by flow recirculation due to the lower pressure behind the damper. This storage was particularly undesirable since it was difficult to remove on-line, as well as limited the range of the dampers. The solution to this problem was to trim the bottom of each damper to create a small gap. This allowed a small portion of the air to sweep under the damper and prevent powder from accumulating behind the damper. Following this modification, no solids storage of any kind was observed behind the dampers.

9.0 EDUCTOR EVALUATION

9.1 Test Objectives

The primary objective of the eductor tests was to characterize eductor operation in terms of flow requirements, coal/gas outflow uniformity, and impact on other DCFS components.

Due to pressure difference between the precombustor and the slagging stage, it may be necessary to boost the precombustor coal line pressure through the use of an eductor system in order to properly balance the system. In anticipation of this, a sub-scale eductor was tested in the cold flow model. Key concerns is whether a sufficient pressure boost can be obtained at an acceptable eductor supply pressure, whether the presence of the eductor adversely affects the operation of the coal feed system, and also to verify the analytical model of the eductor system.

9.2 Test Configuration

The test configuration for the eductor evaluation tests was similar to that for the splitter evaluation, except that a transparent eductor was installed in the right cyclone blowdown leg. An additional compressed air supply line was connected to the eductor motive fluid injector, with the compressed air measured with a sonic orifice. Pressures were measured on each side of the eductor in order to determine boost performance. During powder tests, all pressure and flow measurements were recorded with a video camera for post-test data reduction. A second video camera was used to record powder flow patterns in the eductor.

The rest of the details are TRW proprietary and excluded in this report.

9.3 Test Results

The test matrix followed during eductor testing is shown in Table 9-1. Three air-only tests were first conducted in order to compare actual eductor performance against an in-house eductor performance code. Tests were run at two different locations downstream of the 90° elbow (L/D = 3 and 9) to effectively bracket the range of eductors locations being considered for CTS testing. Two additional eductor tests were run with the nominal powder addition used for the splitter tests (solids-to-gas ratio = 1:4). The first test was run with symmetric cyclone dampers, while the second was run with the left cyclone damper partially closed.

During the air-only tests, the eductor flow ratio, defined as the eductor motive fluid flow divided by the eductor inlet flow, was varied over the range of 9-17%. The nominal eductor flow ratio during CTS testing is expected to be 15%. The results of eductor test #1 (EDUCT1) indicated that the actual eductor boost was

TABLE 9-1. EDUCTOR EVALUATION TEST MATRIX

TEST	EDUCTOR FLOW RATIO (PERCENT)	EDUCTOR POSITION (L/D)	DAMPER POSITION (a)	SPLITTER POSITION (b)	POWDER INJECTION	MASS SPLIT LEFT CYCLONE	PERCENT RIGHT CYCLONE
EDUCT 1	9-17	3.3	100/100	50/50	NO	N/A	N/A
EDUCT 2	9-15	3.3	100/100	50/50	NO	N/A	N/A
EDUCT 3	9-15	9.0	100/100	50/50	NO	N/A	N/A
EDUCT 4	12-15	3.3	100/100	50/50	YES	49.4	50.6
EDUCT 5	14-18	3.3	57/100	50/50	YES	45.0	55.0

a - AIR INLET FRACTION (CYC1/CYC2)

b - INLET FLOW SPLIT (CYC1/CYC2)

significantly below that expected based on model calculations. Following the test, the eductor was inspected and it was determined that the injector at the center of the eductor was slightly misaligned. Subsequent troubleshooting revealed that the eductor performance was quite sensitive to injector positioning, at least for eductor flow ratios in the range of interest. Thus, prior to the next text the eductor injector was carefully aligned along the centerline of the eductor.

The results of EDUCT2 indicated much better agreement between the data and model calculations.

Test EDUCT3 was conducted to determine the effect of eductor location on performance. For this test, the eductor was moved six duct diameters downstream away from the 90° elbow to effectively reduce the swirl at the inlet of the eductor. The results of EDUCT3 indicated good agreement between the data and calculation.

During tests EDUCT4 and EDUCT5, powder was introduced into the flow upstream of the splitter in order to verify eductor performance during two-phase flow operation. During these tests, the eductor motive flow was held constant, however the inlet flow (cyclone blowdown flow) tended to decrease slightly as the particulate filter located in the powder collection tank started to clog. This effect allowed for collection of data over a range of eductor flow ratios. The results of EDUCT4 and EDUCT5 indicated that both the measured and calculated values are lower than those obtained during air-only testing, due to the effect of powder addition. However, the difference between the measured eductor boost and the calculated values is approximately 10-15%, which is the same as that observed during air-only testing.

In general, the flow of air and powder through the eductor was observed to be steady at the nominal eductor conditions. A swirl pattern was observed both upstream and downstream of the eductor, however, the presence of swirl does not appear to significantly affect eductor performance. The swirl was observed to tighten in the throat of the eductor, and then stretch out again in the diffuser section.

The presence of the eductor also did not appear to adversely affect the operation of either the splitter or the cyclones. For symmetric inlet dampers, a powder split of 49.4/50.6 was obtained, which is slightly unusual since the nominal powder split for symmetric dampers was 51.3/48.7. The powder split obtained when the left cyclone damper was partially closed was 45.0/55.0 which agrees well with the previous splitter calibration data. A complete calibration of the splitter was not performed during eductor testing due time and budgetary constraints as well as the uncertainty of whether an eductor system will be required for the Healy DCFS.

10.0 SLAGGING COMBUSTOR SPLITTER AND TRANSPORT LINES EVALUATION

10.1 Test Objectives

The primary objective of the slagging combustor splitter and transport lines tests was to help select a configuration for the Healy DCFS that could reliably and stably split the slagging combustor coal flow into six individual streams feeding the six coal injectors located at the head end of the slagging combustor. This test phase was particularly important since the slagging stage coal feed line and splitter will not be verified with hot-fired tests at CTS prior to installation at Healy.

Some of the important selection criteria for the slagging combustor splitter include low pressure drop, split distribution, lack of solids accumulation, low wear characteristics, and the fit within the coal feed line topology. One additional consideration is the relationship between the injector coal flow distribution and the mixing patterns within the head end of the combustor. Previous cold flow studies showed that asymmetric mixing patterns exist in the head end of the combustor as a result of the single tangential air inlet. Coal that is injected on the same side as the air inlet has a greater tendency to travel down the centerline of the combustor, with a corresponding lower residence time and a lower probability of slag particle capture. Thus, a splitter which feeds a larger proportion of the total coal to the injectors on the opposite side of the air inlet is desirable.

A number of different splitter concepts were considered prior to cold flow testing, including a scroll-type splitter similar to the precombustor coal burner, a ring-type splitter, a rectangular, or "cobra" splitter, and a cone-like splitter.

For the cold flow evaluation, the cobra splitter was given top priority due to its success in providing a uniform powder and air distribution in previous tests with the primary DCFS splitter. The cone splitter was also tested since it had been successfully demonstrated during Cleveland hot-fired testing, although in a different orientation.

10.2 Test Configuration

The test configuration is TRW proprietary, and is excluded in this report.

10.3 Test Results

The test results are TRW proprietary, and are excluded in this report.

11.0 CONCLUSIONS AND RECOMMENDATIONS

11.1 Twin Cyclone Characterization Testing

1. A total of 12 cold flow tests were conducted during this test phase, including 7 air-only tests and 5 powder tests.

2. Key test parameters were cyclone blowdown ratio, cyclone air flow rate, cyclone inlet area, cyclone exit pipe diameter and powder loading.

3. Cyclone pressure drop, measured from cyclone inlet to vent was found to be independent of cyclone blowdown ratio over the range of interest (0-40%).

4. Blowdown pressure drop, measured from cyclone inlet to blowdown exit, increases linearly with blowdown ratio. For the cyclone geometry of interest, the blowdown pressure drop is 20-40% higher than the cyclone pressure drop depending on blowdown ratio.

5. Cyclone pressure drop was observed to be proportional to the square of cyclone inlet velocity, for a constant cyclone inlet area.

6. Both the cyclone and blowdown pressure drops were observed to decrease when powder was injected upstream of the cyclones. This decrease in pressure drop is attributed to an increase in effective wall roughness, which in turn reduces the average tangential velocity and subsequently the overall pressure drop.

7. Both the cyclone and blowdown pressure drop were found to decrease as the cyclone inlet area was reduced, for a constant inlet cyclone velocity. This reveals that the cyclone pressure drop was not only dependent on cyclone inlet velocity, but on inlet mass flow as well.

11.2 Splitter Evaluation

1. The 360° degree upstream cylindrical splitter was eliminated from consideration due to significant powder storage in the bottom of the splitter drum.

2. The 135° degree splitter configuration with a contoured splitter plate effectively minimized powder storage within the splitter drum.

3. The flow conditioning sections located upstream of the splitter drum were observed to uniformly distribute incoming powder prior to entering the splitter.

4. The majority of the powder was observed to flow along the

outer wall of the splitter, however a small recirculation zone was observed just above each of the splitter outlets.

5. Some temporary powder storage was observed in the connecting ducts for flow velocities below approximately 40 ft/s.

6. A number of different powder injection methods were investigated in order to assess the sensitivity of the splitter to inlet powder distributions. In all cases, the actual powder split stayed between 45 and 55%, even in the extreme case in which the powder was purposely biased to the left and right wall of the inlet duct.

7. For a given inlet powder distribution, the powder split was found to be very repeatable, with a relative standard deviation of 1.3%.

8. The powder split is primarily controlled by the positioning of the cyclone inlet dampers. The position of the splitter plate was found to play only a secondary role for splitter plate positions in the range of 40-60%.

9. For a given mass flow rate, cyclone pressure drop was observed to increase as one or both of the dampers were closed.

10. The splitter pressure drop was measured to be small relative to the cyclone pressure drop (~10%).

11. The total cyclone blowdown was found to be independent of cyclone flow split over the range of interest. This indicates that the coal flow split can be controlled independent of the total carrier flow rate.

12. The pressures at the bottom of each cyclone were found to be equal throughout the flow split control range. Thus, as the coal split is varied, the individual carrier flows will automatically adjust to preserve this pressure balance. In other words as the coal to one line is increased, the corresponding blowdown air flow will decrease in order to maintain a constant pressure drop between the cyclones and the coal injectors. The opposite effect will occur in the other line.

13. Overall cyclone efficiency for the twin cyclone system was found to be essentially constant over the required flow split range.

14. Two different methods of measuring cyclone air flow split were investigated: (1) inferring the split from direct measurement of cyclone inlet velocity and (2) inferring the split from cyclone pressure drop and damper position. Very good agreement was found between the two methods.

15. Very good agreement was also found between inferred cyclone air splits and actual cyclone powder splits. This result confirmed that the powder splits according to the air split and that the powder split can be measured indirectly on-line thorough measurement of the individual cyclone pressure drops and damper position.

16. If possible, the CTS and Healy cyclones should be calibrated at the nominal solids-to-gas ratio, due to the dependence of cyclone pressure drop on powder loading. However, based on the results of cold flow testing, the level of powder addition was observed to have only a secondary effect on the calculated air split curves. Thus, if powder calibration is not possible, then a correction can be added to account for the effects of powder addition based on cold flow test data.

11.3 Eductor Evaluation

1. The eductor performance is sensitive to the alignment of the motive fluid injector. If the injector is misaligned or extends into the throat section, eductor pressure boost can be decreased by as much as 50%.

2. Once the injector was properly located, good agreement was obtained between measured and calculated eductor performance.

3. Eductor performance decreased slightly when the eductor was relocated form 3.3 to 9.0 diameter downstream of the cyclone blowdown leg.

4. The addition of powder did not change the basic performance of the eductor, with measured pressure boost remaining approximately 10-15% below calculations which is the same as that observed during air-only testing.

5. In general, the flow of air and powder through the eductor was observed to be steady at the nominal eductor conditions. A swirl pattern was observed both upstream and downstream of the eductor, however, the presence of swirl does not appear to significantly affect eductor performance.

6. The presence of the eductor also did not appear to adversely affect the operation of either the splitter or the cyclones.

11.4 Slagging Combustor Splitter and Transport Line Evaluation

1. A cobra-type splitter with a horizontal transition section is susceptible to solids accumulation. Vertical orientation of the transition section is preferred however this is not possible within the space constraints of the Healy plant.

2. A vertical cone-like splitter is recommended for the Healy DCFS as it eliminates the need for a horizontal transition

section. A similar cone splitter was successfully operated during Healy coal tests at the Cleveland facility.

3. The vertical cone splitter configuration delivers a greater proportion of the total coal to injectors located opposite the coal-fired precombustor. This may be desirable to promote better mixing of the coal and air in the head end of the combustor.